PB86-241551

# Studies in Geophysics
# Active Tectonics

National Research Council, Washington, DC

Prepared for

Geological Survey, Washington, DC

1986

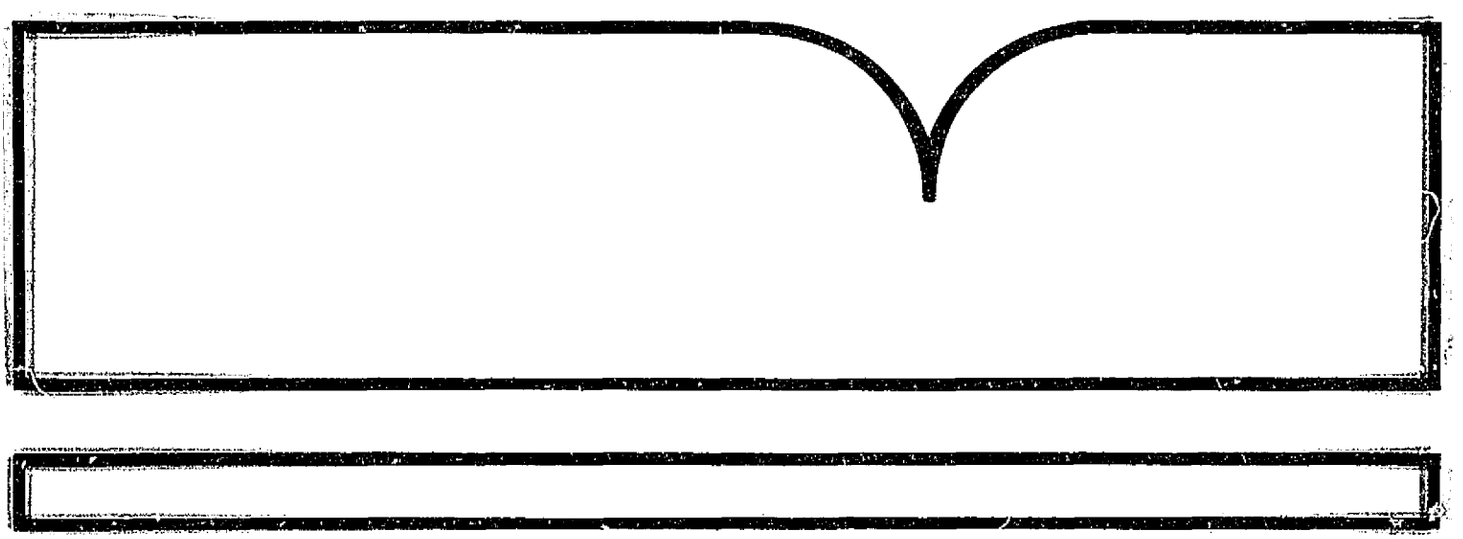

U.S. Department of Commerce
National Technical Information Service
NTIS

STUDIES IN GEOPHYSICS

NRC NAS NAE IOM

# Active Tectonics

50272-101

| REPORT DOCUMENTATION PAGE | 1. REPORT NO. ISBN 0-309-03638-0 | 2. | 3. Recipient's Accession No. PB86 224351/AS |
|---|---|---|---|

**4. Title and Subtitle**
ACTIVE TECTONICS

**5. Report Date**
April 1986

**6.**

**7. Author(s)**

**8. Performing Organization Rept. No.**
ISBN 0-309-03638-0

**9. Performing Organization Name and Address**
National Research Council
Commission on Physical Sciences, Mathematics, & Resources
2101 Constitution Ave., N.W.
Washington, DC 20418

**10. Project/Task/Work Unit No.**

**11. Contract(C) or Grant(G) No.**
(C) DE-FG02-82ER12018
(G) EAR-8216205

**12. Sponsoring Organization Name and Address**
U.S. Geological Survey, Department of Energy, National Science Foundation, National Aeronautics & Space Adm., National Oceanic & Atmospheric Administration, Defense Advanced Research Project

**13. Type of Report & Period Covered**
Final

**14.**

**15. Supplementary Notes**
Report is part of series of "Studies in Geophysics". Preliminary findings presented at a symposium of the American Geophysical Union held in June 1983 in Baltimore, MD. Report includes an index.

**16. Abstract (Limit: 200 words)**

Active tectonics is defined within the study as tectonic movements that are expected to occur within a future time span of concern to society. Such movements and their associated hazards include earthquakes, volcanic eruptions, and land subsidence and emergence.

The entire range of geology, geophysics, and geodesy is, to some extent, pertinent to this topic. The needs for useful forecasts of tectonic activity, so that actions may be taken to mitigate hazards, call for special attention to ongoing tectonic activity--its rates, styles, and patterns. Many of these processes cannot be described reasonably using the limited instrumental or historical records; however, most can be adequately described for practical purposes using the geologic record of the past 500,000 years. In this context, further progress in understanding active tectonics depends on continued research on a range of geologic, geophysical, and geodetic topics; particularly important is improvement in the accuracy of dating techniques for recent geologic materials.

**17. Document Analysis a. Descriptors**
geology, geophysics, seismology, geodesy, earthquakes, volcanoes, deformation, geomorphology, tectonics, neotectonics, hazards, faulting, folding, dating, hillslopes, tilt, strain, soils

**b. Identifiers/Open-Ended Terms**
San Andreas Fault, Mississippi River, California, Ventura uplift,

**c. COSATI Field/Group**

| 18. Availability Statement | 19. Security Class (This Report) | 21. No. of Pages |
|---|---|---|
| "Distribution is unlimited." | Unclassified | 280 |
| | 20. Security Class (This Page) Unclassified | 22. Price |

STUDIES IN GEOPHYSICS

# Active Tectonics

Geophysics Study Committee
Geophysics Research Forum
Commission on Physical Sciences,
Mathematics, and Resources
National Research Council

NATIONAL ACADEMY PRESS
Washington, D.C. 1986

NATIONAL ACADEMY PRESS 2101 Constitution Avenue, N.W. Washington, DC 20418

NOTICE: The project that is the subject of this report was approved by the Governing Board of the National Research Council, whose members are drawn from the Councils of the National Academy of Sciences, the National Academy of Engineering, and the Institute of Medicine. The members of the committee responsible for this report were chosen for their special competences and with regard for appropriate balance.

This report has been reviewed by a group other than the authors according to procedures approved by a Report Review Committee consisting of members of the National Academy of Sciences, the National Academy of Engineering, and the Institute of Medicine.

The National Research Council was established by the National Academy of Sciences in 1916 to associate the broad community of science and technology with the Academy's purposes of furthering knowledge and of advising the federal government. The Council operates in accordance with general policies determined by the Academy under the authority of its congressional charter of 1863, which establishes the Academy as a private, nonprofit, self-governing membership corporation. The Council has become the principal operating agency of both the National Academy of Sciences and the National Academy of Engineering in the conduct of their services to the government, the public, and the scientific and engineering communities. It is administered jointly by both Academies and the Institute of Medicine. The National Academy of Engineering and the Institute of Medicine were established in 1964 and 1970, respectively, under the charter of the National Academy of Sciences.

The Geophysics Study Committee is pleased to acknowledge the support of the National Science Foundation, the Defense Advanced Research Projects Agency, the National Aeronautics and Space Administration, the National Oceanic and Atmospheric Administration, the U.S. Geological Survey, and the Department of Energy (Grant #DE-FG02-82ER12018) for the conduct of this study.

Library of Congress Cataloging-in-Publication Data

Main entry under title:

Active tectonics.

(Studies in geophysics)
Includes index.
1. Geology, Structural—Addresses, essays, lectures.
I. Geophysics Research Forum (U.S.) Geophysics Study Committee. II. Series.
QE601.A25 1986 551.8 85-32026
ISBN 0-309-03638-0

Printed in the United States of America


National Academy Press

The National Academy Press was created by the National Academy of Sciences to publish the reports issued by the Academy and by the National Academy of Engineering, the Institute of Medicine, and the National Research Council, all operating under the charter granted to the National Academy of Sciences by the Congress of the United States.

# Panel on Active Tectonics

ROBERT E. WALLACE, U.S. Geological Survey, Menlo Park, *Chairman*
CLARENCE R. ALLEN, California Institute of Technology
LARRY D. BROWN, Cornell University
LLOYD S. CLUFF, Pacific Gas & Electric
BRUCE M. CROWE, Los Alamos National Laboratory
JOHN C. CROWELL, University of California, Santa Barbara
EDWARD A. KELLER, University of California, Santa Barbara
KENNETH R. LAJOIE, U.S. Geological Survey, Menlo Park
LARRY MAYER, Miami University
DAVID NASH, University of Cincinnati
DONALD W. PETERSON, U.S. Geological Survey, Vancouver
KENNETH L. PIERCE, U.S. Geological Survey, Denver
STANLEY A. SCHUMM, Colorado State University
DAVID P. SCHWARTZ, Woodward-Clyde Consultants
D. BURTON SLEMMONS, University of Nevada, Reno
ARTHUR G. SYLVESTER, University of California, Santa Barbara
WAYNE THATCHER, U.S. Geological Survey, Menlo Park
ROBERT S. YEATS, Oregon State University

*Staff*

THOMAS M. USSELMAN

# Geophysics Study Committee

ARTHUR E. MAXWELL, The University of Texas at Austin, *Chairman*
†ALLEN F. AGNEW, Geological Consultant, Corvallis, Oregon
†RICHARD A. ANTHES, National Center for Atmospheric Research
*COLIN BULL, Mercer Island, Washington
GORDON P. EATON, Texas A&M University
DEVRIE S. INTRILIGATOR, Carmel Research Center
*NICHOLAS C. MATALAS, U.S. Geological Survey, Reston
J. MURRAY MITCHELL, National Oceanic and Atmospheric Administration
*V. RAMA MURTHY, University of Minnesota
†RICHARD J. O'CONNELL, Harvard University
†MARTIN WALT, Lockheed Missiles and Space Company, Inc.
FERRIS WEBSTER, University of Delaware

*Liaison Representatives*

RALPH ALEWINE, Defense Advanced Research Projects Agency
BRUCE B. HANSHAW, U.S. Geological Survey, Reston
GEORGE A. KOLSTAD, Department of Energy
MICHAEL MAYHEW, National Science Foundation
NED OSTENSO, National Oceanic and Atmospheric Administration
SHELBY TILFORD, National Aeronautics and Space Administration

*Staff*

THOMAS M. USSELMAN

*Terms ended June 30, 1985.
†Terms began July 1, 1985.

# Geophysics Research Forum

*Ex Officio*

JOHN D. BOSSLER, National Geodetic Survey
ROBERT K. CRANE, Dartmouth College
FRANK D. DRAKE, University of California, Santa Cruz
ROBERT HOFSTADTER, Stanford University

*Staff*

PEMBROKE J. HART

# Commission on Physical Sciences, Mathematics, and Resources

"Page missing from available version"

# Studies in Geophysics*

ENERGY AND CLIMATE
Roger R. Revelle, *panel chairman*, 1977, 158 pp.
CLIMATE, CLIMATIC CHANGE, AND WATER SUPPLY
James R. Wallis, *panel chairman*, 1977, 132 pp.
ESTUARIES, GEOPHYSICS, AND THE ENVIRONMENT
Charles B. Officer, *panel chairman*, 1977, 127 pp.
THE UPPER ATMOSPHERE AND MAGNETOSPHERE
Francis S. Johnson, *panel chairman*, 1977, 169 pp.
GEOPHYSICAL PREDICTIONS
Helmut E. Landsberg, *panel chairman*, 1978, 215 pp.
IMPACT OF TECHNOLOGY ON GEOPHYSICS
Homer E. Newell, *panel chairman*, 1979, 121 pp.
CONTINENTAL TECTONICS
B. Clark Burchfiel, Jack E. Oliver, and Leon T. Silver, *panel co-chairmen*, 1980, 197 pp.
MINERAL RESOURCES: GENETIC UNDERSTANDING FOR PRACTICAL APPLICATIONS
Paul B. Barton, Jr., *panel chairman*, 1981, 118 pp.
SCIENTIFIC BASIS OF WATER-RESOURCE MANAGEMENT
Myron B. Fiering, *panel chairman*, 1982, 127 pp.
SOLAR VARIABILITY, WEATHER, AND CLIMATE
John A. Eddy, *panel chairman*, 1982, 106 pp.
CLIMATE IN EARTH HISTORY
Wolfgang H. Berger and John C. Crowell, *panel co-chairmen*, 1982, 197 pp.
FUNDAMENTAL RESEARCH ON ESTUARIES: THE IMPORTANCE OF AN INTERDISCIPLINARY APPROACH
Charles B. Officer and L. Eugene Cronin, *panel co-chairmen*, 1983, 79 pp.

*Published to date.

EXPLOSIVE VOLCANISM: INCEPTION, EVOLUTION, AND HAZARDS
Francis R. Boyd, Jr., *panel chairman*, 1984, 176 pp.
GROUNDWATER CONTAMINATION
John D. Bredehoeft, *panel chairman*, 1984, 179 pp.
ACTIVE TECTONICS
Robert E. Wallace, *panel chairman*, 1986, 266 pp.

# Preface

This study is part of a series of *Studies in Geophysics* that have been undertaken for the Geophysics Research Forum by the Geophysics Study Committee. One purpose of each study is to provide assessments from the scientific community to aid policymakers in decisions on societal problems that involve geophysics. An important part of such assessments is an evaluation of the adequacy of current geophysical knowledge and the appropriateness of current research programs as a source of information required for those decisions.

This study on active tectonics was initiated by the Geophysics Study Committee and the Geophysics Research Forum in consultation with the liaison representatives of the agencies that support the Geophysics Study Committee, relevant committees and boards within the National Research Council, and members of the scientific community.

The study addresses our current scientific understanding of active tectonics—particularly the patterns and rates of ongoing tectonic processes. Many of these processes cannot be described reasonably using the limited instrumental or historical records; however, most can be described adequately for practical purposes using the geologic record of the past 500,000 years. A program of fundamental research focusing especially on Quaternary tectonic geology and geomorphology, paleoseismology, neotectonics, and geodesy is recommended to better understand ongoing, active tectonic processes.

The preliminary scientific findings of the authored background chapters were presented at an American Geophysical Union symposium in San Francisco in December 1983. In completing their chapters, the authors had the benefit of discussion at this symposium as well as the comments of several scientific referees. Ultimate responsibility for the individual chapters, however, rests with their authors.

The Overview of the study summarizes the highlights of the chapters and formulates conclusions and recommendations. In preparing the Overview, the panel chairman and the Geophysics Study Committee had the benefit of meetings that took place at the symposium and of the comments of the panel of authors and other referees. Responsibility for the Overview rests with the Geophysics Study Committee and the chairman of the panel.

"Page missing from available version"

# Contents

# Active Tectonics

"Page missing from available version"

# Overview and Recommendations

Ninety-two thousand people were killed in the Tambora, Indonesia, eruption of 1815; over 820,000 were killed in the Sian, China, earthquake of 1556; 240,000 were killed by the earthquake of 1976 at Tangshan, China; and about 6000 were killed in the 1985 earthquake in Mexico City. Less spectacular, but economically serious, are the effects of slower tectonic processes or tectonic events of smaller amplitude that can, for example, disrupt river channels or warp coastlines and harbors. Only the most stable blocks of the Earth's crust provide suitable long-term repositories for the disposal of radioactive waste, yet almost no region is completely free of tectonic changes over millenia. Thus, the evaluation of active tectonic processes is critical to many of mankind's activities, so that hazards can be minimized and structures can be sited and constructed in ways that serve their functions most effectively, economically, and safely.

To fully evaluate ongoing tectonic activity and its associated hazards requires knowledge of the rates, styles, and patterns of tectonic processes. Many of these processes cannot be described reasonably using the limited instrumental or historical records; however, most can be described adequately for practical purposes using the geologic record of the past 500,000 yr.

In the following discussion *active tectonics* is defined as tectonic movements that are expected to occur within a future time span of concern to society, and the significance of active tectonism to society is of special concern. The entire range of geology, geophysics, and geodesy is, to some extent, pertinent to this topic; but the needs for useful forecasts of tectonic activity, so that actions may be taken to mitigate hazards, call for special attention to ongoing tectonic activity, its rates, styles, and patterns. The question of what constitutes ongoing is itself addressed because the patterns of activity leading to some catastrophic events cannot necessarily be delineated by a few-year-long data base or even by all of recorded history. For example, some of the largest earthquakes that have occurred were generated along segments of great faults that are now seismically very quiet. In some places, the historical seismic record suggests, inaccurately, an inverse pattern of what the long-term geologic record demonstrates.

Understanding the period from the present to about 500,000 yr ago (the late Quaternary) forms the best basis for analyzing active tectonics of concern to society. To study this period of time calls for a special mix of geologic, seismological, geophysical, and geodetic techniques, many of which need major research efforts to achieve their full potential. Some of the most critical needs are highlighted in this Overview. Detailed discussions of recent advances in understanding active tectonic processes and their rates appear in the authored chapters that follow this Overview.

Many research programs that can provide background for the study of active tectonics have been considered in earlier reviews by the National Research Council, including such reports as *Geophysical Predictions* (1978), *Earthquake Research for the Safer Siting of Critical Facilities* (1980), *Geodetic Monitoring of Tectonic Deformation—Toward a Strategy* (1981), *Effective Use of Earthquake Data* (1983), *Seismographic Networks: Problems and Outlook for the 1980s* (1983), *Explosive Volcanism: Inception, Evolution, and Hazards* (1984), and *Seismological Studies of the Continental Lithosphere* (1984). Research needs in, for example, seismological and geodetic techniques of importance to active tectonics are well formulated in these documents. The present study makes no attempt to review all these previous analyses but builds on them and specifically endorses some previous recommendations. For the most part, the previous reports have not addressed the premodern part of the time frame of the past few hundred thousand years, which must be understood to evaluate ongoing tectonic activity fully.

Some potentially powerful techniques that should be developed by accelerated research are considered in this study. The recently emerging subdiscipline of paleoseismology—in which geologic techniques are used to identify and evaluate prehistoric earthquakes—has provided some of the most important recent advances in earthquake prediction. Similar techniques have also permitted evaluation of seismic hazards for urban areas and for critical facilities such as dams and nuclear reactors. Essential to such geologic research and evaluations are the ages of geologic units. Only by having the geologic history calibrated by known dates can we calibrate the (1) recurrence intervals of earthquakes and volcanic eruptions and (2) continuing rates and changes of rates of all tectonic processes. The determination of rates of processes and means of dating materials of late Quaternary age (past 500,000 yr) thus are considered of high priority for research attention.

Among other facets of geology that have been underused in studying active tectonics is geomorphology. Landforms are everywhere; they are extremely sensitive to active tectonics; and geomorphic analysis has the potential for providing insights into active tectonic rates, styles, and patterns of deformation available through almost no other approach. Serious efforts are needed to accelerate research in quantitative geomorphology.

The need is recognized for improving geodetic measurements of active tectonics through new land-based instruments, such as two-color laser distance-measuring devices, and space-related techniques, such as the Global Positioning System (GPS). Regional seismic networks are considered essential to track the patterns of ongoing strain release, to assist in mapping the activity of faults, and to assist in tracking the movement of magmas under volcanoes. Rapid data gathering, processing, and analyses are imperative. Great volumes of data from regional seismic networks and a variety of strain meters and geodetic networks must be handled quickly if useful forecasts (with lead times up to a few weeks) of earthquakes, volcanic eruptions, and landslides are to be made successfully.

In summary, this study addresses tectonic processes, their rates, and methods of identifying and evaluating active tectonics by analysis of events, especially in the time frame from the present to about 500,000 yr ago. Except for brief comments, the socioeconomic and engineering accommodations for coping with the problems created by

active tectonic processes are not addressed; they are in the domain of other specialists and other reports.

## ACTIVE TECTONICS

In the earth sciences "tectonics" refers to the deformational structures and architecture of the outer parts of the Earth and to the evolution of these features through time. Examples include folds, warpings and tiltings of crustal blocks, and displacement on faults. In this study we define "active tectonics" as "tectonic movements that are expected to occur within a future time span of concern to society."

This definition of active tectonics has evolved from the many definitions of active fault that have been used in the past. The lack of agreement on a single definition of an active fault has caused confusion and attendant engineering, social, and legal difficulties. Many of the definitions inappropriately have mixed elements including criteria for identifying faults, criteria for estimating degree of activity, and value judgments about the level of activity that constitutes acceptable risk to mankind.

The terms *active faults* and *active tectonics* imply that events are currently happening, but here the term *currently* is ambiguous. The *present* is a moving instant that progresses ever forward in time. To most people currently very likely is thought of in minutes, or at most in years, whereas to a geologist a time sample that appropriately represents currently or present might span many thousands of years. Focusing the definition of active tectonics on the future avoids selecting a single period of time to represent the present and emphasizes the prediction of future tectonic events, which has the greatest potential benefit in guiding hazard-reduction actions.

The frequency of occurrence of specific faulting events has been incorporated in some definitions of active faults. Thus, various public agencies define an active fault as having had displacements (a) in 10,000 yr, (b) in 35,000 yr, (c) in 150,000 yr, or (d) twice in 500,000 yr. Such definitions have come to carry legal significance, and the great range in time frame has caused confusion. The differences reflected in these definitions relate principally to the degree of activity and to the levels of risk that are acceptable to various agencies. A far less confusing approach is to simplify the definition itself, to describe the rates of processes separately from the processes themselves, and to judge what risk is acceptable to society separately from the description of processes and their rates.

Geologists, geophysicists, and geodesists can identify the geologic structures and can describe and evaluate the degree of activity and the patterns of activity. It is the role of engineers to try to accommodate and minimize the deleterious effects of tectonic activity; policymakers must decide whether the rates of processes and engineering accommodations of those processes result in an acceptable situation or level of risk.

## TECTONIC PROCESSES

Tectonic deformation may occur as broad warping of the Earth's surface, termed epeirogeny, to produce or reshape the larger features of continents and ocean basins, or it may be orogenic, that is, in more localized regions and belts to form mountain chains. The vertical movements of epeirogeny may result in plateaus and basins, whereas the more complex deformational processes of orogeny, or mountain building, include, for example, folding, faulting, plastic deformation, plutonism, and volcanism.

The styles and rates of tectonic processes range widely; the most active and complex tend to occur along the margins of lithospheric plates. The continental margin of western North America, where the Pacific, North American, and Juan de Fuca-Gorda plates join, exemplifies the complexity that can exist at such boundaries. Strike slip predominates where the Pacific and North American plates are in contact in Califor-

nia; convergence and subduction occur where the oceanic Juan de Fuca-Gorda plates slide beneath the continental North American plate in Oregon and Washington; and, where the three join at the Mendocino triple junction, several directions and rates of plate motion must be accommodated in a complex geometric pattern. The oblique relative movements of the Pacific and North American plates farther south in Mexico result in the shifting of Baja California northwestward away from continental Mexico. A similar pattern of crustal extension is present across the intraplate Basin and Range province.

Examples of epeirogenic movements include the broad uplift of the Colorado Plateau, the Monroe Uplift across the lower Mississippi River Valley, the isostatic rebound of the Canadian and Scandinavian shields following deglaciation, and the depression of parts of the East Coast of North America.

Active orogenic movements are well characterized by active faulting and active folding. Major strike-slip faults, such as the San Andreas Fault system in California, disrupt the landscape by offsetting streams, sedimentary basins, and mountain masses. The lateral movements are almost always accompanied by at least some vertical movement of crustal blocks. Irregularities in the fault trend, or on the fault surface, cause local rotation of stress; crustal blocks may be forced upward or downward—generally with the vertical movement accommodated along either reverse or normal faults—or the blocks may be rotated between branches of a fault.

Extension of the Earth's crust dominates in some provinces, and, as in the Basin and Range province of the western United States, extension is accompanied by vertical adjustments of range-sized blocks under the influence of gravity. Horsts and grabens develop as individual crustal blocks rise or drop, or the range blocks tilt so that one edge drops downward while the other edge rises.

Many ranges along plate boundaries are the products of folding of stratified sediments. Folding generally represents processes of crustal shortening; crustal shortening also may involve the thrusting of one block over or under another, along relatively gently inclined faults.

Where crustal plates collide rather than slide laterally past one another, the oceanic plate tends to slide beneath the continental plate in a process known as subduction, although not uncommonly part of an oceanic plate rises and slides over the continental plate (obduction). During collision with the Asiatic crustal plate, the Indian subcontinental plate has been thrust perhaps more than a thousand kilometers beneath the Himalayas and the Tibetan Plateau.

Many smaller crustal blocks, or microplates, have collided with and have been accreted to the major continental plates. Investigations during the past decade suggest that some microplates have migrated at rates of tens of centimeters per year and have traveled across several tens of degrees of latitude. Such mobility of the Earth's crust is an important aspect of active tectonics.

In the overall crustal shortening process, large thrust faults emerge from the lower crust and flatten as they near the surface so that slabs of crust kilometers thick move tens of kilometers over underlying parts of the crust. In addition, large slabs (kilometers thick) of the Earth's crust may slide or glide off regionally uplifted terranes under the influence of gravity or as the result of widespread crustal stretching. Surfaces of decoupling or detachment along which sliding takes place may involve tens of thousands of square kilometers, and the scale of folds and faults in the deformed plate above this detachment surface may be complex and measured in tens of kilometers. Growth faults, which are similarly gravity driven, can produce hazardous ruptures both at the surface and at depth. It is difficult to distinguish between those structures driven by gravity from those resulting from either shortening or stretching of the upper mantle and lower crust, and the distinction in places is moot.

Other gravity-driven movements of smaller masses of Earth materials are initiated in

regions of high relief, including, for example, landslides, debris flows, and mud flows, as well as volcanic-related lava flows, ash flows, and lahars. Even though such movements of masses result from active tectonism and may constitute severe hazards, they are considered to be secondary to the more fundamental active tectonic processes and thus are not discussed extensively in this study.

## RATES OF ACTIVE-TECTONIC AND GEOMORPHIC PROCESSES

Even the most stable intracontinental and intraoceanic basin areas of the Earth's surface are constantly changing, although at rates difficult to detect by classical geodetic techniques. But along the margins of continents and ocean basins where plates of the Earth's crust collide or interact, the rates can be rapid and even catastrophic and, for volcanic eruption, explosive.

Explosive rates are represented by such dramatic volcanic eruptions of historical times as Tambora (1815) and Krakatau (1883), in Indonesia, Mount St. Helens, Washington (1980), and El Chichon, Mexico (1982). Along great faults lateral displacements of about 10 m, along tens of kilometers of fault length, have occurred abruptly and suddenly to generate great earthquakes. Eyewitnesses of the 1983 Borah Peak, Idaho, earthquake reported that a meter-high scarp formed in less than a second. Laboratory and field analyses show that fault ruptures propagate at rates of 2-3 km/sec.

Longer-term average rates of processes are exemplified by as much as 10 cm per year of relative motion between the major plates of the Earth's crust. Geodetic nets a few tens of kilometers wide across the plate-bounding San Andreas Fault in California show relative motion of up to 3.5 cm/yr; this rate is confirmed close to the fault using creepmeters spanning only a few tens of meters across creeping segments of the fault. This rate contrasts with a rate of between 5.5 and 6 cm/yr for the relative plate motion between the North American and Pacific plates, as determined from the rate of seafloor spreading calculated from the positions of the magnetic stripes that lie symmetrically on the two sides of the East Pacific Rise. The difference of 2 to 2.5 cm/yr between the rate of motion on the fault and that of the plates is distributed across the western part of the North American continent, possibly affecting areas as far inland as 1000 km.

Vertical displacements of the Earth's crust can involve a sudden uplift of as much as 10 m, as occurred at Montague Island during the Alaskan earthquake of 1964. In the active regions of the Great Basin province of the western United States, average vertical displacement rates of mountain blocks relative to basin blocks not uncommonly have been as high as several tenths of a millimeter per year for several millions of years. In Japan, near the Kozo-Matsuda Fault, average displacement rates as high as 5 mm/yr over thousands of years are recorded. Although the centers of continents are generally thought to be relatively stable, average uplift rates may range from 0.01 to 1.0 mm/yr for several tens of thousands of years. Uplift rates on the Monroe Uplift, in the Mississippi Valley, for example, have been of this general rate. It is estimated that the crest of the Ventura anticline in southern California has been rising at a rate of about 10-15 mm/yr for a few hundred thousand years.

Optimism about improving our capability of making meaningful short-term predictions of volcanic eruptions and developing methods to predict earthquakes is predicated primarily on improving our ability to measure and to recognize significant changes in rates of deformation. Among the signals used for successful prediction of eruptions at Mount St. Helens were increases in the rate of displacement of the surface of the new lava dome and the rate of thrusting on the crater floor adjacent to the lava dome (Figure 1). Increased rates of tilt of the flanks of Kilauea volcano in Hawaii have been recognized for several decades as indicators of magmatic filling of shallow reservoirs and impending eruptions of the volcano. Interpretations of increased seismicity—

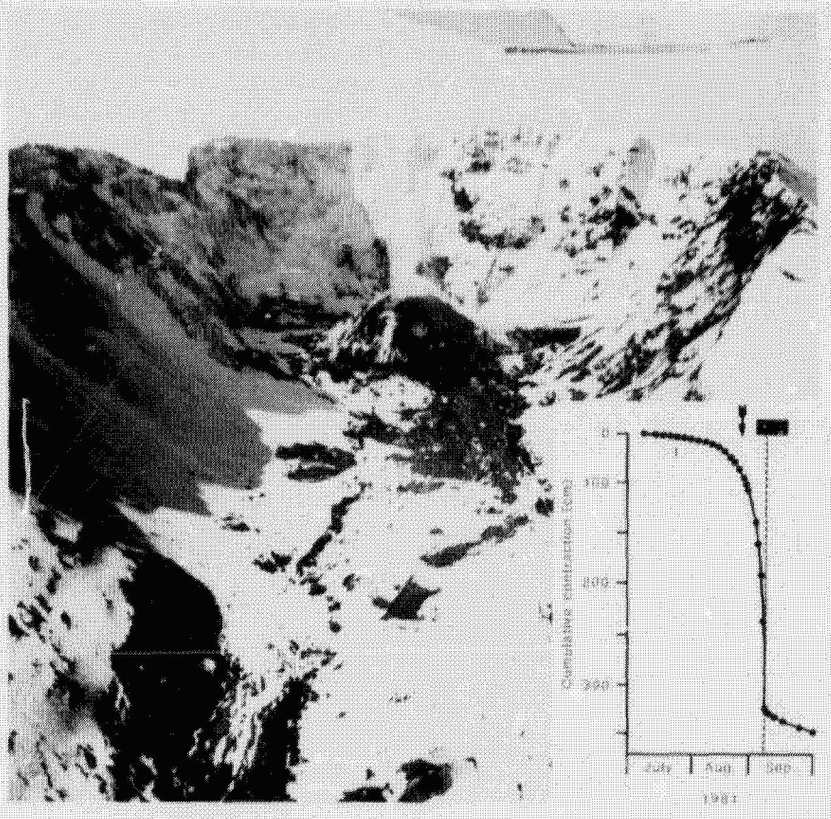


FIGURE 1 **Prediction of eruptions.** More than a dozen eruptions have been successfully predicted at Mount St. Helens, Washington. One of the important data sets for the predictions is the rate of thrusting in the floor of the crater adjacent to the lava dome. The crater formed during the explosive eruption of 1980 and the lava dome that subsequently developed are shown in this photograph of April 17, 1981. The graph shows contraction across a thrust fault on the crater floor prior to the September 1981 eruption. The black rectangle is the period within which the eruption was predicted to occur. The prediction was made at the arrow, and the eruption occurred at the vertical dashed line [graph from D. A. Swanson, T. J. Casadevall, D. Dzurisin, S. D. Malone, C. G. Newhall, and C. S. Weaver (1983), *Science* 221, 1369-1376; photograph by R. E. Wallace, U.S. Geological Survey].

a manifestation of strain release—have played a key role in successful predictions of volcanic eruptions in Hawaii, Washington State, and elsewhere.

The concept that elastic strain must accumulate in brittle rock before rupture occurs is the underlying rationale for earthquake prediction. Changes in the rate and patterns of strain just before rupture that are seen in laboratory experiments suggest that marked changes—either decreases or increases in rates of strain or in sense of strain—may signal an impending rupture and earthquake. A 2-yr halt in fault creep at one point on the Calaveras Fault prior to the Coyote Lake earthquake of 1979 in central California may have been a precursor to that earthquake. Regional tilts of land surfaces in Japan before the 1964 Niigata earthquake may represent the type of strain to be expected, but questions have been raised about older surveys and their adequacy for accurately recording such changes. However, few, if any, recognized changes that have been documented are widely acknowledged as having been clear premonitory signals for earthquakes.

Tectonic rates are reflected in rates and patterns of geomorphic processes and forms. For example, fault-generated range fronts on which displacement rates average tenths of a millimeter per year for a million or more years are characterized by low sinuosity of the topographic boundary between the range and basin and by faceted spurs. The range margin sinuosity increases with slower rates, and the pattern of faceted spurs gives way to more highly dissected and less planar landforms along range fronts.

The rates of geomorphic processes range dramatically from climate to climate, and different processes may be dominant in each. For example, fluvial processes are dominant in semiarid areas, whereas wind action may be dominant in arid regions and mass movement in some humid or tropical regions. In humid climates the potential for sediment production could be great, but vegetation reduces erosion rates. These and other

processes of erosion, such as aeolian, raindrop impact, ice, and geochemical processes, interact in different climates to affect collectively the overall degradation and destruction of landforms constructed by tectonic processes.

Slopes of fault scarps or wave-cut cliffs may be modified rapidly by gravitational processes. The near-vertical free face of a few-meter-high scarp may disappear within a few hundred years, as material falls off the steep face to rest at the angle of repose in a debris slope covering the free face. The scarp later becomes modified by downslope movement of material according to a diffusion model, which operates at slower and slower rates. However in a desert climate, a meter-high fault scarp may be clearly recognizable for a hundred thousand years.

## TECHNIQUES FOR EVALUATING ACTIVE TECTONICS

The entire range of geologic, geophysical, and geodetic techniques may have a bearing on evaluating active tectonics, but for studying ongoing processes some are more useful than others.

The period of past behavior of tectonic movements that is significant to predict future movements may range from days to thousands, or even millions, of years. In general, however, the predictive value of events of the past decreases with age, but *the length of time analyzed must be sufficiently long to sample adequately a particular series of events, changes in rates of events, or changes in patterns of tectonics.* For example, large intraplate earthquakes generally recur on a given fault at intervals of several thousands of years, and, thus, an estimate of earthquake potential based on only a century or two of recorded history may mistakenly suggest quiescence in regions that hold the most severe threat of great earthquakes. Each sample interval of time provides different insight into tectonic processes. Repeated geodetic measurements made over days or decades provide details of tectonism unidentifiable in most geologic studies, but only from the longer-term geologic record can many tectonic movements be identified and their rates determined.

In regard to active tectonics, the segment of the future of greatest concern to mankind generally is only the next few years to few decades, although for safe disposal of some radioactive waste the period is thousands or tens of thousands of years.

Events of the past 100,000 to 200,000 yr, and especially of the past 10,000 to 20,000 yr, are particularly significant as a basis for predicting future trends. Geodetic techniques can be used to identify and quantify very recent historical tectonism, and real-time geology and geophysics have already been used to provide predictions of specific future events. Some of the greatest successes have been achieved in predicting eruptions of volcanoes. The basic physical and chemical models that can be translated into geophysical, geochemical, and geologic predictions are in the process of rapid evolution, and many advances seem to be just over the horizon.

Though this emphasis is on events of late Quaternary time, we do not exclude significant evidence about tectonic history and processes obtainable from longer periods of geologic time. for example, the past few million years, or latest Neogene and Quaternary time. Neotectonics, which pertains to the tectonics of this longer period of time, is the focus of the Neotectonic Map Project under the Geological Society of America's Decade of North American Geology (DNAG) project. For this review, *neotectonics* is distinct from *active tectonics* but is recognized as providing an important set of data.

Even the longer record cannot be ignored, because to a large extent those structures that originated in Mesozoic and Tertiary time greatly influence the patterns of Quaternary structures. Paleozoic and older structures have less influence. Stress orientations may have changed, but during any period of strain the prefractured nature of the Earth's crust and other anisotropism affect the response of the crust. Furthermore, the tectonics of old features now inactive can cast light on those currently active.

A strategy for geodetic monitoring of active tectonics was concisely presented in *Geodetic Monitoring of Tectonic Deformation—Toward a Strategy* (1981), and a few highlights of that study serve to indicate the suggested types of problems, monitoring techniques, and evaluation procedures.

Questions exist, for example, about the relationship between the Chandler wobble of the Earth and earthquakes and whether major earthquakes cause a discernible change in the polar path. Up to a point, classical astronomical observations can be used to study such problems. However, improved geodetic space techniques such as very-long-baseline radio interferometry and satellite laser ranging are rapidly advancing our understanding of plate motions; such observational techniques are beginning to allow the direct measurement of present-day plate motion. Such studies can cast light on the rheological properties of the asthenosphere, its viscosity, and whether gross strain is rather more impulsive than continuous. Regional strain measurements are currently made by laser-ranging techniques in which measurements are infrequent. By employing two-color laser-ranging techniques, corrections for atmospheric conditions are made automatically in data processing and very frequent observations are practical. Small trilateration nets, level lines, and stretched-wire creepmeters spanning only a few tens of meters are used for studying localized deformation along faults. Tiltmeters, linear strain meters, and volumetric strain meters are among instruments currently used to study tectonic strain. The precision required is of the order of a few parts in ten million, but some measurements of the order of a few parts in a billion or smaller are desirable. Most instruments do not have, or barely have, such capabilities. Noise near the Earth's surface, furthermore, exacerbates the problem of recognizing tectonic signals of such small size. Long-term stability of instruments is a special problem.

The historical record prior to modern instrumentation can provide important insight into longer-term rates and patterns of volcanism, earthquakes, and crustal deformation. In an area of active uplift in Iran, for example, a canal built 1700 yr ago has cut down about 5 m below its original bed, indicating an uplift rate of about 2 mm/yr. In western North American, the historical record of earthquakes is not even 200 years long, but in China it is almost 4000 yr long, although reasonably complete for only about 1000 yr. Similarly there is a historical record of volcanism that is useful as a measure of the frequency and characteristics of eruptions.

Because of low rates of tectonic strain accumulation in many places, the periods of time represented even by recorded history do not adequately sample longer-term trends and cycles. The historically most inactive sections of great faults, indeed, may be candidates for generating the largest future earthquakes. Geologic techniques provide the only means to sample sufficiently long time spans during which many rates and patterns of tectonic processes must be analyzed.

The stratigraphic record contains clear physical evidence of past events. In Japan, for example, bountiful evidence of complex volcanism is preserved by layer upon layer of volcanic ash, breccias, and lava flows. Furthermore, abundant tephra layers—each of which has a distinctive chemical and mineralogic characteristic and was deposited within a few days or weeks—over large areas provide distinctive time markers that permit many local and regional tectonic events to be analyzed in the context of a time frame.

Stratigraphic relations along active faults may reveal a sequence of successive offsets and deposition of sediments that permit the reconstruction of the history of faulting, the recurrence intervals, and size of faulting events. Sedimentary structures such as sand blows, clastic dikes, and deformed beds related to liquefaction may reveal the history of strong ground shaking and add to the evidence of prehistoric earthquakes. Repeated deposition of colluvial wedges along the bases of fault scarps creates unique stratigraphic relations from which an interpretation of the paleoseismological record can be derived.

Analysis of gross stratigraphy—the composition of the lithologic units and the deformation of beds—can indicate whether rates of uplift nearby were rapid or slow, whether volcanic arcs were nearby, or whether terranes that contributed clasts to the sediments had later moved away. At small scales, as in excavations dug across active faults, the sequence of sedimentation and faulting can be analyzed to determine how often large prehistoric earthquakes occurred. The patterns and rates of silting of rivers are extremely sensitive to tectonic changes.

Landforms, created by the competition between tectonic constructional and erosional destructional processes, contain abundant evidence of active tectonics. Classical geomorphology, however, has concentrated primarily on descriptions of landforms, and process and stages of erosion were stated in only generalized terms. In the past decade or so, quantitative, process-oriented geomorphology has been directed toward problems of active tectonics. Studies of marine terraces, river geomorphology, fault scarps, and eruptive volcanic features have demonstrated a rich and readily available source of information about active tectonics recorded in landforms. Coseismically uplifted marine terraces may provide evidence of prehistoric earthquakes. Direct measurement of fault-scarp morphology, for example, when analyzed according to an error-function solution of a diffusion model, can approximate the date of a great prehistoric earthquake. From such analysis, the pattern and recurrence interval of large earthquakes can be determined even where average recurrence intervals are measured in thousands of years. In summary, as more research is carried out on the effect of active tectonics on landforms, geomorphology can become one of the most powerful tools for evaluating active tectonics.

Clearly, tectonic processes are complex, often nonuniform, and the emphasis given here on predicting future tectonic activity introduces the important problem of how best to state the likelihood of future events. A variety of formal mathematical methods is currently available for expressing probability, but further study is warranted into techniques of conveying to both lay and technical audiences the likelihood and consequences of complex tectonic activity.

Applications of such techniques as described above have recently led to some new insights about active tectonics. The findings described below, furthermore, indicate some areas of research that are worthy of further attention.

- Individual or groups of large prehistoric earthquakes can be clearly identified by geologic means, such as by microstratigraphy and microgeomorphology. The research efforts so directed are now termed paleoseismology. By such methods the long-term patterns and timing of some great earthquakes have been analyzed.
- Coherence of signals among gravitational changes, lateral changes, and vertical changes confirm that tectonic changes on a time scale of months or years are real and are amenable to analysis. From such studies the normal dynamic behavior of the Earth's crust may be determined, and the predictive value of unusual changes can be assessed.
- A variety of active-tectonic realms of diverse sizes has been recognized and defined; each realm is characterized by distinctive patterns and rates of deformation. Such analysis provides a basis for zonation to assist in the reduction of geologic hazards.
- Folding can be an important active-tectonic process. In the past, folding has been ignored to a large extent in active-tectonic studies even though a rich and voluminous mass of information about folding has been in existence for a long time in the classical tectonic literature. Further analysis will permit evaluation of the strain budget, that is, the distribution of strain, between faulting and folding.
- Some well-known physical models such as the diffusion or heat-flow model have been applied successfully to the analysis of geomorphic processes.
- Determining the distribution of microseismicity has proven to be one of the best

techniques for defining the pattern of active faulting. Such studies can "paint" the three-dimensional time-space relation and show how strain is propagated. Additionally, digitally recorded data from broadband, wide dynamic-range seismometers have permitted greatly improved analysis of the faulting process.

- Broad vertical changes in elevation that occur on an historical time scale, within what are generally thought of as stable intracontinental regions, have been found to affect dramatically the regimes of major rivers, bank stability and silting, and navigation and flood control.

## IMPACT ON SOCIETY

Only when an infrequent paroxysm of the Earth's crust occurs in the form of an earthquake, volcanic eruption, or landslide is the dynamic nature of the Earth's crust brought clearly to public attention. Largely unnoticed are slower movements of the Earth's crust, which, nevertheless, are costly in terms of engineering countermeasures required or the constraints that are placed on land uses. The demands for safety and continuity of service required of modern-day critical facilities, such as nuclear reactors, large dams, and structures for defense, require a knowledge of the Earth's crust well beyond the current state of geophysical and geologic information. As a result, costly mistakes have been made, and high-priority programs have been delayed or canceled. Without a doubt the future will call for more such uses in projects having even greater sophistication, greater potential hazard, and more complex interactions with the environment.

### *The Tragedy of Ignorance*

For the want of information about active tectonics, numerous mistakes and extremely costly delays or cancellations of major engineering projects have resulted. A few case histories will serve as examples.

In the early 1960s, the Pacific Gas and Electric Company began to develop a site for a nuclear reactor at Bodega Bay in northern California. The first site selected was astride the part of the San Andreas Fault that caused the great San Francisco earthquake of 1906. Soon, however, it became recognized that the fault might pose problems, and the site was moved a few kilometers west, but still near the fault zone. During the excavation of the giant pit (Figure 2) that was to contain the reactor, faults were found and concern was raised that movement on these secondary faults might rupture the reactor and cause a major disaster.

At that time, and to a major extent even today, the geologic and geophysical communities simply had no scientifically based answers to such fundamental questions as: Will the next rupture recur on the 1906 break of the San Andreas Fault, or will it occur on some other fault branch or strand within the kilometer-wide fault zone? How much displacement can be expected on branch faults and parallel faults at distances of several kilometers from the main break? How does a history of one displacement in 10,000 or 35,000 yr on a branch fault factor into a calculation of probability of a future displacement on that branch fault?

In 1969 the Bodega Bay nuclear reactor project was canceled after several years of acrimonious debate, because no one had the needed scientific information with which to assess the stability of the site. As a result millions of dollars were spent unproductively. The lack of understanding of active tectonics has caused problems in the development of similar facilities.

As an additional example, in 1979 the building of a large thin-arch dam at Auburn, California, in the foothills of the Sierra Nevada was stopped. Although much had been learned about earthquake hazards in the ensuing years since the Bodega Bay nuclear

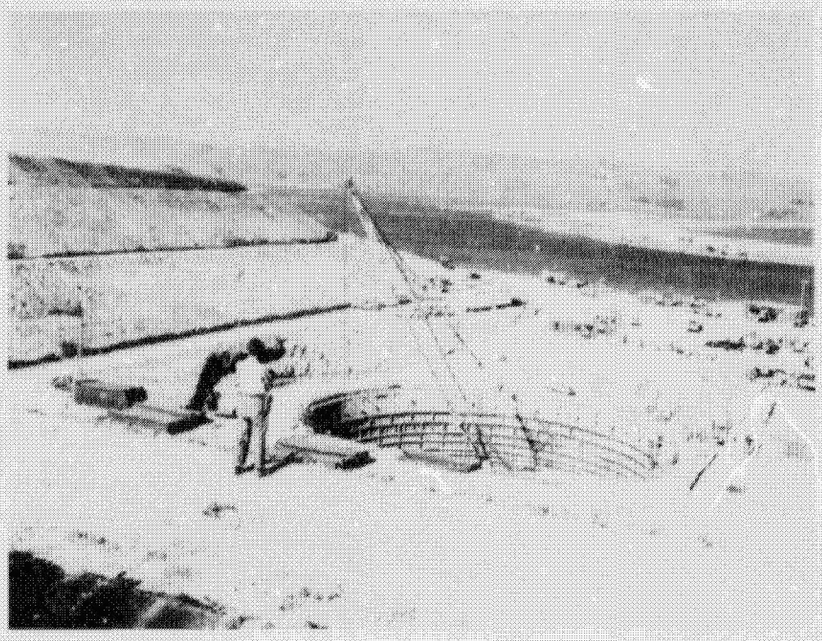

FIGURE 2 **Wasted effort!** Excavation at Bodega Bay, California, for a proposed nuclear reactor began in the early 1960s. The San Andreas Fault lies under Bodega Bay in the background, and branch faults were found in the excavation. Concern over faulting events that might rupture the reactor caused cancellation of the project. Because of the infancy of the science of faulting and relation to earthquakes, scientists could not agree on the probability of a faulting event or the size of such an event under the site (photograph by R. E. Wallace, U.S. Geological Survey).

reactor project was canceled, data about the earthquake and fault-displacement potential of the Sierra Nevada foothills belt were almost nonexistent.

A team of earth-science consultants studied the problem for the U.S. Bureau of Reclamation and estimated that several inches of displacement along the fault was very possible within the lifetime of the dam. Government geologists, serving in a review capacity, estimated that 3 feet of displacement might occur on the faults during an earthquake. Clearly, there was no satisfactory scientific basis for agreement on the exact amount of displacement to be expected, but both groups of specialists did agree that fault displacement during the lifetime of the dam must be considered a distinct possibility. After review of the fault data and the engineering characteristics of the dam, officials of the U.S. Bureau of Reclamation concluded that even the smaller estimated displacement would exceed the accommodation capabilities of the dam as planned. After 10 yr of preliminary site development at a cost of over $200 million, the project was halted (Figure 3).

### *Benefits from Understanding*

The veil of ignorance, at least with regard to earthquake hazards in the United States, has been rolled back to some extent as a result of the National Earthquake Hazard Reduction Program, which formally began in 1977. Fundamental studies of volcanic processes at the Hawaiian Volcano Observatory, similarly, have resulted in practical guidelines for reducing the hazards of volcanic eruption. Examples of successes can serve to illustrate the kinds of benefits that are likely to accrue from long-term fundamental research in active tectonics.

On October 28, 1983, an earthquake of magnitude 7.3 occurred in central Idaho. A spectacular fault scarp 36 km long formed along the west flank of the Lost River Range, a typical Basin and Range fault-block mountain (Figure 4).

Significantly the 1983 rupture occurred exactly where it was expected in that it replicated a fault displacement of similar size that occurred in late Holocene time, possibly within the last 5000 yr. Only in the past decade had the tendency been demonstrated

clearly that historical breaks occur along the traces of Holocene breaks. The fault along the Lost River Range had been studied in 1977 to evaluate the earthquake hazards at the Idaho National Engineering Laboratory (INEL), and Holocene displacement had been identified. As a result of correctly anticipating the location and size of the 1983 earthquake, automatic shut-off systems functioned effectively at INEL and closed down nuclear reactors, and a potentially hazardous situation was countered.

An impact on policy and decision making that can result when a significant new set of data and some basic understanding about active tectonics replace almost total ignorance can be illustrated by discoveries of the late 1970s and early 1980s in the Mississippi Valley. There, until about 1981-1982, the causative structures of the great New Madrid earthquakes of 1811-1812 were mysteries. As a result, in planning an engineering project, the earthquakes were considered random events that could occur anywhere over a vast area of the midcontinent. A combination of geophysical explorations including

FIGURE 3 **Canceled!** After years of site preparation the thin-arch dam planned near Auburn, California, was canceled because faults of the Foothills Fault zone were found to cut the rocks under the foundation. Analyses indicated the possibility of displacements too large to be accommodated by the planned design of the dam. Almost nothing was known about the Foothills Fault zone before the dam was started (photograph courtesy of the U.S. Bureau of Reclamation).

FIGURE 4 **Faulting site predicted.** The vertical bare slope is the fault scarp that formed during the 1983 earthquake at Borah Peak, Idaho. An older, degraded scarp is represented by the more gradual slope between the man's feet and the top of the vertical scarp. Analysis of the slope of the older scarp and microstratigraphy exposed in 1977 in a trench through this site indicated previous displacement on the fault within the past several thousand years (Holocene time). Recently gained understanding of fault behavior strongly indicated that such Holocene fault scarps are candidate sites for future displacement, and this theory was confirmed here. As a result of the studies, nuclear reactors at the nearby Idaho National Engineering Laboratory were equipped with automatic shut-off systems that functioned successfully during the earthquake (photograph by R. E. Wallace, U.S. Geological Survey).

gravity, magnetic, and seismic reflection techniques revealed a buried but clearly definable rift zone (Figure 5). Faults of the rift zone were shown to be ancient geologic features that originated as extensional features but that were being reactivated by compressional stresses in the current tectonic regime. Geologic studies suggested a recurrence period of 600-1000 yr for such great earthquakes.

Although much is yet to be learned, the structures of the rift zone that caused the 1811-1812 earthquakes, and which will likely generate future earthquakes, now are clearly recognizable. Thus, potential future earthquakes to be accounted for in the design of engineering projects need not be considered possible everywhere in the midcontinent; engineering designs can be much more realistic and cost-effective, and regional planning can be conceived on a more rational basis.

Much of the central part of the United States has been considered to be free of major earthquake hazards. Surprisingly, however, in a seismically very quiet part of central Oklahoma, the Meers Fault has recently been discovered to have had displacement of several meters in Holocene time, presumably accompanied by one or more major earthquakes [M. C. Gilbert, *Earthquake Notes* 55(1), 1-3 (1985)]. A remarkably fresh fault scarp is still preserved, and the last event may have occurred within the past few thousand years. The discovery raises the question as to how many other unidentified active faults exist in seismically quiet regions of intracontinental regions. Newly developed methods in paleoseismology now permit investigation of this question.

### *Socioeconomic Measures*

Measures to counter the effects of earthquakes, volcanic eruptions, and slower forms of tectonic deformation fall into four categories: engineering accommodations, sensible

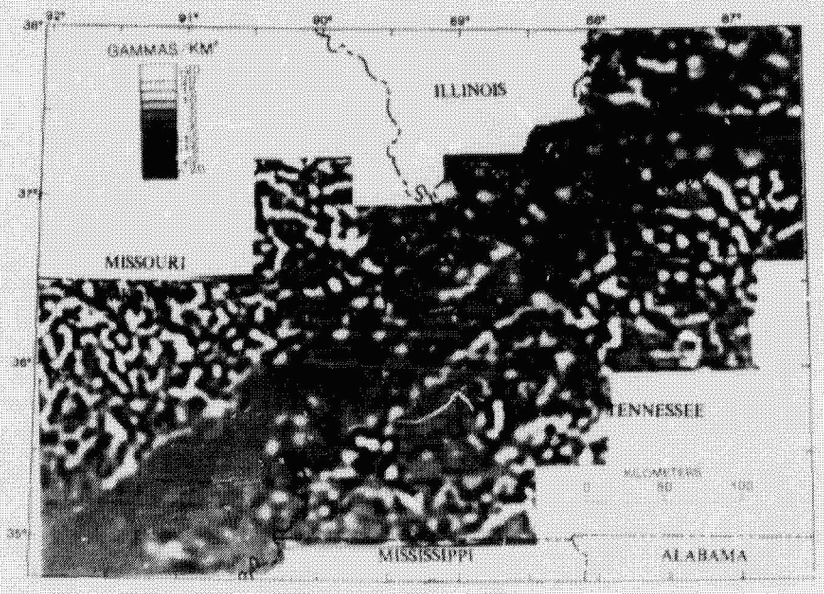


FIGURE 5 **Causative structures revealed.** Until various geophysical techniques were brought to bear in the search for possible buried faults that could have caused the great 1811-1812 earthquakes, similar earthquakes were presumed to be possible over a vast area of the Mississippi Valley. As a result, concern was raised about major engineering projects. This map of the second vertical derivation of the total magnetic-field intensity reveals a northeast-trending magnetic feature that is interpreted as a completely masked graben. Historical seismicity has been concentrated within the graben, and thus the rift structure is presumed to be responsible for the generation or control of seismicity. [Figure from T. G. Hildenbrand, M. F. Kane, and J. D. Hendricks (1982), Magnetic basement in the upper Mississippi Embayment region--A preliminary report, in *Investigations of the New Madrid, Missouri, Earthquake Region*, U.S. Geol. Surv. Prof. Paper 1236-E, pp. 38-53.]

use of the land, event prediction, and disaster preparedness. Engineering design and construction of structures to resist earthquake shaking, offset by faulting, and differential settlement can greatly reduce the hazard of structural collapse. Planning the use of land so that structures, especially those for dense occupancy, are not built astride active faults or in the potential paths of volcanic lava flows or lahars is prudent and effective, and yet such obvious methods of reducing hazards commonly have been ignored.

In many states and countries, building codes and standards are followed to some extent, but in practice the craftsman or builder, through ignorance or neglect, too often fails to incorporate the specified design features in the final structure. Simple factors such as the lime content of mortar and the proper wetting of bricks before application of mortar in masonry construction greatly affect the strength of buildings. Special studies are required when building near active faults in California. Disaster plans for responding to potential hazards from volcanic eruptions have been prepared in California, Washington, Japan, and Italy, among others.

Successful prediction of at least a few dozen volcanic eruptions undoubtedly has reduced the hazard to life and property. Among damaging earthquakes for which claims of prediction have been made, only the Haicheng, China, earthquake of 1974 seems to be widely credited by the scientific community as having had a valid scientific basis. For the first time in the United States, a long-term earthquake prediction was reviewed and approved as scientifically valid by both the National Earthquake Prediction Evaluation Council and the California Earthquake Prediction Evaluation Council. The prediction was announced officially by the Director, U.S. Geological Survey, on April 5, 1985, and the announcement stated that "an earthquake of magnitude 5.5 to 6 is likely to occur in the Parkfield, California, area within the next several years (1985-1993). . . ."

Identification of the most stable tectonic blocks and prediction of the degree of stability, or lack of active tectonism, have been even more difficult than predicting tectonic events. Few methods of analysis and little understanding of the long-term processes are at hand.

The past two decades have seen a major acceleration in disaster preparedness. One example is the Southern California Earthquake Preparedness Project, which was

started in 1980 under joint state and federal support. Preliminary prototype response plans have been completed for an industry, a county, a large city, and a small city. Elements of the prototype plan include, for example, voluntary self-help, communications, special problems of schools, law enforcement, and concerns of financial institutions. An early requirement for the project was an accurate scenario of the tectonic process, in this case the detailed effects of a major earthquake when it happened and the likely content of an earthquake prediction if it were made. These needs could be fulfilled only poorly or not at all because of the state of earthquake science. All administrative, societal, economic, and other steps to cope with the impact of active-tectonic processes hinge on understanding those processes and the rates at which they operate.

## RECOMMENDATIONS FOR RESEARCH PRIORITIES AND ACTIONS

A program of fundamental research focusing especially on Quaternary tectonic geology and geomorphology, paleoseismology, neotectonics, and geodesy is recommended to better understand ongoing, active-tectonic processes. Capability should be developed to assess the potential for, or to predict, tectonic activities up to several thousand years in the future. To accomplish these goals, special attention should be given to the following research areas that constitute especially powerful techniques or gaps or areas of weakness within the complex matrix of scientific disciplines needed.

We stress strongly, however, that the priorities given here are predicated on the existence of a healthy level of fundamental research in related, broad subjects including understanding the continental lithosphere, plate tectonics, energetics of tectonic processes, seismology, and volcanism. Other National Research Council reports have already addressed many of these topics.

### *Research Priorities*

- *Dating Techniques*: The greatest need is for data and models concerning the rates of active-tectonic processes. Public-policy decisions, for example, about what levels of earth-hazard risks are acceptable, rest largely on evaluations of the rates (and the variability of rates) of processes, the frequency of events, and the prediction of when hazards might become critical. To this end, new and improved techniques of dating materials and events of Quaternary age are needed. For example, thermoluminescence, uranium trend, beryllium-10, aluminum-26, and soil development are among two dozen or more potentially useful dating techniques currently being investigated as alternatives to the more widely used techniques, including radiocarbon dating. Tandem accelerator mass spectrometry may permit several of these new techniques to become practical and may improve the usefulness of older techniques. The breadth of applicability and precision of each technique need improvement.
- *Tectonic Geomorphology*: Research in tectonic geomorphology aimed at documenting rates, styles, and patterns of movements is recommended as one of the potentially most effective means of analyzing ongoing tectonic processes. Research in quantitative geomorphology is especially important.
- *Geodesy*: Research using geodetic techniques should be expanded to delineate the patterns and scales of ongoing deformation. We endorse the recommendations in the 1981 report *Geodetic Monitoring of Tectonic Deformation—Toward a Strategy* by the Committee on Geodesy/Committee on Seismology. Techniques described in that report range from ground techniques using strain meters and laser-ranging devices to space techniques using very-long-baseline radio interferometry (VLBI) and the Global Positioning System (GPS).
- *Paleoseismology*: Because major tectonic processes such as those manifested by seismicity are commonly grossly misrepresented by the historical time sample, pa-

leoseismic techniques should be furthered. Physical exploration, such as trenching to expose and permit microstratigraphic analysis in critical places, and geomorphic techniques aimed at paleoseismology are of high priority.

- *Real-Time Geology*: Recording, processing, and interpreting of geologic changes in a time frame of seconds to weeks—which can be termed "real-time geology"—are needed for the development of short-term predictive capability. Special instrumentation, automation, and rapid computer processing of data are required. A far more detailed understanding than currently exists of certain real-time Earth processes is needed.
- *Probability Studies*: Methods for expressing the probability of future tectonic activity need much improvement. Incomplete data and debatable interpretations of data will continue to be a problem, and yet both conclusions and uncertainties must be communicated as precisely as possible within the technical community as well as to nontechnical decision makers.

### *Recommendations for Specific Actions*

In order to advance these research areas of high priority, the following institutional considerations and technical approaches are emphasized:

- Research in dating techniques suitable for analysis of Quaternary geology should be (a) recognized as a high priority for support by funding groups—both governmental and private and (b) encouraged through workshops and symposia under the auspices of professional societies.
- Studies of Quaternary geology useful in analyzing active tectonics should be more effectively integrated into the earth-science curricula of universities. Special attention should be given to tectonic geomorphology including the observational, experimental, and quantitative-theoretical elements.
- Emphasis should be given to research programs that employ geodesy to analyze the dynamic as well as the static features of the Earth's crust.
- Clear and specific identity should be given to research concerning Quaternary structures, processes, and rates of processes.
- Research programs to develop short-term (up to a few weeks) predictive capabilities for active tectonics, along with the ability for rapid data analysis, should be established or accelerated by those federal and state agencies responsible for issuing geologic hazard warnings. To this end, regional seismic networks and systems for monitoring strain and stress in real time are critical.
- Preplanning is needed to assure the effective study of events of opportunity. The observation of volcanic eruptions, earthquakes, or landslides while they are occurring can reveal facts about Earth processes unavailable at any other time. For example, recording of strong ground motion during an earthquake, measurement of changes in pore pressure during a landslide, or the changes in composition of gases during volcanic eruptions can be carried out only at specific critical moments.
- The continuity of carefully selected programs aimed at gathering long-term baseline data with temporal significance is desirable.
- The importance of regional seismic networks to the study of active tectonics should be considered and should continue to be evaluated by the appropriate institutions.
- Wider use of trenches, tunnels, drill holes, and other artificial excavations to reveal structural and age relations of tectonic units is desirable. Instrumentation of tunnels and boreholes, furthermore, can avoid spurious signals (noise) found near the Earth's surface and thus permit recording of smaller signals significant to active tectonics.
- The further and more complete use of aerial photography and remote sensing at

many scales and in many radiation bands can reveal or clarify geomorphic and geologic relations otherwise unavailable. Side-looking radar, which permits illumination of the landscape from angles impossible by natural sunlight, can enhance selected geomorphic and tectonic trends. New, sophisticated technology, such as used in the airborne profiling of terrain (APT) system, may provide previously unobtainable data on geodetic and geophysical changes that are a direct reflection of active tectonics.

## BIBLIOGRAPHY

*U.S. Program for the Geodynamics Project: Scope and Objectives*, U.S. Geodynamics Committee, National Research Council, National Academy of Sciences, Washington, D.C., 235 pp., 1973.

*Predicting Earthquakes*, Committee on Seismology, National Research Council, National Academy of Sciences, Washington, D.C., 62 pp., 1976.

*Trends and Opportunities in Seismology*, Committee on Seismology, National Research Council, National Academy of Sciences, Washington, D.C., 158 pp., 1977.

*Earthquake Hazards Reduction: Issues for an Implementation Plan*, Office of Science and Technology Policy Executive Office of the President, Washington, D.C., 230 pp., 1978.

*Geophysical Predictions*, Geophysics Study Committee, National Research Council, National Academy of Sciences, Washington, D.C., 215 pp., 1978.

*An Assessment of the Consequences and Preparations for a Catastrophic California Earthquake: Findings and Actions Taken*, Federal Emergency Management Agency, Washington, D.C., 59 pp., 1980.

*Continental Tectonics*, Geophysics Study Committee, National Research Council, National Academy of Sciences, Washington, D.C., 197 pp., 1980.

*Earthquake Research for the Safer Siting of Critical Facilities*, Committee on Seismology, National Research Council, National Academy of Sciences, Washington, D.C., 49 pp., 1980.

*Dynamics and Evolution of the Lithosphere: The Framework for Earth Resources and the Reduction of Hazards*, Inter-Union Commission on the Lithosphere, International Council of Scientific Unions, 62 pp., 1981.

*Geodetic Monitoring of Tectonic Deformation—Toward a Strategy*, Committee on Geodesy/Committee on Seismology, National Research Council, National Academy Press, Washington, D.C., 109 pp., 1981.

*Goals and Tasks of the Landslide Part of a Ground-Failure Hazards Reduction Program*, U.S. Geological Survey, 49 pp., 1982.

*Effective Use of Earthquake Data*, Committee on Seismology, National Resource Council, National Academy Press, Washington, D.C., 51 pp., 1983.

*The Lithosphere, Report of a Workshop*, U.S. Geodynamics Committee, National Research Council, National Academy Press, Washington, D.C., 84 pp., 1983.

*Multidisciplinary Use of the Very Long Baseline Array*, Board on Physics and Astronomy, National Research Council, National Academy Press, Washington, D.C., 202 pp., 1983.

*Opportunities for Research in the Geological Sciences*, Board on Earth Sciences, National Research Council, National Academy Press, Washington, D.C., 95 pp., 1983.

*Seismographic Networks: Problems and Outlook for the 1980s*, Committee on Seismology, National Research Council, National Academy Press, Washington, D.C., 62 pp., 1983.

*Explosive Volcanism: Inception, Evolution, and Hazards*, Geophysics Study Committee, National Research Council, National Academy Press, Washington, D.C., 176 pp., 1984.

*National Earthquake Hazards Reduction Program: Overview*, M. L. Schnell and D. G. Heard, eds., U.S. Geological Survey Circular 918, 65 pp., 1984.

*Seismological Studies of the Continental Lithosphere*, Committee on Seismology, National Research Council, National Academy Press, Washington, D.C., 144 pp., 1984.

*Geodesy: A Look to the Future*, Committee on Geodesy, National Research Council, National Academy Press, Washington, D.C., 179 pp., 1985.

*Safety of Dams: Flood and Earthquake Criteria*, Water Science and Technology Board, National Research Council, National Academy Press, Washington, D.C., 321 pp., 1985.

# 1 Active Tectonics Along the Western Continental Margin of the Conterminous United States

JOHN C. CROWELL
*University of California, Santa Barbara*

ABSTRACT

Active-tectonic deformation along the continental margins of Baja California, California, Oregon, and Washington is the result of crustal mobility at the joining of the North American, Pacific, and Juan de Fuca lithospheric plates. South of the Mendocino triple junction, strike slip predominates along a broad and braided system of both major and minor faults with a roughly northwesterly strike. Blocks between faults are warped, folded, uplifted, depressed, and rotated as shown by deformed erosional surfaces and stratigraphic markers, by geodetic and geophysical measurements, and by earthquakes. On the southeast, this wide transform belt merges with the divergent boundary at the head of the Gulf of California. Farther to the northwest, the belt joins the convergent plate margin near Cape Mendocino. On northwestward, vertical tectonic movements predominate.

Geophysical, geologic, and geomorphic investigations of the coastal belt extending from the deep Pacific Ocean on the west to well within the continental cordillera on the east are revealing much concerning the manner of deformation along such a wide plate boundary. Data come both from intensive study of local sites, including those for engineering projects, and from broader regional studies. Melded results from many types of investigation, skillfully summarized on special maps depicting tectonic behavior, will aid in evaluating sites for construction projects and will contribute to basic tectonic understanding. Toward these ends, stimulation is needed to coordinate symbiosis among all geoscientists, ranging from engineering geologists to global tectonicists.

## INTRODUCTION

The western margin of North America is tectonically active. Here rugged mountains and deep valleys are associated with earthquakes and ground warping, which attest to the mobility of the crust. This is the belt where giant lithospheric plates meet—the North American plate on the east and the Pacific and Juan de Fuca plates on the west. This mobility is measured and documented by employing many approaches, some instrumental and others through geomorphic and geologic mapping, which are described elsewhere in this volume. In this short paper I review briefly the nature of the crustal deformation taking place at present and back into the geologic past for the past half-million years or so along the western continental margin.

Studies of crustal deformation are important in that they provide information useful in the siting and design

of critical engineering structures. But they also reveal much concerning the nature of crustal deformation and contribute to our understanding of the strength of the crust and the way structural flaws or ancient weak zones influence where faulting and folding take place. Local studies reveal the style, rates, episodicity, or clustering of deformational events. They document the style and distribution of strain features such as faults, folds, warpings, rotations, translations, and earthquakes. This information needs then to be dovetailed with regional investigations focused on arriving at better plate-tectonic generalizations. The latter research aids in arriving at improved geologic models, and these in turn will aid in understanding what is controlling deformation at local sites. To the extent that the models are applicable they will aid in extrapolating concepts to regions where engineering structures are needed and planned but where direct information on active deformation is missing because of the piecemeal and incomplete nature of the pertinent geologic record.

The question arises: How far back into the geologic past are deformational data useful in understanding the ongoing flexings and breakings of the crust that affect human enterprises? A first answer to this question is: as far back as the deformational style and strain pattern are essentially the same as those operating today. Except within limited areas, the plate-tectonic control of deformation has been the same during the past million years or so. The limited areas where strain patterns and styles of deformation have changed significantly are at plate boundaries, and especially at junctures such as near the Mendocino triple junction. Locally within major plates, as along braided fault zones, deformation styles evolve through time but across limited areas.

## ACTIVE-TECTONIC REALMS OF CALIFORNIA, OREGON, AND WASHINGTON

In general, the active-tectonic realms correspond to the physiographic provinces of the western conterminous United States because tectonic activity is primarily responsible for mountains and valleys, the shape of coastlines, and the boundaries of regions such as the Basin and Range province. An active tectonic realm is, therefore, defined as a region where the tectonic deformation in progress at present and for the past half million years or so has the same style and pattern. This means that the orientation of folds and faults undergoing growth and the locations and type of earthquakes and volcanic centers are nearly the same throughout the realm. Several maps have already been published that show features such as earthquake distribution, stress patterns, and elevation changes (e.g., Buchanan-Banks *et al.*, 1978; Zoback and Zoback, 1980, 1981; Sbar, 1982; Gable and Hatton, 1983). The boundaries between some realms are sharp, but most are transitional. In addition, the concept involves scale. In working with an area the size of a city or county, small difference may be significant and may warrant separation into different subrealms. When dealing with a region as large as the three Pacific Coast states and adjacent portions of Baja California and British Columbia, however, generalizations are appropriate and local differences are smoothed.

In Figure 1.1, only the main provinces are demarcated. They are described briefly from south to north because of the convenience of picturing the sliding of western North America obliquely away from the divergent plate boundary in the Gulf of California. The main splintered boundary is the San Andreas transform system, upon which most of this sliding takes place. The Basin and Range physiographic province is primarily a broad region of stretching in this scheme and is the region north of the Mendocino triple junction where oblique plate convergence is taking place. The floor of the Pacific Ocean west of northernmost California, Oregon, and Washington is both moving relatively northwestward with respect to the continent (Pacific plate) and also eastward beneath it (Juan de Fuca plate). All these movements are relative, however, with respect to the North American lithospheric plate, which is by no means fixed. For example, as the Atlantic Ocean widens, North America may be viewed as moving relatively westward.

### *Gulf of California*

The peninsula of Baja California, as it moves northwestward, is in the process of being rifted from the mainland of Mexico, thereby opening the Gulf of California. The crust flooring the Gulf is expanding as new seafloor is formed at depth along a series of spreading segments defined by a pattern of oblique transform faults (Figure 1.1). The peninsula broke away from the Mexican mainland on the east about 4 million years (m.y.) ago (Larson *et al.*, 1968; Moore and Buffington, 1968), and the spreading process is still continuing. This movement pattern results in several superimposed styles at a local scale within the region: strike-slip displacements near the major transform faults, sagging and warping over pull-apart basins where the rift floor is stretching, and downslope displacements along the margins of the Gulf of California where high-standing terrain of the old continent is relatively unsupported at the edge of the rift.

The Salton Trough lies at the northwestern end of the

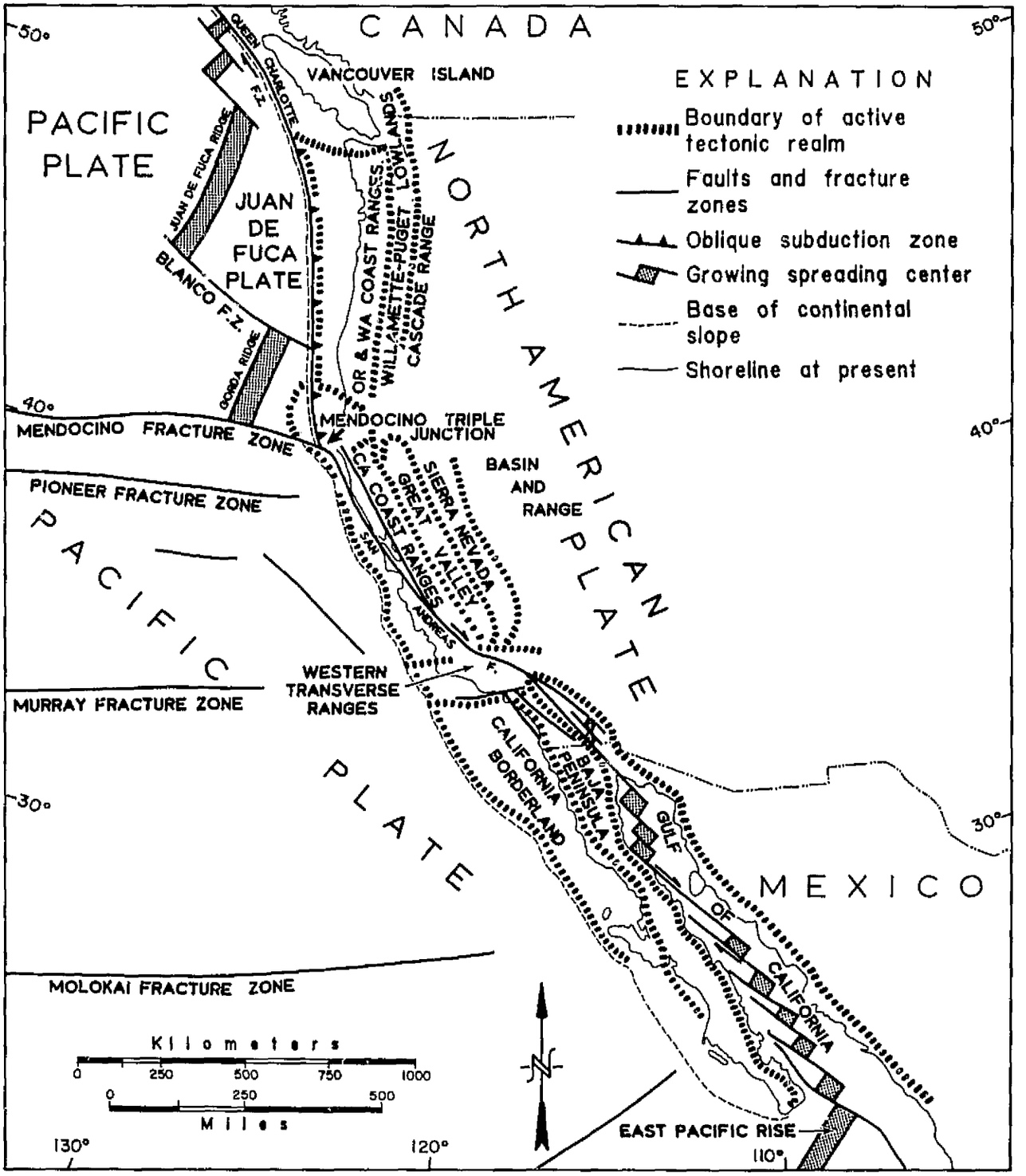


FIGURE 1.1 Map showing active-tectonic realms along the western margin of the conterminous United States. Boundaries between realms are transitional. Base map modified from Drummond *et al.* (1981).

Gulf of California rift and reflects transition into the San Andreas transform system (Crowell and Sylvester, 1979; Crowell, 1981; Johnson *et al.*, 1982). Within this region several complex fault zones (Elsinore, San Jacinto, and San Andreas), characterized by braided slices, extend northwestward from spreading centers within the head of the Gulf. Crustal blocks and slices within and between these fault zones rise and sink ("porpoise structure") as lithospheric displacements continue; some mountain blocks move upward and now stand high as the result of squeezing and shortening, whereas, not far away, other sectors are depressed to form basinal receptacles for sediments washed in from adjacent highlands. Even alluvial surfaces formed but a few millenia ago are warped and disturbed in this tectonically active region. Such a pattern of deformation is shown by earthquakes, geodetic measurements, and the interpretation of landforms (Sharp *et al.*, 1972; Keller *et al.*, 1982). The crustal deformation to be expected beneath a local site the size of a few city blocks—an area appropriate for most engineering structures—will therefore depend critically on exactly where it is sited in such a region.

### *Baja California Peninsula and Peninsular Ranges*

West of the Gulf of California lies the peninsula of Baja California and its northwestern extension into southern California constituting the Peninsular Ranges (Gastil *et al.*, 1981). This is primarily a region of deeply eroded basement rocks, broken into only a few long slices that are tipped westward. Compared with most of California the region is relatively intact and stable, except for belts along the major fault zones such as the Elsinore and San Jacinto. Its western margin is transitional into the California Borderland province along splays of the Newport-Inglewood Fault zone, which parallels the present shoreline just offshore. The northwestern margin of the Peninsular Ranges borders one of California's most complex tectonic regions, a region abutting the Transverse Ranges. Here, bordering the Los Angeles Basin, Miocene and more recent crustal extensions and rotation of blocks have not yet been completely investigated. It is a region where at places folds are currently forming and faults are actively displacing alluvial surfaces (Harding, 1976). In rough terms, the northwestern margin of the Peninsular Ranges block is being forced into the Transverse Ranges as it is carried northwestward during the opening of the Gulf of California.

### *California Borderland*

The topography of the seafloor to the west of southern California and the northern part of the Baja California Peninsula is characterized by basins and ranges (Moore, 1969; Howell and Vedder, 1981). Some of the ranges are surmounted by islands, others reach up to near sea level to form shoals. Many of the ranges are bordered by long, straight, discontinuous fault scarps as shown by subsea topography and the linear arrangement of earthquake epicenters. The region is one where the topography reflects the structure closely: the subsea mountains, formed mainly in post-mid-Miocene times, have been only slightly eroded. Basins, on the other hand, are being infilled by turbidity currents that are bringing sediment down submarine canyons from source areas on land well to the east. The flat floors of basins have been smoothed by sedimentation processes.

### *Transverse Ranges*

One of the most active regions tectonically in western North America lies athwart the northwestern trend of mountain ranges fringing the continent and is appropriately named the Transverse Ranges. To the southeast the Peninsular Ranges parallel the trend of the continental margin, and to the northwest so do the Coast Ranges, Great Valley of California, and the Sierra Nevada.

In this east-west trending province, marine terraces near the city of Ventura, for example, are moving upward at rates of as much as 7.5 mm per year (Lajoie *et al.*, 1982). In the same region, strata laid down at marine depths of several thousand feet only a half-million years ago are now warped and uplifted well above sea level and are deeply eroded (Yeats, 1977). The region, which extends both east and west of the Big Bend in the San Andreas Fault system, is one where different parts have had different tectonic histories during the past million years or so (Jahns, 1973; Allen, 1981; Crowell, 1982; Yeats, 1983). Some faults root at depths where earthquakes originate, others are related to sliding of beds across each other during folding and are relatively shallow and not so likely to generate dangerous earthquakes. The region also includes the area of the enigmatic Palmdale Bulge, where geodetic measurements show either general uplift during the last few decades or episodic uplift, although the interpretation of the measurements is controversial (Castle *et al.*, 1976; Jackson and Lee, 1979; Mark *et al.*, 1981; Strange, 1981, 1984; Stein, 1984). Moreover, the Transverse Ranges and parts of bordering realms include tectonic blocks that have been rotated clockwise during Miocene

times (Luyendyk *et al.*, 1980). Although these tectonic rotations are not known to be going on today, they have contributed to the heterogeneity of the bedrock, and so affect strain patterns now under development.

The San Fernando earthquake of February 9, 1971, was located within the Transverse Ranges on a fault dipping northward beneath the San Gabriel Mountains (Grantz *et al.*, 1971; Oakeshott, 1975a). The fault was one of many known to have broken young deposits and with fault landforms along it, such as the Raymond, Cucamonga, Sierra Madre, San Andreas, and San Jacinto. But it was not known beforehand that this fault, nor the segment where the ground was broken, was most likely to be the site of a disruptive earthquake. Most of the active faults in this region, and elsewhere around the Los Angeles metropolitan region, have now been demarcated, but tectonic understanding has not yet progressed far enough for geoscientists to pinpoint with confidence which fault is most likely to break next. Faults known to be recently active are most likely to rupture again, but more research to learn which are the most dangerous is required.

The geologic situation in the vicinity of the San Fernando earthquake serves to illustrate problems in appraising future earthquake hazards. Young and datable sedimentary deposits, such as alluvium and terrace deposits, are needed to ascertain the time of movement of tectonic features that disrupt them. Faults are commonly known to be active where they cut deposits only a few thousand years old. Faults are suspected of being active where the youngest strata or geomorphic features cut are several tens of thousand or a hundred thousand years old. In the absence of datable young beds that are clearly cut by faults or warped and distorted by folding, there is at present no satisfactory way to determine whether a fault should be labeled as active and is likely to break again in the near future. Many faults are mappable in older rocks, but they may have been formed by geologically ancient deformations under tectonic regimes and stress situations long abandoned.

The difficulties are illustrated in Figure 1.2, a cross section through the region of the San Fernando earthquake and extending northeastward into ancient rocks, including those of Precambrian age. Along the edge of the valley, transected young deposits prove that the faulting is young, but faults within the higher mountains underlain only by basement rocks may have been active at intervals any time since the rocks were consolidated over a billion years ago. These ancient rocks have also been tilted and folded as shown by layering in igneous rocks formed by settling of crystals on the flat floor of a magma chamber in Precambrian time. Whether the tilting of the layering, which was originally nearly horizontal, took place not long after crystallization or but recently cannot be determined from examining local outcrops. Regional understanding of the tectonic history, however, may provide a basis for useful inferences.

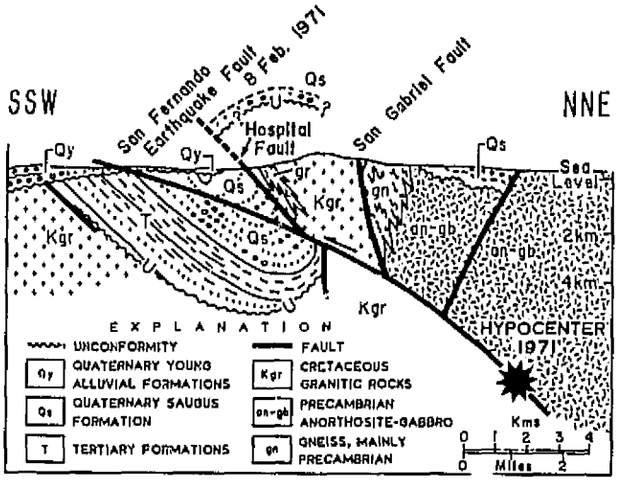


FIGURE 1.2 Geologic cross section through the hypocenter of the San Fernando earthquake of February 9, 1971. Refer to text for discussion. Modified from Oakeshott (1975b, Fig. 4).

That the basement rocks in this region have been folded and displaced recently is also shown by the shape of the unconformity between young deposits and the basement (Figure 1.2; Oakeshott, 1975b). The syncline beneath the San Fernando earthquake fault is accompanied by an anticline above it, even though along the plane of the cross section there are no outcrops of the unconformity for about 8 km northward. The folded unconformity, dated as young because the deposits just above it are geologically young, proves that the latest deformation of the basement block took place in recent times. But this interpretation does not preclude many other deformational events, including several episodes of folding and faulting in the geologically remote past. During the earthquake the San Gabriel Fault did not rupture the ground surface so far as is known; this major ancient fault was ignored in the modern stress regime. Old faults may well become reactivated if they are oriented so that the resolved shear stress on them is sufficient for slip within the present-day tectonic situation. For this reason it is desirable for investigators to learn as much as they can concerning the style of deformation so that they can advance reasonable inferences concerning which faults are dangerous. Models of crustal structure and behavior that are well substantiated may be helpful in this task.

*California Coast Ranges*

Northwest of the Transverse Ranges, and reaching into the area near the Mendocino triple junction, are several low but rugged ranges interspersed with long intermontane valleys. The region constitutes the Coast Ranges. They break off sharply both at the shoreline on the west and with the topographically flat Great Valley on the east. Throughout the mountain belt, the ranges are uplifted and deformed as shown by warped young terraces and surfaces (Buchanan-Banks *et al.*, 1978; Page, 1981). The Coast Ranges are also constructed of ancient rocks that have been involved in a complicated history through geologic time. For example, many of the older strata were formed at a convergent tectonic boundary between lithospheric plates coming in against the continent from Pacific regions. Many faults in such areas have moved again and again, and some may now be active, although it is difficult to document the timing of the most recent displacements owing to the paucity of young offset strata.

The stretch of the San Andreas Fault through the central Coast Ranges is straight and constitutes the near-surface boundary between the lithospheric plates. Activity along it is shown in two ways. First, it is the locus of continuous slow creep, and, second, from time to time noticeable earthquakes take place upon it, such as the Parkfield earthquake of 1966 (Brown *et al.*, 1967). The reach of the fault subject to creep and frequent small earthquakes extends on northwestward from near the town of Parkfield into the San Francisco Bay area. This is the part of the fault system that is under close watch instrumentally by the U.S. Geological Survey. Seismographs and instruments of other types are monitoring the behavior of the walls on either side of the fault in a search for premonitory changes in strain, tilt, magnetism, electrical field, the depth and character of small earthquakes, and the gas contents and water levels in wells (Raleigh *et al.*, 1982). When a major earthquake occurs along this segment of the San Andreas, geoscientists hope to have gathered many kinds of information pertinent to understanding when, where, and why the earthquake happened.

The Coalinga earthquake of May 1983 took place in the central California Coast Ranges, with its epicenter near their margin with the Great Valley and about 30 km from the San Andreas Fault (Eaton *et al.*, 1983; Namson *et al.*, 1983; Wentworth *et al.*, 1983). Although the tectonic setting of the earthquake is still under study, it appears that relatively rigid crustal layers are deforming differently from those at depth. The occurrence of the earthquake at distance from the San Andreas Fault attests to the mobility of a broad belt near the lithospheric plate boundary and also that geologists have much to learn concerning its dynamics.

To the south of Parkfield the fault last ruptured during the Fort Tejon earthquake of 1857, one of the strongest earthquakes in California recorded history (Sieh, 1978a,b). This earthquake displaced ground features about 30 feet right laterally along the fault from the southernmost Coast Ranges, through the Big Bend region of the San Andreas Fault and the central Tranverse Ranges, to the vicinity of the city of San Bernardino.

Within the San Francisco Bay region elongate crustal blocks are separated by several major faults of the San Andreas transform system, such as the San Gregorio, San Andreas (proper), Hayward, and Calaveras (Crowell, 1976; Page, 1981, 1982). These faults are neither exactly parallel to each other nor to the direction of movement between the Pacific and North American lithospheric plates. Where the faults diverge or converge in map view, blocks between them may be either squeezed or stretched. Where they are stretched, the terrain sags to form valleys and sedimentary basins, and where squeezed, terrain rises to make mountains. San Francisco Bay itself may well owe its origin to the sagging of the block between the San Andreas and Hayward Faults so that ocean waters from the Pacific are able to flood eastward upon the continent. In this region, terrains between major faults are undergoing deformation as shown by out-of-place old-erosional surfaces—some have been much uplifted and dissected; others, such as marine terraces, are now depressed far below the levels where they were formed (Atwater *et al.*, 1977). Soft mélanges of the ancient Franciscan Complex stand high and are prone to severe landsliding. The region as a whole is undergoing deformation, but deformation is even more concentrated along the major fault zones (Brabb and Hanna, 1981; Prescott *et al.*, 1981).

North of San Francisco Bay several terrains between discontinuous active faults are recognized (Herd, 1978; Fox, 1983). Shear stress between the two lithospheric plates is apparently spread across a region running through broad lowlands near the city of Santa Rosa. The belt of displacements includes the San Andreas Fault on the west and extends well to the east into the high Coast Ranges, roughly on line northwestward from the active Calaveras and Concord Faults. This region is one where the active plate boundary is broad and diffuse and where crustal slices within it also show "porpoise structure." Geologic mapping with an emphasis on documenting recent deformation is hampered in the northern California Coast Ranges by widespread dense forests and brush, steep terrain subject to landsliding, and the paucity of datable young rocks.

*Mendocino Triple Junction*

The region onshore from the Mendocino triple junction, where the the Juan de Fuca, Pacific, and North American lithospheric plates meet, is complex tectonically (Atwater, 1970). It lies transitionally between terrains on the south undergoing transform displacements and those to the north undergoing oblique convergence. Moreover, the relative movement between the major plates is carrying the triple junction slowly northwestward relative to the continent on the east, so that through time, transform-belt tectonic features are being overprinted on those formed under a regime of oblique convergence. Investigation of a few patches of Quaternary strata show both folding and faulting. In fact, wrench faulting forming ahead of the arrival of the San Andreas transform system is recognized 120 km north of the triple junction (Kelsey and Cashman, 1983).

*Oregon and Washington Coast Ranges*

From the Mendocino triple junction, coastal mountain ranges extend on northward from within California through Oregon and Washington. Farther inland in Oregon lies the Willamette Valley and still farther eastward the Cascade Range. Active volcanoes surmount the Cascade Range, including Mount St. Helens (Lipman and Mullineaux, 1981), and are inferred to be the consequence of subduction of the Juan de Fuca plate beneath the continent. The belt of active volcanoes extends from Mount Lassen on the south, onshore to the southeast from the Mendocino triple junction, through Mount Shasta, and on northward through both Oregon and Washington and southernmost British Columbia. Along this trend, active deformation associated with volcanism therefore also requires evaluation, but the volcanic belt lies well to the east of the coastline.

Along the coast, uplifted marine terraces attest to vertical tectonic movements, but active-tectonic investigations are sparse. The coastal ranges, including the Olympic Mountains in Washington, were uplifted beginning in Pliocene time and are still rising (Snavely and Wagner, 1963; Gable and Hatton, 1983). Fault scarps of Quaternary age have been identified on the southeastern part of the Olympic Peninsula (Wilson *et al.*, 1979) and on the seafloor (Snavely *et al.*, 1980). Earthquakes, such as those near Mount Rainier in 1973 and 1974 (Crosson and Frank, 1975; Crosson and Lin, 1975), and geodetic measurements prove recent deformation (Ando and Balazs, 1979). Investigations stimulated by the 1980 eruption of Mount St. Helens are adding much to understanding of the tectonics of the region (e.g., Weaver and Smith, 1983).

In northwestern Washington the tectonic style of active deformation changes gradually from one of oblique convergence to one of transform displacements associated with the Queen Charlotte Fault zone. This zone, which lies off the coast of British Columbia, forms the boundary between the Pacific and North American plates northwest of the Juan de Fuca Rise. The transition zone lies inboard primarily of the fragmented Juan de Fuca plate (Figure 1.1; Clowes *et al.*; 1983). High river terraces and upland surfaces of Quaternary age attest to active uplift in the Coast Mountains of British Columbia, inferred to be due chiefly to vertical expansion after heating of a thick crustal slab; this active uplift is documented by the unroofing and setting of fission-track dates (Parrish, 1983). Active tectonics in this region appear to be the consequence of isostatic adjustments to a previous history of oblique subduction that has thickened the crustal slab.

*Other Active-Tectonic Realms*

Several other provinces lie to the east of the coastal belt and locally display active deformation but are not dealt with in detail here (Figure 1.1). They include the Great Valley of California, the Willamette-Puget Sound Lowlands of Oregon and Washington, Sierra Nevada, Cascade Ranges, and Basin and Range province. In fact, from a global viewpoint, the whole of western North America constitutes the deformed margin of the North American plate (Atwater, 1970). The eastern edge of this belt corresponds to the abrupt eastern escarpment of the Rocky Mountains where they meet the Great Plains. The relatively stable craton lies still farther east and underlies the middle of the continent.

## DISCUSSION

These brief descriptions of active-tectonic realms along the Pacific Coast emphasize the mobility of the region. Earthquakes, geodetic surveys, other geophysical measurements of several types, geomorphic studies, and geologic observations document irregular ground movement both vertically and horizontally. Many small areas the size of cities have been intensively studied, so that their deformational history is well known, but these areas are scattered and unevenly distributed. In addition, the kind and quality of data documenting active deformation is unsatisfactorily variable.

Documentation of recent deformation from earthquakes and from most geophysical measurements deals with the present and the past few decades only. It does not span time intervals long enough to reveal an understanding of average conditions—the time sampling is

just too short (Allen, 1975). Therefore basic documentation of recent deformation is lacking both areally and temporally. The former can be remedied only in part by adding many instruments throughout a region. Despite the huge cost, only short-time-span information can result.

However, widespread studies in tectonic geomorphology—locally quantified by appropriate regional studies involving geophysical measurements and isotopic and soil dating—will add useful information on averages over several millenia. Investigations of these sorts have been most fruitful in local areas, especially around San Francisco Bay and in the Santa Barbara-Ventura regions (Atwater *et al.*, 1977; Keller *et al.*, 1982; Lajoie *et al.*, 1982; Yeats, 1983). These types of study need to be extended throughout the coastal belt wherever there are young datable strata to work with. By means of such investigations, deformational histories extending back into geologic time for tens of thousands of years will provide better understanding of the episodicity or continuity of rates of uplift, sinking, warping, folding, and faulting.

A long look at the late Cenozoic geologic history of the tectonically mobile belt shows that activity along major fault strands of the San Andreas Fault system, for example, has switched from fault to fault (Crowell, 1979). Studies of critical areas using geomorphic data should aid in understanding the timing of these switchings. They will also help in characterizing the style and timing of crustal movements on slices within fault zones themselves.

Vast proportions of the mobile belt extending inland from the Pacific Coast are not continuously underlain by young datable strata or datable geomorphic surfaces and so do not lend themselves to geomorphic or geologic study aimed at demarcating episodes of active deformation through time. Documentation of deformation in such regions will therefore always be piecemeal and incomplete. Many of these intervening regions are underlain by older rocks deformed many times through the geologic ages. Tectonic overprinting of one style on another makes it difficult to separate the results of those crustal movements now under way from the results of ancient ones. Conclusions concerning deformation in these regions will therefore have to come largely from extrapolation from where data are available to intervening areas where there are none. These extrapolations need to be based on understanding of the regional tectonic behavior and on well-constrained tectonic models. With this information in hand we may be able to place geophysical instruments, such as strain gauges, at critical locations where they can provide warnings of impending earthquakes.

The classification of active-tectonic realms in this brief paper is built on the plate-tectonic concept, and much local research at present is striving to add details to this concept and to improve models. In fact, maps at scales ranging from local areas to large regions, showing the style of active deformation, will provide a useful way to synthesize and portray data from both observations and models. More subsurface data are also needed to improve the models. Much crustal extension and shortening prevails in the upper few tens of kilometers of the crust. Profiles using the reflection seismograph will be especially helpful in outlining the structure at depth, including the position and character of décollement zones. The fine structure and behavior of small crustal units or blocks in three dimensions is not yet fully melded into global plate-tectonic theory.

Progress in tectonic understanding will be strongly accelerated if there is better coordination among many types of geoscientist whose professional focus initially differs widely. Local studies by engineering geologists will improve understanding of the way small sectors behave through time. They reveal the style, rates, episodicity, or clustering of deformational events, that is, they reveal the strain pattern under development in limited areas. Investigations undertaken to evaluate the safety and suitability of sites for major engineering structures such as high-rise buildings, nuclear power plants, bridges, tunnels, and dams provide examples of such local studies. Data and inferences from these investigations will add significantly to tectonic models, which in turn will aid in extrapolating to areas where active-tectonic data are sparse or lacking. All geoscientists need to find ways to stimulate coordination leading to mutual symbiosis.

During the decades ahead geoscientists foresee a marked improvement in the applicability of tectonic models, thanks to the integration of data from local detailed studies, both geologic and geophysical. Geoscientists are challenged to monitor these local studies and strive to place them into a regional synthesis. Both data and inferences can be depicted on maps and diagrams that are especially designed to show and discriminate between basic information and interpretation and to show active-tectonic realms more satisfactorily. Science and society will both benefit significantly.

## REFERENCES

Allen, C. R. (1975). Geological criteria for evaluating seismicity, *Geol. Soc. Am. Bull. 86*, 1041-1057.

Allen, C. R. (1981). The modern San Andreas Fault, in *The Geotectonic Development of California*, W. G. Ernst, ed., Prentice-Hall, Englewood Cliffs, N.J., pp. 511-534.

Ando, M., and E. I. Balazs (1979). Geodetic evidence for aseismic

subduction of the Juan de Fuca plate, *J. Geophys. Res. 84*, 3023-3028.

Atwater, T. (1970). Implications of plate tectonics for the Cenozoic tectonic evolution of western North America, *Geol. Soc. Am. Bull. 81*, 3513-3516.

Atwater, B. F., C. W. Hedel, and E. J. Helley (1977). Late Quaternary depositional history, Holocene sea-level changes, and vertical crustal movement, southern San Francisco Bay, California, *U.S. Geol. Surv. Prof. Paper 1014*, 15 pp.

Brabb, E. E., and W. F. Hanna (1981). Maps showing aeromagnetic anomalies, faults, earthquake epicenters, and igneous rocks in the southern San Francisco Bay Region, California, *U.S. Geol. Surv. Map GP-932*.

Brown, R. D., Jr., J. G. Vedder, R. E. Wallace, E. F. Roth, R. F. Castle, A. O. Waananen, R. W. Page, and J. P. Eaton (1967). The Parkfield-Cholame, California, earthquakes of June-August, 1966, *U.S. Geol. Surv. Prof. Paper 579*, 66 pp.

Buchanan-Banks, J. M., E. H. Pampeyan, H. C. Wagner, and D. S. McCulloch (1978). Preliminary map showing recency of faulting in coastal south-central California, *U.S. Geol. Surv. Map MF-910*.

Castle, R. O., J. P. Church, and M. R. Elliot (1976). Aseismic uplift in southern California, *Science 192*, 251-253.

Clowes, R. M., R. M. Wallis, Z. Hajnal, and I. F. Jones (1983). Seismic reflections from subducting lithosphere? *Science* 223, 668-670.

Crosson, R. S., and D. Frank (1975). The Mt. Rainier earthquake of July 18, 1973, and its tectonic significance, *Bull. Seismol. Soc. Am. 65*, 634-645.

Crosson, R. S., and J. Lin (1975). A note on the Mt. Rainier earthquake of April 20, 1974, *Bull. Seismol. Soc. Am. 65*, 549-556.

Crowell, J. C. (1976). Implications of crustal stretching and shortening of coastal Ventura Basin, California, *Pacific Sec., Am. Assoc. Petrol. Geol. Misc. Publ. 24*, 365-382.

Crowell, J. C. (1979). The San Andreas Fault system through time, *J. Geol. Soc. 136*, 293-302.

Crowell, J. C. (1981). Juncture of San Andreas transform system and Gulf of California rift, *Oceanol. Acta 3* (Proc. 26th Inter. Geol. Congress, Geology of Continental Margins), pp. 137-141.

Crowell, J. C. (1982). The tectonics of Ridge Basin, southern California, in *Geologic History of Ridge Basin, Southern California*, J. C. Crowell and M. H. Link, eds., Pacific Sec., Soc. Econ. Paleontol. Mineral., pp. 25-41.

Crowell, J. C., and A. G. Sylvester, eds. (1979). *Tectonics of the Juncture Between the San Andreas Fault System and the Salton Trough, Southeastern California*, Dept. Geol. Sci., Univ. Calif., Santa Barbara, 193 pp.

Drummond, K. J., *et al.* (1981). Plate-tectonic map of the circum-Pacific region, northeast quadrant, *Am. Assoc. Petrol. Geol. Map*.

Eaton, J., R. Cockerham, and R. Lester (1983). Setting, distribution, and focal mechanisms of the 1983 Coalinga earthquake and its aftershocks, *EOS 64*, 740.

Fox, K. F., Jr. (1983). Tectonic setting of late Miocene, Pliocene, and Pleistocene rocks in part of the Coast Ranges north of San Francisco, California, *U.S. Geol. Surv. Prof. Paper 1239*, 33 pp.

Gable, D. J., and T. Hatton (1983). Maps of vertical crustal movements in the conterminous United States over the last 10 million years, *U.S. Geol. Surv. Map I-1315*.

Gastil, G., C. Morgan, and D. Krummenacher (1981). The tectonic history of peninsular California and adjacent Mexico, in *The Geotectonic Development of California*, W. G. Ernst, ed., Prentice-Hall, Englewood Cliffs, N.J., pp. 284-305.

Grantz, A., *et al.* (1971). The San Fernando, California, earthquake of February 9, 1971, *U.S. Geol. Surv. Prof. Paper 733*, 254 pp.

Harding, T. P. (1976). Tectonic significance and hydrocarbon trapping consequences of sequential folding synchronous with San Andreas faulting, San Joaquin Valley, California, *Am. Assoc. Petrol. Geol. Bull. 60*, 356-378.

Herd, D. G. (1978). Intracontinental plate boundary east of Cape Mendocino, California, *Geology 6*, 721-725.

Howell, D. G., and J. G. Vedder (1981). Structural implications of stratigraphic discontinuities across the southern California borderland, in *The Geotectonic Development of California*, W. G. Ernst, ed., Prentice-Hall, Englewood Cliffs, N.J., pp. 535-558.

Jackson, D. D., and W. B. Lee (1979). The Palmdale bulge—An alternate interpretation, *EOS 60*, 810.

Jahns, R. H. (1973). Tectonic evolution of the Transverse Ranges province as related to the San Andreas Fault system, *Stanford Univ. Publ. Geol. Sci. 13*, 149-170.

Johnson, C. E., *et al.* (1982). The Imperial Valley, California, earthquake of October 15, 1979, *U.S. Geol. Surv. Prof. Paper 1254*, 451 pp.

Keller, E. A., M. S. Bonkowski, R. J. Korsch, and R. J. Shlemon (1982). Tectonic geomorphology of the San Andreas Fault zone in the southern India Hills, Coachella Valley, California, *Geol. Soc. Am. Bull. 93*, 46-56.

Kelsey, H. M., and S. M. Cashman (1983). Wrench faulting in northern California and its tectonic implications, *Tectonics 2*, 565-576.

Lajoie, K. R., A. M. Sarna-Wojcicki, and R. F. Yerkes (1982). Quaternary chronology and rates of crustal deformation in the Ventura area, California, in *Neotectonics in Southern California*, Cordilleran Sec., Geol. Soc. Am., Volume and Guidebook, pp. 43-51.

Larson, R. L., H. W. Menard, and S. Smith (1968). Gulf of California: A result of ocean-floor spreading and transform faulting, *Science 161*, 781-784.

Lipman, P. W., and D. R. Mullineaux, eds. (1981). The 1980 eruptions of Mount St. Helens, Washington, *U.S. Geol. Surv. Prof. Paper 1250*, 844 pp.

Luyendyk, B. P., M. J. Kammerling, and R. Terres (1980). Geometric model for Neogene crustal rotations in southern California, *Geol. Soc. Am. Bull. 91*, 211-217.

Mark, R. K., J. C. Tinsley III, E. B. Newman, T. D. Gilmore, and R. O. Castle (1981). An assessment of the accuracy of the geodetic measurements that define the southern California uplift, *J. Geophys. Res. 86*, 2783-2808.

Moore, D. G. (1969). Reflection profiling studies of the California Continental Borderland, *Geol. Soc. Am. Spec. Paper 107*, 138 pp.

Moore, D. G., and E. C. Buffington (1968). Transform faulting and growth of Gulf of California since the late Pliocene, *Science 161*, 1238-1241.

Namson, J., T. Davis, and M. B. Lagoe (1983). Thrust-fold deformation style of seismically active structures near Coalinga, California, *EOS 64*, 749-750.

Oakeshott, G. B., ed. (1975a). San Fernando, California, earthquake of 9 February 1971, *Calif. Div. Mines Geol. Bull. 196*, 463 pp.

Oakeshott, G. B. (1975b). Geology of the epicentral area, in *San Fernando Earthquake of 9 February 1971*, G. B. Oakeshott, ed., *Calif. Div. Mines Geol. Bull. 196*, pp. 19-30.

Page, B. M. (1981). The southern Coast Ranges, in *The Geotectonic Development of California*, W. G. Ernst, ed., Prentice-Hall, Englewood Cliffs, N.J., pp. 329-417.

Page, B. M. (1982). Modes of Quaternary tectonic movement in the San Francisco Bay region, California, *Calif. Div. Mines Geol. Spec. Publ. 62*, pp. 1-10.

Parrish, R. R. (1983). Cenozoic thermal evolution and tectonics of the Coast Mountains of British Columbia, I. Fission track dating, apparent uplift rates, and patterns of uplift, *Tectonics 2*, 601-632.

Prescott, W. H., M. Lisowski, and J. C. Savage (1981). Geodetic mea-

surements of crustal deformation on the San Andreas, Hayward, and Calaveras Faults near San Francisco, California, *J. Geophys. Res. 86*, 10853-10869.

Raleigh, C. B., K. Sieh, L. R. Sykes, and D. L. Anderson (1982). Forecasting southern California earthquakes, *Science 217*, 1097-1104.

Sbar, M. L. (1982). Delineation and interpretation of seismotectonic domains in western North America, *J. Geophys. Res. 87*, 3919-3928.

Sharp, R. V. *et al.* (1972). The Borrego Mountain earthquake of April 9, 1968, *U.S. Geol. Surv. Prof. Paper 787*, 207 pp.

Sieh, K. E. (1978a). Prehistoric large earthquakes produced by slip on the San Andreas Fault at Pallett Creek, California, *J. Geophys. Res. 83*, 3907-3939.

Sieh, K. E. (1978b). Slip along the San Andreas Fault associated with the great 1857 earthquake, *Seismol. Soc. Am. Bull. 68*, 1421-1448.

Snavely, P. D., Jr., and H. C. Wagner (1963). Tertiary geologic history of western Oregon and Washington, *Wash. Div. Mines Geol. Rep. Invest. 22*, pp. 25.

Snavely, P. D., Jr., H. C. Wagner, and D. L. Lander (1980). Geologic cross section of the central Oregon continental margin, *Geol. Soc. Am. Map Chart Ser. MC-28J*.

Stein, R. S. (1984). Comment on "The impact of refraction correction on leveling interpretations in southern California" by W. E. Strange, *J. Geophys. Res. 89*, 559-561.

Strange, W. E. (1981). The impact of refraction correction on leveling interpretations in southern California, *J. Geophys. Res. 86*, 2809-2824.

Strange, W. E. (1984). Reply [to Stein, 1984], *J. Geophys. Res. 89*, 562-564.

Weaver, C. S., and S. W. Smith (1983). Regional tectonic and earthquake hazard implications of a crustal fault zone in southwestern Washington, *J. Geophys. Res. 88*, 10371-10383.

Wentworth, C. M., M. D. Zoback, and J. A. Bartow (1983). Thrust and reverse faults beneath the Kettleman Hills anticlinal trend, Coalinga earthquake region, California, inferred from deep seismic-reflection data, *EOS 64*, 747.

Wilson, J. R., M. J. Bartholomew, and R. J. Carson (1979). Late Quaternary faults and their relationship to tectonism in the Olympic Peninsula, Washington, *Geology 7*, 235-239.

Yeats, R. S. (1977). High rates of vertical crustal movement near Ventura, California, *Science 196*, 295-298.

Yeats, R. S. (1983). Large-scale Quaternary detachments in Ventura Basin, southern California, *J. Geophys. Res. 88*, 569-583.

Zoback, M. D., and M. L. Zoback (1981). State of stress and intraplate earthquakes in the United States, *Science 213*, 96-104.

Zoback, M. L., and M. D. Zoback (1980). State of stress in the conterminous United States, *J. Geophys. Res. 85*, 6113-6156.

# 2 Epeirogenic and Intraplate Movements

LARRY D. BROWN
*Cornell University*

ROBERT E. REILINGER*
*Air Force Geophysics Laboratory*

ABSTRACT

Major deformations of the Earth's surface are largely consistent with the tenets of plate tectonics, which predict that such activity should be focused at the various boundaries along which massive lithospheric plates collide, pull apart, or slide past one another. Yet crustal deformations also occur well into the interior of these plates. Some may represent the "distributed" effects of distant plate boundaries, as, for example, the earthquakes of the intermontane western United States. Some, such as the geodetically observed uplift over a deep magma chamber in the Rio Grande rift of New Mexico, may correspond to incipient formation of a new plate boundary. Others, like the subtle, broad uplifts and subsidences in the nominally "stable" cratonic interiors, are much more puzzling. Such motions often appear estranged, if not divorced, from accepted plate-tectonic processes. Postglacial rebound, a well-known phenomenon in portions of North America and Europe, also appears to be an inadequate explanation for many observations.

Understanding contemporary motions of plate interiors is often hindered by the paucity and uncertain accuracy of relevant geophysical and geodetic observations. Yet intraplate tectonics constitutes more than a scientific enigma. Even seemingly slow vertical motions may threaten river courses or seafront properties on socially relevant time scales, and the subtle strains accumulating elsewhere may portend future earthquakes or volcanoes in the least predictable places.

## INTRODUCTION

Even a cursory glance at global earthquake activity makes clear that much of the world's tectonic activity is concentrated in relatively narrow belts (Figure 2.1). According to the theory of plate tectonics, these earthquake belts, and the similar patterns of volcanic activity, mark the currently active boundaries between large, lithospheric plates that are moving relative to one another (e.g., Dewey, 1975). The Pacific "Ring-of-Fire," for example, is associated primarily with subduction of the lithospheric plates carrying the Pacific Ocean beneath other plates carrying Asia, North America, and South America. In the United States, the San Andreas Fault is considered a classic example of active tectonics associated with two plates (Pacific and North America) sliding past one another.

However, plate boundaries are far from being the

*Robert E. Reilinger is now at the Massachusetts Institute of Technology.

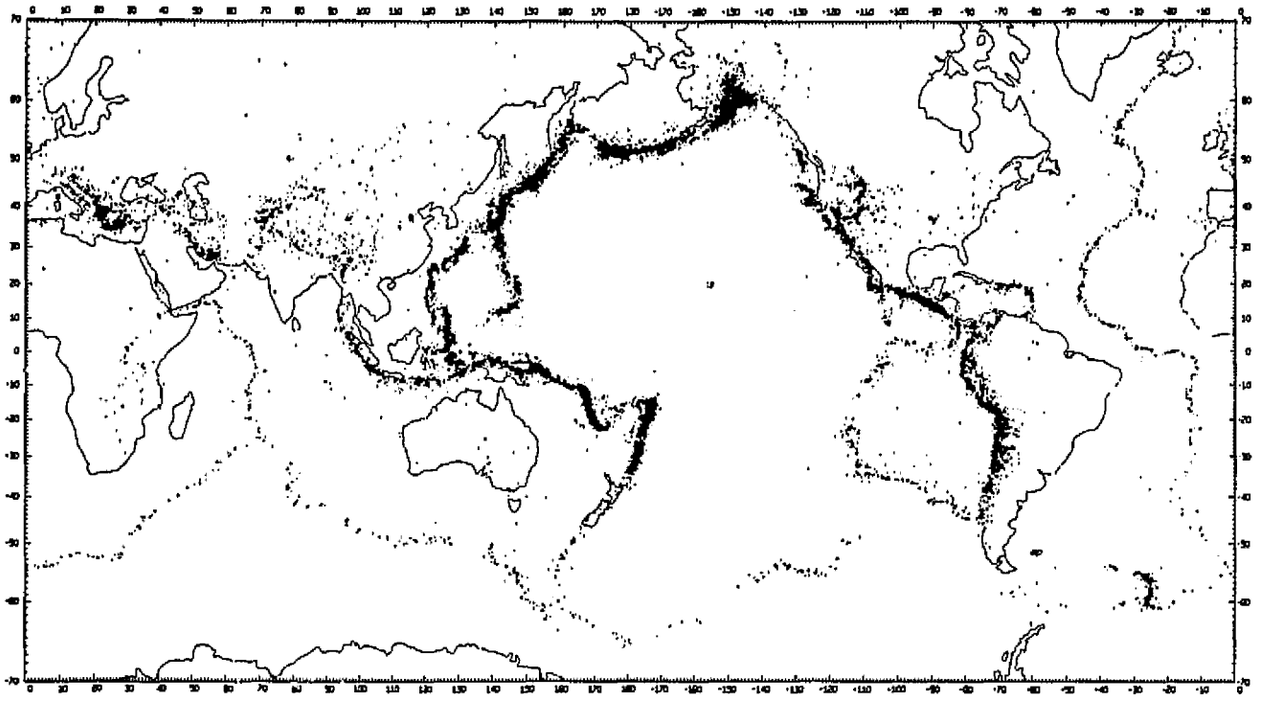

FIGURE 2.1 Global seismicity. Earthquakes tend to be concentrated along relatively narrow belts that define the boundaries of active lithospheric plates. However, some earthquakes also occur well within the plates thus defined. Examples include southeast Asia and the intermontane western United States (after Barazangi and Dorman, 1968).

whole story as far as active tectonics is concerned. In many parts of the world, within both ocean basins as well as continental interiors, there are concentrations of earthquake and volcanic activity that seem divorced from plate-tectonic precepts. Hawaii is a dramatic example. The volcanoes of the Hawaiian Islands-Emperor Seamount chain are generally believed to result from upwelling of magmas from a source beneath the Pacific lithospheric plate. Although the geometry of the volcanic chain appears to be due to the motion of this plate over the underlying mantle "hot spot," the hot spot itself is arguably a phenomenon independent from the overlying global plate framework.

Regions such as southeast Asia and the western United States, where plate boundaries cut into continents, seem especially prone to intraplate tectonics. The volcanic and seismic activity in such areas is conspicuous (Figure 2.1) and often dramatic (Figure 2.2). The semantics of whether tectonic activity in such areas should be be considered truly intraplate or treated as some kind of distributed effect of a distant plate boundary largely begs the issue. Regardless of nomenclature, the fundamental causes of many such phenomena remain unclear, and their place in the plate-tectonic framework unresolved.

The ancient Precambrian cores of the world's continents contain special problems for understanding active tectonics. Although the most obvious manifestations of contemporary tectonics, such as seismicity, are decidedly less pronounced than along the plate boundaries, or even in the geologically younger intraplate regions, earthquakes do occur in the craton and near its periphery. In the United States, two of the most destructive earthquakes in history occurred not along the San Andreas Fault but in the nominally "stable" eastern United States near New Madrid, Missouri, in 1811-1812, and near Charleston, South Carolina, in 1886. Seismicity continues in many parts of the eastern United States, and faults of relatively recent geologic vintage have been identified (York and Oliver, 1976).

That parts of the cratonic interior are tectonically active in the present time should perhaps not be surprising in view of the geologic record. Features such as the Michigan Basin and the Adirondack Dome (Figure 2.3) are incontrovertible evidence that the cratons were subject to major vertical motions in the past that lack a clear connection to the plate-tectonic scenarios of those times. Geologic strata attest to many gentle inundations and uplifts of the interior platforms that reflect relative mo-

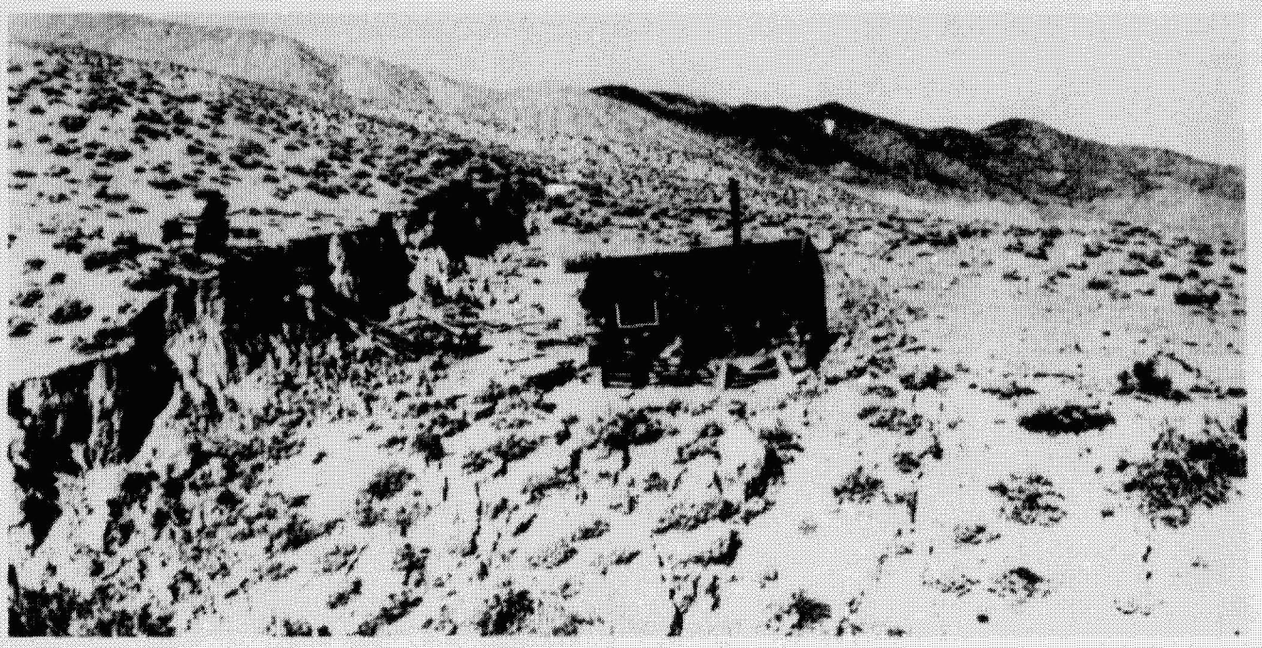

FIGURE 2.2 Faulting associated with the 1944 Dixie Valley, Nevada, earthquake (from Stewart, 1980).

tion of land and sea (Sloss, 1963), motions that are usually referred to as epeirogenic to distinguish them from the more severe forms of deformation associated with mountain building. Geodetic surveys over the cratons of North America and Eurasia appear to indicate that these regions are still going up and down at remarkable rates, although the significance of some of these observations is obscured by an ongoing debate over their accuracy.

Any consideration of the active deformation of intraplate interiors must, of course, recognize the importance of vertical motions associated with the retreat of the ice sheets since the last major continental glaciation. Studies of the contemporary uplift of Fennoscandia as documented by leveling observations and tilted beach terraces are now classic (e.g., Niskanen, 1939). The effects of postglacial rebound are not restricted to areas in proximity to the former ice sheets but are global in extent and of particular importance in coastal areas.

In the following discussion, we outline some of the evidence for active tectonics in intraplate areas, review some of the obstacles to our fuller understanding of their causes, and assess their potential impact on society.

## EARTHQUAKE DEFORMATION

While the underlying causes of intraplate earthquakes remain problematical, some are clearly associated with large and, in some cases, destructive surface movements. Such earthquakes are not limited to continental areas (Wiens and Stein, 1984). Surface faulting is but one of the more obvious expressions of earthquake deformation (Figure 2.2). In some cases, geodetic measurements delineate more subtle patterns of motion. It is reasonable to assume, and the limited evidence available suggests, that intraplate earthquakes are characterized by a deformation cycle with preseismic, coseismic, postseismic, and interseismic phases similar to that inferred for interplate events (Thatcher, Chapter 10, this volume). Coseismic, and to a lesser extent, postseismic deformation have been documented by geodetic measurements for a number of intraplate earthquakes in the United States (Table 2.1). Movements of several centimeters are common, and several meters are possible. Undoubtedly similar movements have accompanied other intraplate events both in the United States and elsewhere but have gone undetected owing to the lack of appropriately timed or spaced observations.

Where sufficiently detailed geodetic observations are available, coseismic movements are roughly consistent with the deformation predicted by simple dislocation theory (e.g., Savage and Hastie, 1966). Intraplate postseismic deformation has been attributed to afterslip on the earthquake fault (e.g., Savage and Church, 1974) or to subsequent viscoelastic relaxation (Koseluk and Bischke, 1981).

FIGURE 2.3 The Adirondack Dome (Courtesy Land Care, Inc., Boonville, New York). Plate interiors often contain isolated geologic structures that are difficult to relate to ancient plate boundaries. The Michigan Basin is another classic example.

TABLE 2.1 Vertical Deformation Associated with U.S. Intraplate Earthquakes

| | | Coseismic | | Postseismic | | |
|---|---|---|---|---|---|---|
| Earthquake | Magnitude | Amplitude | Extent, km | Amplitude | Extent, km | References |
| Hebgen Lake, Montana (1959) | 7.5 | 6 m (15 cm) | 20 × 50 (80 × 140) | 30 cm (7 cm)[a] | 100 (40)[a] | Myers and Hamilton, 1964<br>Savage and Hastie, 1966<br>Reilinger *et al.*, 1977<br>Reilinger, 1985<br>Savage *et al.*, 1985 |
| Borah Peak, Idaho (1983) | 7.3 | 1.5 m | 50 | | | Stein and Barrientos, 1985 |
| Dixie Valley, Nevada (1954) | 7.1 | 1.5 m (1–2 m)[a] | 10 | 7.5 cm | 8 | Savage and Hastie, 1966<br>Savage and Church, 1974 |
| Valentine, Texas (1931) | 6.4 | 10 cm | 50 | | | Ni *et al.*, 1981 |
| Yellowstone Park, Wyoming (1975) | 6 | 10 cm | | | | Pitt *et al.*, 1979 |
| Oroville, California (1975) | 5.7 | 10 cm | 15 | | | Savage *et al.*, 1977 |

[a]Horizontal movement, 1971-1984.

Preseismic deformation, with its obvious implications for prediction, has proven elusive to capture in the more active interplate zones (e.g., Thatcher, 1981), so it is not surprising that it has not yet been unambiguously observed in the intraplate environment. Measurement of coseismic and postseismic deformation is guided by the known time and location of a specific earthquake. In contrast, preseismic motion is likely to be observed more by chance than design, as when repeated geodetic surveys, often carried out for other reasons, happen to cover the location of and a time interval immediately preceding some later earthquake.

Interseismic deformation, the slow buildup of strain during the time periods between earthquakes, is difficult to measure for similar reasons, but also because it accumulates at rates much slower than the other deformation phases. In his review of evidence for horizontal strain accumulation from geodetic measurements, Savage (1983) found significant strain rates in a number of areas, including the Watsatch Fault near Salt Lake City, Utah, the area near Hebgen Lake, Montana, the main seismic belt of western Nevada, and the Seattle, Washington, area. Some of these deformations may well reflect the secular accumulation of interseismic strain.

Earthquakes in the stable interior pose a special problem. It has proven extremely difficult to associate intraplate earthquakes, even large ones, with specific faults in areas like the eastern United States. The easternmost example of Table 2.1 is that of inferred coseismic deformation associated with the 1931 Valentine, Texas, earthquake, which is arguably still within the seismic regime of the active Rio Grande rift system (Ni *et al.*, 1981). Although Schilt and Reilinger (1981) reported some curious vertical motions near the New Madrid seismic zone that may be earthquake related, the connection remains speculative. Aggarwal and Sykes (1978) related low-level seismicity in the New York area to the Ramapo Fault, while recent studies near Charleston (Talwani *et al.*, 1984) may have identified subsurface faulting associated with the major nineteenth century earthquake there. Zoback *et al.* (1980) found

FIGURE 2.4 Damage caused by the 1886 Charleston, South Carolina, earthquake [from U.S. Geol. Surv. Prof. Paper 1028 (1977)]. The historical record makes clear that earthquakes are a threat even in the nominally "stable" interior.

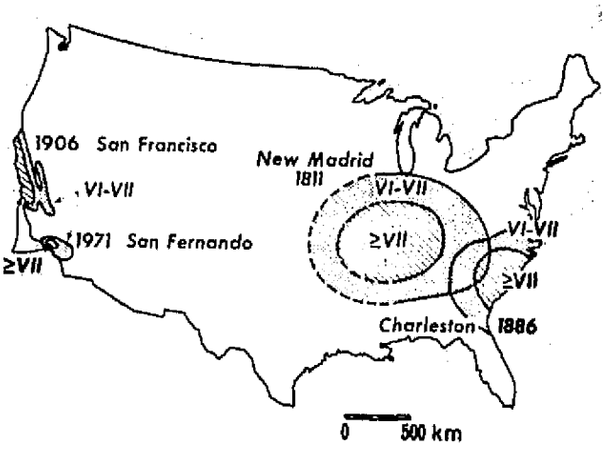


FIGURE 2.5 Area affected by the 1886 Charleston earthquake compared with other major U.S. earthquakes (modified after Rankin, 1977). Earthquakes in the eastern United States are felt over a larger area than an equivalent-sized earthquake in the west owing to more efficient propagation of seismic energy. Intensities are given using the Modified Mercali scale.

evidence of surprisingly large horizontal strains in southeastern New York, which may reflect ongoing ductile deformation at depth. However, an examination of the limited number of horizontal resurveys in other areas of the eastern United States associated with seismicity failed to detect any significant motion (Krueger *et al.*, 1983).

This paucity of surface manifestation, together with the comparatively low recurrence rate of earthquakes and relatively short historic record, makes seismic-hazard mapping an especially difficult endeavor in the stable interior. Yet earthquake hazard can by no means be neglected in these areas. Major earthquakes in the New Madrid, Missouri, area in 1811-1812 and near Charleston, South Carolina (Figure 2.4), are well-known testaments to the uncertain vulnerability of major population centers in such nominally quiescent regions (Sykes, 1978). Potential seismic hazard in the stable interior is exacerbated by the more efficient transmission of seismic energy. An earthquake in the eastern United States is likely to be felt over or damage a much larger area than an equivalent earthquake along the San Andreas Fault, for example (Figure 2.5). Mitigating hazards from earthquakes in the stable interior remains one of least tractable yet most important problems in contemporary tectonics.

## MAGMA INFLATION

Another dramatic demonstration of intraplate tectonics are the oceanic volcanic chains such as Hawaii, which unequivocably confirm that not all volcanoes lie over subduction zones. Movements associated with such volcanoes have been closely monitored for some time (e.g., Wilson, 1935) and are generally thought to reflect the episodic inflation and deflation (eruption) of subsurface magma chambers (e.g., Decker, 1969). Observations of ground motion near volcanoes, together with attendant seismic activity, have proven to be effective predictors for future eruptions.

Somewhat less well known, perhaps, are other results that suggest subsurface magma injection in areas of not-so-recent volcanism. One example of surface deformation attributed to magma at depth comes from the Rio Grande rift of central New Mexico. A variety of geophysical measurements near Socorro, New Mexico, indicate the existence of a thin, but extensive, mid-crustal magma layer (Sanford *et al.*, 1977). Precise leveling over this magma body indicates vertical uplift of about 15 cm over a 40-yr period (Reilinger and Oliver, 1976). Recent measurements indicate (Figure 2.6) that the cen-

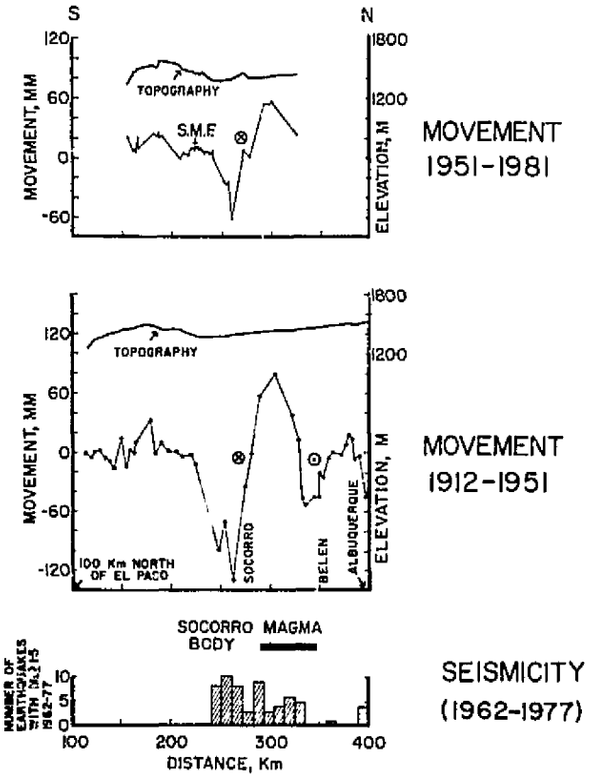


FIGURE 2.6 Uplift in central New Mexico measured by repeated leveling (Larsen *et al.*, 1985). This movement is attributed to inflation of a mid-crustal magma body. This inflation may also be responsible for seismicity of this area.

tral uplift over the magma chamber is flanked by a zone of subsidence, the overall pattern suggesting withdrawal of magma from one reservoir and injection into another (Larsen *et al.*, 1985). An intriguing aspect of this uplift is that it occurs in an area where there have been no historical eruptions, although volcanic rocks in the rift attest to such activity as recently as 100,000 yr ago (Lipman and Mehnert, 1975). Whether this ground motion portends some future eruption or is part of some normal cycle of magma transfer at depth with little chance of breaking out at the surface has yet to be ascertained.

Geodetic observations have been linked to possible intracrustal magmatism in other parts of the Rio Grande rift (e.g., Reilinger *et al.*, 1979), in Yellowstone National Park (Pelton and Smith, 1982), and, most recently, near Mammoth Lakes in eastern California (Savage and Clark, 1982; Castle *et al.*, 1984). In the latter example, changes in elevation and horizontal strain have been interpreted to indicate magmatic resurgence of the Long Valley caldera by inflation of an approximately 10-km-deep magma chamber. This inflation may be responsible for a series of four magnitude-6 earthquakes in the area in 1980. Because there have been several explosive eruptions and extrusion of rhyolite domes in this area during the past 400 yr, and because Long Valley is less than 200 miles from major cities like Sacramento and San Francisco, deformation and seismic activity are being monitored in order to predict possible future activity.

The local and regional doming near Yellowstone is difficult to relate to standard plate-boundary processes. Magma injection is thought to result from a "hot spot" that can be traced into the North American continent along the Snake River Plain (e.g., Suppe *et al.*, 1975). In this sense it is clearly an intraplate phenomena. On the other hand, it could be argued that the apparent magma uplifts near Mammoth Lakes and in the Rio Grande rift really represent plate-boundary processes. The former may be a relict of the subduction-related volcanism, which for the most part ceased when the West Coast converted from a convergent to a strike-slip margin. Likewise the New Mexico activity could well represent the beginnings of a new plate boundary, a rift that may evolve into a new ocean basin by splitting off the southwestern United States.

Semantics notwithstanding, such examples must be considered in order to understand intraplate phenomena. After all, neither lies upon a currently active plate boundary per se. More to the point, the geologic processes that they represent may well pertain to other "intraplate" phenomena whose association with similarly defunct or precursor boundaries is simply not yet so apparent.

## CRUSTAL LOADING

Contemporary deformation of the stable interior is virtually synonymous in many minds with postglacial rebound. The broad doming of recently deglaciated parts of North America and Scandinavia has long been documented by geologic studies of warped beach terraces and geodetic measurements of continued uplift (Figure 2.7). This motion is perhaps the best understood, geomechanically speaking, of any type of intraplate deformation, although controversy still revolves around distinguishing those possible deep-earth rheologies that are most consistent with the observed rebound effects (e.g., Kaula, 1980).

An important aspect of recent studies of postglacial phenomena, especially sea-level changes, is that this is a global phenomenon, not restricted to the immediate area of glacial retreat. Concepts such as the collapse of a peripheral bulge (e.g., Walcott, 1972) have been re-

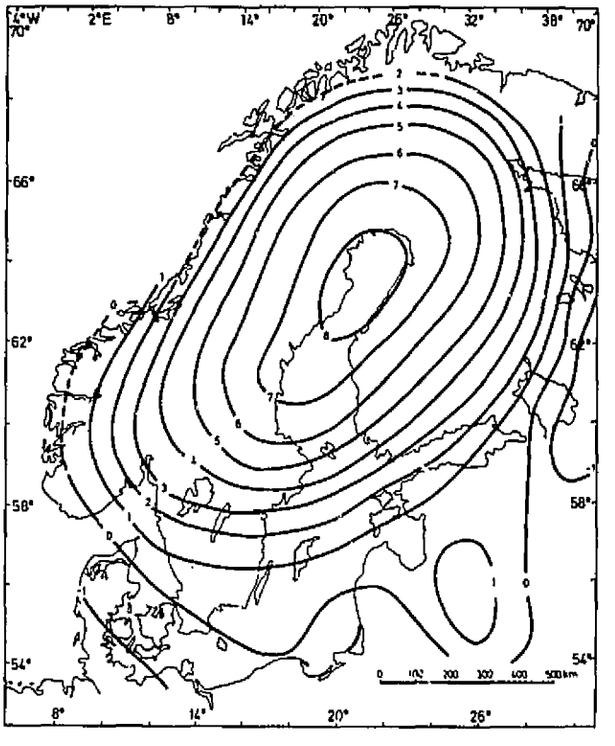


FIGURE 2.7 Postglacial rebound of Fennoscandia (Balling, 1980). Contours represent uplift in millimeters per year measured by precise leveling.

fined to predict a complex pattern of relative motion of land and sea the world over (e.g., Clark, 1980).

A persistent suspicion is that the stresses associated with postglacial rebound may be sufficient to trigger seismic activity in deglaciated regions (e.g., Stephansson and Carlsson, 1980). However, the correlation between rebound and earthquakes seems tenuous at best.

Land uplift following glacial unloading has also been reported on a more local scale. Hicks and Shofnos (1965) correlated an anomalous drop in sea level in southeastern Alaska with recent retreat of a small ice sheet. The rate of this local land uplift is on the order of 4 mm/yr.

Ice is not the only crustal load capable of driving surface deformation. Crittenden (1963), for example, reported both geologic (deformed shorelines) and leveling evidence of continued local uplift in the area of former Lake Bonneville. This rebound is inferred to follow the removal of the water load associated with climatic changes in postpluvial periods. Depression of the land surface by filling of new reservoirs is well known (e.g., Longwell, 1960). Holzer (1979) even reported evidence that drawdown of aquifers in southern Arizona has been followed by a rebound effect. In addition, Opdyke *et al.* (1984) attributed post-Pleistocene uplift in northern Florida to crustal unloading associated with limestone dissolution in Karst areas.

Redistribution of crustal loads by erosion, sedimentation, and faulting is fundamental in geology. Sedimentary infilling clearly augments thermal subsidence to form some of our major basins (e.g., Sleep, 1971), and the importance of crustal loading by thrust sheets is being recognized as a major factor in the formation and evolution of foreland basins and basement arches (Quinlan and Beaumont, 1984). Perhaps a contemporary example is found in the south central United States, where leveling results (Figure 2.8) have been interpreted to show uplift of a forebulge associated with sedimentary loading of the Mississippi delta (Jurkowski *et al.*, 1984; Nunn, 1985).

## EPEIROGENY

Sedimentary strata that overlie large areas of the stable interiors like the central United States and eastern Europe record a history of broad upwarping and downwarping relative to sea level (e.g., King, 1977). In some cases, large basins or domes have formed, apparently unrelated—except by age—with distant plate boundaries. Formation of these relatively gentle tectonic features is called epeirogeny, a term that still carries an aura of mystery. Indeed, there is no widespread agreement on what causes these interior motions.

One of the most surprising results to arise from the analyses of precise leveling data is that many of these platform areas seem still to be going up or down at geologically rapid rates. For example, a map of vertical crustal motion in eastern Europe (Figure 2.9) published not long ago shows parts of the Russian platform going up and down at differential rates of several millimeters per year. Leveling in the eastern United States (Figure 2.10) likewise seems to suggest that vertical neotectonic motion is the norm, not the exception, in these areas, in spite of a long-term geologic record of relative tranquillity (e.g., Brown and Oliver, 1976). Although some of these apparent motions may be remnants of postglacial rebound, as in the Baltic Shield or the Great Lakes area of the United States, most lack a clear-cut neotectonic explanation.

However, before ascribing these motions to some new, unheralded form of intraplate tectonics, it is important to recognize that there are major outstanding questions about the accuracy of the geodetic measurements on which most such studies are based. Recent work has shown, for example, that systematic errors are more serious than previously thought and that apparent changes in elevation once believed to be neotectonic in origin are now perceived by some to be artifacts of observational errors (Strange, 1981).

Unfortunately, assessing the influence of geodetic errors on estimates of vertical crustal motion in areas like eastern North America is still in an early stage, and initial results are too few and inconclusive (e.g., Fadaie and Brown, 1984). Yet even a cursory glance at Figure 2.10 provides grounds for skepticism. In this figure are two independent estimates of crustal motion, one based on water level and leveling in southeastern Canada and one based on leveling and sea-level data for the eastern United States. Although the rates are similar, these estimates show a disturbing degree of inconsistency where they join along the United States-Canada border. Until these data sets are reduced jointly and uniformly it is perhaps unfair to expect complete agreement; yet, the question remains as to whether some of these patterns are more the result of statistical smearing of unrecognized and inadequately treated systematic errors than real ground motion.

A prominent trend of the map in Figure 2.10 is the apparent uplift of the Appalachians relative to the coastal regions and interior plains. Yet this relict mountain belt is generally thought to have last been active over 200 m.y. ago (Williams and Hatcher, 1983). Since certain types of leveling error are known to correlate with height, is the Appalachian "uplift" really the accumulation of such errors? Is the similarly inferred con-

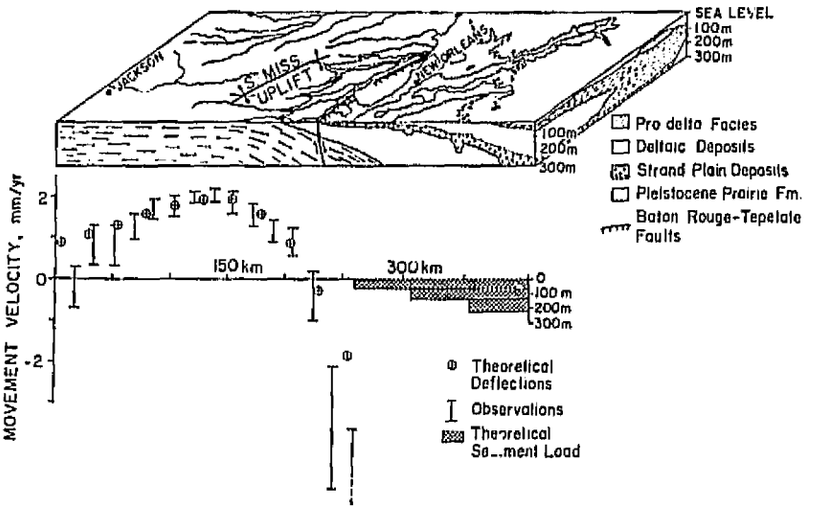


FIGURE 2.8 Arching of the Gulf Coastal Plain north of New Orleans indicated by precise leveling data. This arching may be a forebulge-type response to sediment loading of the Mississippi delta (Jurkowski *et al.*, 1984).

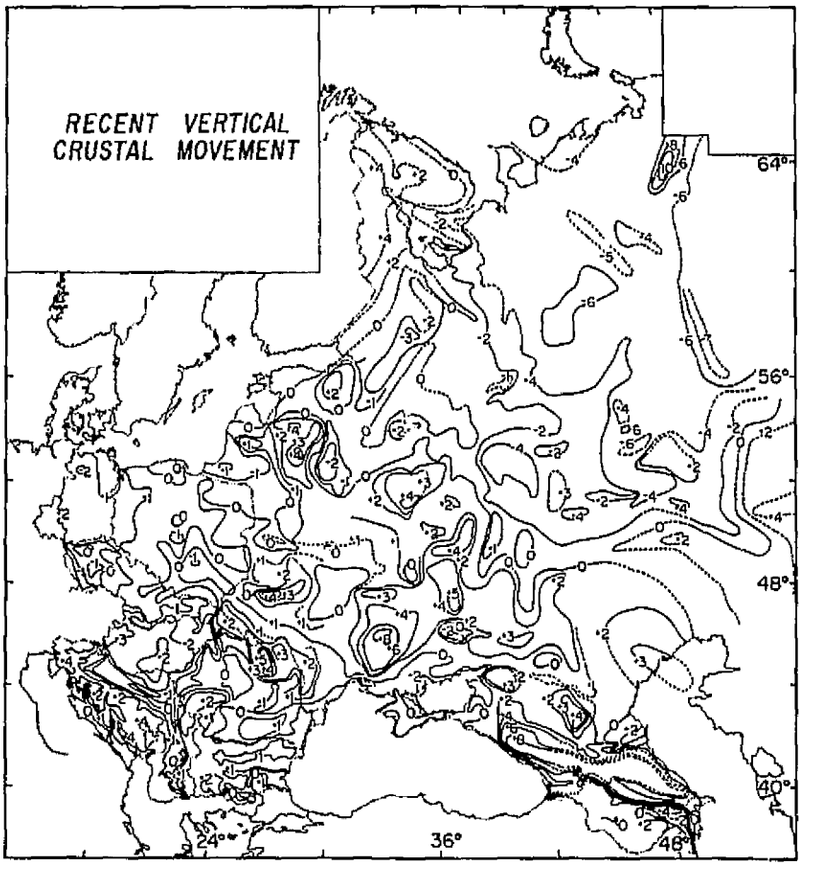


FIGURE 2.9 Contemporary vertical crustal motion (millimeters per year) of eastern Europe inferred from precise releveling (after Mescherikov, 1973).

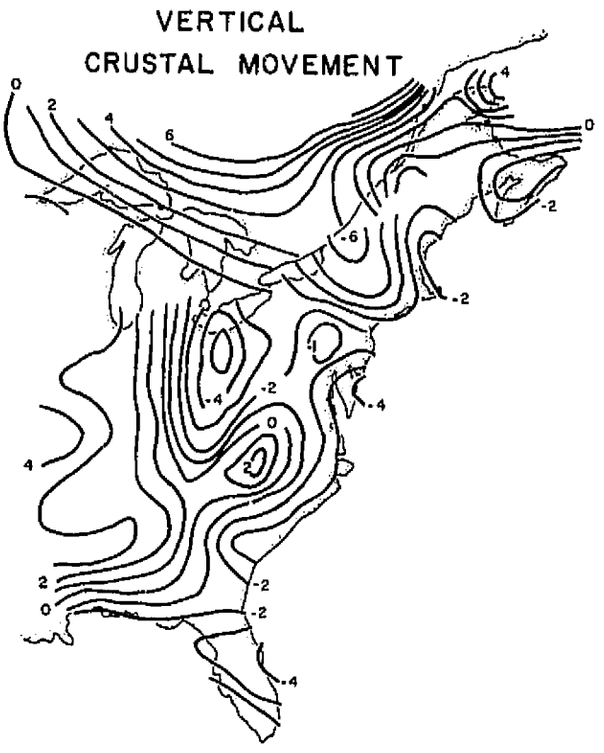


FIGURE 2.10 Apparent vertical motion (millimeters per year) of the eastern United States from precise releveling (Eastern United States results from unpublished map by G. Jurkowski; Great Lakes and Canadian results from Vanicek and Nagy, 1980). Some of these patterns have been questioned because of uncertainties about the accuracy of the geodetic measurements on which they are based.

temporary uparching of the Adirondack Dome in New York State (Isachsen, 1975) likewise suspect, or are real and important neotectonic motions being revealed?

Until thorough error analyses are completed, proper reservations about the reality of significant neotectonic motion in at least parts of the stable interiors seem warranted. However, evidence for neotectonic motion in such areas does not hinge solely on geodetic data. Holocene motions along the East Coast have been inferred from tilted beach terraces (Winker and Howard, 1977) and from submarine geomorphology (Officer and Drake, 1981). Adams (1980) has even attempted to correlate the relatively detailed changes in river drainage in the deep interior of the United States to contemporary tilts indicated by leveling. Anderson *et al.* (1984) cited a correlation between patterns of modern subsidence indicated by leveling and post-Pleistocene deformation of wave-cut terraces near Eastport, Maine. Albeit many, if not all, of these inferences of motion could be challenged to some degree, the issue of neotectonics of the interior remains unresolved. In fact it is the continuing uncertainty about what is really going up and down in many parts of the interior that constitutes perhaps the dominant problem of active intraplate tectonics.

## DISCUSSION

Although intraplate motions are remote almost by definition from plate boundaries, it does not necessarily follow that they are unrelated to plate-boundary forces. The concept that lithospheric plates are rigid is a first-order treatment at best, and the geologic record is replete with evidence that interiors respond and deform to the actions at their edges. The tectonic collage that is now southeast Asia, formed by the collision of the Indian subcontinent into the Asian underbelly, is elegant proof that plate-boundary forces exert an influence hundreds of kilometers into the interior (e.g., Molnar and Tapponnier, 1978).

Some of the intraplate stress patterns mapped by Zoback and Zoback (1980) for the United States (Figure 2.11) suggest affinities with activity at boundaries of the North American plate. The extensional stresses of the Basin and Range, for example, have been interpreted as distributed shear from the San Andreas Fault system (Atwater, 1970). East-west compression of the eastern United States has been argued to reflect plate-driving forces (Sbar and Sykes, 1973), although other explanations have also been discussed (Zoback and Zoback, 1980, 1981). Yet neither intraplate stress patterns nor seismicity are by any means simple, and the link, if any, to distant plate boundaries is more often obscure than not.

One possible reason for complexity in intraplate tectonics is reactivation, i.e., the concept that present tectonics is guided by crustal heterogeneities formed during much earlier times. Woollard's (1958) appeal to reactivation of older geologic structures as an explanation of eastern United States seismicity has been echoed in various guises ever since. Sykes (1978) surveyed an array of evidence suggesting that intraplate neotectonics is influenced by structures inherited from earlier times, when plate boundaries may have been more directly involved (Figure 2.12). For example, Zoback *et al.* (1980) reported seismic reflection data that documents continued Cenozoic motion on Cretaceous faults in the Mississippi Valley region. Ancient crustal flaws may well serve to guide and focus plate-boundary forces in locally diverse, perhaps destructive ways, although the mechanics of this process are not completely understood (e.g., Zoback *et al.*, 1980).

However, reactivation is at best only part of the picture for active tectonics in intraplate regions. Postglacial rebound is another, and hot spots are undoubtedly a

third. None of these, however, seems to explain all the observations, such as the geodetic indications of contemporary intraplate ups and downs or geologic structures like the Michigan Basin. Although some of the geodetic evidence may be open to doubt, the geologic record is unequivocal. Thus the question remains as to whether there exist heretofore unrecognized mechanisms of intraplate deformation. Menard (1973), for example, postulated the existence of asthenospheric bumps to explain anomalous ocean-floor bathymetry. Jacoby (1972) looked to densification of the mantle due to magma separation as a possible means of inducing vertical motion by increasing continental buoyancy. McKenzie (1984) considered the intrusion of magma into the lower crust as another means of driving vertical motion. These and other possibilities deserve critical consideration and testing with observations.

One of the problems with geodetic indications of vertical movement within plates has to do with their apparent rates, typically on the order of a few millimeters per year (Figures 2.9 and 2.10). Although these would seem to be minute motions, they are extremely large from the geologic perspective. One millimeter per year corresponds to 1 km every million years. For comparison, rates of contemporary erosion in intraplate areas are usually estimated to be at least an order of magnitude less (Schumm, 1963). If such rates were sustained, we should expect imposing mountain ranges to be thrown up within relatively short periods, geologically speaking. That we do not see such topography leads to the argument that these motions are oscillatory or episodic, so that there is no net accumulation of relief. In some respects, such an explanation seems a bit ad hoc, and skeptics might infer that the inconsistency between some geodetically measured rates and the more subdued geologic record is further reason to question the accuracy of the former. However, it should be remembered that rates of vertical motion on the order of a few millimeters per year are much smaller that the commonly accepted rates of a few centimeters per year for the hori-

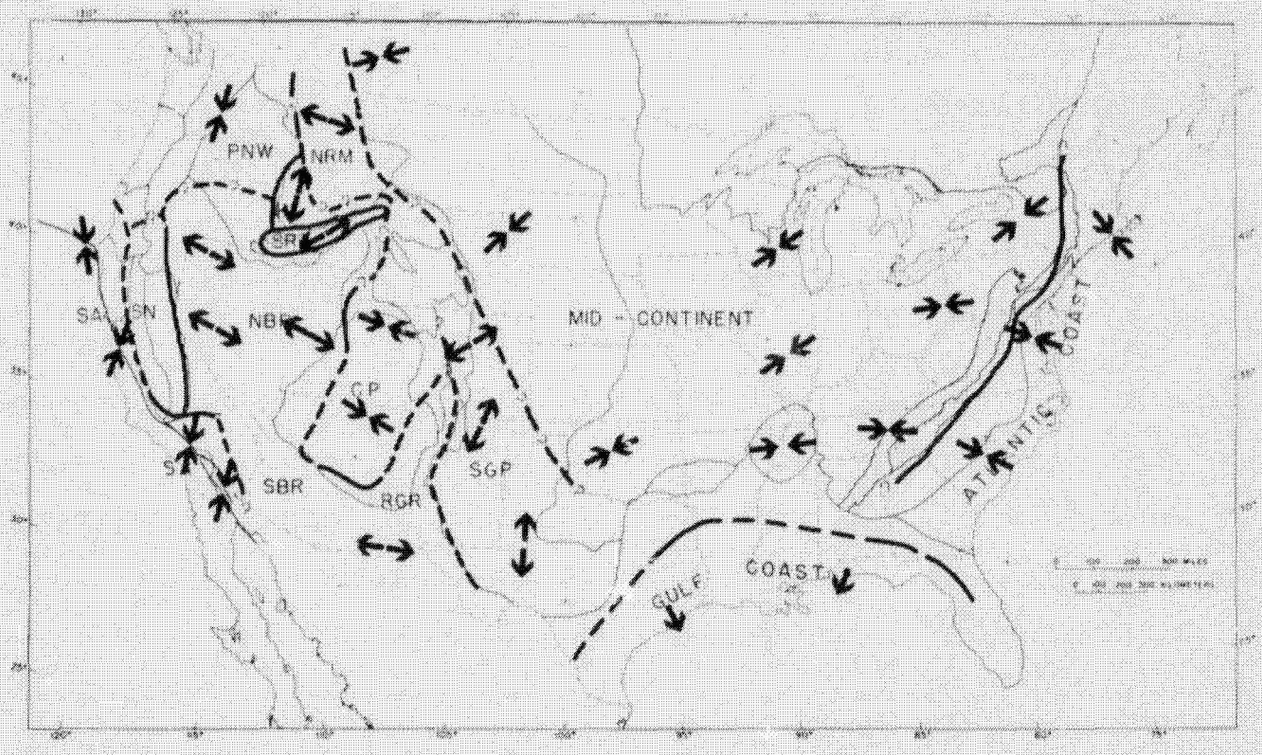


FIGURE 2.11 State of stress in the United States (Zoback and Zoback, 1980).

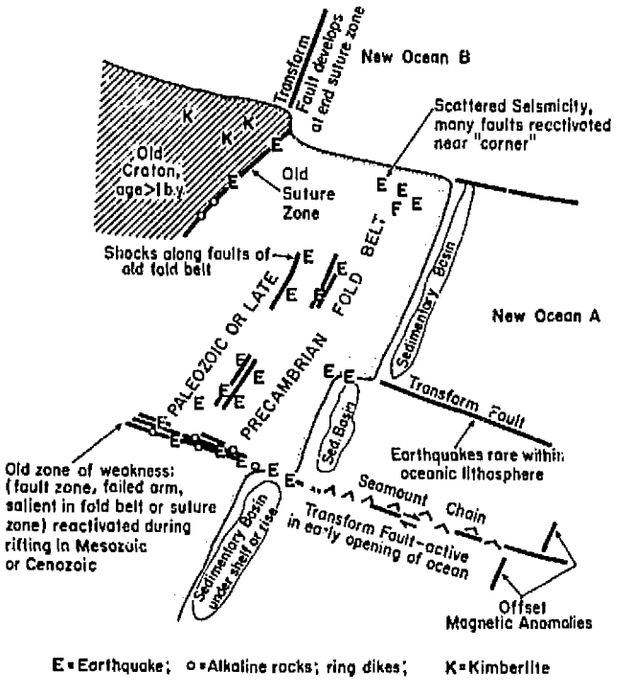


FIGURE 2.12 Intraplate tectonics may be influenced by inherited tectonic structures. In this example, relict transform faults left behind from the opening of the Atlantic may serve as weaknesses that concentrate modern intraplate stresses, thus constituting potential foci of seismic activity (Sykes, 1978).

zontal motions associated with plate tectonics (Minster and Jordan, 1978). Moreover, the geologic record is full of cyclicity (Vail *et al.*, 1977).

## SOCIAL IMPACT

The social ramifications of contemporary intraplate deformations are various. Some are relatively obvious: co-seismic deformations can damage nearby structures and disrupt or sever support services such as water or communication lines. Other types of deformation may have more subtle impact. The apparently slow vertical motions in the stable interior may yet be significant in planning long-term engineering projects. For example, a differential rate of only a centimeter per year will accumulate to a meter in a century. In a coastal region, a meter change in average elevation can translate into major shifts in effective shoreline positions, positions that have fundamental economic and legal significance (Bossler, 1984).

Intraplate deformation can also have indirect significance. For example, movements that precede and are related to earthquakes clearly have value in prediction. Generally speaking, to the extent that intraplate motions provide clues for our understanding of the state and evolution of stress in plate interiors, they are potentially critical guides for mitigating hazards from more obvious phenomena such as earthquakes and volcanoes.

## NEEDS AND TRENDS

Current understanding of the active tectonics in intraplate regions is mixed. On the one hand, broad concepts have been developed for areas like Hawaii (hot spots), Scandinavia (postglacial rebound), the Basin and Range of the western United States (distributed shear), and southeast Asia (India as a rigid indentor) that provide useful frameworks for monitoring, relating, and mitigating hazards from specific phenomena like earthquakes or volcanoes. Yet observations from other areas, such as the eastern United States, remain difficult to relate to any encompassing tectonic theory.

Although much has been learned about intraplate phenomena, basic questions remain. How are stresses in the plate interior related to forces at plate boundaries? To what extent are contemporary tectonics influenced by pre-existing structures? How accurate are the geodetic measurements that are often our primary source of information on contemporary deformations in such areas? How do we recognize the influence of subtle levels of active tectonics in the geologic (geomorphic) record? What are the best observational strategies for monitoring motions in areas of varying degrees of tectonic activity? What is an appropriate level of effort for tectonic investigations in intraplate areas in relation to the more active interplate zones?

It is easy to become complacent on the issue of intraplate tectonics. After all, damaging earthquakes are usually few and far between, and the secular motions seem too slow to warrant much concern, even if they prove to be real and not artifacts of measurement error. However, the relatively low frequency with which intraplate events seem to affect our lives does not alter the fact that they can have and will continue to have major economic and social impact. There is more than sufficient reason to justify efforts to fill our considerable gaps in understanding intraplate motions.

Future progress in studying intraplate tectonics requires many things. Many areas of the United States lack any geodetic resurveys with which to estimate contemporary deformation. This is especially true of horizontal measurements outside the well-known seismic zones of the western United States. Issues of accuracy in geodetic measurements must be satisfactorily resolved. Monitor-

ing programs that most effectively address issues of contemporary dynamics must be designed and funded at an adequate level. Furthermore, it must be recognized that these monitoring programs must be long term. New technologies must be brought to bear and integrated with conventional techniques. And certainly more research is needed to integrate and cross-calibrate seismologic, geodetic, and geomorphic measures of active tectonics to broaden our base of observations.

In many respects these demands are being addressed. For example, the National Aeronautics and Space Administration, the U.S. Geological Survey, the National Geodetic Survey (NGS), and others have been developing and/or applying new techniques such as very-long-baseline interferometry (VLBI), satellite laser ranging (SLR), and the Global Positioning System (GPS) to monitoring crustal deformations (e.g., Coates *et al.*, 1985). The NGS has made an important effort to develop new corrections for geodetic leveling (e.g., Holdahl, 1981), and research has become much more meticulous as far as evaluating the accuracy of measurements (Jackson *et al.*, 1980). Yet much remains to be done. Funding agencies and investigators alike must realize that proper resolution of critical issues concerning active tectonics of plate interiors will require a long-term commitment because of the very nature of the processes involved.

## ACKNOWLEDGMENTS

Contribution No. 6 from the Institute for the Study of the Continents.

## REFERENCES

Adams, J. (1980). Active tilting of the United States midcontinent: Geodetic and geomorphic evidence, *Geology 8*, 442-446.

Aggarwal, Y. P., and L. R. Sykes (1978). Earthquakes, faults and nuclear powerplants in southern New York-northern New Jersey, *Science 200*, 425-429.

Anderson, M. A., J. T. Kelley, W. B. Thompson, H. W. Borns, Jr., D. Sanger, D. C. Smith, D. A. Tyler, R. S. Anderson, A. E. Bridges, K. J. Crossen, J. W. Ladd, B. G. Andersen, and F. T. Lee (1984). Crustal warping in coastal Maine, *Geology 12*, 677-680.

Atwater, T. (1970). Implications of plate tectonics for the Cenozoic evolution of western North America, *Geol. Soc. Am. Bull. 81*, 3513-3536.

Balling, N. (1980). The land uplift in Fennoscandia, gravity field anomalies and isostasy, in *Earth Rheology, Isostasy and Eustasy*, N.-A. Morner, ed., Wiley, New York, pp. 297-326.

Barazangi, M., and J. Dorman (1968). World seismicity map of ESSA Coast and Geodetic Survey epicenter data for 1961-1967, *Bull. Seismol. Soc. Am. 59*, 369-380.

Bossler, J. D. (1984). The administrative, economic, and political aspects of the North American datum 1988 adjustment, Tech. Papers, 44th Annual Meeting, Am. Soc. Surv. Mapping, p. 185.

Brown, L. D., and J. E. Oliver (1976). Vertical crustal movements from leveling data and their relation to geologic structure in the eastern United States, *Rev. Geophys. Space Phys. 14*, 13-35.

Castle, R. O., J. E. Estrem, and J. C. Savage (1984). Uplift across Long Valley Caldera, California, *J. Geophys. Res. 89*, 11507-11516.

Clark, J. A. (1980). A numerical model of worldwide sea level change on a viscoelastic Earth, in *Earth Rheology, Isostasy and Eustasy*, N.-A. Morner, ed., Wiley, New York, pp. 525-534.

Coates, R. J., H. Frey, J. Bosworth, and G. D. Mead (1985). Space age geodesy: The NASA Crustal Dynamics Project, *IEEE Trans. Geosci. Remote Sensing*.

Crittenden, M., Jr. (1963). New data on the isostatic deformation of Lake Bonneville, *U.S. Geol. Surv. Prof. Paper 454E*, 1-31.

Decker, R. W. (1969). Land surface deformation related to volcanic activity in Hawaii, *Am. Phil. Soc. Yearb.* 295.

Dewey, J. F. (1975). Plate tectonics—A global view of the dynamics of the Earth, in *The Rediscovery of the Earth*, L. Motz, ed., Van Nostrand Reinhold, New York, pp. 164-180.

Fadale, K., and L. Brown (1984). Contemporary tilting in the central Atlantic coastal plain, *J. Geol. 92*, 547-559.

Hicks, S. D., and W. Shofnos (1965). The determination of land emergence from sea level observations in southeast Alaska, *J. Geophys. Res. 70*, 3315-3320.

Holdahl, S. R. (1981). A model of temperature stratification for correction of leveling refraction, *Bull. Geodesique 55*, 231-249.

Holzer, T. L. (1979). Elastic expansion of the lithosphere caused by groundwater depletion, *J. Geophys. Res. 84*, 4689-4698.

Isachsen, Y. W. (1975). Possible evidence for contemporary doming of the Adirondack Mountains, New York, and suggested implications for regional tectonics and seismicity, *Tectonophysics 29*, 169-181.

Jackson, D. D., W. B. Lee, and C. C. Liu (1980). Aseismic uplift in southern California: An alternative interpretation, *Science 210*, 534-536.

Jacoby, W. R. (1972). Plate theory, epeirogenesis and eustatic sea-level changes, *Tectonophysics 15*, 187-196.

Jurkowski, G., J. Ni, and L. Brown (1984). Modern uparching of the Gulf coastal plain, *J. Geophys. Res. 89*, 6247-6255.

Kaula, W. K. (1980). Problems in understanding vertical movements and earth rheology, in *Earth Rheology, Isostasy and Eustasy*, N.-A. Morner, ed., Wiley, New York, pp. 577-589.

King, P. B. (1977). *The Evolution of North America*, Princeton Univ. Press, Princeton, N.J.

Koseluk, R. A., and R. E. Bischke (1981). An elastic rebound model for normal fault earthquakes, *J. Geophys. Res. 86*, 1081-1090.

Krueger, S. W., W. H. Prescott, and M. D. Zoback (1983). Constraints on strain rates in intraplate seismic regions of the eastern United States as inferred from geodetic survey measurements, *EOS 64*, 842.

Larsen, S., R. Reilinger, and L. Brown (1985). Evidence of ongoing crustal deformation related to magmatic activity near Socorro, New Mexico, *J. Geophys. Res.*

Lipman, P. W., and H. H. Mehnert (1975). Late Cenozoic basaltic volcanism and development of the Rio Grande depression in the southern Rocky Mountains, *Geol. Soc. Am. Mem. 144*, 119-154.

Longwell, C. R. (1960). Interpretation of the levelling data, *U.S. Geol. Surv. Prof. Paper 295*, 33-38.

McKenzie, D. (1984). A possible mechanism for epeirogenic uplift, *Nature 307*, 616-618.

Menard, H. W. (1973). Epeirogeny and plate tectonics, *Trans. Am. Geophys. Union 54*, 1246-1255.

Mescherikov, Y. A., ed. (1973). Map of the recent vertical crustal movements of Eastern Europe (1:2,500,000), Main Admin. Geodesy and Cartography, Moscow.

Minster, J. B., and T. H. Jordan (1978). Present-day plate motions, *J. Geophys. Res. 83*, 5331-5354.

Molnar, P, and P. Tapponnier (1978). Active tectonics of Tibet, *J. Geophys. Res. 83*, 5361-5375.

Myers, W. F., and W. Hamilton (1964). Deformation accompanying the Hebgen Lake earthquake August 17, 1959, *U.S. Geol. Surv. Prof. Paper 435*, 55-98.

Ni, J. F., R. E. Reilinger, and L. D. Brown (1981). Vertical crustal movements in the vicinity of the 1931 Valentine, Texas, earthquake, *Bull. Seismol. Soc. Am. 71*, 857-863.

Niskanen, E. (1939). On the upheaval of land in Fennoscandia, *Ann. Acad. Sci. Fenn. Ser. A3. 53*, 1-30.

Nunn, J. A. (1985). State of stress in the northern Gulf Coast, *Geology 13*, 429-432.

Officer, C. B., and C. L. Drake (1981). Epeirogenic plate movements, *J. Geol. 90*, 139-153.

Opdyke, N. D., D. P. Spangler, D. L. Smith, D. S. Jones, and R. C. Lindquist (1984). Origin of the epeirogenic uplift of Pliocene-Pleistocene beach ridges in Florida and development of the Florida Karst, *Geology 12*, 226-228.

Pelton, J. R., and R. B. Smith (1982). Contemporary vertical surface displacements in Yellowstone National Park, *J. Geophys. Res. 87*, 2745-2781.

Pitt, A. M., C. S. Weaver, and W. Spence (1979). The Yellowstone Park earthquake of June 30, 1975, *Bull. Seismol. Soc. Am. 69*, 187-205.

Quinlan, G. M., and C. Beaumont (1984). Appalachian thrusting, lithospheric flexure, and the Paleozoic stratigraphy of the eastern interior of North America, *Can. J. Earth Sci. 21*, 973-995.

Rankin, D. W. (1977). Studies related to the Charleston, South Carolina, earthquake of 1886—Introduction and discussion, *U.S. Geol. Surv. Prof. Paper 1028*, 1-15.

Reilinger, R. (1985). Vertical movements associated with the 1959 M = 7.1 Hebgen Lake, Montana, earthquake, in *Proceedings of Workshop XXVII on the Borah Peak, Idaho, Earthquake*, R. S. Stein and R. C. Bucknam, eds., U.S. Geol. Surv. Open-File Rep. 85-290, pp. 519-530.

Reilinger, R. E., and J. E. Oliver (1976). Modern uplift associated with a proposed magma body in the vicinity of Socorro, New Mexico, *Geology 4*, 583-586.

Reilinger, R. E., G. P. Citron, and L. D. Brown (1977). Recent vertical crustal movements from precise leveling data in southwestern Montana, western Yellowstone National Park, and the Snake River Plain, *J. Geophys. Res. 82*, 5349-5359.

Reilinger, R. E., L. D. Brown, J. E. Oliver, and J. E. York (1979). Recent vertical crustal movements from leveling observations in the vicinity of the Rio Grande rift, in *Rio Grande Rift: Tectonics and Magmatism*, R. E. Riecker, ed., American Geophysical Union, Washington, D.C., pp. 223-236.

Sanford, A. R., R. J. P. Mott, Jr., P. J. Shuleski, E. J. Rinehart, R. J. Caravella, R. M. Ward, and T. C. Wallace (1977). Geophysical evidence for a magma body in the crust in the vicinity of Socorro, New Mexico, in *The Earth's Crust*, J. E. Heacock, ed., American Geophysical Union Monograph 20, Washington, D.C., pp. 385-403.

Savage, J. C. (1983). Strain accumulation in western United States, *Ann. Rev. Earth Planet. Sci. 11*, 11-43.

Savage, J. C., and J. P. Church (1974). Evidence for post-earthquake slip in the Fairview Peak, Dixie Valley, and Rainbow Mountain Fault areas of Nevada, *Bull. Seismol. Soc. Am. 64*, 687-698.

Savage, J. C., and N. M. Clark (1982). Magmatic resurgence in Long Valley caldera, California: Possible cause of the 1980 Mammoth Lakes earthquakes, *Science 217*, 531-533.

Savage, J. C., and L. M. Hastie (1966). Surface deformation associated with dip slip faulting, *J. Geophys. Res. 71*, 4897-4904.

Savage, J. C., M. Lisowski, W. H. Prescott, and J. P. Church (1977). Geodetic measurements of deformation associated with the Oroville, California earthquake, *J. Geophys. Res. 82*, 1667-1671.

Savage, J. C., M. Lisowski, and W. H. Prescott (1985). Strain accumulation in the Rocky Mountain States, *J. Geophys. Res. 90*.

Sbar, M. L., and L. R. Sykes (1973). Contemporary compressive stress and seismicity in eastern North America: An example of intra-plate tectonics, *Geol. Soc. Am. Bull. 84*, 1861-1882.

Schilt, F. S., and R. E. Reilinger (1981). Evidence for contemporary vertical fault displacement from precise leveling data near the New Madrid seismic zone, western Kentucky, *Bull. Seismol. Soc. Am. 71*, 1933-1942.

Schumm, S. A. (1963). The disparity between present rates of denudation and orogeny, *U.S. Geol. Surv. Prof. Paper 454-H*, 1-13.

Sleep, N. H. (1971). Thermal effects of the formation of Atlantic continental margins by continental breakup, *Geophys. J. 24*, 325-350.

Sloss, L. L. (1963). Sequences in the cratonic interior of North America, *Geol. Soc. Am. Bull. 74* 93-114.

Stein, R. S., and S. E. Barrientos (1985). Planar high-angle faulting in the Basin and Range: Geodetic analysis of the 1983 Borah Peak, ID, earthquake, *J. Geophys. Res. 90*.

Stephansson, O., and H. Carlsson (1980). Seismo-tectonics in Fennoscandia, in *Earth Rheology, Isostasy and Eustasy*, N.-A. Morner, ed., Wiley, New York, pp. 327-337.

Stewart, J. H. (1980). *The Geology of Nevada*, Nevada Bureau of Mines Spec. Publ. 4, 136 pp.

Strange, W. B. (1981). The impact of refraction correction on leveling interpretations in southern California, *J. Geophys. Res. 86*, 2809-2824.

Suppe, J., C. Powell, and R. Berry (1975). Regional topography, seismicity, Quaternary volcanism, and the present-day tectonics of the western United States, *Am. J. Sci. 275A*, 397-431.

Sykes, L. R. (1978). Intraplate seismicity, reactivation of pre-existing zones of weakness, alkaline magmatism, and other tectonism postdating continental fragmentation, *Rev. Geophys. Space Phys. 16*, 621-688.

Talwani, P., D. J. Colquhoun, C. M. Poley, J. Cox, and G. Lennon (1984). Seismotectonic framework for the Charleston earthquakes, *EOS 65*, 990.

Thatcher, W. (1981). Crustal deformation studies and earthquake prediction research, in *Earthquake Prediction: An International Review*, D. W. Simpson, and P. G. Richards, eds., Maurice Ewing Ser. 4, American Geophysical Union, Washington, D.C., pp. 394-410.

Vail, P. R., R. M. Mitchum, Jr., and S. Thompson III (1977). Seismic stratigraphy and global changes of sea level, Part 4; Global cycles of relative changes of sea level, in *Seismic Stratigraphy—Applications to Hydrocarbon Exploration*, C. E. Payton, ed., Am. Assoc. Petrol. Geol. Mem. 26, pp. 83-97.

Vanicek, P., and D. Nagy (1980). The map of contemporary vertical crustal movements in Canada, *EOS 61*, 145-147.

Walcott, R. I. (1972). Late Quaternary vertical movements in eastern North America: Quantitative evidence of glacio-isostatic rebound, *Rev. Geophys. Space Phys. 10*, 849-884.

Wiens, D. A., and S. Stein (1984). Intraplate seismicity and stresses in young oceanic lithosphere, *J. Geophys. Res. 89*, 11442-11464.

Williams, H., and R. D. Hatcher, Jr. (1983). Appalachian suspect terranes, in *Contributions to the Tectonics and Geophysics of Moun-*

*tain Chains*, R. D. Hatcher, Jr., H. Williams, and I. Zietz, eds., Geol. Soc. Am. Mem. 158, pp. 33-54.

Wilson, R. H. (1935). Ground surface movement at Kilauea volcano, Hawaii, *Univ. Hawaii Res. Publ. 10*.

Winker, C. D., and J. D. Howard (1977). Correlation of tectonically deformed shorelines on the southern Atlantic Coastal Plain, *Geology 5*, 123-127.

Woollard, G. P. (1958). Areas of tectonic activity in the United States as indicated by earthquake epicenters, *Trans. Am. Geophys. Union* 39, 1135-1150.

York, J. E., and J. E. Oliver (1976). Cretaceous and Cenozoic faulting in eastern North America, *Geol. Soc. Am. Bull. 87*, 1105-1114.

Zoback, M. D., and M. L. Zoback (1981). State of stress and intraplate earthquakes in the United States, *Science 213*, 96-104.

Zoback, M. D., R. M. Hamilton, A. J. Crone, D. P. Russ, F. A. McKeown, and S. R. Brockman (1980). *Science 209*, 971-976.

Zoback, M. L., and M. D. Zoback (1980). State of stress in the conterminous United States, *J. Geophys. Res. 85*, 6113-6156.

# 3 Evaluation of Active Faulting and Associated Hazards

D. BURTON SLEMMONS *and* CRAIG M. DEPOLO
*University of Nevada, Reno*

ABSTRACT

Active faulting is a geologic hazard with a causative relation to earthquakes and associated strong ground motion, surface faulting, tectonic deformation, landslides and rockfalls, liquefaction, tsunamis, and seiches. Plate-tectonic models for the Earth's crust show that most active faults occur near plate boundaries, and research has been concentrated in interplate regions. Intraplate regions have less fault activity and represent a potential hazard that only recently has been recognized. Faults are delineated by geologic, remote-sensing, seismic reflection, gravity, magnetic, and trenching methods. Fault activity is assessed using geologic, geomorphic, geodetic, and seismologic data. Correlations of fault length, displacement, and area with earthquake magnitude are utilized to assess earthquake hazards of faults and form the principal data for risk analysis. Estimation of earthquake recurrence rates and characterization of fault behavior provide additional input data for risk analysis.

Recent attention has been focused on the character of subduction in the northwestern United States. An absence of large seismic events along this convergent zone has led to the speculation that the zone is aseismic. Recent studies indicate, however, that if this is true, this zone may be unique when compared with other subduction zones of the world. Ongoing studies are trying to determine if this region has had large earthquakes in the geologic past. The recent discovery of the active geomorphic features along the Meers Fault in Oklahoma has prompted studies of this and adjoining regions.

## INTRODUCTION

The assessment of earthquake hazards involves consideration of earthquake magnitude, intensity, frequency, recency of the last event, probability of occurrence, and human experience and values.

The appraisal of earthquake potential is feasible because historical data show a good correlation between earthquake size and the fault rupture parameters of length, maximum displacement, and fault rupture area. Most earthquakes have proportional tectonic effects, with earthquakes of below magnitude 6 having fault ruptures of up to 10-km length and a few centimeters maximum displacement, but magnitude 8+ earthquakes have up to 400-km length and 10 m of displacement. This relation also can be used for paleoseismicity evaluations to infer from prehistorical evidence the potential size of future activity on the same fault segments.

The historical record of worldwide earthquakes

shows an excellent spatial correlation with plate-tectonic movements. Most of the historical or geologically young fault ruptures are located on or near boundaries between plates and microplates.

### *Importance to Society*

Most evaluations of active faults are conducted at or near plate boundaries, where consideration of design, siting, zoning, communication, and response to earthquake hazards is necessary for all types of major engineering structures in order to reduce potential loss of life, injury, or property damage. The seismic motion or deformation effects on facilities such as nuclear generators, dams, communication centers, and other lifelines is critical because of great potential harm to society.

The importance of earthquake evaluation in intraplate regions has been recognized recently. In the intraplate region east of the Rocky Mountains, earthquakes affect larger areas than in the western United States. Although intraplate earthquakes are more infrequent and unexpected, the impact of earthquakes on society can be greater than is generally perceived because of the large affected areas and greater population density in the eastern United States.

### *Difficulties in Making Evaluations*

The evaluation of faults, particularly assessment of their seismic potential, is often difficult because of the following factors: poor conditions of surface exposure (concealment by bodies of water or young sediments); plastic deformation of near-surface materials; transitional or branching rupture character; detachment, décollement, or listric faulting of shallow materials; conflicting or incomplete geologic, seismologic, or geophysical observations; incomplete bases for analysis; and basic assumptions about activity or nonactivity of faults. These factors have led to smaller, shorter, more discontinuous expression of surface faulting parameters in almost one-fourth of the historical examples of surface faulting in North America.

### *Approach for Earthquake Evaluation*

Two approaches for earthquake-hazard assessment have been used in the United States. The western United States is dominated by active-tectonic processes and many active faults. Those faults with proper orientations or connections to plate boundaries may be active and can be evaluated by methods that are discussed in this paper. Faults within this region are commonly assumed to be active unless there are contrary data.

In the central and eastern United States—in intraplate regions east of the Rocky Mountains—most faults are inactive and rarely have the potential for being sources of damaging and hazardous earthquakes. Earthquakes of these zones may not show characteristics typical of active faults, with lower magnitudes (commonly less than 5.75 or 6), and may be assumed to have random or "floating" epicenters within a province. Man's structures may need to be designed conservatively for the largest historical earthquake of the region or province or may be designed conservatively for a higher magnitude or intensity. Most faults for such regions are commonly assumed, or may appear to be inactive, although the Meers Fault (Oklahoma) and the scarp at Reelfoot Lake (near New Madrid, Missouri) suggest that some faults of central United States may be active, and deterministic assessments should be used.

Many different disciplines are used for studying active faults. Some of these are shown in Figure 3.1 in a time perspective.

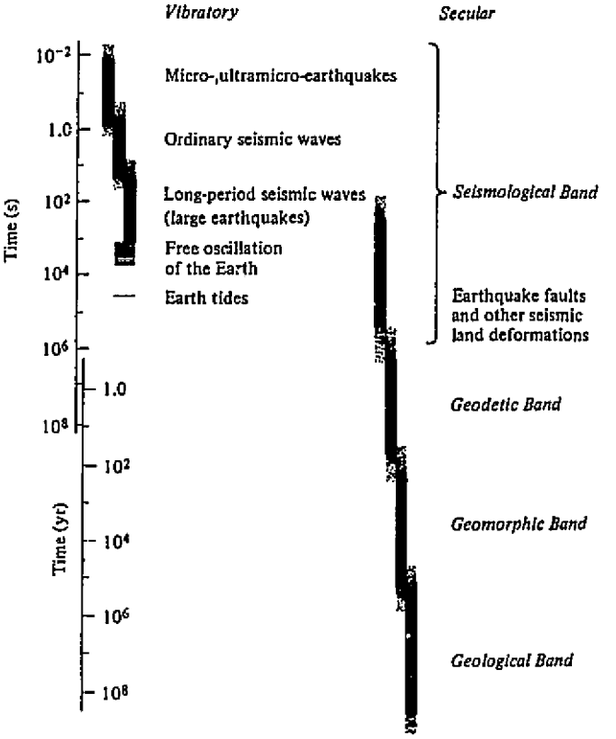


FIGURE 3.1 Time relations of different disciplines associated with active faulting. (From Kasahara, 1981.)

## SEISMOGENIC MODEL

Earthquakes are generally assumed to be elastic waves radiating out from a rupture in the Earth that slips suddenly and generally in a brittle manner. Most evaluations of the potential for surface faulting and earthquakes assume that earthquakes of above magnitude $M_S = 6$ are by brittle failure and are represented by fault-rupture parameters. This simple model is effective for many examples of surface faulting, particularly for faults with moderate to steep dips and with good surface exposure. The release of energy is a function of fault rupture parameters and is also affected by the elastic rebound of the strained volume of rock, associated folding (King and Stein, 1983; Hill, 1984; Molinari, 1984), detachment faulting (Hardyman, 1978; Berberian, 1982), fault type and attitude (low angle thrust faults), and surface exposure.

## HAZARDS RELATED TO FAULTS

### *Earthquake and Ground Motion*

Perhaps the best-known hazards of active faulting are the destructive effects of earthquake shaking, often called "strong ground motion." Sudden movement along a fault or fault zone radiates elastic waves that are generally strongest near the causative fault and taper off or attenuate away from the fault. Strong ground motion is the single largest natural factor in causing earthquake damage, including loss of life and property, failure of structures, disruption of utilities, and numerous secondary effects such as landsliding and liquefaction.

The characteristics and intensity of strong ground motion at different sites usually varies with a number of factors, including earthquake size, attentuation, and local ground response. Variation of strong ground motion with distance from a causative fault has been one of the most discussed factors, based on many analyses of strong-motion records from historical earthquakes and various theoretical considerations. Recent studies by McGarr (1984) show that the intensity of strong ground motion may vary with the type of motion along a fault (e.g., reverse motion versus normal motion). Details of the geometry of fault zones can have a large influence on strong ground motion. Local areas where the fault is not so free to slide concentrate stress (Bakun *et al.*, 1980, 1984; Aki, 1984); when these places are broken and the stress is released a large amount of high-frequency energy is generated resulting in high-frequency ground motion.

Source directivity, a phenomenon involving the propagating fault rupture and its relationship with the elastic waves being radiated, can have a pronounced effect on the frequency and amplitudes of the radiating waves and should be addressed for sites near the causative fault (Singh, 1981). Other factors such as the radiated wave's travel path characteristics (Singh, 1981), topographic effects at a site (Davis and West, 1973), and site materials and geology (Rogers *et al.*, 1983) can also affect strong ground motion. Many siting and design studies use a sophisticated approach to strong ground motion estimation involving the combined expertise of the seismologist, the geologist, and the engineer for deterministic and probabilistic studies.

The effect of strong ground motion is incorporated into building codes and may influence zoning (Berg, 1983). Geotechnical studies of soils as well as geologic and seismologic fault studies are vital to this ground motion potential assessment.

### *Surface Rupture*

One of the most direct hazards (effects) of active faulting is displacement or offset at the foundation of a structure (Swiger, 1978). Ruptures can occur suddenly during earthquakes or slowly or gradually by creep. Three main types of fault movements associated with a faulting event are primary, secondary, and sympathetic movements. A primary rupture occurs along the main fault responsible for the earthquake and can be estimated from observations and regression analyses (Slemmons, 1982b; Bonilla *et al.*, 1984) of historical earthquakes and fault displacement. These are commonly based on rupture length or maximum displacement; actual observed effects can be reduced by drag and distributed rupture, plastic failure, detachment, and other causes.

The construction of some brittle structures may not tolerate even small fault rupturing. The proposed Auburn Dam in California was in advanced stages of site preparation when the possibility of fault displacement of about 15 cm in the foundation was estimated by Woodward-Clyde Consultants (1977). The consultants and a special review panel essentially concurred that, although the recurrence interval was very long, the maximum expected ground displacement of about 15 cm could occur with an associated earthquake of magnitude 6.5. The concrete double arch dam could not accommodate this large a foundation displacement, and the proposed dam was abandoned as inappropriate for the site even though $200 million was spent for site preparation.

Secondary ruptures are those that occur along branch faults and other faults subordinate to the principal fault trace. These faults locally accommodate deformation

from the main fault and generally have lesser displacements. Bonilla (1970) showed that secondary rupture displacements decrease with increasing distance from the fault.

Sympathetic offsets occur when strain release along the main fault or vibratory ground motion disturbs the state of stress of another fault, causing it to undergo displacement. During the 1968 Borrego Mountain earthquake, sympathetic displacement occurred on three faults, the Imperial, Superstition Hills, and San Andreas. Investigations by Allen *et al.* (1972) reported sympathetic offsets of 1- to 2.5-cm right-lateral displacement and that the longest of these ruptures was 30 km long and 50 km from the epicenter.

Surface displacement can occur gradually in areas of tectonic creep and nontectonic fluid withdrawal. In California, several faults are undergoing tectonic creep, with a maximum reported creep of 3.2 cm/yr along the San Andreas Fault in San Benito County (Burford and Harsh, 1980).

### *Tectonic Deformation*

Tectonic deformation refers to areal or regional deformation that may or may not be associated with moderate or large earthquakes. Dramatic effects of tectonic deformation have been noted by observing the vertical displacement and tilting of shorelines during the 1964 Alaskan earthquake, which shows evidence of land movement relative to sea level. An area of south central Alaska, of probably over 110,000 $mi^2$ of land and sea bottom, was affected by warping, horizontal distortion, and faulting (Plafker, 1972). The upper growth limit of barnacles showed a maximum of 37.8 feet of vertical displacement when the pre-earthquake and post-earthquake shorelines at Montague Island were compared (Plafker, 1972). In the Kodiak Islands, a maximum subsidence of 6.3 feet of the shoreline was recorded (Plafker, 1972). Plafker commented, "Regional uplift and subsidence occurred mainly in two nearly parallel elongate zones, together about 600 miles long and as much as 250 miles wide, that lie along the continental margin." Earth movements, detected by geodetic measurements, were recorded after the 1971 San Fernando, California, earthquake ($M_L$ = 6.5). These measurements showed the mountains to the northeast of the causative fault shifted upward as much as 2 m and horizontally as much as 2 m (Savage *et al.*, 1975).

Folds and large crustal uplifts and tilts have generally been assumed to be aseismic and to represent gradual plastic failure. Recent activity at Coalinga, California, has shown that this, however, is not always the case. The damaging 1983 Coalinga earthquake ($M_S$ = 6.6) occurred in an area where active faults and large-magnitude earthquakes were previously unrecognized. Post-earthquake investigations concluded that no surficial faulting accompanied the earthquake (Clark *et al.*, 1984). Studies by King and Stein (1983) showed that uplifted Holocene terraces on the main fold associated with the earthquake could be identified and are consistent with the regional deformation accompanying the earthquake (Stein, 1983). Other earthquakes that were associated with folding and compressional regimes are the 1978 Tabas-e-Golshan, Iran, earthquake ($M_S$ = 7.5) and the 1980 El Asnam, Algeria, earthquake ($M_S$ = 7.25).

The relationships recognized at Coalinga have led to a re-examination of major folds of the California Coast and Transverse Ranges and adjustment of seismic design of nearby major engineering structures. Yeats (1982) suggested that surface faults along anticlines may be weakly seismic or low-shake faults. These faults, also called flexural-slip faults, are thought to be related to the folding structure, with displacement occurring along bedding planes of the units being folded (see Yeats, Chapter 4, this volume). Hill (1984) suggested that some of the Coalinga earthquakes may be related to flexural-slip events. Late Quaternary fault scarps are associated with the Toppenish anticline of the Yakima fold belt in Washington (Campbell and Bentley, 1981), but whether these are seismogenic has not been resolved.

Criteria for discriminating between seismogenic and aseismic geologic structures have yet to be developed for evaluating folds or areas actively undergoing tectonic deformation. Resolution of these issues is important for seismic evaluation of many engineering structures in areas with Late Cenozoic folding. Tectonic tilting or warping must also be considered for level or gradient-sensitive structures, such as aqueducts in Owens Valley and also on the western edge of the San Joaquin Valley.

### *Secondary Effects*

Secondary effects associated with earthquakes include landslides and rockfalls, liquefaction, seiches, and tsunamis. These effects can cause severe and widespread damage; although the effects may be severest in the epicentral region, they may extend out to distances of as much as 1000 km. Landslides are often induced by earthquake shaking. The scale of these features can vary from slides a few meters long to slides kilometers in length. During the 1976 Guatemalan earthquake ($M_S$ = 7.5) over 10,000 landslides were generated in an area of 16,000 $km^2$ (Harp *et al.*, 1981). One of the most notable slides occurred in Peru in 1970, where a large, seismi-

cally induced landslide originating 130 km from the earthquake claimed at least 18,000 and possibly as many as 25,000 lives (Gere and Shah, 1984). Splashes or waves caused by landslides may also have extensive effects; the 1958 earthquake induced a landslide into Lituya Bay, which caused a giant wave reaching 1720 ft above sea level (Miller, 1960).

Liquefaction is a phenomenon in which near-surface water-saturated sediments are shaken, lowering their rigid strength and behaving as a semiliquid material. Structures such as buildings and pipelines built on ground that liquifies can tilt or sink or may be moved as the ground flows. This phenomenon has been noted in many earthquakes including classic effects of large apartment houses tilting in Niigata, Japan, during the June 1964 earthquake and spectacular effects during the March 1964 earthquake at Turnagain Heights and Valdez Harbor, Alaska. Liquefaction effects can be predicted in a gross way using simple linear diagrams (Youd, 1978) or more precisely with sophisticated computer models for specific sites (Youd *et al.*, 1978).

A seiche is a wave set up in a body of water in response to earthquake waves and also can occur great distances from the earthquake source. The danger of seiche is temporary flooding of areas near lakes and reservoirs and overtopping of dams. During the 1954 Dixie Valley-Fairview Park, Nevada, earthquakes, a seiche was set up in a covered water reservoir in Sacramento, California, 300 km away, damaging support pillars, concrete walls, and gunite panels (Steinbugge and Moran, 1957).

Large ocean waves created by uplift or downdropping of the seafloor during an earthquake are called tsunamis. Tsunamis can move hundreds of kilometers per hour and destroy facilities and structures along the coast, thousands of kilometers from the earthquake. Warnings are issued when there is a large earthquake in oceanic areas, which allows coastal residents to go to safety on higher ground until the tsunami danger has passed.

Detailed observations and investigations of secondary effects have led to the understanding, prediction, and mitigation of these effects in many areas. Today, secondary effects can often be identified and risks assessed thanks to geologic, geophysical, and engineering laboratory and field studies.

## TECTONIC SETTING

### *Plate-Tectonic Relationships*

Plate-tectonic concepts are accepted by most earth scientists as a working model of the crustal behavior of the Earth. This model suggests that the Earth's surface is composed of several large plates and numerous smaller plates that are slowly moving and rotating with respect to each other. Since this behavior is dynamic, faulting, earthquake activity, and rates of fault slip and folding are closely related to the rate of movement between plates. Most seismic activity occurs along plate boundaries, areas known as interplate areas. Intraplate areas are areas within plates and have less seismic activity and lower rates of tectonic activity than interplate areas. Closer inspection of interplate regions reveals smaller "microplate" tectonic domains characterized by a particular faulting style, such as the Basin and Range province in the western United States.

### *Interplate Regions*

These regions have many active faults with a potential for future displacements and associated earthquake activity. The methods described in this chapter are especially appropriate for many faults in these regions. There is a great range in rates of fault activity with recurrence intervals that range from decades to hundreds of thousand years. Additionally, the plate and microplate boundaries vary from sharp and narrow to broad ("soft") zones that may extend hundreds to thousands of kilometers from the main boundary, including most of the western United States, although there are "islands" of inactive subplates within this region and variations in rate of activity within active provinces. Wallace and Whitney (1984) described an example of variable rates of tectonic activity within the Great Basin province. Complete evaluations of a fault are needed to assess the following characteristics: seismogenic character, segmentation, recurrence interval and slip rate, recency of fault activity, and the relation to the site or area being evaluated.

The maximum magnitude of earthquakes varies with seismotectonic province or fault and includes a range in values for each type of plate boundary. The maximum historical values include $M_w$ (moment magnitude) values of over 9 for some subduction zones, $M_S$ (surface wave) magnitudes of up to about 8.3 for strike-slip faults, and $M_S$ magnitudes of up to about 7.5 or 8 for extensional zones.

### *Intraplate Regions*

Seismic hazard evaluation of intraplate regions has evolved rapidly in the last few years, although processes will become more refined and better understood. Rates of activity are generally orders of magnitude lower within intraplate areas as compared with interplate areas. The low rates of faulting and warping and sub-

dued geomorphic expression of deformation may be due to broad basinal or domal uplift. These lower tectonic rates are generally accompanied by less earthquake activity than for interplate regions. In general this has caused more focus and awareness of earthquake hazard in interplate regions and less concern in the intraplate regions. An excellent summary of intraplate seismicity (and other intraplate tectonism) is given by Sykes (1978), who noted that intraplate seismicity appears to be localized along pre-existing zones of crustal weakness. Seismicity in the eastern United States within the North American plate exemplifies this concept.

Seismic activity in the New Madrid area, where the large earthquakes of 1811 and 1812 occurred, appears to be localized along a pre-existing rift structure in the continent (Sykes, 1978). Although at the time the rift was formed the continent was under extension in that region, recent activity appears to be related to compression. This change in stress regime shows how a pre-existing structure (e.g., rift) can be reactivated in later, different strain episodes. The crustal weakness appears to be the locus of earthquake-related strain release. The 1886 Charleston earthquake was located in a Paleozoic orogenic belt, an inactive or relic interplate region on the eastern edge of the continent. Low seismicity and cover of young sediments has not allowed the tectonics and source zones of the Charleston earthquake to be understood as well as in the New Madrid area.

The Meers Fault of Oklahoma is another example of reactivation of an ancient geologic structure. The Meers Fault, a segment of the Frontal Fault zone, was formed about 500 m.y. ago as part of the southern Oklahoma rift. During a later orogeny it underwent extensive compressional (reverse) as well as left-lateral displacement. Studies of the Meers Fault show that the fault is currently active and has a dominant lateral component (Ramelli and Slemmons, 1985; Slemmons *et al.*, 1985).

The potential size of intraplate earthquakes, although they are infrequent, is great. The New Madrid, Missouri, earthquakes of 1811 and 1812 are estimated to have $M_S$ magnitudes of over 8; the Charleston, South Carolina, earthquake of 1886 was about $M_S = 7$. The recently discovered Meers Fault has characteristic features that suggest $M_S = 6.5$ to 7.5 earthquakes in the late Quaternary (Slemmons *et al.*, 1985).

## IDENTIFICATION AND DELINEATION OF ACTIVE FAULTS

### *Geologic Methods*

Many active faults are poorly delineated on most pre-1950 geologic, structural, or tectonic maps. These commonly emphasize ancient and inactive tectonic features rather than neotectonic structures. Recognition and detailed mapping of historical and Quaternary faults in many zones of neotectonic activity, particularly at or near plate boundaries, have led to recent improvements in the delineation of active faults. In addition, the possible reactivation of intraplate faults such as the Meers Fault has emphasized the need to re-examine other faults and folds in central and eastern United States.

### *Remote-Sensing Methods*

Remote-sensing methods can be effective in detecting, delineating, and describing the character of active faults and neotectonic features. The most effective methods accentuate fault scarps by employing imaging techniques using special illumination angles, wavelengths, or stereographic effects. Some of the methods for earthquake-hazard analysis are summarized by Glass and Slemmons (1978), but newer equipment and methods and rapid developments in analytical techniques require continued adaptation of many of these concepts. Examples of instrumental and structural analysis are in Williams (1983) in the section on geological applications, and for applications in nuclear power-plant site investigations in McEldowney and Pascucci (1979).

Low Sun angle and radar imagery methods are especially effective in detecting and delineating active faults and folds. Special low-Sun angle photography of faults can have the advantages of relatively low cost and appropriate scale and optimum shadowing or highlighting of scarps by selection of solar azimuth and altitude. Since this is the most effective single method of assessment of active faults, it is one of the most widely used methods for aerial photography and reconnaissance (Glass and Slemmons, 1978). Radar imagery of some areas is available at much higher cost and on smaller scales, may have the advantages of some ground penetration in arid regions, and can be taken at any azimuth, time of day or night, and in cloud or fog cover.

Recent studies using ground penetrating radar for fault trace identification have been very successful. Black *et al.* (1983) studied an area along the San Andreas Fault zone that has been extensively trenched and found good correlation of the ground penetrating radar records and the trench logs. Bilham and Seeber (1985) used subsurface radar profiling to detect colluvial wedges associated with former movements along the Lost River Fault and wide zones of faulting along the San Andreas Fault system. As this method is refined it will become an even more powerful method of fault detection and delineation.

### *Geophysical Methods*

Observations of seismicity can sometimes help to delineate active faults. Persistent alignments of seismicity, especially at the ends of identified faults, can occasionally be considered seismic sources or seismogenic extensions of a fault. Many active faults have associated seismicity, including the Calaveras, Hayward, and central San Andreas Fault zones of central California, which, however, may only indicate the creeping segments of these faults. Other sections of the San Andreas Fault system that are not currently creeping are not clearly delineated by small earthquakes. Areas of relatively high seismicity may warrant examination for active faults.

In the eastern United States, alignments of high seismicity such as near New Madrid are associated active subsurface faults. Other major basement faults are associated with seismicity and may be active (Gordon, 1985); these also could be examined.

Seismic reflection techniques can help to delineate subsurface faults in sedimentary basins, both on land and beneath lakes and oceans. These techniques are used for recent fault detection and delineation studies, particularly in offshore California (Greene *et al.*, 1973) and along the central California coastal margin near the Hosgri Fault (Crouch *et al.*, 1984) near Point Conception (Pipkin and Ploessel, 1985), and in the offshore zone of deformation between the Inglewood Fault and Rose Canyon Fault (San Diego). Seismic reflection profiling by the Consortium for Continental Reflection Profiling (COCORP) has revealed the down-dip nature of many faults and a major detachment surface under the Sevier Desert of Utah (Allmendinger *et al.*, 1983).

Gravity methods are most effective for studying fault zones where a strong density contrast exists between materials on either side of the fault. This situation occurs along faults where basement rocks are displaced against sediments or fault offsets in basins where the thickness of sediment differs across the fault. These methods are especially effective for regions of extensional faulting. Zoback (1983) used gravity techniques to delineate the geometry of range bounding normal faults in the Basin and Range province along the Wasatch Fault zone in Utah.

Application of surface magnetic and aeromagnetic survey methods for evaluation of active faults is discussed by Cluff *et al.* (1972), Krinitzsky (1974), and Sherard *et al.* (1974). These methods can be used to detect and delineate faults concealed by recent sediments and provide a relatively inexpensive method of contouring the thickness of basin fill. Smith (1967) located intrabasin, largely concealed, major fault grabens within the Dixie Valley graben using aeromagnetic methods. Some of these graben boundary faults were also accurately delineated by the faulting of the 1954 Dixie Valley earthquake. Smith provided a detailed outline for applying magnetic methods to the Basin and Range province with normal- and oblique-slip faults.

Bailey (1974) used a magnetometer to determine the surface fault location of the Chabot Fault, California, where anomalous drops in magnetism suggested locations of fracturing and subsequent leaching related to faulting. The eastern limit of the Chabot Fault zone was identified so that buildings could be sited to avoid potential surface rupture. Similar applications may be useful in defining active faults that are concealed by young alluvium or bodies of water.

### *Exploratory Methods*

Exploratory methods for fault assessment advocated by Louderback (1950) were little used until the late 1960s when they assumed an important role in fault evaluations to assess such features as for activity, age dating, paleorupture and liquefaction events, slip direction, recurrence intervals, and slip rates. An adequate exploratory trenching and borehole program is critical in evaluation of active faults and is a major part of both domestic and foreign assessments. Specific applications to fault assessment are included in Taylor and Cluff (1973). The use of trenching as an exploratory method for nuclear power plant siting is discussed in Hatheway and Leighton (1979).

## DETERMINATION OF FAULT ACTIVITY

### *Definition of Activity*

Before 1950, most geologists did not distinguish between inactive faults and those with a potential for renewed displacements and associated earthquake activity, yet this is a critical part of man's planning and design. Slemmons (1982a) listed over 30 definitions for "active" or "capable" faults of which only three were made before 1950. No definition for active faults is universally accepted, although two elements are present in most definitions: (1) the potential or probability of future displacements in the present tectonic setting and (2) the time of most recent displacement (e.g., historical, Holocene, Quaternary, or "in the present seismotectonic regime"). The first element, potential, is critical to all assessments for larger earthquakes; the second, recency, relates indirectly to rate of activity, which provides a more quantitative measure of degree of fault activity. Fault activity can also be classified by fault slip rate. Figure 3.2 shows the general relationships between

three factors: (1) the time since the last event or recurrence interval, (2) the surface wave magnitude, and (3) fault slip rate. This figure also shows the general geomorphic expression for each interval of fault slip rates, although such factors as climate, time since the last event, variations in fault slip rate, or noncharacteristic activity can affect the landforms. Cluff and Cluff (1984) noted that the common current use of "active" and "inactive" can be a scientific oversimplification that may lead to improper siting or design of engineered structures. Use of quantitative measures for degree of activity, such as fault slip rate and recurrence interval with probabilities and variance, can lead to deterministic values providing meaningful numbers for analysis by probabilistic methods.

### *Geologic Indicators*

One of the most convincing arguments or evidence of fault activity is the cross-cutting or non-cross-cutting relationship with a datable unit. If Holocene activity is the criterion for activity, then a Holocene age unit crossing the fault could be an ideal location for a trench site. If the unit is offset, then the age of the unit and the amount of offset can be used to estimate a slip rate and a recurrence interval if the nature of characteristic earthquake is known. A wide variety of types of Holocene deposits have been used for evaluation of fault activity, most commonly alluvial and volcanic deposits. Deposits are dated by carbon-14 radiometric methods, tephrochronology, soil development, fossil stratigraphy, and many other techniques. Pierce (Chapter 13, this volume) presents a good summary and review of Quaternary dating methods. Exposures of faulted units may be found in stream cuts and landslide scars or in road cuts or other man-made excavations. To prove whether a fault or strand of a fault system is active, a trench may be dug at the proposed site and the geologic units and soils inspected for faults. If no demonstrated fault activity has taken place in these geologic units within the defined "active" fault period, the proposed structure can be considered reasonably safe from damage from surface faulting.

The structural aspects of young geologic units adjacent to faults may also provide information about activity of a fault. Adjacent units may be brecciated and shattered, have open fissures, be tilted or warped, or have secondary effects of faulting and liquefaction effects (e.g., sand boils and sand dikes). In a detailed study of a fault, the youthful geologic units should be described, delineated, and inspected for evidence of young faulting.

### *Geomorphic Indicators*

The freshness of appearance and type of geomorphic expression of faults is related to the age of faulting (Matsuda, 1975; Slemmons, 1977, 1982a; Wallace, 1977, 1978). Geomorphic investigations into faulting are relatively easy and can yield considerable information. Many landforms such as depressions and sag ponds, open rifts, and prominent high-angle scarps suggest youthfulness and further help to identify the active traces or strands of faults zones (Figure 3.3).

A geomorphic investigation begins with examination of aerial photographs or an aerial reconnaissance. Overview of the geomorphology allows delineation of key lo-

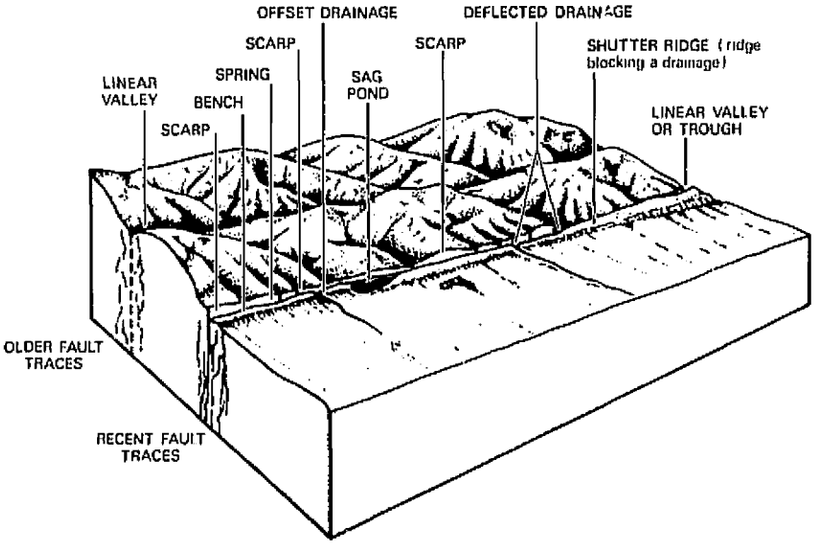


FIGURE 3.2 Relation between time or recurrence interval between earthquakes, earthquake magnitude, and slip rate across the fault zone. This chart assumes that most of the energy is released by seismogenic rather than aseismic activity and that the average displacement is one half the maximum. [Modified from Matsuda (1975) and Slemmons (1977).]

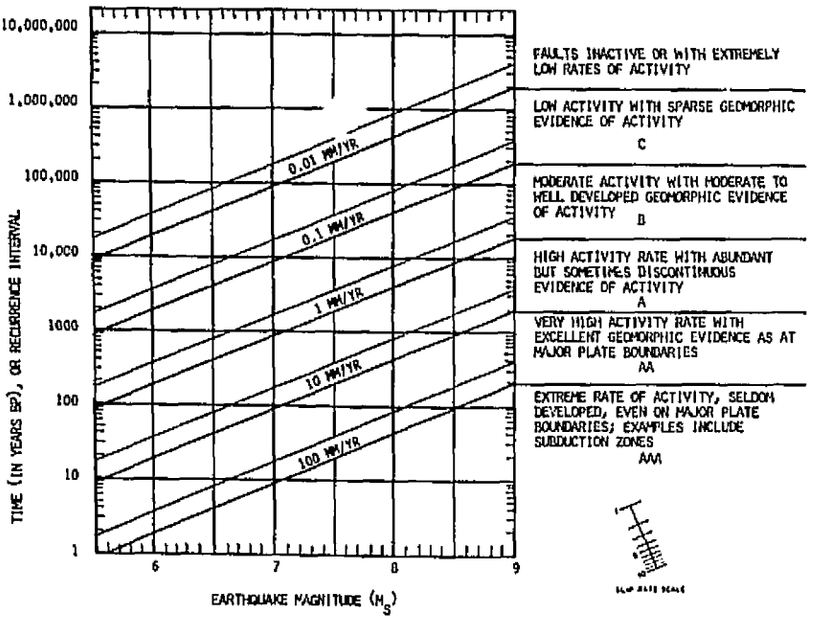


FIGURE 3.3 Geomorphic features related to active faulting.

cations for ground investigations. Low-Sun-angle techniques for reconnaissance or photography have been extremely useful in detecting subtle geomorphic features that would have otherwise been missed (Glass and Slemmons, 1978), such as in cities where geomorphic expression of scarps may have been smoothed out or altered, but general elevation differences still exist.

Key areas found through geomorphic investigation are often used as sites for further geologic investigations as exploratory trenching. Geomorphic investigations form a large part of the data base used in paleoseismic investigations. Freshness and continuity of geomorphic expression in space strongly suggest a surface rupture created during one event or over multiple events closely spaced in time.

Recently there have been numerous efforts to quantify the degree of degradation of fault scarps relative to age (see Chapters 7, 8, and 12, this volume).

### *Geodetic Indicators*

Recognition of activity along some faults is possible by repeated geodetic surveys. Geodetic methods are capable of detecting and measuring tectonic strain of regions or across active faults. Reduction of the geodetic data permits determination of rate and direction of ground movement. The data provide another measure of fault displacement, both seismic or aseismic, and can assist in locating active branch faults or focus on areas of current movement within complex zones of faulting. Sylvester (Chapter 11, this volume) presents several methods of near-field geodetics including level lines, alignment surveys, trilateration, triangulation, and creepmeters. Regional geodetic leveling and trilateration surveys are made to monitor regional strain accumulation and release (Prescott *et al.*, 1979; Vanicek *et al.*, 1980).

Advances using satellite geodesy, e.g., the Navstar Global Positioning System (GPS), offer surveying techniques with a precision superior to classic surveying at one-twentieth the cost (Kerr, 1985).

### *Seismologic Indicators*

Detailed studies of earthquake epicentral and hypocentral distributions of many fault zones can indicate the activity, continuity, location, dip and strike, seismogenic depth, and possible stress regime of the fault zone. However, this is often a difficult task. The quality of seismic data must be scrutinized and understood. The best-quality data come from dense seismometer networks that are limited to a few areas and are often temporary. Quarry blasts and possible geothermal, volcanic, and reservoir-induced seismicity must be separated from fault-related seismicity and can be analyzed as an additional seismic hazard. The remainder may be a well-defined zone of activity or a diffuse pattern of distributed activity. Well-defined zones of activity are common in aftershock areas and along creeping sections of faults. Diffuse patterns are harder to interpret but at least indicate that some strain is taking place in the area. A diffuse pattern of historical

seismicity suggests a maximum historic earthquake (for the area including the fault) and warrants further investigation of faulting in the area.

Earthquake activity along a fault zone clearly indicates that the fault zone is active at least at seismogenic depths. However, the type of activity needs to be evaluated to assess the hazard and risk. A fault that slips aseismically represents a different type of risk than a fault that slips with large rupture events. Adjoining sections of the same fault may behave differently and, for example, the San Andreas Fault between Parkfield and San Juan Bautista appears to be characterized by creep and frequent lower magnitude (less than 6) earthquakes, whereas the adjoining section to the south has abrupt brittle failures, about 150-yr recurrence intervals, and up to magnitude 8.3 earthquakes.

### *Rates of Activity*

Rates of activity may be learned from the study of geomorphic features (Matsuda, 1975); faults with high slip rate have abundant and well-developed landforms and steep scarps (Wallace, 1977; Hanks *et al.*, 1984; Chapters 7, 12, and 14, this volume). The interrelationships of time between characteristic earthquakes (the recurrence interval), fault slip rate, and earthquake magnitude are shown in Figure 3.2. Slip rates presented in this figure are based on average displacement, which is more likely to be measured during field studies, rather than maximum displacement. We have assumed that the average displacement is one-half the maximum displacement.

## EARTHQUAKE SIZE AND ACTIVE FAULT PARAMETERS

### *Earthquake Magnitudes and Moment Magnitude*

Earthquake magnitude scales are one of the most important earthquake size source parameters used today in seismology and active-tectonic studies. Magnitude scales have different forms such as local magnitude ($M_L$), surface-wave magnitude ($M_S$), body-wave magnitude ($M_b$), and coda-duration magnitude ($M_c$) (Kanamori, 1977; Bath, 1981; Chung and Bernreuter, 1981). These different forms were originally created to accommodate different kinds of seismic networks (e.g., near field versus far field) in the magnitude determination of earthquakes. One of the principal differences between the magnitude scales is the period of the wave measured. This difference of measured frequency arises from the variety of instrument responses of seismometers used and the changing frequency spectrum of the waves reaching seismometers at various distances from the earthquake sources. The local magnitude scale was introduced by C. F. Richter for earthquakes in southern California with epicentral distances of 600 km or less and focal depths of 15 km or less. Both $M_L$ and $M_b$ are determined from the amplitude of waves with a period of about 1 sec, and the values of these magnitudes are thought to saturate at about magnitude 7.25 (Chung and Bernreuter, 1981). Thus, as the rupture gets larger in area from that of a magnitude 7.25 earthquake, the values of $M_L$ and $M_b$ increase very little and do not represent the entire energy released from the earthquake.

The surface wave magnitude is suitable for global distances and is measured at periods near 20 sec. The $M_S$ scale saturates at about magnitude 8.6 (Chung and Bernreuter, 1981).

Another useful seismic estimate of earthquake size, the seismic moment ($M_0$), is defined as the product of the rupture area ($A$), the average displacement of the rupture ($D$), and the shear modulus ($\mu$) along the rupture (Brune, 1968),

$$M_0 = \mu AD.$$

Hanks and Kanamori (1979) developed a moment magnitude scale ($M_w$) based on seismic moment, where

$$M_w = 2/3 \log M_0 - 10.7.$$

The moment magnitude is an important scale because it relates directly with the physical properties of the rupture and does not, by definition, saturate.

Earthquake size is one of the most important factors in seismic-hazard analysis and can be estimated using specific fault parameters. When using magnitude data, it is important to understand the characteristics of the scale being used, such as saturation, and to understand the quality or range in errors and uncertainties of the data used for the magnitude estimate.

### *Fault Rupture Parameters and Earthquake Size*

Tocher (1958) recognized that there was a good relationship in large historical earthquakes between size or magnitude and the logarithmic parameters of total surface rupture length, maximum displacement, or length times maximum displacement. Subsequent reports by Iida (1959, 1965), Bonilla (1967, 1970), and Bonilla and Buchanan (1970) refined the original linear regressions. Bonilla with his colleagues (Bonilla and Buchanan, 1970; Mark, 1977; Mark and Bonilla, 1977) and Slemmons (1977) added new data points and rejected poor data, improved magnitude values and statistical practices, and scrutinized the quality of field measurements of faulting parameters. More compatible linear regres-

sions with lower standard deviations and better fit were obtained by Slemmons (1982b) and using more sophisticated magnitude values and statistical methods by Bonilla *et al.* (1984). Where there is good field expression of the length and/or maximum displacement from geomorphic expression of fault scarps, or where these parameters can be measured from soil-stratigraphic relations, it is possible to infer the approximate magnitude of paleoseismic events. These correlations between fault parameters and earthquake magnitude have been made for siting and engineering design of vital structures in many parts of the world for diverse tectonic settings, including extensional areas such as the Basin and Range province (Wallace, 1977, 1978; Cluff *et al.*, 1980; Schwartz and Coppersmith, 1984) and regions of strike-slip faulting (Sieh, 1984; Sieh and Jahns, 1984) and for thrust faulting in regions with compressional tectonics (Woodward-Clyde Consultants, 1984). An application to intraplate locations is shown by the left-oblique faulting of the Meers Fault zone in Oklahoma. There a 26- to 38-km-long fault scarp can be mapped. Using correlations of length to $M_S$ magnitude, the scarp can be inferred to have formed during prehistoric earthquakes of between 6.5 to 7.5 magnitude (Slemmons *et al.*, 1985). This paleoseismic evidence is especially important since no historical earthquakes have been recorded in the area. Elsewhere in this zone a general alignment of epicenters of small earthquakes has been noted (Gordon, 1985).

In summary, active fault parameters such as length and displacement can be used to estimate earthquake magnitudes through the regression formula presented by Slemmons (1982b) or Bonilla *et al.* (1984), and the parameters can be used directly in a moment magnitude calculation. An example of these correlations is shown in Figure 3.4.

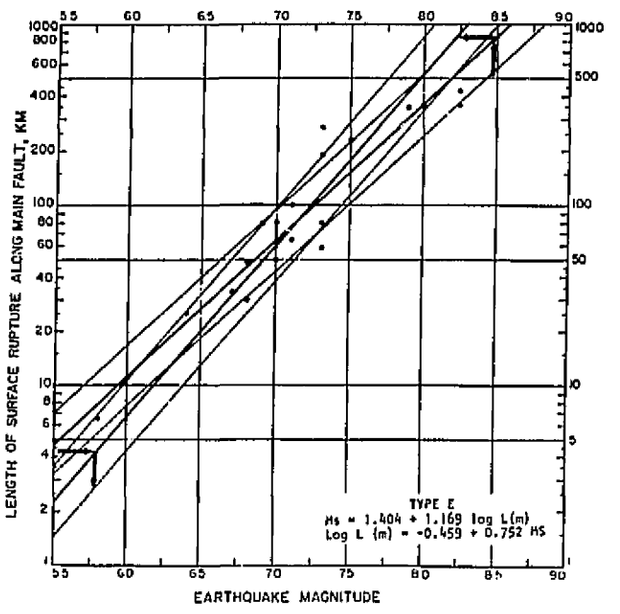


FIGURE 3.4 Relationship between earthquake magnitude ($M_S$) and maximum displacement for strike-slip faults. (From Slemmons, 1982b.)

*Segmentation*

The segmentation of fault systems involves the identification of individual fault segments that appear to have continuity, character, and orientation; these suggest that a segment will rupture as a unit (Slemmons, 1982b). Individual fault segments have different characteristics relative to adjacent segments or are separated from adjacent segments by identifiable discontinuities.

Figure 3.5 illustrates the concept that fault zones rupture in segments with an example from Turkey. During the period 1939 to 1967, the North Anatolian Fault system ruptured as segments and not as a single throughgoing event.

The delineation of segments involves the identification of discontinuities in the fault system. Discontinuities can be divided into two categories, geometric and inhomogeneous; these categories are borrowed from seismologists who have used these terms for asperities and barriers (Aki, 1984). Examples of geometric discontinuities include fault intersections, such as branch faults or cross-fault terminations; fault-zone features, such as en echelon segments, separations, and changes in attitude; and fault terminations. Inhomogeneous discontinuities include variations in fault width, local stress regimes, and rates of displacement.

Segall and Pollard (1980), acknowledging that fault traces consist of numerous discrete segments, have developed a two-dimensional mathematical solution for nonintersecting cracks. Their solution describes the mechanical behavior of left-stepping versus right-stepping en echelon cracks in a right lateral stress regime. Segall and Pollard state, "for right lateral shear and left-stepping cracks, normal tractions on the overlapping crack ends increase and inhibit frictional sliding, whereas for right-stepping cracks, normal tractions decrease and facilitate sliding." Bakun *et al.* (1980) studied the seismicity and behavior of the San Andreas Fault zone in central California where strain release is characterized by creep and moderate earthquakes. In their analysis, they modeled fault segments in an en echelon fashion (Figure 3.6). Behavior of these segments was as would be pre-

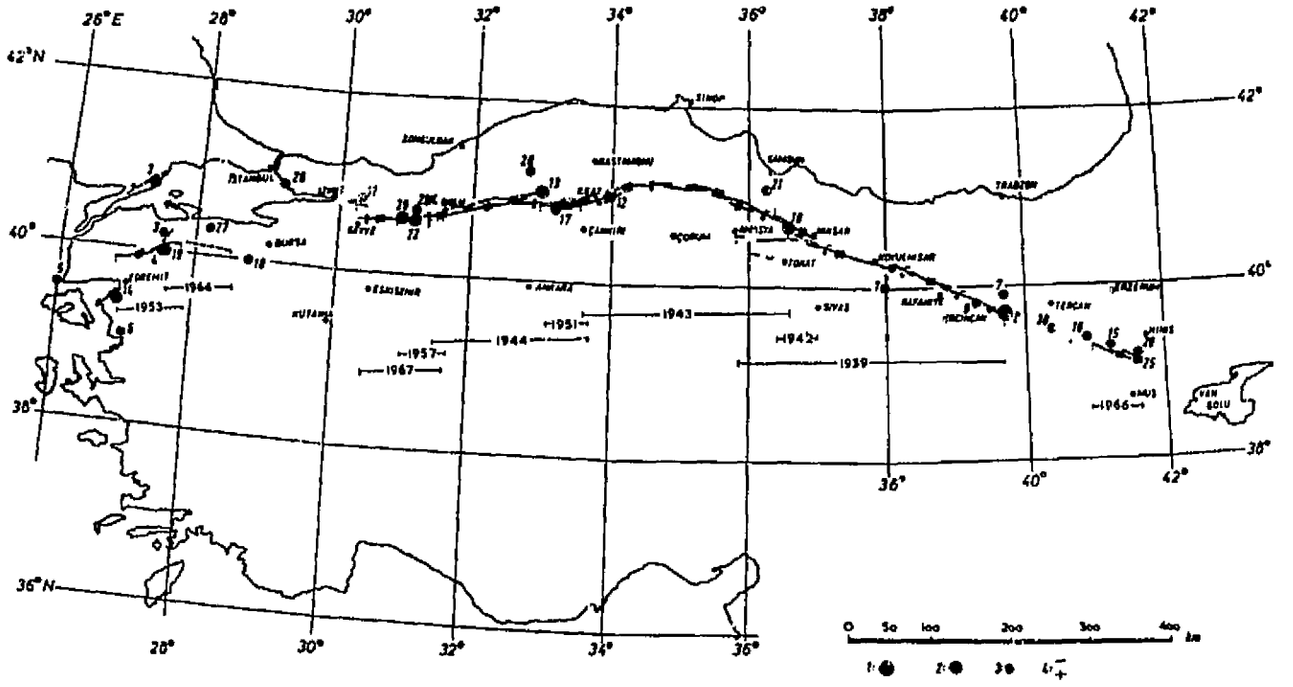


FIGURE 3.5 Sequence of faulting along the North Anatolian Fault zone, Turkey, for the period 1939-1983. (Modified from Am[illegible] 1978.)

dicted by Segall and Pollard's model, strengthening the idea that fault systems behave in a segmented manner.

If the discontinuities are large enough, segmentation of a fault system may be intuitively easy (e.g., a 10-km en echelon step appears to be a substantial discontinuity with a good chance of stopping a rupture). In less clear cases of discontinuities, several lines of geologic, seismologic, and geometric evidence must be gathered to suggest or substantiate the existence of the discontinuity. An understanding and delineation of the entire earthquake history of a fault can be used as relatively strong evidence of segmentation. Once convinced that a particular segmentation is reasonable, various approaches including correlation with faulting parameters can be used to estimate earthquake magnitudes. Schwartz and Coppersmith (1984; Chapter 14, this volume) suggested examples of fault zones for which the segmentation model may be applicable.

## EARTHQUAKE RECURRENCE ESTIMATION

### *Recurrence Models*

Earthquake recurrence intervals can vary markedly from fault to fault. Historical seismicity of the Parkfield segment of the San Andreas Fault system suggests a recurrence rate of 21 ± 4 yr (Bakun and McEvilly, 1984), whereas soils and trenching data suggest to Machette (1978) that the County Dump Fault in New Mexico has a recurrence interval of 90,000 to 190,000 yr. As pointed out by Wallace (1970) and Schwartz and Coppersmith (1984; Chapter 14, this volume), the slip rate of a fault directly affects recurrence rates.

Various models have been used to explain earthquake recurrence, including the time-predictable (Shimazaki and Nakata, 1980; Bufe *et al.*, 1977), slip-predictable (Shimazaki and Nakata, 1980), and the periodical model (Bakun and McEvilly, 1984).

### *Recurrence Data*

Wallace (1970) discussed recurrence for the San Andreas Fault. Subsequent refinements in dating, exploratory trenching, geomorphic expression, and low-Sun-angle aerial reconnaissance or photography have greatly expanded knowledge of faulting recurrence, paleoseismicity, and scarp morphologic change. These new methods are critical to active fault evaluations and timing and probability analyses.

Studies determining paleoseismic history have been conducted recently at Pallett Creek (Sieh, 1984) and Wallace Creek (Sieh and Jahns, 1984) and at Cajon Pass (Weldon and Sieh, 1985) along the San Andreas Fault zone. Cross-cutting relationships and radiocarbon dates

limit the ages of the prehistoric ruptures, and can be used to determine a local recurrence interval and slip rate for the fault. Although the 1886 Charleston earthquakes apparently did not rupture the ground surface, preventing a direct analysis of recurrence rate, studies of liquefaction-related sand blows in the Charleston area by Obermeier *et al.* (1985) suggest at least two prehistoric events occurred that may be used to establish the recurrence interval of large earthquakes for the area. Thatcher (1984) noted examples in which geodetic measurements may also lead to recurrence estimates.

### *Seismic Gaps*

Mogi (1979) pointed out that the term "seismic gap" has been used to describe two different phenomena. Mogi termed a seismic gap of the first kind as a gap in the spatial distribution of rupture zones of the largest earthquakes in a seismic belt. A second kind of seismic gap is a gap in the seismicity of smaller-magnitude earthquakes before larger earthquakes.

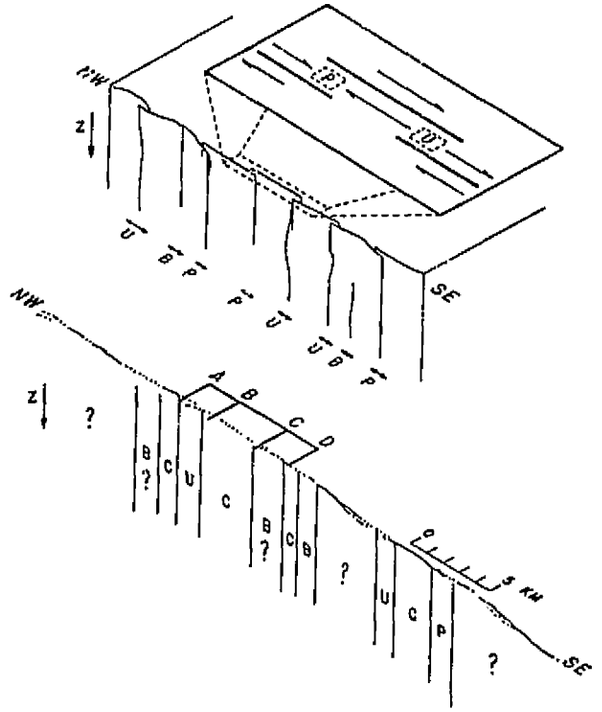


FIGURE 3.6 (Top) Schematic fault model structure. Interior of the smooth, continuous, nearly planar segments are creeping patches (C). Stuck patches are classified as pinned (P), unpinned (U), or bent (B) if they occur at a left-stepping offset, a right-stepping offset, or a change in strike, respectively. (Bottom) Specific model for the Bear Valley-Limekiln Road section of the San Andreas Fault in central California. (From Bakun *et al.*, 1980.)

Wallace (1981) described seismic gaps as active-tectonic zones between recently active fault segments with high potential for reactivation in the near future. Wallace and Whitney (1984) examined the paleoseismic history of three segments of the Central Nevada Seismic Belt—the Dixie Valley Fault segment, the Stillwater Fault segment, and the Pleasant Valley Fault zone segment. They found that scarps $10^4$ to $10^5$ yr of age and approximately Holocene age (less than $10^4$ yr) are present in places along all three segments. However, within historical time, only the Pleasant Valley faults in 1915 and the Dixie Valley faults in 1954 ruptured. Within the intervening Stillwater seismic gap there are no free faces preserved on Holocene scarps, indicating that they are probably older than 300 yr. Wallace and Whitney (1984) commented that "the Stillwater gap is a likely site for future major faulting, but the low level of seismicity in the gap area suggests that the next major earthquake is not imminent."

Other fault systems where seismic gaps of the first kind have been identified are plate boundary systems. McCann *et al.* (1979) conducted a comprehensive study of large earthquakes and seismic gaps along major plate boundaries. Figure 3.7 shows large earthquakes and seismic gaps along the major plate boundaries near Alaska. The second type of seismic gap applies mainly to the earthquake prediction and management.

## CASE STUDIES

### *Character of the Subduction in Northwestern United States—Seismic or Aseismic?*

Several lines of evidence suggest the Juan de Fuca and Gorda plates are being subducted underneath the North American plate in the northwestern United States. These include (1) the Cascade Range, an active andesitic chain of volcanoes; (2) seismicity related to the Benioff-Wadati zone (Smith and Knapp, 1980; Cockerham, 1984; Tabor and Smith, 1985); (3) geodetic deformation consistent with subduction (Ando and Balazs, 1979; Savage *et al.*, 1981); and (4) deformation of marine terraces consistent with subduction (Adams, 1984). Although active subduction seems clear, this system has been relatively aseismic with respect to great subduction-zone earthquakes. Subduction is either proceeding with relatively little coupling with the overriding plate and thus large elastic strains are not being stored, or the subducting Juan de Fuca/Gorda plate is strongly coupled with the overriding plate, producing conditions in which a large earthquake could occur in the future and the historical period is a period between

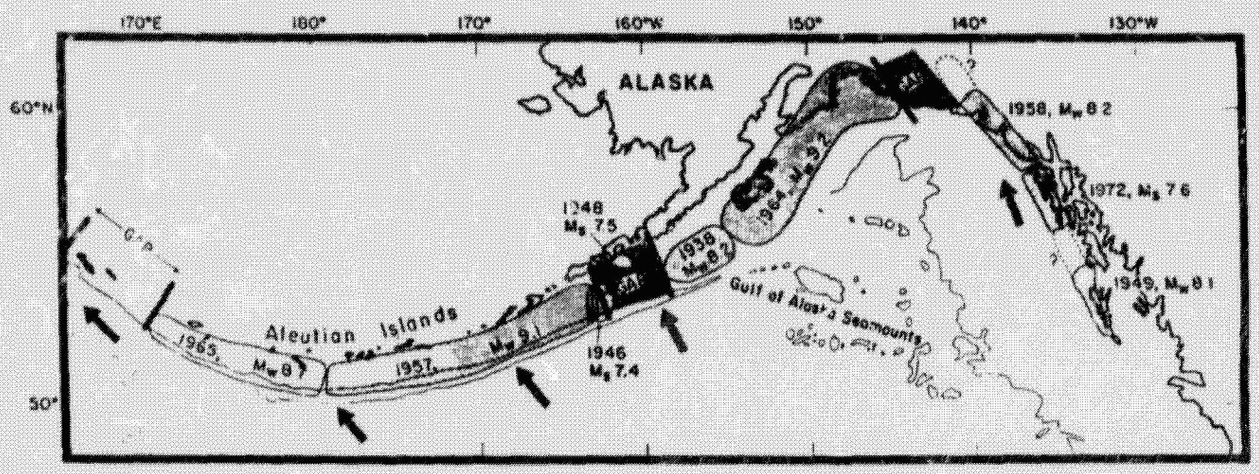


FIGURE 3.7 Recent large earthquakes along the Alaska-Aleutian seismic zone. Areas along this zone that have not ruptured are considered seismic gaps and may be the locations of future large earthquakes. (From McCann *et al.*, 1979.)

earthquakes (Ando and Balazs, 1979; Weaver and Smith, 1983; Adams, 1984).

Recent studies have been undertaken to assess the seismic potential associated with subduction in this region (Heaton and Kanamori, 1984; Adams, 1984). Heaton and Kanamori examined the seismic coupling process and compared the Juan de Fuca subduction zone with subduction of other young oceanic plates. In particular, they compared convergence rates, ages of lithosphere, presence of active back-arc basins, depth of oceanic trench, dip of the Benioff-Wadati zone, topography of the subducted slab, and seismic quiescence. Present-day convergence across the Juan de Fuca subduction zone has been estimated as 3 to 4 cm/yr, a moderate rate for subduction zones. The age of the subducted slab has been estimated at 10 to 15 m.y., a relatively young lithospheric plate (Heaton and Kanamori, 1984). They associated the young buoyant crust with strong coupling with the overriding plate; and when rates of plate movement and the age of ocean floor are used (Ruff and Kanamori, 1980), they estimated a maximum moment magnitude of $M_w = 8.3 \pm 0.5$. They also proposed that other parameters such as the dip of the Benioff-Wadati zone (10 to 15° beneath Puget Sound), topography of the subducted slab, absence of a back-arc basin, and depth of trench suggest strong coupling of the plates. In their worst-case model of strong coupling, the Juan de Fuca subduction zone could rupture in one event (approximately 600 km by 200 km; convergence rate = 4 cm/yr), with an estimated maximum moment magnitude of $M_w = 9.0$.

Heaton and Kanamori (1984) commented, "this 500-km gap in seismic activity is one of the most remarkable to be found anywhere in the Circum-Pacific belt," and "if slip is occurring aseismically on the shallow part of the subduction zone, then this particular example would have to be considered unique." They concluded, "that there is sufficient evidence to warrant further study of the possibility of a great subduction zone earthquake in the Pacific Northwest."

Adams (1984) suggested types of geologic investigations of paleoseismic activity that could help resolve the seismic hazard. A possible example is Sims's (1975) study of disturbances of glacio-lacustrine deposits in the western Puget Sound area, which considered 14 disturbed zones in the 40,000-yr-old sediments to be caused by earthquakes. Such evidence needs to be verified as truly seismogenic, synchronous with earthquakes, and distributed over a larger part of the Pacific Northwest.

Definitive studies have yet to resolve the issue of whether this Benioff-Wadati zone is seismogenic or aseismic. Resolution is important to future building, siting, design, and zoning within Washington and Oregon. Many existing engineered structures may have inadequate design for earthquakes of magnitude 7.5, 8.0, or 8.5.

### *Implications of the Meers Fault, Oklahoma*

The Meers Fault (Figure 3.8) is a relatively short fault of about 75-km length in the Frontal Fault zone between the Amarillo-Wichita Uplift and the Anadarko Basin. It was previously recognized to be a major ancient fault with about 3 km of total vertical component of offset in a zone of faults that has a total, mainly Paleozoic, offset of over 10 km. Gilbert (1983) recognized that

FIGURE 3.8 Aerial view of the late Holocene Meers Fault in Oklahoma. The fault scarp is about 5 m high and shows left-lateral offset of drainage lines and ridges.

this fault showed well-defined steep scarps suggesting late Quaternary to prehistorical activity with earthquakes of magnitude 6 to 7. This statement was unexpected, as this area has no historical seismicity and is almost 600 km east of the nearest recognized Quaternary faults of the Rio Grande-Rocky Mountain Belt. Previous seismic assessments of earthquake risk assumed that maximum future earthquakes would be of magnitude 5.5 or less, the maximum historical earthquake within the region. As noted by Kerr (1985), this area would have been an ideal one for vital engineering structures, because the fault appeared to be inactive and not a seismic threat. Studies by Ramelli and Slemmons (1985) and Tilford and Westen (1985) confirmed that there is a young fault scarp of about 26- to 28-km length along part of the Meers Fault zone. Ramelli and Slemmons subsequently identified another scarp that extends the main scarp for a total length of about 38 km. The compound scarp of 5-m height developed from repeated surface fault offsets. Donovan (1985), Kerr (1985), Slemmons *et al.* (1985), and other workers also showed that the fault also had a left-lateral component. Past offsets were at least 1 or 2 m per event. These data suggest that past offsets were accompanied by earthquakes of surface wave magnitude of 6.5 to 7.5. The Holocene activity is confirmed by radiometric dating (Madole and Meyer, 1985) and youthful scarp morphology (Ramelli and Slemmons, 1985). The lack of significant historical seismicity is indicated by Gordon (1985), Gordon and Dewey (1985), and Lawson (1985), although Gordon recognized a general epicentral alignment with the Wichita-Ouachita zone, with left-lateral focal mechanisms in this trend.

This unexpected young fault leads to the speculation that there are possible connections between the Frontal Fault zone and the Mississippi trend of epicenters in the New Madrid, Missouri, area (with short zones of surface faulting in 1811–1812). Further connections were suggested by Hinze *et al.* (1980, 1985) between the New Madrid area and the east-west trending zone of faults in the complex group of faults in the Cottage Grove-Moorman Syncline-Rough Creek-Kentucky River Fault zone. Pleistocene fault activity along the Kentucky River Fault zone has been suggested by VanArsdale and Sergeant (1985). They examined trenches in the Plio-Pleistocene terrace deposits along the Kentucky River Fault zone and found the deposits folded, faulted, and injected with clay dikes. These connections suggest a possible extensive Quaternary breakup of the midcontinental region along reactivated faults; a potential for high-magnitude earthquakes may be present. In addition it indicates the need for more studies of tectonic activity in Central and Eastern United States and the reassessment of the current rationale for evaluating earthquake activity in this intraplate region.

## ACKNOWLEDGMENTS

Much of the research that contributed to this paper is related to special studies for the U.S. Nuclear Regulatory Commission. We gratefully acknowledge their support and encouragement. We are especially grateful to Jim Lienkaemper of the U.S. Geological Survey in Menlo Park; his careful and perceptive review led to many discussions and beneficial changes in the paper. Barbara Matz of the Mackay School of Mines provided

both word processing and editorial assistance. We also benefitted from technical and editorial comments from Steve Brocoum, Tom Usselman, David R. Slemmons, Sunny Meriweather, and Hank Ohlin.

## REFERENCES


Adams, J. (1984). Active deformation of the Pacific Northwest continental margin, *Tectonics 3*(4), 449-472.

Aki, K. (1984). Asperities, barriers, characteristic earthquakes and strong motion prediction, *J. Geophys. Res. 89*, 5867-5872.

Allen, C. R., M. Wyss, J. N. Brune, A. Grantz, and R. E. Wallace (1972). Displacements on the Imperial, Superstition Hills and the San Andreas Faults triggered by the Borrego Mountain earthquake, *U.S. Geol. Surv. Prof. Paper 787*, 87-104.

Allmendinger, R. W., J. W. Sharp, D. Von Tish, L. Serpa, L. Brown, S. Kaufman, J. Oliver, and R. B. Smith (1983). Cenozoic and Mesozoic structure of the eastern Basin and Range province, Utah, from COCORP seismic-reflection data, *Geology 11*, 532.

Ambraseys, N. N. (1978). Studies in historical seismicity and tectonics, in *The Environmental History of the Near and Middle East*, W. C. Brice, ed., Academic Press, New York, pp. 185-210.

Ando, M., and E. I. Balazs (1979). Geodetic evidence for aseismic subduction of the Juan de Fuca plate, *J. Geophys. Res. 84*, 3023-3027.

Bailey, A. D. (1974). Near surface fault detection by magnetometer, *Calif. Geol. 27*, 274.

Bakun, W. H., and T. V. McEvilly (1984). Recurrence models and the Parkfield, California, earthquakes, *J. Geophys. Res. 89*, 3051-3058.

Bakun, W. H., R. M. Stewart, C. G. Bufe, and S. M. Marks (1980). Implication of seismicity for failure of a section of the San Andreas Fault, *Bull. Seismol. Soc. Am. 70*, 185.

Bakun, W. H., M. M Clark, R. S. Cockerham, W. L. Ellswork, A. G. Lindh, W. H. Prescott, A. F. Shakal, and P. Spudich (1984). The 1984 Morgan Hill, California, earthquake, *Science 225*, 288.

Bath, M. (1981). *Earthquake Magnitude—Recent Research and Current Trends*, Elsevier, Amsterdam.

Berberian, M. (1982). Aftershock tectonics of the 1978 Tabas-e-Golshan (Iran) earthquake sequence: A documented active (thin- and thick-skinned) tectonic case, *Geophys. J. R. Astron. Soc. 68*, 499-530.

Berg, G. V. (1983). Seismic design codes and procedures, *Earthquake Engineering Research Institute Monograph*, 119 pp.

Bilham, R., and L. Seeber (1985). Paleoseismic studies using subsurface radar profiling, in *Summaries of Technical Reports*, Vol. XIX, U.S. Geol. Surv. Open-File Report 85-22, p. 47.

Black, W. E., J. P. Singh, F. C. Kresse, P. Bilham, and L. Seeber (1983). Ground penetrating radar for fault trace identification, *Assoc. Eng. Geol., Abstr. Prog., 26th Ann. Mtg.*

Bonilla, M. G. (1967). Historic surface faulting in continental United States and adjacent parts of Mexico, *U.S. Geol. Surv. Open-File Report.*

Bonilla, M. G. (1970). Surface faulting and related effects, in *Earthquake Engineering*, R. L. Wiegel, ed., Prentice-Hall, Englewood Cliffs, N.J., pp. 47-74.

Bonilla, M. G., and J. M. Buchanan (1970). Interim report on worldwide historic surface faulting, *U.S. Geol. Surv. Open-File Report*, 32 pp.

Bonilla, M. G., R. K. Mark, and J. J. Lienkaemper (1984). Statistical relations among earthquake magnitude, surface rupture length, and surface fault displacement, *Bull. Seismol. Soc. Am. 74*, 2379-2411.

Brune, J. N. (1968). Seismic movement, seismicity and rate of slip along major fault zones, *J. Geophys. Res. 73*, 777-784.

Bufe, C. G., P. W. Harsh, and R. D. Burford (1977). Steady-state seismic slip—A precise recurrence model, *Geophys. Res. Lett. 4*, 91-94.

Burford, R. O., and P. W. Harsh (1980). Slip on the San Andreas Fault in central California from alinement surveys, *Bull. Seismol. Soc. Am. 70*, 1233.

Campbell, N. P., and R. D. Bentley (1981). Late Quaternary deformation of the Toppenish Ridge uplift in southcentral Washington, *Geology 9*, 519-524.

Chung, D. H., and D. L. Bernreuter (1981). Regional relationships among earthquake magnitude scales, *Rev. Geophys. Space Phys. 19*, 649-663.

Clark, M. M., K. K. Harms, J. J. Lienkaemper, J. A. Perkins, M. J. Rymer, and R. V. Sharp (1984). The search for surface faulting after the May 2 earthquake, in *Coalinga, California, Earthquake of May 2, 1983*, R. E. Scholl and J. L. Stratta, eds., Earthquake Engineering Research Institute Report 84-03, San Francisco, Calif., pp. 54-56.

Cluff, L. S., and J. L. Cluff (1984). Importance of assessing degrees of fault activity for engineering decisions, in *Proceeding of the 8th World Conference on Earthquake Engineering*, Vol. 2, Prentice-Hall, Englewood Cliffs, N.J., pp. 629-636.

Cluff, L. S., W. R. Hansen *et al.* (1972). Site evaluation in seismically active regions—An interdisciplinary team approach, in *International Conference on Microzonation*, Seattle, 1972.

Cluff, L. S., A. S. Patwardhan, and K. J. Coppersmith (1980). Estimating the probability of occurrences of surface faulting earthquakes on the Wasatch Fault zone, Utah, *Bull. Seismol. Soc. Am. 70*, 463-478.

Cockerham, R. S. (1984). Evidence for a 180 km long subducted slab beneath northern California, *Bull. Seismol. Soc. Am. 74*, 569.

Crouch, J. K., S. B. Bachman, and J. T. Shay (1984). Post-Miocene compressional tectonics along the central California margin, in *Tectonics and Sedimentation Along the California Margin*, J. K. Crouch and S. B. Bachman, eds., Pacific Section, Soc. Econ. Paleontologists and Mineralogists 38.

Davis, L. L., and L. R. West (1973). Observed effects of topography on ground motion, *Bull. Seismol. Soc. Am. 63*, 283.

Donovan, R. N. (1985). The Meers Fault as a hinge to the Wichita Frontal Fault Zone, *Seismol. Soc. Am. Abstr., 80th Ann. Mtg.*

Gere, J. M., and H. C. Shah (1984). *Terra Non Firma*, W. H. Freeman and Co., New York.

Gilbert, M. C. (1983). The Meers Fault of southwestern Oklahoma: Evidence for possible strong Quaternary seismicity in the mid continent, *EOS 64*(18), 313.

Glass, C. E., and D. B. Slemmons (1978). Imagery in earthquake analysis, U.S. Army Engineers Waterways Exp. Stn., Vicksburg, Miss., Report 11, 221 pp.

Gordon, D. W. (1985). Revised instrumental hypocenters and correlations of earthquake locations and tectonics in the central United States, *U.S. Geol. Surv. Prof. Paper* (draft).

Gordon, D. W., and J. W. Dewey (1985). The Wichita-Ouachita seismic zone—southern Oklahoma seismicity in a regional context, *Seismol. Soc. Am. Abstr., 80th Ann. Mtg.*

Greene, H. G., *et al.* (1973). Faults in the Monterey Bay region, California, *U.S. Geol. Survey Map MF-518.*

Hanks, T. C., and H. Kanamori (1979). A moment magnitude scale, *J. Geophys. Res. 84*, 2981-2987.

Hanks, T. C., R. C. Bucknam, K. R. Lajoie, and R. E. Wallace (1984). Modification of wave-cut and fault-controlled landforms, *J. Geophys. Res. 89*, 5771-5790.

Hardyman, R. F. (1978). Volcanic Stratigraphy and Structural Geol-

ogy of Gillis Canyon Quadrangle, Northern Gillis Range, Mineral County, Nevada, Ph.D. thesis, Univ. Nev., Reno.

Harp, E. L., R. C. Wilson, and G. F. Wieczorek (1981). Landslides from the February 4, 1976, Guatemala earthquake, *U.S. Geol. Surv. Prof. Paper 1204A*, 35 pp.

Hatheway, A. W., and F. B. Leighton (1979). Trenching as an exploratory method, in *Geology in the Siting of Nuclear Power Plants*, A. W. Hatheway and C. R. McClure, Jr., eds., Geol. Soc. Am. Rev. in Eng. Geol. IV, pp. 169-196.

Heaton, T., and H. Kanamori (1984). Seismic potential associated with subduction in the northwestern United States, *Bull. Seismol. Soc. Am. 74*, 933.

Hill, M. L. (1984). Earthquakes and folding, Coalinga, California, *Geology 12*, 711-712.

Hinze, W. J., L. W. Braile, G. R. Keller, and E. G. Lidiak (1980). Models for midcontinent tectonism, in *Continental Tectonics*, NRC Geophysics Study Committee, National Academy of Sciences, Washington, D.C., pp. 73-83.

Hinze, W. J., L. W. Braile, G. R. Keller, and E. G. Lidiak (1985). Geophysical-geological studies of possible extensions of the New Madrid Fault zone, U.S. Nuclear Reg. Comm. NUREG/CR-3174 2.

Iida, K. (1959). Earthquake energy and earthquake fault, *Nagoya Univ. J. Earth Sci. 7*, 98-107.

Iida, K. (1965). Earthquake magnitude, earthquake fault, and source dimensions, *Nagoya Univ. J. Earth Sci. 13*, 115-132.

Kanamori, H. (1977). The energy release in great earthquakes, *J. Geophys. Res. 82*, 2981-2987.

Kasahara, K. (1981). *Earthquake Mechanics*, Cambridge University Press.

Kerr, R. A. (1985). Unexpected young fault found in Oklahoma, *Science 227*, 1187-1188.

King, G., and R. Stein (1983). Surface folding, river terrace deformation rate and earthquake repeat time in a reverse faulting environment: The Coalinga, California earthquake of May 1983, in *The 1983 Coalinga, California, Earthquake*, J. H. Bennett and R. W. Sherburne, eds., Calif. Div. Mines and Geol. Special Publ. 66, Sacramento, Calif., pp. 261-274.

Krinitzsky, E. L. (1974). State-of-the-art for assessing earthquake hazards in the United States: Fault assessment in earthquake engineering, U.S. Army Engineers Waterways Exp. Stn., Vicksburg, Miss., Misc. Paper S-73-1, Report 2.

Lawson, J. E., Jr. (1985). Seismicity at the Meers Fault, *Seismol. Soc. Am. Abstr., 80th Ann. Mtg.*

Louderback, G. O. (1950). Faults and engineering geology, in *Application of Geology to Engineering Practice*, S. Paige, ed., Geological Society of America, Boulder, Colo., pp. 125-150.

Machette, M. N. (1978). Dating Quaternary faults in the southwestern United States by using buried calcic paleosols, *J. Res. U.S. Geol. Surv. 6*(3), 369-381.

Madole, R. F., and R. Meyer (1985). Holocene movement on the Meers Fault, southwest Oklahoma, *Seismol. Soc. Am. Abstr., 80th Ann. Mtg.*

Mark, R. K. (1977). Application of linear statistical models of earthquake magnitude versus fault length in estimating maximum acceptable earthquakes, *Geology 5*, 464-466.

Mark, R. K., and M. G. Bonilla (1977). Regression analysis of earthquake magnitude and surface fault length using the 1970 data of Bonilla and Buchanan, *U.S. Geol. Surv. Open-File Report 77-614*, 8 pp.

Matsuda, T. (1975). Magnitude and recurrence interval of earthquakes from a fault (in Japanese), *Earthquake, Ser. 2, 28*, 269-283.

McCann, W. R., S. P. Nishenko, L. R. Sykes, and J. Krause (1979). Seismic gaps and plate tectonics: Seismic potential for major plate boundaries, *Pure Appl. Geophys. 117*, 1082-1147.

McEldowney, R. C., and R. F. Pascucci (1979). Application of remote sensing data to nuclear power plant site investigations, in *Geology in the Siting of Nuclear Power Plants*, A. W. Hatheway and C. R. McClure, Jr., eds., Geol. Soc. Am. Rev. in Engineer. Geol. IV, pp. 121-139.

McGarr, A. (1984). Scaling of ground motion parameters, state of stress, and focal depth, *J. Geophys. Res. 89*, 6969.

Miller, D. J. (1960). The Alaskan earthquake of July 10, 1958: Giant wave in Lituya Bay, *Bull. Seismol. Soc. Am. 50*, 217-322.

Mogi, K. (1979). Two kinds of seismic gaps, *Pure Appl. Geophys. 117*, 1172-1186.

Molinari, M. P. (1984). Late Cenozoic geology and tectonics of Stewart and Monte Cristo Valleys, West-Central Nevada, M.S. thesis, Univ. Nev., Reno, 124 pp.

Obermeier, S. F., G. S. Gohn, R. E. Weems, R. L. Gelinas, and R. Meyer (1985). Geologic evidence for recurrent moderate to large earthquakes near Charleston, South Carolina, *Science 227*, 408.

Pipkin, B. W., and M. Ploessel (1985). Submarine geologic investigation for liquified natural gas facility, Southern California borderland, *Bull. Assoc. Eng. Geol. 22*, 193-200.

Plafker, G. (1972). Tectonics, in *The Great Alaskan Earthquake of 1964: Seismology and Geodesy*, National Academy of Sciences, Washington, D.C., pp. 113-188.

Prescott, W. H., J. C. Savage, and W. T. Kinoshita (1979). Strain accumulation rates in the western United States between 1970 and 1978, *J. Geophys. Res. 84*, 5423-5435.

Ramelli, A. K., and D. B. Slemmons (1985). Surface offsets and scarp morphology, Meers Fault, Oklahoma, *Seismol. Soc. Am. Abstr., 80th Ann. Mtg.*

Rogers, A. M., J. C. Tinsley, and W. W. Hays (1983). The issues surrounding the effects of geologic conditions on the intensity of ground shaking, in *A Workshop on "Site-Specific Effects of Soil and Rock on Ground Motion and the Implications for Earthquake-Resistant Design,"* W. W. Hays, ed., U.S. Geol. Surv. Open-File Report 83-845.

Ruff, L., and H. Kanamori (1980). Seismicity and the subduction process, *Phys. Earth Planet. Int. 23*, 240.

Savage, J. C., R. O. Burford, and W. T. Kinoshita (1975). Earth movements from geodetic measurements, in *San Fernando, California, Earthquake of 9 February 1971*, Calif. Div. Mines Geol. Bull. 196, p. 175.

Savage, J. C., M. Lisowski, and W. H. Prescott (1981). Geodetic strain measurements in Washington, *J. Geophys. Res. 86*, 4929-4980.

Schwartz, D. P., and K. J. Coppersmith (1984). Fault behavior and characteristic earthquakes: Examples from the Wasatch and San Andreas Faults, *J. Geophys. Res. 89*, 5681-5698.

Segall, D., and D. D. Pollard (1980). Mechanics of discontinuous faults, *J. Geophys. Res. 85*, 4337-4350.

Sherard, J. L., L. S. Cluff, and C. R. Allen (1974). Potentially active faults in dam foundations, *Geotechnique 24*(3), 367-428.

Shimazaki, K., and T. Nakata (1980). Time-predictable recurrence model for large earthquakes, *Geophys. Res. Lett. 7*, 279-282.

Sieh, K. E. (1984). Lateral offset and revised dates of large earthquakes along the San Andreas Fault system at Pallett Creek, southern California, *J. Geophys. Res. 89*, 7641-7670.

Sieh, K. E., and R. Jahns (1984). Holocene activity of the San Andreas Fault at Wallace Creek, California, *Geol. Soc. Am. Bull. 45*, 883-896.

Sims, J. (1975). Determining earthquake recurrence intervals from deformation structures in young lacustrine sediments, *Tectonophysics 29*, 141-152.

Singh, J. P. (1981). The influence of seismic source directivity on strong ground motion, Ph.D. thesis, Univ. Calif., Berkeley.

Slemmons, D. B. (1977). Faults and earthquake magnitude, U.S.

Army Engineers Waterways Exp. Stn., Vicksburg, Miss., Misc. Paper S-73-1, Report 6, 166 pp.

Slemmons, D. B. (1982a). A procedure for analyzing fault-controlled lineaments and the activity of faults, in *Proceedings 3rd International Conference on Basement Tectonics*, D. W. O'Leary and J. L. Earle, eds., International Basement Tectonics Association, p. 33.

Slemmons, D. B. (1982b). Determination of design earthquake magnitudes for microzonation, in *3rd International Earthquake Microzonation Conference Proceedings*, pp. 119-130.

Slemmons, D. B., A. R. Ramelli, and S. Brocoum (1985). Earthquake potential of the Meers Fault, Oklahoma, *Seismol. Soc. Am. Abstr., 80th Annu. Mtg.*

Smith, T. E. (1967). Aeromagnetic measurements in Dixie Valley, Nevada: Implications regarding Basin-and-Range structure, *J. Geophys. Res.* 73, 1321-1331.

Smith, S. W., and J. S. Knapp (1980). The northern termination of the San Andreas Fault, in *Studies of the San Andreas Fault Zone in Northern California*, R. Streitz and R. Sherburne, eds., Calif. Div. Mines and Geol. Spec. Report 140, 153.

Stein, R. S. (1983). Reverse slip on a buried fault during the 2 May 1983 Coalinga earthquake: Evidence from geodetic elevation changes, in *The 1983 Coalinga, California, Earthquakes*, J. H. Bennett and R. W. Sherburne, eds., Calif. Div. Mines and Geol. Spec. Publ. 66, Sacramento, Calif., pp. 151-163.

Steinbugge, K. V., and D. F. Moran (1957). Engineering aspects of the Dixie Valley-Fairview Peak Earthquakes, *Bull. Seismol. Soc. Am.* 47, 335-348.

Swiger, W. F. (1978). Specialty session on design for fault displacement, in *Earthquake Engineering and Soil Dynamics*, American Society of Civil Engineers, Pasadena, Calif., p. 1464.

Sykes, L. R. (1978). Intraplate seismicity, reactivation of pre-existing zones of weakness, alkaline magmatism, and other tectonism postdating continental fragmentation, *Rev. Geophys. Space Phys.* 16, 621-688.

Tabor, J. J., and S. W. Smith (1985). Seismicity and focal mechanisms associated with the subduction of the Juan de Fuca plate beneath the Olympic Peninsula, Washington, *Bull. Seismol. Soc. Am.* 75, 237.

Taylor, C. L., and L. S. Cluff (1973). Fault activity and its significance assessed by exploratory excavation, in *Proceedings Conference on Tectonic Problems of the San Andreas Fault System*, R. L. Kovach and A. Nur, eds., Stanford University Publ. Geol. Sci. 13, pp. 239-248.

Thatcher, W. (1984). The earthquake deformation cycle, recurrence, and the time-predictable model, *J. Geophys. Res.* 89, 5674-5680.

Tilford, N. R., and D. P. Westen (1985). Morphological evidence for recent multiple surface ruptures along the Meers Fault, southwestern Oklahoma, *Seismol. Soc. Am. Abstr., 80th Ann. Mtg.*

Tocher, D. (1958). Earthquake energy and ground breakage, *Bull. Seismol. Soc. Am.* 48, 147-153.

VanArsdale, R. B., and R. E. Sergeant (1985). Post Pliocene displacement on faults within the Kentucky River Fault zone of east-central Kentucky, *Geol. Soc. Am. Abstr. Programs 17*, 739.

Vanicek, P., R. O. Castle, and E. I. Balazs (1980). Geodetic leveling and its applications, *Rev. Geophys. Space Phys. 18*, 505-524.

Wallace, R. E. (1970). Earthquake recurrence intervals on the San Andreas Fault, California, *Geol. Soc. Am. Bull. 81*, 2875-2890.

Wallace, R. E. (1977). Profiles and ages of young fault scarps, north-central Nevada, *Geol. Soc. Am. Bull. 88*, 1267-1281.

Wallace, R. E. (1978). Geometry and rates of change of fault generated range fronts, north-central Nevada, *J. Res. U.S. Geol. Surv. 6*, 637-650.

Wallace, R. E. (1981). Active faults, paleoseismology, and earthquake hazards in the western United States, in *Earthquake Prediction: An International Review*, D. W. Simpson and T. G. Richards, eds., Maurice Ewing Ser. 4, American Geophysical Union, Washington, D.C., pp. 209-216.

Wallace, R. E., and R. A. Whitney (1984). Late Quaternary history of the Stillwater seismic gap, Nevada, *Bull. Seismol. Soc. Am. 74*, 301-314.

Weaver, C. S., and S. W. Smith (1983). Regional tectonic hazard implications of a crustal fault zone in southwestern Washington, *J. Geophys. Res. 88*, 10371-10383.

Weldon, R. J., II and K. E. Sieh (1985). Holocene rate of slip and tentative recurrence interval for large earthquakes on the San Andreas Fault, Cajon Pass, Southern California, *Geol. Soc. Am. Bull. 96*, 793-812.

Williams, R. S., ed. (1983). *Geologic Hazards in Geological Applications*, American Society of Photogrammetry.

Woodward-Clyde Consultants (1977). Earthquake Evaluation Studies of the Auburn Dam Area—Summary Report, Vol. 1, Woodward-Clyde Consultants, San Francisco, Calif.

Woodward-Clyde Consultants (1984). Seismic Microzonation of Ech Cheliff Region Algeria, Vol. 1, Woodward-Clyde Consultants, San Francisco, Calif.

Yeats, R. C. (1982). Low-shake faults of the Ventura Basin, California, in *Neotectonics in Southern California*, J. D. Cooper, compiler, Cordilleran Section, Geol. Soc. Am. field trip guidebook, pp. 3-15.

Youd, T. L. (1978). Mapping liquefaction-induced ground failure potential, *Proc. Am. Soc. Civil Eng. 104*(GT4), 433-446.

Youd, T. L., J. C. Tinsley, B. M. Perkins, and R. F. Preston (1978). Liquefaction potential map of San Fernando Valley, California, in *Proceedings of the Second International Conference on Microzonation*, pp. 267-278.

Zoback, M. L. (1983). Structure and Cenozoic tectonism along the Wasatch Faultzone, Utah, in *Tectonic and Stratigraphic Studies in the Eastern Great Basin*, Geol. Soc. Am. Mem. 157.

# 4 Active Faults Related to Folding

ROBERT S. YEATS
*Oregon State University*

ABSTRACT

Active convergent zones contain fold-and-thrust belts that deform a sedimentary wedge by low-angle thrusting and flexural-slip folding over a subjacent, more rigid basement. Flexural-slip faults form by bedding slip during flexural-slip folding and are observed when unconformably overlying deposits are deformed by renewed folding. These faults are upthrown toward synclinal axes and die out in fold hinges. Bending-moment faults are produced because the convex side of a folded layer is lengthened normal to the fold axis and placed in tension, forming normal faults and extension fractures, whereas the concave side is shortened and placed in compression, forming reverse faults. Neither class of fault is likely to extend downward to rocks of such high strength that enough elastic strain energy could be stored to produce a large earthquake when released suddenly. However, all known historical examples are coseismic, and age relations on such second-order faults may apply to subjacent first-order seismogenic faults. Some folds such as Anticline Ridge at Coalinga, California, apparently are surface expressions of buried seismogenic faults. Regionally, fold-and-thrust belts may be modeled by the snow plow model of Davis *et al.* (1983) if the slope of the upper and lower boundaries of the forward-tapering wedge, the coefficients of basal and internal friction, and the ratio of pore pressure to hydrostatic pressure are known. This model implies that the deformation migrates toward the margin of the thrust belt such that youngest structures are at the edge; and pore pressures within individual folds, even those back from the edge, probably exceed hydrostatic.

## INTRODUCTION

Folds and low-angle thrust faults are an important component of ancient mountain belts. Thus it is surprising that they are not more widely reported in the literature on active tectonics. Part of the reason for this is that mountain belts characterize zones of plate convergence, and most of these zones comprise the accretionary wedges confronting island arcs and are, accordingly, offshore. The southern margin of the convergence zone of southern Asia extending west from the Himalaya to the Zagros Mountains is perhaps the most notable exception on land.

Most of the literature on active tectonics deals with zones of strike slip: the San Andreas Fault system of California, the Alpine Fault system of New Zealand, and the North Anatolian Fault system of Turkey, among others. Yet even in these zones, there are smaller regions dominated by tectonic convergence: the Transverse Ranges of California and the ranges and basins of the

northwestern South Island and central Otago, New Zealand, for example. Both the full-scale convergence zones, such as the Himalaya, and the zones subordinate to transform faulting, such as the Transverse Ranges, contain examples of active folds and low-angle thrust faults, and future research is likely to discover that active folds and thrust faults are as widespread in the active convergent zones as they are in extinct mountain belts. This chapter reviews the state of knowledge of structures related to folding in light of their impact on society.

## MECHANICAL BACKGROUND

The mechanical properties of fold-and-thrust belts were considered by Elliott (1976) and Chapple (1978), building on the earlier work of Hubbert and Rubey (1959). Chapple (1978) noted that fold-and-thrust belts, whether on land or offshore, should show (1) a basal surface of décollement below which there is little or no deformation; (2) an overall shape in cross section of a wedge tapering toward the edge of the mountain belt with its base, the basal décollement, sloping toward the interior of the mountain belt; and (3) extensive horizontal contraction in the tapered wedge above the basal décollement. Davis *et al.* (1983) considered the mechanics of a fold-and-thrust wedge to be analogous to that of the wedge of snow that forms ahead of the blade of a moving snow plow. The snow deforms until the wedge attains a critical taper, then slides stably, growing as new snow is accreted at the front of the wedge. Parameters essential to an understanding of the mechanics of a fold-and-thrust wedge include the angle of topographic slope of the wedge toward the frontal edge of the deformed belt, the angle of rearward slope of the basal décollement, the coefficient of internal friction within the wedge, the coefficient of sliding friction on the base (about 0.85 according to Byerlee, 1978), and the ratio of pore fluid pressure to the vertical stress imposed by overburden ($\lambda$). Davis *et al.* (1983) applied their mechanical model to the active fold-and-thrust belt of western Taiwan, where extensive subsurface information is available, and they determined the critical parameters to be angle of forward topographic slope 2.9 $\pm$ 0.3°, rearward slope of the décollement 6°, and $\lambda$ equal to 0.7. The fold-and-thrust wedge is above sea level, and the topography is at steady state: thickening of the wedge by contractile tectonics is balanced by erosion, which proceeds at a rate of 5 to 6 mm/yr (Li, 1976; Suppe, 1981). The model is sensitive to the nature of material comprising the décollement, where it is assumed that essentially pure frictional sliding occurs. However, evaporites characterize the fold-and-thrust wedges of the Zagros Mountains (Stöcklin, 1968) and the Salt Range of Pakistan (Seeber *et al.*, 1981), and these may yield plastically rather than by pressure-dependent Coulomb friction. The snowplow model has two important implications for active tectonics: (1) the age of deformation should migrate outward toward the front of the wedge, and (2) rocks within the wedge are near the point of critical failure and are likely to exhibit pore pressures greater than hydrostatic.

Yeats *et al.* (1981) pointed out that faults that do not extend downward into rocks of high strength will not be expected to produce large-amplitude ground acceleration that is due to seismic shaking because such rocks under near-surface confining pressures are not capable of storing enough elastic strain energy to generate a large earthquake when that strain energy is released instantaneously. Because fold-and-thrust belts terminate downward at a basal décollement over an undeformed rigid basement, the question of their seismotectonic signature is an important one. Where the décollement contains rocks of such low strength that deformation may occur plastically under low confining pressure, as in the Zagros Mountains and the Pakistan Salt Range, internal deformation is probably not accompanied by large earthquakes (Berberian, 1981; Seeber *et al.*, 1981; Seeber, 1983). In the thinner portions of fold-and-thrust wedges, the rocks are probably not under sufficient confining pressure to possess much shear strength, even though they behave according to Coulomb friction laws. However, in the thicker portions of wedges, the earthquake potential is not so clear. Seeber *et al.* (1981) suggested that the greatest earthquakes of the Indian Himalaya occur in front of the range in the Ganges foredeep, even though this area has been characterized by low instrumental seismicity in recent years. The large isoseismal areas of these earthquakes and lack of surface rupture in great historical earthquakes of the Ganges flood plain suggest that a large part of the décollement surface moves as a blind thrust, producing a detachment earthquake. The 1964 Prince William Sound, Alaska, earthquake also may be of detachment type (Seeber *et al.*, 1981).

## FLEXURAL-SLIP FAULTS

### *General Statement*

Most folds characteristic of foreland fold-and-thrust belts form by flexural slip. A stack of stiff beds alternating with thin, less stiff layers is end-loaded, and these beds buckle by slip on inherently weaker bedding surfaces separating stiffer beds (Ramsay, 1967, pp. 392-393). Slickensides on these weak surfaces are perpendic-

ular to the fold axis. Thickness of individual competent beds remains constant from hinge to limbs of folds. Rock layers are flexed, and upper layers slip over underlying layers toward anticlinal hinges and away from synclinal hinges. Slip is zero at fold hinges. On the limbs of the fold, the amount of slip on bedding faults depends on the maximum dip of the limbs and the thickness of each flexed layer. Because such bedding faults, called *flexural-slip faults* by Yeats *et al.* (1981), do not produce stratigraphic separation, they are not likely to be recognized unless there is a sequence overlying the flexural-slip fold with angular unconformity, and continued folding causes displacement of these younger deposits. Such deposits are cut by faults that are parallel to bedding in the folded sequence and upthrown toward the subjacent synclinal axis. The younger deposits are likely to be tilted toward the synclinal axis so that their dip is in the same direction as that in the subjacent, more strongly folded beds. Because flexural-slip faults remain in bedding, they do not extend to depths greater than the amplitude of the flexural-slip fold. Furthermore, displacement vanishes in the axis of the syncline where the faulted bedding plane is deepest. Beds at these depths, which would in most cases not exceed a few kilometers, are likely to have shear strength too low under such low confining pressures for bedding faults to generate large earthquakes, particularly in view of the fact that such faults form along the structurally weakest layers.

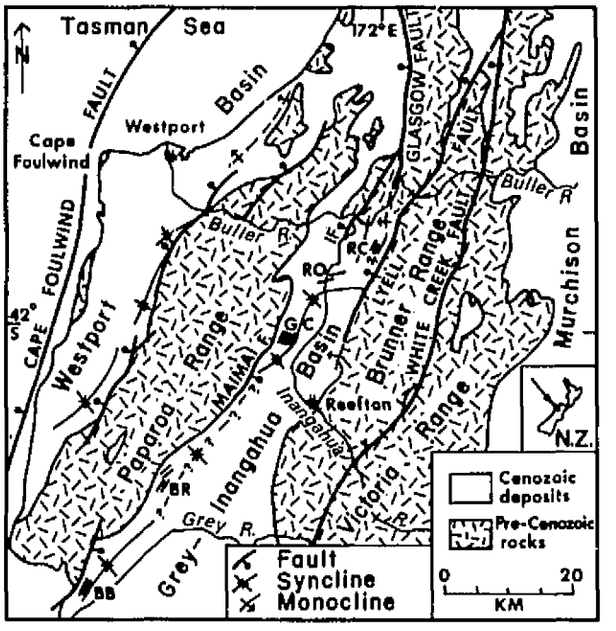


FIGURE 4.1 Tectonic map of the Buller region, South Island, New Zealand. Heavy lines are faults with bar and ball on downthrown side. Arrows on monoclines point to downwarped side. Short heavy lines show flexural-slip fault sets in Grey-Inangahua Basin: BB, Blackball; BR, Big River; GC, Giles Creek; RC, Rough Creek (active in 1968); RO, Rotokohu (active in 1968); IF, Inangahua (active in 1968).

### *Grey-Inangahua Basin, New Zealand*

Flexural-slip faulting was first described (although not named) by Suggate (1957) and Young (1963) in the Grey-Inangahua Basin of the northwestern South Island, New Zealand (Figure 4.1). The Grey-Inangahua Basin is a northeast-trending structural depression filled with Cenozoic strata resting with angular unconformity on a terrane consisting of Mesozoic and older rocks, including granitic basement. The Cenozoic strata are folded asymmetrically on the west side of the basin against the Paparoa Range. The folded strata are overlain with angular unconformity by glacial outwash gravels that form prominent surfaces above present river level. South of Giles Creek, one of these surfaces is cut by faults parallel to bedding in subjacent strata and upthrown toward the subjacent synclinal axis (Suggate, 1957). The surface is also tilted toward the synclinal axis (shown diagrammatically in Figure 4.2).

A terrace riser cuts across the faults, and the fault scarps are higher on the more elevated terrace surface (Suggate, 1957; Yeats, in press; Figure 4.2). The changes in scarp height may be explained using Lensen's (1968) reasoning at Branch River, New Zealand. Faulting occurred after the outwash stream had abandoned the terrace surface southwest of the terrace riser and while it still flowed across the lower terrace surface to the northeast. Further erosion removed the fault scarps northeast of the terrace riser where the stream still flowed but preserved the scarps on the abandoned, higher surface to the southwest. Renewed faulting occurred after the stream had abandoned the outwash surface altogether. The scarps northeast of the terrace riser reflect only the later faulting whereas the scarps southwest of the terrace riser reflect both episodes of faulting.

### *Transverse Ranges, California*

Flexural-slip faulting is also documented in the Ventura Basin, California, northeast of Santa Paula, where Pliocene-Pleistocene strata are strongly folded and locally overturned on the north flank of the Santa Clara syncline and are overlain by alluvial fans derived from mountains to the north (Figure 4.3) (Keller *et al.*, 1982; Rockwell, 1983). Surfaces of these fans are tilted toward the Santa Clara synclinal axis and are cut by faults that are parallel to bedding in the subjacent, strongly folded

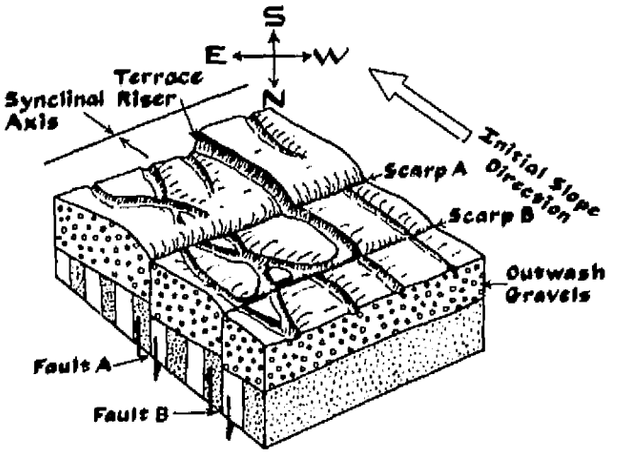


FIGURE 4.2 Block diagram showing relations at Giles Creek, South Island, New Zealand. Outwash gravels overlie steeply dipping strata on limb of syncline in which synclinal axis is southeast of diagram. Gravels are tilted toward synclinal axis. Bedding-plane (flexural-slip) faults propagate upward through gravels and appear as scarps facing away from synclinal axis. Fault scarps are higher on high side of terrace riser, indicating that some faulting occurred after outwash drainage had abandoned the high side of the terrace riser but still occupied the low side. Additional faulting occurred after the drainage had abandoned the terrace altogether. Fault scarp A faces up the depositional slope and is ungullied, indicating that it formed so suddenly that the rills occupying old outwash channels were ponded at base of scarp. Fault scarp B also formed instantaneously, but it is small enough that rill drainage was maintained across it, thereby gullying the scarp.

strata and are upthrown toward the synclinal axis. The faults show normal separation where the subjacent bedding is overturned and reverse separation where bedding is upright (Figure 4.3). Fan emplacement during tilting resulted in a cycle starting with fan deposition, then tilting followed by fan entrenchment, then deposition of a new fan surface, which was itself subsequently tilted. Seven geomorphic surfaces ranging in age from present day to an estimated 120,000 yr are recognized by Keller *et al.* (1982) and Rockwell (1983) on the basis of degree of soil development calibrated in part by $^{14}C$ dates and on the amount of tectonic deformation. Four of the older surfaces show increasing tilt and scarp height with increasing age.

Other examples of flexural-slip faulting in the Transverse Ranges are recognized in the Oakview area of the Ventura Basin (Keller *et al.*, 1982) and Point Conception, west of Santa Barbara, California (Cluff *et al.*, 1981).

### *Shinano River, Niigata Prefecture, Japan*

Active folding has been recognized in Japan for many years (Otuka, 1942), and attempts have been made to compare rates of folding of river terraces with rates of folding of subjacent strata (Sugimura, 1967; Kaizuka, 1967; Nakamura and Ota, 1969). The most extensively documented active folds occur in central Japan along the Shinano River (Ota, 1969), which flows northward across folded strata of the Pliocene-Pleistocene Uonuma Group. These folds are overlain with angular unconformity by fluvial terraces that are themselves folded. Strike faults cut the terraces at Yamamoto-yama (cross section 6 of Figure 6 of Ota, 1969) and northwest of Ojiya town (cross section 7 of Figure 6 of Ota, 1969). At Yamamoto-yama, Ota observed that the faults are upthrown in the direction of the synclinal axis of the folded Uonuma Group and of the oldest fluvial terrace. In a recent visit to the area with the author, she confirmed that the terrace remnants between the strike faults slope toward the synclinal axis, indicating that the faults are probably flexural-slip faults.

The early work northwest of Ojiya town had suggested that the strike faults there are downthrown toward the synclinal axis. However, Ota and Suzuki (1979) described a new quarry exposure near Katakai, which exposed the faulted terrace and the underlying Uonuma Group (Figure 4.4). Four faults parallel to bedding in the Uonuma Group cut the overlying terrace and are upthrown toward the synclinal axis. In the quarry exposure, the steeply dipping Uonuma Group

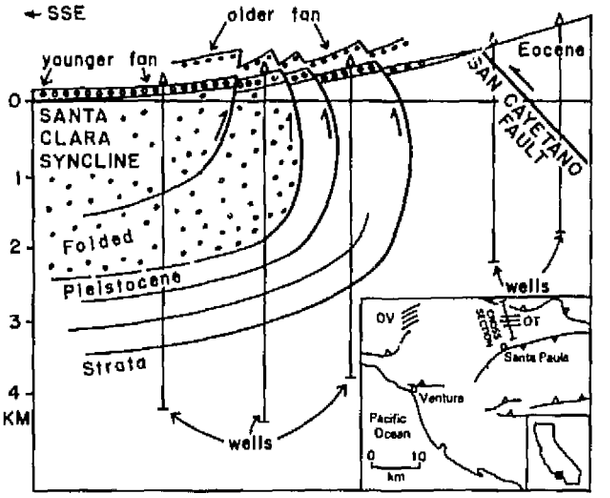


FIGURE 4.3 Diagrammatic cross section across north flank of Santa Clara syncline east of Santa Paula, Ventura Basin, California. Flexural-slip faults have normal separation where subjacent strata are overturned, reverse separation where subjacent strata are upright. Older fan has more separation and tilt than younger fan. Modified from Yeats *et al.* (1981) and Keller *et al.* (1982). No vertical exaggeration. Inset: OT, Orcutt-Timber Canyon flexural-slip faults; OV, Oakview flexural-slip faults.

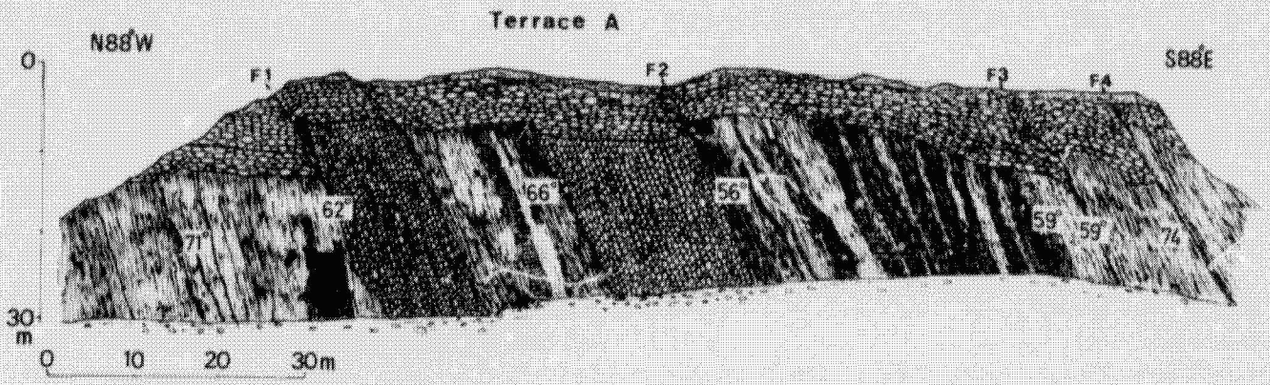


FIGURE 4.4 Quarry exposure of tilted and faulted Shinano River stream terrace unconformably overlying steeply dipping Uonuma Group near Katakai, Niigata Prefecture, Japan. Two faults in gravel (F1 and F2) are propagated upward into terrace material from contacts between conglomerate and fine-grained strata of Uonuma group (from Ota and Suzuki, 1979).

consists of fine-grained nonmarine strata with two interbeds of conglomerate. Two of the four faults occur at the contact between a gravel interbed and the finer grained strata, suggesting that the faults are localized by lithology contrasts in the underlying, folded strata.

### *Examples of Coseismic Flexural-Slip Faulting*

There are no known examples of flexural-slip faults formed by aseismic creep. However, there are examples of such faults accompanying earthquakes at Lompoc, California; El Asnam, Algeria; and possibly Inangahua, New Zealand. On April 7, 1981, an earthquake of $M_L$ = 2.5 in a diatomite quarry near Lompoc, California, produced a zone of reverse fault scarps at least 575 m long, with the fault plane formed in clay interbeds in diatomite and diatomaceous shale on the north flank of a syncline (Yerkes *et al.*, 1983). Maximum net slip was 25 cm, with maximum dip slip of 23 cm and right-lateral strike slip of 9 cm. The earthquake is best explained by removal of diatomite during quarrying under conditions in which maximum principal compressive stress is horizontal and normal to the synclinal axis. Removal of overburden increased the shear stress on the bedding plane enough to cause the earthquake 2 yr after the end of quarrying (Yerkes *et al.*, 1983).

The El Asnam, Algeria, earthquake reactivated a reverse fault and was accompanied by extensive internal deformation of the rocks adjacent to the surface trace of this fault (Philip and Meghraoui, 1983). At Kef el Mes, near the northeastern limit of 1980 surface rupture, the reverse fault was accompanied by renewed flexural-slip folding of Pliocene strata in an adjacent syncline (Figure 4.5). Flexural-slip faulting on bedding planes produced fault scarps that produced displacement in an opposite sense to that on the main fault.

The Inangahua, New Zealand, earthquake of May 24, 1968, was apparently generated on the Inangahua reverse fault, which joins the Glasgow Fault to the northeast (Figure 4.1; Lensen and Suggate, 1968; Lensen and Otway, 1971; Nathan, 1978a). The Rotokohu and Rough Creek Faults were formed during this earthquake by slip parallel to bedding on the north flank of a syncline in folded Neogene strata, producing scarps in late Pleistocene outwash gravels that overlie the folded strata unconformably (Lensen and Otway, 1971). Vertical leveling profiles across the Rotokohu Fault also showed this displacement (Boyes, 1971). Lensen (1976) later used the surface faulting accompanying the Inangahua earthquake to classify faults as *earthquake-generating* (Inangahua) and *earthquake-generated* (Rotokohu and Rough Creek). However, the Rotokohu and Rough Creek Faults are parallel to a sharp linear gradient in isostatic gravity anomalies (Anderson, 1979), and they may be the surface expression of a structure involv-

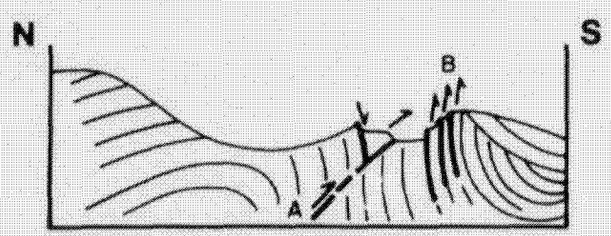


FIGURE 4.5 Diagrammatic cross section of coseismic flexural-slip faulting at Kef el Mes, El Asnam earthquake, 1980, after Philip and Meghraoui (1983). Earthquake-generating reverse fault at A; earthquake-generated faults at B produced by renewed folding of syncline.

ing basement rocks rather than faults produced by flexural-slip folding.

Field evidence suggests that at least the larger flexural-slip faults at Giles Creek and Blackball in the Grey-Inangahua Basin are coseismic (Yeats, in press). The flexural-slip faults at both these localities face west, up the depositional slope of the outwash surfaces that they cut (Figure 4.2). The surface at Giles Creek is grooved by braided channels that formerly carried outwash gravels from glaciers on the east side of the Paparoa Range. After abandonment of the outwash surface, the braided channels remained, but they now carry only the runoff derived from the surface itself whereas formerly they carried detritus from the Paparoa Range. Most of the west-facing fault scarps are ungullied, even though they are very old; the faults cut surfaces more than 100,000 yr old (Suggate, 1965; Nathan, 1978b; R. P. Suggate, New Zealand Geological Survey, personal communication, 1984), but they do not cut an outwash surface at Blackball considered to be 18,000 to 23,000 yr old (Nathan, 1978b; Suggate, 1965; Suggate and Moar, 1970).

The ungullied west-facing scarps at Giles Creek are in contrast to extensively gullied east-facing scarps on the same surface, scarps presumably related to range-front faulting (Yeats, in press). Rill drainage down the old outwash channels dissects the scarps that face east, down the depositional slope, but collects at the base of the west-facing scarps, forming small bogs or small streams that drain parallel to the scarp and off the surface. The only west-facing scarps that are gullied are those in which scarp heights are relatively low, such as the southern parts of scarps B and D of Suggate (1957) and scarp C of Young (1963). If the west-facing scarps had formed by aseismic creep on flexural-slip faults, the rill drainage should have been able to maintain itself across the slowly rising fault scarps (Figure 4.2), just as it does when scarp height is very low. However, the drainage is blocked by the scarps, suggesting that the scarps formed suddenly, accompanying an earthquake. To be ungullied by the drainage, a scarp must appear instantaneously and must be high enough that the former drainage, even at maximum stream flow, is unable to overtop the new scarp. The flexural-slip fault scarps northeast of Santa Paula, California, face up the depositional slope of the fans that they cut (Figure 4.3), but the high initial slope of the fan surface and the high-volume stream flow under the occasional torrential rainfall experienced in southern California result in gullying of the newly formed scarps, even if they do form suddenly.

## BENDING-MOMENT FAULTS

Deformation of a flexed layer can be treated as bending an elastic plate around a fold axis. If the plate is bent by equal and opposite moments applied at its ends, the convex side is lengthened and placed in tension, and the concave side is shortened and placed in compression (Figure 4.6; cf. photoelastic experiments of Currie *et al.*, 1962). The compression and tension of the sides are produced by a couple or bending moment (Johnson, 1970, pp. 41-50). Between that portion of the plate in compression and that portion in tension, there is a neutral surface on which there is neither compression nor tension (Figure 4.6). The strain within a bent plate is approximately proportional to the distance from the neutral surface and inversely proportional to the radius of curvature of the plate.

On the convex surface, the minimum principal compressive stress ($\sigma_3$) is tangent to the plate surface but perpendicular to the axis of bending, whereas on the concave surface, the maximum principal compressive stress ($\sigma_1$) has this orientation. If the neutral surface is located at the center of the plate, the deviatoric stress ($\sigma_1 - \sigma_3$) is zero at the neutral surface and maximum at the convex and concave surfaces. If the beam is structurally isotropic and homogeneous, and folding is upright, initial rupture above the yield stress will be by extension fractures or normal faults at the convex surface and by reverse faults at the concave surface (Figure 4.6). These faults are small scale because they extend to no greater depth than the neutral surface of the flexed plate. Such faults should not be capable of large earthquakes if the flexed plate is a sedimentary bed of low strength and the radius of curvature of the flexure is relatively small.

The importance of bending-moment faults in seismic-risk evaluations is in the fact that these faults are likely to

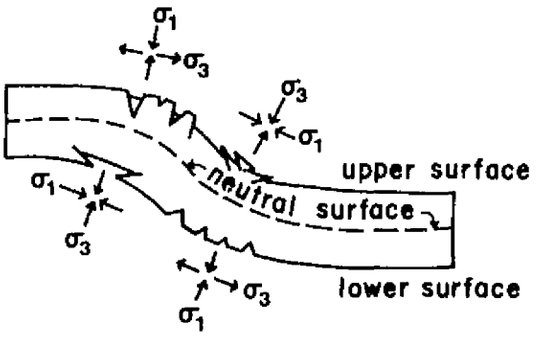


FIGURE 4.6 Bending moment faults developed on the concave and convex sides of a flexed layer. Faults should occur on both upper and lower surfaces, but they have only been observed on upper surface.

be encountered in trenches across scarps suspected of being faults. The trench is dug with the strategy of encountering late Quaternary deposits cut by a suspected fault. To be recognized as bending-moment faults, fault displacement must be normal on the convex side of a fold and reverse on the concave side. Two examples from trench investigations follow.

The Ventura Fault in the Ventura Basin of California forms a linear, south-facing scarp that trends eastward along the foot of the hills bordering the city of Ventura on the north (Sarna-Wojcicki *et al.*, 1976). In east Ventura, the scarp diverges from the foothills and maintains an easterly strike whereas the edge of the hills trends more to the east-northeast (Figure 4.7). In this area, the surface of the Harmon alluvial fan is cut by a south-facing scarp attributed to the Ventura Fault. The scarp forms the boundary between an uplifted bench of older deformed deposits on the north and young undeformed sediments on the south (Sarna-Wojcicki *et al.*, 1976). The seismotectonic setting of this fault in a region of north-south horizontal contraction predicts that it should have reverse displacement. However, two trenches across the Ventura scarp (Figure 4.7) show several normal faults that offset all but latest Holocene sediments (Sarna-Wojcicki *et al.*, 1976; Gardner and Stahl, 1977). The normal faults are concentrated in the flexed region and are interpreted as bending-moment faults. These faults are secondary features apparently produced by displacement on the subjacent Ventura Fault. Age of youngest sediments displaced by the normal faults can be assumed to date the latest movement on the Ventura Fault, but the orientation and sense of displacement on these normal faults cannot be extrapolated to infer sense of displacement on the Ventura Fault.

In the city of Camarillo, south of Ventura, trenches dug by Geotechnical Consultants, Inc., across a linear, south-facing scarp (Gardner, 1982) were dug to shed light on late Quaternary movement history of the Camarillo Fault, a north-side-up member of the Simi reverse-fault system (Figure 4.8). The trenches (Figure 4.8) revealed an increase in south dip northward toward the scarp, but instead of a high-angle reverse fault dipping north, a low-angle, north-dipping reverse fault and a set of high-angle, south-dipping reverse faults were found. These faults are interpreted as being produced by bending moment on the concave side of a monoclinal bend in Quaternary sediments that are either draped over a buried fault or are part of a pressure ridge. This interpretation makes it unlikely that the faults exposed in the trenches are seismogenic, and it also implies that the trenches provide no evidence about whether the Camarillo Fault itself is seismogenic. As in the case of the Ventura Fault, the youngest sediments warped across the scarp or cut by bending-moment faults can be assumed to have been deposited prior to latest movement on the subjacent Camarillo Fault.

Bending-moment faults are also found at Toppenish Ridge, an east-trending anticline in Miocene basalts and Quaternary sediments in south-central Washington State (Campbell and Bentley, 1981; Figure 4.9). On the north side of Toppenish Ridge, surface ruptures near the hinge of the overturned Satus Peak anticline in basalt cut late Quaternary alluvium and landslide material. These ruptures were interpreted by Campbell and Bentley (1981) as related to bending moment in the hinge of the fold. The hinge of the overturned syncline immediately to the north is characterized by thrust faults that cut Quaternary alluvium. Campbell and Bentley (1981) interpreted these as the surface expression of a décollement thrust (Mill Creek thrust) passing underneath the anticline. I consider it to be more likely that they are due to bending moment on the concave side of the syncline.

Finally, Philip and Meghraoui (1983) present evidence that normal faulting on the hanging wall of the 1980 El Asnam thrust fault (Figure 4.10) is produced by bending moment as the strata in the hanging wall are folded. These are called "extrados fractures" by Philip and Meghraoui (1983). In addition to normal faults, tension cracks appear close to the surface with edges vertically offset and with dip-slip slickensides. Two cases are presented. Where thrusting is dip-slip (Figure 4.10A and 4.10B), normal faults are parallel to the thrust fault trace and to the anticlinal axis. Where thrusting is oblique-slip (Figure 4.10C and 4.10D), the normal-fault grabens develop at an angle to the thrust fault trace and the anticlinal axis. In plan view, they resemble pull-apart basins. The extension is due not only to anticlinal bending but also to left-oblique slip in the hanging wall. As in the case of the bedding-slip faults at Kef el Mes, these faults are low-seismic although they are coseismic—that is, they are part of the deformation accompanying a major thrust-fault earthquake, but they themselves do not deform strata that are strong enough to store much elastic strain energy.

## FOLDS RELATED TO FAULTING

The discussion above has concentrated on faults that are by-products of folding. They are near-surface structures, hence they are small scale and unlikely to generate large earthquakes. However, the flexural-slip and bending-moment faults at El Asnam accompanied the 1980 earthquake (Philip and Meghraoui, 1983). They accompanied near-surface folding that was itself a by-product

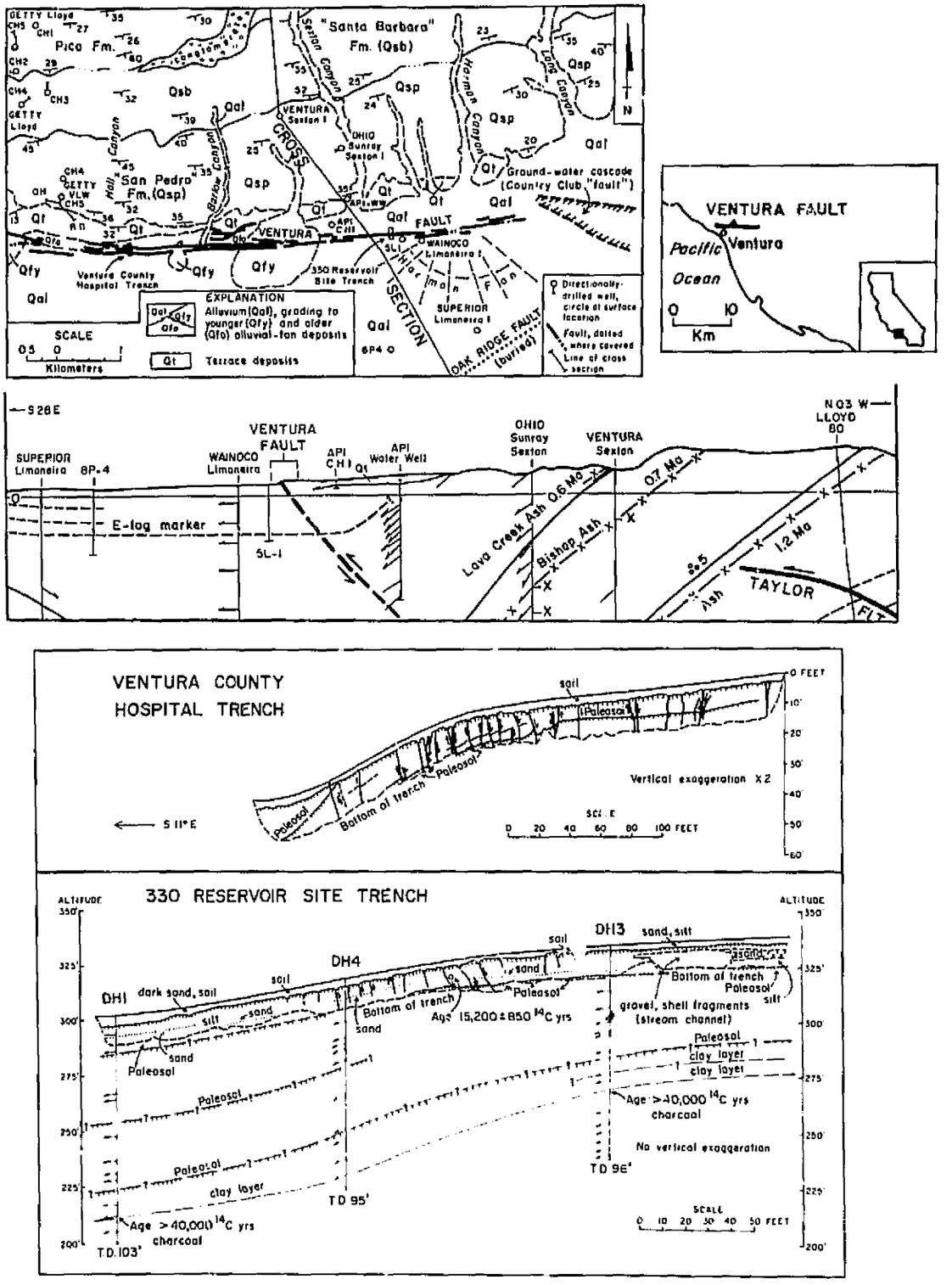


FIGURE 4.7 Sketches of two trenches across Ventura Fault simplified from Sarna-Wojcicki *et al.* (1976) and Geotechnical Consultants, Inc. Ventura Fault is expressed as a flexure with slopes and dips steeper than areas to the north and south. Hospital trench has vertical exaggeration ×2; reservoir trench has no vertical exaggeration. In both trenches, fractures are concentrated where strata are flexed. Most fractures are normal faults or soil-filled extension fractures, as would be expected if fractures are related to bending moment.

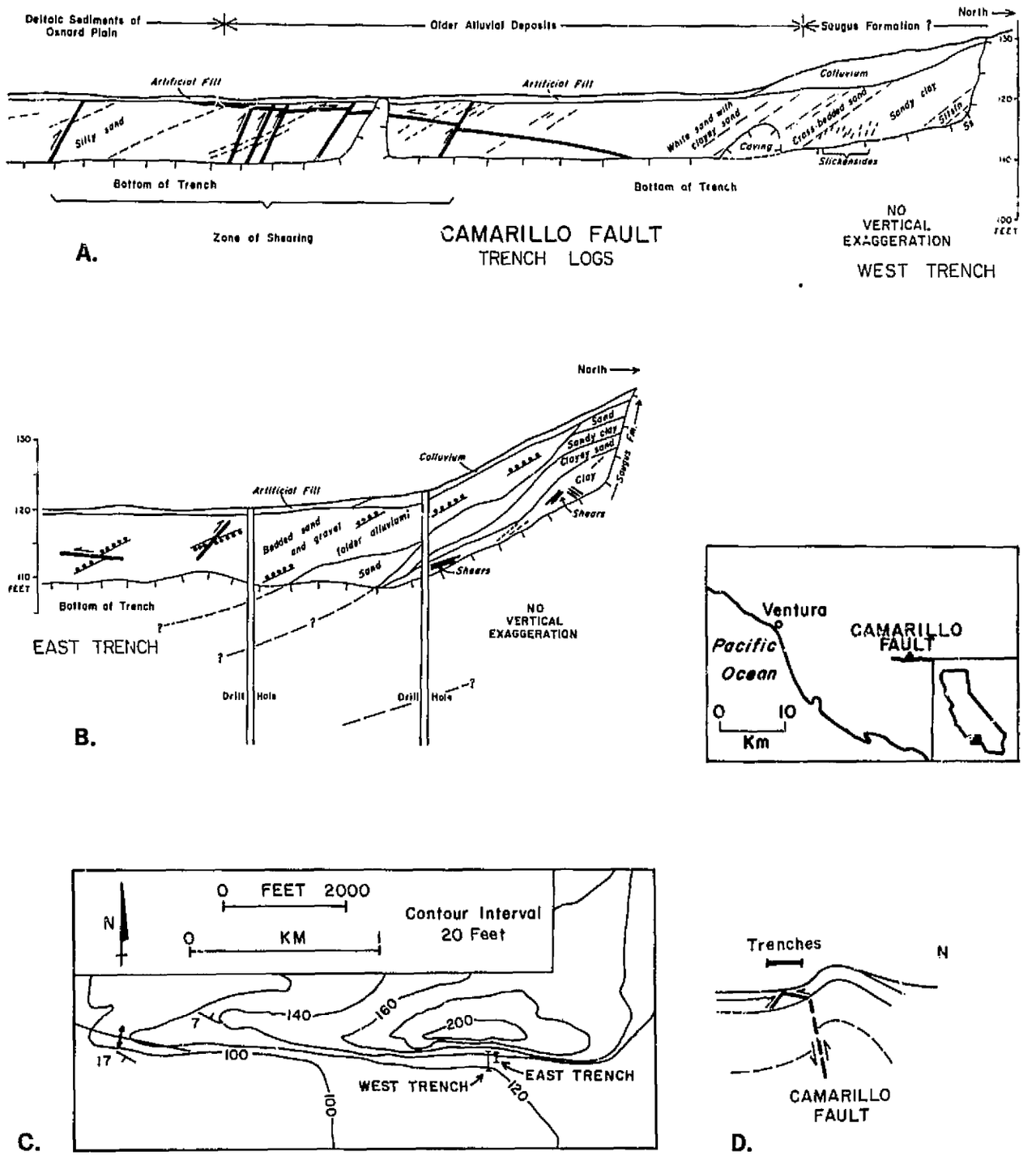


FIGURE 4.8 A and B, Simplified sketches of trenches across Camarillo Fault, after D. A. Gardner (1982; unpublished technical reports by Geotechnical Consultants, Inc.). No vertical exaggeration. C, Topography of ridge in downtown Camarillo from U.S. Geological Survey Camarillo 7 ½-minute quadrangle, locating two trenches. Camarillo Fault is presumed to control steep south flank of this ridge. D, Sketch of presumed relation between bending-moment faults in trenches and subjacent Camarillo Fault.

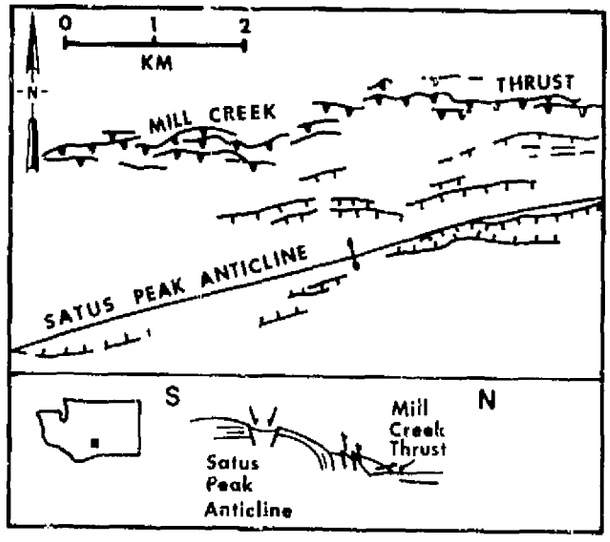


FIGURE 4.9 Tectonic sketch and diagrammatic cross section of Satus Peak anticline at Toppenish Ridge, Washington, redrawn and modified from Campbell and Bentley (1981). Sawteeth mark the hanging-wall side of reverse faults; ticks mark the hanging-wall side of assumed normal faults.

of a deep-seated left-lateral reverse fault that generated the 1980 mainshock (Philip and Meghraoui, 1983) (Fault A of Figure 4.5). In a similar fashion, the folds generating the flexural-slip faults in the Grey-Inangahua Basin, New Zealand, may themselves be related to deep-seated reverse faulting at the margin of the Paparoa Range (Figure 4.1). The seismogenic Newport-Inglewood Fault in the Los Angeles Basin, California, is for the most part not exposed at the surface. The fault cuts basement rocks, but the fault zone is expressed at the surface as *en echelon* anticlines formed as pressure ridges along the fault (Barrows, 1974; Yeats *et al.*, 1981). Near Ventura, California, the Montalvo Mounds are late Quaternary anticlinal ridges that mark the surface expression of the Oak Ridge high-angle reverse fault that does not itself reach the surface (Yeats *et al.*, 1981).

The May 1983 earthquake at Coalinga, California ($M_S$ = 6.5), did not rupture the ground surface (although one aftershock did) but instead augmented a fold at Anticline Ridge, as based on geodetic data (Stein and King, 1984). Deformation of the stream bed of Los Gatos Creek, an antecedent stream that cuts across the

FIGURE 4.10 Coseismic bending-moment faults associated with 1980 El Asnam earthquake, after Philip and Meghraoui (1983). Displacement on the main seismogenic thrust fault was accompanied by anticlinal folding in the hanging wall, which was itself accompanied by grabens along the anticlinal crest. These grabens are parallel to the anticlinal crest (A, B) or oblique to the anticlinal crest and stepped right where thrusting had a left-slip component (C, D). Map symbols: 1, normal fault; 2, tensile crack; 3, *en echelon* cracks; 4, thrust faults and pressure ridges; 5, attitude of dipping bed; 6, attitude of horizontal bed.

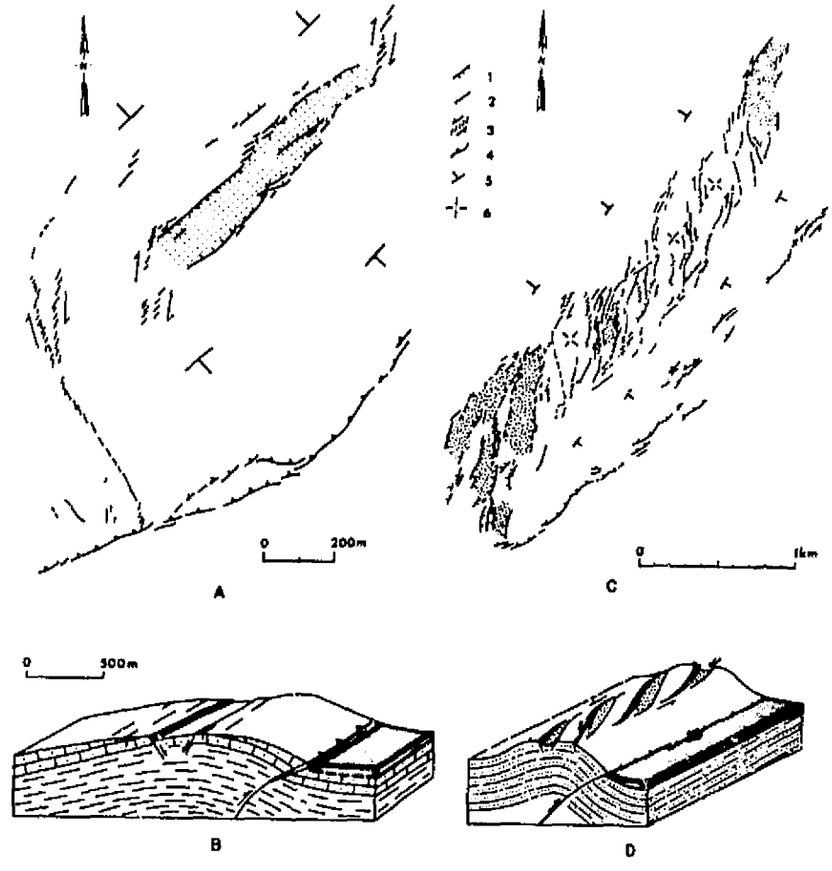

anticline, and an alluvial fan surface indicates that folding similar to the 1983 event has been taking place for the past 2500 to 10,000 yr at a rate of surface uplift of 1 to 4 mm/yr. The folding resembles that of subjacent strata and indicates that the folding may have been taking place for at least the past 2 m.y. Stein and King (1984) modeled the folding as having been generated by a reverse fault with a slip rate of 3 to 12 mm/yr based on the deformation of Los Gatos Creek and 1 to 4 mm/yr based on the deformation of underlying strata. Folding is coseismic with an average recurrence interval of earthquakes the size of the 1983 event of 200 to 1500 yr (Stein and King, 1984). In dissent, Hill (1984) noted the failure of the 1983 aftershocks to define a subsurface fault plane. Focal mechanisms of 10 earthquakes at Coalinga have nodal planes that are parallel to folded bedding at the epicenter of each event, leading Hill (1984) to suggest that the Coalinga earthquake was produced by deep-seated flexural-slip folding.

## ACTIVE TECTONICS OF ON-LAND FOLD-AND-THRUST BELTS

Flexural-slip faults and bending-moment faults are secondary features related to flexural-slip folding, which itself characterizes foreland fold-and-thrust belts. Davis *et al.* (1983) developed their mechanical model from a study of western Taiwan (cf. Suppe and Wittke, 1977; Suppe and Namson, 1979; Suppe, 1980a,b, 1981; Namson, 1982). The active-tectonic setting of fold-and-thrust belts is illustrated in this paper by a discussion of the active foreland thrust belt of northern Pakistan and India, part of the Himalayan convergence zone between the Indian and Eurasian plates, and the central Ventura Basin of California, where the convergence zone is limited in length, apparently controlled by the big bend of the San Andreas Fault. These two regions offer the possibility of determining rates of convergence directly from the geologic record.

Active foreland thrusting occurs on a continental scale in the foothills of the Himalaya as the Indian shield is overridden by its own northern margin in a series of south-verging thrusts (Yeats and Lawrence, 1984). The Precambrian Indian shield slopes gently northward beneath the Indo-Ganges floodplain and is overlain by flat-lying molasse deposits (Siwalik Group), which are older versions of the modern drainage system (Figure 4.11). In India, the alluvial plain consists of a northern domain in which large rivers break out of the mountains and flow south across broad distributary fans, a central domain in which the south-flowing streams merge with the east-southeastward flow of the main Ganges River and flow parallel to the Himalayan front, and a southern domain in which small-volume rivers flow northward from the Indian shield into the Ganges (Geddes, 1961; Figure 4.11A). The depositional axes of Pleistocene and older Siwalik molasse basins are parallel to the Ganges River but north of it; the older the molasse, the farther north its depositional axis (Acharyya and Ray, 1982). The molasse basins are forced southward owing to the southward advance of Himalayan thrust sheets such that it may be possible at a given site to progress upsection from southerly, shield-derived sediments to northerly, Himalaya-derived sediments (Figure 4.11B; Tandon, 1976; Parkesh *et al.*, 1980) and finally to the appearance of the thrust sheets themselves. Lyon-Caen and Molnar (1985) suggested that the age of the basal molasse sediments overlying the Indian Shield decreases southward at a rate of 10-15 mm/yr.

Active faults are found in the interior of the Himalaya of Nepal and India as well as the southern mountain front, but only the mountain-front fault (Himalayan Frontal thrust) shows north-over-south thrusting (Nakata, 1972, 1982; Nakata *et al.*, 1984). Major thrusting in the Kathmandu intermontane basin predates deposition of the Lukundol Formation, which is Pliocene in age as based on magnetostratigraphy and vertebrate fossils (Yoshida and Igarashi, 1984; M. Yoshida, personal communication, 1984).

The southward advance of décollement thrusting may be better calibrated in northern Pakistan (Figure 4.12) where the molasse basin is wider and subsurface evidence more abundant. New thrusts appear within the previously undeformed foreland sediments resting on top of the northward-sloping Indian shield. The Salt Range overrides its own fan material and alluvium along the newest thrust—the Salt Range thrust of late Quaternary age—and most of the major deformation is younger than 0.4 m.y. ago (Ma) (Yeats *et al.*, 1984; Point A, Figure 4.12). Farther north, near Rawalpindi, major deformation is dated as between 1.9 and 2.1 Ma on the basis of molasse deposits calibrated by magnetostratigraphy and tephrochronology above and below the major angular unconformity (Raynolds and Johnson, in press) (point B, Figure 4.12), and the Soan syncline began to control deposition about 3 Ma (Raynolds, 1980). The distance between points A and B projected perpendicular to strike is 100 km, and the age difference between the end of deposition of subsequently deformed molasse deposits at the two points (2.1-0.4 Ma) is 1.7 m.y., a rate of southward migration of deformation of 60 mm/yr. Farther north, at the southern edge of the Peshawar Basin (point C, Figure 4.12), major thrusting predates deposition of nonmarine deposits as old as 2.8 Ma as dated by magnetostratigraphy and tephrochronology (Burbank, 1983; Burbank and Tahirkheli, 1985; Yeats and Hussain, 1985). The distance between points B and C projected perpendicular to strike is 70 km, and

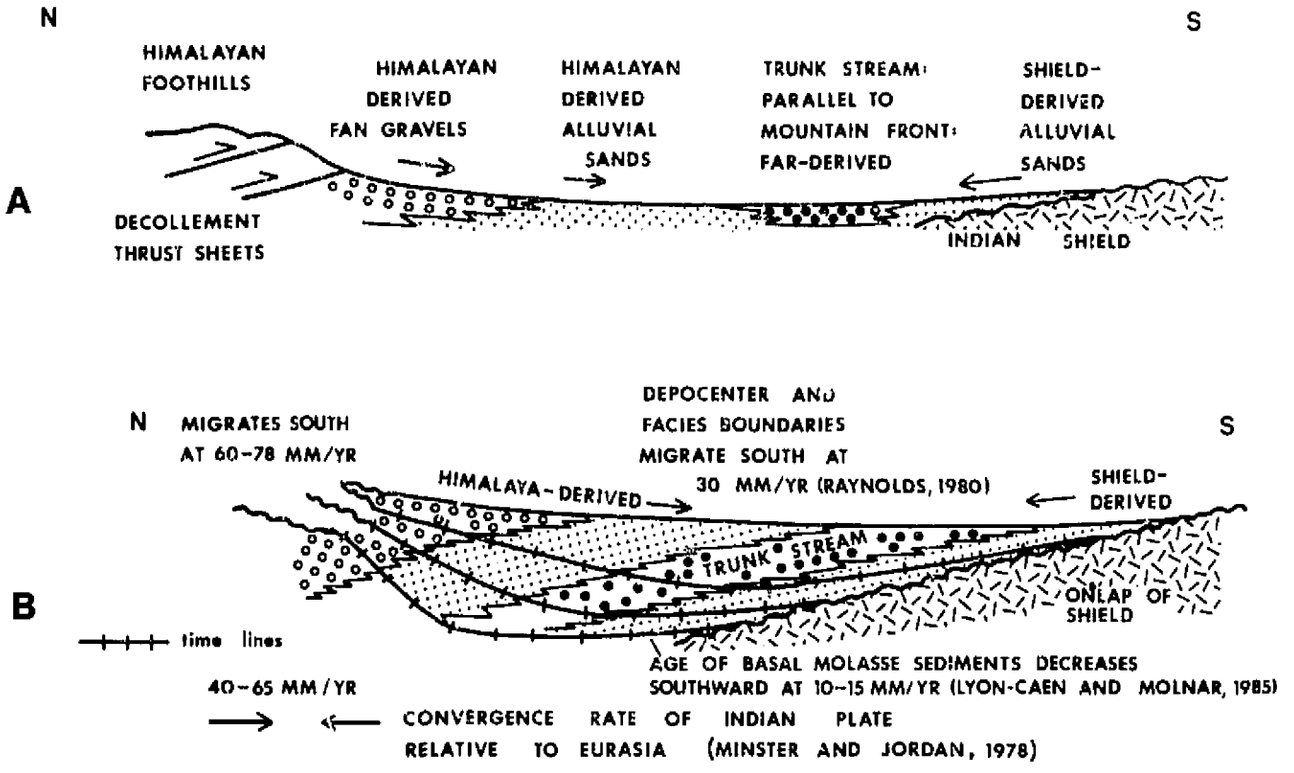


FIGURE 4.11 A, Typical profile of the Himalayan thrust front and molasse sediments controlled by it. The Himalaya undergoes uplift as a consequence of foreland thrusting, shedding sediments into the flanking molasse basin. These side tributaries are collected by a master stream (Indus, Jhelum, Ganges) flowing parallel to mountain front. Tributaries on the south are derived from Indian shield. B, Southward migration of deformation front and sedimentary facies boundaries of molasse due to advancing foreland thrust sheets, compared to plate convergence rate. Depocenters and facies migrate south at 30 mm/yr (Raynolds, 1980), basal molasse sediments become younger southward at 10-15 mm/yr (Lyon-Caen and Molnar, 1985), and deformation as dated by angular unconformities migrates south at a poorly controlled rate of 60-78 mm/yr.

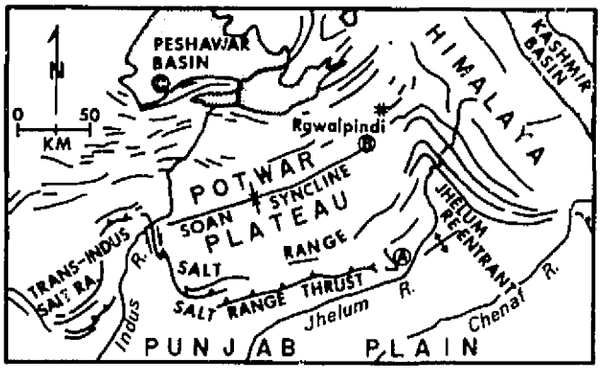


FIGURE 4.12 Tectonic map of southern margin of Himalaya in northern Pakistan. Intermontane basins are shaded. Points A, B, and C are localities where age of major deformation may be dated; see text. Sawteeth mark late Quaternary thrusts; arrows mark late Quaternary strike-slip fault.

the age difference between the oldest deposits after major deformation at the two points (2.8-1.9 Ma) is 0.9 m.y., a southward younging of 78 mm/yr. Those rates imply that new thrusts appear and propagate in the previously undeformed molasse basin at rates higher than the convergence between the Indian and Eurasian plates.

Southward migration of the Siwalik foredeep in the Jhelum re-entrant, eastern Potwar Plateau, as based on southward progradation of conglomerate facies (Raynolds, 1980), takes place at a rate of 30 mm/yr. This progradation was influenced by increased uplift rates in the source areas as well as southward advance of Himalayan thrust sheets, so the rate of advance of thrust sheets would be less than 30 mm/yr. These rates may be compared with the northward motion of the Indian plate with respect to Eurasia of 40 mm/yr at the western end of the Himalaya to 65 mm/yr at the eastern end (Minster and Jordan, 1978). Either most of the conver-

gence between Eurasia and India is being accommodated at the southern margin of the thrust belt rather than being more uniformly distributed between the thrusts at the southern margin and more interior and more poorly dated thrust zones, such as the Main Central Thrust, or southward propagation of thrusts takes place faster than the rate of plate convergence. The rate of underthrusting of India beneath the Himalaya is 18 mm/yr based on data from large earthquakes since the year 1900 (Molnar and Deng, 1984), suggesting that only part of the Indian-Eurasian convergence is being taken up within the Himalaya, with the remainder being taken up by escape-block tectonics farther north.

The Transverse Ranges of California are controlled by north-south contractile tectonics related to the big bend in the San Andreas Fault. In the Ventura Basin, continuous sedimentation throughout most of Quaternary time was strongly influenced by contractile tectonics. These sediments have been age-calibrated by tephrochronology, magnetostratigraphy, and radiometric dating (Izett *et al.*, 1974; Blackie and Yeats, 1976; Lajoie *et al.*, 1979, 1982; Liddicoat and Opdyke, 1981). Based on this calibration and on the construction of balanced cross sections across the Ventura Basin, the rate of convergence of the northern edge of the Ventura Basin against its southern edge is 23 mm/yr over the past 0.2 m.y. at Ventura (Yeats, 1983), over half the north-south component of Pacific-American plate motion in this area, which is 42 mm/yr (Bird and Rosenstock, 1984). Most of this shortening occurred across the Ventura Avenue anticline and the adjacent syncline to the north (Yeats, 1982).

The Ventura Avenue anticline contains a giant oil field with more than 1460 wells, resulting in an extensive, detailed data set on its internal structure (Figure 4.13). Prior to formation of the anticline, the Taylor low-angle thrust fault set began to form 1.3 Ma along a weak layer in the Pliocene turbidite sequence, moved up a 45° ramp, and stopped motion about 0.65 Ma. Maximum net slip rate was 2.8 mm/yr to the southeast (Yeats, 1983). Following the end of deposition of nonmarine coarse-grained strata of the San Pedro Formation about 0.2 Ma, the anticline began to buckle. The Ventura River was antecedent to this buckle, and uplift of the crest of the fold is calibrated by deformed river terraces that have been dated by $^{14}C$, with age extrapolations beyond the limits of $^{14}C$ dating based on a soils chronosequence (Keller *et al.*, 1982; Rockwell, 1983). Uplift rates on the anticlinal crest were 4.3 to 5.2 mm/yr for the last 29,600 yr, 10.5 to 11.5 mm/yr from 80,000 to 29,600 yr ago, and 15 to 16 mm/yr from 200,000 to 80,000 yr ago (Keller *et al.*, 1982). Rockwell (1983) demonstrated that a rootless buckle fold formed by end loading would undergo rapid displacement normal to its loading direction early in its formation, and this displacement would slow down as the fold became more fully developed [Rockwell, 1983; Yeats, 1983; cf. theoretical considerations by Currie *et al.* (1962) and Adams (1984)]. The fold is still under high horizontal stress because it is overpressured, with the ratio of fluid pressure to overburden pressure increasing from 0.55 to 0.8 as radius of curvature decreases from 300 to 30 m in the core of the fold (Yeats, 1983).

If the fold is still undergoing contraction as uplift of its crest continues at a decreasing rate, how is this contraction being accommodated? The limbs may still be steepening, but an alternative way to accommodate contraction may be the Ventura Fault (Figure 4.7). The south-facing fault scarp occurs at the sharp boundary between flat-lying strata of the Santa Clara syncline and south-dipping strata of the south flank of the Ventura Avenue anticline. This sharp boundary dips 45° north to depths of several kilometers and is planar, and it is assumed that this boundary is the Ventura Fault at depth (Figures 4.7 and 4.13). It is younger than most of the folding because it is planar, in contrast to other reverse faults that curve over the crest of the anticline and, therefore, formed as low-angle thrusts during the early stages of folding (Figure 4.13). Although the fault scarp is linear and well documented, subsurface well correlations indicate little or no stratigraphic separation across the fault. As shown in Figures 8, 10, and 11 of Yeats (1982), horizons can be correlated across the fault with a sharp change in dip, but no displacement. This led me to propose earlier that the Ventura Fault formed by bending moment (Yeats, 1982), a conclusion that is probably wrong. My present view is that the fault formed so recently that it has not had time to accumulate enough displacement to be documented without ambiguity in the subsurface. The evidence for this is the planar nature of the boundary between flat-lying and steeply dipping strata. The Ventura Avenue fold may have acquired a configuration that is stable to continued horizontal stress if there is a zone south of the fold along which further displacement may take place. If displacement occurs by southward sliding of the Pliocene-Pleistocene turbidite sequence over a subjacent Miocene ductile sequence, this displacement may break through to the surface as the Ventura Fault, as illustrated in the inset to Figure 4.13.

## SOCIETAL IMPLICATIONS OF ACTIVE FAULTS AND FOLDS

Yeats *et al.* (1981) suggested that flexural-slip faults of the Ventura Basin would cause ground-rupture prob-

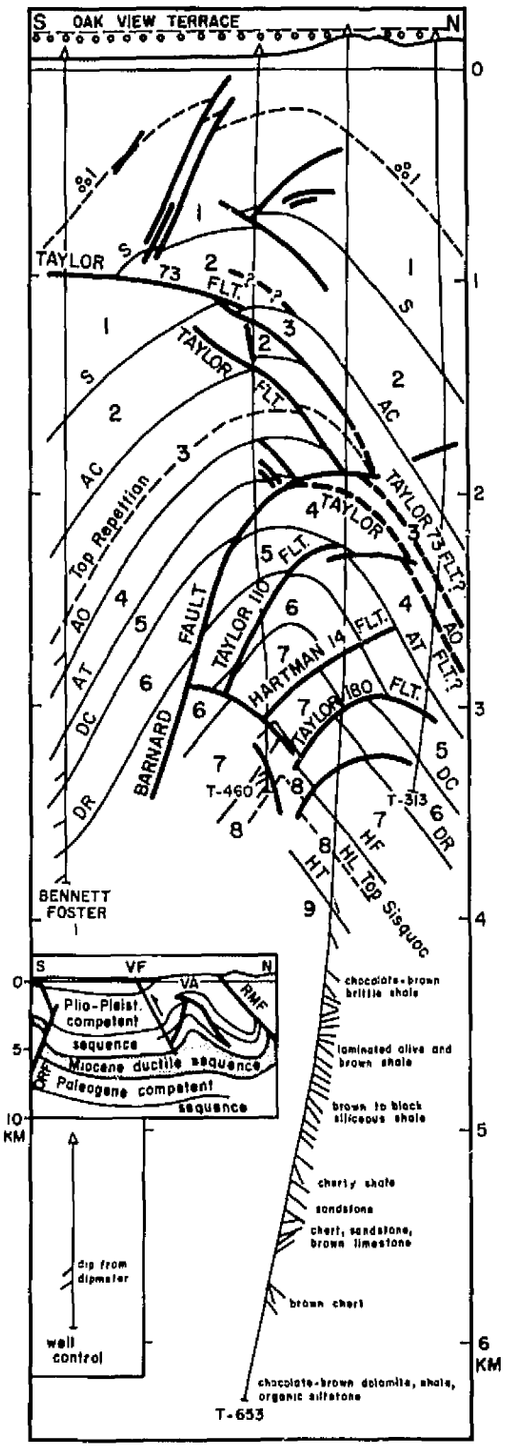


FIGURE 4.13 North-south cross section across Ventura Avenue anticline near Ventura River, showing the 6553 m deep test well, Shell-Taylor 653 (T-653). In inset: ORF, Oak Ridge Fault; RMF, Red Mountain Fault; VA, Ventura Avenue anticline; VF, Ventura Fault. Oak View terrace dated as 32,000 yr before present.

lems, but would not result in large earthquakes with major seismic shaking. These faults curve into bedding in flexural-slip folds, and they do not extend downward into rocks of such high strength that sudden release of stored elastic strain energy would cause a large earthquake. The 1981 Lompoc earthquake showed that flexural-slip faults are not aseismic, and Yeats (1982) referred to them as *low-shake faults*. Bending-moment faults are also low-shake faults, as are at least some thrust faults involving only the sedimentary cover.

But all known historical examples of bending-moment and flexural-slip faults accompany earthquakes, so if they are low-seismic, they are also coseismic. There are no known examples of flexural-slip faults forming by creep. The Giles Creek, New Zealand, flexural-slip faults show evidence of at least two episodes of faulting within a few thousand years, then no evidence of additional faulting in the last 20,000 yr, despite the fact that the Grey-Inangahua Basin where they occur produced a large earthquake in 1968. Flexural-slip faults (and perhaps bending-moment faults as well) that cut late Quaternary deposits may be used to monitor the recurrence of stick-slip faulting on subjacent seismogenic faults that may not cut late Quaternary deposits. The relations between coseismic flexural-slip and bending-moment faults to the seismogenic El Asnam thrust are instructive to this point. The flexural-slip faults northeast of Santa Paula, California, may provide information about movement on the nearby San Cayetano Fault (Figure 4.3), and the flexural-slip faults in the Grey-Inangahua Basin may document displacement on seismogenic reverse faults bounding the basin on the west. Finally, the coseismic growth of the Anticline Ridge anticline during the 1983 Coalinga, California, earthquake may provide information on the recurrence interval of a subjacent seismogenic reverse fault.

An implication of the mechanical model of Davis *et al.* (1983) is that folds in active fold-and-thrust belts are likely to be overpressured, and Davis *et al.* (1983) summarize evidence that overpressured folds exist in subaerial fold-and-thrust belts in Taiwan and the Himalaya and in submarine accretionary wedges adjacent to the Middle America, Aleutian, and eastern Caribbean trenches and off the coasts of Oregon and the Pakistani Makran. The Ventura Avenue anticline, in a somewhat similar contractile environment, is perhaps the most extensively documented overpressured structure in the world. Future oil exploration in active fold-and-thrust belts offshore and onshore should expect overpressured reservoirs and adopt necessary techniques to prevent blowouts.

Another implication of the model of Davis *et al.* (1983) is that folds migrate out toward the edge of the

fold belt, and therefore the most frontal folds and thrusts are most likely to be still growing. Accordingly, ground rupture is most likely in these frontal structures and less likely in those structures farther back. However, even these more internal structures are likely to be overpressured, and changes of fluid pressure due to water flooding may produce failure, because the tapered wedge is assumed to be on the verge of shear failure throughout (Davis *et al.*, 1983).

Where the basal décollement in fold-and-thrust wedges is composed of material that deforms plastically, displacement may not be accompanied by large earthquakes. Where the basal décollement yields by Coulomb friction, its ability to produce large earthquakes may depend on the thickness of the wedge. Where the wedge is thick, very large earthquakes may occur (Seeber *et al.*, 1981).

## ACKNOWLEDGMENTS

My work has been supported principally by contracts from the Earthquake Hazards Reduction Program of the U.S. Geological Survey. Work in New Zealand was supported by the U.S. Geological Survey, by Grant INT-82-19897 from the National Science Foundation, and by Oregon State University. Work in Pakistan was supported by Grant INT-81-18403 from the National Science Foundation, and my visit to Japan was sponsored by Grant EAR-83-18194 from the National Science Foundation. R. P. Suggate reviewed an early draft to the paper.

## REFERENCES

Acharyya, S. K., and K. K. Ray (1982). Hydrocarbon possibilities of concealed Mesozoic-Paleogene sediments below Himalayan nappes—reappraisal, *Am. Assoc. Petrol. Geol. Bull. 66*, 57-70.

Adams, J. (1984). Active deformation of the Pacific Northwest continental margin, *Tectonics 3*, 449-472.

Anderson, H. J. (1979). A geophysical study of the Westport, Inangahua and Murchison Basins, west coast South Island, Geophysics Division (New Zealand) Department of Scientific and Industrial Research Report 148, 53 pp.

Barrows, A. A. (1974). A review of the geology and earthquake history of the Newport-Inglewood structural zone, southern California, *Calif. Div. Mines Geol. Spec. Rep. 114*, 115 pp.

Berberian, M. (1981). Active faulting and tectonics of Iran, in *Zagros-Hindu Kush-Himalaya Geodynamic Evolution*, H. K. Gupta and F. M. Delany, eds., Am. Geophys. Union Geodynamics Series, Vol. 3, Washington, D.C., pp. 33-69.

Bird, P., and R. W. Rosenstock (1984). Kinematics of present crust and mantle flow in southern California, *Geol. Soc. Am. Bull. 95*, 946-957.

Blackie, G. W., and R. S. Yeats (1976). Magnetic reversal stratigraphy of Pliocene-Pleistocene producing section of Saticoy oil field, Ventura Basin, California, *Am. Assoc. Petrol. Geol. Bull. 60*, 1985-1992.

Boyes, W. S. (1971). Horizontal and vertical crustal movement in the Inangahua earthquake of 1968, in Recent Crustal Movements, B. W. Collins and R. Fraser, eds., *R. Soc. N.Z. Bull. 9*, 61-72.

Burbank, D. W. (1983). The chronology of intermontane-basin development in the northwestern Himalaya and the evolution of the Northwest Syntaxis, *Earth Planet. Sci. Lett. 64*, 77-92.

Burbank, D. W., and R. A. K. Tahirkheli (1985). The magnetostratigraphy, fission-track dating, and stratigraphic evolution of the Peshawar intermontane basin, northern Pakistan, *Geol. Soc. Am. Bull. 96*, 539-552.

Byerlee, J. (1978). Friction of rocks, *Pure Appl. Geophys. 116*, 615-626.

Campbell, N. P., and R. D. Bentley (1981). Late Quaternary deformation of the Toppenish Ridge uplift in south-central Washington, *Geology 9*, 519-524.

Chapple, W. M. (1978). Mechanics of thin-skinned fold-and-thrust belts, *Geol. Soc. Am. Bull. 89*, 1189-1198.

Cluff, L. S., *et al.* (1981). Seismic safety review of the proposed liquefied natural gas facility, Santa Barbara County, California, Report to California Public Utilities Commission by Liquefied Natural Gas Seismic Review Panel, 4 pp.

Currie, J. B., H. W. Patnode, and R. P. Trump (1962). Development of folds in sedimentary rocks, *Geol. Soc. Am. Bull. 73*, 655-674.

Davis, D., J. Suppe, and F. A. Dahlen (1983). Mechanics of fold-and-thrust belts and accretionary wedges, *J. Geophys. Res. 88*, 1153-1172.

Elliott, D. (1976). The motion of thrust sheets, *J. Geophys. Res. 81*, 949-963.

Gardner, D. A. (1982). Seismic/ground rupture hazards associated with the Camarillo Fault, in *Neotectonics in Southern California*, J. D. Cooper, compiler, Cordilleran Section, Geol. Soc. Am. field trip guidebook, pp. 59-60.

Gardner, D. A., and I. Stahl (1977). Geotechnical-seismic investigation of the proposed 330 Zone Water Storage Reservoir and Water Conditioning Facilities Site for the City of San Buenaventura, California, Report V77151, Geotechnical Consultants, Inc., 19 pp., 2 plates, 2 appendices.

Geddes, A. (1961). The alluvial morphology of the Indo-Gangetic Plain: Its mapping and geographical significance, *Trans. Inst. Brit. Geogr. 29*, 253-276.

Hill, M. L. (1984). Earthquakes and folding, Coalinga, California, *Geology 12*, 711-712.

Hubbert, M. K., and W. W. Rubey (1959). Role of fluid pressure in mechanics of overthrust faulting: I. Mechanics of fluid-filled solids and its application to overthrust faulting, *Geol. Soc. Am. Bull. 70*, 115-166.

Izett, G. A., C. W. Naeser, and J. D. Obradovich (1974). Fission track age of zircon from an ash bed in the Pico Formation (Pliocene-Pleistocene) near Ventura, California, *Geol. Soc. Am. Abstr. Programs 6*, 197.

Johnson, A. M. (1970). Physical processes in geology, Freeman, Cooper & Co., San Francisco, Calif., 577 pp.

Kaizuka, S. (1967). Rate of folding in the Quaternary and the present, *Geogr. Rep. Tokyo Metropolitan Univ. 2*, 1-10.

Keller, E. A., T. K. Rockwell, M. N. Clark, G. R. Dembroff, and D. L. Johnson, (1982). Tectonic geomorphology of the Ventura, Ojai and Santa Paula areas, western Transverse Ranges, California, in *Neotectonics in Southern California*, J. D. Cooper, compiler, Cordilleran Section, Geol. Soc. Am. field trip guidebook, pp. 25-42.

Lajoie, K. R., J. P. Kern, J. F. Wehmiller, G. L. Kennedy, S. A. Mathieson, A. M. Sarna-Wojcicki, R. F. Yerkes, and P. F. McCrory

(1979). Quaternary marine shorelines and crustal deformation, San Diego to Santa Barbara, California, in *Geological Excursions in the Southern California Area*, P. L. Abbott, ed., San Diego State University, Calif., pp. 3-15.

Lajoie, K. R., A. M. Sarna-Wojcicki, and R. F. Yerkes (1982). Quaternary chronology and rates of crustal deformation in the Ventura area, California, in *Neotectonics in Southern California*, J. D. Cooper, compiler, Cordilleran Section, Geol. Soc. Am. field trip guidebook, pp. 43-51.

Lensen, G. J. (1968). Analysis of progressive fault displacement during downcutting at the Branch River terraces, South Island, New Zealand, *Geol. Soc. Am. Bull. 79*, 545-556.

Lensen, G. J. (1976). Earth deformation in relation to town planning in New Zealand, *Int. Assoc. Eng. Geol. Bull. 14*, 241-247.

Lensen, G. J., and P. M. Otway (1971). Earthshift and post-earthshift deformation associated with the May 1968 Inangahua earthquake, New Zealand, in *Recent Crustal Movements*, B. W. Collins and R. Fraser, eds., *R. Soc. N.Z. Bull. 9*, pp. 107-116.

Lensen, G. J., and R. P. Suggate (1968). Inangahua earthquake—preliminary account of the geology, *N.Z. Dept. Sci. Ind. Res. Bull. 193*, 17-36.

Li, Y. H. (1976). Denudation of Taiwan island since the Pliocene epoch, *Geology 4*, 105-107.

Liddicoat, J. C., and N. D. Opdyke (1981). Magnetostratigraphy of sediments in the Atlantic Coastal Plain and Pacific Coast of the United States as an aid for dating tectonic deformation, Tech. Rep. Summary, Contract 14-08-0001-18377, U.S. Geol. Surv., Menlo Park, Calif.

Lyon-Caen, H., and P. Molnar (1985). Gravity anomalies, flexure of the Indian Plate, and the structure, support, and evolution of the Himalaya and Ganga Basin, *Tectonics 4*, 513-538.

Minster, J. B., and T. H. Jordan (1978). Present-day plate motions, *J. Geophys. Res. 83*, 5331-5354.

Molnar P., and Deng Qidong (1984). Faulting associated with large earthquakes and the average rate of deformation in central and eastern Asia, *J. Geophys. Res. 89*, 6203-6227.

Nakamura, K., and Y. Ota (1969). Study of active fold in Japan—a review, *Quaternary Res. (Tokyo) 7*, 200-211 (in Japanese).

Nakata, T. (1972). Geomorphic history and crustal movements of the foothills of the Himalayas, *Sci. Rep. Tohoku Univ. 7th Ser. (Geogr.) 22*, 39-177.

Nakata, T. (1982). A photogrammetric study on active faults in the Nepal Himalaya, *J. Nepal Geol. Soc. 2*, 67-80.

Nakata, T., S, Iwata, H. Yamanaka, H. Yagi, and H. Maemoka (1984). Tectonic landforms of several active faults in the western Nepal Himalayas, *J. Nepal Geol. Soc. 4*, 177-199.

Namson, J. (1982). Studies of the structure, stratigraphic record of plate interaction and role of pore-fluid pressure in the active fold and thrust belt of Taiwan and a study of manganese deposits from northern California, Ph.D. thesis, Princeton Univ., N.J., 302 pp.

Nathan, S. (1978a). Geol. Map of New Zealand 1:63360, Sheets S31 and pt. S32, Buller-Lyell, N.Z. Geol. Surv. map, report, 32 pp.

Nathan, S. (1978b). Geol. Map of New Zealand 1:63360, Sheet S44, Greymouth, N.Z. Geol. Surv. map, report, 36 pp.

Ota, Y. (1969). Crustal movements in the late Quaternary considered from the deformed terrace plains in northeastern Japan, *Jpn. J. Geol. Geogr. 40*, 41-61.

Ota, Y., and I. Suzuki (1979). Notes on active folding in the lower reaches of the Shinano River, central Japan, *Geogr. Rev. Jpn. 52*, 592-601 (in Japanese).

Otuka, Y. (1942). Active rock folding in Japan, *Proc. Imp. Acad. Jpn. 17*, 518-522.

Parkesh, B., R. P. Sharma, and A. K. Roy (1980). The Siwalik Group (molasse) sediments shed by collision of continental plates, *Sediment. Geol. 25*, 127-159.

Philip, H., and M. Meghraoui (1983). Structural analysis and interpretation of the surface deformations of the El Asnam earthquake of October 10, 1980, *Tectonics 2*, 17-49.

Ramsay, J. G. (1967). *Folding and Fracturing of Rocks*, McGraw-Hill Book Co., New York, 568 pp.

Raynolds, R. G. H. (1980). The Plio-Pleistocene structural and stratigraphic evolution of the eastern Potwar Plateau, Pakistan, Ph.D. thesis, Dartmouth Coll., Hanover, N.H.

Raynolds, R. G. H., and G. D. Johnson (in press). Rates of Neogene depositional and deformational processes, northwest Himalayan foredeep margin, Pakistan, *Geol. Soc. Lond.* (volume on Geochronology and the Geological Record).

Rockwell, T. K. (1983). Soil chronology, geology and neotectonics of the north central Ventura Basin, Ph.D. thesis, Univ. Calif., Santa Barbara, 424 pp.

Sarna-Wojcicki, A. M., K. M. Williams, and R. F. Yerkes, R. F. (1976). Geology of the Ventura Fault, Ventura County, California, *U.S. Geol. Surv. Misc. Field Studies Map MF-781*.

Seeber, L. (1983). Large scale thin-skin tectonics, *Rev. Geophys. Space Phys. 21*, 1528-1538.

Seeber, L., J. G. Armbruster, and R. C. Quittmeyer (1981). Seismicity and continental subduction in the Himalayan arc, in *Zagros-Hindu Kush-Himalaya Geodynamic Evolution*, H. K. Gupta and F. M. Delany, eds., Am. Geophys. Union Geodynamics Series, Vol. 3, Washington, D.C., pp. 215-242.

Stein, R. S., and G. C. P. King (1984). Seismic potential revealed by surface folding: 1983 Coalinga, California, earthquake, *Science 224*, 867-872.

Stöcklin, J. (1968). Structural history and tectonics of Iran: A review, *Am. Assoc. Petrol. Geol. Bull. 52*, 1229-1258.

Suggate, R. P. (1957). The geology of Reefton subdivision, *N.Z. Geol. Surv. Bull. 56*, 146 pp.

Suggate, R. P. (1965). Late Pleistocene geology of the northern part of the South Island, New Zealand, *N.Z. Geol. Surv. Bull. 77*, 91 pp.

Suggate, R. P., and N. T. Moar (1970). Revision of the chronology of the late Otira glacial, *N.Z. J. Geol. Geophys. 13*, 742-746.

Sugimura, A. (1967). Uniform rates and duration period of Quaternary earth movements in Japan, *J. Geosci. Osaka City Univ. 10*, 25-35.

Suppe, J. (1980a). A retrodeformable cross section of northern Taiwan, *Geol. Soc. China Proc. 23*, p. 46-55.

Suppe, J. (1980b). Imbricated structure of western foothills belt, south-central Taiwan, *Petrol. Geol. Taiwan 17*, 1-16.

Suppe, J. (1981). Mechanics of mountain building and metamorphism in Taiwan, *Geol. Soc. China Mem. 4*, 67-89.

Suppe, J., and J. Namson (1979). Fault-bend origin of frontal folds of the western Taiwan fold-and-thrust belt, *Petrol. Geol. Taiwan 16*, 1-18.

Suppe, J., and J. H. Wittke (1977). Abnormal pore-fluid pressure in relation to stratigraphy and structure in the active fold-and-thrust belt of north-western Taiwan, *Petrol. Geol. Taiwan 14*, 11-24.

Tandon, S. K. (1976). Siwalik sedimentation in a part of the Kumaon India, *Sediment. Geol. 16*, 131-154.

Yeats, R. S. (1982). Low-shake faults of the Ventura Basin, California, in *Neotectonics in Southern California*, J. D. Cooper, compiler, Cordilleran Section, Geol. Soc. Am. field trip guidebook, pp. 3-15.

Yeats, R. S. (1983). Large-scale Quaternary detachments in Ventura Basin, southern California, *J. Geophys. Res. 88*, 569-583.

Yeats, R. S. (in press). Faults related to folding, including examples from New Zealand, *R. Soc. N.Z. Bull.*

Yeats, R. S., and A. Hussain (1985). Timing of structural events in the

Himalayan foothills of northwestern Pakistan, *Geol. Soc. Am. Abstr. Programs 17*, 756.

Yeats, R. S., and R. D. Lawrence (1984), Tectonics of the Himalayan thrust belt in northern Pakistan, in *Marine Geology and Oceanography of Arabian Sea and Coastal Pakistan*, B. U. Haq and J. D. Milliman, eds., Van Nostrand Reinhold Co., New York, pp. 177-198.

Yeats, R. S., M. N. Clark, E. A. Keller, and T. K. Rockwell (1981). Active fault hazard in southern California: Ground rupture versus seismic shaking, *Geol. Soc. Am. Bull. 92* (Part I), 189-196.

Yeats, R. S., S. H. Khan, and M. Akhtar (1984). Late Quaternary deformation of the Salt Range of Pakistan, *Geol. Soc. Am. Bull. 95*, 958-966.

Yerkes, R. F., W. L. Ellsworth, and J. C. Tinsley (1983). Triggered reverse fault and earthquake due to crustal unloading, northwest Transverse Ranges, California, *Geology 11*, 287-291.

Yoshida, M., and Y. Igarashi (1984). Neogene to Quaternary lacustrine sediments in the Katmandu Valley, Nepal, *J. Nepal Geol. Soc. 4*, 73-100.

Young, D. J. (1963). A faulted and tilted late Pleistocene terrace near Blackball, *N.Z. J. Geol. Geophys. 6*, 721-724.

# 5 Alluvial River Response to Active Tectonics

STANLEY A. SCHUMM
*Colorado State University*

ABSTRACT

Alluvial rivers are influenced by changes of valley floor slope, and therefore deformation of the valley floor by active tectonics can cause pattern change, aggradation, and degradation.

Canals have been abandoned owing to uplift in Iran, and major floods and avulsive shift of the Indus River has been attributed to earthquake-generated dams and tilting of the Indus Valley. Streams crossing the Monroe uplift in Louisiana and the Wiggins uplift in Mississippi show pattern, gradient, and depth changes that indicate that these uplifts are active. The Mississippi River shows effects of the Lake County and Monroe uplifts.

Slow deformation of a valley floor will eventually affect channel stability. This poses hazards to structures on or near the river banks as well as to bridges and pipeline and powerline crossings. Navigation may be impaired, and the variability of overbank flooding along the river can cause legal problems.

## INTRODUCTION

Alluvial rivers, those that flow between banks and on a bed composed of sediment that is transported by the river, are sensitive to changes of sediment load, water discharge, and variations of valley floor slope (Schumm, 1977). Therefore, in addition to the dramatic effects when stream channels and terraces are offset along faults (Wallace, 1967; Stevens, 1974), other more subtle effects should be recognizable when deformation is vertical, slower, and aseismic.

Many of the major rivers of the world follow structural lows and major geofracture systems (Potter, 1978). In fact, Melton (1959) suspected that streams that have adjusted to tectonic activity are numerous, and the lower Mississippi River and Rio Grande are clearly in areas of structural instability as are the lower Amazon, Niger, Tigrus, Euphrates, Rhine, and Indus, among others. The high discharge of these rivers should permit them to maintain their courses in spite of active tectonics. However, large rivers, because of their low gradients, may, in fact, be the most significantly affected by the minor changes in slope caused by active deformation.

In spite of the practical significance of active tectonics, only a few investigators have considered its effects on alluvial rivers (Tator, 1958; Schumm, 1972, 1977; Adams, 1980; Russ, 1982; Burnett and Schumm, 1983). It is possible that this situation exists because variations of channel morphology and behavior can also be attributed to downstream variations of discharge and to the quantity and type of sediment load; therefore, the effects of active tectonics are difficult to detect. In ad-

dition, the attention of geomorphologists and photogeologists generally has been concentrated on the identification of geologic structures that are assumed to be quiescent (Howard, 1967; Ollier, 1981, p. 180) rather than on the effect of ongoing deformation on alluvial channels. Nevertheless, geomorphologists working in petroleum exploration, e.g., DeBlieux (1951, 1962) and Tator (1958), indicated that fluvial anomalies, such as local development of meanders or a braided pattern, local widening or narrowing of channels, anomalous ponds, marshes or alluvial fills, variations of levee width or discontinuous levees, and any anomalous curve or turn, are possible indicators of active tectonics. In addition, active tectonics can produce nickpoints, convexities or concavities of the longitudinal profile, channel depth variations, and, of course, either aggradation or degradation.

Another problem is that active tectonics takes several forms. Deformation can be along faults (shear, normal, or reverse in a downstream sense) or pairs of faults (horst and graben). These faults should have the same effect as a monocline, dome, or basin. In addition to local structural features, the entire valley may be tilted upstream, downstream, or laterally. The possibilities are great, but, in reality, the primary effect of tectonics will be local steepening or reduction of gradient or cross-valley tilting.

In addition to these primary influences on channel and valley gradient and configuration, there will be secondary effects, as the rivers respond to the changed gradient (aggradation or degradation), and there will be tertiary effects, as decreased or increased sediment loads influence reaches downstream of the deformed reach and as aggradation or degradation in the deformed reach progresses upstream. In addition to tectonic effects, there can be similar influences as a result of differential compaction of sediments (draping) over buried topographic highs.

## TECTONIC EFFECTS

Where tectonism has been persistent for long periods of time active deformation will produce a channel response that will be superimposed on the long-term tectonic effects. Major valley deformation or total disruption of the river system can be the result of long-term tectonism.

### *Valley Change*

The most commonly cited evidence for deformation is the warping of alluvial terraces in a valley. If the deformation has persisted the oldest terrace is the most deformed by uplift (convex) or subsidence (concave), and it will show the greatest offset by faulting (Machida, 1960; Zuchiewicz, 1979, 1980). Where there has been uplift or subsidence, terraces are warped upward or downward, and the extent of the displacement can be determined by comparison with the longitudinal profile of the present river if, indeed, the river has adjusted to the past deformation. Machida (1960) assumed that the longitudinal profile of a terrace is described by a negative exponential function in a downstream direction and that deviations from this curve indicate deformation. Valley-floor deformation can also be indicated by depth to bedrock. Alluvium will be thickest over downfaulted or downfolded zones and thinnest over areas of uplift (Kowalski and Radzikowska, 1968).

### *River Changes*

When uplift is too rapid to be accommodated by a river there will be disruption of the drainage pattern (Sparling, 1967; Twidale, 1971, pp. 133-136; Ollier, 1981). For example, Freund *et al.* (1968) have evidence that movement along the Dead Sea rift in Israel disrupted streams that formerly drained from Jordan and crossed what is now the Dead Sea Valley to the Mediterranean Sea. Portions of the channels of these rivers are now displaced about 43 km as a result of movement along the boundary faults of the Dead Sea rift. The Murray River on the Riverine Plain near Echuca (Victoria, Australia) is an impressive example of channel modification by tectonic activity (Bowler and Harford, 1966). The Cadell Fault block has converted the Murray River from a single channel to an anastomosing system of channels that surround the obstruction. The abandoned segment of the Murray River is preserved on the dipslope of the fault block. A particularly active tectonic area is the eastern side of the East African rift valley near Lake Victoria. Doornkamp and Temple (1966) described the formation of lakes in some valleys, as a result of gradient reduction, and this could be the first stage of drainage disruption.

In many cases, incising channels will encounter resistant strata, which may retard or prevent the maintenance of an antecedent condition. Incised meander patterns can also indicate deformation because the alluvial river pattern is affected by the deformation before it becomes fixed by incision into bedrock (Gardner, 1975).

## EVIDENCE FOR ACTIVE TECTONICS

The preceding discussion reviews evidence for past deformation but not necessarily for active tectonics. Modern river and valley-floor morphology and geodetic

surveys provide the best geomorphic evidence of ongoing deformation.

In those areas where the rate of deformation is low, active tectonics is reflected by geomorphic features that react to small changes of slope, for example, the gradient of terraces and stream channels and meander characteristics (Radulescu, 1962; Neef, 1966). One of the most sensitive indicators of change is the valley-floor profile and longitudinal profile of the stream (Bendefy *et al.*, 1967; Zuchiewicz, 1979).

Degradation and aggradation can be evidence of active tectonics, and these processes will be accompanied by changes of channel morphology (depth and width) as the channel incises or as it aggrades. Therefore, progressive changes of thalweg or water-surface elevation can provide information on vertical changes of the channel. When a long gaging-station record is available, it can be used to determine water-surface change with time. When the gage height or water-surface elevation for a specific discharge [e.g., 100 cubic feet/second (cfs)] is plotted against time, any rise or fall of the specific gage height indicates a change of either channel capacity (area) or elevation (see Figure 5.16 below). For example, on the axis of an active uplift both the river bottom and water surface at a given discharge should be lowered, as the channel scours in response to increased slope (Volkov *et al.*, 1967). When the water surface and river bottom rise through time, either very rapid uplift or a decrease of channel capacity by aggradation can be the cause.

### *Channel Patterns*

Stream patterns are sensitive indicators of valley-slope change (Schumm, 1972, 1977; Schumm *et al.*, 1972). Adams (1980) demonstrated a relation between measured tilt rates and downstream changes of sinuosity for the Mississippi River between St. Louis and Cairo and for the lower Missouri River. That is, in order to maintain a constant gradient a river that is being steepened by a downstream tilt will increase its sinuosity, whereas a reduction of valley slope will lead to a reduction of sinuosity. However, Twidale (1966) reported that both the Flinders and Leichardt Rivers have changed to a braided pattern as a result of the steepening of their gradient by the Selwyn Upwarp in northern Queensland.

Another cause of meander growth and river shift is the lateral or transverse tilting of the valley. In general, a river should shift in a downtilt or a downslope direction and concentrate its attack on the valley side that has been downtilted (Cotton, 1941). Nanson (1980) showed that the south-flowing Beatton River in British Columbia is affected by isostatic tilt to the east, which caused a deviation from the normal downstream migration of the meanders. The tilting has augmented the easterly directed flow velocities, thereby resulting in an easterly bias to channel migration. However, although meander loops tend to migrate toward the east, frequent channel cutoffs leave the channel close to the west wall of the valley. The Beatton River is confined within a valley and is not free to shift laterally for an appreciable distance. This is unlike the situation on the Hungarian Plain, where the Tiza River has shifted laterally for long distances, as a result of deformation of the surface of the plain (Mike, 1975).

### *River Types*

It is not possible to predict consistently the pattern and channel changes because different types of alluvial channel will respond differently to active tectonics; therefore, the characteristics of alluvial channels must be reviewed before their potential response can be evaluated. This can best be done by discussing a simple classification of alluvial channels that is based on type of sediment load (bed load, mixed load, suspended load) and pattern (Figure 5.1).

Five basic channel patterns exist (Figure 5.1). These are straight channels with either migrating sand waves (pattern 1) or with a sinuous thalweg and alternate bars (pattern 2). There are two types of meandering channels, a highly sinuous channel of equal width (pattern 3a) and channels that are wider at bends than in crossings (pattern 3b). The meandering-braided transition

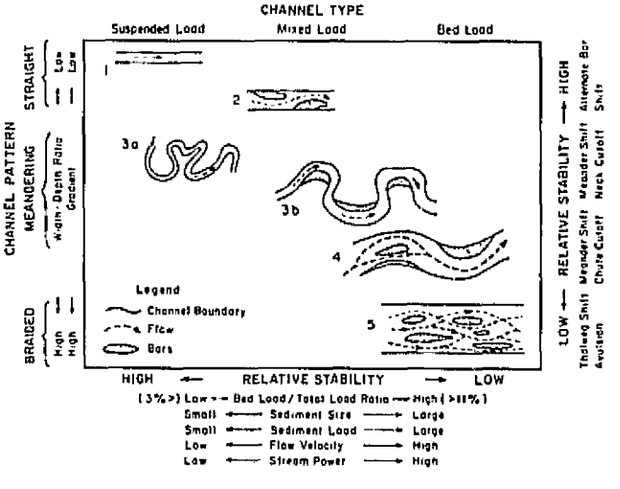


FIGURE 5.1 Channel classification based on pattern and type of sediment load with associated variables and relative stability indicated. From Schumm (1981).

(pattern 4) and a typical braided-stream (pattern 5) complete the sequence. The relative stability of these channels in terms of their normal erosional activity and the shape and gradient of the channels, as related to relative sediment size, load, velocity of flow, and stream power, are also indicated on Figure 5.1. It has been possible to develop these patterns experimentally by varying the gradient, sediment load, stream power, and type of sediment load transported by the channel (Schumm and Khan, 1972).

The range of channels from straight through braided forms a continuum (Figure 5.1), but experimental work and field studies have indicated that the pattern changes between braided, meandering, and straight occur at river-pattern thresholds (Figure 5.2). The pattern change takes place at critical ranges of valley slope, stream power, and sediment load (Schumm and Khan, 1972).

Observed rivers can be placed within the five general categories. However, within the meandering stream group there is considerable range of sinuosity (1.25 to 3.0), which is the ratio of channel length to valley length. In addition, in the braided-stream category there are bar-braided and island-braided channels. Islands are vegetated bars. There are also multiple channel patterns termed anastomosing, anastomosed, or anabranch channels (Schumm, 1977, p. 155; Smith and Smith, 1980). In fact, it has been suggested that 14 channel patterns can be recognized (Figure 5.3).

Experimental studies and field observations confirm that a change of valley-floor slope will cause a change of channel pattern and dimensions. The change will differ, however, depending on (1) where the channel lies on a plot such as that of Figure 5.2, (2) the type of channel (Figures 5.1 and 5.3), and (3) the amount and rate of deformation.

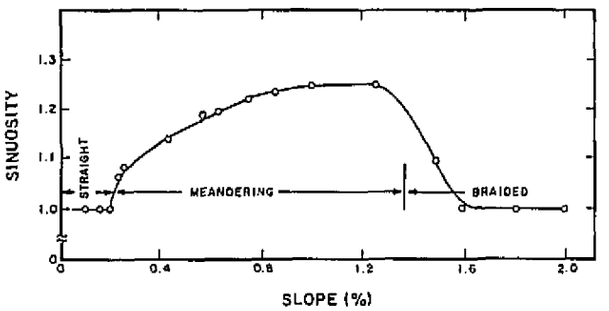


FIGURE 5.2 Relation between valley (flume) slope and sinuosity (channel length/valley slope or valley slope/channel slope) during experiments at constant discharge. Sediment load, stream power, and velocity increase with slope, and a similar relation can be developed with these variables. From Schumm and Khan (1972).

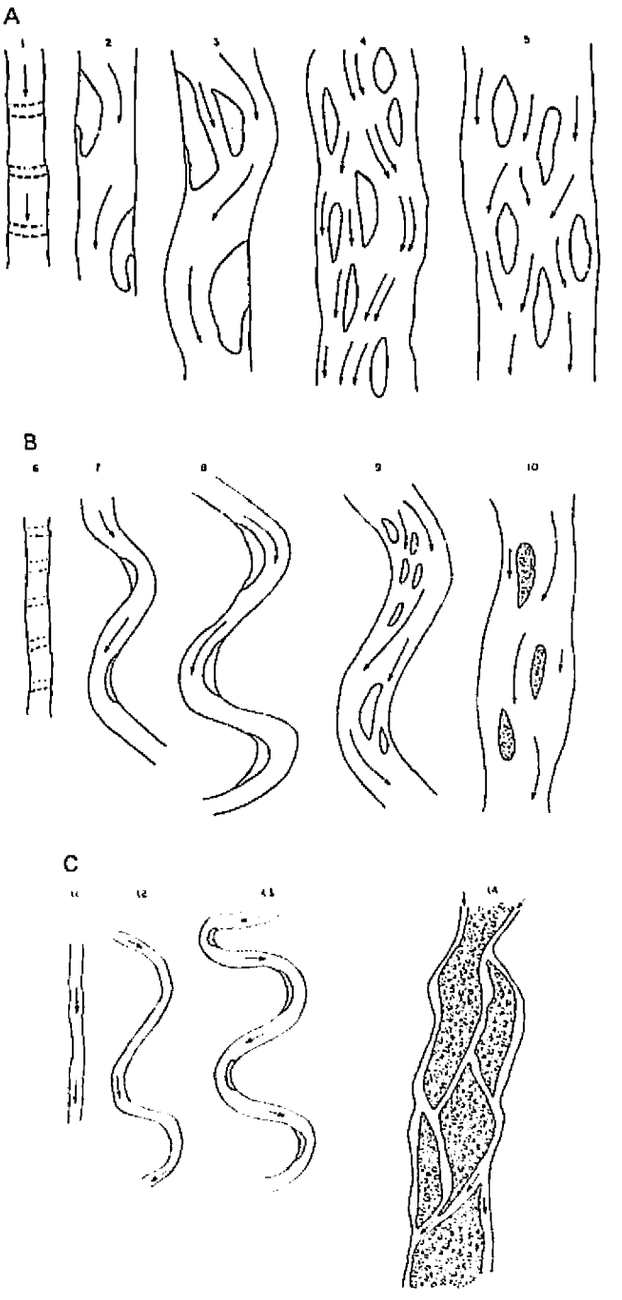


FIGURE 5.3 The range of alluvial channel patterns for the three channel types shown in Figure 5.1. A, Bed-load channel patterns; B, mixed-load channel patterns; C, suspended-load channel patterns. From Schumm (1981).

Slight increases of valley slope will shift river patterns from left to right on Figures 5.2 and 5.3, as the river adjusts its gradient by pattern change. With greater changes of valley slope, incision may produce sufficient sediment to cause a change from one type of channel to another with a metamorphosis of a mixed-load channel to bed-load channel (Figure 5.3). In addition, significant reductions of slope or greatly increased sediment loads will produce aggradation and very likely a braided channel, as a result of sediment deposition.

Braided channels are the result of high bed-load transport on steep gradients or of deposition. Therefore, a braided channel can be in equilibrium or unstable. The anastomosing pattern (pattern 14 of Figure 5.3) is still an enigma. It may be a relatively steep gradient suspended-load channel analogous to the bed-load and mixed-load braided channels (Figure 5.3), or it may be the suspended-load equivalent of the unstable braided channel that forms where overbank flow produces multiple channels in a valley.

In an effort to determine the effects of active tectonics on alluvial channels experimental studies were performed by Ouchi (1983, 1985) and Jin (1984) in a large flume (8.5 m × 2.4 m), the center section of which could be raised or lowered by hydraulic jacks. Figure 5.4 summarizes the results for braided and meandering channels during uplift and downwarping. Because the braided channel could not change its pattern, as a result of uplift, it degraded forming terraces. The sediment produced by the incision caused aggradation downstream, and the reduced gradient upstream also caused aggradation.

During downwarping the experimental braided channel degraded in the upper steepened reach, and it aggraded downstream. Adjustment was much slower during subsidence because during uplift channel incision is concentrated in a channel, whereas adjustment by aggradation requires deposition not only in the channel but over the valley floor. The aggradation in zones B and C reduced downstream sediment loads and induced degradation in zone D (Figure 5.4).

Adjustment of the meandering channel was as expected with increased overbank flooding upstream and an increase of sinuosity on the steeper reaches during uplift. Jin's (1984) results also show clearly the meandering-channel response to uplift (Figure 5.5).

Note that in each case (Figure 5.4) the secondary response to the primary deformation causes tertiary effects in zones A and D both upstream and downstream of the zones of deformation (B and C). Figure 5.4 is presented to illustrate the complexity of the channel response to active tectonics. In each case if the experiment had continued without further deformation there

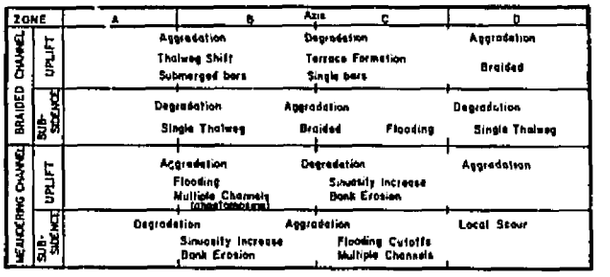


FIGURE 5.4 Effect of uplift and subsidence on braided and meandering experimental channels. Zones of active deformation (B, C) are separated by the axis of deformation. Zone A upstream and Zone D downstream from the zones of active deformation show tertiary effects of valley slope change. The position of the descriptive term indicates generally where the process or channel form is present. Modified from Ouchi (1983).

would be additional channel adjustment. For example, in the uplift experiments degradation, which was concentrated at the axis of uplift (Figure 5.4), would have extended upstream to at least the boundary between zones A and B.

Alluvial channels are sensitive indicators of change. However, they adjust to changes of hydrology and sediment load as well as to active tectonics. Therefore, it may be difficult to determine the cause of channel change because man's activities and climatic variations both act to alter discharge and sediment load during historic time. Channel pattern change alone is not sufficient evidence for active tectonics, rather it is one bit of

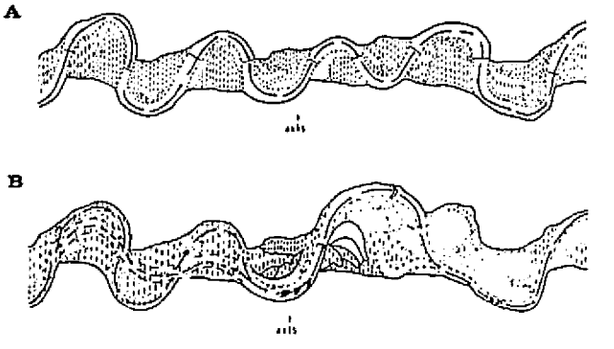


FIGURE 5.5 Meandering channel pattern change, as a result of uplift in center of figure. A shows meandering channel developed after 400-h run time, B shows effect of uplift on this 3.5-m reach of experimental channel after an additional 100 h. Upstream reach shows evidence of overbank flooding, development of multiple channels, and aggradation. Downstream reach shows increase of meander amplitude, wavelength, and sinuosity as well as degradation and a cutoff. Flow is from left to right. Stippled pattern represents sand on floodplain. Vertical-line pattern represents silt and clay deposits on floodplain. From Jin (1984)

evidence that must be supported with other morphologic evidence of aggradation, degradation, or survey data. In many areas the evidence will be circumstantial. Nevertheless, anomalous reaches that are not related to artificial controls or to tributary influences may reasonably be assumed to be the result of active tectonics.

## EXAMPLES

Examples from the Near East, Pakistan, and the lower Mississippi Valley illustrate the impact of active tectonics on the effective utilization of rivers and canals.

### *Near East*

Where man has built long-lasting structures, active-tectonic effects are recorded by displacement of these features. For example, in the southeastern corner of Iran, the Shaurn anticline forms a range of low hills. Folding began in late Pliocene, and it still continues (Ambraseys, 1978). In the first or second century A.D. two canals were cut across the anticline in order to lead water from a canal system on the northeast flank to the more extensive and fertile plains on the southwest. These channels afford a unique opportunity for measuring the uplift of the anticlines since the canals were built. One canal still carries water, but, where it crosses the anticline it has cut down about 3.5 m below its original bed. The other canal has been abandoned. An accurate survey along its alignment shows that, along the anticlinal axis, the bed of the canal has risen at an average rate of approximately 1 m per century (Lees, 1955).

In the Tigrus and Euphrates Valley, where there is active tectonics (Lees, 1955; Adams, 1965; Mirjayar, 1966), canals have also been abandoned. They show reversed gradients and incision.

### *Indus Valley*

There are numerous active faults in the Indus Valley (Kazmi, 1979). The most spectacular effect of active faulting is due to the Rann of Cutch Fault zone in the lower Indus Valley. In 1819 a severe earthquake resulted in the 6-m uplift of a 16-km-wide and 81-km-long tract of alluvial land. This feature was locally known as Alah Bund (Oldham, 1926), and it blocked an eastern branch of the Indus River. The channel at that time was dry, but flow was re-established during a flood in 1828.

Lyell (1857, p. 462) stated that "for several years after the convulsion of 1819, the course of the Indus was very unsettled, and at length, in 1826, the river threw a vast body of water into its eastern arm, forcing its way in a more direct course to the sea, burst through all the artificial barriers that had been thrown across the channel, and at length cut right through the Alah Bund." For discussion of recent history of the Indus see Holmes (1968), and for an interesting hypothesis concerning the decline of an Indus civilization see Dales (1966), who suggested that one ancient [illegible] valley city (Mohenjo-daro) was flooded as a r[illegible] major tectonic activity forming a dam in the Ind[illegible] alley. This is possible as a result of valley-floor warpin[illegible], but not as the result of a major natural alluvial dam (Lambrick, 1967). Finally, the westward shift of the Indus River during the last few thousand years suggests major avulsive changes owing to westward tilting of the Indus River valley (Wilhelmy, 1969).

### *Mississippi Valley*

*Lake County Uplift* The great 1811-1812 earthquakes near New Madrid, Missouri, have created considerable concern about the possibility of a recurrence. Therefore, extensive studies have been carried out in this area, and the literature relating to the geophysics and geology of the Mississippi Embayment between Memphis and Cairo is abundant (McKeown and Pakiser, 1982).

The area of deformation near New Madrid is referred to as the Lake County Uplift (Figure 5.6). The surface of the uplift is as much as 10 m above the general level of the Mississippi River Valley. The deformed area has a maximum length of about 50 km and a maximum width of about 23 km. Its relief is uneven, and the surface is dominated by two elongated bulges.

The Lake County Uplift consists of part of four different geomorphic surfaces, the modern Mississippi meander belt and three separate Mississippi River braided-stream terraces. Lateral migration of the Mississippi River during and following the most active periods of deformation has eroded a considerable amount of the uplifted surface. During great floods of the past, the as yet uneroded portions of the Lake County Uplift existed as islands on the Mississippi River alluvial plain.

Russ (1982) cited the following evidence of active deformation of the Lake County Uplift: (1) profiles of the Lake County Uplift reveal that the structure is significantly higher than the natural occurring landforms of the modern meander belt (Figure 5.7A); (2) the longitudinal profiles of abandoned river channels and natural levees have been significantly warped, some to the extent that the original river flow direction has been reversed; (3) the modern floodplain is also warped (Figure 5.7B); and (4) the Reelfoot scarp vertically offsets abandoned Mississippi River channels, which once flowed across the area.

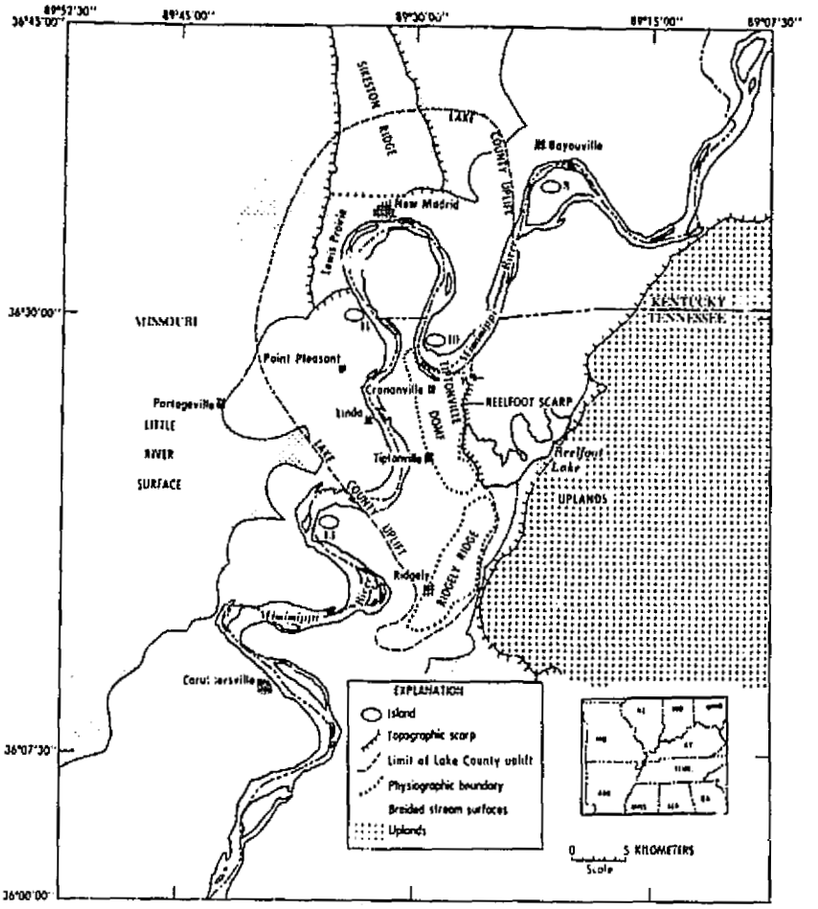


FIGURE 5.6 Map of New Madrid region showing the Lake County Uplift. From Russ (1982).

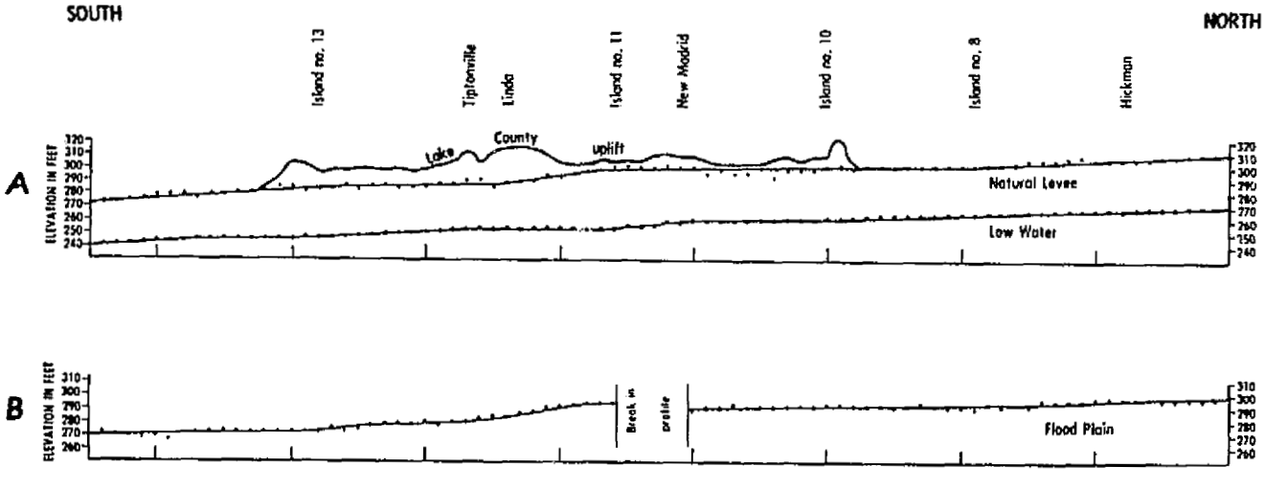


FIGURE 5.7 Longitudinal profiles between Mississippi River miles 845 to 930. Locations are shown on Figures 5.6 and 5.8. A, Natural-levee profile and low-water profiles: B, floodplain profile. From Russ (1982).

An examination of Figure 5.7 reveals that all the profiles have a similar shape, suggesting that they may be the result of the same events. The profiles are convex upward, a configuration that is commonly associated with uplift, and Russ (1982) concluded that this shape may be due to recent and even current deformation. Russ also stated that several aspects of the meander pattern of the Mississippi River suggest control by tectonic processes. Above the uplift axis, between Cairo, Illinois, and Hickman, Kentucky, the river is currently relatively straight. From Hickman south to Arkansas, however, it is sinuous (Figure 5.8). It is possible that the river straightened its course to increase its gradient in an area where tilting is reducing it, whereas downstream the high sinuosity reflects steepening (Figures 5.2 and 5.3). The river is constrained by the topographically high Sikeston Ridge to the north and the Tiptonville Dome to the south.

The position of the Mississippi River course within its meander belt also suggests the possibility of tectonic influence. Between Cairo, Illinois, and Hickman, Kentucky, and in general between Blytheville, Arkansas, and Memphis, Tennessee, the river flows along the eastern edge of its meander belt (Figure 5.8). However, between Hickman and Blytheville the river shifts to the west. It is conceivable that the river has been deflected to the west as a result of the uplift. However, old maps indicate that the position of the river in 1765 is similar to that of today. Thus, any significant tectonic deflection must have occurred before 1765.

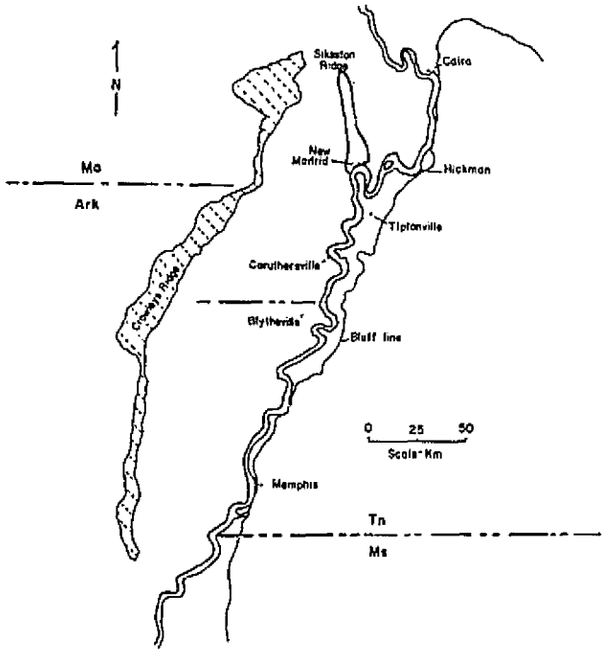


FIGURE 5.8 Map of Mississippi Valley between Memphis, Tennessee, and Cairo, Illinois.

The effect of the New Madrid earthquake on the Mississippi River provides an extreme example of the tertiary effects of active tectonics on a major river during a long period of time. For example, Walters and Simons (1984) studied the history of the river, and they summarized as follows: From 1765 to the winter of 1811-1812 the lower Mississippi was a graded river, and there were four neck cutoffs during that period. Beginning on December 16, 1811, and continuing intermittently through February 1812, the New Madrid earthquake shocks caused bank caving, which introduced tremendous quantities of sediment into the channel. The most severe caving occurred in the reach from the confluence of the Ohio and Mississippi Rivers to below Blytheville, Arkansas (Figure 5.8). The increased sediment load caused excessive shoaling, enlargement of islands, and at some locations new islands and point bars were formed. During the years following the earthquake (1818-1874), the sediment began to move gradually downstream. This increase in sediment load caused reduction in meandering, and the number of cutoffs doubled. From 1875 to 1932 the number of neck cutoffs decreased. Above Osceola the introduction of sediment was almost instantaneous, and the response was the formation of a wider aggrading channel. Below Osceola the response was a steepening of the gradient by meander cutoffs and sinuosity reduction.

From the examination of gaging-station records and especially specific-gage relations, Walters and Simons (1984) concluded that the lower Mississippi River channel from above New Madrid, Missouri, to Red River Landing, Louisiana, was aggrading after about 1880, perhaps as a result of the sediment introduced by the New Madrid earthquakes.

*Monroe Uplift* The Monroe Uplift, the extent of which is defined by deformed Cretaceous and Tertiary strata, is a dome approximately 120 km in diameter. It is situated mostly in northeastern Louisiana (Figure 5.9), but it extends into southeastern Arkansas and west central Mississippi (Wang, 1952). Its eastern-most extension includes the Mississippi River between Greenville and Vicksburg.

Geologic evidence that the Monroe Uplift was active since the Tertiary has been presented by several authors. Veatch (1906) discussed the existence of two active linear structures, which pass through the uplift. He further claimed that recent movement along the west end of the flexure has resulted in the formation of a series of shoals

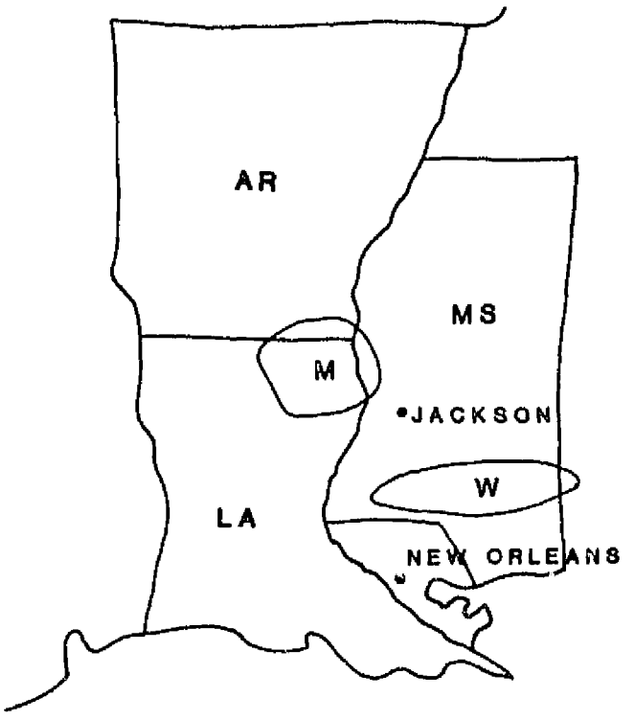


FIGURE 5.9 Index map showing location of Monroe (M) and Wiggins (W) Uplifts.

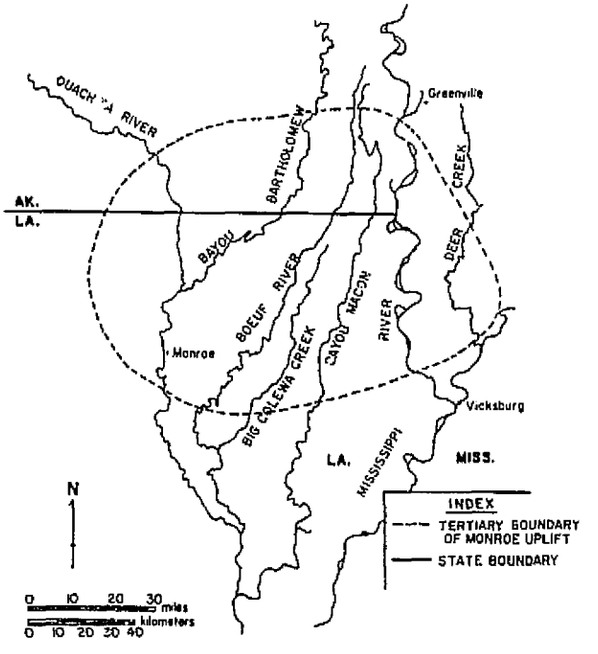


FIGURE 5.10 Index map of Monroe Uplift. From Burnett and Schumm (1983).

on the Sabine and Angelina Rivers and swamping of an area in the Angelina River Valley in eastern Texas.

The uplift consists of the Boeuf and Tensas Basins as well as Macon Ridge and the Mississippi River from mile 450 to 530. The basins are composed of large backswamp areas crossed by several old Arkansas River channels with well-developed natural levees. Macon Ridge in the center of the uplift is composed of five mid-Wisconsin glacial outwash terraces (Saucier and Fleetwood, 1970), which form a narrow, north-south trending, elongated area of high ground.

Several streams—Ouachita River, Bayou Bartholomew, Boeuf River, Big-Colewa Creek, Bayou Macon, and Deer Creek (Figure 5.10)—that cross the Monroe Uplift in northeastern Louisiana and generally parallel the Mississippi River were studied by Burnett (1982). They flow generally to the southwest across the uplift, and they locally occupy old abandoned courses of the Arkansas River.

The Mississippi River has a highly irregular thalweg profile through the Monroe Uplift (Winkley, 1980). The thalweg slope is significantly reduced or even reversed in part of the uplift zone. At river mile 485, the mean thalweg slope is $-0.00004$, but it increases downstream to $+0.0001$. This suggests that deformation is occurring and that it is affecting a major river.

Evidence of recent surface movement on the Monroe Uplift is indicated by precise geodetic surveys. The geodetic surveys do not cross the uplift axis, but they suggest uplift of the southern part of the area between 1934 and 1966 (Burnett, 1982). The longitudinal profiles of Pleistocene and Holocene terraces show convexities, which are due to uplift. If the Monroe Uplift is still active today, the modern stream and valley-floor profiles should exhibit the effects of the uplift similar to those shown by terrace profiles. Indeed, valley profiles of the Monroe Uplift streams shows an obvious zone of upward convexity (Figure 5.11).

Comparing the amounts of vertical deformation of the terraces and floodplains in the Monroe Uplift area to their ages of formation provides a means of estimating contemporary rates of uplift in this area. By this method, the convexity in the oldest and highest Macon Ridge terrace profile ($Qtb_1$) indicates that about 3.8 m of vertical deformation has occurred at the uplift axis since this terrace was formed (Figure 5.11). Saucier (1970) estimated the age of this terrace to be 33,000 yr old. Therefore, the maximum rate of uplift is estimated to be about 1.0 mm per year during the last 33,000 yr. For the other profiles the rates vary from 0.01 to 1.4 mm/yr.

Sinuosity for the five rivers is plotted with reference to

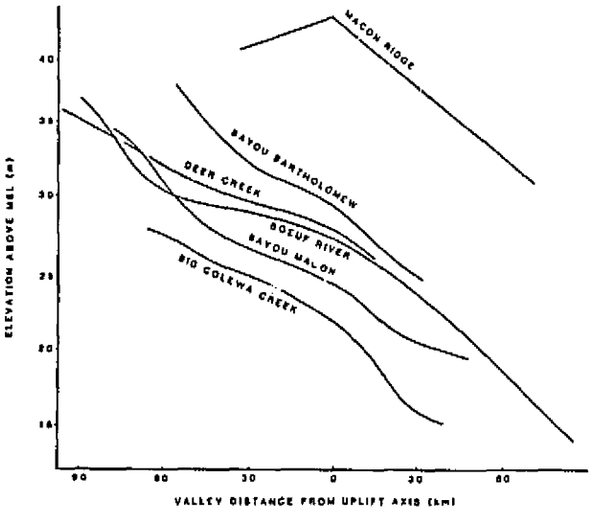


FIGURE 5.11 Longitudinal valley profiles of streams crossing the Monroe Uplift, and Macon Ridge, which is a remnant of a Pleistocene Mississippi River terrace. From Burnett and Schumm (1983).

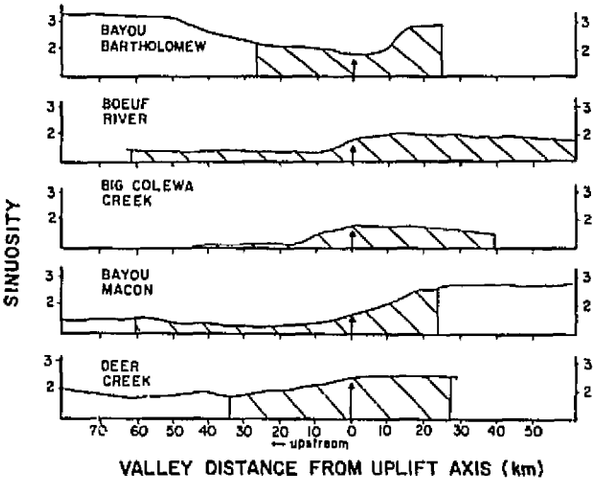


FIGURE 5.12 Variations of sinuosity along six streams crossing the Monroe Uplift. Distance above and below uplift axis is shown. Downstream is to the right. Arrows indicate axis of uplift, and cross hatching shows zones of modern uplift. From Burnett (1982).

the position of the uplift axis (Figure 5.12). In each case sinuosity increases as the axis is approached or crossed. Where sinuosity is high above the axis, there is a decrease of sinuosity as the axis is approached (Bayou Bartholomew). The results are as suggested by Figures 5.2 and 5.3.

To examine the variability of the channel-bed elevation and also changes in the bank height along the streams that cross the Monroe Uplift, channel thalweg elevations were plotted in relation to the valley distance along Boeuf River and Big Colewa Creek (Figure 5.13). These projected channel profiles are not affected by changes in sinuosity because the thalweg elevation (or low water elevation) at a given location is plotted with reference to valley distance rather than channel distance (Burnett, 1982).

In Figure 5.13, the difference in the elevation of the projected channel profile and that of the valley profile at a given location represents the depth of the channel below the valley surface at that location. The reaches with large differences in elevation between the valley surface and channel (high banks) are those where the channel has downcut or degraded. Also, where average bank height is small the channel has not degraded, or it has, in fact, aggraded. The projected channel profiles do not parallel the valley profiles, indicating that varying amounts of degradation or aggradation have occurred along the channel. The Boeuf River has apparently compensated for the uplift, but the Big Colewa Creek profile contains a major convexity (Figure 5.13). At the axis of the uplift and in the downvalley zone of the uplift, the average bank heights are, in general, high (11 to 13 m for the Boeuf River and 6 m for Big Colewa Creek). These observations indicate that degradation has occurred at and below the uplift axis, but above the axis

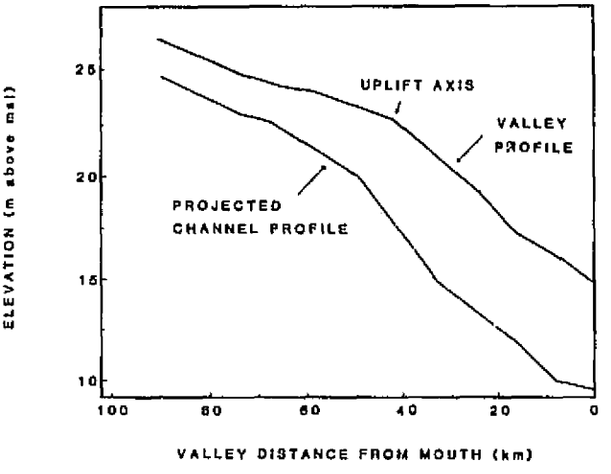


FIGURE 5.13 Valley and projected-channel profiles of Boeuf River and Big Colewa Creek. From Burnett (1982).

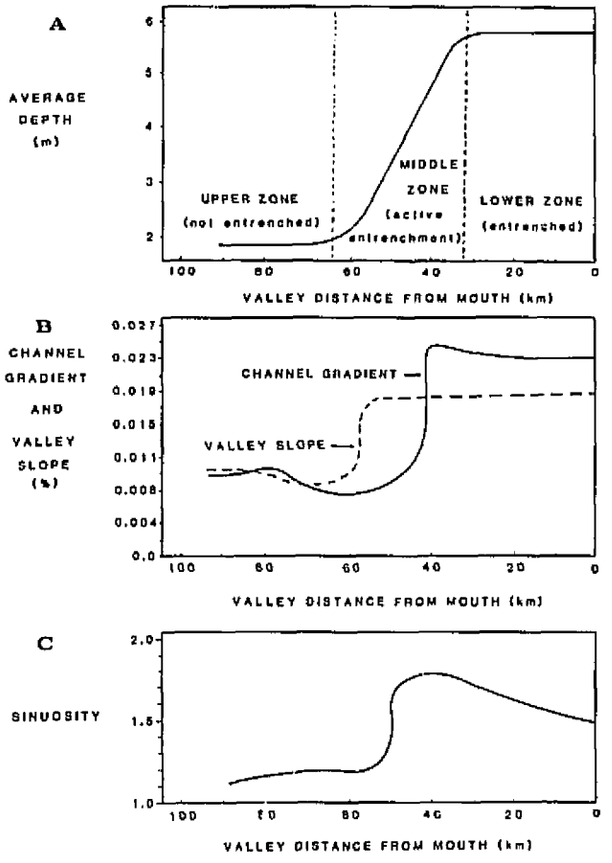


FIGURE 5.14 Effect of Monroe Uplift on Big Colewa Creek. A, Change of channel depth. Three reaches show different degrees of response to uplift. B, Change of channel gradient and slope of valley floor. C, Change of sinuosity. From Burnett and Schumm (1983).

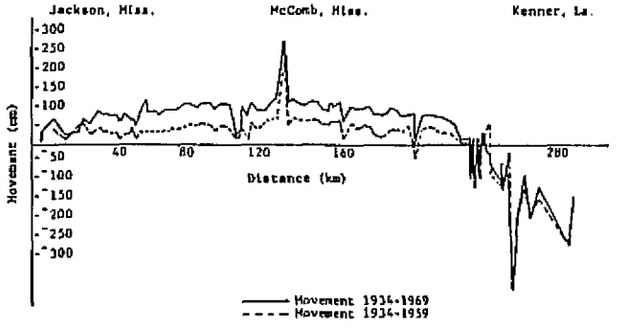


FIGURE 5.15 Vertical benchmark movement along a National Geodetic Survey route between Jackson, Mississippi, and New Orleans, Louisiana. From Brown and Oliver (1976) with permission of the American Geophysical Union.

degradation has yet to affect the profile of Big Colewa Creek.

The Big Colewa Creek channel can be used to summarize the effect of uplift on an alluvial channel. It can be divided into three zones of activity along its valley (Figure 5.14A). The lower zone, from the mouth to valley km 32, has a high average bank height of about 6 m. The middle zone, from valley km 32 to 65, shows a clear upstream decrease in the average bank height from 6 to 2 m. The upper zone, above valley km 65, has a constant low average bank height of 2 m. Degradation may have occurred in the lower zone, whereas entrenchment is still in progress in the middle zone, and in the upper zone entrenchment has not yet occurred.

Figure 5.14B shows changes in valley slope and channel thalweg slope with valley distance. The valley slope remains high from the mouth to valley km 40, and then it suddenly decreases. The break in slope, at valley km 40, defines the apparent location of the uplift axis. The thalweg slope is high from the mouth to valley km 55, and then it also suddenly decreases. The fact that the two curves do not coincide suggests that the channel has incised through the axis of uplift.

Sinuosity is approximately 1.2 in the upstream stretch of Big Colewa Creek (Figure 5.14C). Downstream between valley km 50 and 55, sinuosity increases to about 1.7, and then it gradually decreases to 1.5 at the mouth.

In summary, numerous relations between the morphology of the streams and terraces and the underlying Cretaceous and Tertiary structures of the Monroe Uplift indicate that the area is still active tectonically. The patterns of changes and the present stream morphology provide information on the response of streams to active uplift within their valleys.

*Wiggins Uplift* In contrast to the Monroe Uplift, active displacement of the Wiggins Uplift (Figure 5.9) is clearly displayed by geodetic surveys (Figure 5.15). Bogue Homo Creek is analogous to Big Colewa Creek in this area, and it displays similar morphologic differences. Above the axis of uplift the channel is anastomosing, and the main channel is relatively straight. Immediately below the axis the channel has incised below the former floodplain to form a low terrace, and sinuosity is higher. Numerous cutoffs have occurred, and locally braided reaches have developed as a result of increased sediment loads resulting from incision.

A gaging station on Tallahala Creek provides evidence of channel incision at an average rate of 12 mm/yr since 1940 (Figure 5.16). This is three times the rate of measured uplift; however, a channel probably adjusts episodically to continuous uplift (Ouchi, 1983).

A factor that makes comparison of channel behavior

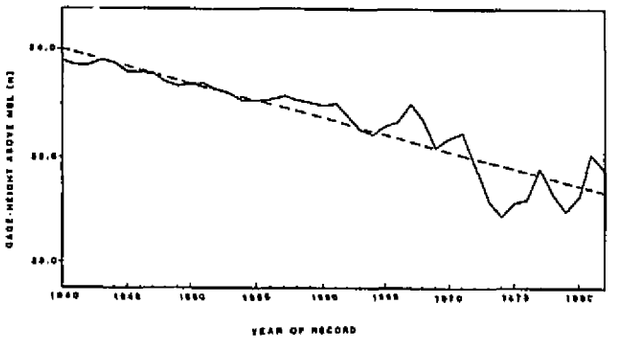

FIGURE 5.16 Specific gage plot for Tallahala River near Runnelstown, Mississippi. The water-surface elevation was determined for a specific discharge of 78 cfs for each year of record. This discharge is base flow and reflects change of bed elevation. From Burnett and Schumm (1983).

difficult is the size or the energy of the channel. Small channels such as Big Colewa Creek and Bogue Homo Creek have been unable to keep pace and incise across the uplift axis. Streams of intermediate size such as Tallahala Creek have incised across the axis, but their long profile still shows a convexity. Large rivers such as the Pearl River (19,900 km$^3$) have been able to keep pace with the uplift, and its projected-channel profile is relatively straight, although terraces and the valley floor are deformed (Figure 5.17). Above the axis of uplift the Pearl River is not anastomosing, but it has developed a new floodplain below the axis of uplift, and the former floodplain is a low terrace.

Changes of channel morphology can frequently be attributed to tributary contributions of water discharge and sediment load, but on the Monroe and Wiggins Uplifts, the patterns of channel change are related to active

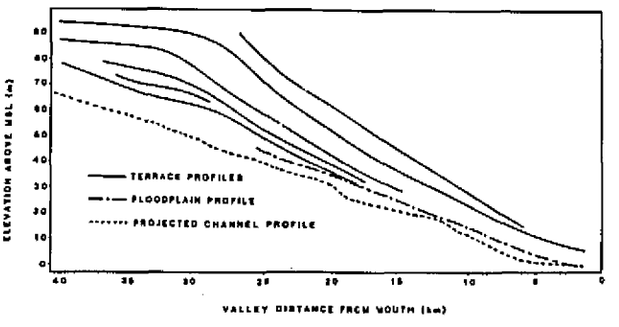


FIGURE 5.17 Longitudinal profiles of terraces and floodplain and a projected-channel profile of the Pearl River, a major river crossing the Wiggins Uplift. A projected-channel profile is a plot of channel-bed elevation against valley distance, which eliminates the effect of sinuosity of the channel long profile. From Burnett and Schumm (1983).

tectonic deformation of the alluvial valley of streams crossing the uplifts (Burnett, 1982).

*Mississippi River* In the preceding discussion of the Mississippi River Valley, three areas of active tectonics have been identified, the Lake County Uplift, the Monroe Uplift, and the Wiggins Uplift. Russ (1982) demonstrated an effect of the Lake County Uplift on the Mississippi River gradient and pattern. Maps (Fisk, 1944) of the old Mississippi River meander courses show that the Mississippi River has maintained very high sinuosity values in this area during the last 2000 to 6000 yr (Figure 5.18).

Winkley (1980) discussed the possible effects of the Monroe Uplift on the past and present morphology of the Mississippi River in the vicinity of Greenville Bridge (mile 531.3), where the Monroe Uplift has exposed Tertiary bedrock in the Mississippi River channel near Greenville. Meander loops have grown and cut off at the same location several times, and the sinuosity has been consistently high near Greenville (Figure 5.18). In this sinuous zone, the Mississippi River has shifted laterally across the Yazoo Clay, being unable to cut through it. Watson *et al.* (1984) suggested that the Wiggins Uplift has increased sinuosity farther south near Natchez (Figure 5.18).

As the average slope of the Mississippi River low-water surface is about 56 mm per river kilometer, with even slow uplift rates of from 3 to 5 mm/yr the effects on this great river can be significant. Studies are under way to determine the extent of the effects of active tectonics on this major commercial artery. Obviously if there is a significant influence on the river, it will have implications for navigation, flood control, and the taxpayer.

## SIGNIFICANCE

Some alluvial rivers are currently adjusting to active tectonics, and this must be considered as an additional explanation for river instability. Furthermore, geomorphic studies provide independent support for the results of the National Geodetic Survey resurveys because river response to uplift conforms to that expected from field and experimental studies of river morphology elsewhere.

As noted above, active tectonics can be responsible for aggradation, degradation, channel avulsion, and pattern change, both downstream and upstream of the deformed reach. Therefore, the net result of active tectonics is unstable river reaches that are characterized by incision, deposition, bank erosion, meander cutoffs, or the development of meandering, braided, or anastomosing patterns (Figure 5.4).

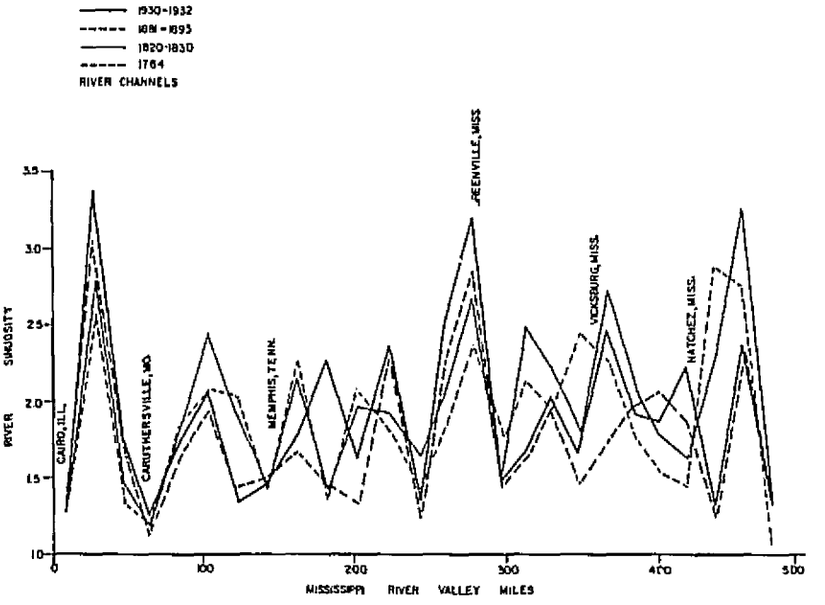


FIGURE 5.18 Variations of Mississippi River sinuosity below Cairo, Illinois, as determined from maps prepared in 1764, 1820-1830, 1881-1893, and 1930-1932. Note consistently high values of sinuosity in reaches affected by Lake County Uplift (Cairo, Illinois-Caruthersville, Missouri); Monroe Uplift (Greenville, Mississippi); and Wiggins Uplift (?) below Natchez, Mississippi. From Schumm *et al.* (1982).

Navigation can be affected by aggradation and the development of bars. Bank erosion, incision, and pattern change can impact riparian use and cause loss of valuable structures (bridges, loading docks) as well as agricultural land and homes. The frequency of overbank flooding will be increased in reaches of aggradation and reduced gradient. Changes in the frequency of overbank flooding through a zone of active tectonics will change the position of "ordinary high water," which is usually a legal boundary, and this may lead to confusion and litigation concerning the location of the river bank.

If rivers are affected by active tectonics then obviously canals will be. Canals are usually constructed to carry relatively clear water on gentle slopes. As in the Middle East, a slight warping can seriously affect the efficiency of the canal (Leary *et al.*, 1981).

The evidence of river response to active tectonics can be used to evaluate the tectonic stability of hazardous waste-disposal sites. For example, in addition to the criteria presented earlier, studies of salt domes in eastern Texas suggest that the Oakwood Salt Dome may be active because channels on the central dome are incised up to 4 *m*, and there are three abandoned channel reaches that suggest lateral movement of the channels away from the dome (Collins *et al.*, 1981). Furthermore, as in the past, fluvial evidence can be used to identify those areas most favorable for exploration for gas and oil. The geomorphic techniques can be used to aid in planning geophysical surveys and the selection of drilling sites.

Active tectonics in some areas has had a disastrous effect. Earthquakes in the upper Indus Basin have triggered massive landslides that impounded vast amounts of water that eventually overtopped the natural dam and caused catastrophic flooding downstream. In addition, valley-floor deformation could lead to major avulsive shifts of a river. The effects discussed herein are primarily related to aseismic deformation, but it is this slow deformation that has been ignored when river behavior is studied. Clearly more detailed studies of the effects of active tectonics on alluvial rivers are needed to establish the within-channel hydraulic changes that can be expected and the engineering response that is required to mitigate the detrimental effects on river stability and use.

## ACKNOWLEDGMENTS

The field work was carried out by Adam Burnett in Louisiana and Mississippi and was performed under research grants from the National Science Foundation (EAR-7727573) and the U.S. Army Corps of Engineers, Potamology Division, Vicksburg. I thank Larry Lattman and David Russ for their helpful reviews.

## REFERENCES

Adams, J. (1980). Active tilting of the United States midcontinent: Geodetic and geomorphic evidence, *Geology 8*, 442-446.

Adams, R. M. (1965). *Land Behind Baghdad*, University of Chicago Press, Chicago, Ill., 187 pp.

Ambraseys, N. N. (1978). Studies in historical seismicity and tectonics, in *The Environmental History of the Near and Middle East*, W. C. Brice, ed., Academic Press, New York, pp. 185-210.

Bendefy, L., J. Dohnalik, and K. Mike (1967). Nouvelles methodes de l'etude genetique des cours de eau, *Int. Assoc. Sci. Hydrology, Publ. 75* (Bevue), pp. 64-72.

Bowler, J. M., and L. B. Harford (1966). Quaternary tectonics and the evolution of the Riverine Plain near Echuca, Victoria, *Geol. Soc. Austral. 13*, 339-354.

Brown, L. D., and J. E. Oliver (1976). Vertical crustal movements from leveling data and their relation to geologic structure in the eastern United States, *Rev. Geophys. Space Phys. 14*, 13-35.

Burnett, A. W. (1982). Alluvial stream response to neotectonics in the lower Mississippi Valley, unpublished M.S. thesis, Colo. State Univ., Fort Collins, Colo.

Burnett, A. W., and S. A. Schumm (1983). Active tectonics and river response in Louisiana and Mississippi, *Science* 222, 49-50.

Collins, E. W., O. R. Dix, and D. K. Hobday (1981). Oakwood Salt Dome, East Texas, surface geology and drainage analysis, *Univ. of Tex., Bur. Econ. Geol. Circular 81-6*, 23 pp.

Cotton, C. A. (1941). Notes on two transverse profile geomorphic problems, *Trans. R. Soc. N.Z. 71*, 1-5.

Dales, G. T. (1966). The decline of the Harappans, *Sci. Am. 214*, 92-100.

DeBlieux, C. (1951). Photogeologic study in Kent County, Texas, *J. Oil Gas 50*, 86.

DeBlieux, C. (1962). Photogeology in Louisiana coastal marsh and swamp, *Gulf Coast Assoc. Geol. Soc. Trans. 12*, 231-241.

Doornkamp, J., and Temple, B. (1966). Surface drainage and tectonic instability in part of southern Uganda, *Geogr. J. 132*, 238-252.

Fisk, H. N. (1944). *Geologic Investigations of the Alluvial Valley of the Lower Mississippi River*, Mississippi River Commission, Vicksburg, Miss., 78 pp.

Freund, R., I. Zak, and Z. Garfunkel (1968). Age and rate of the seismal movement along the Dead Sea rift, *Nature* 220, 253-255.

Gardner, T. W. (1975). The history of part of the Colorado River and its tributaries, an experimental study, *Four Corners Geol. Soc. Guidebook, 8th Field Conference (Canyonlands)*, pp. 87-95.

Holmes, D. A. (1968). The recent history of the Indus, *Geogr. J. 134*, 367-382.

Howard, A. D. (1967). Drainage analysis in geologic interpretation, *Am. Assoc. Petrol. Geol. 51*, 2246-2259.

Jin, De Sheng (1984). Unpublished report on experimental studies, Colo. State Univ., Fort Collins, Colo., 15 pp.

Kazmi, A. H. (1979). Active fault systems in Pakistan, in *Geodynamics of Pakistan*, A. Farah and K. A. DeJong, eds., Geol. Surv. of Pakistan, Quetta, pp. 285-294.

Kowalski, W. C., and H. Radzikowska (1968). The influence of neotectonic movements on the formation of alluvial deposits and its engineering-geological estimation, *Proc. 23rd Inter. Geol. Congr. Prague Czech., Section 12*, pp. 197-203.

Lambrick, H. T. (1967). The Indus flood plain and the "Indus" civilization, *Geogr. J. 133*, 483-495.

Leary, P. C., P. E. Malin, R. A. Strelitz, and T. L. Henyey (1981). Possible tilt phenomena observed as water level anomalies along the Los Angeles aqueduct, *Geophys. Res. Lett. 8*, 225-228.

Lees, G. M. (1955). Recent earth movements in the Middle East, *Geol. Runds. 43*, 221-226.

Lyell, C. (1857). *Principles of Geology*, Appleton and Co., New York, 834 pp.

Machida, T. (1960). Geomorphological analysis of terrace plains-fluvial terraces along the River Kuji and the River Ara, Kanto District, Japan, *Science Reports Section C 7*, Tokyo Kyoiku Daigaku (Tokyo University of Education), pp. 137-194.

McKeown, F. A., and L. C. Pakiser, eds. (1982). *Investigations of the New Madrid, Missouri Earthquake Region*, U.S. Geol. Surv. Prof. Paper 1236, 201 pp.

Melton, F. A. (1959). Aerial photographs and structural geology, *J. Geol. 67*, 352-370.

Mike, K. (1975). Utilization of the analyses of ancient riverbeds for the detection of Holocene crustal movements, *Tectonophysics 29*, 359-368.

Mirjayar, K. M. (1966). Recent tectonic movements and the development of the Euphrates River Valley, *Izv. Akad. Nauk SSSR Ser. Geogr. Geofiz. 5*, 80-85.

Nanson, G. C. (1980). A regional trend to meander migration, *J. Geol. 88*, 100-107.

Neef, E. (1966). Geomorphologische Moglichteiten für festellung junger Erdkrustenbewengungen, *Geologie (Berlin) 15*, 97-101.

Oldham, R. D. (1926). The Cutch earthquake of 16 June 1819 with a revision of the great earthquake of 12 June 1897, *Geol. Surv. India Mem. 46*, 1-77.

Ollier, C. C. (1981). *Tectonics and Landforms*, Longmans, New York, 324 pp.

Ouchi, S. (1983). Response of alluvial rivers for active tectonics, unpublished Ph.D. dissertation, Colo. State Univ., Fort Collins, Colo., 205 pp.

Ouchi, S. (1985). Response of alluvial rivers to slow active tectonic movement, *Geol. Soc. Am. Bull. 96*, 504-515.

Potter, P. E. (1978). Significance and origin of big rivers, *J. Geol. 86*, 13-33.

Radulescu, G. (1962). Deciphering of tectonic movements in the Quaternary territory of Rumania by means of geomorphical methods, in *Problems de Geographie*, pp. 9-19.

Russ, D. P. (1982). Style and significance of surface deformation in the vicinity of New Madrid, Missouri, *U.S. Geol. Surv. Prof. Paper 1236*, pp. 45-114.

Saucier, R. T. (1970). Quaternary geology of the lower Mississippi River Valley, *Research Series No. 6, Arkansas Archaeol. Surv.*, Fayetteville, Ark., 26 pp.

Saucier, R. T., and A. R. Fleetwood (1970). Origin and chronologic significance of late Quaternary terraces, Quachita River, Arkansas and Louisiana, *Geol. Soc. Am. Bull. 81*, 869-890.

Schumm, S. A. (1972). Geologic implications of river pattern variability (abstract), *Am. Assoc. Petrol. Geol. 56*, 652 pp.

Schumm, S. A. (1977). *The Fluvial System*, John Wiley & Sons, New York, 338 pp.

Schumm, S. A. (1981). Evolution and response of the fluvial system, sedimentologic implications, *Soc. Econ. Paleontol. Mineral. Spec. Publ. 31*, pp. 19-29.

Schumm, S. A., and H. R. Khan (1972). Experimental study of channel patterns, *Geol. Soc. Am. Bull. 83*, 1755-1770.

Schumm, S. A., H. R. Khan, B. R. Winkley, and L. G. Robbins (1972). Variability of river patterns, *Nature* 237, 75-76.

Schumm, S. A., C. C. Watson, and A. W. Burnett (1982). Investigation of neotectonic activity within the Lower Mississippi Valley Division: Phase I, U.S. Army Corps of Engineers, Lower Mississippi Valley Division (Vicksburg), Potamology Program, Report 2, 158 pp.

Smith, D. G., and N. D. Smith (1980). Sedimentation in anastomosed river systems, examples from alluvial valleys near Banff, Alberta, *J. Sediment. Petrol. 50*, 157-164.

Sparling, D. R. (1967). Anomalous drainage pattern and crustal tilting in Ottowa County, Ohio, *Ohio J. Sci. 67*, 378-381.

Stevens, G. R. (1974). *Rugged Landscape, the Geology of Central New Zealand*, A. H. and A. W. Reed, Wellington, 286 pp.

Tator, B. A. (1958). The aerial photograph and applied geomorphology, *Photogramm. Eng. 24*, 549-561.

Tanner, W. F. (1974). The incomplete flood plain, *Geology* 2, 105-106.

Tricart, J. (1974). *Structural Geomorphology*, Longmans, New York, 305 pp. (translation of 1968 French edition).

Twidale, C. R. (1966). Late Cainozoic activity of the Selwyn Upwarp, northwest Queensland, *J. Geol. Soc. S. Austral.* 13, 491-494.

Twidale, C. R. (1971). *Structural Landforms*, Australian National University Press, Canberra.

Veatch, A. C. (1906). Geology and underground water resources of nothern Louisiana and southern Arkansas, *U.S. Geol. Surv. Prof. Paper* 46, 422 pp.

Volkov, N. G., I. L. Sokolovsky, and A. L. Subbotin (1967). Effect of recent crustal movement on the shape of longitudinal profiles and water levels in rivers, *Int. Union Geodesy Geophys. Publ.* 75, pp. 105-116.

Wallace, R. E. (1967). Notes on stream channels offset by the San Andreas Fault, southern Coast Ranges, California, *Stanford Univ. Publ. (Geol. Sci.)* 11, 6-20.

Walters, W. H., and D. B. Simons (1984). Long-term changes of Lower Mississippi River meander geometry, in *River Meandering*, C. M. Elliott, ed., Am. Soc. Civil Eng., New York, pp. 318-329.

Wang, K. K. (1952). Geology of Ouachita Parish, *La. Geol. Surv. Bull.* 28, Baton Rouge, La., 126 pp.

Watson, C. C., S. A. Schumm, and M. D. Harvey (1984). Neotectonic effects on river pattern, in *River Meandering*, C. M. Elliott, ed., Am. Soc. Civil Eng., New York, pp. 55-66.

Wilhelmy, H. (1969). Das Urstromtal am Ostrand der Indusebene und das sarasvati Problem, *Z. Geomorphol.* (suppl. 6 and 8), 76-93.

Winkley, B. R. (1980). Analysis of River Conditions to Improve Navigation at the Greenville, Mississippi Bridge, Mississippi River, Potamology Section, Hydraulics Branch, Vicksburg District, U.S. Army Corps of Engineers, Vicksburg, Mo., 55 pp.

Zuchiewicz, W. (1979). A possibility of application of the theoretical longitudinal river's profile analysis to investigations of young tectonic movements, *Ann. Soc. Geol. Pologne* 49, 327-342.

Zuchiewicz, W. (1980). Young tectonic movements and morphology of the Pieniny Mountains (Polish Western Carpathians), *Ann. Soc. Geol. Pologne* 50, pp. 263-300.

# 6 Coastal Tectonics

KENNETH R. LAJOIE
*U.S. Geological Survey, Menlo Park*

## INTRODUCTION

Between one-third and one-half of the Earth's marine coastlines lie along or near tectonically and seismically active plate boundaries (Inman and Nordstrom, 1971). Many of the world's major population centers lie along these active coastlines and, therefore, are vulnerable to adverse impacts of large earthquakes. Fortunately, there has been remarkable progress over the past two decades in the field of coastal tectonics, the study of recent crustal deformation and paleoseismicity in coastal regions. Of particular importance is progress in establishing earthquake recurrence, dating recent fault activity, and measuring rates of recent crustal deformation, all of which are crucial in determining earthquake potential and assessing seismic hazards and risk. Much of the recent progress in coastal tectonics stems directly from the development of new dating techniques that have led to a better understanding of Quaternary [past 2 million years (m.y.)] sea-level fluctuations and their relationship to marine strandlines (abandoned or relict marine shorelines), which are among the most numerous and widespread tectonic markers in the Quaternary geomorphic record (Figures 6.1, 6.2, and 6.3).

Sea level is the common and unifying element of coastal tectonics. Present sea level, the universal datum for measuring elevation, is the most convenient reference for detecting ongoing vertical crustal movement and assessing short-term tectonic stability in coastal areas. Accordingly, coastal tectonics often includes analysis of tide-gauge data (Figure 6.4) and other historical and archeological information that might reveal apparent sea-level changes. Past sea levels derived from the geologic record comprise a composite datum for measuring long-term crustal movement. Consequently, coastal tectonics also includes mapping and dating marine strandlines and separating the vertical crustal movements from the past sea-level fluctuations they si-

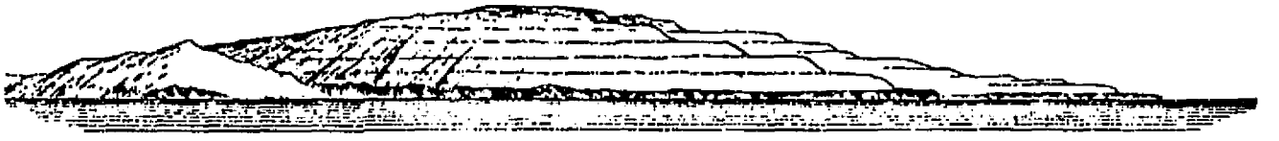

FIGURE 6.1 Emergent marine strandlines form steplike terraces on the Palos Verdes Peninsula of southern California. These and similar strandlines on tectonically active coastlines record both crustal uplift and major glacio-eustatic sea-level fluctuations (see Figure 6.6). The lowest strandline terrace is about 100 ka and the highest is about 1000 ka. The highest point on the peninsula is about 450 m above sea level. Modified from Davidson (1889).

multaneously record. Because marine strandlines are the physical records of past sea levels, the study of sea-level history is an integral part of coastal tectonics.

Time-transgressive sequences of displaced and deformed Pleistocene [2 m.y. to 10,000 yr (10 ka) ago] marine strandlines document patterns of and, where dated, yield rates of continual, long-term crustal deformation (Figures 6.1 and 6.2). Sequences of emergent Holocene (past 10 ka) strandlines (Figure 6.3), which occur only along the most rapidly uplifting coastlines, commonly record abrupt coseismic uplift events of 1-15 m (see Figures 6.25-6.28 below) that cumulatively comprise the long-term deformation recorded by Pleistocene strandlines. Consequently, sequences of Holocene strandlines often record past earthquakes and, where dated, yield earthquake periodicity and provide a means of forecasting future seismic events. In many areas, apparent sea-level changes documented by tide-gauge records (Figure 6.4) or subtle shifts in the location of the modern shoreline reflect ongoing vertical crustal movement. Frequently, this movement is opposite in sense to long-term trends and, therefore, may represent postearthquake crustal relaxation or pre-earthquake strain accumulation.

Coastal tectonics includes the study of both onshore (emergent) and offshore (submergent) marine strandlines and structural features. However, offshore coastal tectonics is a highly specialized field and is beyond the scope of this brief review, which focuses mainly on the formation and deformation of emergent marine strandlines and stresses their importance in determining the style and measuring the rates of recent crustal deformation, especially in highly active coastal regions. Most examples of strandline displacement and deformation cited in this review reflect sustained tectonic processes, but a few, included mainly for comparative purposes, reflect transitory volcanic and glacio-isostatic crustal deformation.

## COASTAL MORPHOLOGY AND TECTONIC SETTING

On global and regional scales coastal morphology correlates closely with tectonic setting (Inman and Nordstrom, 1971). The greatest geomorphic contrast is between the subdued coastlines along passive continental margins and the rugged coastlines along convergent plate boundaries. Along most coastlines modern (active) coastal landforms are similar to their Pleistocene counterparts, which suggests that current tectonic and coastal processes have been fairly uniform over considerable periods of time.

Most exposed coastlines along passive continental

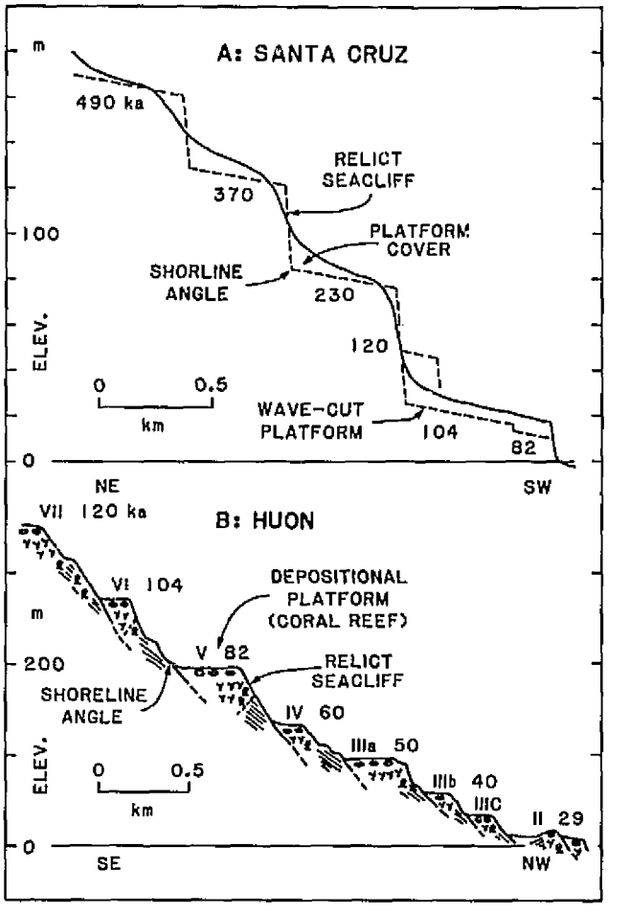


FIGURE 6.2 Cross-sectional profiles of emergent Pleistocene strandline terraces.

A, Erosional strandlines near Santa Cruz, California. Solid line is existing topographic profile. Dashed line represents original profile of each strandline terrace, which consists of a relict wave-cut platform backed by a relict sea cliff. The intersection of the platform and the sea cliff is the shoreline angle, which closely approximates the paleoshoreline. Seaward thinning wedges of alluvial sediment derived from the degrading sea cliffs overlie the wave-cut platforms. A 120-ka strandline was removed from this section when the next lower (104 ka) platform was cut; the 120-ka strandline occurs a few kilometers north of this site and is projected onto this cross section. The three lowest strandlines were dated by paleontological, amino acid, and geomorphic techniques. The average uplift rate (0.35 m/ka) was derived from the vertical displacement (28 m) of the 82-ka strandline. The three highest strandlines were dated by extrapolation of this uplift rate and by numerical analysis of the progressively gentler slopes of successively higher (older) relict sea cliffs. Modified from Hanks *et al.* (1984).

B, Depositional strandline terraces on the Huon Peninsula, Papua New Guinea. Each platform is a relict coral reef. U-series dates on fossil corals from these strandlines yield a history of glacio-eustatic fluctuations that serves as a tectonic datum for measuring vertical tectonic movements on other coastlines throughout the world (see Figure 6.6). The maximum average uplift rate of 4 m/ka on the Huon Peninsula was derived from the maximum vertical displacement (500 m) of the 120-ka strandline. Note that the three lowest strandlines on the Santa Cruz coastline correlate with the three highest strandlines in this sequence. Modified from Chappell (1974a).

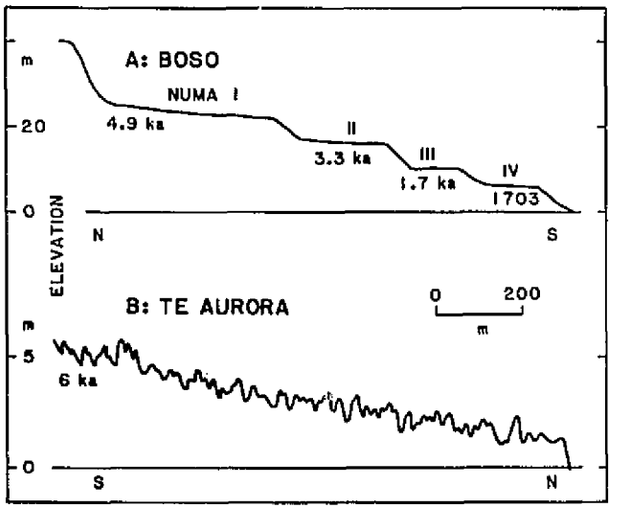


FIGURE 6.3 Cross-sectional profiles of Holocene strandlines.

A, Erosional terraces on the Boso Peninsula of Honshu, Japan. These strandlines, unlike their Pleistocene counterparts, represent periodic coseismic uplift events, not sea-level fluctuations (see Figures 6.7, 6.25, 6.26, 6.27, and 6.28). The lowest platform (IV) records uplift that accompanied two major earthquakes in 1703 and 1923, and the three highest strandlines were dated by radiocarbon analysis of fossil shells. The average uplift rate is 3.9 m/ka (see Figure 6.25). Modified from Matsuda *et al.* (1978).

B, Depositional strandlines (beach ridges) at Te Araroa on North Island, New Zealand. Each ridge most likely represents a storm event not a coseismic uplift event. If uplift events are recorded in this sequence of strandlines, they are indistinguishable from storm events. The average uplift rate derived from the highest beach ridge (6 ka) is 1 m/ka. Modified from Garrick (1979).

margins consist of broad coastal plains bordered offshore by wide continental shelves and gentle continental slopes. These relatively stable coastlines are characterized by depositional landforms such as broad sandy beaches and offshore barrier bars and at low latitudes by broad coral reefs. The southeast coast of North America and the northeast coast of Australia are typical passive-margin coastlines with low-to-moderate topographic relief and subdued depositional landforms. Much of the former is bordered offshore by barrier bars (Oaks and Du Bar, 1974), and most of the latter by extensive coral reefs (Hopley, 1983).

Long-term tectonic stability along most passive-margin coastlines is expressed stratigraphically by undeformed continental and marine sediments that underlie flat coastal plains and continental shelves and geomorphically by broad accretionary strandline terraces that consist of subdued beach ridges separated by abandoned tidal flats (Oaks and Du Bar, 1974). However, rapid sediment accumulation, such as at the mouth of a large river, may isostatically depress an otherwise stable passive-margin coastline (Figure 6.4C) (Fisk and McFarlan, 1955; Hicks and Crosby, 1974). Also, occasional large earthquakes, such as the 1886 Charleston, South Carolina, seismic event on the Atlantic coast of North America (Hays and Gori, 1983), indicate that passive continental margins are not completely aseismic, even though there is little stratigraphic or geomorphic evidence in these areas of recent, near-surface crustal deformation.

In contrast to the subdued coastlines along passive plate boundaries, most coastlines along or near active continental margins consist of coastal hills or mountains bordered offshore by narrow continental shelves and

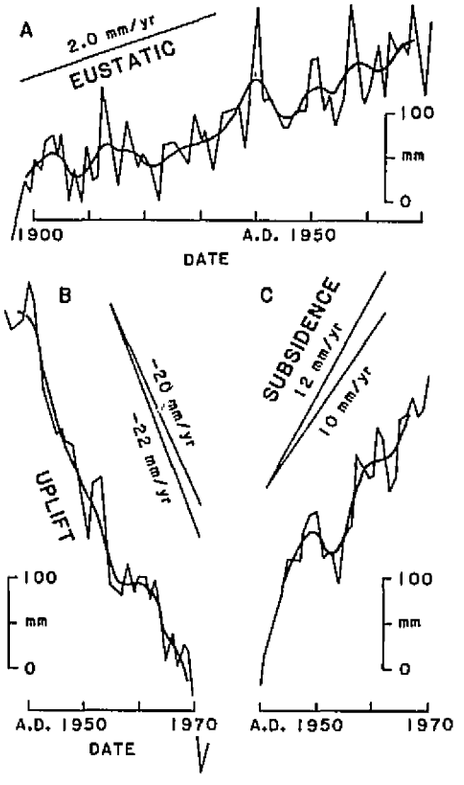


FIGURE 6.4 Tide-gauge records.

A, San Francisco, California—the secular drift of this record (−2 mm/yr) is similar to that found in other parts of the world and, therefore, probably represents eustatic rise in sea level.

B, Juneau, Alaska—the extreme apparent drop in sea-level represents crustal uplift due to either tectonic uplift or residual glacio-eustatic rebound.

C, Mississippi delta—the apparent rise in sea-level represents subsidence due to sediment compaction and isostatic adjustments of the crust to the sediment load of the Mississippi delta. The eustatic rise (2 mm/yr) was subtracted from the relative rates to obtain the uplift and subsidence rates. Modified from Hicks and Crosby (1974).

deep submarine trenches, particularly in the circum-Pacific region. These tectonically active coastlines are characterized by rugged erosional landforms such as steep sea cliffs and rocky headlands, islands and sea stacks. However, at low latitudes coral reefs commonly form narrow depositional platforms even along rugged coastlines (Figure 6.2B)(Chappell, 1974a). The mountainous west coast of South America is an active-tectonic coastline that geomorphically reflects regional crustal uplift and subsidence related to rapid plate convergence and resultant subduction along the offshore Peru-Chile Trench (Plafker, 1972). The hilly-to-mountainous coast of California in western North America is an active-tectonic coastline that geomorphically reflects slower regional uplift and local basin subsidence related to oblique plate convergence and resultant large-scale, right-lateral displacement across the San Andreas Fault system.

Long-term crustal instability along most active-tectonic coastlines is expressed stratigraphically by folded and faulted marine sediments that fill youthful structural basins and geomorphically by narrow uplifted and deformed Pleistocene strandline terraces that notch steep coastal slopes (Figures 6.1 and 6.2). Short-term instability along extremely active coastlines is expressed geomorphically by emergent Holocene strandline terraces (Figure 6.3) and by dramatic changes in the location and configuration of modern shorelines that result from rapid vertical crustal movements (Figure 6.4). Most of the Earth's seismicity occurs along or near active-tectonic coastlines (Tarr, 1974), and many large earthquakes in these areas are recorded geomorphically by emergent Holocene strandline terraces (Figure 6.3A; also see Figures 6.25-6.28 below).

The subdued coastlines bordering the shallow epicontinental seas in North America (Hudson Bay) and Fennoscandia (Bay of Bothnia) are exceptions to the general rule that coastal regions undergoing rapid crustal deformation are characterized by marked topographic relief. However, the rapid crustal uplift recorded so dramatically by sequences of highly emergent Holocene strandlines in these recently deglaciated areas reflects transitory isostatic rebound (see Figure 6.10 below) not sustained tectonic deformation.

## MARINE STRANDLINES

Marine strandlines are the geological and historical records of former sea levels. In the geologic record marine strandlines are the depositional and erosional remains of abandoned marine shorelines (Figures 6.1, 6.2 and 6.3), and in the historical record they are most commonly tide-gauge measurements (Figure 6.4) or high-water marks on man-made coastal structures.

A strandline, or a sequence of strandlines, is a relative sea-level record that potentially represents both *real* and *apparent* sea-level changes (Figure 6.5):

$$relative = real + apparent. \qquad (6.1)$$

Real sea-level changes are absolute vertical movements of the ocean's surface and may be local to worldwide in extent; if worldwide, they are called eustatic changes.

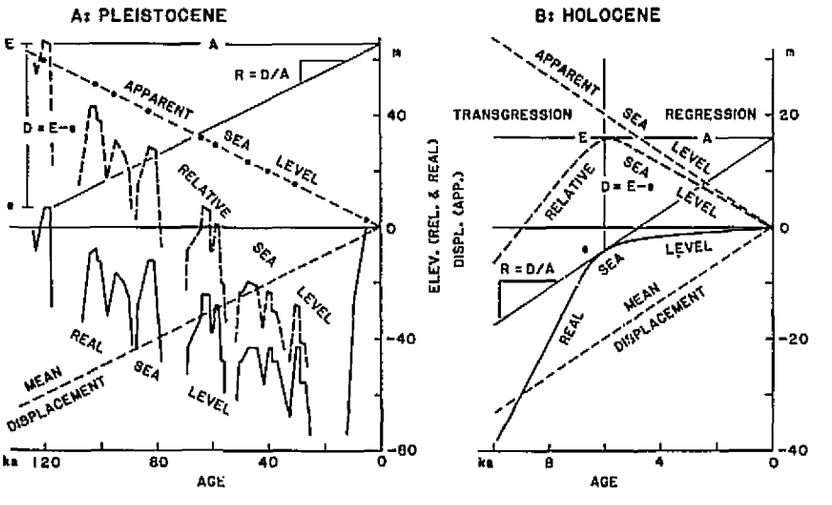


FIGURE 6.5 Relative, apparent, and real sea-level changes.

A, Late Pleistocene.

B, Holocene.

All sea-level records (strandlines or tide-gauge measurements) are relative, which means they potentially represent both apparent and real sea-level changes (*relative = real + apparent*). Apparent sea-level changes are the inverse of the vertical crustal (or ground) movements that produce them and, therefore, are the focus of all coastal tectonic studies. The apparent sea-level history is obtained by algebraically or graphically subtracting the real sea-level history from the relative record of marine strandlines. In effect, the real sea-level history is a composite tectonic datum. The real sea-level history is obtained by subtracting apparent sea level changes from a relative sea-level record. In this case, the uplifting coastline is a moving sea-level datum. $E$ is the present elevation of a strandline; $e$ is the original elevation of a strandline; $D$ is the vertical displacement ($D = E - e$); $A$ is the age of a strandline; $R$ is the crustal displacement rate ($R = D/A$).

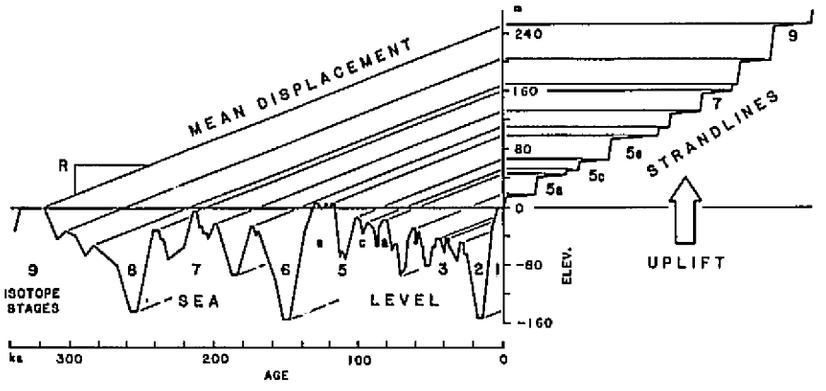


FIGURE 6.6 Pleistocene sea-level fluctuations and origin of emergent Pleistocene strandlines. Emergent strandlines simultaneously record tectonic uplift and major sea-level highstands. The rising coastline is a moving strip chart on which sea-level highstands are recorded sequentially as strandlines whose ages increase with elevation. The slope ($R$) of the diagonal line connecting each highstand to the elevation of its strandline is the average uplift rate. If the uplift rate was constant, the uplift lines for all strandlines are parallel. Strandlines formed during lowstands are usually destroyed by subsequent sea-level fluctuations and rarely appear in the emergent geologic record. Strandlines younger than 60 ka appear above sea level only where the uplift rate is greater than 1 m/ka. The sea-level fluctuation curve was derived from a sequence of U-series dated coral-reef strandlines on the Huon Peninsula, Papua New Guinea (Figure 6.2B) by subtracting tectonic uplift from the relative strandline record (Figure 6.5A). Sea-level curve modified from Chappell (1983); oxygen-isotope stages (1-9) from deep-sea cores (Shackleton and Opdyke, 1973).

Quaternary sea-level history was characterized by periodic eustatic fluctuations of 100-150 m caused by the advance and retreat of continental glaciers. Apparent sea-level changes are not real but result from and are the inverse of vertical ground movements. Consequently, apparent sea-level changes are only local or regional in extent.

The primary task in coastal tectonics is separating the apparent component from the real component of a relative sea-level record. This is done graphically or algebraically by subtracting the real sea-level history from a relative sea-level record:

$$apparent = relative - real. \qquad (6.2)$$

In effect, the real sea-level history is a fluctuating tectonic datum to which each strandline (tectonic marker) must be correlated by age (Figures 6.5, 6.6, and 6.7).

The real sea-level history is obtained by subtracting apparent sea-level changes (the inverse of vertical crustal movements) from a detailed and well-dated relative sea-level record (Figure 6.5):

$$real = relative - apparent. \qquad (6.3)$$

In this case, the tectonic history is an absolute sea-level datum and can be either moving or stationary. A rapidly and steadily rising coastline is the best datum for measuring major, long-term sea-level fluctuations (Figures 6.5A and 6.6) (Chappell, 1983), whereas a stable coastline is the best datum for measuring minor, short-term sea-level changes (Figures 6.5B and 6.7) (Bloom, 1970; Scholl *et al.*, 1970). Generally, the greatest uncertainties in most long-term sea-level histories derived from strandline data stem from the simplifying assumption of constant uplift. However, on a tilted coastline where Pleistocene strandlines converge, constant long-term uplift at a particular locality can be demonstrated empirically (Chappell, 1983). The greatest uncertainties in short-term sea-level histories stem from the assumption of coastal stability. Where short-term stability at a coastal locality cannot be demonstrated by independent geodetic data, subtle sea-level changes can be expressed in only relative terms. An additional complication is

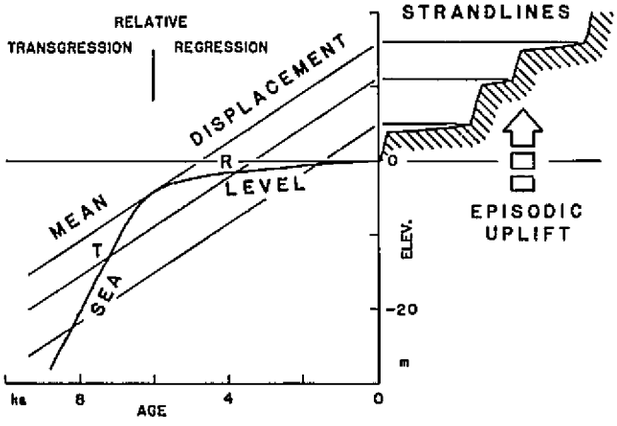


FIGURE 6.7 Holocene sea-level changes and origin of emergent Holocene strandlines. In contrast to Pleistocene strandlines, emergent Holocene strandlines represent discrete uplift events or storm events, not sea-level fluctuations. The highest strandline correlates with the tangent point at the sea-level inflection between 7 ka and 5 ka BP. All lower strandlines represent two paleoshorelines, one occupied during the transgressive phase and one during the regressive phase (see Figure 6.5B for relative sea-level changes). The sea-level curve is general and may vary slightly from region to region owing to minor geoidal distortions.

that different measurement techniques (e.g., geodetic, tide gauge) occasionally yield conflicting results for short-term sea-level changes (Brown, 1978).

*Pleistocene Strandlines*

Along steep coastal slopes in uplifting areas Pleistocene strandlines occur most commonly as narrow (< 1 km), steplike terraces within a few hundred meters above present sea level. Consequently, a vertical sequence of uplifted strandline terraces resembles a flight of stairs (Figures 6.1 and 6.2). Each strandline terrace consists of a virtually horizontal erosional or depositional platform backed by a steep sea cliff along its landward margin. The shoreline angle, the intersection of the relict platform and sea cliff, closely approximates the location and elevation of the abandoned marine shoreline and is the linear structural marker depicted on most longitudinal profiles of deformed strandlines (for examples see Figures 6.8A, 6.13, 6.17, 6.20, and 6.21). The shoreline platform, also referred to as the terrace platform, is the planar tectonic marker depicted on most cross-sectional profiles and detailed isobase maps of deformed strandlines (Figures 6.2 and 6.3A; also see Figures 6.19 and 6.21 below).

Commonly, a thin (1-3 m) veneer of shallow-water sand, gravel, and cobbles, which locally contains fossil marine shells used for dating, overlies the terrace platform. Where subaerial slope degradation is rapid, a seaward-thinning prism of alluvium derived from upland streams and abandoned sea cliffs overlies the platform and its associated marine sediments and buries the shoreline angle (Figure 6.2A). In these areas the geomorphic expression of successively higher (older) Pleistocene strandline terraces is progressively subdued, and the position and configuration of both the shoreline angle and the terrace platform must be derived from borehole or shallow seismic data (see Figure 6.21 below) (Bradley and Griggs, 1976; Lajoie *et al.*, 1979b). However, in some areas the progressively greater degradation of successively older relict sea cliffs provides a means of dating emergent strandlines (Figure 6.2A) (Hanks *et al.*, 1984). Along gentle coastal slopes in slowly uplifting areas emergent strandlines commonly consist of broad (1-10 km) terrace platforms backed by low sea cliffs obscured by relict beach ridges and dune fields (Hoyt and Hails, 1974; Lajoie *et al.*, 1979a).

A general consensus has developed over the past two decades that a flight of emergent Pleistocene strandlines is the geologic record of periodic glacio-eustatic sea-level highstands superimposed on a rising coastline (Figure 6.6) (Broecker *et al.*, 1968; Mesolella *et al.*, 1969; Matthews, 1973). In this model, a rising coastal landmass is a moving strip chart on which brief sea-level highstands were successively recorded as depositional or erosional strandlines. Strandlines also formed during sea-level lowstands (Emery, 1958; Lewis, 1971a,b, 1974; Ridlon, 1972), but along uplifting coastlines most of these strandlines were destroyed by wave erosion during subsequent sea-level fluctuations and, therefore, rarely appear in the emergent marine record (Figure 6.6). An important exception is found in the deeply incised sequence of emergent strandline terraces on the Huon Peninsula of Papua New Guinea, where sea-level lowstands are recorded as deltaic accumulations preserved beneath a protective cover of coral reefs deposited during subsequent sea-level highstands (Chappell, 1974a, 1983). Along many subsiding coastlines, strandlines formed during sea-level lowstands probably dominate the submergent geomorphic record but are difficult to distinguish from strandlines formed during highstands (Moore and Fornari, 1984).

The most detailed tectonic datum for deriving uplift from emergent Pleistocene strandlines on coastlines throughout the world is the paleosea-level curve obtained by subtracting well-documented constant tectonic uplift from the relative sea-level record of emergent coral-reef strandlines on the Huon Peninsula of Papua New Guinea (Figures 6.2B and 6.6) (Veeh and Chappell, 1970; Bloom *et al.*, 1974; Chappell, 1983). There, uranium-series dates on fossil corals yield a paleosea-level curve back to about 340 ka before present (BP) that agrees with longer, but less detailed, sea-level curves derived from emergent coral-reef strandlines on the island of Barbados in the West Indies (Broecker *et al.*, 1968; Mesolella *et al.*, 1969; Matthews, 1973; Bloom *et al.*, 1974; Bender *et al.*, 1979) and from oxygen-isotope data from deep-sea cores (Shackleton and Opdyke, 1973). The uplift rate (maximum 4.0 m/ka) of the Huon Peninsula was derived from the elevation of the prominent 120-ka strandline that formed 2-10 m above present sea level during the last major interglacial sea-level highstand (Thurber *et al.*, 1965; Veeh, 1966; Ku *et al.*, 1974; Neumann and Moore, 1975; Marshall and Thom, 1976; Stearns, 1976; Harmon *et al.*, 1978; Shubert and Szabo, 1978; Szabo *et al.*, 1978; Szabo, 1979). The most important features of the New Guinea paleosea-level curve as a tectonic datum are the periodic interglacial highstands at approximately 100 ka intervals and the successively lower interstadial highstands at approximately 20 ka intervals over the past 120 ka. Virtually all Pleistocene strandlines along emergent coastlines throughout the world were formed during these brief paleosea-level highstands. The longer paleosea-level records on Barbados and in the deep-sea cores indicate that the main 100-ka cycle of interglacial high-

stands extends back to at least 700 ka (Shackleton and Opdyke, 1973; Bender *et al.*, 1979).

Morner (1976, 1983) argued that no locally derived Pleistocene sea-level curve should be used as a worldwide tectonic datum because the sea surface, an approximate geoid or equipotential gravitational surface, is grossly distorted by gravitational fluctuations on a time scale of 10-100 ka. If correct, this supposition implies that major, glacially induced changes in ocean volume were expressed by neither synchronous nor uniform sea-level fluctuations. However, similar absolute ages of Pleistocene strandlines on emergent coastlines throughout the world and, more importantly, similar elevations of sea-level highstands on several independently derived late Pleistocene sea-level curves demonstrate that, within reasonable margins of uncertainty (±5 ka and ±10 m; Stearns, 1976, 1984; Harmon *et al.*, 1979; Chappell, 1983), major sea-level fluctuations were synchronous and relatively uniform over at least the past 300 ka, and most likely much longer (Veeh and Valentine, 1967; Bloom *et al.*, 1974; Konishi *et al.*, 1974; Ku and Kern, 1974; Moore and Samayajulu, 1974; Chappell and Veeh, 1978; Harmon *et al.*, 1978; Marshall and Launay, 1978; Bender *et al.*, 1979; Dodge *et al.*, 1983; Ward, 1985; also see references on elevation of 120-ka highstand in preceding paragraph). Also, reasonable graphical correlations of undated strandline sequences in Japan (see Figure 6.14 below) (Miyoshi, 1983), New Zealand (W. Buli, University of Arizona, personal communication, 1983), and California (Hanks *et al.*, 1984) with 120-ka to 40-ka highstands on the New Guinea paleosea-level curve indicate that strandlines from all four areas were synchronous and had a common datum. An apparent exception is found along the southeast Atlantic coast of North America, where the ages, but not the relative heights, of late Pleistocene highstands agree with paleosea-level data from New Guinea and other parts of the world (Belknap, 1979; Cronin *et al.*, 1981). However, the discrepancies of 20-30 m found along this passive continental margin may represent subtle tectonic or isostatic crustal movements not regional sea-level variations. In any event, although rapid geoidal distortion is a potential problem that requires further investigation, most existing data indicate that geoidal distortion could not have been significant over late Pleistocene time. Consequently, there is no compelling reason not to use the New Guinea sea-level curve worldwide as a first-order tectonic datum, at least over the past 120 ka.

Because virtually all emergent Pleistocene strandlines were formed during sea-level highstands (Figure 6.6), the task of dating a particular strandline is reduced to correlating it with a specific peak on the New Guinea paleosea-level curve using one or more absolute (isotopic) or relative (geomorphic, paleontologic, and chemical) dating techniques (Chappell and Veeh, 1978; Kennedy *et al.*, 1982; Sutherland, 1983; Hanks *et al.*, 1984). Uranium-series analyses of fossil corals yield the most reliable absolute dates for Pleistocene strandlines (Broecker and Bender, 1973; Harmon *et al.*, 1979), but because fossil corals are virtually restricted to tropical latitudes, less-reliable dating techniques must be used at higher latitudes.

Frequently, only one or two Pleistocene strandlines in an emergent sequence can be dated independently, but the ages of other strandlines can be inferred from the resultant uplift rate (Chappell and Veeh, 1978; Hanks *et al.*, 1984; Ward, 1985). Occasionally, an entire sequence of undated late Pleistocene strandlines can be correlated with the paleosea-level curve by trial and error if different, but constant, uplift rates are assumed; the best graphical correlation of strandline elevations and paleosea-level highstands simultaneously yields the most reasonable uplift rate and strandline ages (see Figure 6.6). In effect, the uplift rate itself is a useful dating tool, even if not independently derived. However, in some complexly deformed coastal areas no strandlines can be dated confidently using this graphical technique (Weber, 1983), which suggests that the uplift rate varied with time. Generally, for strandlines dated between 700 ka and 200 ka BP by either absolute or relative techniques the uncertainty in correlation with the Pleistocene paleosea-level curve is at least one major glacio-eustatic cycle (±100 ka), and for strandline dated between 120 ka and 30 ka the uncertainty is commonly one minor cycle (±20 ka) (Harmon *et al.*, 1979; Stearns, 1984).

The best-preserved and most reliably dated Pleistocene strandlines along most emergent coastlines correlate with the 120-ka, 104-ka, and 82-ka sea-level highstands (see Figure 6.11B below). These three highstands correlate with deep-sea oxygen-isotope substages 5e, 5c, and 5a, respectively (Shackleton and Opdyke, 1973; Chappell, 1983), and their strandlines are often referred to by these alphanumeric designations. Strandlines that correlate with younger (lower) highstands appear in the emergent geologic record only where uplift rates are sufficiently high (>0.3-1.0 m/ka) to elevate them above present sea level (Figure 6.6). Along most erosional coastlines some emergent Pleistocene strandlines are missing or are laterally discontinuous owing to sea-cliff retreat during the formation of younger strandlines (see Figures 6.17B and 6.20A below). Generally, strandlines older than 400 ka are poorly preserved owing to subaerial slope degradation and stream incision; exceptions are found on stable or slowly rising coastlines where strandlines as old as 2.4 m.y. are commonly preserved

(Ward, 1985). In areas of rapid uplift (greater than 4 m/ka), subaerial erosional processes are greatly accelerated and strandlines older than 120 ka are rarely preserved. However, in areas of rapid uplift the fine structure of late Pleistocene sea-level history is most clearly and completely recorded by strandlines younger than 120 ka (Chappell, 1983).

*Holocene Strandlines*

Radiocarbon dates on fossil wood, peat, and shell from sedimentary deposits on continental shelves and in shallow coastal embayments throughout the world indicate that sea level stood about 100-150 m below its present position during the last glacial maximum between 20 ka and 15 ka BP, and then rose rapidly to within 4-6 m of its present position by about 7-5 ka BP as the major ice sheets retreated at the end of Pleistocene time (Bloom, 1977). Although sea-level changes over the past 5 ka may have varied regionally owing to minor geoidal distortion and hydro-isostatic crustal loading (Clark *et al.*, 1978), the most reliable data indicate that sea level has not fluctuated significantly (±2 m), nor has it been higher than its present position, over this period of time (Figure 6.7) (Thom *et al.*, 1969; Bloom, 1970; Scholl *et al.*, 1970; Omoto, 1979; Faure *et al.*, 1980; Thom and Roy, 1983; Sneh and Klein, 1984; Gibb, in press). Consequently, Holocene strandlines, unlike Pleistocene strandlines, do not represent eustatic sea-level fluctuations but rather episodic crustal movements or major storm events. However, the highest strandlines in most Holocene strandline sequences usually represent the sudden and drastic decrease in postglacial sea-level rise between 7 ka and 5 ka BP (Figure 6.7). Along erosional coastlines emergent Holocene strandlines form and survive only where crustal uplift is sufficiently rapid (>1-2 m/ka) to offset the destructive effects of subsequent wave erosion. However, along prograding coastlines depositional strandlines survive even where there is little or no crustal uplift (Figure 6.3B) (Schofield, 1973, Garrick, 1979).

Most emergent Holocene strandlines of both erosional and depositional origin are similar in configuration to their Pleistocene counterparts but usually are smaller in scale, finer in geomorphic expression, and better preserved (Figure 6.3). Also, because of their relatively youthful age, most Holocene strandlines lie within tens rather than hundreds of meters above present sea level, even along the most rapidly uplifting coastlines. In protected embayments and near the mouths of large streams and rivers, Holocene strandlines commonly consist of bouldery to sandy beach ridges that are relatively imprecise paleosea-level indicators (Figure 6.3B) (Schofield, 1973; Garrick, 1979). However, along many wave-resistant coastlines with small tidal ranges (less than 1 m) emergent Holocene strandlines consist of horizontal solution notches and faint waterlines on rocks and sea cliffs that are extremely precise paleosea-level indicators (Machida *et al.*, 1976; Pirazzoli *et al.*, 1982). Along some recently uplifted coastlines, strandlines consist of horizontal bands of fossil intertidal sessile organisms such as barnacles, which are also precise paleosea-level indicators (Sawamura, 1953) even in areas with large tidal ranges (Plafker, 1965). In the historical record, emergent Holocene strandlines most commonly consist of points on tide-gauge records (Figures 6.4 and 6.9B) (Hicks and Crosby, 1974; Berrino *et al.*, in press), but in a few areas they consist of waterlines and burrows of intertidal organisms on recently uplifted or downdropped man-made coastal structures (see Figure 6.9A below)(Grant, 1970; Flemming, 1972; Berrino *et al.*, in press).

Along many rapidly uplifting coastlines, prehistoric Holocene strandlines are similar to strandlines produced by abrupt vertical crustal movements associated with major historical earthquakes (Sugimura and Naruse, 1954; Plafker, 1965; Wellman, 1969; Matsuda *et al.*, 1978). This similarity suggests that all emergent Holocene strandlines are of coseismic origin. However, along stable or steadily uplifting coastlines, both erosional and depositional strandlines probably form during infrequent major storms (Schofield, 1973; Garrick 1979; Hillaire-Marcel, 1980). A major uncertainty in deriving a history of paleoseismicity from a sequence of emergent Holocene strandlines is that coseismic and storm-produced strandlines may be indistinguishable. Consequently, if coseismic and storm-produced strandlines occur together (Sandweiss and Rollins, 1981; Lajoie *et al.*, 1982a), the number of past earthquakes could be overestimated from the geologic record. On the other hand, wave erosion may remove coseismic strandlines from the geologic record (see Figure 6.27B below) (Plafker *et al.*, 1981), in which case the number of earthquakes represented by a sequence of emergent Holocene strandlines could be underestimated.

Because of minor regional or subregional geoidal distortions, local hydro-isostatic adjustments, variable oceanographic conditions (currents, water temperature, salinity), and climatic fluctuations, there is probably no locally derived late Holocene sea-level curve that can be used as a precise universal tectonic datum for measuring minor (less than 2 m) vertical crustal movements (Clark *et al.*, 1978; Newman *et al.*, 1978). At best, a locally derived curve is a regional tectonic datum. However, data from coastlines throughout the world indicate that relative sea-level changes greater than 2-4 m over the past 6 ka are either apparent (caused by tectonic and isostatic crustal movements or sediment

compaction) or spurious (caused by reworking or contamination of dated fossil materials), not real. Therefore, present sea-level or a generalized sea-level curve (Figure 6.7) is often used as an approximate tectonic datum for measuring late Holocene crustal movements, especially where rates of deformation are very high (see Figures 6.25, 6.26, and 6.27 below) (Matsuda *et al.*, 1978; Plafker and Rubin, 1978; Plafker *et al.*, 1981).

Most Holocene strandlines in the geologic record are dated directly or indirectly by radiocarbon techniques. However, the sudden and drastic decrease in the sea-level rise between 7 ka and 5 ka BP occasionally leads to incorrect or misleading radiocarbon dates on fossil materials (particularly marine shells) from emergent Holocene strandlines. This potential problem exists because all but the highest strandline in a sequence of emergent Holocene strandlines represent two different paleoshorelines—a transgressive shoreline older than about 6 ka and a regressive shoreline younger than 6 ka (Figure 6.7). Consequently, marine shells deposited on the older, transgressive shoreline could be reworked into sediments deposited on the younger, regressive shoreline.

On the other hand, the two-part configuration of the Holocene sea-level curve provides an independent means of approximating the ages of emergent Holocene strandlines and deriving minimum uplift rates. On a plot of strandline elevation versus sea-level history (Figure 6.7), the straight line connecting the elevation of the highest strandline on the vertical axis and the tangent point at the break on the sea-level curve represents the average uplift since that strandline formed. The coordinates of the tangent point are the tentative age and original elevation of the highest strandline, and the slope of the line is the tentative average uplift rate. If constant uplift is assumed, interpolation of the uplift rate yields age estimates for any lower strandlines (see Figure 6.28 below) (Wellman, 1969). Because the highest Holocene strandline on most coastlines represents the break in sea-level rise, its age is usually between 7 ka and 5 ka, depending on the uplift rate; because the break is rounded, the age of the highest strandline increases from 5 ka to 7 ka as the uplift rate increases. However, if subsequent cliff erosion destroyed the 7-5-ka strandline, the highest surviving strandline would be somewhat younger. Obviously, other dating techniques are needed to test for this possibility.

## STRANDLINE DISPLACEMENT AND DEFORMATION

Regional patterns of vertical strandline displacement (uplift or subsidence) and deformation (folding and faulting) commonly reflect primary tectonic processes (subduction and rifting) related directly to horizontal plate motions. Important exceptions are found in the northernmost continental areas of North America and Europe where regional patterns of latest Pleistocene and Holocene strandline displacement reflect major but transitory isostatic responses of the crust and mantle to geologically recent glacial unloading.

Local patterns of strandline displacement and deformation generally involve minor tectonic structures (folds, faults, horsts, and grabens) that reflect secondary tectonic processes related to subregional stress patterns. Available data indicate that most secondary and some primary tectonic deformation recorded by marine strandlines extends no farther than a few tens of kilometers inland from the coastline. In many areas, vertical ground displacements on a local scale also reflect nontectonic processes such as volcanic tumescence (Kaizuka *et al.*, 1983; Berrino *et al.*, in press), isostatic adjustments due to sediment accumulation (Fisk and McFarlan, 1955), and sediment compaction due to natural processes (Atwater *et al.*, 1977) or fluid extraction (Poland, 1971; Buchanan-Banks *et al.*, 1975). In many cases, especially those involving minor vertical displacements, it is difficult, if not impossible, to distinguish tectonic from nontectonic apparent sea-level changes.

It is noteworthy that on both local and regional scales sequences of marine (and lacustrine) strandlines constitute the longest and most detailed and areally extensive records of late Quaternary crustal deformation. Indeed, the magnitudes and rates of tectonic, isostatic, and volcanic processes derived from deformed and displaced strandlines are commonly used as references for comparing and interpreting tectonic data from less complete or shorter records in other geological environments.

### *Vertical Displacement*

Because marine strandlines define horizontal lines and planes (where curved or closed), they record vertical crustal displacements (uplift or subsidence) more clearly than horizontal displacements. Net vertical displacement ($D$) is the difference between the present elevation ($E$) and the original elevation ($e$) of a strandline and is also the product of the strandline's age ($A$) and the average displacement rate ($R$) (Figure 6.5):

$$D = E - e = AR. \tag{6.4}$$

The average displacement rate ($R$) is the displacement ($D$; $E - e$) of a strandline divided by its age ($A$):

$$R = D/A = (E - e)/A. \tag{6.5}$$

An isobase is a locus of points on a planar tectonic marker (a marine platform or a plane defined by a curved or closed strandline) along which the vertical

displacement rate ($R$) is equal (see Figures 6.12, 6.15A, 6.16A, 6.18, and 6.21 below). The history of vertical crustal displacements at a coastal locality is derived graphically by plotting the displacement ($D$) of each independently dated strandline as a function of its age ($A$) (Figure 6.5). The resultant locus of points is the apparent sea-level history, which, as stated previously, is the inverse of the displacement history. If this locus of points defines a straight line, the displacement rate ($R$), which is the inverse of the slope of the line, was constant. If it does not define a straight line, the displacement rate was variable (see Figures 6.9A and 6.10B below). Commonly, only one strandline in a sequence can be dated independently, and, therefore, only an average displacement rate can be derived from a relative sea-level record.

A plot of strandline elevation ($E$) as a function of age ($A$) yields the relative sea-level history, which is the inverse of the approximate displacement history where vertical displacements are large compared to sea-level changes. Frequently, uplift histories based on highly emergent Holocene strandlines (see Figures 6.25, 6.26, and 6.27 below) or very old Pleistocene strandlines (Bender *et al.*, 1979) are approximated by relative sea-level curves. In other words, present sea level can be used as an approximate datum.

The presence of emergent marine strandlines along most active-tectonic coastlines suggests that crustal uplift is more common than subsidence. However, subsidence is probably underestimated merely because most geologic evidence for downward crustal movements is buried in sedimentary basins (Atwater *et al.*, 1977) or is submerged offshore (Lewis, 1974). Many studies of long-term crustal movements in coastal areas focus on uplift mainly because the emergent strandline record is better exposed and easier to interpret than the submergent record.

Most long-term crustal movements recorded by marine strandlines reflect sustained tectonic deformation along active plate boundaries, but the most rapid known rates of vertical crustal displacement reflect transitory volcanic tumescence and glacio-isostatic rebound. Both processes are noteworthy primarily for comparative purposes, but also because they are, themselves, related to tectonic processes in various ways.

*Volcanic Displacements* The highest known rates of sustained vertical ground displacement exceed 100 mm/yr and are recorded by marine strandlines on the flanks of active insular and coastal volcanoes. For example, on the island of Iwo Jima, the tip of a large volcano in the western Pacific Ocean, radiometrically and historically dated emergent strandlines yield an average uplift rate

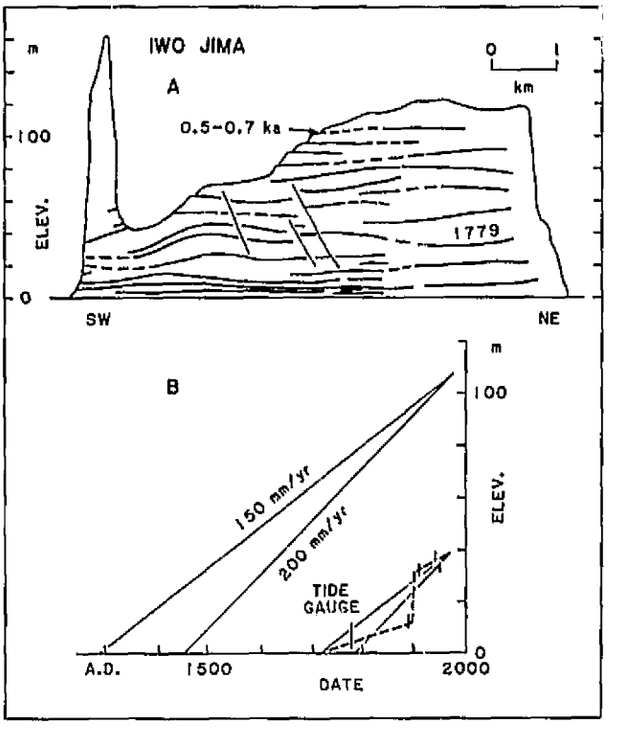


FIGURE 6.8 Recent volcanic uplift of Iwo Jima, a volcanic island 1200 km south of Tokyo, Japan.

A, Longitudinal strandline profiles. The strandline labeled 1779 was the active shoreline mapped in 1779 by the crew of the English explorer, Captain Cook. The age and maximum elevation of this strandline yield an average uplift rate of 200 mm/yr, which is similar to the rate of 170-240 mm/yr derived from radiocarbon dates of 0.5-0.7 ka on the 110-m strandline. The well-defined strandlines were formed by wave action during brief pauses in uplift or during periodic storms.

B, Average uplift rates derived from 110-m (0.5-0.7 ka) and 40-m (0.2 ka) strandlines. Tide-gauge data record variable uplift that reached 800 mm/yr over the past 80 yr. Both modified from Kaizuka *et al.* (1983).

of 200 mm/yr over the past 800 yr (Figure 6.8) (Kaizuka *et al.*, 1983). However, tide-gauge data suggest that uplift rates on the island probably fluctuated between 100 and 800 mm/yr over this period of time (Figure 6.8B), during which only minor phreatic eruptions are known to have occurred (Corwin and Foster, 1959).

An even longer record of vertical ground displacements related to volcanic processes is found in the Phlegraean Fields caldera on the Mediterranean coast near Naples, Italy, where historically dated strandlines on man-made structures document alternating subsidence and uplift that averaged 12 mm/yr over the past 2 ka (Figure 6.9) (Berrino *et al.*, in press). However, uplift and subsidence exceeded 150 mm/yr for a few decades before and after a minor eruption in A.D. 1538. Tide-

gauge records at Pozzuoli, a coastal suburb of Naples, yield uplift rates of 350 and 500 mm/yr for two brief periods between 1970 and 1983 (Figure 6.9B), which suggests that another eruption is imminent. However, the data from Iwo Jima indicate that rapid uplift and even short surges of extremely rapid uplift are not by themselves definite indicators of imminent eruption.

*Glacio-Isostatic Displacements* Highly emergent latest Pleistocene and Holocene marine (and lacustrine) strandlines in the deglaciated areas of northern North America and Europe record the highest known rates of regional vertical crustal displacement (Figure 6.10). Around Hudson Bay in Canada (Farrand and Gajda, 1962; Andrews, 1970; Peltier and Andrews, 1983) and the Gulf of Bothnia in Fennoscandia (Lundqvist, 1965; Donner, 1965, 1980), which were the regions of thickest ice accumulation during the last major glacial advance, rates of postglacial isostatic rebound reached 100 m/ka (100 mm/yr) between 13 ka and 7 ka BP and decreased quasi-exponentially to the present rates of 6-9 mm/yr (Barnett, 1966; Balling, 1980). Even these rates of residual glacio-isostatic rebound are extremely high compared with most rates of vertical tectonic displacement. Along the margins of these deglaciated areas, Holocene strandlines and tide-gauge data record complex histories of rapid subsidence as well as uplift, which probably reflect the collapse and inward migration of a crustal forebulge peripheral to the retreating ice front (Grant, 1980; Morner, 1980; Clague *et al.*, 1982).

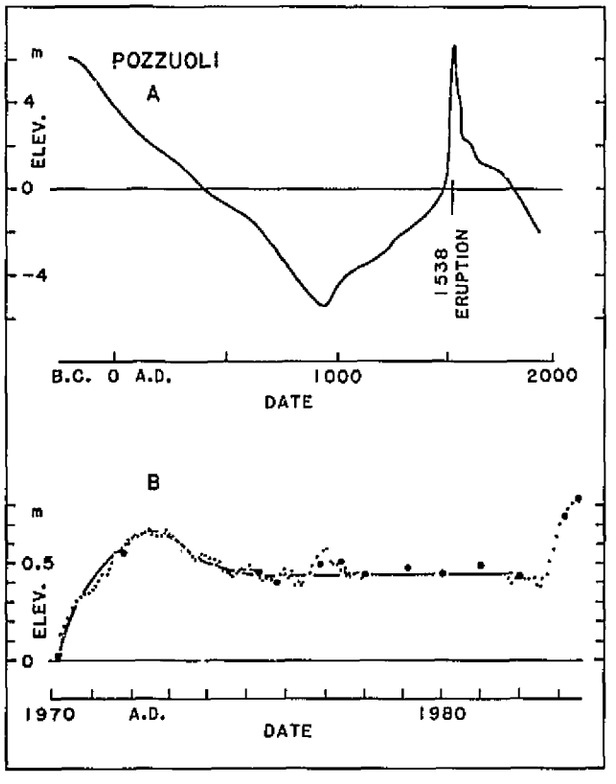


FIGURE 6.9 Recent volcanic displacements at Pozzuoli, a coastal suburb of Naples, Italy, in the Phlegraean Fields caldera.

A, Vertical displacement based on historical data such as water marks on Roman buildings. Mount Nuovo, a small cinder cone nearby, erupted in A.D. 1538, about 40 yr after the uplift rate increased from 10 mm/yr to about 100 mm/yr. The general subsidence that followed this small eruption has now reversed.

B, Tide-gauge data at Pozzuoli Harbor from 1970 to 1983. During two brief periods (1970-1973 and 1982-1983) uplift reached 800 mm/yr. Because of this rapid uplift, increased fumerole activity, and ground cracking, parts of Pozzuoli have been evacuated in anticipation of another eruption. Modified from Berrino *et al.* (in press).

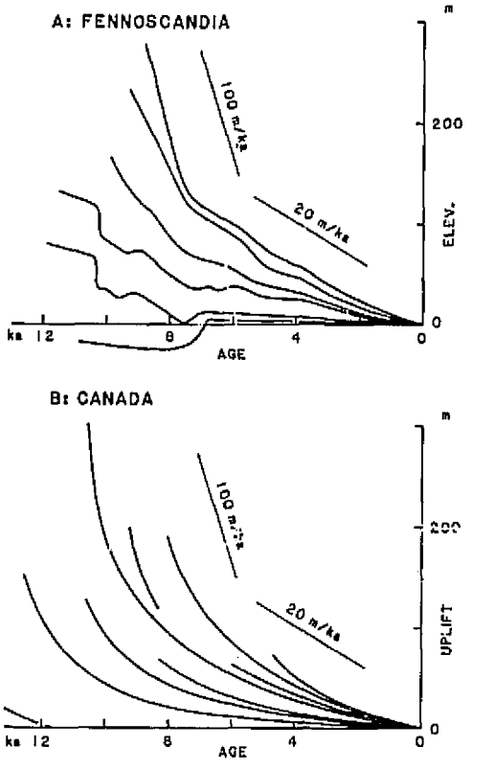


FIGURE 6.10 Postglacial isostatic rebound curves derived from dated marine and lacustrine strandlines.

A, Relative sea-level changes (minimum apparent sea-level changes), Gulf of Bothnia, Scandinavia. Modified from Lundqvist (1965).

B, Apparent sea-level changes, Hudson Bay, North America. Modified from Farrand and Gajda (1962).

In both areas crustal movement is the inverse of the curves. Regional crustal uplift exceeded 100 m/ka shortly after deglaciation in both areas.

In some deglaciated areas rapid vertical crustal movements recorded by strandlines probably reflect tectonic as well as isostatic processes (Grant, 1970; Mathews *et al.*, 1970; Clague *et al.*, 1982; Anderson *et al.*, 1984), and in a few areas the two processes apparently interact. For example, in western Scotland successively older emergent Holocene strandlines are offset progressively greater amounts across a series of local vertical faults (Sissons and Cornish, 1982), which indicates that the rate of glacio-isostatic rebound differed on either side of each fault. Also, in both North America and Europe, concentrations of recent seismic activity are closely associated with residual glacio-isostatic adjustments (Oliver *et al.*, 1970; Morner, 1978, 1980; Thompson *et al.*, 1983; Anderson *et al.*, 1984). Apparently, even residual isostatic movements trigger earthquakes along zones of crustal weakness, even in areas of relative tectonic stability. Rapid glacio-isostatic displacements are also important in a general tectonic context because they yield valuable information on the strength of the Earth's crust and the visco-elastic properties of the underlying mantle (Walcott, 1970; Peltier and Andrews, 1983).

*Tectonic Displacements* In marked contrast to the extremely rapid rates of volcanic and glacio-isostatic crustal displacement (>100 m/ka), the highest known rates of sustained vertical tectonic displacement recorded by marine strandlines are only 4 to 10 m/ka (Figure 6.11). Furthermore, these rapid displacement rates are recorded only by Holocene and latest Pleistocene strandlines, which suggests that they are of fairly limited duration. Also, virtually all rapid tectonic displacements recorded by marine strandlines occur along the axes of youthful anticlines above thrust-type faults in compressional tectonic regimes. Consequently, rapid vertical displacements of tectonic origin mainly reflect secondary deformation and are of limited importance in studies of regional crustal movements. However, because these rapid displacements are usually produced by episodic coseismic uplift events that are sufficiently large (1-15 m) to be expressed in the geologic record as emergent Holocene strandlines, they are extremely important in studies of paleoseismicity (see Figures 6.25-6.28 below). The episodic nature of rapid displacements recorded by marine strandlines suggests that maybe all tectonic deformation occurs in discrete increments. If this model is correct, these increments are too small or too infrequent at low deformation rates to be clearly expressed or preserved in the long-term geologic record.

Data from emergent Pleistocene strandlines throughout the world indicate that most rates of long-term tectonic uplift are less than 2 m/ka (Figure 6.11B), even along rapidly converging plate boundaries. Evidently,

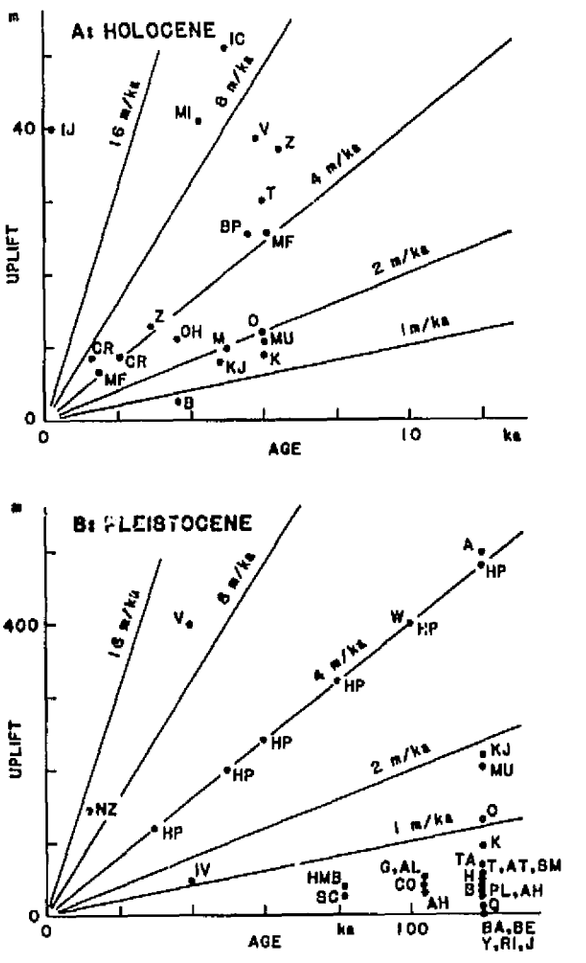


FIGURE 6.11 Rates of vertical crustal displacement (uplift only).

A, Holocene: IJ, Iwo Jima, volcanic uplift included for comparative purposes (Kaizuka *et al.*, 1983); CR, Crete (Angelier, 1979); Z, Zagros (Vita-Finzi, 1979); B, Bahrein (Ridley and Seeley, 1979); MI, Middleton Island (Plafker and Rubin, 1978); IC, Icy Cape (Plafker *et al.*, 1981); M, Makran (Page *et al.*, 1979); T, Turakirae (Wellman, 1969); BP, Boso Peninsula (Matsuda *et al.*, 1978; MF, Miller Flat; OH, Ocean House; V, Ventura; (Lajoie *et al.*, 1982a, 1983); O, Osado, K, Kosado (Tamura, 1979); MP, Muroto Peninsula (Kanaya, 1978); KJ, Kikai Jima (Nakata *et al.*, 1978).

B, Pleistocene: NZ, New Zealand (Wellman, 1979); V, Ventura (Lajoie *et al.*, 1982b); A, Arauco (Kaizuka *et al.*, 1973); HP, Huon Peninsula (Chappell, 1983); W, Wairarapa (Cahni, 1978); KJ, Kikai Jima (Konishi *et al.*, 1974); MV, Muroto (Yoshikawa *et al.*, 1964); O, Osado; K, Kosado (Tamura, 1979); HMB, Half Moon Bay (Lajoie *et al.*, 1979b); SC, Santa Cruz (Hanks *et al.*, 1984); RI, Royalty Islands (Marshall and Launay, 1978); TA, Taaanaki (Pillans, 1983); T, Timor; AT, Atauro (Chappell and Veeh, 1978); H, Haiti (Dodge *et al.*, 1983); B, Barbados (Bender *et al.*, 1979); AH, Arroyo Hondo; CO, Cojo; Al, Algeria; IV, Isla Vista; SM, Santa Monica (Lajoie and Sarna-Wojcicki, 1982); PL, Point Loma (Ku and Kern, 1974); J, Jamaica (Moore and Samayajulu, 1974); BA, Bahamas (Neumann and Moore, 1975); Y, Yucatan (Szabo *et al.*, 1978); BE, Bermuda (Harmon *et al.*, 1979, 1981); Q, Queensland (Ward, 1985).

in most areas isostatic adjustments are sufficiently rapid to compensate for (and thus prevent) higher rates of vertical crustal movement on a regional scale.

Although most short-term, vertical tectonic displacements recorded by Holocene marine strandlines are episodic or otherwise variable (see Figures 6.25-6.28 below) (Matsuda *et al.*, 1978; Plafker and Rubin, 1978; Plafker *et al.*, 1981), most average, long-term displacements recorded by Pleistocene strandlines appear to be relatively constant, at least over the past 100-500 ka (Bloom *et al.*, 1974; Konishi *et al.*, 1974; Moore and Samayajulu, 1974; Chappell and Veeh, 1978; Bender *et al.*, 1979; Harmon *et al.*, 1981; Dodge *et al.*, 1983; Chappell, 1983; Hanks *et al.*, 1984). Along some slowly uplifting coastlines, strandline data indicate that vertical displacement was fairly constant over the past 2-2.5 m.y. (Ward, 1985). Constant uplift can be demonstrated by comparing actual strandline elevations with those predicted by assuming constant uplift and using the New Guinea sea-level curve as a tectonic datum. Close agreement supports both the assumption of constant uplift and, of course, the assumption that the sea-level curve was a common tectonic datum.

Along a few coastlines, strandline data indicate that long-term tectonic uplift was clearly variable. For example, in the Christchurch area on the island of Barbados radiometrically dated Pleistocene strandlines yield an average uplift rate of 0.5 m/ka between 300 ka and 200 ka BP, and a lower rate of 0.3 m/ka after 200 ka BP (Bender *et al.*, 1979). Interestingly, in the nearby Saint George's Valley area uplift was relatively constant and averaged 0.3 m/ka over the past 640 ka.

Where data from marine strandlines and other tectonic markers are sufficiently abundant, regional compilations of vertical crustal movements provide valuable insights into both local and regional tectonic processes. Regional data are most conveniently and clearly expressed planimetrically by isobases (Figure 6.12) (Research Group for Quaternary Tectonics Map of Japan, 1969; Dambara, 1971; Wellman, 1979). Not surprisingly, most long-term regional isobases closely mimic general topographic contours, which simply means that the highest uplift rates occur in mountainous areas and the lowest rates or subsidence occur in low-lying regions. Usually, short-term isobases derived from historical information (tide-gauge and geodetic data) agree with longer-term isobases derived from geologic information, but locally short-term and long-term displacement rates differ drastically or the sense of displacement is reversed. For example, along the coastlines of northern California, Oregon, and Washington, net (long-term) displacement rates derived from Pleistocene strandlines are very low (0-0.5 m/ka; derived from dates

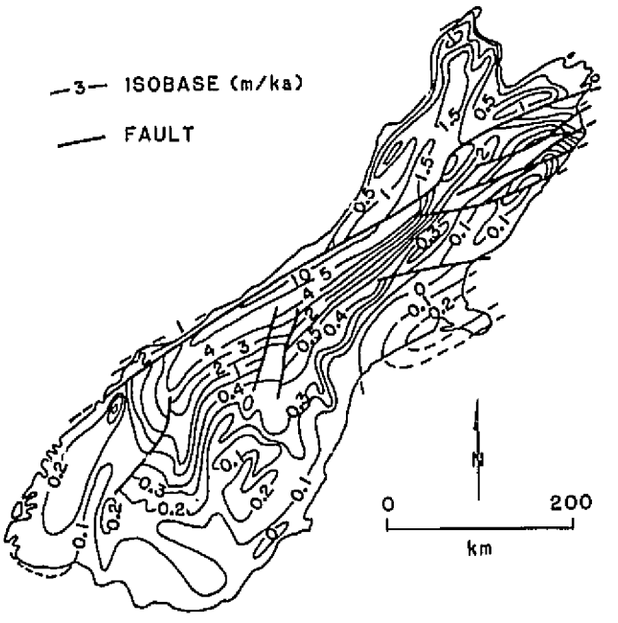


FIGURE 6.12 Isobase map of South Island, New Zealand, summarizing uplift data from marine strandlines and other vertically displaced geomorphic features. An isobase is a locus of points along which the uplift rate was equal. Isobases of South Island generally mimic topographic contours. Modified from Wellman (1979).

given in Kennedy *et al.*, 1982), but short-term rates derived from tide-gauge data locally reach 3 mm/yr (3 m/ka) (Hicks and Crosby, 1974). Some differences and reversals between short-term and long-term displacement rates probably represent pre-earthquake strain accumulation (Matsuda, 1976) or postearthquake crustal relaxation and, therefore, are important in determining earthquake potential (Thatcher, 1984). On the Muroto Peninsula of Shikoku, Japan, the 120-ka and 6-ka strandlines yield similar long-term uplift rates of 1.7 and 2.0 ka, respectively (Yoshikawa *et al.*, 1974)(see Figure 6.16A below), whereas episodic uplift associated with earthquakes over the past 300 yr averaged 12.5 mm/yr (see Figure 6.26A below). Geodetic and tide-gauge data show that the peninsula actually subsided between these coseismic uplift events (see Figure 6.16B below).

### *Tilt*

Crustal tilt ($T$) is the differential vertical displacement ($D_{\mathrm{I}} - D_{\mathrm{II}}$) of a horizontal tectonic marker (strandline or platform) divided by the horizontal distance ($d$) between any two observation points (I and II)

along a coastline. The resultant dimensionless ratio is, of course, the tangent of the tilt angle ($\theta$):

$$T = (D_I - D_{II})/d = \tan\theta. \qquad (6.6)$$

The tilt rate ($R$) is the tilt ($T$) divided by the age ($A$) of the marker:

$$R = T/A = \tan\theta/A. \qquad (6.7)$$

Even minor crustal tilt is clearly expressed in the longitudinal and cross-sectional profiles of marine strandlines. If the profiles of two or more tilted strandlines are parallel (Figure 6.13A), the differential vertical displacement took place at the time or after the youngest strandline formed. If the profiles converge (Figures 6.13B and 6.13C), which is the most common case, the differential displacement was progressive and took place over the period of time during which the strandlines formed.

If the tilt rate is constant, the geometric relationships of converging strandline profiles (Figures 6.13B and 6.13C) provide a useful means of correlating Pleistocene strandlines from widely separated areas, even where no independent age data are available. The algebraic expression relating the present elevation ($E_1$) of one strandline to the present elevation ($E_2$) of a second strandline at the same coastal locality is

$$E_1 = (A_1/A_2)E_2 - [(A_1/A_2)\,e_2 - e_1], \qquad (6.8)$$

where the first constant ($A_1/A_2$) is the ratio of the strandline ages, and the second constant $[(A_1/A_2)\,e_2 - e_1]$ is the difference between the original strandline elevations ($e_1$ and $e_2$). This equation defines a straight line generated by graphically plotting the elevation of the first strandline ($E_1$) as a function of the elevation of the second ($E_2$) at two or more localities along a tilted coastline or from different coastlines with different uplift rates (Figure 6.14). The first constant ($A_1/A_2$) is the slope of the line, and the second constant $[(A_1/A_2)\,e_2 - e_1]$ is its intercept on the vertical axis. The numerical values of these two constants are unique for any pair of Pleistocene strandlines and remain fixed regardless of the differential uplift rates. Therefore, the graphically derived values for these constants can be used to correlate undated strandline pairs from widely separated areas, such as from one island to another (Figure 6.14) (Miyoshi, 1983). These graphical correlations are possible only if the strandline pairs had common datums and were synchronous, and furthermore, only if the tilt rate at each locality was constant (but not necessarily equal). Consequently, Holocene strandlines cannot be correlated using this graphical technique because they are not necessarily synchronous along different coastlines.

Along straight coastlines, emergent strandlines are

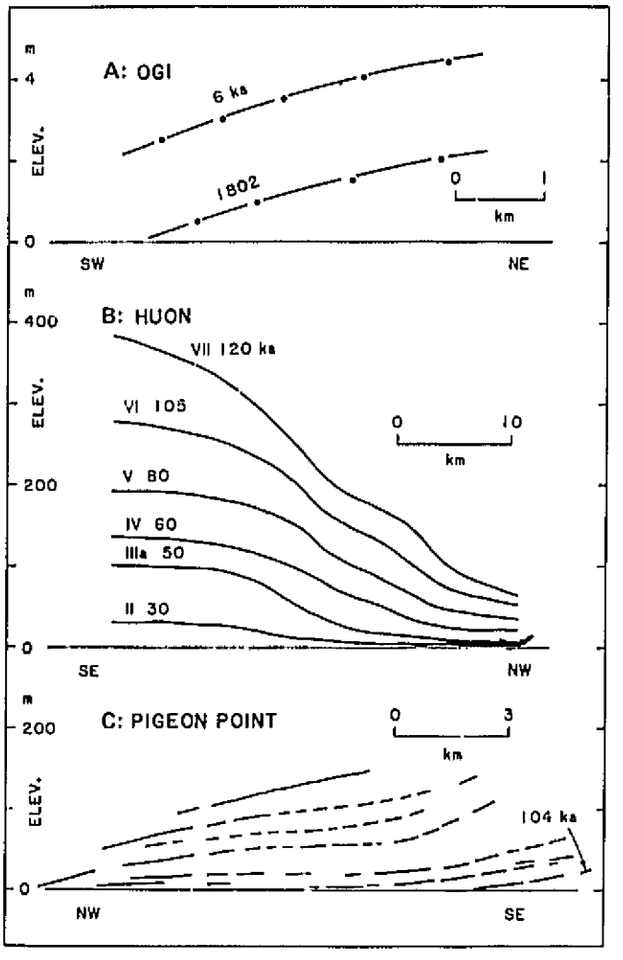


FIGURE 6.13 Tilted longitudinal profiles of emergent marine strandlines.

A, Parallel Holocene strandlines on Ogi Peninsula of Sado Island, Japan. The lowest strandline was formed by differential uplift associated with a large earthquake in 1802. The 6-ka strandline is parallel to this historical strandline, which indicates that no other tilt event has occurred in the past 6 ka. The 2 m separating these strandlines probably represents either gradual or abrupt uplift after 6 ka BP but before 1802. See Figure 6.24 for location. From data in Ota *et al.* (1976).

B, Converging Pleistocene strandlines on the Huon Peninsula, Papua New Guinea (see Figure 6.2B for cross-sectional profile). These converging strandlines record continual tilt over the past 120 ka. Ages are U-series dates on fossil corals. Minor irregularities in vertical spacing represent local variations in tilt rate. Modified from Chappell (1974b).

C, Converging Pleistocene strandlines near Point Año Nuevo on the central California coastline. Modified from Lajoie *et al.* (1979b).

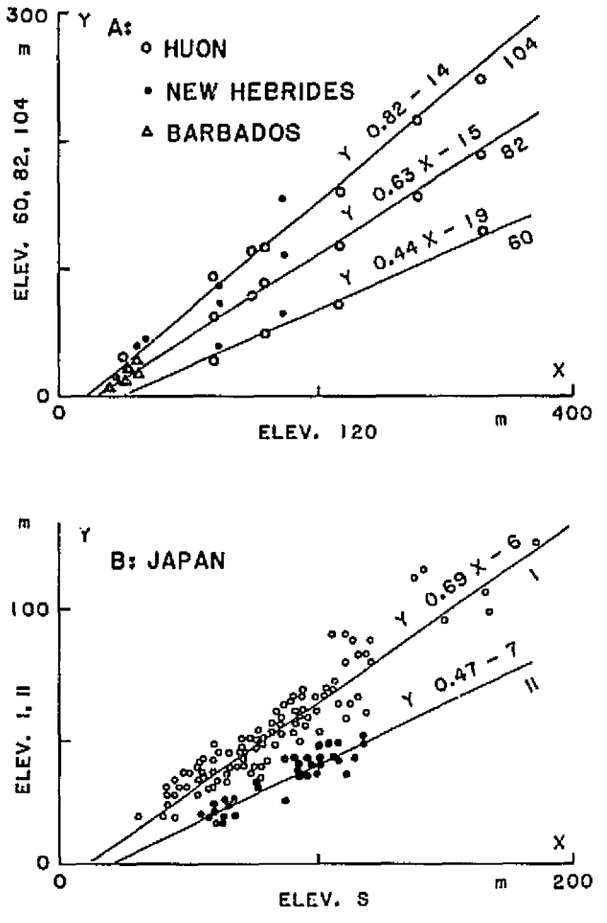


FIGURE 6.14 Correlation of Pleistocene strandlines by graphical techniques. The elevation of one strandline ($E_1$) is related to the elevation of a second strandline ($E_2$) at the same locality by the general equation $E_1 = (A_1/A_2)E_2 - [(A_1/A_2)\,e_2 - e_1]$. The constants $(A_1/A_2)$ and $[(A_1/A_2)\,e_2 - e_1]$ are unique for any pair of late Pleistocene strandlines and, therefore, can be used as a means of correlating strandline pairs from widely separated areas. The general equation (here simplified to $Y = Ax + B$) defines a straight line generated by plotting the elevation of one strandline ($E_1$) as a function of the elevation a second ($E_2$); the strandline pairs must be from localities with different but constant uplift rates, such as along a tilted coastline (Figure 6.13B), or on widely separated islands.

A, A plot of elevations of dated strandlines (60 ka, 82 ka, 104 ka, and 120 ka) from different parts of the world illustrate the relationship.

B, Undated strandline pairs (I and S; II and S) from throughout the Japanese archipelago. The constants for the two plots indicate that the S, I, and II strandlines correlate with the 120-ka, 80-ka, and 60-ka strandlines, respectively. Modified from Miyoshi (1983).

linear tectonic markers that record components of crustal tilt parallel to the shoreline. One of the best examples of tilt along a straight coastline is found on the Huon Peninsula of Papua New Guinea where the converging longitudinal profiles of six coral-reef strandlines record continual northwestward tilt of a large structural block over late Pleistocene time (Figure 6.13B) (Chappell, 1974b). There, as in other areas (Figure 6.13C) (Lajoie *et al.*, 1979b), minor irregularities in the converging profiles of Pleistocene strandlines reflect slight variations in the patterns and rates of long-term differential uplift.

Along straight, curved, and irregular coastlines, marine platforms are planar and virtually horizontal structural markers that record the actual direction of local tilt. In some areas progressively greater slopes of successively higher (older) marine platforms clearly record continual crustal tilt in both seaward and landward directions (Bradley and Griggs, 1976; Sarna-Wojcicki *et al.*, 1976; Gahni, 1978; Pillans, 1983).

Along irregular coastlines, curved or closed strandlines around small coastal embayments, peninsulas, or islands define broad planes that also record crustal tilt on a local, but slightly larger, scale (Figures 6.15 and 6.16A) (Ota, 1964, 1975; Tamura, 1979). A particularly instructive example of tilt is found on the Muroto Peninsula of southeast Shikoku, Japan, where structural contours on the planes defined by 120-ka and 6-ka strandlines yield similar rates of landward (northward) tilt of $6.1 \times 10^{-5}$/ka and $5.5 \times 10^{-5}$/ka, respectively (Figure 6.16) (Yoshikawa *et al.*, 1964; Kanaya, 1978). Significant landward tilt of the peninsula accompanied the 1947 Nankai earthquake, which suggests that long-term tilt in that area is episodic, not continuous. Gradual short-term seaward tilt documented by geodetic and tide-gauge data prior to the 1947 seismic event (Figure 6.16B)(Yoshikawa *et al.*, 1964) probably reflected pre-earthquake strain accumulation (1984).

Synchronous strandlines on widely separated islands or on distant parts of deeply embayed coastlines define areally extensive planes that record crustal tilt on a regional scale. For example, two planes defined by the 120-ka and 6-ka strandlines on numerous islands of the Ryukyu archipelago in southern Japan may record general eastward tilt over an area of 100,000 km$^2$ (Konishi *et al.*, 1974; Ota and Hori, 1980).

### *Folds*

Folds are merely compound tilts and, therefore, are similarly expressed by emergent marine strandlines in the coastal geologic record (Figures 6.17 and 6.18). In some areas folds expressed by deformed strandlines oc-

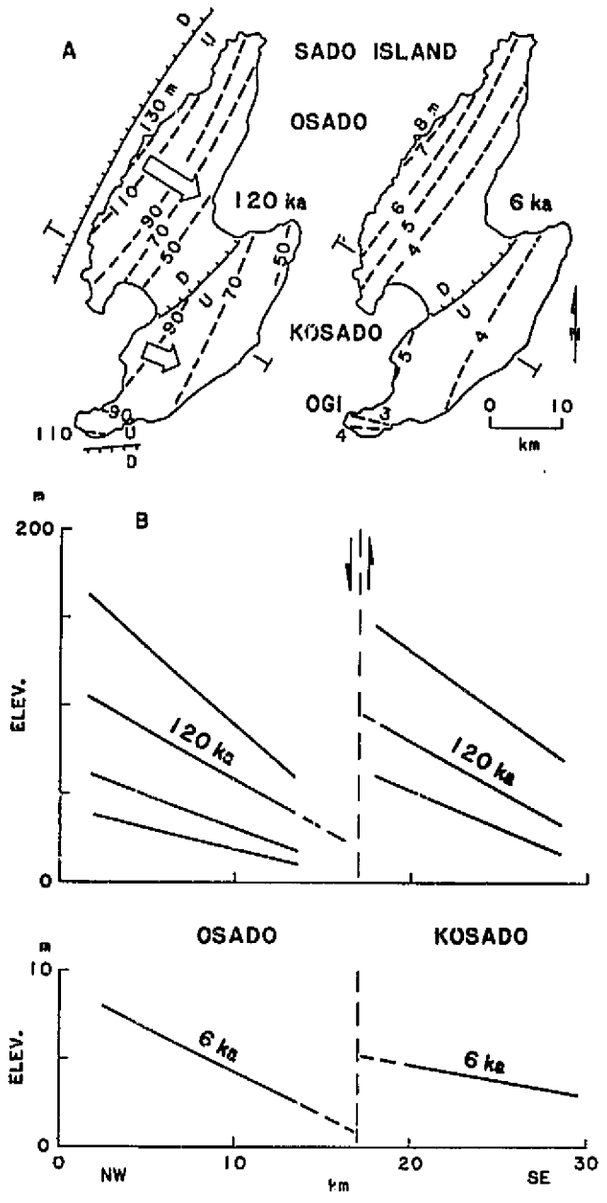


FIGURE 6.15 Tilted strandlines on Sado Island, Japan.

A, Isobases defined by 120-ka and 6-ka strandlines reveal continuous southeastward tilt of two structural blocks (Osado and Kosado) that constitute the island. Note—data points occur only along coastlines; isobases interpolated across inland areas.

B, Longitudinal profiles of Pleistocene and Holocene strandlines also reveal continual tilt. The strandline data indicate that the tilt rates of the two blocks have been constant but significantly different. If the fault separating the two parts of the island is vertical, the 120-ka strandline is offset about 75 m and the 6-ka strandline is offset about 4 m, which yield similar average slip rates of 0.6 m/ka and 0.7 m/ka, respectively. See Figure 6.24 for location. Modified from Tamura (1979).

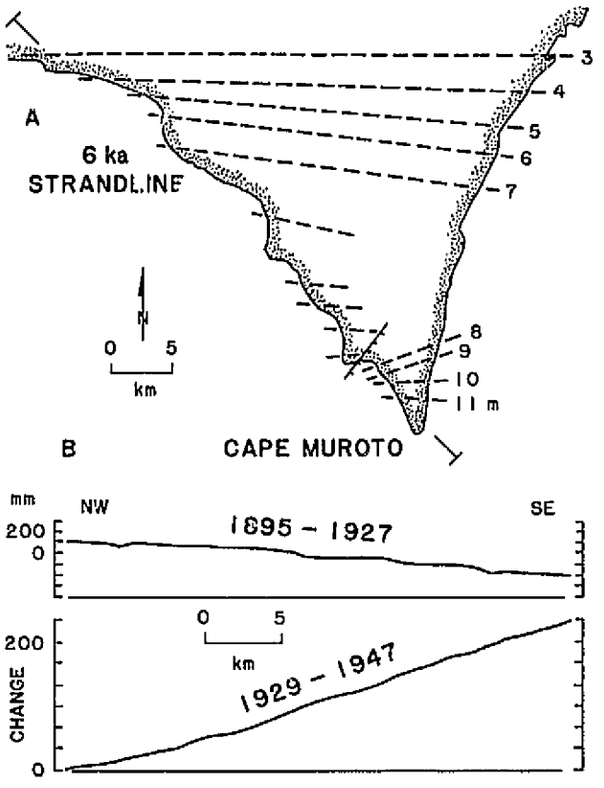


FIGURE 6.16 Tilted strandlines on the Muroto Peninsula, Japan.

A, Isobases on 6-ka strandline reveal short-term northward (landward) tilt of peninsula at the rate of $5.5 \times 10^{-5}$/ka, which is similar to the long-term rate derived from the 120-ka strandline but much lower than the $5.3 \times 10^{-4}$/ka rate produced by historical earthquakes. Note—data points occur only along coastlines; isobases interpolated across inland areas.

B, Geodetic data show that significant landward tilt accompanied the 1947 Nankai earthquake. This coseismic movement indicates that tilt in this area is episodic not continuous. Gradual southward (seaward) tilt documented by geodetic data prior to the 1947 earthquake probably reflected pre-earthquake strain accumulation. See Figure 6.24 for location. Modified from Yoshikawa *et al.* (1964) and Kanaya (1978).

cur above and closely mimic tighter bedrock structures, which indicates that strandline deformation represents the most recent increment of long-term crustal movement (Figures 6.17A and 6.18B) (Wellman, 1971a,b; Gahni, 1978; Lajoie *et al.*, 1982b). In many areas, however, folded strandlines are not associated with obvious bedrock structures and, therefore, are the only clear evidence for recent crustal folding (Figure 6.17B; also see Figure 6.21 below) (Plafker, 1972; Kaizuka *et al.*, 1973; Lajoie *et al.*, 1979a). In either case, progressively tighter folds in successively older strandlines reflect continual differential crustal movement (Figure 6.17). Along

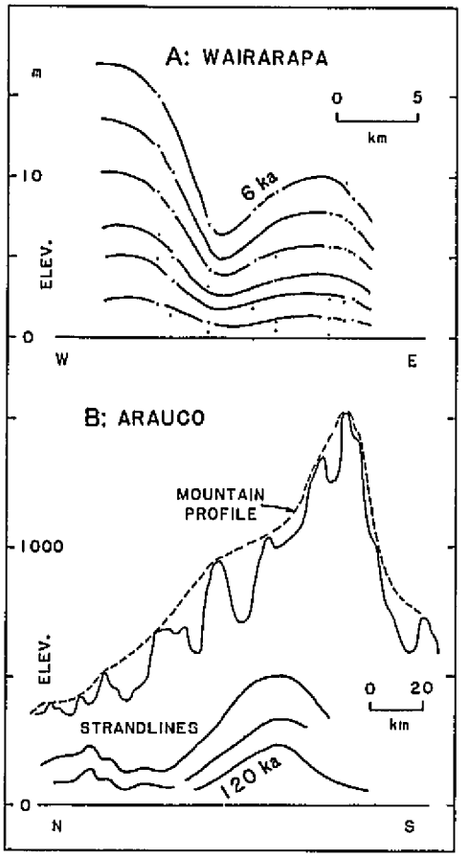


FIGURE 6.17 Crustal folds recorded by strandlines and illustrated by profiles.

A, Longitudinal profiles of Holocene strandlines on Wairarapa coast of North Island, New Zealand, reveal tight folds clearly expressed in underlying Tertiary rocks. Each strandline is probably of coseismic origin, which indicates that folding was incremental not continuous. Highest (6 ka) strandline dated by graphical techniques. Modified from Wellman (1971b).

B, Longitudinal profiles of Pleistocene strandlines along the Arauco coast of Chile reveal a broad warp not expressed in bedrock units but generally expressed in the generalized skyline profile of the local mountain range. Age of lowest strandline estimated to be 120 ka. Modified from Kaizuka *et al.* (1973).

C, Profiles of historical coseismic strandlines reveal broad crustal warps in the Gulf of Alaska (1964) and on the Chilean coast (1960). These profiles are not continuous but are defined by numerous points on highly irregular coastlines. See Figure 6.18A for isobase map of warp in Gulf of Alaska. Modified from Plafker (1972).

some highly active coastlines coseismic strandlines are warped into progressively tighter folds (Figure 6.17A) (Wellman, 1971a,b; Kaizuka *et al.*, 1973; Gahni, 1978), which suggests that tectonic folding, like uplift and tilt, is incremental, not continuous.

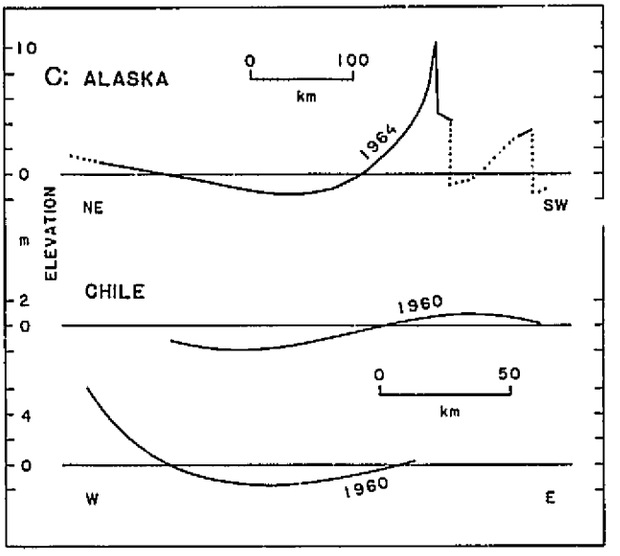


On local to regional scales, vertical displacement data from deformed marine strandlines are conveniently summarized as structural contours and isobases that express folds planimetrically (Figure 6.18; also see Figure 6.21 below). Structural contours and standard isobases depict deformation of a single tectonic marker (Figure 6.18A; also see Figure 6.21A below), whereas integrated isobases depict deformation normalized from two or more tectonic markers of different ages (Figure 6.18B) (Gahni, 1978).

Isobases on the surface defined by the 1964 strandline in the Gulf of Alaska (Figure 6.18A) reveal broad, gentle warps produced by coseismic crustal deformation over an area of 200,000 km$^2$ (Plafker, 1965). These isobases indicate that during the great 1964 earthquake an area of 60,000 km$^2$ was uplifted an average of 1-2 m and was tilted northward; maximum uplift was 3-10 m above local, north-dipping secondary faults (Figure 6.17C) (Plafker and Rubin, 1978). The isobases also show that an area of 110,000 km$^2$ north of the uplifted zone subsided a maximum of 2 m during the earthquake. The pattern of coseismic crustal warping associated with the earthquake is similar to the general pattern of long-term deformation documented by older Holocene strandlines. However, drowned vegetation in the uplifted area south of the epicenteral region documents subsidence during the 1.4 ka prior to the earthquake (Plafker and Rubin, 1978). This subsidence was probably pre-earthquake strain accumulation above the interplate megathrust on which the slip occurred.

The general pattern of coseismic uplift and subsidence that accompanied the 1964 earthquake in the Gulf of Alaska is similar to the pattern of crustal defor-

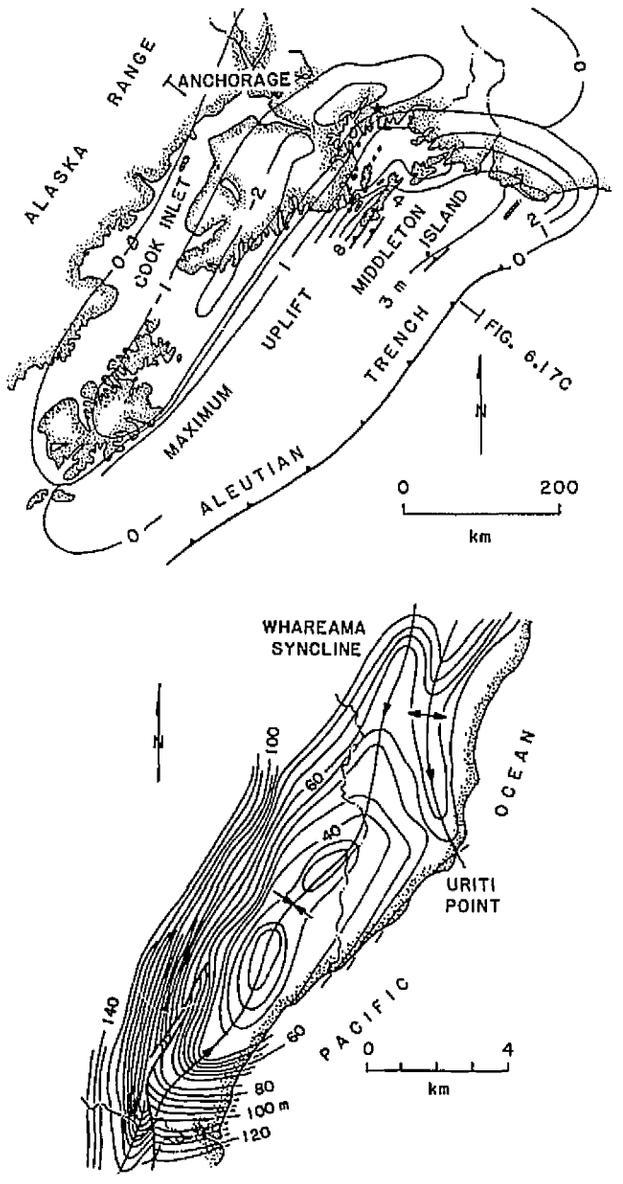


FIGURE 6.18 Crustal folds recorded by strandlines and illustrated by isobases. An isobase is a locus of points along which the rate of vertical crustal movement is equal.

A, 1964 strandline records subtle crustal warps associated with large megathrust earthquake in Gulf of Alaska. See Figure 6.17C for profile of warped surface. Modified from Plafker (1972).

B, Integrated isobases on 100-ka surface of the Wairarapa coast of North Island, New Zealand. Elevation data from 120-ka and 80-ka strandlines normalized to 100-ka surface. Complex folds and faults revealed by these isobases mimic structures in Tertiary bedrock. Intense folding is due to crustal shortening in sedimentary prism at leading edge of overthrust plate. Modified from Gahni (1978).

mation that accompanied the great 1960 megathrust earthquake in coastal Chile (Figure 6.17C) (Plafker and Savage, 1970; Plafker, 1972). These two well-documented examples of coseismic crustal deformation suggest that broad warping (subsidence as well as uplift) in the overthrust plate is characteristic of great megathrust earthquakes. It is noteworthy that the subtle coseismic crustal deformation expressed by vertically displaced strandlines in both Alaska and Chile would not have been recorded in such great detail nor over such large areas in noncoastal regions, nor even along coastlines without deep embayments and offshore islands.

An interesting contrast to the broad, regional warps depicted by isobases on the coseismic strandline in the Gulf of Alaska is found in the tight, local folds and related faults depicted by integrated isobases on Pleistocene and Holocene strandlines along the Wairarapa Coast of North Island, New Zealand (Figure 6.18B). The former reflect primary crustal deformation near the leading edge of a major overthrust plate (Plafker, 1972), and the latter reflect intense secondary deformation due to rapid crustal shortening within an accretionary prism in a similar tectonic setting (Gahni, 1978; Cole and Lewis, 1981).

An interesting aspect of crustal folds, which commonly is ignored or misunderstood in tectonic studies, is that the rate of vertical displacement along the axis of a fold and the rate of tilt along its limbs both decrease as the fold matures. If this apparent decrease in crustal deformation is documented by successively older strandlines, it could be misinterpreted as a reduction in local or regional tectonic strain.

### *Vertical Fault Movement*

Because marine platforms and strandlines are virtually horizontal structural markers, they record vertical fault movement more clearly than lateral movement. Often, vertical discontinuities in cross-sectional profiles of platforms (Figure 6.19) (Ota, 1975; Lajoie *et al.*, 1979b; Dames and Moore Consultants, 1981; Sarna-Wojcicki *et al.*, 1986) and in longitudinal profiles of strandlines (Figures 6.15B and 6.20) (Yoshikawa *et al.*, 1964; Ota, 1975; Lajoie *et al.*, 1979a,b; Tamura, 1979; Sissons and Cornish, 1982; Pillans, 1983) express even minor vertical fault movements, even where there is no other evidence of fault activity. Jogs in isobases and structural contours on marine platforms also express vertical fault movements and, where aligned, define local fault traces (Figures 6.12, 6.18B, and 6.21A) (Gahni, 1978; Lajoie *et al.*, 1979b). However, not all vertical offsets of marine strandlines and platforms doc-

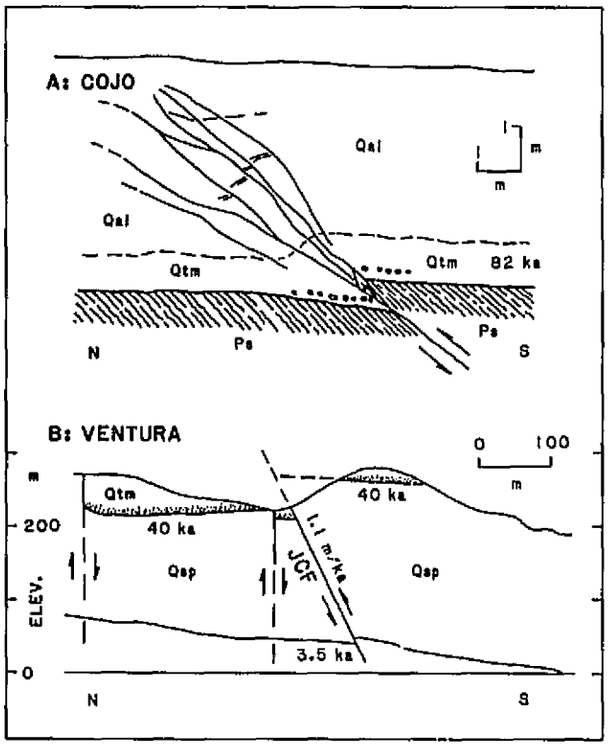


FIGURE 6.19 Vertical component of fault displacement recorded by offsets in cross-sectional profiles of marine strandlines.

A, Wave-cut platform and overlying marine (Qtm) and alluvial (Qal) sediment offset about 1 m across a minor bedding-plane fault near Point Conception in southern California. Platform dated at 82 ka by graphical and amino-acid techniques. Overlying terrace cover may be as young as latest Pleistocene or early Holocene. Modified from Dames and Moore consultants (1981) and Lajoie and Sarna-Wojcicki (1982).

B, 40-ka wave-cut platform and overlying marine sediment offset 45 m across Javon Canyon fault (JCF) near Ventura, California, yields a long-term displacement rate of 1.1 m/ka. A stream-cut platform graded to a 3.5-ka marine strandline is offset 4 m across the same fault, which yields a similar short-term displacement rate of 1.2 m/ka. See Figure 6.22A for coseismic slip events on this fault. Modified from Sarna-Wojcicki *et al.* (1986).

ument fault movement. Some, especially along steep coastal slopes, represent large, block-type slope failures.

Along many coastlines marine strandlines and platforms provide relative age control for recent fault activity. If a wave-cut strandline truncates a bedrock fault, the latest movement on the fault is, of course, older than the strandline. Conversely, if a strandline is offset across a fault, the latest movement is younger (Figures 6.15 through 6.21). Both the U.S Nuclear Regulatory Commission and the State of California Public Utilities Commission use relative strandline-fault relationships indirectly to define active faults in their assessment of seismic hazards to critical engineered structures in coastal regions. Both agencies consider a fault potentially active if it has moved in the past 100 ka. This somewhat arbitrary age is used specifically because the 120-ka to 82-ka strandlines are the most prominent and most accurately dated tectonic markers along most coastlines.

Where dated, faulted strandlines also yield rates of fault movement. The offset of a strandline or platform divided by its age is, of course, the average slip rate since the strandline formed. In some areas, progressively greater offsets of successively older strandlines document continual fault activity and yield long-term average slip rates (Figures 6.15B, 6.19B, and 6.20) (Sissons and Cornish, 1982; Pillans, 1983; Sarna-Wojcicki *et al.*, 1986). For example, on Sado Island off the west coast of Honshu, Japan, vertical discontinuities in the profiles of five Pleistocene and Holocene strandlines record continuous differential movement across the steeply dipping fault that separates the two mountainous parts of the

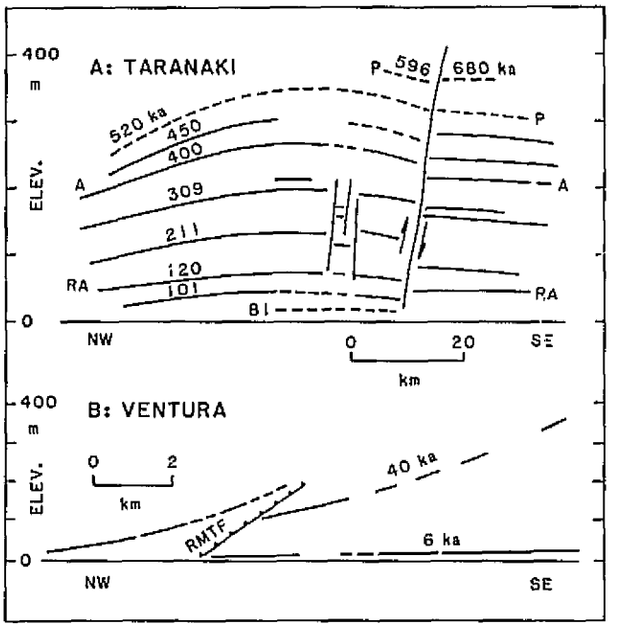


FIGURE 6.20 Vertical component of fault displacement recorded by offsets in longitudinal profiles of marine strandlines.

A, Progressively greater vertical offset of successively older marine strandlines documents continual fault activity over at least the past 700 ka on the Taranaki coast of North Island, New Zealand. Strandline ages (81-596 ka) derived from tephrochronology, amino-acid data, and uplift rates. Modified from Pillans (1983).

B, Vertical offset of 40-ka strandline across Red Mountain thrust fault (RMTF) near Ventura, California. Strandline age based on amino-acid data from fossil shells. Modified from Lajoie *et al.* (1982b).

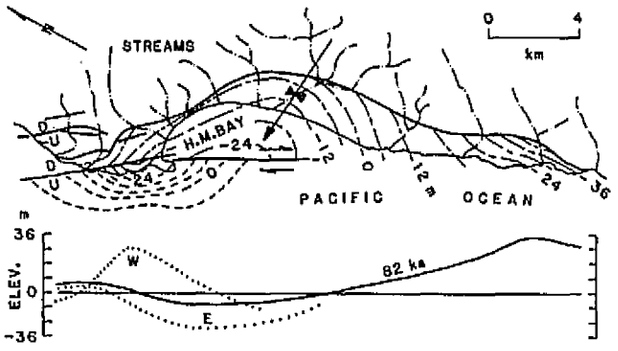


FIGURE 6.21 Closely related folding and faulting recorded by deformed 82-ka strandline at Half Moon Bay, California. Structural contours on wave-cut platform depict drag folds that plunge obliquely into and away from the vertical fault plane. Orientation of folds indicates predominant right-lateral fault movement, which is consistent with regional fault movements. Longitudinal profiles of strandline and faulted platform record gentle warps and vertical offset across fault. Shoreline angle of strandline does not intersect fault plane so local slip vector and slip rate are not known. Vertical separation of wave-cut platform across fault revealed by platform profiles on fault plane (dotted lines; E, east; W, west). Structural contours derived mainly from shallow borehole and seismic refraction data. Modified from Lajoie *et al.* (1979b).

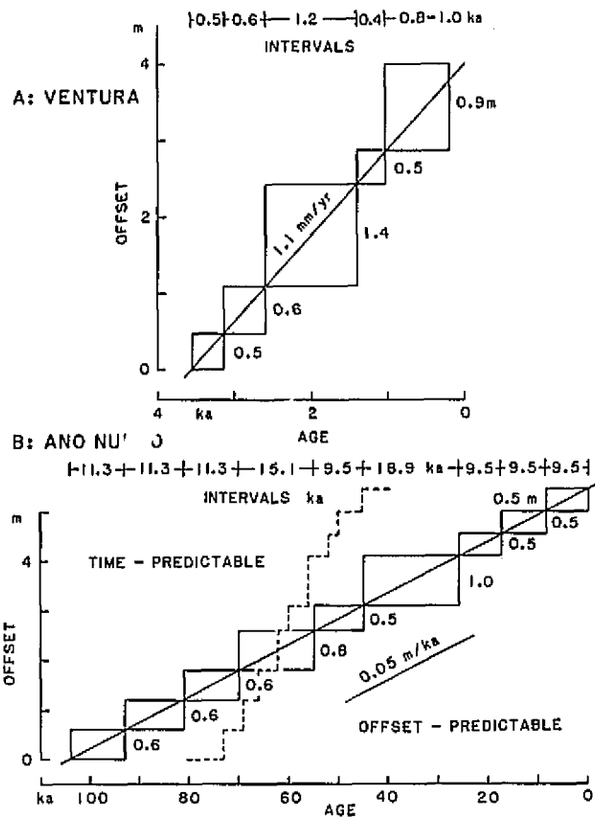


FIGURE 6.22 Coseismic slip events on faults recorded by scarp-derived talus.

A, Stream-cut platform graded to 3.5-ka marine strandline offset 4 m across Javon Canyon fault near Ventura, California (see Figure 6.19B). At least five discrete slip events (0.5-1.4 m) are recorded by lenses of scarp-derived talus preserved below the upthrown block. If these slip events are coseismic, the average earthquake recurrence interval for this fault is about 700 yr. Modified from Sarna-Wojcicki *et al.* (1986).

B, Vertical component of fault displacement recorded by offset of 104-ka wave-cut platform at Point Año Nuevo, California. At least nine discrete slip events are recorded by lenses of scarp-derived talus and faulted sediment preserved on the wave-cut platform beneath the upthrown block. If slip events are coseismic, the average earthquake recurrence interval is about 12 ka. It should be stressed, however, that average recurrence intervals have little meaning if total fault movement occurred during a short period of time (dotted line). Independently derived ages for each event are needed to resolve this potentially serious problem. Modified from Weber and Cotton (1981).

island (Figure 6.15) (Tamura, 1979). If this fault is vertical, the 120-ka strandline is offset about 75 m, which yields a long-term slip rate of 0.6 m/ka. The 6-ka strandline is offset about 4 m, which yields a similar short-term slip rate of 0.7 m/ka. Another excellent example of continuous fault slip recorded by progressively greater offset of successively older marine strandlines is found near the town of Ventura on the southern California coastline (Figure 6.19B) (Sarna-Wojcicki *et al.*, 1986). There, the wave-cut platform of the 40-ka strandline (Kennedy *et al.*, 1982) is vertically offset about 45 m across a high-angle reverse fault, which yields an average slip rate of 1.1 m/ka. Nearby, a stream-cut platform graded to an emergent 3.5-ka strandline is offset 4 m across the same fault, which yields a similar shorter-term slip rate of 1.2 m/ka.

If the size of an average coseismic slip event is assumed or is known from a historical seismic event, it can be divided into the slip rate to yield the average earthquake recurrence interval. However, where discrete slip events are recorded geologically, earthquake recurrence can be determined more directly. For example, lenses of scarp-derived Holocene talus preserved beneath the upthrown block of the high-angle reverse fault near Ventura, California (Figure 6.19B), record at least five discrete slip events during the past 3.5 ka (Figure 6.22A) (Sarna-Wojcicki *et al.*, 1986). If these slip events were of coseismic origin, the average vertical displacement was 0.8 m and the average earthquake recurrence interval was 700 yr.

An even longer history of discrete slip events is recorded where a 104-ka marine platform is offset across a strand of a complex fault zone at Point Año Nuevo about 100 km south of San Francisco on the central California coastline (Lajoie *et al.*, 1979b). This wave-cut platform

is offset 5.5 m (dip-slip component), which yields an average long-term slip rate of 0.05 m/ka. More importantly, however, scarp-derived talus that accumulated on the marine platform below the periodically rejuvinated fault scarp records at least nine slip events over the past 104 ka (Figure 6.22B) (Weber and Cotton, 1981). If coseismic, these slip events, which averaged 0.6 m, yield an average earthquake recurrence interval of about 12 ka. It should be stressed, however, that if total fault movement was restricted to relatively short periods of time (Figure 6.22B), average recurrence intervals are of little use in predicting the time of the next event. Each event must be dated independently to make meaningful predictions of future events.

### *Lateral Fault Movement*

As indicated previously, lateral fault movement is rarely recorded by marine strandlines, even where strandlines clearly cross active strike-slip faults. Usually, the amount of offset is ambiguous because of irregularities in or poor preservation of the paleoshoreline. For example, at Point Año Nuevo on the central California coastline, two Pleistocene strandlines that cross a major right-lateral fault system appear to be offset across several fault strands (Weber and Lajoie, 1977; Weber and Cotton, 1981). However, because these strandlines must be projected considerable distances (up to 1.0 km) at low angles across some of the fault strands, the individual and cumulative offsets of each strandline are too uncertain to yield meaningful rates of lateral fault movement.

In some areas, the sense but not the amount of lateral fault movement is expressed by the orientation of drag folds recorded by marine strandlines. For example, the 82-ka strandline at Half Moon Bay about 60 km northwest of Point Año Nuevo on the central California coastline records broad crustal warps on both sides of a major fault strand within the coastal fault system (Figure 6.21) (Lajoie *et al.*, 1979b; Kennedy *et al.*, 1981). Structural contours on the warped wave-cut platform define a broad syncline that plunges obliquely into the vertical fault plane from the east and a broad anticline that plunges away from the fault plane to the west. These structural relationships suggest that the syncline and anticline are drag folds related to right-lateral fault movement, which is consistent with regional fault movements. Unfortunately, the strandline of this deformed marine platform does not intersect the fault plane and, therefore, neither the local slip vector nor the slip rate is known. However, where latest Pleistocene stream courses cross the warped marine terrace northeast of the fault they are deflected toward the axis of the syncline (Figure 6.21), which suggests that fault movement and related crustal warping were continual over the past 82 ka.

## COSEISMIC UPLIFT AND EARTHQUAKE RECURRENCE

In several seismically active coastal areas historical coseismic uplift has produced conspicuous emergent marine strandlines 1-15 m above sea level. The best documented examples of historical coseismic strandlines are found in Japan (Sugimura and Naruse, 1954; Nakamura *et al.*, 1965; Ota *et al.*, 1976; Matsuda *et al.*, 1978; Shimazaki and Nakata, 1980), New Zealand (Wellman, 1969; Stevens, 1973), Alaska (Plafker, 1965, 1972), Chile (Plafker and Rubin, 1967; Plafker and Savage, 1970; Plafker, 1972), and Iran (Page *et al.*, 1979). The historical coseismic strandlines in these areas suggest that similar higher (older) Holocene strandlines in these and other active-tectonic areas are also of earthquake origin. If this interpretation is correct, a sequence of emergent Holocene strandlines is a physical record of past earthquakes from which it should be possible to predict the size and date of the next seismic event.

If the average uplift rate is constant, coseismic uplift events may follow a time-predictable or displacement-predictable pattern (Figure 6.23) (Shimazaki and Nakata, 1980). In a time-predictable pattern the time between events is proportional to the size of the preceding event, and, therefore, the date, but not the size, of the next event can be predicted. In a displacement-predictable pattern the time between events is proportional to the size of the succeeding event, and the size of the next event can be predicted for any future date, but that date cannot be predicted. Of course, if the period and size of uplift events are regular, both can be predicted for the next event. In practice, however, strandline elevations and dates are usually too variable or imprecise to fit any pattern exactly, and, therefore, only average displacements and recurrence intervals can be derived from sequences of emergent Holocene strandlines. In some cases, the uplift rate is so variable that no reasonable predictions can be made.

A few examples of coseismic uplift from Japan, Alaska, and New Zealand illustrate some of the possibilities and limitations in deriving detailed seismic histories from sequences of emergent Holocene strandlines.

### *Japan*

The Japanese archipelago, which lies along the leading, overthrust margin of the Eurasian tectonic plate in the western Pacific Ocean, is one of the most seismically

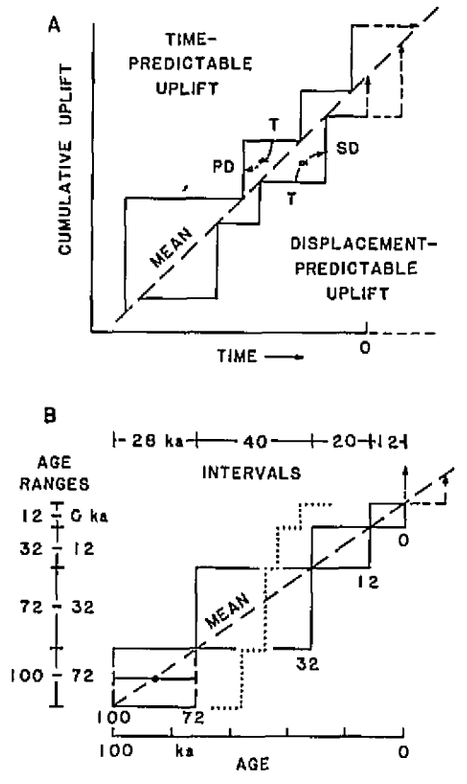


FIGURE 6.23 Theoretical patterns of coseismic uplift (or fault movement).

A, If average uplift rate is constant, the incremental coseismic uplift events may follow either a time-predictable or a displacement-predictable pattern. In a time-predictable pattern the time between events ($T$) is proportional to the size of the preceding displacement ($PD$). In this case, the time, but not the size, of the next event can be predicted. In a displacement-predictable pattern the time between events is proportional to the size of the succeeding displacement ($SD$). In this case, the size of the next event can be predicted for any future date, which cannot be predicted. In practice, strandline elevations and ages are usually too uncertain to reveal precise patterns of uplift. Modified from Shimazaki and Nakata (1980).

B, If a displaced marker (e.g., wave-cut platform) is dated but individual events are not dated independently, their intervals and age ranges can be estimated from the average displacement rate. However, if total displacement is highly irregular (dotted line), average displacement intervals, rates, and age values are meaningless. Independent ages of events are needed to establish displacement pattern.

active areas on Earth (Tarr, 1974). Great intraplate megathrust earthquakes occur along the major subduction zone that forms the eastern boundary of the archipelago, and smaller, but still potentially destructive, interplate earthquakes occur along its complexly faulted eastern boundary. Particularly good examples of coseismic strandlines are found on the Boso Peninsula, the Muroto Peninsula, and Kikai Island along the overthrust Pacific Coast and on Awashima Island and the Ogi Peninsula of Sado Island along the block-faulted Japan Sea Coast (Figure 6.24).

Four emergent Holocene strandlines (Numa I-IV) form prominent terraces around the southern tip of the Boso Peninsula about 80 km south of Tokyo (Figures 6.3A, 6.24, and 6.25) (Sugimura and Naruse, 1954; Matsuda *et al.*, 1978). Isobases on the planes defined by these curved strandlines reveal progressive uplift and northward tilt of the southernmost part of the peninsula. Radiocarbon dates on fossil shells from the three highest strandlines (Numa I-III terraces) yield an average uplift rate of 3.9 m/ka (Figure 6.25A). The lowest major strandline (Numa IV or Genroku terrace) at 5 m and a minor strandline at 1.0 m were formed by uplift during the great Kanto earthquakes of 1703 and 1923, respectively. The ages and vertical distances between successively higher pairs of dated strandlines yield an average uplift per event of about 6 m and an average recurrence interval of about 1.5 ka. More importantly, however, the uplift and age data appear to follow a

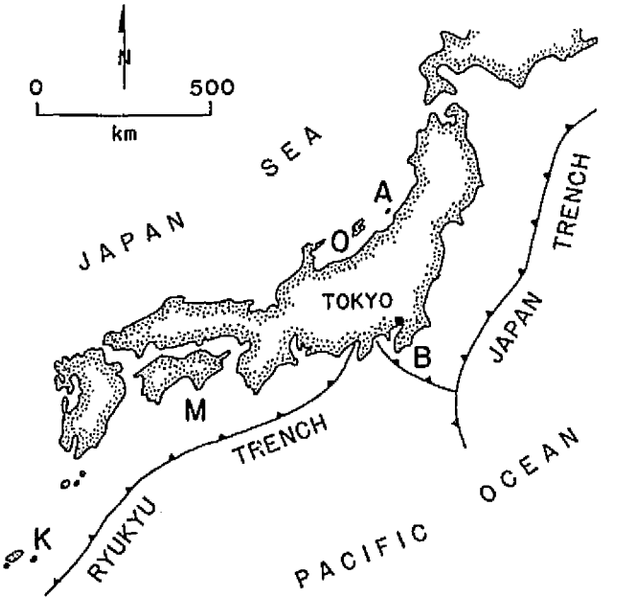


FIGURE 6.24 Generalized tectonic map of Japan showing locations of emergent marine strandlines produced by historical coseismic uplift. O, Ogi Peninsula of Sado Island, 1802 earthquake (see Figure 6.13A for strandline profiles and Figures 6.15A and 6.24 for location); A, Awashima Island, 1964 Niigata earthquake; B, Boso Peninsula, 1703 and 1923 Kanto earthquakes (see Figure 6.25 for uplift history); M, Muroto Peninsula, 1707, 1855, and 1947 Nankaido earthquakes (see Figure 6.26A for uplift history; see Figure 6.16 for strandline and geodetic data); K, Kikai Jima, no historical coseismic strandlines, but see Figure 6.26B for Holocene uplift history.

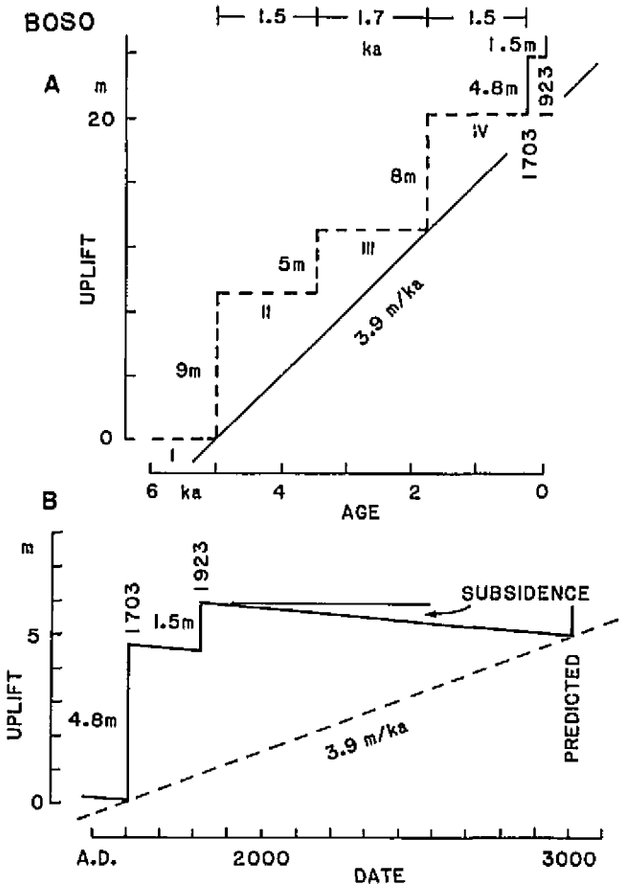


FIGURE 6.25 Coseismic uplift, Boso Peninsula, Japan.

A, Average uplift appears to be constant, and coseismic uplift events appear to follow a time-predictable pattern.

B, Uplift pattern indicates that the next event (or sequence of events) will occur in A.D. 3000. Interearthquake subsidence (strain accumulation) from geodetic data is incorporated into prediction model. See Figure 6.24 for location and Figure 6.3A for profile of strandlines. Modified from Matsuda *et al.* (1978).

time-predictable pattern. After being corrected for probable postearthquake subsidence (currently 1-2 mm/yr), the strandline data from the Boso Peninsula indicate that the next uplift event similar to the combined 1703 and 1923 events will occur in 0.8-1.3 ka (Figure 6.25B). Other workers (Nakata *et al.*, 1980; and Shimazaki and Nakata, 1980; Yonekura and Shimazaki, 1980) also studied the emergent Holocene strandlines on the Boso Peninsula and reached similar conclusions. However, some of these workers (Yonekura and Shimazaki, 1980) suggested that the largest uplift events may have accompanied moderate-sized earthquakes on steep, secondary faults within the overthrust plate of the Sagami subduction zone and that the smallest uplift events may have accompanied larger earthquakes on the main but more gently dipping thrust fault. If this interpretation is correct, the 1703 Kanto earthquake may have been smaller than the 1923 event, even though the relative coseismic uplift would suggest otherwise. Interestingly, at Oiso, a densely populated suburb of Tokyo, about 70 km northwest of the Boso Peninsula, the sum of the uplifts that accompanied the 1703 and 1923 earthquakes is less than the uplift required to maintain the long-term uplift rate derived from older strandlines. This relationship suggests that the next uplift event in the Oiso area is overdue. Consequently, the Oiso area may currently be at greater seismic risk than the southern Boso Peninsula (Matsuda *et al.*, 1978).

At Murotsu harbor on the southern tip of the Muroto Peninsula on the island of Shikoku (Figure 6.24), the uplifts associated with the great Nankaido earthquakes of 1707 (1.8 m), 1855 (1.2 m), and 1947 (1.2 m) were determined by primitive but reasonably accurate harbor soundings and by a vertically displaced strandline defined by barnacles (Figures 6.16 and 6.26A) (Sawamura, 1953; Shimazaki and Nakata, 1980). These historical data yield a constant short-term uplift rate of 12.5 mm/yr, which is about six times higher than the

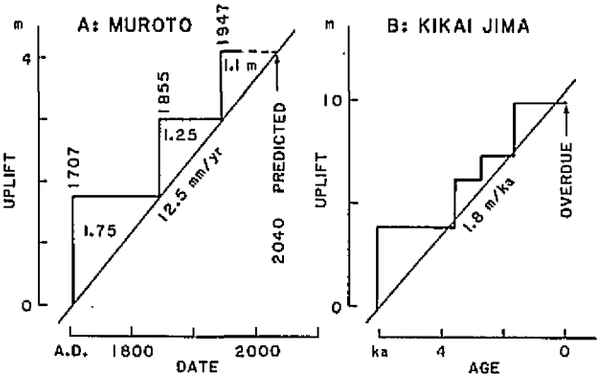


FIGURE 6.26 Coseismic uplift on Muroto Peninsula and Kikai Jima, Japan.

A, Historical coseismic strandlines at Murotsu Harbor. Uplift events appear to follow a time-predictable pattern and yield an average short-term uplift rate of 12.5 mm/yr, which is about six times higher than the long-term rate of 1.7-2.0 m/ka derived from 6-ka and 120-ka strandlines. If the short-term rate prevails, the next coseismic event should occur in the year 2040. If the long-term rate prevails, the next event (or sequence of closely spaced events) will not occur for another 3 ka. (See Figure 6.16 for more uplift data.)

B, Radiocarbon-dated strandlines on Kikai Island, Japan, appear to follow a time-predictable pattern. If correct, a large coseismic uplift event should have occurred between 1400 and 1600. There is no geologic or historical evidence for such an event, so the area may be overdue for a large earthquake. Modified from Shimazaki and Nakata (1980). See Figure 6.24 for locations.

long-term rate of 1.7-2.0 m/ka derived from the 6-ka and 120-ka strandlines (Yoshikawa *et al.*, 1964; Kanaya, 1978). If the exceptionally high uplift rate produced by historical coseismic events is maintained, the next large earthquake should occur in 2040 (Shimazaki and Nakata, 1980). However, if the long-term rate prevails, which seems more likely, the next event, or a series of closely spaced events, should not occur for another 3 ka. Tide-gauge and geodetic data from central Japan, which reveal the spatial and temporal patterns of interearthquake crustal deformation between the 1855 and 1947 events, indicate that because of the nonlinearity of strain buildup and the significant permanent deformation, simple recurrence calculations from strandline data may overestimate the true interval between major earthquakes by a factor of 2-3 in the Nankai area (Thatcher, 1984). On the other hand, the three closely spaced historical uplift events on the Muroto Peninsula and the two closely spaced events on the Boso Peninsula suggest that the large vertical spacing between emergent Holocene strandlines in these and possibly other areas may represent multiple, not single, earthquakes. If this interpretation is correct, earthquakes at a particular locality on a convergent plate boundary may occur in relatively tight clusters separated by considerable periods of time (1-3 ka), in which case the date of the next event would be difficult if not impossible to predict.

On Kikai Island, the easternmost island in the Ryukyu archipelago of southern Japan, radiocarbon dates of fossil corals from four Holocene strandlines yield a uniform uplift rate of 1.8 m/ka over the past 6 ka and indicate that coseismic uplift followed a time-predictable pattern (Figures 6.24 and 6.26B) (Nakata *et al.*, 1978, 1979; Shimazaki and Nakata, 1980). If the time-predictable model is correct, there should have been a large earthquake between A.D. 1400 and 1600. The lack of historical or geological evidence for an earthquake of this age suggests that Kikai Island, like the Oiso area near Tokyo, is overdue for a major earthquake (Shimazaki and Nakata, 1980).

Two very different earthquake recurrence intervals are recorded by emergent Holocene strandlines on Sado and Awashima Islands in the intensely faulted area off the west coast of central Honshu, the largest Japanese island (Figure 6.24). Seven emergent Pleistocene and Holocene strandlines occur on the Ogi Peninsula, the southernmost tip of Sado Island (Figure 6.15A) (Ota *et al.*, 1976). The lowest (2 m) strandline was formed by uplift during a major earthquake in 1802 (Figure 6.13A). This strandline and the next higher (4 m) 6-ka strandline are both tilted northward about $2.5 \times 10^{-2}$, which indicates that the 1802 event was the only tilt event in the past 6 ka. The uniform difference of 2 m between these two strandlines is ascribed to a 2-m highstand of sea level at about 6 ka BP (Ota *et al.*, 1976). A more likely explanation is that the area was uplifted uniformly after 6 ka BP but before the 1802 tilt event. In any case, dividing the coseismic tilt produced in 1802 into the long-term tilt rate derived from the 120-ka strandline yields a recurrence interval for seismic events of 5-9 ka, which is consistent with the >6-ka interval documented by the two lowest strandlines.

At Awashima, which lies about 70 km northeast of Sado Island (Figure 6.24), tilted strandlines yield a much shorter recurrence interval (Nakamura *et al.*, 1965). Awashima was uplifted a maximum of 1.8 m and tilted northward about $2.4 \times 10^{-4}$ during the 1964 Niigata earthquake. The long-term tilt rate derived from the 82-ka strandline at 50-70 m above sea level is $4.3 \times 10^{-4}$/ka. Dividing this tilt rate by the 1964 tilt yields an average recurrence interval of about 1.5 ka. The different earthquake recurrence intervals for the faults near the Ogi Peninsula and Awashima Island demonstrate that similar faults within the same tectonic province can have very different displacement histories.

### *Alaska*

The narrow zone comprising the Aleutian archipelago and the south coast of mainland Alaska lies along the overthrust margin of the North American tectonic plate in the north Pacific Ocean. At numerous localities in this seismically active area, great interplate megathrust earthquakes are recorded by emergent Holocene and historical strandlines.

On Middleton Island (Figure 6.18A) emergent Holocene strandlines record six coseismic uplift events over the past 4.5 ka (Figure 6.27A) (Plafker and Rubin, 1967, 1978). The lowest strandline at 3.5 m above sea level was produced by uplift associated with the great 1964 earthquake in southern Alaska. Radiocarbon dates on peat and wood from the wave-cut platforms of the five highest strandlines indicate that the time interval between uplift events increased gradually from about 0.5 ka to 1.4 ka and that the uplift rate decreased from 14 m/ka to 5.6 m/ka. If the island subsided slightly between major earthquakes, the uplift that accompanied each earthquake was greater than the vertical spacing between strandlines. It is not clear if the uplift events, which ranged from 7-12 m and averaged about 9 m, followed a displacement-predictable or a time-predictable pattern, but it is obvious that the 3.5-m uplift associated with the 1964 earthquake was not sufficiently large to maintain even the diminishing uplift rate (Figure 6.27A). In effect, at least half of the stress accumulated since the formation of the second lowest strandline at

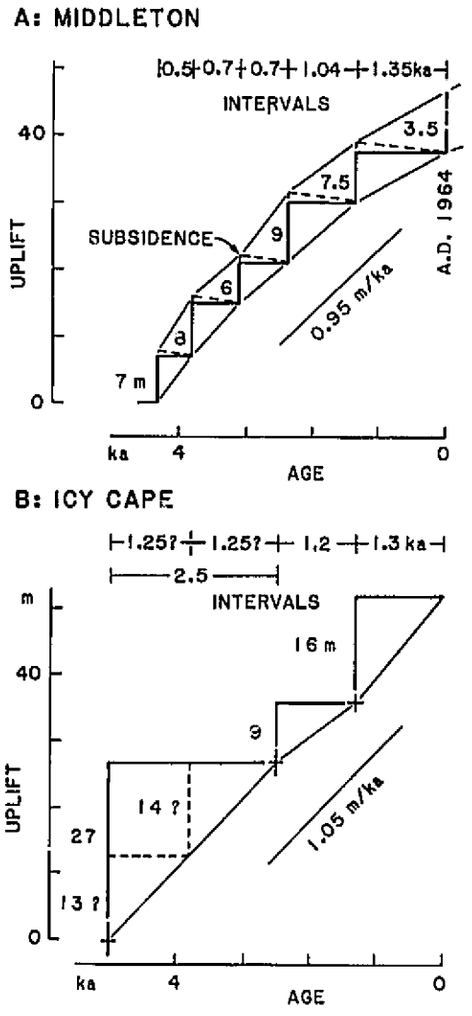


FIGURE 6.27 Coseismic uplift, Gulf of Alaska.

A, Radiocarbon-dated and historical coseismic strandlines on Middleton Island, Alaska. Average uplift rate is decreasing and interval between events is increasing while the size of each event has remained fairly constant. Average uplift is 0.95 m/ka. The 1964 coseismic uplift did not bring the island up to the long-term rate, which suggests that another event is due in the near future. Present sea level used as tectonic datum. Modified from Plafker and Rubin (1978).

B, Radiocarbon-dated coseismic strandlines at Icy Cape (about 300 km east of Middleton Island on the Alaska mainland) yield a fairly constant uplift of about 1 m/ka. Uplift events appear to follow a time-predictable pattern. If this pattern continues, the next event is due in the near future. Modified from Plafker *et al.* (1981). See Figures 6.17C and 6.18A for 1964 coseismic strandline deformation.

about 1.4 ka BP has yet to be released. Consequently, if the Holocene trend continues, coseismic uplift at least as large as the 1964 event should occur on Middleton Island sometime in the near future (Plafker and Rubin, 1978).

The focal region of the 1964 Alaskan earthquake lies north and west of Middleton Island (Figure 6.18A), and a seismic gap lies to the east. Consequently, the next uplift event to affect the island may accompany a megathrust earthquake in the area of the seismic gap, possibly on the submarine Pamplona Fault (Plafker and Rubin, 1978). This interpretation is supported by data from Icy Cape, a broad sedimentary headland about 300 km east of Middleton Island on the Alaska mainland and within the area of the seismic gap. There, depositional strandlines dated at 4.9 ka, 2.4 ka, and 1.3 ka BP by radiocarbon techniques record at least three uplift events that followed a time-predictable pattern over the past 5 ka (Figure 6.27B) (Plafker *et al.*, 1981). The lowest (1.3 ka) strandline may have been formed during the same seismic event that produced the second lowest strandline dated at 1.35 ka on Middleton Island (Figure 6.27A). If the 1.2-1.3-ka time span between strandlines at Icy Cape is the recurrence interval for the area of the present seismic gap, the next uplift event is overdue. Presumably, this event would make up some or all of the apparent deficiency in uplift on Middleton Island. An interesting aspect of the strandline sequence at Icy Cape is that the vertical distance between the 4.9-ka and 2.4-ka strandlines is 27 m (Figure 6.27B), which seems too large for a single uplift event. If uplift averaged 10-15 m per event, a 14-m uplift at about 3.8 ka BP may not have been recorded or its strandline may have been destroyed by subsequent wave erosion (Plafker *et al.*, 1981).

### *New Zealand*

The large southwest Pacific islands of New Zealand straddle the convergent boundary between the Australia-India tectonic plate to the west and the Pacific plate to the east. Northeast of the islands, the Australia-India plate is being thrust eastward over the Pacific plate, and southwest of the islands the relationship is reversed. The islands themselves are a manifestation of the uplift along the transition between the two opposing subduction zones on the same interplate boundary (Walcott, 1984). Within this complex structural area both interplate and intraplate earthquakes are common. At several localities, especially along the southeast coast of North Island, large earthquakes are recorded by emergent Holocene strandlines.

At least five coseismic uplift events are recorded by six

bouldery beach ridges up to 27 m above sea level on the rapidly uplifting coastline at Turakirae Head, the southernmost tip of North Island (Figure 6.28) (Wellman, 1969; Stevens, 1973). The two lowest strandlines at 7 and 3 m above sea level, which were formed during historical earthquakes in 1460 and 1855, respectively, appear to record regional northwestward tilt across the entire southern tip of the island, whereas the four highest strandlines appear to record intense crustal warping between two local faults parallel to the offshore subduction zone (Wellman, 1969). However, all six strandlines may reflect regional tilt (Stevens, 1973). In either case, the five coseismic uplift events represented by these strandlines range from 2.5 to 9 m, and average 5.4 m (Figure 6.28). An assumption of constant uplift yields tentative ages for the four highest strandlines and also yields an average uplift rate of about 4 m/ka (see Figure 6.7) (Wellman, 1969). These graphically derived dates appear to indicate that uplift events follow a time-predictable pattern, which would indicate that the next event should occur in about 500 yr (Wellman, 1969). However, the pattern of uplift is inherent in the assumption of constant uplift—it is not independently demonstrated. Consequently, no firm estimate for the date of the next coseismic uplift event can be made.

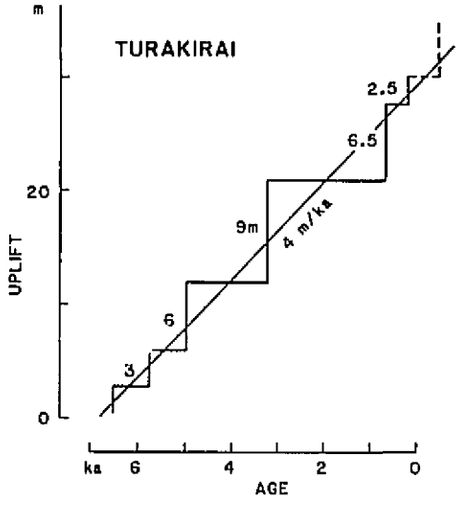


FIGURE 6.28 Coseismic Holocene strandlines at Turakirae Head, North Island, New Zealand. Highest (6 ka) strandline dated by graphical techniques (see Figures 6.5B and 6.7) assuming constant uplift rate (4 m/ka). Rate interpolated to estimate ages of lower strandlines. If uplift follows a time-predictable pattern, the next event should occur in 0.5 ka. It should be stressed, however, that these strandlines must be dated independently to demonstrate constant uplift and the time-predictable pattern. Modified from Wellman (1969).

The often disparate and inconclusive estimates of past and future seismic events derived from sequences of emergent Holocene strandlines in the three areas discussed here (Japan, Alaska, and New Zealand) illustrate many of the difficulties encountered in interpreting even excellent historical and geological strandline data. However, in spite of these difficulties sequences of coseismic strandlines are among the most complete records of past earthquakes and in many coastal areas provide extremely valuable insights into the distribution of earthquakes in both space and time.

## FUTURE RESEARCH

This brief review of coastal tectonics illustrates the breadth and scope of neotectonic deformation and seismic history that can be derived from the study of marine strandlines, which so conspicuously record the dynamic interaction between the fluctuating sea level and mobile tectonic plates along many of the world's active coastlines. Without sea-level changes, discrete strandlines would not be produced and the long-term record of Pleistocene crustal movements in coastal areas would be extremely difficult if not impossible to extract from a relative sea-level record. Conversely, without vertical crustal movements, a detailed history of sea-level fluctuations would be virtually impossible to reconstruct. As our understanding of this complex interaction increases we discover new problems that require the reinterpretation of existing data and the acquisition of new, more precise information. It should be stressed, however, that even at our present level of understanding the uncertainties inherent in extracting past crustal movements and seismic histories from relative sea-level records are far outweighed by the wealth of useful information obtained.

Following is a list of some of the most pressing problems and needs that must be addressed if we are to progress in the new and rapidly evolving field of coastal tectonics.

- Theoretical models relating sea-level changes and vertical crustal movements should be developed. General relationships are expressed by Eqs. (6.1) and (6.8) and Figures 6.5, 6.6, and 6.7. Theoretical models will provide a framework in which tectonic and sea-level data can be interpreted and evaluated. They will also provide graphical and mathematical means of correlating and dating strandlines. Models will also provide a coherent framework for compiling and comparing strandline data from different areas.
- The resolution of existing radiometric, chemical, and paleontologic dating techniques should be im-

proved and the ranges of these techniques extended. New dating techniques should be developed, especially for the period between 100-1000 ka BP.

- Both Pleistocene and Holocene (including historical) strandlines on many more coastlines throughout the world should be mapped and dated. Particular attention should be paid to precise ages and elevations. These data are needed to resolve potentially serious problems of geoidal distortion and regional hydro-isostatic crustal movements. If geoidal distortion is significant on a time scale of 10-100 ka, regional sea-level curves should be developed as tectonic datums. If geoidal distortion is relatively insignificant, its magnitude will help to establish uncertainty limits for rates of crustal deformation. In short, both Pleistocene and Holocene sea-level curves should be improved to provide more accurate estimates of tectonic deformation.
- More effective tide-gauge stations and geodetic networks to monitor ongoing crustal movements and regional sea-level changes should be developed. Particular care should be taken in comparing data from these two sources and from other historical and geological sources.
- Detailed studies of coseismic strandlines on rapidly deforming coastlines should be undertaken to establish patterns of paleoseismicity. Particular attention should be placed on precise dating.
- Existing data on the age and elevation of coastlines throughout the world should be compiled to establish regional patterns of crustal deformation and sea-level change.
- Submerged strandlines should be mapped and dated. New techniques for conducting these difficult and expensive investigations should be developed.

## REFERENCES


Anderson, W. A., J. T. Kelley, W. B. Thompson, H. W. Borns, D. Sanger, D. C. Smith, D. A. Tyler, R. S. Anderson, A. E. Bridges, K. J. Crossen, J. W. Ladd, B. G. Anderson, and F. T. Lee (1984). Crustal warping in coastal Maine, *Geology 12*, 677-680.

Andrews, J. T. (1970). Present and postglacial rates of uplift for glaciated northern and eastern North America derived from postglacial uplift curves, *Can. J. Earth Sci. 7*, 703-715.

Angelier, J. (1979). Recent Quaternary tectonics in the Hellenic Arc: examples of geologic observations on land, *Tectonophysics 52*, 267-275.

Atwater, B. F., C. W. Hedel, and E. J. Helley (1977). Late Quaternary depositional history, Holocene sea-level changes, and vertical crustal movement, southern San Francisco Bay, California, *U.S. Geol. Surv. Prof. Paper 1014*, 15 pp.

Balling, N. (1980). The land uplift in Fennoscandia, gravity field anomalies and isostasy, in *Earth Rheology, Isostasy and Eustasy*, N.-A. Morner, ed., John Wiley & Sons, New York, pp. 297-310.

Barnett, D. M. (1966). A re-examination and re-interpretation of tide-gauge data for Churchill, Manitoba, *Can. J. Earth Sci. 3*, 77-88.

Belknap, D. F. (1979). Application of amino-acid geochronology to stratigraphy of late Cenozoic marine units of the Atlantic Coastal Plain, unpublished Ph.D. dissertation, Univ. Del.

Bender, M. L., R. G. Fairbanks, F. W. Taylor, R. K. Matthews, J. G. Goddard, and W. S. Broecker (1979). Uranium-series dating of the Pleistocene Indies, *Geol. Soc. Am. Bull. 90*, 577-594.

Berrino, G., G. Corrado, G. Luongo, and B. Toro (in press). Surface deformation and gravity changes accompanying the 1982 Pozzuoli uplift, *Bull. Volcan.*

Bloom, A. L. (1970). Holocene submergence in Micronesia as the standard for eustatic sea-level changes, *Geol. Soc. Am. Bull. 81*, 145-154.

Bloom, A. L. (1977). Atlas of sea-level curves, IGCP Project 61 Sea Level Project, UNESCO, Paris.

Bloom, A. L., W. S. Broecker, J. Chappell, R. K. Matthews, and K. J. Mesolella (1974). Quaternary sea-level fluctuations on a tectonic coast: New $^{230}Th/^{234}U$ dates from the Huon Peninsula, New Guinea, *Quat. Res. 4*, 185-205.

Bradley, W. C., and G. B. Griggs (1976). Form, genesis and deformation of central California wave-cut platforms, *Geol. Soc. Am. Bull. 87*, 433-449.

Broecker, W. S., and M. L. Bender (1973). Age determination on marine strandlines, in *Calibration of Hominoid Evolution*, W. W. Bishop and J. A. Miller, eds., Scottish Academic Press, pp. 19-35.

Broecker, W. S., D. L. Thurber, J. Goddard, T.-L. Ku, R. K. Matthews, and K. J. Mesolella (1968). Milankovitch hypothesis supported by precise dating of coral reefs and deep-sea sediments, *Science 159*, 297-300.

Brown, L. D. (1978). Recent vertical crustal movement along the east coast of the United States, *Tectonophysics 44*, 205-231.

Buchanan-Banks, J. M., R. O. Castle, and J. I. Ziony (1975). Elevation changes in the central Transverse Ranges near Ventura, California, *Tectonophysics 29*, 113-125.

Chappell, J. M. (1974a). Geology of coral terraces, Huon Peninsula, New Guinea: A study of Quaternary tectonic movements and sea-level changes, *Geol. Soc. Am. Bull. 85*, 553-570.

Chappell, J. M. (1974b). Upper mantle rheology in a tectonic region: Evidence from New Guinea, *J. Geophys. Res. 79*, 390-398.

Chappell, J. M. (1983). A revised sea-level record for the last 300,000 years from Papua New Guinea, *Search 14*, 99-101.

Chappell, J. M., and H. H. Veeh (1978). Late Quaternary tectonic movements and sea-level changes at Timor and Atauro Island, *Geol. Soc. Am. Bull. 89*, 356-368.

Clague, J., J. R. Harper, R. J. Hebda, and D. E. Howes (1982). Late Quaternary sea levels and crustal movements, coastal British Columbia, *Can. J. Earth Sci. 19*, 597-618.

Clark, J. A., W. E. Farrell, and W. R. Peltier (1978). Global changes in postglacial sea level: A numerical calculation, *Quat. Res. 9*, 265-287.

Cole, J. W., and K. B. Lewis (1981). Evolution of the Taupo-Hikurangi subduction system, *Tectonophysics 72*, 1-21.

Corwin, G., and H. L. Foster (1959). The 1957 explosive eruption on Iwo Jima, Volcano Islands. *Am. J. Sci. 257*, 161-171.

Cronin, T. M., B. J. Szabo, T. A. Ager, J. E. Hazel, and J. P. Owens (1981). Quaternary climates and sea levels of the U.S. Atlantic coastal plain, *Science 211*, 233-239.

Dambara, T. (1971). Synthetic vertical movements in Japan during recent 70, *J. Geod. Soc. Jpn. 17*, 100-108.

Dames and Moore Consultants (1981). Marine terrace studies and age dating: Final geoseismic investigation for proposed LNG terminal at little Cojo Bay, California, unpublished consultant's report prepared for Western LNG Terminal Associates, Los Angeles, Calif.

Davidson, G. (1889). *Coast Pilot of California, Oregon and Washington*, 4th ed., U.S. Coast and Geodetic Survey.

Dodge, R. E., R. G. Fairbanks, L. K. Benninger, and F. Maurrasse (1983). Pleistocene sea levels from raised coral reefs of Haiti, *Science 219*, 1423-1425.

Donner, J. J. (1965). The Quaternary of Finland, in *The Quaternary 1*, K. Rankama ed., Interscience, New York, pp. 221-272.

Donner, J. J. (1980). The determination and dating of synchronous late Quaternary shorelines in Fennoscandia, in *Earth Rheology, Isostasy and Eustasy*, N.-A. Morner ed., John Wiley & Sons, New York, pp. 285-293.

Emery, K. O. (1958). Shallow submerged marine terraces of southern California, *Geol. Soc. Am. Bull. 69*, 39-60.

Farrand, W. R., and R. T. Gajda (1962). Isobases on the Wisconsin marine limit in Canada, *Geogr. Bull. 17*, 5-22.

Faure, H., J. C. Fontes, L. Hebrard, J. Moteillet, and P. A. Piazzoli (1980). Geoidal changes and shore-level tilt along Holocene estuaries: Senegal River area, West Africa, *Science 210*, 421-423.

Fisk, H. N., and E. McFarlan, Jr. (1955). Late Quaternary deltaic deposits of the Mississippi River, in *Crust of the Earth*, A. Poldervaart, ed., Geol. Soc. Am. Spec. Paper 62, pp. 269-302.

Flemming, N. C. (1972). Eustatic and tectonic factors in the relative vertical displacements of the Aegean Coast, in *The Mediterranean Sea: A Natural Sedimentary Laboratory*, D. J. Stanley, ed., Dowden, Hutchinson and Ross, Inc., Stroudsburg, Pa.

Gahni, M. A. (1978). Late Cenozoic vertical crustal movements in the southern North Island, New Zealand, *N.Z. J. Geol. Geophys. 21*, 117-125.

Garrick, R. A. (1979). Late Holocene uplift at Te Araroa, East Cape, North Island, New Zealand, *N.Z. J. Geol. Geophys. 22*, 131-139.

Gibb, J. G. (in press). A New Zealand regional Holocene eustatic sea-level curve and its application to vertical tectonic movements, in *Proceedings Volume for 1984 Recent Crustal Movements Conference*, Wellington, N.Z.

Grant, D. R. (1970). Recent coastal submergence of the Maritime Provinces, Canada, *Can. J. Earth Sci. 7*, 676-680.

Grant, D. R. (1980). Quaternary sea-level changes in Atlantic Canada as an indication of crustal deleveling, in *Earth Rheology, Isostasy and Eustasy*, N.-A. Morner, ed., John Wiley & Sons, New York, pp. 201-214.

Hanks, T. C., R. C. Bucknam, K. R. Lajoie, and R. E. Wallace (1984). Modification of wave-cut and faulting-controlled landforms, *J. Geophys. Res. 89*, 5771-5790.

Harmon, R. S., H. P. Schwarcz, and D. C. Ford (1978). Late Pleistocene sea-level history of Bermuda, *Quat. Res. 9*, 205-218.

Harmon, R. S., T.-L. Ku, R. K. Matthews, and P. L. Smart (1979). Limits of U-series analysis: Phase 1 results of the uranium-series intercomparison project, *Geology 7*, 405-409.

Harmon, R. S., S. L. Lynton, R. M. Mitterer, P. Garrett, H. P. Schwarcz, and J. L. Larson (1981). Bermuda sea level during the last interglacial, *Nature 289*, 481-483.

Hays, W. W., and P. L. Gori (1983). The 1886 Charleston, South Carolina, earthquake and its implications for today, *U.S. Geol. Surv. Open-File Rep. 83-843*, 508.

Hicks, S. D., and J. E. Crosby (1974). Trends and variability of yearly mean sea level 1893-1972, *U.S. Natl. Ocean. Atmos. Admin. Tech. Mem. NOS 13*, 1-14.

Hillaire-Marcel, C. (1980). Multiple component postglacial emergence eastern Hudson Bay, Canada, in *Earth Rheology, Isostasy and Eustasy*, N.-A. Morner, ed., John Wiley & Sons, New York, pp. 215-230.

Hopley, D. (1983). Deformation of the North Queensland continental shelf in the late Quaternary, in *Shorelines and Isostasy*, D. E. Smith and A. G. Dawson, eds., Academic Press, New York, pp. 347-368.

Hoyt, J. H., and J. R. Hails (1974). Pleistocene stratigraphy of southeastern Georgia, in *Post-Miocene Stratigraphy, Central and Southern Atlantic Coastal Plain*, R. Q. Oaks, ed., Utah State University Press, pp. 191-205.

Inman, D. L., and C. E. Nordstrom (1971). The tectonic and morphologic classification of coasts, *J. Geol. 79*, 1-21.

Kaizuka, S., T. Matsuda, M. Nogami, and N. Yonekura (1973). Quaternary tectonic and recent seismic crustal movements in the Arauco Peninsula and its environs, central Chile, *Geogr. Rep. Tokyo Met. Univ. 8*, 1-49.

Kaizuka, S., T. Miyauchi, and S. Nagaoka (1983). Marine terraces, active faults and tectonic history of Iwo Jima, *Ogasawara Res. Comm. of Tokyo Met. Univ. 9*, 13-45.

Kanaya, A. (1978). Holocene terraces and tectonic movements of Muro'o Peninsula, southern Shikoku, Japan, *Geogr. Rev. Jpn. 51*, 451-463.

Kennedy, G. L., K. R. Lajoie, S. A. Mathieson, and D. J. Blunt (1981). Half Moon Bay terrace, California, and the age of its Pleistocene invertebrate faunas, *S. Calif. Assoc. Malacol. Proc. 1981*.

Kennedy, G. L., K. R. Lajoie, and J. F. Wehmiller (1982). Aminostratigraphy and faunal correlations of late Quaternary marine terraces, Pacific Coast, U.S.A., *Nature 299*, 545-547.

Konishi, K., A. Omura, and O. Nakamichi (1974). Radiometric coral ages and sea level records from the late Quaternary reef complexes of the Ryukyu Islands, in *Proceedings Second International Coral Reef Symposium*, pp. 595-613.

Ku, T.-L., and J. P. Kern (1974). Uranium-series age of the upper Pleistocene Nestor Terrace, San Diego, California, *Geol. Soc. Am. Bull. 85*, 1713-1716.

Ku, T.-L., M. A. Kimmel, W. H. Eastan, and T. J. O'Neil (1974). Eustatic sea level 120,000 years ago on Oahu, Hawaii, *Science 6*, 959-962.

Lajoie, K. R., and A. M. Sarna-Wojcicki (1982). Late Quaternary coastal tectonics in the central and western Transverse Ranges, southern California, *Geol. Soc. Am. Abstr. Programs 14-4*, 179.

Lajoie, K. R., J. P. Kern, J. F. Wehmiller, G. L. Kennedy, S. A. Mathieson, A. M. Sarna-Wojcicki, R. F. Yerkes, and P. F. McCrory (1979a). Quaternary marine shorelines and crustal deformation, San Diego to Santa Barbara, California, in *Geological Excursions Southern California Area*, P. L. Abbott, ed., San Diego State University, pp. 3-15.

Lajoie, K. R., G. E. Weber, S. A. Mathieson, and J. Wallace (1979b). Quaternary tectonics of coastal Santa Cruz and San Mateo Counties, California, as indicated by deformed marine terraces and alluvial deposits, in *Coastal Tectonics and Coastal Geologic Hazards in Santa Cruz and San Mateo Counties, California*, G. E. Weber, K. R. Lajoie, and G. B. Griggs, eds., Geol. Soc. Am. Guidebook.

Lajoie, K. R., A. M. Sarna-Wojcicki, and Y. Ota (1982a). Emergent Holocene marine terraces at Ventura and Cape Mendocino, California—indicators of high tectonic uplift rates, *Geol. Soc. Am. Abstr. Programs 14-4*, 178.

Lajoie, K. R., A. M. Sarna-Wojcicki, and R. F. Yerkes (1982b). Quaternary chronology and rates of crustal deformation in the Ventura area, California in *Neotectonics of Southern California*, J. D. Cooper, comp., Geol. Soc. Am. Guidebook, pp. 43-51.

Lajoie, K. R., G. L. Kennedy, S. A. Mathieson, A. M. Sarna-Wojcicki, A. A. Morrison, and M. K. Tobish (1983). Emergent Holocene marine terraces at Cape Mendocino and Ventura, California, U.S.A., in *Proceedings International Symposium on Development of Holocene Shorelines*, Tokyo, Japan.

Lewis, K. B. (1971a). Erosion and deposition on a tilting continental shelf during Quaternary oscillations of sea level, *N.Z. J. Geol. Geophys. 2*, 281-301.

Lewis, K. B. (1971b). Growth rate of folds using tilted wave-planed

surfaces: Coast and continental shelf, Hawke's Bay, *R. Soc. N.Z. Bull. 9*, 225-231.
Lewis, K. B. (1974). The continental terrace, *Earth Sci. Rev. 10*, 37-71.
Lundqvist, J. (1965). The Quaternary of Sweden, in *The Quaternary*, K. Rankama, ed., Interscience, New York, pp. 139-198.
Machida, H., H. Nakagawa, and P. Pirazzoli (1976). Preliminary study on Holocene sea levels in the central Ryukyu Islands, *Rev. Geomorph. Dynamique 25*, 49-62.
Marshall, J. F., and J. Launay (1978). Uplift rates of the Loyalty Islands as determined by $^{230}Th/^{234}U$ dating of raised coral terraces, *Quat. Res. 9*, 186-192.
Marshall, J. F., and B. G. Thom (1976). The sea level in the last interglacial, *Nature 263*, 120-121.
Mathews, W. H., J. G. Fyles, and H. W. Nasmith (1970). Postglacial crustal movements in southwestern British Columbia and adjacent Washington State, *Can. J. Earth Sci. 7*, 690-702.
Matsuda, T. (1976). Empirical rules on sense and rate of recent crustal movements, *J. Geod. Soc. Jpn. 22*, 252-263.
Matsuda, T., Y. Ota, M. Ando, and N. Yonekura (1978). Fault mechanism and recurrence time of major earthquakes in southern Kanto district, Japan, as deduced from coastal terrace data, *Geol. Soc. Am. Bull. 89*, 1610-1618.
Matthews, R. K. (1973). Relative elevation of late Pleistocene high sea-level stands: Barbados uplift rates and their implications, *Quat. Res. 3*, 147-153.
Mesolella, K. J., R. K. Mathews, W. S. Broecker, and D. L. Thurber (1969). The astronomical theory of climatic change: Barbados data, *J. Geol. 77*, 250-274.
Miyoshi, M. (1983). Estimated ages of late Pleistocene marine terraces in Japan, deduced from uplift rate, *Geogr. Rev. Jpn. 56*, 819-834.
Moore, J. E., and D. J. Fornari (1984). Drowned reefs as indicators of subsidence of the island of Hawaii, *J. Geol. 92*, 752-759.
Moore, W. S., and B. L. K. Samayajulu (1974). Age determinations of fossil corals using $^{230}Th/^{234}Th$ and $^{230}Th/^{227}Th$, *J. Geophys. Res. 79*, 5065-5068.
Morner, N.-A. (1976). Eustasy and geoid changes, *J. Geol. 84*, 123-151.
Morner, N.-A. (1978). Faulting, fracturing and seismic activity as a function of glacial-isostasy in Fennoscandia, *Geology 6*, 41-45.
Morner, N.-A. (1980). The Fennoscandian uplift: Geological data and their geodynamical implication, in *Earth Rheology, Isostasy and Eustasy*, N.-A. Morner ed., John Wiley & Sons, New York, pp. 251-283.
Morner, N.-A. (1983). Comment on tectonic uplift of a middle Wisconsin marine platform near Mendocino triple junction, California, *Geology 11*, 621.
Nakamura, K., K. Kasahara, and T. Matsuda (1965). Tilting and uplift of an Island, Awashima, near the epicentre of the Niigata earthquake in 1964, *J. Geod. Soc. Jpn. 10*, 111-214.
Nakata, T., T. Takahashi, and M. Koba (1978). Holocene-emerged coral reefs and sea-level changes in the Ryukyu Islands, *Geogr. Rev. Jpn. 51*, 87-108.
Nakata, T., M. Koba, W. Jo, T. Imaizumi, H. Matsumoto, and T. Suganuma (1979). Holocene marine terraces and seismic crustal movement, *Sci. Rep. Tohoku Univ., 7th Ser. (Geogr.) 29*, 195-204.
Nakata, T., M. Koba, T. Imaizumi, W. Jo, H. Matsumoto, and T. Suganuma (1980). Holocene marine terraces and seismic crustal movements in the southern part of Boso peninsula, Kanto, Japan, *Geogr. Rev. Jpn. 53*, 29-44.
Neumann, A. C., and W. S. Moore (1975). Sea-level events and Pleistocene coral ages in the northern Bahamas, *Quat. Res. 5*, 3215-224.
Newman, W. W., L. J. Cinquemani, R. R. Pardi, and L. L. Marcus (1978). Holocene deleveling of the United States' east coast, in *Earth Rheology, Isostasy and Eustasy*, N.-A. Morner, ed., John Wiley & Sons, New York, pp. 449-463.
Oaks, R. Q., Jr., and J. R. Du Bar, eds. (1974). *Post Miocene Stratigraphy Central and Southern Atlantic Coastal Plain*, Utah State University Press, 275 pp.
Oliver, J., T. Johnson, and J. Dorman (1970). Postglacial faulting and seismicity in New York and Quebec, *Can. J. Earth Sci. 7*, 579-590.
Omoto, K. (1979). Holocene sea-level change: A critical review, *Sci. Rep. Tohoku Univ., 7th Ser. 29*, 205-222.
Ota, Y. (1964). Coastal terraces of the Sado Island, Japan, *Geogr. Rev. Jpn. 37*, 226-242.
Ota, Y. (1975). Late Quaternary vertical movement in Japan estimated from deformed shorelines, in *Quaternary Studies*, R. P. Suggate and M. M. Creswell, eds., Royal Society of New Zealand, pp. 231-239.
Ota, Y., and N. Hori (1980). Late quaternary tectonic movement of the Ryukyu Islands, Japan, *Quat. Res. 18*, 221-240.
Ota, Y., T. Matsuda, and K. Naganuma (1976). Tilted marine terraces of the Ogi Peninsula, Sado Island, central Japan, related to the Ogi Earthquake of 1802, *Seismol. J. Soc. Jpn. II-29*, 55-70.
Page, W. D., J. N. Alt, L. S. Cluff, and G. Plafker (1979). Evidence for the recurrence of large-magnitude earthquakes along the Makran coast of Iran and Pakistan, *Tectonophysics 52*, 533-547
Peltier, W. R., and J. T. Andrews (1983). Glacial geology and glacial isostasy of the Hudson Bay region, in *Shorelines and Isostasy*, D. E. Smith and A. G. Dawson, eds., Academic Press, New York, pp. 285-320.
Pillans, B. (1983). Upper Quaternary marine terrace chronology and deformation, South Taranaki, New Zealand, *Geology 11*, 292-297.
Pirazzoli, P. A., J. Thommeret, Y. Thommeret, J. Laborcal, and L. F. Montaggioni (1982). Crustal block movements from Holocene shorelines: Crete and Atikythira (Greece), *Tectonophysics 86*, 27-43.
Plafker, G. (1965). Tectonic deformation associated with the 1964 Alaska earthquake, *Science 148*, 1675-1687.
Plafker, G. (1972). Alaskan earthquake of 1964 and Chilean earthquake of 1960: Implications for arc tectonics, *J. Geophys. Res. 77*, 901-924.
Plafker, G., and M. Rubin (1967). Vertical tectonic displacements in south-central Alaska during and prior to the great 1964 earthquake, *J. Geosci. Osaka City Univ. 10*, 53-66.
Plafker, G., and M. Rubin (1978). Uplift history and earthquake recurrence as deduced from marine terraces on Middleton Island, Alaska, in *Proceedings of Conference VI Methods and Identification of Seismic Gaps*, pp. 687-721.
Plafker, G., and J. C. Savage (1970). Mechanism of the earthquakes of May 21 and 22, 1960, *Geol. Soc. Am. Bull. 81*, 1001-1030.
Plafker, F., T. Hudson, M. Rubin, and K. Dixon (1981). Holocene marine terraces and uplift history in the Yakataga seismic gap near Icy Cape, Alaska, *U.S. Geol. Surv. Cir. 844*, 111-115.
Poland, J. F. (1971). Land subsidence in the Santa Clara Valley, Alameda, San Mateo and Santa Clara Counties, California, *U.S. Geol. Surv. MF-336*, 1:125,000.
Research Group for Quaternary Tectonic Map (1969). Quaternary tectonic map of Japan, 1:2,000,000, National Research Center for Disaster Prevention, 6 sheets.
Ridley, A. P., and Seeley, M. W. (1979). Evidence for recent coastal uplift near Al Jubail, Saudia Arabia, *Tectonophysics 52*, 319-327.
Ridlon, J. B. (1972). Pleistocene-Holocene deformation of the San Clemente Island crustal block, California, *Geol. Soc. Am. Bull. 83*, 1831-1844.
Sandweiss, D. H., and H. B. Rollins (1981). A single large magnitude

uplift in the Holocene record of the Peruvian north coast, *Geol. Soc. Am. Abstr. Programs 13*, 545.

Sarna-Wojcicki, A. M., K. M. Williams, and R. F. Yerkes (1976). Geology of the Ventura fault, Ventura County, California, *U.S. Geol. Surv. Map MF-781*, 1:6,000.

Sarna-Wojcicki, A. M., K. R. Lajoie, and R. F. Yerkes (1986). Recurrent Holocene displacement on the Javon Canyon fault: A comparison of fault movement history with calculated average recurrence intervals, *U.S. Geol. Surv. Prof. Paper 1339*.

Sawamura, T. (1953). Relation between the activities of the outer earthquake zone in southwestern Japan and the geologic structures and crustal movements of Shikoku and its vicinity, *Res. Rep. Kochi Univ. 2*(15), 1-46.

Schofield, J. E. (1973). Post-glacial sea levels of Northland and Auckland, *N.Z. J. Geol. Geophys. 16*, 359-366.

Scholl, D. W., F. C. Craighead, and M. Stuiver (1970). Florida curve revised: Its relation to coastal sedimentation rates, *Science 163*, 562-564.

Shackleton, N. J., and N. D. Opdyke (1973). Oxygen isotope and paleomagnetic stratigraphy of equatorial Pacific core V28-238, *Quat. Res. 3*, 39-55.

Shimazaki, K., and T. Nakata (1980). Time-predictable recurrence model for large earthquakes, *Geophys. Res. Lett. 7*, 279-282.

Shubert, C., and B. J. Szabo (1978). Uranium-series ages of Pleistocene marine deposits on the islands of Curacao and La Blanquilla, Caribbean Sea, in *Caribbean Geol. Conf. 8th Proc.*, H. J. MacGillavry and D. J. Beets, eds., *Geol. Mijnbouw 57*, 325-332.

Sissons, J. B., and R. Cornish (1982). Rapid localized glacio-isostatic uplift at Glen Roy, Scotland, *Nature 297*, 213-214.

Sneh, Y. and M. Klein (1984). Holocene sea-level changes at the coast of Dor, southeast Mediterranean, *Science 226*, 831-832.

Stearns, C. E. (1970). Estimates of the position of sea level between 140,000 and 75,000 years ago, *Quat. Res. 6*, 445-429.

Stearns, C. E. (1984). Uranium-series dating and the history of sea level, in *Quaternary Dating Methods*, W. C. Mahaney, ed., Elsevier, New York, pp. 53-66.

Stevens, G. R. (1973). Late Holocene marine features adjacent to Port Nicholson, Wellington, New Zealand, *N.Z. Geol. Surv. 16*, 455-484.

Sugimura, A., and Y. Naruse (1954). Changes in sea level, Seismic upheavals and coastal terraces in the southern Kanto Region, Japan, *Jpn. J. Geol. Geogr. 24*, 101-113.

Sutherland, D. C. (1983). The dating of former shorelines; in *Shorelines and Isostasy*, D. E. Smith, and A. G. Dawson, eds., Inst. Brit. Geogr. Spec. Publ. 16, pp. 129-160.

Szabo, B. J. (1979). Uranium-series age of coral reef growth on Rottuest Island, western Australia, *Mar. Geol. 29*, M11-M15.

Szabo, B. J., W. C. Ward, A. E. Weidie, and M. J. Brady (1978). Age and magnitude of the late Pleistocene sea-level rise on the eastern Yucatan Peninsula, *Geology 6*, 713-715.

Tamura, A. (1979). Holocene marine terraces and crustal movements of Sado Island, central Japan, *Geogr. Rev. Jpn. 52*, 339-355.

Tarr, A. C. (1974). World Seismicity map, U.S. Geological Survey.

Thatcher, W. (1984). The earthquake deformation cycle at the Nankai Trough, southwest, Japan, *J. Geophys. Res. 89*, 3087-3101.

Thom, B. G., and P. S. Roy (1983). Sea-level changes in New South Wales over the past 15,000 years, *Geogr. Dept. James Cook Univ. Monogram Series, Occasional Paper 3*, 64-84.

Thom, G. G., R. H. Hails, and A. R. H. Martin (1969). Radiocarbon evidence against higher postglacial sea levels in eastern Australia, *Mar. Geol. 7*, 161-168.

Thompson, W. B., K. J. Borns, H. W. Borns, Jr., and B. C. Anderson (1983). Glacial-marine deltas and late Pleistocene-Holocene crustal movements in southern Maine, in *New England Seismotectonic Study Activities in Maine during Fiscal Year 1982*, W. B. Thompson and J. T. Kelley, eds., Maine Geol. Surv. Rep., U.S. Reg. Comm., pp. 153-171.

Thurber, D. L., W. S. Broecker, W. S. Blanchard, and H. A. Protratz (1965). Uranium-series ages of Pacific atoll coral, *Science 149*, 55-58.

Veeh, H. H. (1966). $^{230}Th/^{238}U$ and $^{234}U/^{238}U$ ages of Pleistocene high sea-level stand, *J. Geophys. Res. 71*, 3379-3386.

Veeh, H. H., and J. Chappell (1970). Astronomical theory of climate change: Support from New Guinea, *Science 167*, 862-865.

Veeh, H. H., and J. W. Valentine (1967). Radiometric ages of Pleistocene fossils from Cayucos, California, *Geol. Soc. Am. Bull. 78*, 547-550.

Vita-Finzi, C. (1979). Rates of Holocene folding in the coastal Zagros near Bandar Abbas, Iran, *Nature 278*, 632-634.

Walcott, R. I. (1970). Isostatic response to loading of the crust in Canada, *Can. J. Earth Sci. 7*, 716-734.

Walcott, R. I. (1984). The major structural elements of New Zealand, in *An Introduction to the Recent Crustal Movements of New Zealand*, R. I. Walcott comp., *R. Soc. N.Z. Misc. Ser. 7*, 1-6.

Ward, W. T. (1985). Correlation of east Australian Pleistocene shorelines with deep-sea core stages: A basis for a coastal chronology, *Geol. Soc. Am. Bull. 96*, 1156-1166.

Weber, G. E. (1983). Geologic investigation of the marine terraces of the San Simeon region and Pleistocene activity of the San Simeon fault zone, San Luis Obispo County, California, *U.S. Geol. Surv. Tech. Rep. 66*.

Weber, G. E., and Cotton, W. R. (1981). Geologic investigation of recurrence intervals and recency of faulting along the San Gregorio fault zone, San Mateo County, California, *U.S. Geol. Surv. Open-File Rep. 81-263*.

Weber, G. E., and K. R. Lajoie (1977). Late Pleistocene and Holocene tectonics of the San Gregorio fault zone between Moss Beach and Point Año Nuevo, San Mateo County, California, *Geol. Soc. Am. Abstr. Programs 9*, 524.

Wellman, H. W. (1969). Tilted marine beach ridges at Cape Turakirae, N.Z., *Tuatara 17*, 82-93.

Wellman, H. W. (1971a). Holocene tilting and uplift of the Glenburn coast, Wairarapa, New Zealand, *R. Soc. N.Z. Bull. 9*, 221-223.

Wellman, H. W. (1971b). Holocene tilting and uplift on the White Rocks coast, Wairarapa, New Zealand, *R. Soc. N.Z. Bull. 9*, 211-215.

Wellman, H. W. (1979). An uplift map for the South Island of New Zealand, and a model for uplift of the Southern Alps, *R. Soc. N.Z. Bull. 18*, 13-21.

Yonekura, N., and K. Shimazaki (1980). Uplifted marine terraces and seismic crustal deformation in arc-trench systems: A role of imbricated thrust faulting, *EOS 61*, 1111.

Yoshikawa, T., S. Kaizuka, and Y. Ota (1964), Mode of crustal movement in the late Quaternary of the southeast coast of Shikoku, southwestern Japan, *Geogr. Rev. Jpn. 37*, 627-648.

# 7 Tectonic Geomorphology of Escarpments and Mountain Fronts

LARRY MAYER
*Miami University*

ABSTRACT

The morphology of fault-generated mountain fronts and escarpments can indicate relative tectonic activity. Fault slip rates can be estimated using erosion rates or dated landform elements. The use of landforms to solve for the timing and magnitude of tectonic perturbations is analogous to an inverse problem where given a landform morphology one must solve for the variables that caused or affected it. Models that predict the rate of landform evolution can be used to solve for the ages of uplifts when properly calibrated with independent age determinations. Basalt flows or air fall tuffs are useful for establishing a denudation chronology and permit erosion rates to be calculated. Future research should develop additional relations among tectonics and landforms rendering the solution to this inverse problem as unique as possible.

## INTRODUCTION

Tectonic geomorphology is the study of landforms that result from tectonism and the interaction between tectonic and geomorphic processes. Tectonic geomorphologic studies constrain solutions to an inverse problem: given selected morphologic attributes of tectonic landforms, can one determine the corresponding tectonic history; or similarly, given information about the tectonic history, can one determine how landforms will evolve? Studies of tectonic geomorphology can discern the nature, timing, and distribution of faulting and seismicity that have occurred over tens of thousands of years, and in the case of mountain fronts and escarpments, an order of magnitude longer. Instrumental recordings of seismic data are available for a very short time; historical records of earthquakes are also useful. Studies of paleoseismicity, which is past seismicity based on interpretation of small-scale geomorphic or stratigraphic features, enable scientists to determine the past behavior of seismogenic structures and, hence, better evaluate the risk to society resulting from future earthquakes. The length of time a landform records depends on its survival time, or how rapidly the landform evolves.

Two types of landform that have long survival times are escarpments and mountain fronts. Other tectonic landforms may have considerably shorter survival times. The relation among the different types of tectonic records is illustrated in Figure 7.1. The precision of the record is inversely proportional to the length of record so that as the time recorded increases we cannot be certain about short-term variations in uplift. In addition, each type of record measures the uplift history of a landform differently. This difference is sometimes expressed by different average uplift rates, which are calculated by

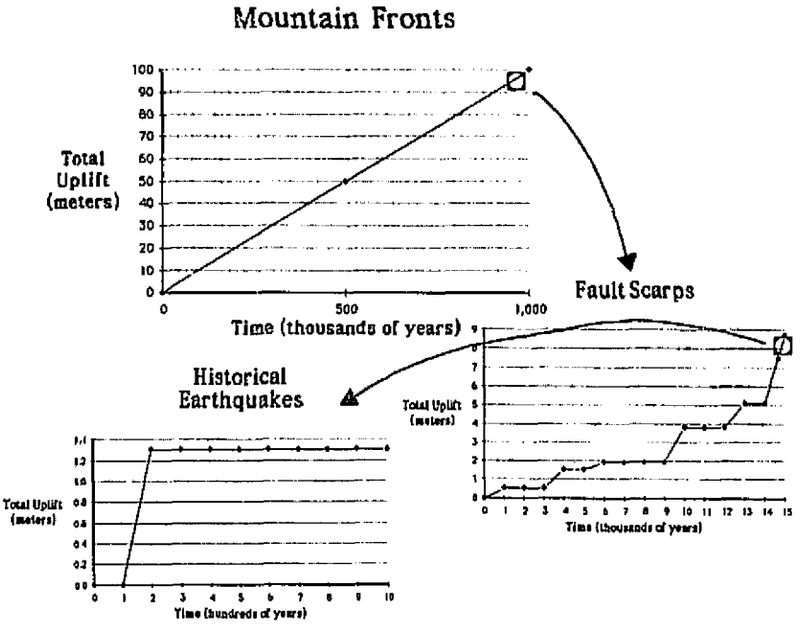


FIGURE 7.1 Graphs showing hypothetical uplift history by plotting cumulative uplift versus the length of record. Mountain fronts record long periods of time, whereas fault scarps and historical earthquake data record progressively shorter time periods. The circle-in-square on the mountain fronts graph outlines the time period shown on the fault scarp graph. Likewise, the circle on the fault scarps graph indicates the time period covered by the historical earthquakes graph.

dividing the total (cumulative) uplift by the period of record. The variation of uplift rate estimates reflects short-term tectonic fluctuations that may be superimposed on long-term trends. Thus, long-term averages of past uplift rates serve to constrain forecasts of uplift. How mountain fronts and escarpments evolve and several methods for their use in tectonic geomorphology are discussed below.

The most popular early attempt to relate landform morphology with tectonics was William Morris Davis' cycle of erosion. Davis (1899) envisioned a closed geomorphic system where, following a pulse of rapid uplift, landforms evolved through a sequence of characteristic landforms. Each landform assemblage in the Davisian sequence of "youth," "maturity," and "old age" stages differed morphologically from the others. Davis' cycle of erosion was highly intuitive and logical but suffered under the blow of equifinality. In other words it was possible to produce the landform assemblages in each stage by variables other than sequential denudation following rapid uplift. For example, rock types and geologic structure differ from area to area, and the effectiveness of erosional geomorphic processes also varies; yet these differences were not accounted for in the cycle of erosion. Despite the shortcomings of the Davisian scheme, the basic concept of landform adjustment following tectonism remains intact. The controversy surrounding the Davisian cycle of erosion may have provided the impetus for quantitative field investigations, the key to unraveling landform history.

Recent studies (Bull and McFadden, 1977; Wallace, 1977, 1978; Bucknam and Anderson, 1979) have examined the interaction of tectonics and landforms using an empirical approach. In these studies dating or determining rates of change of a landform or landform assemblage is an ultimate goal on which tectonic interpretations may be based. Data that allow the rates of landform change to be estimated can be used to determine how landforms may respond to tectonic perturbations. Hillslopes can result from tectonism such as faulting, and, therefore, hillslope evolution and slope processes are fundamental to understanding how erosion and tectonics interact to produce any given landform.

## SLOPES

Slopes are basic landform elements that are naturally combined to form landform assemblages. Hillslopes are that portion of the sloping landscape within a drainage basin that contribute sediment (by several transport processes) and runoff to streams. Slope systems denote landform assemblages that operate or evolve as an integrated package of surficial processes and are commonly delineated by their topographic expression.

Equilibrium in slope systems can refer either to slope

forms that tend to persist over time or to conditions where the rate at which regolith or soil develops is balanced by the rate of soil removal. In the latter context, equilibrium slopes are suggested by field observations that show soil (sensu lato) thickness to be relatively constant over a slope. Constant soil thickness requires a balance between production of soil by weathering and its removal by erosion. Departures from this balance are either tipped toward erosion or weathering, and the resulting slopes are termed, respectively, weathering-limited and transport-limited slopes (Young, 1972).

Weathering-limited slopes denote a condition where the rate of soil removal exceeds that of soil production. Bare rock slopes are an example of a weathering-limited slope. Transport-limited slopes refer to a condition where the rate of soil production does not limit the rate of soil removal. A valley-side slope cut by drainages on the erodible materials of "badlands" is an example of a transport-limited slope.

As a slope erodes, its forms may change. Four types of slope evolution that describe some common patterns of slope change are decline, replacement, retreat, and rounding. Each type of slope evolution is the geometric result of the distribution of net erosion along a slope. During the history of some slopes, more than one type of slope evolution can take place. The relation between slope evolution and erosion can be described using a mass-flux diagram (Figure 7.2). Mass flux is a rate of material movement per unit of slope area and is analogous to the concept of erodibility.

A mass-flux diagram illustrates the position on a slope where either erosion or deposition is most efficient. Slope decline is important in areas with stable base-level and mature topography. Though characterized by erosion throughout the length of the slope, decline results from more effective erosion near the upper portions adjacent to the drainage divides. The situation of parallel retreat occurs when erosion is constant along a slope and therefore vertical lowering of the slope occurs everywhere at the same rate. Parallel retreat is common, but not restricted to, areas where the upper surface is protected from erosion by a resistant cap rock. Slope replacement describes the replacement of the original slope by one controlled by deposition. Material eroded from the escarpment is deposited at the base of the slope and accumulates at a slope less steep than the original escarpment. With time, the depositional slope replaces the original slope.

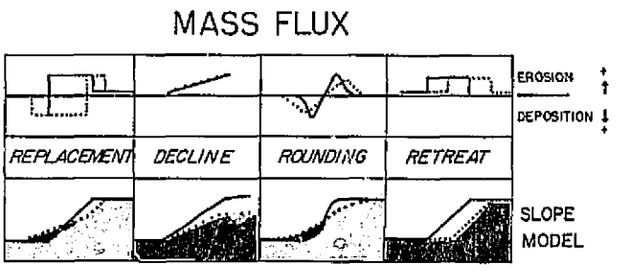


FIGURE 7.2 Mass-flux diagram illustrating the differences in slope models in terms of how erosion or deposition is distributed along the profile. The solid lines mark the initial condition, and the dotted lines indicate profile change after some time. On the lower portion of the figure, white areas of the profile indicate erosion while the dark areas (for rounding and replacement) indicate deposition.

Slope rounding describes a symmetric erosion-deposition feature of some slopes that decreases the curvature all along a slope. Fault scarps in alluvium show this form of evolution. Other models of slope evolution can be envisioned by relating the amount of material eroded on a slope to some morphologic factor such as slope gradient or slope curvature. Slope rounding and decline are similar except for the deposition that is found in slope-rounding evolution. In addition, as a slope evolves, the dominant pattern of evolution may change. For example, a slope may initially change by slope replacement and later by some other evolutionary type. In the case of fault scarps formed in alluvium, early slope development is characterized by slope replacement and later by slope rounding (see Nash, Chapter 12, this volume).

## FAULT-GENERATED MOUNTAIN FRONTS

The Basin and Range physiographic province of the United States is characterized by fault-bounded mountain blocks. These mountains, formed where faults displaced the topographic surface, are termed fault-generated mountains (Figure 7.3). The morphology of mountain fronts is strongly affected by the width of the range. The range width determines the maximum possible drainage basin size that can develop. As virtually all of the area within the mountain block is sloping (i.e., draining), drainage basins fill all available space. For a given mountain range, larger watersheds that tend to have a characteristic shape also have a regular spacing along the mountain front. The spacing depends on basin shape. Regular spacing of basins measured as a ratio between the distances of the basin mouths along the range front to length of the basin was noted by Wallace (1978).

Drainage basin characteristics within the mountain range, primarily shape and size, affect the morphology of the mountain front and how that front may evolve. Large circular watersheds do not effectively fill space at

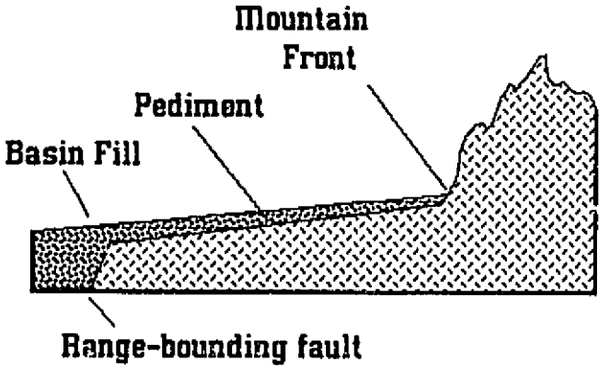


FIGURE 7.3 Idealized fault-bounded mountain front and related terminology.

the mountain front and therefore, depending on other factors, may allow for extensive triangular facets (Figure 7.4). In some instances, triangular facets represent the eroded plane of faulting at the mountain front, and the existence of facets indicates that sufficient time to obliterate them has not elapsed.

The overall morphology of typical Basin and Range mountain blocks reflects their integrated erosional-tectonic history. Because a lag time exists between the time of faulting at the structural front and transmission of this base-level perturbation upstream, the tectonic history may be reflected differently in different parts of the drainage basin. For this reason, morphologic studies have emphasized the geomorphic features near the mountain front.

Several morphologic features of mountain blocks may reflect recent tectonism. Bull and McFadden (1977) suggested that the sinuosity of a mountain front is related to the time elapsed since active high-angle faulting ceased (see Keller, Chapter 8, this volume). Linear or curvilinear mountain fronts have low sinuosity and may represent recent fault movement, while mountain fronts

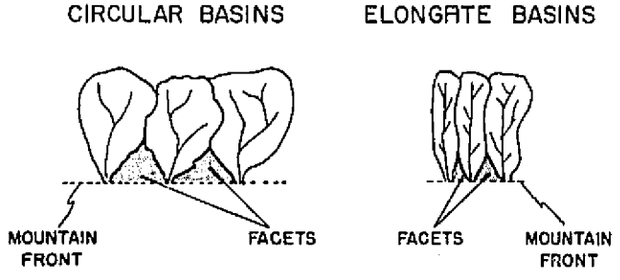


FIGURE 7.4 Relation between basin shape and morphology of the mountain front.

deeply embayed by pediments have high sinuosity and may represent tectonic quiescence or rock control.

A maximum limit on sinuosity is achieved where the spur ridges separating adjacent drainage basins are not eroded away. This relation is shown schematically in Figure 7.5. Using simple geometric shapes for hypothetical pediment embayments one can show that the maximum possible sinuosity is dependent on drainage-basin spacing. Given a drainage-basin spacing and given the constraint that the spur ridges do not erode back, sinuosity increases as erosion progresses, and, therefore, sinuosity increases with time. Unfortunately, the constraint that spur ridges do not erode is not valid. Spur ridges do erode but at rates that are much slower than the stream erodes it valley. With decreasing stream length and, hence, decreasing mountain width, the rate of stream valley erosion may approach that of the spur ridges. Thus for narrow ranges, sinuosity may be low and practically independent of time since faulting. In general, sinuosity is dependent on basin spacing, time, and range width.

Stream valley erosion, and particularly the morphology of a stream valley in cross section, has also been proposed as a tool in interpreting tectonic activity. Bull and McFadden (1977) suggested that the width of the valley floor near the mountain front is a useful index that measures effectiveness of stream downcutting (see Keller, Chapter 8, this volume). Bull and McFadden suggested that a simple ratio of valley floor width to average height of the adjacent divides be used as this index and demonstrated statistically significant variation in the ratio for different tectonic settings.

Stream-valley morphology affords a fruitful ap-

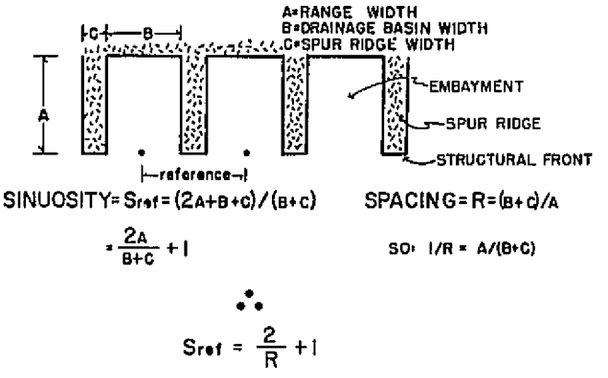


FIGURE 7.5 Hypothetical mountain front used to derive a relation among sinuosity, range width, and basin spacing. In this derivation it is assumed that the spur ridges do not erode back. Different geometric shapes for the embayment can be used but show a similar linear relationship between sinuosity and basin spacing.

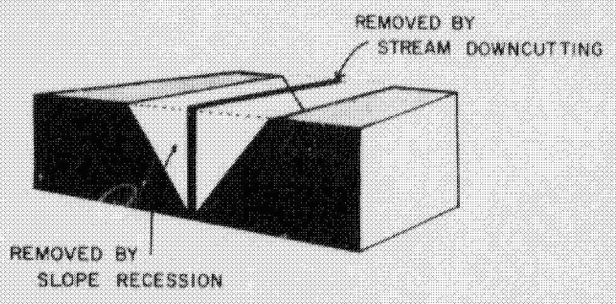


FIGURE 7.6 Conceptual representation of valley erosion. The relative rates of two processes, stream downcutting and slope recession, determine the morphology of the resultant valley.

proach to tectonic history based on several geomorphic postulates proposed in the context of Basin and Range physiography. First, streams downcut in response to vertical uplift, and downcutting becomes less important as the stream gradient readjusts to the new lowered base level. Second, when the mode of erosion of the valley-side slopes is dominated by slope retreat, then morphology of the stream valley is related to both the rate of stream downcutting and the rate of slope retreat. This concept is illustrated on Figure 7.6 and simply states that the volume of material removed when a stream valley is formed is related to both stream and hillslope erosional processes and that the resultant valley depends on the relative rates of the two processes.

Morphologic descriptions of stream valleys, within the context of the specific postulates noted above, can then be used to make some meaningful interpretation. A simple scheme for describing stream-valley morphology is shown on Figure 7.7. The V ratio incorporates information about shape of the valley that can, in turn, be related to vertical uplift. V ratios near 1 indicate a U-shaped valley. Ratios greater than 1 indicate a valley much wider than deep, whereas very small ratios represent active downcutting that is common for streams flowing in V-shaped valleys.

V ratios, shown in Figure 7.8, are not unique. The same V ratio may describe valleys with different morphology; however, these ratios are generally comparable when the valley depths are about equal between groups or are normalized for valley depth. Larger V ratios may indicate relatively less active vertical tectonism.

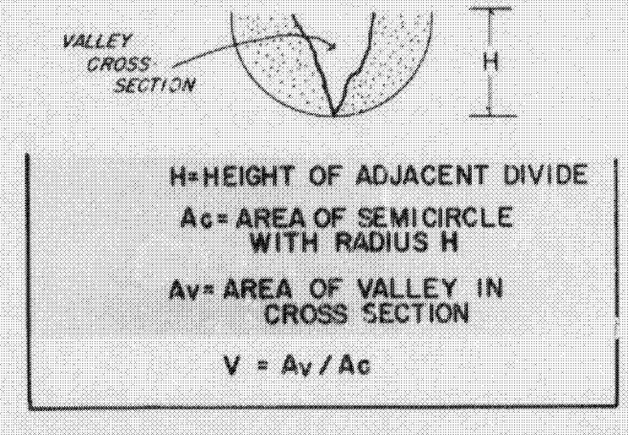


FIGURE 7.7 A numerical index of valley morphology can be calculated by comparing the area of the actual valley cross section with the area of a semicircle with radius equal to the height of the adjacent drainage divide.

## FAULT-GENERATED ESCARPMENTS

Fault-generated escarpments are characterized by a cliff or free face and an associated talus slope. Rock materials fall off the free face and accumulate on the talus slope. Free-face slope angles are commonly greater than 40°, whereas the angles on the talus slopes are largely controlled by the angle of repose of the materials comprising the talus. Some escarpments show a slope-replacement mode of evolution (Figures 7.9 and 7.10), while others show slope retreat.

The location of drainage divides with respect to the cliff face in large part determines the morphologic evolution or escarpments. The spatial relationships be-

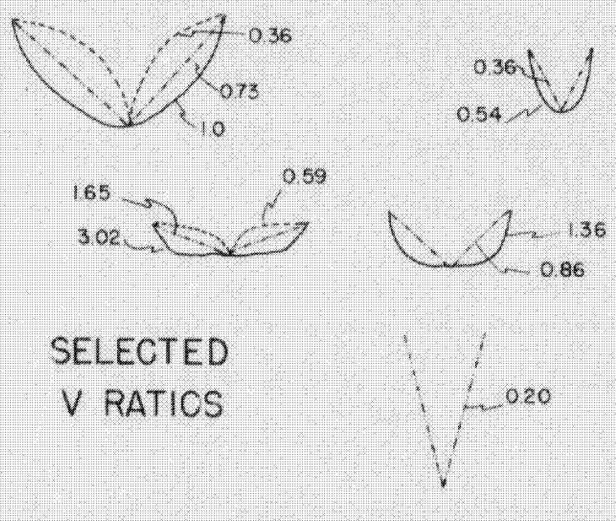


FIGURE 7.8 Comparison between generalized valley morphologies and their associated V ratios. The V ratio is defined on Figure 7.7. Larger ratios indicate that slope recession is more important than stream downcutting and, depending on the actual rates, may indicate tectonic quiescence.

FIGURE 7.9 The 1887 rupture along the Pitaycachi Fault scarp in Sonora, Mexico, that shows the early stages of profile evolution to be characterized by slope replacement.

tween drainage networks, discharge, and the escarpment physically limit such morphologic characteristics as linearity, hypsometry, and dissection. Where an escarpment is also a drainage divide (Figure 7.11) there is a tendency toward maintaining linearity and also for a slope-retreat mode of escarpment evolution. The Mogollon Rim in central Arizona is an example of a high escarpment that is also a drainage divide (Figure 7.11), separating flow onto the Colorado Plateau from flow into the Basin and Range province. The Hurricane Cliffs are another example where linearity is maintained to some extent by the coincidence of drainage divide and escarpment. The Grand Wash Cliffs, in contrast, are deeply embayed (Figure 7.12). This is due in part to their antiquity, but also because the main drainage divide did not coincide with the escarpment. Significant drainages cut the Grand Wash Cliffs, the largest of which is the Colorado River.

Streams flowing across fault-generated escarpments erode valley embayments. Many of the embayments in their most simplified planimetric form resemble triangular cuts into the uplifted escarpment. We can consider the embayment length (the distance upstream from escarpment front to the head of the embayment) to be the height of the triangle and the width of the embayment at the escarpment front to be the base of the triangle. The geometry of these embayments is dependent on the size of the stream in the valley. The relationship between stream length and embayment length is linear. For embayments eroded into cliffs around the Grand Canyon, embayment length is proportional to the length of the stream. These relations imply that the regression line relating stream length and embayment length for an escarpment has temporal significance and can be used for relative dating of escarpments. Older escarpments should plot above younger escarpments, all else being comparable.

Another factor influencing the geometry of escarpment embayments is the rate of slope retreat. The more rapid the slope retreat relative to headward advance of the embayment, the wider the embayment mouth. Because the embayment's length and width dimensions grow at different rates, the resulting geometry can be referred to as anisometric and, where well described by

FIGURE 7.10 The Vermillion Cliffs in northern Arizona is at this locale characterized by slope replacement. The talus slope consists of debris that forms at the expense of the cliff face.

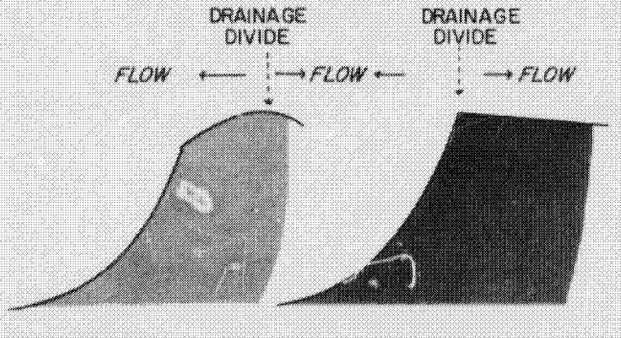


FIGURE 7.11 Profiles of two escarpments. The one on the left has drainage over the escarpment face, a situation that promotes dissection of the escarpment. The profile on the right shows that the escarpment and the drainage divide are one and the same, a situation that promotes linearity regardless of age.

a power function, as allometric. The allometric characteristics of embayment growth may permit morphology-derived dating of certain fault-generated escarpments. In any event, the width of the embayment mouth of larger streams, it seems reasonable to assume, is a function of time.

## RATES OF GEOMORPHIC PROCESSES

Rates of stream downcutting, escarpment retreat, pedimentation, and other geomorphic processes permit estimates of the rates of tectonic processes such as vertical uplift. Pediments, for example, are bedrock surfaces formed by erosion of a mountain block that gently slope toward the basin and commonly are covered by some

FIGURE 7.12 Computer-enhanced topographic image of the Shivwitz Plateau in northwestern Arizona. North is at top of photo. The north-south trending upper Grand Wash Cliffs shows deep embayment by streams traversing. The canyons in the south and eastern portions of the photo are tributaries to the Colorado River in the Grand Canyon.

thickness of gravel (Figure 7.13). They form only under conditions where the rate of piedmont erosion is greater than the rate of uplift across a range-bounding fault. Where rock control is not a factor, pediments represent a period of tectonic inactivity and thus are binary in nature. Pediment widths are dependent on the time since active faulting along the range front and also on drainage basin slope and length. Estimates of pedimentation rates are generally in the range of 300-1000 m per million years (m.y.) (Young and Brennan, 1974; Wallace 1978). A pediment 2 km wide may therefore represent a period of tectonic quiescence that lasted greater than 2 m.y. Pediments that form in conjunction with cliff retreat from fault-generated escarpments can be used in an analogous fashion.

Basalt flows and volcanic ash deposits provide an unique opportunity to determine the ages of tectonic events and the rates of geomorphic processes. They can preserve a datum that records previous river levels or a prefaulting topography. For example, if a basalt flowed down a river channel and subsequent tectonically induced entrenchment results in topographic inversion with the old channel preserved by the basalt, then the amount and geometry of downcutting can be determined (Figure 7.14).

The Grand Wash in northwestern Arizona is an example of topographic inversion (Figure 7.15). Basalts flowed down the Grand Wash valley about 7 m.y. ago (Hamblin *et al.*, 1981). Base-level fall, perhaps related to the downcutting by the Colorado River, resulted in entrenchment. When downcutting by large streams is caused by tectonic uplift, the total amount of downcutting approaches the total amount of uplift. Because a former river level is both preserved and dated by basalt flows, average downcutting rates can be calculated, which turn out to be 26 m/m.y. for the Grand Wash (Hamblin *et al.*, 1981). Similar calculations indicate that the Hurricane fault, near the town of Hurricane, Utah, has a minimum vertical slip rate of 300 m/m.y. for the last 0.3 m.y.

The amount of downcutting, however, decreases upstream from the base-level fall. Rice (1980), using four dated basalt flows, estimated a 95 m/m.y. average downcutting rate of the Little Colorado River over the past 2.5 m.y.

Alternatively, if an area containing basalt flows has

FIGURE 7.13 Pediment surface in the Mohave Desert of California exposing bedrock. The pediment-mountain front junction is abrupt and characterized by a sharp break in slope.

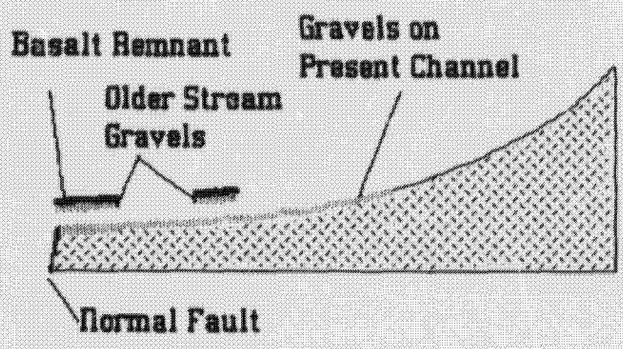


FIGURE 7.14 Profile of stream channel showing the relation between the present channel and portions of an older channel preserved by basalt flows. Downcutting induced by faulting has left the older channel remnants much higher than the present channel.

been tectonically warped or tilted, the basalts may record irregularities, anomalous gradients, or gradient reversals. Classic examples of basalt-filled channels being used as long-term tiltmeters can be found in studies of late Cenozoic tectonism in the Sierra Nevada Mountains of California (Bateman and Wahrhaftig, 1966). Use of volcanic ashes to date erosional or depositional surfaces are also abundant (Young and Brennan, 1974). Field relations using dated basalts have supported tectonic geomorphologic inference regarding classical geomorphic problems including the development of the western margin of the Colorado Plateau and the evolution of the Grand Canyon (McKee and McKee, 1972; Hamblin *et al.*, 1981).

## DISCUSSION

The tectonic geomorphology of fault-generated topographic fronts can be used to describe long-term tectonic

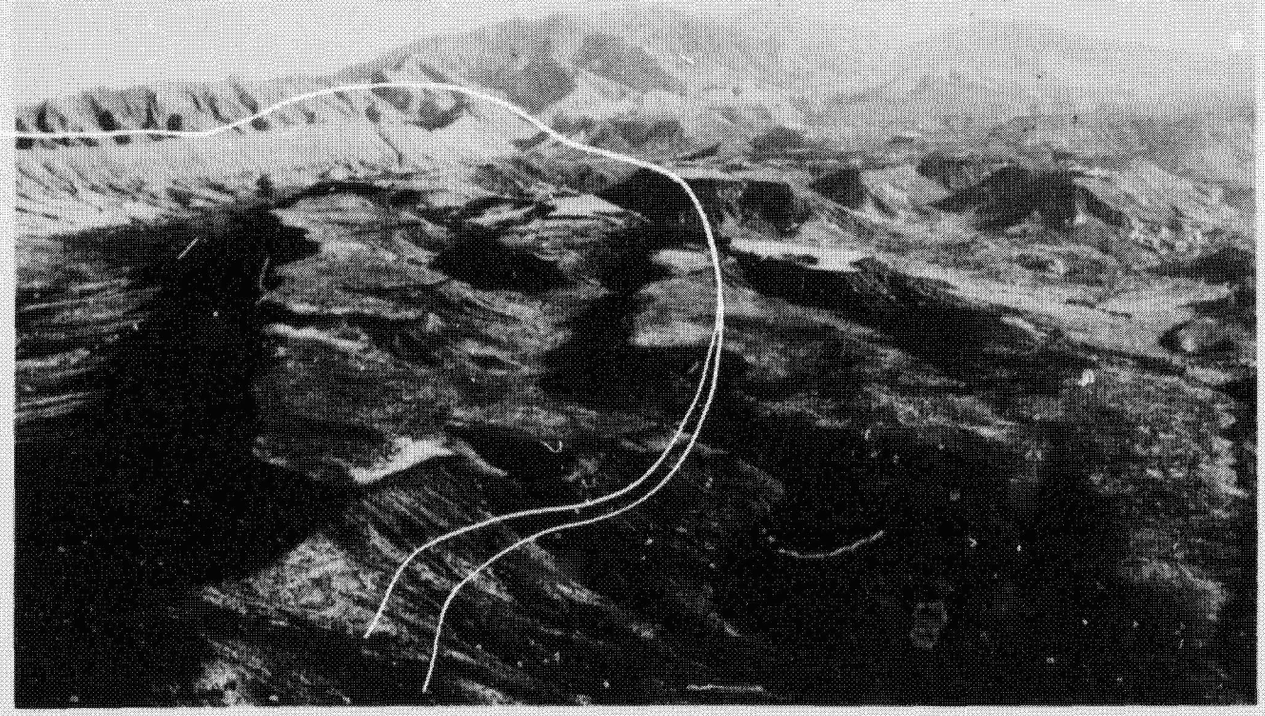

FIGURE 7.15 Aerial oblique view looking north at Grand Wash. The Virgin Mountains are located at the northernmost part of the photograph. The flat-topped mesas are capped by basalt flows that record a time when the base level in Grand Wash was much higher. The basalt flows provide a chronostratigraphic datum that can be used to calculate average rates of stream downcutting and make inferences about tectonic uplift.

history. Forecasting tectonic activity requires a long record, and therefore the tectonic geomorphology of landforms with long survival times will be an important ingredient in estimating tectonic hazards. Rates of geomorphic processes such as pedimentation or stream downcutting can act as a clock that starts ticking following the formation of a tectonic landform. Present limited knowledge of these rates suggests that during periods of active faulting in the Basin and Range province, fault-slip rates of about 0.1-1 m per 10,000 yr or greater are needed to generate high topographic escarpments, and these periods of active faulting may last on the order of a million years.

The Hurricane escarpment, in southern Utah, for example, was formed by an average fault-slip rate of 3 m per 10,000 yr. Landforms, such as scarps, produced by slip rates less than 1 m per 100,000 yr may be sufficiently obliterated by erosion to preclude the accumulation of relief across a mountain front. Relations between the recurrence interval of ground-rupturing earthquakes and mountain front development need closer study. Many of the methods described above can be easily used and rapidly applied, and, therefore, regional studies are both possible and desirable. The need for more data on geomorphic rates is a limiting factor on the interpretation of such analyses, and therefore Quaternary dating is a corequisite for continued research in the field of tectonic geomorphology.

## REFERENCES


Bateman, P. C., and C. Wahrhaftig (1966). Geology of the Sierra Nevada, in *Geology of Northern California*, California Division of Mines and Geology Bull. 190, pp. 107-172.

Bucknam, R. C., and R. E. Anderson (1979). Estimation of fault scarp ages from a scarp-height—slope angle relationship, *Geology 7*, 11-14.

Bull, W. B., and L. D. McFadden (1977). Tectonic geomorphology north and south of the Garlock Fault, California, in *Geomorphology in Arid Regions: Annual Binghamton Conference*, D. O. Doehring, ed., State University of New York at Binghamton, pp. 115-136.

Davis, W. M. (1899). The geographical cycle, *J. Geogr. 14*, 481.

Hamblin, W. K., P. E. Damon, and W. B. Bull (1981). Estimates of vertical crustal strain rates along the western margins of the Colorado Plateau, *Geology 9*, 293-298.

McKee, E. D., and E. H. McKee (1972). Pliocene uplift of the Grand Canyon region—a time of drainage adjustment, *Geol. Soc. Am. Bull. 83*, 1923-1932.

Rice, R. J. (1980). Rates of erosion in the Little Colorado valley, Arizona, in *Timescales in Geomorphology*, R. A. Cullingford *et al.*, eds., John Wiley, New York, pp. 317-331.

Wallace, R. E. (1977). Profiles and ages of young fault scarps in north-central Nevada, *Geol. Soc. Am. Bull. 88*, 107-172.

Wallace, R. E. (1978). Geometry and rates of change of fault-generated range-fronts, north-central Nevada, *J. Res. U.S. Geol. Surv. 6*, 637-650.

Young, A. (1972). *Slopes*, Oliver and Boyd, Edinburgh/London, 288 pp.

Young, R. A., and W. J. Brennen (1974). Peach Springs Tuff—its bearing on the structural evolution of the Colorado Plateau and development of Cenozoic drainage in Mohave county, Arizona, *Geol. Soc. Am. Bull. 85*, 83-90.

# 8 Investigation of Active Tectonics: Use of Surficial Earth Processes

EDWARD A. KELLER
*University of California, Santa Barbara*

ABSTRACT

Evaluation of landforms, soils, and deposits formed by active tectonics is providing basic data necessary for long-term earthquake prediction, seismic-hazard evaluation, and probabilistic seismic-risk assessment.

Investigation of active tectonics based on geomorphic techniques varies from regional reconnaissance work to detailed, site-specific, process-response study. Geomorphic indices and landform assemblages are useful in regional evaluation to identify relative tectonic activity and sites where rates of active-tectonic processes may be evaluated. Process-response studies involve coupling of geologic and geomorphic processes with responses of the landscape. Such an approach involves study of faulted Holocene (less than 10,000-yr-old) deposits; faulted landforms such as offset streams, alluvial fans, marine terraces, river terraces, and glacial moraines; and change in fault-scarp morphology with time.

Rates of active-tectonic processes may be calculated from geomorphic evaluation, provided deformation of a specific landscape feature is measured and chronology of the deformed feature is established. It is usually easier to identify and measure deformation of features than establish chronology, and even if rates of tectonic deformation can be established, evaluation of their significance may be difficult because they often vary in time and space owing to geologic constraints. For examples, slip rates may vary along different segments of the same fault owing to changes in tectonic framework, and rates of uplift of terraces or other landforms may change through time as a function of mechanics of deformation.

## INTRODUCTION

Understanding and long-term prediction of earthquakes associated with active tectonics has experienced remarkable progress in recent years through the study of near-surface processes (geomorphology). Studies of geologically young (less than 10,000-yr-old) and slightly older (less than 125,000-yr-old) landforms, soils, and deposits are providing basic data necessary for long-term earthquake prediction, seismic-hazard evaluation, and probabilistic seismic-risk assessment. A large number of faults capable of producing damaging earthquakes have been identified and evaluated to determine rates of movement and potential earthquake hazard. For a few faults, including the San Andreas Fault north of Los Angeles, California, and the Wasatch Fault near Salt Lake City, Utah, recurrence intervals of recent (prehistoric) earthquakes have been determined (Allen, 1983).

Information concerning rates of movement along

faults, potential earthquake hazard, and recurrence of large earthquakes obtained from quantitative field studies in geomorphology is extremely useful in long-term (tens to hundreds of years) land-use planning, a goal of which is earthquake-hazard reduction. Specifically, studies of active faults are providing critical information necessary for residential and commercial zoning near active faults; establishing building codes; and planning for large dams, nuclear power plants, liquified natural gas facilities, and other critical facilities.

Geomorphic evaluation of active tectonics has taken two approaches depending on whether reconnaissance information or detailed evaluation is desired. Reconnaissance work to identify areas where active tectonics is particularly significant generally involves the use of geomorphic indices (sensitive to rock resistance, climatic change, or tectonic processes) or assemblages of landforms produced or modified by active-tectonic processes. Detailed, site-specific study of active tectonics often involves evaluation of process-response models that attempt to explore relations between landforms, earth materials, geomorphic processes, and active tectonics integrated through time. The concept of time or chronology is introduced here because without establishment of a reliable chronology, process-response models will not yield rates of faulting and recurrence intervals of damaging earthquakes that are necessary in evaluating seismic risk. Much of the remainder of this paper will emphasize these points: use of geomorphic indices in reconnaissance studies of active tectonism; landform assemblages as indicators of active tectonism; and use of process-response models in establishing relations between landforms, earth materials, geomorphic processes, and tectonic processes for devising rates of active tectonics. Figure 8.1 summarizes the two main approaches to studying geomorphologic indicators of active tectonics and use to society.

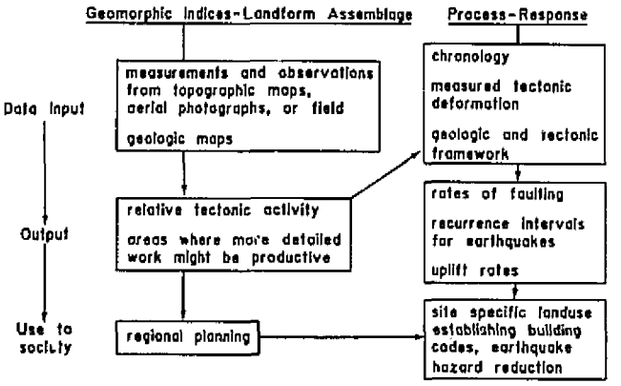


FIGURE 8.1 Active tectonics and geomorphology: data input, output, and use to society.

## GEOMORPHIC INDICES AND ACTIVE TECTONICS

Geomorphic indices are useful tools in evaluating active tectonics because they quickly provide insight concerning specific areas or sites in a region that is adjusting to relatively rapid rates of active-tectonic deformation. Indices that have been most successful are related to erosional and depositional processes associated with fluvial (river) systems. The best known of these are the stream-gradient index (*SL* index) developed by Hack (1973), the mountain-front sinuosity ($S_{mf}$ index) developed by Bull (1977a, 1978), and the ratio of valley-floor width to valley height ($V_f$ index) also developed by Bull (1977a, 1978).

### *Stream-Gradient Index*

The stream-gradient index (Hack, 1973), later applied to the San Gabriel Mountains in southern California by Keller (1977), is defined as

$$SL = (\Delta H/\Delta L)L, \qquad (8.1)$$

where $SL$ is the stream-gradient index, $\Delta H/\Delta L$ is the local gradient of the stream reach where the index is computed ($\Delta H$ is the drop in elevation of the reach and $\Delta L$ is the length of the reach), and $L$ is the total channel length from the drainage divide to the center of the reach, measured along the channel.

The $SL$ index is crudely related to the available stream power, defined as the product of water discharge and water-surface slope, and thus reflects the ability of the stream to transport its load. The index is a surrogate for stream power because the upstream channel length is proportional to bankfull discharge and the slope of the water surface is approximated by the slope of the channel bed.

The stream-gradient index is particularly sensitive to changes in slope and thus is a valuable tool in evaluating active tectonics with a strong vertical component of deformation. However, the index is also sensitive to rock resistance (resistant rock produces a steep channel slope), and differentiating between effects of tectonics and rock resistance may be difficult. That is, values of the index are high in areas where the rocks are particularly resistant or where active tectonics has resulted in vertical deformation at the Earth's surface. Therefore, anomalously high $SL$ indices in rocks of low or uniform resistance is a possible indicator of active tectonics. Figure 8.2 shows stream-gradient indices for the San Ga-

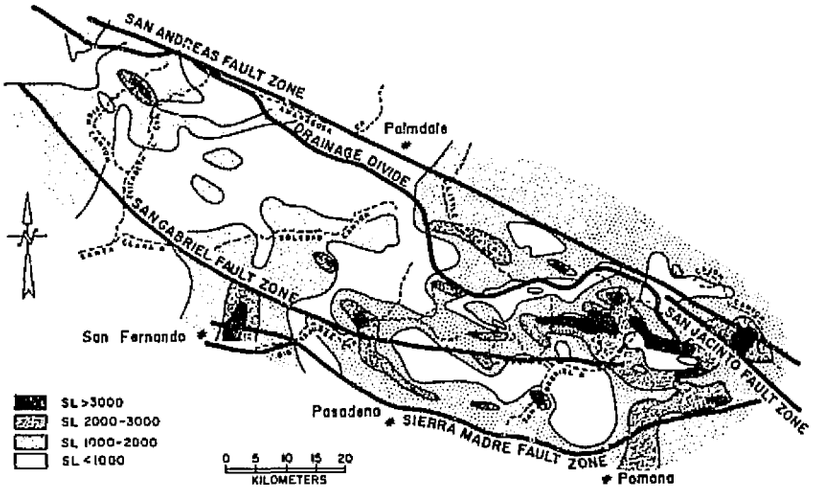


FIGURE 8.2 Stream gradient (*SL*) indices for the San Gabriel Mountains, California. See text for explanation.

briel Mountains in southern California. Areas of anomalously high indices are located along the southern and eastern fronts of the range. Although it was previously known that rates of uplift were relatively high in these areas, the indices verified this and also delineated an area of unusually high indices near the location of the 1971 San Fernando earthquake. Thus a regional evaluation of the San Gabriel Mountains suggests that detailed studies along the southern and eastern fronts of the range as well as near San Fernando have the best chance of yielding rates of vertical tectonics (uplift), slip rates along active faults, and recurrence intervals of damaging earthquakes. Areas where stream-gradient indices are relatively low are associated with two general conditions: areas where soft sedimentary rocks are abundant and along major strike-slip faults (the San Andreas and San Gabriel Faults) where horizontal movement has crushed the rocks producing zones low in resistance to erosion.

The *SL* index over a region can be computed from small-scale topographic maps. The index could also be computed from analyses of elevational data stored in computer systems. Therefore, in theory, large regions may be evaluated quickly, although interpretation of the index will remain crude because it may be difficult to separate effects of rock resistance from active tectonics. Nevertheless, the *SL* index is a valuable reconnaissance tool useful in isolating smaller areas for detailed work.

*Mountain-Front Sinuosity*

Mountain-front sinuosity ($S_{mf}$) is defined as

$$S_{mf} = L_{mf}/L_s, \tag{8.2}$$

where $L_{mf}$ is the length of mountain front along the mountain-piedmont (foot of mountain) junction and $L_s$ is the straight-line length of the front. The $S_{mf}$ index reflects a balance between the tendency of streams and slope processes to produce an irregular (sinuous) mountain front and vertical active tectonics that tends to produce a prominent straight front (Bull and McFadden, 1977). Thus, mountain fronts associated with active uplift are relatively straight, but if the rate of uplift is reduced or ceases, erosional processes will begin to form a sinuous front that becomes more irregular with time.

Mountain-front sinuosity was used by Bull and McFadden (1977) to evaluate the marked contrast in tectonic activity north and south of the Garlock Fault in California. North of the fault the values of $S_{mf}$ are low, suggesting active tectonics, whereas south of the fault the $S_{mf}$ values suggest relative tectonic stability.

Rockwell and Keller (in press) used mountain-front sinuosity in the Ventura Basin, southern California, where $S_{mf}$ values vary from about 1 to 3. Low sinuosity (1.01 to 1.14), characteristic of tectonically active fronts, can be maintained in the Ventura area if a threshold rate of uplift greater than 0.4 mm/yr is maintained.

Mountain-front sinuosity, like the stream-gradient

index, is a valuable reconnaissance tool when evaluating effects of active vertical tectonics. The $S_{mf}$ index is particularly attractive because it can be quickly and easily measured from aerial photographs, satellite or other high-altitude imagery, or topographic maps.

### *Ratio of Valley-Floor Width to Valley Height*

The ratio of the width of valley floor to valley height $V_f$ may be expressed by

$$V_f = 2V_{fw}/[(E_{ld} - E_{sc}) + (E_{rd} - E_{sc})], \quad (8.3)$$

where $V_{fw}$ is the width of valley floor, $E_{ld}$ and $E_{rd}$ are the respective elevations of the left and right valley divides, and $E_{sc}$ is the elevation of the valley floor (Bull and McFadden, 1977). In determining $V_f$, the data are measured at a given distance up from the mountain front. The index reflects differences between broad-floored canyons with relatively high values of $V_f$ and V-shaped canyons with relatively low values. Comparison of $V_f$ values measured from valleys emerging from different mountain fronts or different parts of the same front provides an indication of whether the streams are actively downcutting (forming V-shaped valleys with low $V_f$) in response to active tectonics or are being eroded laterally (forming broad valleys with high $V_f$) in response to relative stability of the front.

The $V_f$ index was tested by Bull and McFadden (1977) for mountain fronts north and south of the Garlock Fault. They found that values of the index varied from 0.05 to 4.7, with the lower values being derived from valleys north of the fault where mountain fronts are tectonically active. The index was also tested by Rockwell and Keller (in press) for mountain fronts near Ventura, California, where $V_f$ ratios show similar trends to that established by Bull and McFadden—being lower for relatively active fronts than for fronts with lesser rates of uplift.

## TECTONIC GEOMORPHOLOGY AND LANDFORM ASSEMBLAGE

A genetic classification of landforms is possible because different geomorphic processes tend to produce a characteristic assemblage of landforms. For example, the discussion of geomorphic indices suggested that active vertical tectonics tends to produce straight mountain fronts with V-shaped canyons and streams with relatively steep gradients for a particular rock type. On a more local scale, as for example along a specific mountain front or fault zone, active tectonics often modifies or produces characteristic landform assemblages. For example, alluvial fans have a variable morphology somewhat dependent on tectonic processes, and active strike-slip faulting produces a specific set of tectonic landforms. A tacit assumption in the evaluation of landform assemblages produced by active tectonics is that the more pristine or fresh appearing the landforms are, the younger the tectonics is assumed to be. Discussion of alluvial-fan morphology and tectonic activity as well as the assemblage of landforms associated with strike-slip faulting will illustrate the above concepts.

### *Alluvial Fans*

An alluvial fan is the end point of an erosional-depositional system in which sediment eroded from a mountain source is transported to the mountain front. There it is deposited as a cone or fan-shaped body of fluvial and/or debris-flow deposits (Bull, 1977b). The stream is the connecting link between the erosional and depositional parts of the system (Bull, 1977b) and therefore has a significant influence on the morphology of the alluvial fan. Radial profiles for most fans are composed of several segments, which together are gently concave. Breaks in slope mark boundaries between segments, and younger segments may be identified from older ones based on relative soil profile development, weathering of alluvial clasts, dissection of the surface by small streams, and development of desert varnish [see Bull (1964, 1977b) for a more detailed discussion of segmented alluvial fans].

Alluvial-fan morphology is an indicator of active tectonics because the fan form reflects varying rates of tectonic processes such as uplift of the source mountain along a range-bounding fault or tilting of the fan surface. When the rate of uplift of the mountain front is high relative to rate of stream-channel downcutting in the mountain and to fan deposition, then fanhead deposition tends to occur, and the youngest fan segment is near the apex of the fan. If the rate of uplift of the mountain front is less than or equal to the rate of downcutting of the stream in the mountain, then fanhead trenching occurs and deposition is shifted downfan. Younger fan segments will then be found well away from the mountain front (Figure 8.3 shows these two conditions). Change in sediment or water yield may also cause fanhead trenching, but this tends to be temporary if mountain-front uplift persists (Bull, 1964).

The above model of segmented alluvial fans relative to active tectonics has been successfully tested for alluvial fans in Death Valley, California (Hooke, 1972). Hooke found that eastward tilting and normal faulting produced segmented alluvial fans. On the east side of

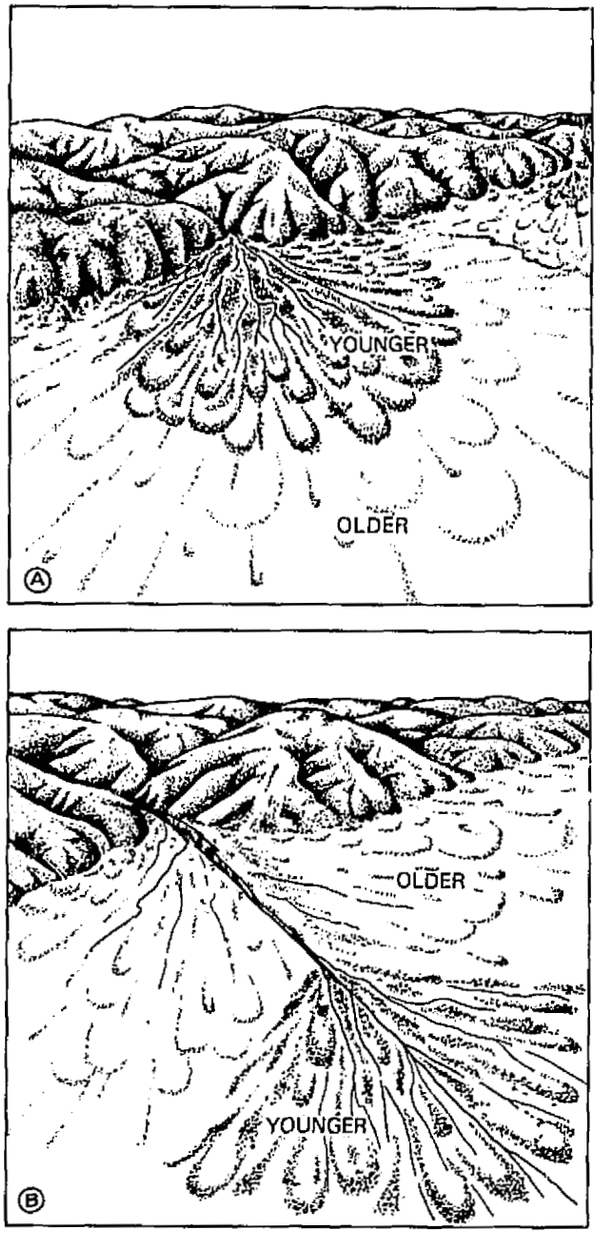


FIGURE 8.3 Alluvial fan morphology: (A) deposition adjacent to mountain front and (B) deposition shifted downfan as a result of fanhead entrenchment. See text for further explanation. From Bull (1977b).

the valley alluvial fans are relatively small and steep, and active normal faulting produces a straight mountain front with young fan segments being deposited on fanhead areas. On the west side of the valley alluvial fans are larger, not so steep, and not so influenced by mountain-front uplift. Lesser uplift and eastward tilting of the fans has shifted to the locus of fan deposition downfan; fanhead trenching occurs, and the younger fan segments are located well away from the fan apex. A similar tendency was noticed for alluvial fans in the Ventura, California, area that are being tilted basinward by active tectonics (Rockwell and Keller, in press). As with the geomorphic indices, the study of alluvial fans provides reconnaissance information concerning relative rates of active tectonics.

### *Landform Assemblage: Strike-Slip Faulting*

Active strike-slip faulting produces a characteristic assemblage of landforms including linear valleys, offset or deflected streams, shutter ridges, sags, pressure ridges, benches, scarps, and small horst and grabens known as microtopography (see Figure 8.4, opposite page). Figure 8.5 shows fault-related landforms associated with an offset alluvial fan located along the San Andreas Fault in the Indio Hills of southern California. The fan is offset about 700 m, and making an assumption concerning the age of the fan from soils (Keller *et al.*, 1982a) the slip rate for this part of the San Andreas Fault is at least 1 cm/yr and probably closer to 3 cm/yr. Small streams at the upper part of the fan are offset several meters, suggesting that tectonic creep or moderate to large earthquakes have occurred in the past few thousand years. There have been no large earthquakes along the southern part of the fault in historical time (several hundred years), but the geomorphology in the fault

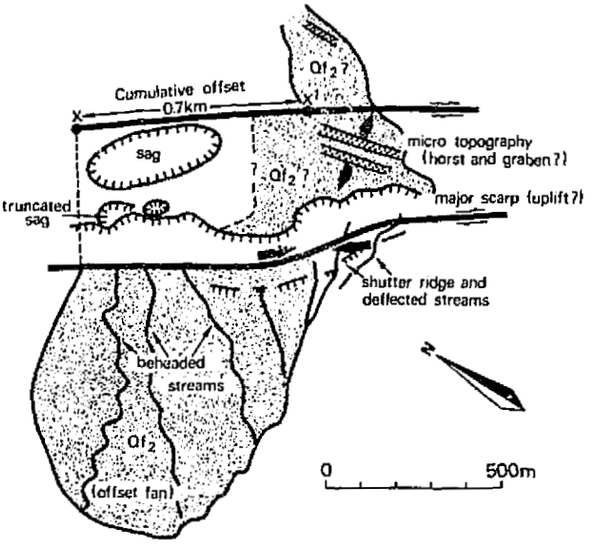


FIGURE 8.5 Sketch map of offset alluvial fan along the San Andreas Fault in the Indio Hills, California. Modified from Keller *et al.* (1982a).

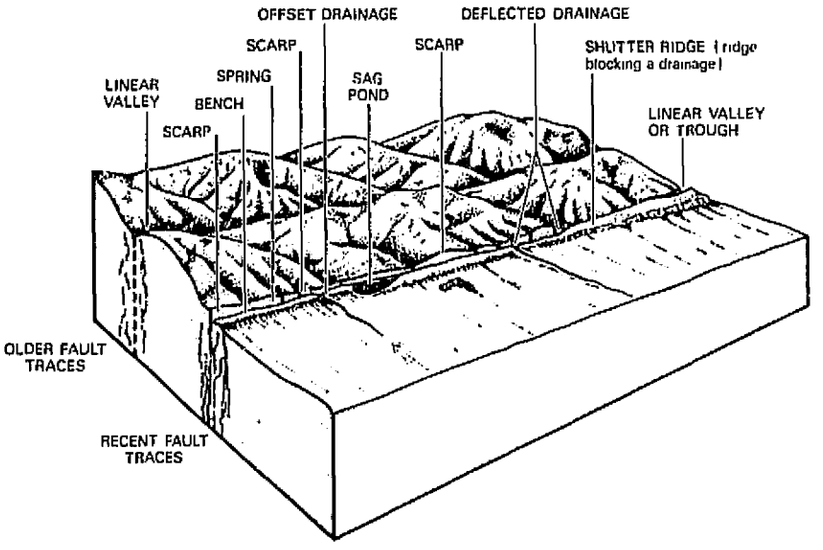


FIGURE 8.4 Assemblage of landforms associated with active strike-slip faulting. Modified from Wesson *et al.* (1975).

zone suggests that earthquakes are likely to be generated there in the future.

Active strike-slip faulting in the offshore southern California continental borderland also has distinctive geomorphic expression characterized by linear troughs, sags, tectonic benches, fault scarps, and offset or deflected channels associated with submarine fans. A recent study of the San Clemente Fault zone (Legg and Luyendyk, 1982), utilizing topographic data from Seabeam surveys, demonstrated that the data base and resolution is now sufficient to begin studying submarine-tectonic geomorphology to improve mapping of active faults and to evaluate long-term earthquake hazard. Figure 8.6 shows topography and tectonic landforms associated with the San Clemente Fault zone (M. R. Legg, University of California, San Diego, personal communication, 1983).

Many of the topographic features associated with active strike-slip faulting such as sags, pressure ridges, and fault scarps can be explained by simple shear that produces contraction and extension as illustrated on Figure 8.7 (Wilcox *et al.*, 1973; Sylvester and Smith, 1976). Others are better explained by extension or contraction associated with releasing or constraining bends or steps of fault traces as illustrated on Figure 8.8 (Crowell, 1974; Dibblee, 1977).

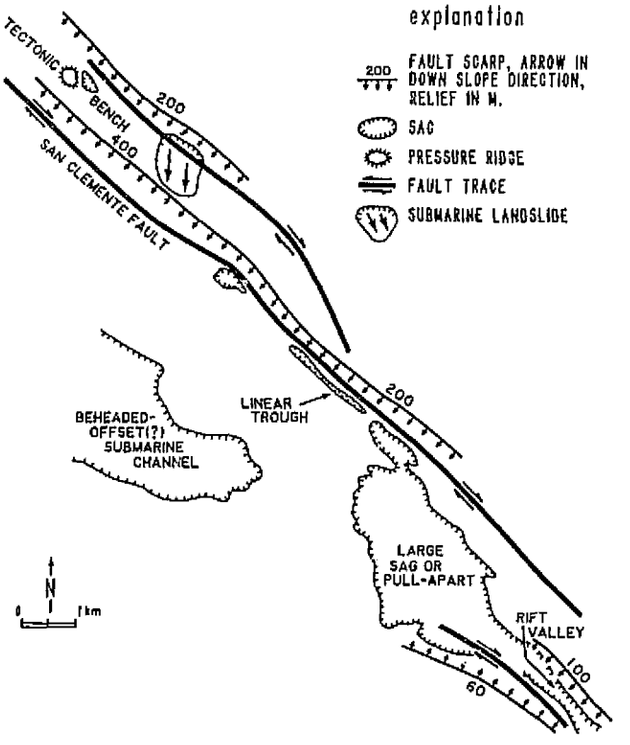


FIGURE 8.6 Sketch map of part of the San Clemente Fault zone. Data are from Seabeam survey. Courtesy of Mark R. Legg, University of California, San Diego.

## PROCESS-RESPONSE MODELS: RATES OF ACTIVE TECTONICS

Process-response models in active tectonics are broadly defined to include the investigation of earth ma-

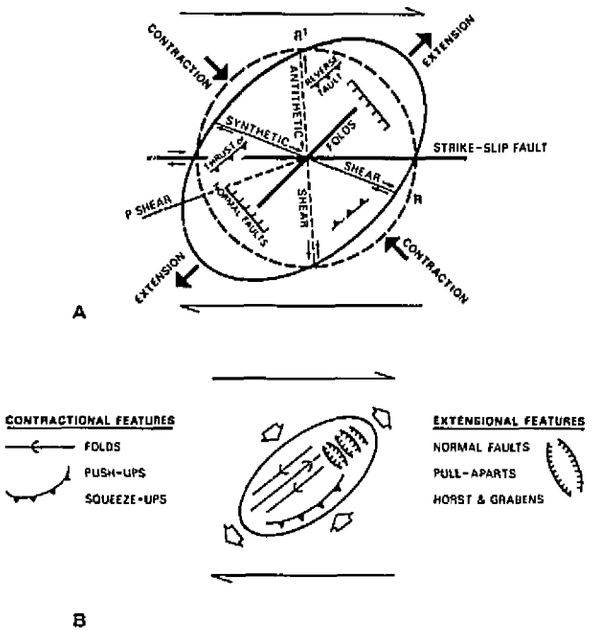


FIGURE 8.7 Simple shear associated with strike-slip faulting produces preferred orientation of fractures, faults and folds (A) as well as extensional and contractional landforms (B). Figure modified from Wilcox *et al.* (1973), Sylvester and Smith (1976), and Keller *et al.* (1982a).

terials, landforms, and late Pleistocene-Holocene chronology, the purpose of which is to derive rates of active tectonics (slip rates on faults, rates of uplift or subsidence, and recurrence intervals of damaging earthquakes). Such investigations have been very successful in recent years and are providing basic data necessary for long-term (tens to hundreds of years) earthquake prediction. Examples include (1) paleoseismic construction (occurrence and recurrence intervals of prehistoric earthquakes) obtained from studying faulted Holocene-alluvial sequences of stream, marsh, lake, or landslide deposits (Clark *et al.*, 1972; Sieh, 1978; Davis, 1981; Rust, 1982); (2) paleoseismic construction based on fault-scarp morphology change with time (Wallace, 1977; Bucknam and Anderson, 1979; Nash, Chapter 11, this volume); and (3) rates of uplift, slip rates on active faults, and/or recurrence intervals of assumed earthquakes based on chronology and offset of landforms such as alluvial fans (Keller *et al.*, 1982a), marine terraces (Matsuda *et al.*, 1978; Lajoie *et al.*, 1979, 1982; Keller *et al.*, 1982b), offset streams (Sharp, 1981; Sieh, 1981), and glacial deposits (Schubert, 1982).

### *Fault-Scarp Morphology*

Slope morphology of scarps produced by faulting is a successful geomorphic indicator of active tectonics. Figure 8.9 shows generalized slope elements associated with a fault scarp. All the elements shown need not be present for a particular scarp, and because slopes are dynamic changing landforms, the dominance of one element relative to others changes with time. Table 8.1 and Figure 8.10 summarize form-process relationships for fault-scarp morphology change with time as discussed by Wallace (1977) for the Great Basin area in Nevada. Wallace was able to develop the chronology shown on Figure 8.10 and Table 8.1 by studying fault scarps that truncate $^{14}C$-dated shorelines of Pleistocene Lake Lahontan, are associated with volcanic ash of known age, were produced by known earthquakes, or can be dated by tree rings (dendrochronology).

Recurrent displacement along the same fault line produces a composite fault scarp. Wallace (1977) stated that multiple displacements on a compound fault scarp

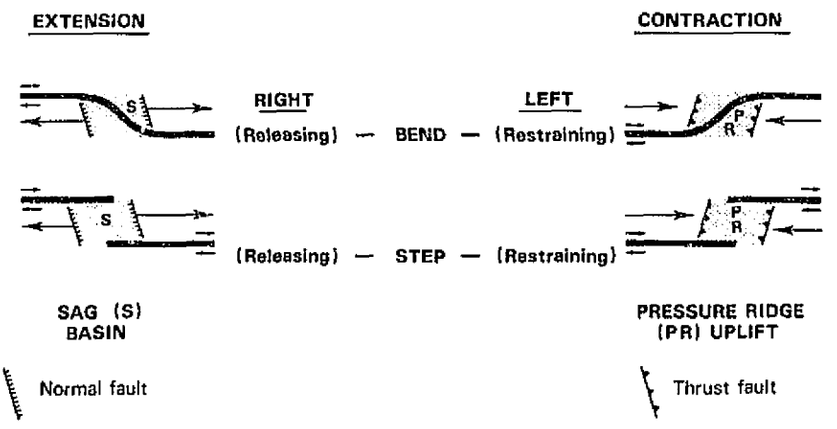


FIGURE 8.8 Pressure ridges and sags associated with restraining and releasing bends and/or steps along strike-slip faults. Modified after Crowell (1974) and Dibblee (1977).

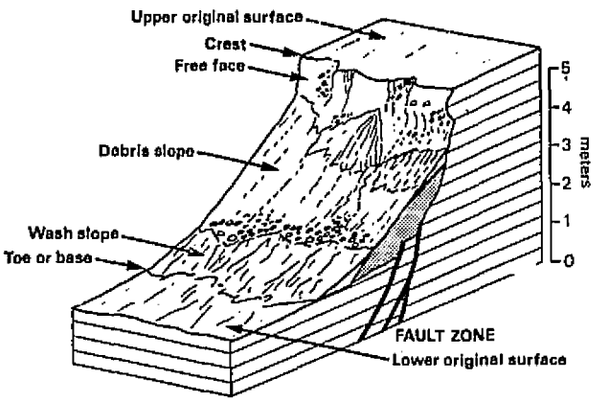


FIGURE 8.9 Basic slope elements that may be present on a fault scarp. After Wallace (1977).

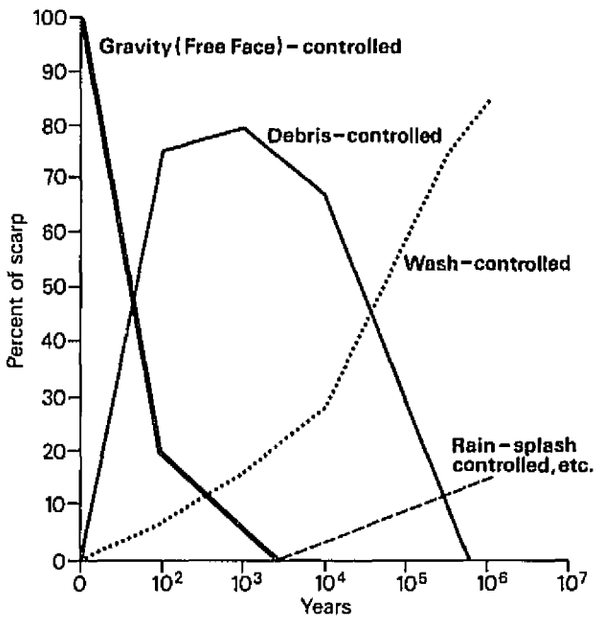


FIGURE 8.10 Change in slope elements (fault-scarp morphology) with time for fault-scarp degradation in the Great Basin area of Nevada. After Wallace (1977).

can be recognized by sharp breaks in slope on the scarp, benches or terraces associated with small channels that have eroded through the fault scarp, knickpoints (short vertical or steep sections) in channels that cross the scarp, scarp height that exceeds that likely produced by a single event, and progressive displacement (older material has been displaced more than younger material).

Change in fault-scarp morphology with time is being treated quantitatively. Bucknam and Anderson (1979) developed relations between scarp height and scarp-slope angle for fault scarps in Utah with estimated ages ranging from 1000 to 100,000 yr (Figure 8.11). Their studies verify Wallace's (1977) conclusion that with

TABLE 8.1 Fault Scarp-Slope Morphology[a]

| Slope Element | Morphology | Process (Formation and/or Modification | Comments and General Chronology |
|---|---|---|---|
| Crest | Top of fault scarp (break in slope); initially sharp, becomes rounded with time | Produced by faulting; modified by weathering, mass wasting | Becomes rounded after free face disappears; usually rounded after about 10,000 yr |
| Free Face | Straight segment; initially 45° to overhanging | Produced by faulting; modified by weathering, gullying, mass wasting; eventually buried from below by accumulation of debris | Dominant element for 100 year or so; disappears after about 1000–2000 yr |
| Debris Slope | Straight segment; at angle of repose of material usually 30° to 38° | Accumulation of material that has fallen down from the free face | Is dominant element after about 100 yr, remains dominant until about 100,000 yr, disappears at about 1,000,000 yr |
| Wash Slope | Straight to gently concave segment; overlaps the debris slope; slope angle generally 3° to 15° | Fluvial erosion and deposition; deposition of wedge or fan of alluvium near toe of the slope; some gullying | Is developed by 100 yr, significant by 1000 yr, and dominant by 100,000 yr |
| Toe | Base of fault scarp (break) in slope) slope; may be initially sharp, but with time may become indeterminate as grades into original slope | Fluvial erosion and deposition; owing to change in process/form from upslope element (free face, debris slope, or wash slope) to original surface below the fault-scarp slope | More prominent in young fault scarps or where wash slope is not present; on scarps older than about 12,000 yr, the basal slope break is sharper than the crestal slope break |

[a]After Wallace (1977) for fault scarps in the Great Basin.

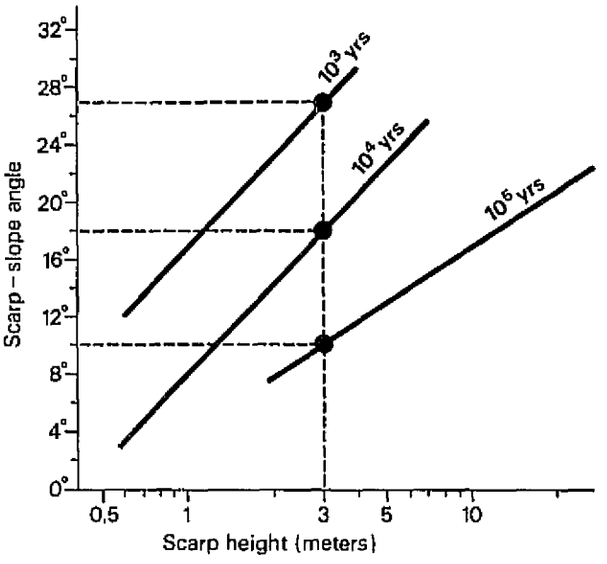


FIGURE 8.11 Relationship between fault-scarp height and scarp-slope angle from scarps ranging in age from $10^3$ and $10^5$ yr. After Bucknam and Anderson (1979).

time the angle of a scarp degrades to a lower-slope angle. For example, for a 3-m-high scarp (shown on Figure 8.11), as the scarp-slope angle decreases from 28° to 10° the scarp age increases from 1000 to 100,000 yr. In theory, once fault-scarp degradation curves, such as those on Figure 8.11, are derived for an area, the investigator can assign estimated ages to fault scarps of known height and slope angle and estimate the earthquake hazard and history. However, care must be taken in making paleoseismic statements because (1) the initial scarp from a single event may vary with materials composing the scarp and local change in pattern of fault displacement, e.g., multiple, composite-overlapping rupture versus single rupture scarps (A. J. Crone, U.S. Geological Survey, personal communication); and (2) temporal and spatial variations in climate may produce a variable fault-scarp morphology.

### *Faulted Holocene Deposits*

Erosional and depositional processes produce stream, marsh, lake, and landslide deposits that, when faulted, may produce valuable information concerning slip rates, rates of uplift or subsidence, and paleoseismicity. Two examples from the San Andreas Fault system in southern California are the Coyote Creek Fault—part of the San Jacinto Fault zone (a major branch of the San Andreas Fault)—and the San Andreas Fault at Pallett Creek (Sieh, 1978).

Holocene paleoseismicity on the Coyote Creek Fault was determined by evaluating progressive vertical displacement of lake deposits. Clark *et al.* (1972) and Sharp (1981) estimated that the recurrence interval for earthquakes similar to the April 9, 1968, Borrego Mountain earthquake ($M$ = 6.7) varies from 50 to several hundred years. The slip rate for the fault is also variable, being 1 to 5 mm/yr for Holocene (less than 10,000 yr) offsets and as high as 8 to 12 mm/yr for a mid-Pleistocene (about 700,000 yr) offset.

Geomorphic investigation of the San Andreas Fault north of Los Angeles has helped answer an important question for understanding the earthquake hazard—how often do large earthquakes occur? Data from Pallett Creek, 55 km northeast of Los Angeles (Sieh, 1978) and two other sites up to 125 km northwest of Pallett Creek (Davis, 1981; Rust, 1982) suggest that three large prehistoric earthquakes since the sixteenth century may be correlated over a long (125 km) segment of the fault. Sieh (1978) believed that evidence from faulted peat deposits at Pallett Creek (dated by $^{14}C$) suggest that there may have been 12 large earthquakes in the past 1700 yr. One of these was historical (1857) and 11 were prehistoric, suggesting an average recurrence interval of 145 yr. However, the length of time between such events may vary from as short as 50 yr to as long as 250 yr (Sieh, 1978). Using the most recent five events, which are well dated and established, the average recurrence interval is about 200 yr (K. E. Sieh, California Institute of Technology, personal communication, 1984). Paleoseismic construction of this segment of the San Andreas Fault, known as the "Big Bend," is providing data useful in long-term earthquake prediction.

### *Faulted Landforms*

Evaluation of faulted landforms (especially those with multiple displacements) including stream channels, river terraces, marine terraces, and glacial moraines is helping answer fundamental questions concerning active tectonics. Some of these questions are: (1) Are rates of faulting constant through time? (2) Which faults produce the greatest earthquake hazard? (3) Are historical rates of faulting, based on first-order leveling, verified in the recent geologic record? (4) What is the potential for seismic shaking or ground rupture at a particular site? (5) What is the likely displacement per event and recurrence interval of earthquakes for specific active faults?

Study of a series of marine terraces (Matsuda *et al.*, 1978) south of Tokyo, Japan—believed to have been produced by a series of sudden uplifts during large earthquakes—suggest that there have been four great

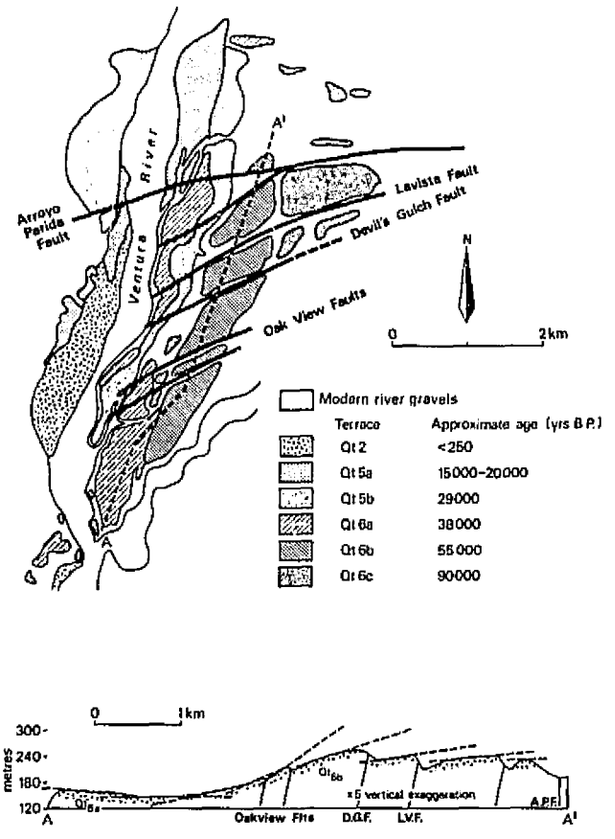


FIGURE 8.12 Faulted terraces of the Ventura River near Oak View, California.

(*M* greater than 8) earthquakes in the last 6000 yr with an average recurrence interval of 1500 yr. The investigators also located an area where they believe a large earthquake is likely in the relatively near future. They base their long-term prediction on the fact that the area near the expected epicenter may be a seismic gap, identified by a local uplift rate that is less than the regional average during the last several thousand years.

Investigation of faulted terraces in New Zealand, Japan, and the United States are yielding estimates of slip rates and recurrence intervals of potential earthquakes. A flight of seven terraces of the Waiohine River, New Zealand, have been progressively offset during the late Pleistocene and Holocene along the Wairarapa Fault (Lensen and Vella, 1971). Making assumptions concerning the chronology the investigators concluded that the horizontal slip rate for the fault is 3.4 to 6 mm/yr, and assuming a 3-m horizontal displacement per earthquake event, a recurrence interval of 500 to 900 yr is obtained. A similar study of a flight of nine terraces of the Kiso River, Japan—progressively displaced (left-lateral) by the Alter Fault—is presented by Yoshikawa *et al.* (1981). A $^{14}C$ date of about 27,000 yr for a terrace with measured horizontal and vertical displacement of 140 and 28 m, respectively, provides a slip rate of about 5 and 1 mm/yr, respectively. Assuming a 8-m displacement per event (based on an $M$ = 8.4 earthquake in 1891 on a similar fault 60 km to the east) yields a recurrence interval of 1600 yr for a similar event on the Alter Fault. As a final example of river terraces, investigation of several late Pleistocene-Holocene terraces of the Ventura River near Oak View, California (Keller *et al.*, 1982b), displaced by flexural-slip faulting (Figure 8.12), yields slip rates that vary from about 0.3 to 1.1 mm/yr. The important aspect of the study was the recognition that the faults produce a ground-rupture hazard rather than seismic-shaking hazard (Yeats *et al.*, 1981; Yeats, Chapter 4, this volume). Assuming a slip event of 25 cm (similar to a flexural-slip event near Lompoc, California, in 1981 that produced a 570-m rupture surface and an $M$ = 2.5 earthquake (Yerkes *et al.*, 1981), the recurrence interval would vary from 250 to 750 yr.

Offset stream channels and glacial moraines are also yielding slip rates for active faults. Sieh (1981) and Sieh and Jahns (1984) estimated from offset stream channels of Wallace Creek along the south-central part of the San Andreas Fault (Figure 8.13) that the slip rate during the latest Pleistocene and Holocene has been about 30 to 40 mm/yr. Finally, Schubert (1982) reported an estimated range of slip rate (3 to 14 mm/yr) for the right-lateral Bocono Fault in western Venezuela. His estimate was based on several measured offsets (60 to 260 m) of

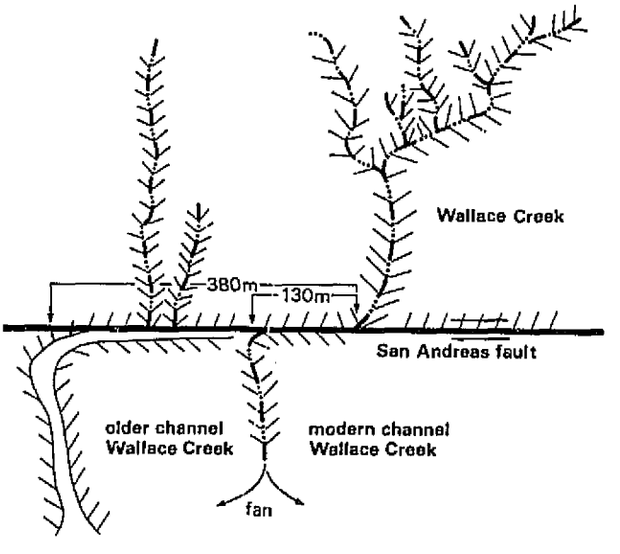


FIGURE 8.13 Channel offset along the San Andreas Fault. See text for explanation. After Sieh (1981).

TABLE 8.2 Uplift and Tilting of Bedrock and River Terraces over the Ventura Avenue Anticline

| Geomorphic Surface | | | Present Height above Ventura River (m)[c] | Potential Range Uplift Rate to Present (mm/yr)[d] | Minimum Possible Uplift Rate to Present (mm/yr)[e] |
|---|---|---|---|---|---|
| Designation | Age (yr)[a] | Sea Level (m)[b] | | | |
| Q5a | 15,800 ± 210 | −110 | 30.5 ± 10 | 5.5 ± 4.2 | 1.9 ± 0.7 |
| Q5a-b | 20,040 ± 590 | − 90 | 85.3 ± 10 | 6.6 ± 2.9 | 4.3 ± 0.5 |
| Q5b | 29,700 ± 1250 | − 41 | 120 ± 10 | 4.8 ± 1.2 | 4.1 ± 0.5 |
| Q6a | 38,000 ± 1500 | − 38 | 175 ± 10 | 5.1 ± 1.0 | 4.7 ± 0.4 |
| Q6c | 80,000 or 105,000 | − 13 | 625 ± 100 | 7.1 ± 2.1 | 7.1 ± 2.0 |
| Bedrock | 200,000 | Present | 2720 ± 200 | 13.6 ± 1.0 (minimum) | 13.6 ± 1.0 |

[a]Based on $^{14}C$ and amino acid racemization chronology (Lajoie *et al.*, 1982).
[b]After Lajoie *et al.* (1979).
[c]Projected to the axis of the anticline.
[d]Assumes complete range of possible adjustment of Ventura River to lower sea level.
[e]Assumes no adjustment of Ventura River to lower sea level.

lateral moraines with an estimated age of 18,000 yr based on palynological, sedimentological, and $^{14}C$ methods.

## RATES, DATES, AND TECTONIC FRAMEWORK: SELECTED OBSERVATIONS RELATIVE TO SOCIETAL NEEDS

Tectonic geomorphology, defined as the application of geomorphic principles to tectonic problems, is significant to society when rates and dates of tectonic events provide the data framework useful in long-term earthquake prediction and land-use planning to reduce the earthquake hazard. Important considerations in developing rates of active tectonics based on geomorphic evaluation are measurement of deformation associated with past tectonic events (such as offset streams, glacial moraines, alluvial deposits, or other features), development of the late Pleistocene to Holocene chronology to derive rates (defined as the ratio of measured deformation to the appropriate time interval), and interpretation of rates of active tectonics that often vary significantly owing to geologic constraints.

The most reliable rates of past tectonic events are derived from well-constrained, measured deformation and chronology. However, it is often easier to measure deformation than to establish the necessary chronology. Methods of establishing chronology are discussed by Pierce (Chapter 13, this volume).

The use of soil geomorphology in establishing late Pleistocene-Holocene chronology is emerging as a powerful tool in deriving rates of active tectonic deformation (see, e.g., Keller *et al.*, 1982a,b; Dembroff, 1982; Rockwell, 1983; Rockwell *et al.*, 1984). The basic idea is to produce a soil chronosequence, defined as a series of soils arranged from youngest to oldest for an area. Relative chronology is based on physical and chemical properties of the soils, and absolute chronology is provided by $^{14}C$ dates and other methods discussed by Pierce (Chapter 13, this volume). Once the chronosequence is established, it may be applied over a large area independent of further absolute dates at sites where deformation is measured; that advantage is the real power of the soil chronosequence.

Rates of active-tectonic deformation must be carefully interpreted because they may vary in time and space owing to geologic constraints such as style of faulting and mechanics of folding. For example, slip rates of flexural-slip faulting near Oak View, California, vary from about 0.3 to 1.1 mm/yr as a function of fault location in a syncline and/or mechanics of folding (Keller *et al.*, 1982b; Rockwell, 1983; and Rockwell *et al.*, 1984), and rate of uplift associated with folding of the Ventura Avenue anticline has decreased from over 10 mm/yr in mid-Pleistocene time to about 5 mm/yr during the late Pleistocene and Holocene (Table 8.2), as a function of mechanics of folding (Keller *et al.* 1982b; Dembroff, 1982; Rockwell, 1983). Thus, there is not necessarily a direct relationship between rate of fault displacement or uplift and earthquake hazard. Understanding the tectonic framework and geologic constraints is necessary to make such a determination.

## ACKNOWLEDGMENTS

Reviews of the manuscript and suggestions for improvement by W. B. Bull and J. G. Dennis are appreciated.

## REFERENCES

Allen, C. R. (1983). Earthquake prediction—past and future, *Geology 11*, 682.
Bucknam, R. C., and R. E. Anderson (1979). Estimation of fault-scarp

ages from a scarp-height-slope-angle relationship, *Geology* 7, 11-14.

Bull, W. B. (1964). Geomorphology of segmented alluvial fans in western Fresno County, California, *U.S. Geol. Surv. Prof. Paper* 352-*E*, pp. 89-129.

Bull, W. B. (1977a). Tectonic geomorphology of the Mojave Desert, U.S. Geol. Surv. Contract Rep. 14-08-001-G-394, Office of Earthquakes, Volcanoes, and Engineering, Menlo Park, Calif., 188 pp.

Bull, W. B. (1977b). The alluvial fan environment, *Prog. Phys. Geogr. 1*, 222-270.

Bull, W. B. (1978). Geomorphic tectonic activity classes of the south front of the San Gabriel Mountains, California, U.S. Geol. Surv. Contract Rep. 14-08-001-G-394, Office of Earthquakes, Volcanoes, and Engineering, Menlo Park, Calif., 59 pp.

Bull, W. B., and L. D. McFadden (1977). Tectonic geomorphology north and south of the Garlock Fault, California, in *Geomorphology in Arid Regions*, D. O. Doehring, ed., Publications in Geomorphology, State University of New York at Binghamton, pp. 115-138.

Clark, M. C., A. Gantz, and M. Rubin (1972). Holocene activity of the Coyote Creek Fault as recorded in sediments of Lake Cahuilla, *U.S. Geol. Surv. Prof. Paper 787*, pp. 112-130.

Crowell, J. C. (1974). Origin of late Cenozoic basins in southern California, in *Tectonics and Sedimentation*, W. Dickinson, ed., Spec. Publ. 22, Soc. Econ. Paleontol. Mineral., pp. 190-204.

Davis, T. (1981). Late Holocene seismic record, western Big Bend of San Andreas Fault, *Geol. Soc. Am. Abstr. Programs 13*, 51.

Dembroff, G. R. (1982). Tectonic Geomorphology and Soil Chronology of the Ventura Avenue Anticline, Ventura, California, unpublished M.S. thesis, Univ. Calif., Santa Barbara, 122 pp.

Dibblee, T. W., Jr. (1977). Strike-slip tectonics of the San Andreas Fault and its role in Cenozoic basin evolvement, in *Late Mesozoic and Cenozoic Sedimentation and Tectonics in California*, San Joaquin Geol. Soc. Short Course, pp. 26-38.

Hack, J. T. (1973). Stream-profile analysis and stream-gradient index, *U.S. Geol. Surv. J. Res. 1*, 421-429.

Hooke, R. L. (1972). Geomorphic evidence for late-Wisconsin and Holocene tectonic deformation, Death Valley, California, *Geol. Soc. Am. Bull. 83*, 2073-2098.

Keller, E. A. (1977). Adjustment of drainage to bedrock in regions of contrasting tectonic framework, *Geol. Soc. Am. Abstr. Programs 9*, 1046.

Keller, E. A., M. S. Bonkowski, R. J. Korsch, and R. J. Shlemon (1982a). Tectonic geomorphology of the San Andreas Fault zone in the southern Indio Hills, Coachella Valley, California, *Geol. Soc. Am. Bull. 93*, 46-56.

Keller, E. A., T. K. Rockwell, M. N. Clark, G. R. Dembroff, and D. L. Johnson (1982b). Tectonic geomorphology of the Ventura, Ojai and Santa Paula areas, western Transverse Ranges, California, in *Neotectonics in Southern California*, J. D. Cooper, ed., Guidebook for 78 Annual Meeting of the Cordilleran Section of the Geol. Soc. Am., pp. 25-42.

Lajoie, K. R., J. P. Kern, J. F. Wehmiller, G. L. Kennedy, S. A. Mathieson, A. M. Sarna-Wojcicki, R. F. Yerkes, and P. F. McCrory (1979). Quaternary marine shorelines and crustal deformation, San Diego to Santa Barbara, California, in *Geological Excursions in the California Area*, P. L. Abbott, ed., San Diego State University, pp. 3-15.

Lajoie, K. R., A. M. Sarna-Wojcicki, and R. F. Yerkes (1982). Quaternary chronology and rates of crustal deformation in the Ventura area, California, in *Neotectonics in Southern California*, J. D. Cooper, compiler, Cordilleran Section, Geol. Soc. Am. field trip guidebook, pp. 43-51.

Legg, M. R., and B. P. Luyendyk (1982). Seabeam survey of an active strike-slip fault in the southern California continental borderland, *EOS 63*, 1107.

Lensen, G. J., and P. Vella (1971). The Waiohine River faulted terrace sequence: Recent crustal movements, *R. Soc. N.Z. Bull. 9*, 117-119.

Matsuda, T., Y. Ota, M. Ando, and N. Yonekura (1978). Fault mechanism and recurrence time of major earthquakes in southern Kanto district, Japan, as deduced from coastal terrace data, *Geol. Soc. Am. Bull. 89*, 1610-1618.

Rockwell, T. K. (1983). Soil Chronology, Geology and Neotectonics of the North Central Ventura Basin, California, unpublished Ph.D. Dissertation, Univ. Calif., Santa Barbara, 424 pp.

Rockwell, T. K., and E. A. Keller (in press). Tectonic geomorphology of alluvial fans and mountain fronts near Ventura, California, in *Proceedings of the 15th Annual Geomorphology Symposium*, M. Morisawa, ed., State University of New York at Binghamton.

Rockwell, T. K., E. A. Keller, M. N. Clark, and D. L. Johnson (1984). Chronology and rates of faulting of Ventura River terraces, California, *Geol. Soc. Am. Bull. 95*, 1466-1474.

Rust, D. J. (1982). Radiocarbon dates for the most recent large prehistoric earthquake and for late Holocene slip rates: San Andreas Fault in part of the Transverse Ranges north of Los Angeles, *Geol. Soc. Am. Abstr. Programs 14*, 229.

Schubert, C. (1982). Neotectonics of Bocono Fault, western Venezuela, *Tectonophysics 85*, 205-220.

Sharp, R. V. (1981). Variable rates of late Quaternary strike slip on the San Jacinto Fault zone, southern California, *J. Geophys. Res. 86*, 1754-1762.

Sieh, K. E. (1978). Prehistoric large earthquakes produced by slip on the San Andreas Fault at Pallett Creek, California, *J. Geophys. Res. 83*, 3907-3938.

Sieh, K. E. (1981). A review of geological evidence for recurrence times of large earthquakes, in *Earthquake Prediction—An International Review*, Am. Geophys. Union, Washington, D.C., pp. 181-207.

Sieh, K. E., and R. H. Jahns (1984). Holocene activity of the San Andreas Fault at Wallace Creek, California, *Geol. Soc. Am. Bull. 95*, 883-896.

Sylvester, A. G., and R. R. Smith (1976). Tectonic transpression and basement-controlled deformation in San Andreas Fault zone, Salton Trough, California, *Am. Assoc. Petrol. Geol. Bull. 60*, 2081-2102.

Wallace, R. E. (1977). Profiles and ages of young fault scarps, north-central Nevada, *Geol. Soc. Am. Bull. 88*, 1267-1281.

Wesson, R. L., E. J. Helley, K. R. Lajoie, and C. M. Wentworth (1975). Faults and future earthquakes, in *Studies for Seismic Zonation of the San Francisco Bay Region*, R. D. Borchardt, ed., *U.S. Geol. Surv. Prof. Paper 941A*, pp. 5-30.

Wilcox, R. E., T. P. Harding, and D. R. Seely (1973). Basic wrench tectonics, *Am. Assoc. Petrol. Geol. Bull. 57*, 74-96.

Yeats, R. S., M. N. Clark, E. A. Keller, and T. K. Rockwell (1981). Active fault hazard in southern California, ground rupture versus seismic shaking, *Geol. Soc. Am. Bull. 92*, 189-196.

Yerkes, R. F., M. G. Bonilla, W. L. Ellsworth, A. G. Lindh, and J. C. Tinsley (1981). Reverse faulting and crustal unloading near Lompoc, northwest Transverse Ranges, California, *Geol. Soc. Am. Abstr. Programs 13*, 586.

Yoshikawa, T., S. Kaizuka, and Y. Ota (1981). *The Landforms of Japan*, University of Tokyo Press, Tokyo, Japan, pp. 39-72.

# Seismological and Paleoseismological Techniques of Research in Active Tectonics

9

CLARENCE R. ALLEN
*California Institute of Technology*

ABSTRACT

Classical seismological techniques such as earthquake hypocentral locations and focal-mechanism studies continue to play an important role in the understanding of active-tectonic processes, but newer techniques such as seismic tomography and the determination of earthquake source parameters are being increasingly utilized. The most spectacular recent progress, however, seems to have been in the area of paleoseismicity and slip-rate studies, where documentation of the ages and displacements of various young geologic features has had great impact on both the understanding of contemporary tectonic processes and on seismic-hazard evaluation. Critical future research needs in seismological and paleoseismological areas include (1) improved local seismic networks, (2) implementation of new worldwide networks utilizing broadband digital recording, (3) increased numbers of strong-motion seismometers in earthquake-prone areas, (4) better understanding of soil development and deformation, (5) improved techniques for absolute age dating of alluvial materials, (6) increased understanding of the rates and nature of modification of surficial neotectonic features such as fault scarps, and (7) continued vigorous field studies of active tectonic processes associated with contemporary large earthquakes.

The study of contemporary and recent earthquakes represents perhaps the major contribution to the understanding of tectonic processes active in the world today. This is not to belittle studies of active folding and warping or of active volcanism, but significant tectonic changes occur so rapidly, dramatically, and over such wide areas during large earthquakes that they seem to represent the most rewarding laboratory for the study of active-tectonic processes. And large earthquakes are of relatively frequent occurrence on a worldwide basis, so that abundant research opportunities exist.

Many of the classical seismological techniques have been—and continue to be—so fundamental to studies of active tectonics that they hardly need discussion. Among these are (1) hypocentral locations of earthquakes, (2) earthquake focal mechanisms, (3) statistical studies of earthquake occurrences, and (4) studies of crustal structure. Indeed, many of the most important ideas of active plate-tectonic processes, such as the transform-fault and subduction-zone concepts, have stemmed directly from studies of earthquake locations and focal mechanisms (e.g., Isacks *et al.*, 1968). Detailed studies of aftershock patterns of major earth-

California Institute of Technology, Division of Geological and Planetary Sciences Contribution No. 4077.

quakes have been critical in developing an understanding the fracture process, and dense seismographic coverage has allowed locations of microearthquakes, sometimes to within a few meters, which in turn permits portrayal of minute details of fault geometry—a geometry that generally turns out to be far more complex than we had ever imagined (e.g., Jamison and Hill, 1982; Reasenberg and Ellsworth, 1983).

But certainly many of the exciting new tectonic implications are coming from those types of relatively new seismological techniques that shed light on the nature and mechanics of the fracture process. An example is the now-widespread use of seismic moment and moment magnitude (e.g., Hanks and Kanamori, 1979), which have a direct tie-in to physical parameters at the earthquake source, such as stress drop, amount of slip, and area of the broken fault surface. The use of such concepts is now widespread in regional syntheses of active-tectonic processes (e.g., Wesnousky *et al.*, 1982; Molnar and Deng, 1984). Still more recent is the introduction of tomographic techniques to seismology (e.g., Anderson and Dziewonski, 1984), in which vast amounts of seismic data are synthesized to reveal heretofore unknown details of three-dimensional crustal structure, which may be very relevant to ongoing tectonic processes (e.g., Humphreys *et al.*, 1984). Increased use of such techniques, together with new broadband and digitally recording seismic instruments (e.g., Alexander, 1983) and dramatically improved data-analysis techniques, is literally revolutionizing the field of seismology. And strong-motion seismology, traditionally visualized as being within the exclusive area of earthquake engineering, is having a rebirth as an interdisciplinary field with surprisingly wide impact in our efforts to understand active tectonic processes close to the center of an earthquake—in the so-called "near field" (e.g., Hanks and McGuire, 1981; Aki, 1982; Hartzell and Helmberger, 1982).

One of the most significant results of recent seismological and geologic studies of contemporary earthquakes is the determination that they are far more different from one to another in their mechanical parameters than we had ever thought. Although this is not particularly good news to those scientists attempting to find methods to predict earthquakes, it surely means that we are gaining a far better understanding of the varied and complex nature of contemporary tectonic processes. We now recognize, for example, that earthquake rupture and associated deformation take place at widely varying rates and that the rupture process, particularly during large earthquakes, is by no means smoothly continuous (e.g., Aki, 1979; Hartzell and Heaton, 1983).

In the author's opinion, however, the most spectacular progress in studies of active-tectonic processes in the past few years has not been in seismology, but instead in the area of paleoseismology, where, in essence, a new research field has been born. Paleoseismology is the study of prehistoric earthquakes based on interpretation of the geologic record that these earthquakes have left behind (e.g., Wallace, 1981). Critical in developing this field have been (1) the recognition that "fossil earthquakes" do indeed leave telltale signs in the geologic column and (2) improved techniques for the absolute age dating of the affected rocks. Thus, it is not now uncommon to identify the specific dates of major earthquakes along a fault over the past few thousands of years, permitting a far better quantitative understanding of the local earthquake hazard than has ever been possible before, albeit on a probabilistic basis (e.g., Tanna Fault Trenching Research Group, 1983; Sieh, 1984).

Along with developments in paleoseismology, major advances in our understanding of slip rates on faults have also occurred. Although both fields involve the establishment of time intervals during which tectonic events have taken place, it is important to recognize the distinction: paleoseismology involves the establishment of dates of individual earthquakes or earthquake sequences, whereas slip-rate studies establish only average rates of deformation. Further assumptions in both are necessary to estimate seismic hazard (e.g., Wesnousky *et al.*, 1984; Youngs and Coppersmith, 1985). Both are important in the understanding of active-tectonic processes.

Slip-rate determination on faults are usually made by observing the offset of features of relatively recent and known ages. Thus the slip rate of the San Andreas Fault of California has been determined by observing the offsets of numerous geologic features such as Holocene stream channels (e.g., Wallace, 1968; Sieh and Jahns, 1984). Offsets of late Pleistocene glacial moraines have permitted the assignment of slip rates to the Bocono Fault of Venezuela (Schubert, 1982), the Tuco Fault of Peru (Yonekura *et al.*, 1979), and the Fairweather Fault of Alaska (Plafker *et al.*, 1978). Offset and deformed river terrace deposits have been used extensively along the Alpine Fault system of New Zealand (e.g., Lensen and Vella, 1971; Adams, 1980), the Median Tectonic Line of Japan (e.g., Okada, 1980), and faults of the Transverse Ranges in California (e.g., Rockwell *et al.*, 1984). Other youthful geologic features that are often offset and can sometimes be dated include soils (e.g., Machette, 1978; Borchardt *et al.*, 1980; Schlemon, 1985), young volcanic rocks (e.g., Roquemore, 1980), offset beach deposits (e.g., Carver, 1970), and offset

landslide deposits (e.g., Sieh, 1978a). Rates of erosional degradation of fault scarps have been used to put limits on slip rates (e.g., Wallace, 1977; Bucknam and Anderson, 1979), and theoretical studies of this phenomenon appear particularly promising (e.g., Nash, 1980; Colman and Watson, 1983; Hanks *et al.*, 1984). Estimated rates of river entrenchment associated with regional uplift have also been used to put limits on slip rates on individual faults within the uplifted area (e.g., Allen *et al.*, 1984). Other examples of slip-rate determinations and recurrence intervals between major earthquakes have been summarized by Sieh (1981).

As opposed to slip-rate determinations, paleoseismological techniques must utilize geologic features associated with *individual* past earthquakes, which is a task that usually constitutes a greater challenge to the geologist. Furthermore, good exposures are almost always critical, which typically implies excavating trenches across the fault under investigation. Among the features that have been used to identify individual paleo-earthquakes from exposures on trench walls are the following:

1. Identification of a fault that can be shown to break older strata but which is, in turn, erosionally truncated and buried by unbroken younger strata that had not yet been deposited at the time of the earthquake (Figure 9.1a), thus bracketing the time interval within which the earthquake must have occurred (e.g., Clark, *et al.*, 1972; Sieh, 1978b).

2. Identification of buried sand-blow deposits or injected sand dikes resulting from soil liquefaction during heavy shaking (Figure 9.1b), usually close to or along the causative fault (e.g., Sieh, 1978b). Such deposits appear to be the only remaining near-surface evidence of the two great historical earthquakes in the eastern United States—the 1811-1812 events near New Madrid, Missouri (Russ, 1979) and the 1886 earthquake at Charleston, South Carolina (Talwani and Cox, 1985). These localities are particularly important to understand, inasmuch as similar deposits elsewhere may be the only surficial geologic clue to eastern U.S. paleoseismicity—and therefore to regional seismic hazard evaluation.

3. Closely related to liquefaction is the phenomenon of intense "rumpling" of newly deposited water-laid sediments (Figure 9.1c), associated with heavy localized shaking, which has also been used as an indication of paleoseismicity (e.g., Sims, 1975; Reches and Hoexter, 1981).

4. Identification of a fault scarp that was subsequently buried by younger unbroken deposits (Figure 9.1d)(e.g., Sieh, 1978b).

5. Closely related to 4, identification of a buried landslide feature or a colluvial apron derived from an eroding fault scarp (Figure 9.1e) (e.g., Swan *et al.*, 1980).

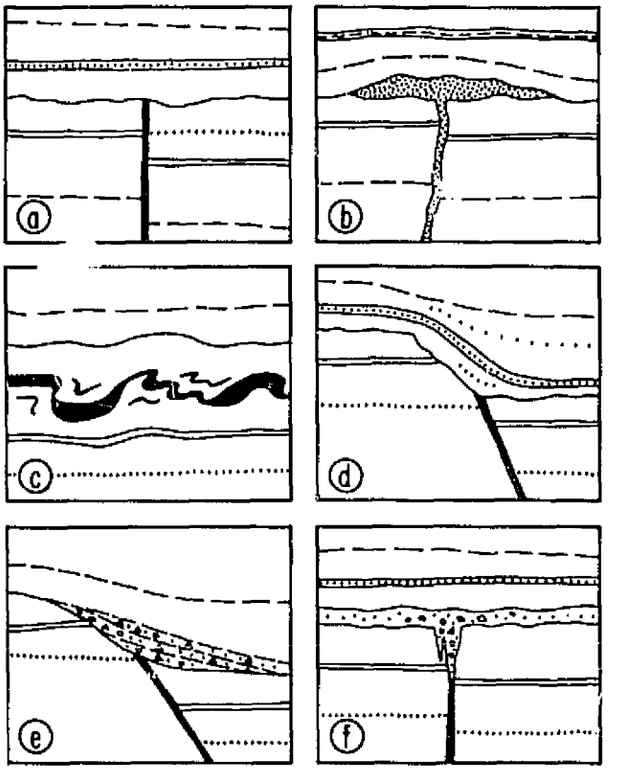


FIGURE 9.1 Sketch diagrams of cross sections of geologic relations that might result from individual paleo-earthquakes. See text for explanation.

6. Identification of a crevice associated with surficial fault movement that was later filled in by surficial materials (Figure 9.1f) (e.g., Allen *et al.*, 1984).

Although each of the above techniques applies ideally to a single paleo-earthquake, as illustrated by the examples in Figure 9.1, a number of repeated earthquakes are likely to be represented in a given exposure, so that the resulting geologic relationships can become exceedingly complex; relationships resulting from one earthquake are modified by subsequent earthquakes along the same fault. Trenches only 5 m deep across the San Andreas Fault in southern California, for example, reveal evidence of 12 individual great earthquakes on the fault within the past 2000 years (Sieh, 1978b, 1984). One might ask how exposures of fault offsets on vertical trench walls can display evidence of displacements along faults such as the San Andreas that have had predominantly horizontal displacements. It turns out that

even strike-slip faults usually have small components of vertical displacements, which tend faithfully to repeat themselves from earthquake to earthquake at a given locality (Allen, 1981). Thus vertical trench walls normally display consistent offsets of strata even along predominantly strike-slip faults. Evidence for the actual amount of strike-slip displacement during individual paleo-earthquakes can sometimes be obtained from horizontal excavations that reveal stream paleochannels or other offset linear features within the displaced strata (e.g., Sieh, 1984).

In all these paleoseismological techniques, optimal bracketing of the time of the earthquake requires dating of (1) the oldest unbroken postearthquake strata and (2) the youngest deformed pre-earthquake strata. Unfortunately, the probability is small of this being practical in any individual exposure. That is, the chances are slim of finding a locality where one of these unique geologic situations can be observed *and* where the adjacent rocks can be radiometrically or otherwise dated. Thus, it is not surprising that many, if not most, trenches excavated for paleoseismological studies have turned out to be inconclusive. But those that have been successful, such as along the San Andreas Fault of California (e.g., Sieh, 1984), the Wasatch Fault of Utah (e.g., Swan *et al.*, 1980), and the Tanna Fault of Japan (Tanna Fault Trenching Research Group, 1983) have had profound implications in terms of seismic-hazard evaluation and the understanding of active-tectonic processes. In commencing a paleoseismological investigation, therefore, one must be aware that the chances of immediate success are not high, and numerous trenches and considerable perseverance are usually called for. It should also be pointed out that many practical difficulties face one attempting to excavate trenches across faults, such as the problems of shallow groundwater, absence of visible stratigraphy, property ownership complications, legally mandated safety precautions, access for equipment, and cost.

In addition to geologic relations that might be observed in excavated trench walls, several other types of geologic relation can be related to individual paleo-earthquakes. Along a strike-slip fault, for example, if abandoned offset stream channels are spaced periodically with respect to their former headwaters (e.g., three abandoned channels laterally offset 10, 20, and 30 m from their former source across the fault) (Figure 9.2), one might conclude that each progressive offset was caused by an individual earthquake with 10 m of displacement, and dating of related alluvium or terrace deposits might permit age assignments to the individual earthquakes (e.g., Sieh and Jahns, 1984). Or in the case of raised marine wave-cut benches, arguments can often

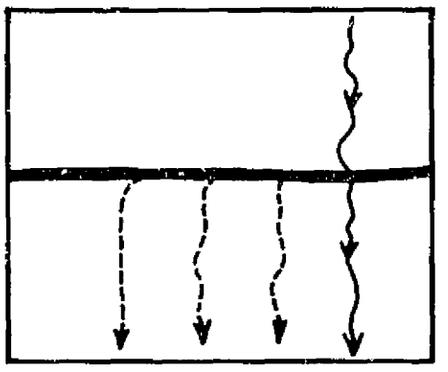

FIGURE 9.2 Sketch of map of offset stream channels that might result from repeated strike-slip displacements during individual paleo-earthquakes.

be made that individual benches are related to abrupt uplifts during individual earthquakes, such as has been well documented from the long historical records in Japan (e.g., Matsuda *et al.*, 1978) and has been important in quantifying seismic hazard in Alaska (e.g., Plafker and Rubin, 1978).

In most paleoseismological investigations, it is necessarily assumed that surficial fault displacement and/or heavy shaking has been limited to infrequent large earthquakes and that moderate-sized earthquakes or continuous fault slippage have not occurred during most of the time interval between the large events. The justification for this assumption lies in the increasing evidence that a given fault at a given locality is in fact typified by a "characteristic earthquake," so that earthquakes of comparable magnitudes tend to repeat one another faithfully and periodically (Schwartz and Coppersmith, 1984). Although relatively continuous fault slippage (or fault "creep") is common during aftershock sequences, continuous fault creep on a long-term basis has been identified only along limited parts of the San Andreas Fault in California (Schulz *et al.*, 1982; Louie *et al.*, 1985) and at one locality along the North Anatolian Fault of Turkey (Aytun, 1982). It does not appear to be as widespread a phenomenon as was postulated when continuous creep was first discovered on the San Andreas Fault only 25 years ago (Steinbrugge *et al.*, 1960), which is encouraging from the point of view of paleoseismological investigations.

What are our seismological and paleoseismological needs, if researches in these fields are to continue to move vigorously forward? In the area of seismology, a number of important needs can be pointed out.

1. Dense local seismographic networks, together with computerized data-analysis facilities, are absolutely essential if detailed studies of earthquake-related active tectonics are to be carried out in a given area. Ideally, the distance between seismometers should be roughly comparable to the average depth of earthquakes in the area if good hypocentral locations (including focal depth) are to be obtained.

2. Modern techniques of seismic analysis, particularly as related to the understanding of fault mechanics, are increasingly dependent on improved instrumentation, such as wideband, digitally recording seismometers. Particularly for the studies of worldwide large earthquakes, which represent our best "window" to contemporary tectonic processes, it is essential that support be obtained and continued for the proposed new Global Seismographic Network (NRC Committee on Seismology, 1983; Incorporated Research Institutes for Seismology, 1984), which will effectively replace the 23-year-old World Wide Standardized Seismographic Network, which has served its purpose well but is now clearly outmoded.

3. Every effort should be made to increase the number of strong-motion accelerographs in areas—anywhere in the world—where large earthquakes are most likely to occur (NRC Committee on Earthquake Enginering Research, 1982). Despite the many years of recording, engineers and seismologists have obtained very few records of the actual ground motion in the close vicinity of a truly great earthquake, and thus we are still deficient in our knowledge of active-tectonic processes in the "near field" of such an event.

In the area of paleoseismology, perhaps our greatest need is simply for more trenches across active faults where significant results might be obtained. But it is also critical that we improve our basic understanding in several of the following areas:

1. Soils are among the geologic features most often disturbed by faulting and earthquakes, but our knowledge of the ages of soils and their rates of development in different climatic environments leaves much to be desired. Furthermore, slow gravity-induced downhill movements of soils (soil "creep"), even on very gentle slopes, can sometimes cause numerous deformational features remarkably similar in appearance to those due to sudden earthquake movements; a better understanding of this phenomenon is important.

2. The most common problem in paleoseismological investigations is that of dating the strata involved, particularly those of an alluvial nature that still defy most of the traditional methods of absolute age dating. Carbon-14 dating, for example, requires the collection of organic materials that are typically rare in alluvial deposits. Improved geochemical techniques of dating young materials are critical, as well as the further development of other promising techniques such as those based on paleomagnetism.

3. Insofar as many prehistoric earthquakes have been associated with the formation of geomorphic features such as fault scarps that are still preserved on the landscape, an improved understanding of the erosional degradation of such features is important if we are to understand their ages of formation. Recent research work in quantitative geomorphology (e.g., Hanks *et al.*, 1984) has been encouraging in this regard and deserves continued vigorous support.

4. Detailed field studies of recent earthquakes, such as the 1980 Algerian disaster (e.g., Philip and Meghraoui, 1983), indicate that many types of surficial deformation other than primary fault scarps may occur in the epicentral area. These features, too, may become buried in the geologic section and be recognizable at a later date, so it is important to understand their origins and possible mechanisms of preservation. Only by studying contemporary earthquakes in the field in great detail will we learn to recognize what is important in identifying and interpreting "fossil" earthqua[illegible]

## REFERENCES


Adams, J. (1980). Paleoseismicity of the Alpine Fault seismic gap, New Zealand, *Geology 8*, 72-76.

Aki, K. (1979). Characterization of barriers on an earthquake fault, *J. Geophys. Res. 84*, 6140-6148.

Aki, K. (1982). Strong motion prediction using mathematical modeling techniques, *Bull. Seismol. Soc. Am. 72*, S29-S41.

Alexander, S. S. (1983). Developments in digital seismology, *Rev. Geophys. Space Phys. 21*, 1132-1142.

Allen, C. R. (1981). The modern San Andreas Fault, in *The Geotectonic Development of California*, W. G. Ernst, ed., Prentice-Hall, Englewood Cliffs, N.J., pp. 511-534.

Allen, C. R., A. R. Gillespie, Y. Han, K. E. Sieh, B. Zhang, and C. Zhu (1984). Red River and associated faults, Yunnan Province, China: Quaternary geology, slip rates, and seismic hazard, *Geol. Soc. Am. Bull. 95*, 686-700.

Anderson, D. L., and A. M. Dziewonski (1984). Seismic tomography, *Sci. Am. 251*, 60-68.

Aytun, A. (1982). Creep measurements in the Ismetpasa region of the North Anatolian Fault zone, in *Multidisciplinary Approach to Earthquake Prediction* 2, A. M. Isakara and A. Vogel, eds., Friedr. Vieweg & Sohn, Braunschweig/Wiesbaden, pp. 279-292.

Borchardt, G., S. Rice, and C. Taylor (1980). Paleosols overlying the Foothills Fault system near Auburn, California, *Calif. Div. Mines Geology Spec. Rep. 149*, 38 pp.

Bucknam, R. C., and R. E. Anderson (1979). Estimation of fault-scarp ages from a scarp-height-slope-angle relationship, *Geology 7*, 11-14.

Carver, G. A. (1970). *Quaternary Tectonism and Surface Faulting in*

*the Owens Lake Basin, California*, Univ. Nev., Mackay School of Mines, Tech. Rep. AT-2, Reno, 103 pp.

Clark, M. M., A. Grantz, and M. Rubin (1972). Holocene activity of the Coyote Creek Fault as recorded in the sediments of Lake Cahuilla, *U.S. Geol. Surv. Prof. Paper 787*, 112-130.

Colman, S. N., and K. Watson (1983). Ages estimated from a diffusion equation model for scarp degradation, *Science 221*, 263-265.

Hanks, T. C., and H. Kanamori (1979). A moment magnitude scale, *J. Geophys. Res. 84*, 2348-2350.

Hanks, T. C., and R. K. McGuire (1981). The character of high-frequency strong ground motion, *Bull. Seismol. Soc. Am. 71*, 2071-2095.

Hanks, T. C., R. C. Bucknam, K. R. Lajoie, and R. E. Wallace (1984). Modification of wave-cut and fault-controlled landforms, *J. Geophys. Res. 89*, 5771-5790.

Hartzell, S. H., and T. H. Heaton (1983). Inversion of strong ground motion and teleseismic waveform data for the fault rupture history of the 1979 Imperial Valley, California, earthquake, *Bull. Seismol. Soc. Am. 73*, 1553-1583.

Hartzell, S., and D. V. Helmberger (1982). Strong-motion modeling of the Imperial Valley earthquake of 1979, *Bull. Seismol. Soc. Am. 72*, 571-596.

Humphreys E., R. W. Clayton, and B. H. Hager (1984). A tomographic image of mantle structure beneath southern California, *Geophys. Res. Lett. 11*, 625-627.

Incorporated Research Institutions for Seismology (1984). *Science Plan for the New Global Seismographic Network*, Incorporated Research Institutions for Seismology, Washington, D.C., 130 pp.

Isacks, B., J. Oliver, and L. R. Sykes (1968). Seismology and the new global tectonics, *J. Geophys Res. 73*, 5855-5899.

Johnson, C. E., and D. P. Hill (1982). Seismicity of the Imperial Valley, *U.S. Geol. Surv. Prof. Paper 1254*, 15-24.

Lensen, G., and P. Vella (1971). The Waiohine River faulted terrace sequence, *R. Soc. N.Z. Bull. 9*, 117-119.

Louie, J., C. R. Allen, D. C. Johnson, P. C. Haase, and S. N. Cohn (1985). Fault slip in southern California, *Bull. Seismol. Soc. Am. 75*, 811-833.

Machette, M. N. (1978). Dating Quaternary faults in the southwestern United States by using buried calcic paleosols, *J. Res. U.S. Geol. Surv. 6*, 369-381.

Matsuda, T., Y. Ota, M. Ando, and N. Yonekura (1978). Fault mechanism and recurrence time of major earthquakes in the southern Kanto district, Japan, as deduced from coastal terrace data, *Geol. Soc. Am. Bull. 89*, 1610-1618.

Molnar, P., and Deng Q. (1984). Faulting associated with large earthquakes and the average rate of deformation in central and eastern Asia, *J. Geophys. Res. 89*, 6203-6227.

Nash, D. B. (1980). Morphological dating of degraded normal fault scarps, *J. Geol. 88*, 353-360.

NRC Committee on Earthquake Engineering Research (1982). *Earthquake Engineering Research—1982*, National Research Council, Washington, D.C., 266 pp.

NRC Committee on Seismology (1983). *Seismographic Networks: Problems and Outlook for the 1980s*, National Research Council, Washington, D.C., 61 pp.

Okada, A. (1980). Quaternary faulting along the Median Tectonic Line of southwest Japan, *Geol. Soc. Jpn. Mem. 18*, 79-108.

Philip, H., and M. Meghraoui (1983). Structural analysis and interpretation of the surface deformations of the El Asnam earthquake of October 10, 1980, *Tectonics 2*, 17-49.

Plafker, G., and M. Rubin (1978). Uplift history and earthquake recurrence as deduced from marine terraces on Middleton Island, Alaska, *U.S. Geol. Surv. Open-File Rep. 78-943*, 687-722.

Plafker, G., T. Hudson, T. Bruns, and M. Rubin (1978). Late Quaternary offsets along the Fairweather Fault and crustal plate interactions in southern Alaska, *Can. J. Earth Sci. 15*, 805-816.

Reasenberg, P., and W. L. Ellsworth (1982). Aftershocks of the Coyote Lake, California, earthquake of August 6, 1979: A detailed study, *J. Geophys. Res. 87*, 10637-10655.

Reches, A., and D. F. Hoexter (1981). Holocene seismic and tectonic activity in the Dead Sea area, *Tectonophysics 80*, 235-254.

Rockwell, T. K., E. A. Keller, M. N. Clark, and D. L. Johnson (1984). Chronology and rates of faulting of Ventura River terraces, California, *Geol. Soc. Am. Bull. 95*, 1466-1474.

Roquemore, G. (1980). Structure, tectonics, and stress field of the Coso Range, Inyo County, California, *J. Geophys. Res. 85*, 2434-2440.

Russ, D. P. (1979). Late Holocene faulting and earthquake recurrence in the Reelfoot Lake area, northwestern Tennessee, *Geol. Soc. Am. Bull. 90*, 1013-1018.

Schubert, C. (1982). Neotectonics of the Bocono Fault, western Venezuela, *Tectonophysics 85*, 205-220.

Schulz, S. S., J. M. Mavko, R. O. Burford, and W. D. Stuart (1982). Long-term fault creep observations in Central California, *J. Geophys. Res. 87*, 6977-6982.

Schlemon, R. J. (1985). Application of soil-stratigraphic techniques to engineering geology, *Assoc. Eng. Geol. Bull. 22*, 129-142.

Schwartz, D. P., and K. J. Coppersmith (1984). Fault behavior and characteristic earthquakes: Examples from the Wasatch and San Andreas Fault zones, *J. Geophys. Res. 89*, 5681-5698.

Sieh, K. E. (1978a). Slip along the San Andreas Fault associated with the great 1857 earthquake, *Bull. Seismol. Soc. Am. 68*, 1421-1448.

Sieh, K. E. (1978b). Prehistoric large earthquakes produced by slip on the San Andreas Fault at Pallett Creek, California, *J. Geophys. Res. 83*, 3907-3939.

Sieh, K. E. (1981). A review of geological evidence for recurrence times of large earthquakes, in *Earthquake Prediction: An International Review*, D. W. Simpson and T. G. Richards, ed., Maurice Ewing Ser. 4, American Geophysical Union, Washington, D.C., pp. 181-207.

Sieh, K. E. (1984). Lateral offsets and revised dates of large prehistoric earthquakes at Pallett Creek, southern California, *J. Geophys. Res. 89*, 7641-7670.

Sieh, K. E., and R. H. Jahns (1984). Holocene activity of the San Andreas Fault at Wallace Creek, California, *Geol. Soc. Am. Bull. 95*, 883-896.

Sims, J. D. (1975). Determining earthquake recurrence intervals from deformational structures in young lacustrine sediments, *Tectonophysics 29*, 141-152.

Steinbrugge, K. V., E. G. Zacher, D. Tocher, C. A. Whitten, and C. N. Claire (1960). Creep along the San Andreas Fault, *Bull. Seismol. Soc. Am. 50*, 389-415.

Swan, F. H., III, D. P. Schwartz, and L. S. Cluff (1980). Recurrence of moderate to large earthquakes produced by surface faulting on the Wasatch Fault zone, *Bull. Seismol. Soc. Am. 70*, 1431-1462.

Talwani, P., and J. Cox (1985). Paleoseismic evidence for recurrence of earthquakes near Charleston, South Carolina, *Science 229*, 379-381.

Tanna Fault Trenching Research Group (1983). Trenching study for Tanna Fault, Izu, at Myoga, Shizuoka Prefecture, Japan, *Earthquake Res. Inst. Bull. 58*, 797-830.

Wallace, R. E. (1968). Notes on stream channels offset by the San Andreas Fault, southern Coast Ranges, California, *Stanford Univ. Publ. Geol. Sci. 11*, 6-21.

Wallace, R. E. (1977). Profiles and ages of young fault scarps, north-central Nevada, *Geol. Soc. Am. Bull. 88*, 1267-1281.

Wallace, R. E. (1981) Active faults, paleoseismology, and earthquake hazards in the western United States, in *Earthquake Prediction: An International Review*, D. W. Simpson and T. G. Richards, ed., Maurice Ewing Ser. 4, American Geophysical Union, Washington, D.C., pp. 209-216.

Wesnousky, S. G., C. H. Scholz, and K. Shimazaki (1982). Deformation of an island arc: Rates of moment release and crustal shortening in intraplate Japan determined from seismicity and Quaternary fault data, *J. Geophys. Res. 87*, 6829-6852.

Wesnousky, S. G., C. H. Scholz, K. Shimazaki, and T. Matsuda (1984). Integration of geological and seismological data for the analysis of seismic hazard: A case study of Japan, *Bull. Seismol. Soc. Am. 74*, 687-708.

Yonekura, N., T. Matsuda, N. Nogami, and S. Kaizuka (1979). An active fault along the western front of the Cordillera Blanca, Peru, *J. Geogr. (Tokyo) 88*, 1-19.

Youngs, R. R., and K. J. Coppersmith (1985). Implications of fault slip rates and earthquake recurrence models to probabilistic hazard estimates, *Bull. Seismol. Soc. Am. 75*, 939-964.

# Geodetic Measurement of Active-Tectonic Processes

10

WAYNE THATCHER
*U.S. Geological Survey*

ABSTRACT

Repeated geodetic measurements are sufficiently precise to detect the growth of mountains, the relative movements of the great lithospheric plates, and present-day rates of fault slip and earthquake strain accumulation. The cyclic buildup and release of strain across major faults can be monitored over the short term (years or less) using precise modern techniques, and longer-term movements can frequently be determined by utilizing the historical record of measurements, which in many active regions extend back into the late nineteenth century. Since about 1970, annual laser-ranging surveys in the western United States and Alaska have delineated the pattern and current rates of deformation in these seismically active regions and have begun to provide accurate fault-slip rates to compare with late Holocene geologic estimates. The imperfect balance between interseismic strain buildup and coseismic strain release introduces a component of permanent deformation into the earthquake cycle that under favorable conditions can be estimated geodetically, providing another link between present-day movements and those preserved in the recent geologic record. Examples include tectonically elevated former shorelines related to great interplate-thrust earthquakes and deformed river profiles observed in intraplate reverse-faulting environments. Despite the relative uniformity of longer-term deformation rates, accumulating evidence indicates considerable short-term irregularity, at least in some regions. Perhaps the best documented example comes from southern California, where rapid, correlated changes among gravity, elevation, and horizontal strain measurements have recently been observed.

## INTRODUCTION

The principle of uniformitarianism leads us to expect that tectonic movements that have occurred in the geologically recent past are taking place at present, and with sufficiently accurate measurements this activity should be observable today. The often spectacular surface deformation that accompanies major earthquakes is readily visible, and precise techniques are not needed for its detection. Most surface movements are, however, more subtle. Typical rates of deformation in tectonically active regions are a few parts in ten million per year (0.1 ppm/yr or 0.1 $\mu$rad/yr). To monitor these faint motions closely, geodetic techniques must measure changes in line length and surface tilt or angular changes between survey monuments to a precision comparable with these annual increments. This capability is within the range of modern methods, and although ear-

lier measurements are less precise, deformation rates of this order, averaged over periods of a decade or longer, are readily obtainable from the earlier historical data.

Because of their high precision and generally wide areal extent (~10 km aperture or greater), geodetic observations made at the Earth's surface provide a measure of the deformation actually occurring at the depths where damaging earthquakes originate (about 20 km or less). Regions of tectonic deformation are invariably seismically active, and it is convenient to characterize the alternating periods of slow aseismic deformation and abrupt earthquake strain release in terms of a simple, repetitive sequence—the *seismic deformation cycle*. Figure 10.1 shows both the idealized model of the cycle first suggested by Reid (1910) and the more refined one accepted today. Both are considerably simplified, showing the time history of cumulative deformation of a single point or localized region, ignoring spatial variations in movement history, and smoothing out temporal fluctuations in deformation rate.

Reid's elastic rebound theory, based on his studies of geodetic measurements related to the great 1906 San Francisco earthquake, postulates that earthquakes represent the release of accumulated elastic strains, and Reid assumed that a major earthquake would not recur until all strains released by the preceding event had reaccumulated [Figure 10.1(a)]. However, geologic field observations certainly demonstrate that not all crustal deformation is elastic and recoverable; indeed, in some seismically active regions inelastic processes such as folding and metamorphic deformation may predominate. As Figure 10.1(b) shows, the existence of a significant component of permanent deformation notably modifies the cycle. Rapid postearthquake deformation, which can persist from years to decades following major events, introduces additional complexity into the simple cycle visualized by Reid.

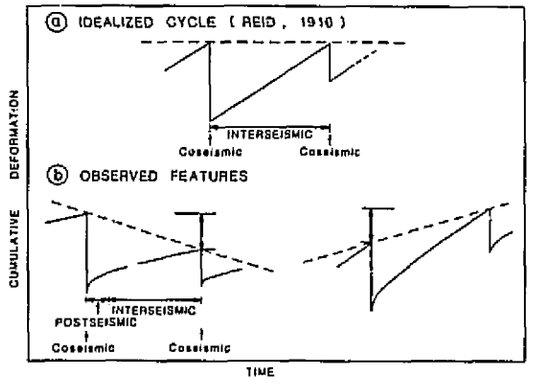


FIGURE 10.1 Simplified forms of the earthquake deformation cycle. Cumulative deformation (e.g., strain, tilt, ground displacement) measured at the Earth's surface is plotted as a function of time. Step offsets correspond to the occurrence times of major earthquakes. Dashed lines give failure level, constant in the idealized cycle (a), and (b) varying with time when the effects of permanent inelastic deformation are included.

Thus, in the modern view the complete cycle consists of the *coseismic* deformation that accompanies the earthquake itself, the *postseismic* transient movements that follow it, and the relatively steady *interseismic* motions that comprise the majority of the cycle. *Permanent deformation* results if the interearthquake strain buildup is not exactly balanced at all points by the coseismic strain release. Where permanent movements have been documented, it has been shown that the coseismic offset can either locally exceed the accumulated interearthquake straining or be less than this amount; both cases are illustrated in Figure 10.1(b).

Geodetic measurements are then capable of delineating major features of the earthquake deformation cycle and closely monitoring current movement patterns. Historical surveys, which typically have repeat times of decades or longer, sample long portions of the cycle, record coseismic and postseismic movements related to past great earthquakes, and provide estimates of the permanent deformation component of the cycle. Modern observations have been most useful in determining interseismic movement rates with high accuracy and refined temporal resolution and are beginning to provide precise estimates of present-day fault slip rates and evidence for hitherto unsuspected short-term irregularities in deformation rate. The purpose of this chapter is to illustrate these capabilities with examples drawn from recent work, especially emphasizing the relation between the geodetic results and those obtained using the geologic measures of deformation and deformation rate discussed elsewhere in this volume.

## PRESENT-DAY DEFORMATION RATES

Rates of deformation have been obtained for much of the seismically active western United States and parts of Alaska; these results have recently been summarized by Savage (1983). In addition, extensive geodetic surveys in active regions elsewhere in the world, notably Japan and New Zealand, have been used to determine patterns and rates of contemporary deformation in tectonic environments similar to those found in this country.

Because of California's high seismicity and population density, intensive measurement efforts are concentrated there. Some typical results, from a laser-ranging (trilateration) network in the southern San Francisco Bay area, are illustrated in Figure 10.2. The network

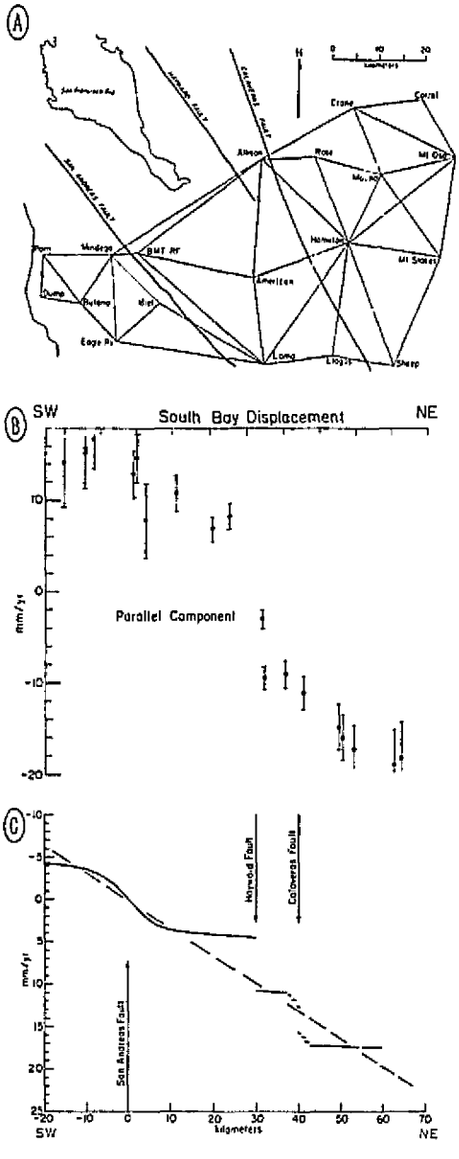


FIGURE 10.2 (A) Stations and lines observed in the southern San Francisco Bay region. Active faults are shown for reference. (B) Displacement rates parallel to N 35° W plotted versus distance normal to strike of San Andreas Fault. (C) Schematic interpretation of (B). Solid curve was drawn for 12 mm/yr slip below 7 km on the San Andreas Fault, 6 mm/yr rigid-block slip on the Hayward Fault, and 6 mm/yr rigid-block slip on the Calaveras Fault. Half of Calaveras fault slip was distributed over 5-km-wide zone. Dashed line is displacement field that would be observed if motion were distributed uniformly. From Prescott *et al.* (1981), with permission of the American Geophysical Union.

contains 43 lines whose lengths have been measured roughly annually since 1970; the precision of each measurement depends on line length but averages about 3 parts in $10^7$. The line length changes during 1970-1980 have been analyzed by Prescott *et al.* (1981), who determined the average displacement rate of each station relative to a fixed center of mass of the network as a whole.

Figure 10.2(B) shows the displacement rate components parallel to the San Andreas Fault plotted versus distance from the fault, and Figure 10.2(C) is a schematic interpretation of this result. Clear offsets occur across the Hayward and Calaveras Faults, and their magnitudes agree well with observed creep rates obtained independently from small-aperture arrays and wire extensometers that span each of these faults (see Sylvester, Chapter 11, this volume, for discussion of these measurement methods).

The displacement-rate profile across the San Andreas Fault is more interesting. The absence of any discontinuity at the fault trace indicates that the San Andreas is locked at the surface; increasing movement rates away from the fault suggest that it is freely slipping below some locking depth, $D$. A simple calculation shows that for such a model the deep slip rate is $12 \pm 4$ mm/yr and $D = 7$ km. This same fault slipped 2 to 3 m from the surface to depths of 5 to 10 km at the time of the great 1906 San Francisco earthquake (Thatcher, 1975), and the current deformation pattern represents strain buildup leading to the repeat of a large or great earthquake like the 1906 shock. If slip rates inferred for the past decade are representative of the long-term rate, and if coseismic offsets of 2 to 3 m per event are typical of this segment of the San Andreas Fault, then the average recurrence interval for such events is 170 to 250 yr.

Geologic data independently support the geodetic results. Although direct evidence is lacking on occurrence times and offsets of past events, measures of late Holocene slip rate confirm the value obtained from geodetic measurements. Dated offsets of late Holocene geomorphic features that cross the San Andreas Fault near Crystal Springs Reservoir, 40 km northwest of the geodetic network shown in Figure 10.2(A), yield a slip rate of 12 mm/yr over the last $1130 \pm 160$ yr (Hall, 1984).

Geodetic estimates of slip rate have been obtained for several other segments of the San Andreas system (see Table 10.1), and more will become available in the future. Several of those listed in Table 10.1 are only approximate and are subject to a number of caveats: often the entire deformation zone of a single fault is not spanned, subsidiary subparallel faults may contribute to observed movements, and deformation rates (see below) may vary notably over time scales of a few years or less.

TABLE 10.1 Geodetic Estimates of Slip Rate on San Andreas Fault System

| Location | Rate (mm/yr) | Reference |
|---|---|---|
| San Francisco | 12 ± 4 | Prescott *et al.* (1981) |
| Central California | 38 ± 5 | Thatcher (1979) |
| Carrizo Plain | 32 | King *et al.* (1983) |
| "Big Bend" Region | 25 | McGarr *et al.* (1982) |

Nonetheless, geodetic measurements can, under favorable conditions, provide accurate estimates of contemporary rates of fault slip. The geodetic estimates complement those obtained by geologic methods. When both are available, late Quaternary or Holocene estimates can be compared with present-day values. When, owing to vagaries of erosion and nondeposition, suitable geomorphic features are absent, geodetic measurements can provide needed constraints.

## SOCIETAL IMPACT, AN EXAMPLE

Networks similar to those in the San Francisco Bay area are located at over 30 other sites elsewhere in California and the western United States, and results from 9 of these are summarized in Figure 10.3.

The strain field obtained for the Seattle network is of special interest because of the light it sheds on interaction between the North American and Juan de Fuca plates (J. F., Figure 10.3). The most important feature of the deformation within this net is the orientation of the direction of maximum compressive strain. Elsewhere along the Pacific coast of North America the compressive strain axis is oriented roughly north-south. Near Seattle, however, it is directed N 70° E, close to the expected convergence direction of N 50° E between the Juan de Fuca and North American plates (Riddihough, 1977). The most straightforward interpretation of this result (Savage *et al.*, 1981) is that the convergent boundary between these two plates is now locked and that current deformation near Seattle represents the accumulation of elastic strains that will eventually be released by the occurrence of a great subduction-zone earthquake off the coast of Washington.

Comparison of the seismicity distribution and plate-tectonic setting of the Pacific Northwest with other subduction zones supports this interpretation, since tectonically similar regions elsewhere accommodate plate convergence by periodic great earthquakes rather than by aseismic subduction (Heaton and Kanamori, 1984). No great earthquake has been recorded off the Washington coast, and the hypothesis that subduction occurs seismically will not be proven until one does. Nonetheless, the arguments favoring this interpretation have had an important impact on land-use planning and have proven sufficiently compelling to effect a major re-evaluation of the seismic hazard that a major subduction-zone earthquake would pose for critical facilities located in the region.

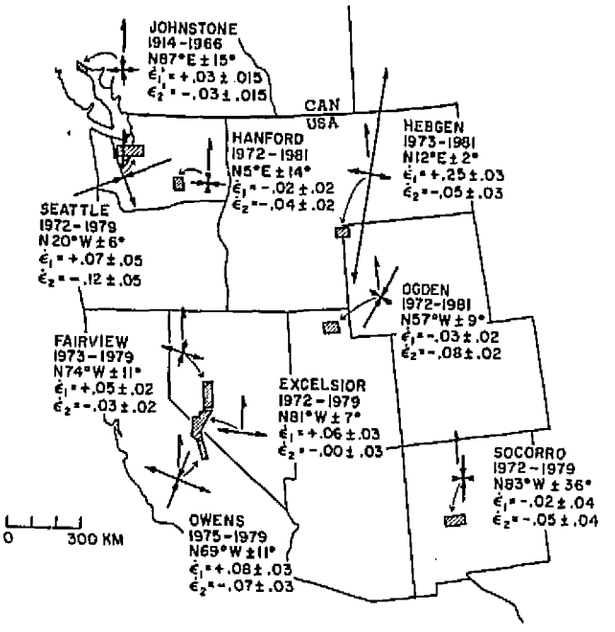


FIGURE 10.3 Location of trilateration networks in western United States and the principal strain rates measured in each. Shown beneath the network name are the time interval covered, the direction of maximum extension, and the principal strain rates (in strain/year). Also shown in the southwest corner of Canada is one triangulation network with the principal deviatoric strain rates measured there. The plate boundaries along the Pacific coast are indicated by the usual symbols (ridge by double line, trench by hachured line, and transform by dashed line). The Juan de Fuca plate is identified by initials J. F. From Savage (1983), copyright Annual Reviews, Inc.

## IRREGULARITIES IN DEFORMATION RATE

The largest variations in movement rate occur during the postseismic phase of the seismic deformation cycle, and once these transients have died out the measured strain rates are, as a rule, at least roughly constant. This constancy is demonstrated by comparisons between historical and modern data, and precise measurements of the past decade also show that year-to-year variations in rate are generally small. Nonetheless, survey-to-survey rate fluctuations nominally above random measurement errors do occur, and in a few cases the variation in deformation rate appears to be quite large.

One of the better documented examples of this kind

comes from southern California, where overlapping observations using three independent measurement systems have been made since 1977 (Jachens *et al.*, 1983). The location of each of these geodetic networks is shown in Figure 10.4. Precise relative gravity measurements have been made twice annually using sets of three to five gravimeters; in each case observations are referenced to a base station located at Riverside (solid dot, Figure 10.4). Elevation differences have been measured annually by leveling surveys carried out over five routes 30 to 100 km long. The horizontal strain field has been monitored by annual surveys of seven trilateration (laser-ranging) networks.

These measurements overlap in three different localities, results for which are shown in Figure 10.5. Four independent parameters are needed to construct this figure; two of them are determined from the data, and two are arbitrary and may be adjusted to improve the match between the three measurement types. The two arbitrary parameters are the absolute levels of two of the time histories relative to the third at each locality. The two constrained parameters are determined from temporally coincident or nearly coincident observations. Comparing changes in gravity with changes in areal strain at all localities establishes a common linear scale

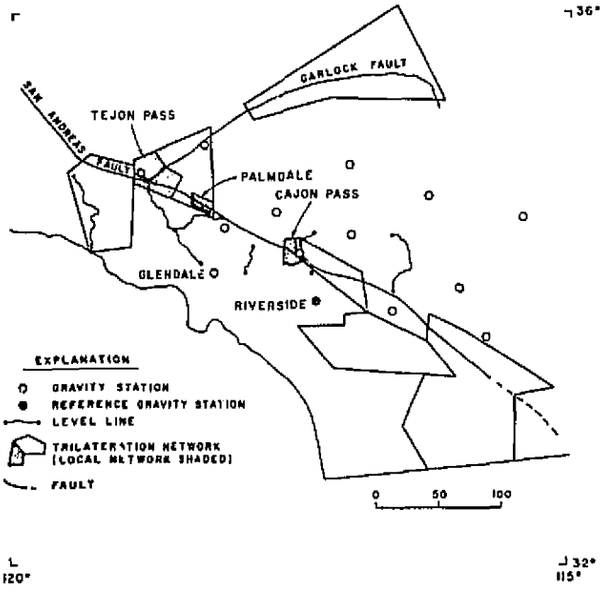


FIGURE 10.4 Index map showing locations of gravity stations, leveling lines, and trilateration networks in southern California that have been surveyed repeatedly during the past 5 to 10 yr. Shaded areas of trilateration networks are local nets used in this study. From Jachens *et al.* (1983), copyright 1983 by the American Association for the Advancement of Science.

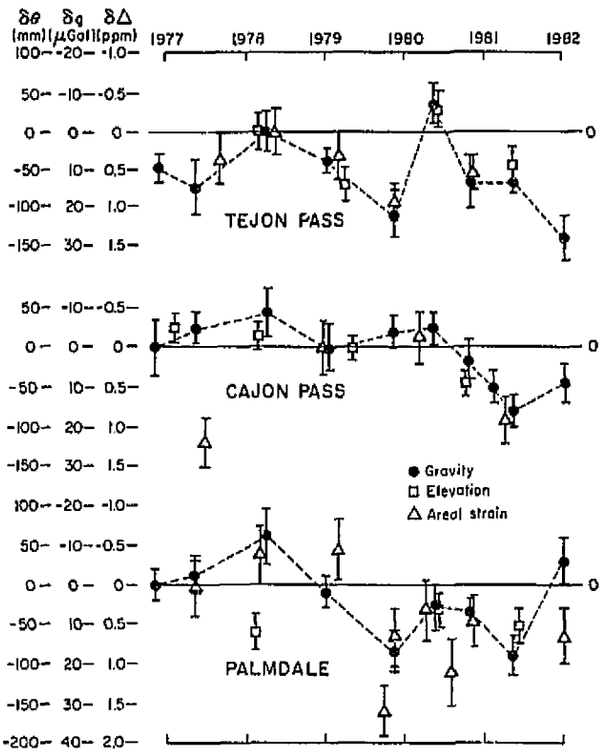


FIGURE 10.5 Temporal changes in gravity ($\delta g$), elevation ($\delta e$), and areal strain ($\delta\Delta$) measurements from three areas of southern California. Error bars on the gravity data represent 1 standard error, and those on elevation and strain data represent 1 standard deviation. Dashed lines connect gravity data. From Jachens *et al.* (1983), copyright 1983 by the American Association for the Advancement of Science.

factor relating the two (0.05 ppm/$\mu$gal), and a similar factor relates gravity and elevation changes ($-0.2$ $\mu$gal/mm). The gravity/areal strain relation is the better determined because more data comparisons are available. However, the coefficient relating gravity and elevation changes agrees with independent determinations obtained using coseismic data from several large earthquakes.

Despite several significant disagreements, the accord among the three independent measurements is rather good. Although the 5-yr record is insufficient to establish a long-term trend in these parameters, departures from uniformity are striking and survey-to-survey fluctuations are large. While other data (e.g., Langbein *et al.*, 1982) exhibit similar short-term variability, not enough measurements of comparable precision and redundancy yet exist to decide clearly whether the irregularities shown in Figure 10.5 are relatively common or extremely rare. Nonetheless, it appears that at least in

some regions a relatively long record is needed to determine representative interseismic movement rates, and caution is thus required in extrapolating a few years of measurements, however precise, to the long term.

## PERMANENT DEFORMATION

Deformed late Quaternary and Holocene structural features are common in seismically active regions. Frequently this permanent deformation is crudely similar to the pattern of coseismic movements observed in historical earthquakes, indicating that the two deformation processes are related and showing that at least in some regions strain accumulation and release are not in perfect balance. Here, two examples are used to demonstrate this imbalance and to illustrate the several links that connect the geologic and geodetic records.

The 1983 Coalinga earthquake ($M$ = 6.5) occurred on a fault lying beneath Anticline Ridge, one of a series of active Quaternary structures that borders the San Joaquin Valley and lies 40 to 80 km east of the San Andreas Fault in central California (Figure 10.6). Seasonal streams that existed prior to the initiation of folding and uplift cross the growing anticlinal structures, and this active tectonism has apparently altered their channels and deformed their streambeds (King and Stein, 1983). Alluvial-fan surfaces that flank Los Gatos Creek where it crosses the southeastern end of Anticline Ridge are about 10 m higher than fan surfaces both upstream and downstream of this region. The streambed profile itself mimics this behavior, but with smaller departures from an inferred undisturbed gradient [Figure 10.7(A)]. King and Stein concluded that both profiles depart from their equilibrium shapes because of recent uplift of Anticline Ridge. However, deposition may also contribute to the profile changes, since a tectonic shallowing of stream gradient will decrease flow velocity and encourage local deposition. If so, this could explain why the maximum fan height is displaced upstream about 3 km from where the inferred crest of Anticline Ridge crosses Los Gatos Creek (R. S. Stein, U.S. Geological Survey, personal communication, 1984). Detrital charcoal dated at 2550 ± 130 yr BP provides a maximum terrace uplift rate (ignoring deposition) of 4 mm/yr.

Leveling surveys show that in 1983, 0.5 m of coseismic uplift took place near the top of Anticline Ridge, and smaller amounts of subsidence occurred to the southwest [Figure 10.7(B)]. No surface faulting associated with the mainshock was observed. As Figure 10.7(B) shows, the pattern of inferred uplift along the

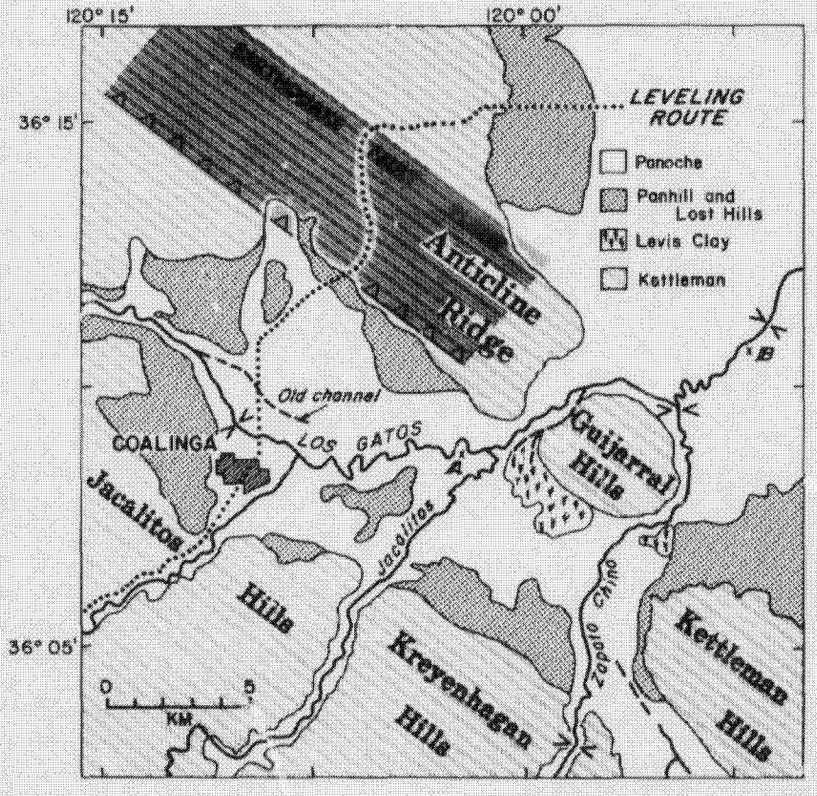


FIGURE 10.6 Simplified map of the surface deposits in the epicentral region of the May 1983 Coalinga earthquake. The approximate surface projection of a fault plane for the earthquake consistent with the seismic and geodetic data is shown. The present river courses are shown by solid lines, and old river courses are shown by dashed lines. A dotted line indicates the course of the geodetic traverse. Note that the width of the structure where it is crossed by the geodetic line is about twice the width of the structure crossed by Los Gatos Creek. From King and Stein (1983).

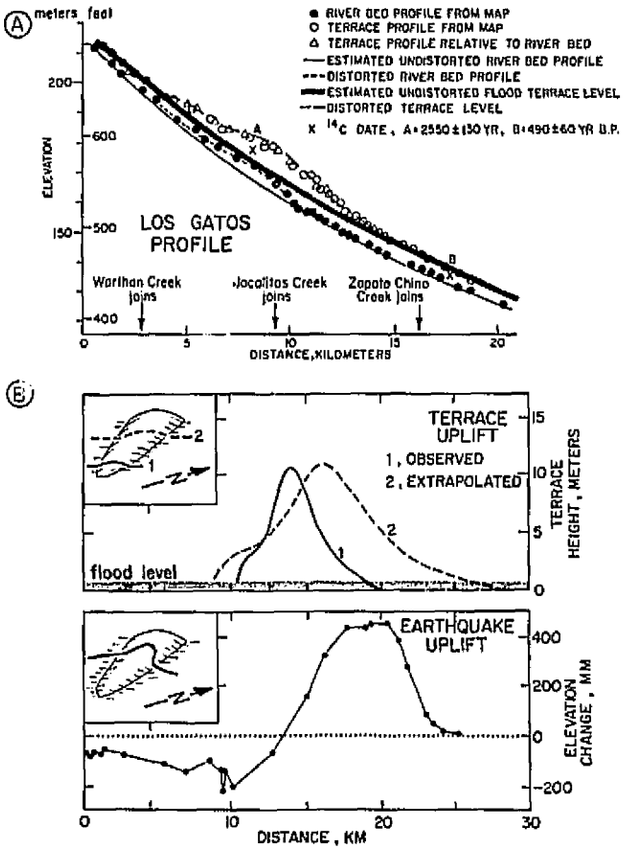


FIGURE 10.7 (A) River terrace and river bed profiles for Los Gatos Creek. All the points except those marked by triangles, which were measured in the field, are taken from the 7.5' topographic maps. The profiles follow the courses of the river except for some of the extreme meanders where the profile follows a direct route. (B) Terrace uplift for Los Gatos Creek, taken from (A) above is indicated by solid line, and a profile extrapolated to the position of the leveling route is indicated by the dotted line. The 1983 earthquake uplift is shown in the lower frame, with uplift projected perpendicular to fault strike. After King and Stein (1983).

stream course is sufficiently similar to the coseismic movements of 1983 to indicate a relation between the two. Of course, the interseismic phase of the cycle will also contribute to observed movements, and erosion and deposition will further modify any tectonically developed topography. However, neither the interseismic movement pattern nor the recurrence interval for 1983-type events is known, and consequently no further constraints on the deformation cycle can be extracted from the available data.

Both the geodetic and geologic records are more complete for the great plate-boundary earthquakes of southwest Japan. The regional tectonic setting is illustrated in Figure 10.8. The Philippine Sea plate underthrusts the Eurasian plate along the Nankai Trough, and a great earthquake occurred along this boundary in 1946. A previous great shock ruptured this same segment of plate boundary in 1854, and historical records indicate an average recurrence interval of 117 years for the past six events on this segment of the Nankai Trough (Ando, 1975).

An extensive leveling network on the island of Shikoku and adjacent Honshu has been surveyed five times or more since about 1890, and numerous tidal gauge stations provide independent constraints on the vertical movement history of the region. In all, the geodetic record is about 90 years long, samples all parts of the deformation cycle, and has a duration comparable with the time interval between the past two events. Although this measurement interval does overlap two adjacent cycles, a single complete cycle can be synthesized provided the last two are similar. Two lines of evidence support the validity of this assumption: (1) the 1854 and 1946 earthquakes are of comparable size, and (2) the current (~1970-1980) patterns and rates of deformation are ap-

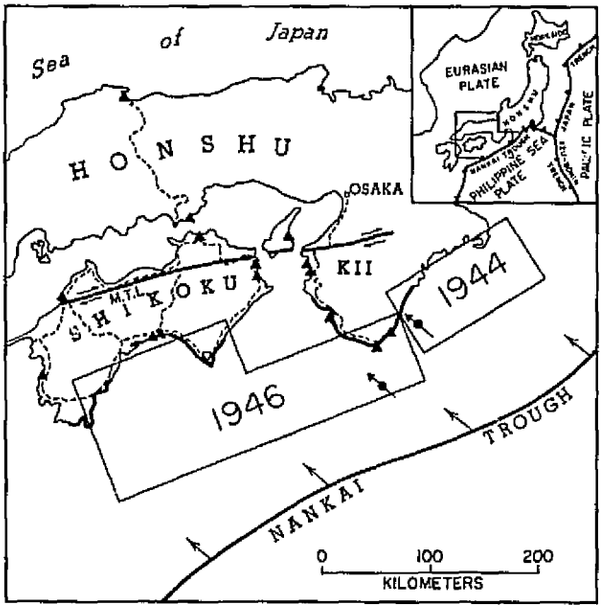


FIGURE 10.8 Location map of southwest Japan. Inset shows plate-tectonic setting. Arrows at Nankai Trough give relative motion of Philippine Sea with respect to Eurasian plate. Rectangles are surface projections of coseismic fault planes of 1944 and 1946 earthquakes, and solid dots with arrows show epicentral locations slip vectors for these two earthquakes. Heavy lines on trench-facing coastlines locate uplifted late Quaternary marine terraces, and solid line with arrows identifies the Median Tectonic Line (M.T.L.), an active right-lateral strike-slip fault. Dashed lines denote leveling routes, and solid triangles locate tidal gauge stations. From Thatcher (1984), with permission of the American Geophysical Union.

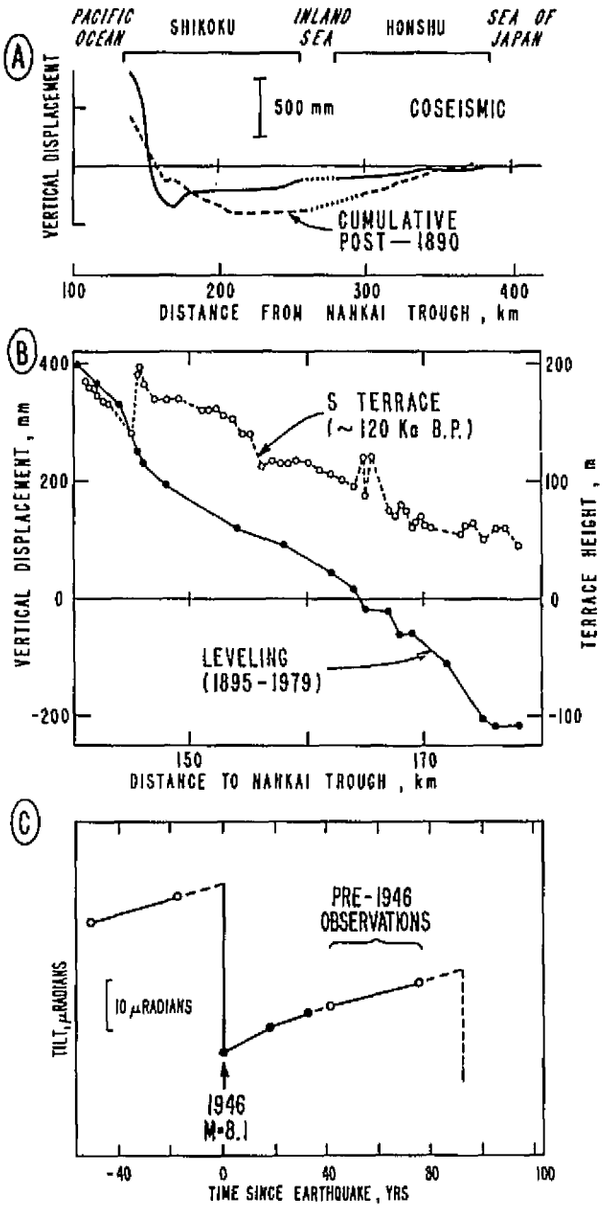


FIGURE 10.9 (A) Summary of observed vertical movements plotted versus distance from Nankai Trough. Solid line shows coseismic movements due to 1946 earthquake, and dashed line shows cumulative deformation inferred for one complete movement cycle. Dotted portions of both curves indicate interpolation across the Inland Sea. (B) Cumulative vertical displacement in millimeters (scale at left), west coast of Muroto Promontory, and marine terrace height in meters (scale at right), both plotted versus distance from Nankai Trough. (C) Synthesized deformation cycle for southeast Shikoku, showing cumulative tilt changes versus time since 1946 Nankaido earthquake. Pre-1946 data (open circles) have been extrapolated to post-1946 time interval. Inferred movements are indicated by dashed lines. From Thatcher (1984), with permission of the American Geophysical Union.

proaching those measured during ~1890-1930, a somewhat later stage of the preceding movement cycle [see Figure 10.9(C)].

The cumulative vertical movements during 1890-1980 are thus representative of the permanent deformation per cycle and Figure 10.9(A) compares these displacements with the coseismic movements of 1946. The two deformation patterns resemble each other, with uplift nearest the Nankai Trough and subsidence further inland. The cumulative movements are also qualitatively consistent with the deformation and areal distribution of late Quaternary-raised shorelines on the southern coasts of Kii Peninsula and Shikoku. Figure 10.9(B) compares the cumulative level changes near southeast Shikoku (Muroto Point) with the heights of a well-preserved marine terrace cut during the last interglacial period and subsequently uplifted tectonically. Although the tilt directions agree, the rates of movement do not. Maximum uplift rates during the past 120,000 yr average 1.5 mm/yr, whereas those since 1890 are three times larger. Tilt rates disagree by comparable amounts, and discrepancies elsewhere are even larger. For example, near the tip of Kii Peninsula cumulative post-1890 uplift is comparable with that measured near Muroto Point, but the S-terrace height is only about 60 m above current sea level. Farther inland, geologically recent submergence is suggested by the indented character of the coastlines. However, no geologic estimates of subsidence rates are available to compare with the post-1890 value of 3 to 4 mm/yr.

In Figure 10.9(C) the near-trench tilt history for a single deformation cycle has been synthesized from available leveling data. The leveling route, in southeast Shikoku, is the same as that used in Figure 10.9(B), and the results of five different surveys have been employed in the reconstruction. The similarity of recent (1964-1980) tilt rates with those obtained prior to 1946 is quite evident, and in Figure 10.9(C) the pre-1946 data have been extrapolated to the current movement cycle. The synthesized cycle is quite similar to the idealized one illustrated in Figure 10.1(B) and clearly exhibits the main elements of the cycle: the postseismic transient, the relatively steady interseismic phase of the cycle, and the significant component of permanent deformation.

## FUTURE DIRECTIONS

During the next decade, full implementation of highly accurate extraterrestrial geodetic surveying methods will have an important impact on crustal deformation measurements in active regions. Satellites of the Global Positioning System (GPS) now being deployed in very well-determined orbits by the U.S. Department of Defense are of particular interest. By rang-

ing to these satellites from the Earth's surface it is anticipated that relative horizontal and vertical positions can be determined within a few centimeters (NRC Panel on Crustal Movement Measurements, 1981). Furthermore, this precision can be obtained at large station separations (hundreds of kilometers), adjacent stations need not themselves be intervisible, and measurements can be made even in overcast conditions.

The precision of GPS measurements degrades for intercontinental station separations (~ 1000-10,000 km). However, other extraterrestrial surveying methods such as Very-Long-Baseline Interferometry (VLBI) and Satellite Laser Ranging (SLR) are expected to be capable of measuring relative positions over these longer ranges to 3 cm or better (NRC Panel on Crustal Movement Measurements, 1981).

Relative to conventional geodetic methods, the most important feature of the new space techniques is the capability for measuring long ranges with high precision. Thus, for station separations greater than about 100 km, GPS methods are expected to become more accurate than land-based surveying. VLBI or SLR measurements over intercontinental baselines will then be capable of resolving relative movements of the Earth's major tectonic plates, and GPS networks with station separations of about 100 km can be used to outline the broad-scale deformation patterns in intracontinental active regions like the western United States and central Asia.

Depending on their ultimately achievable accuracy and measurement costs, extraterrestrial methods may also be competitive with land-based surveying over shorter ranges as well. In remote and inhospitable environments, where clear sighting conditions are rare and station intervisibility is difficult to obtain, GPS methods may also prove to be more feasible and cost-effective than conventional techniques.

Geodetic observations provide a direct measure of strain changes occurring at seismogenic depths, and as a result they will play an important role in determining the degree to which large, destructive earthquakes are predictable. In recent years geodetic monitoring has been intensified in areas of identified high seismic potential both in the United States and elsewhere. Further detailed monitoring can be anticipated in the future. Most of this work comprises annual surveys, but in several parts of California monthly and weekly surveys are now being carried out as well (Langbein *et al.*, 1982; Prescott and Savage, 1984). With a long record of frequent measurements, the patterns and rates of interseismic movement will be outlined in considerable detail. The typical variability of these patterns and rates as a function of time will be determined as well. Eventually, large earthquakes will occur in these closely studied regions. When these events take place, the accumulated data should be sufficient to determine precisely whether diagnostic crustal movement anomalies preceded their occurrence.

## REFERENCES


Ando, M. (1975). Source mechanism and tectonic significance of historical earthquakes along the Nankai Trough, Japan, *Tectonophysics 27*, 119-140.

Hall, N. T., (1984). Holocene history of the San Andreas Fault between Crystal Springs Reservoir and San Andreas Dam, San Mateo County, *Bull. Seismol. Soc. Am. 74*, 281-299.

Heaton, T. H., and H. Kanamori (1984). Seismic potential associated with subduction in the northwestern United States, *Bull. Seismol. Soc. Am. 74*, 933-942.

Jachens, R. C., W. Thatcher, C. W. Roberts, and R. S. Stein (1983). Correlation of changes in gravity, elevation and strain in southern California, *Science 219*, 1215-1217.

King, C., and R. Stein (1983). Surface folding, river terrace deformation rate and earthquake repeat time in a reverse faulting environment: The Coalinga, California earthquake of May 1983, in *The 1983 Coalinga, California, Earthquake*, J. H. Bennett and R. W. Sherburne, eds., Calif. Div. Mines and Geol. Spec. Publ. 66, Sacramento, Calif., pp. 261-274.

King, N. E., C. Gu, and W. H. Prescott (1983). Strain accumulation on the San Andreas Fault south of Parkfield, California, 1970-1983, *EOS 64*, 841.

Langbein, J. O., M. F. Linker, A. McGarr, and L. E. Slater (1982). Observations of strain accumulation across the San Andreas Fault near Palmdale, California, with a two-color geodimeter, *Science 218*, 1217-1219.

McGarr, A., M. D. Zoback, and T. C. Hanks (1982). Implications of an elastic analysis of in situ stress measurements near the San Andreas Fault, *J. Geophys. Res. 87*, 7797-7806.

NRC Panel on Crustal Movement Measurements (1981). *Geodetic Monitoring of Tectonic Deformation—Toward a Strategy*, National Academy Press, Washington, D.C., 109 pp.

Prescott, W. H., and J. C. Savage (1984). Frequent geodolite distance measurements and the detection of temporal variations in strain accumulation, *J. Geophys. Res. 89*.

Prescott, W. H., M. Lisowski, and J. C. Savage (1981). Geodetic measurement of crustal deformation on the San Andreas, Hayward, and Calaveras Faults near San Francisco, California, *J. Geophys. Res. 86*, 10853-10869.

Reid, H. F. (1910). Permanent displacements of the ground, in *The California Earthquake of April 18, 1906*, Report of the State Earthquake Investigation Commission, Carnegie Institution of Washington, Washington, D.C., Vol. 2, pp. 16-28.

Riddihough, R. P. (1977). A model for recent plate interactions off Canada's west coast, *Can. J. Earth Sci. 14*, 384-396.

Savage, J. C. (1983). Strain accumulation in western United States, *Ann. Rev. Earth Planet. Sci. 11*, 11-43.

Savage, J. C., M. Lisowski, and W. H. Prescott (1981). Geodetic strain measurements in Washington, *J. Geophys. Res. 86*, 4929-4940.

Thatcher, W. (1975). Strain accumulation and release mechanism of the 1906 San Francisco earthquake, *J. Geophys. Res. 80*, 4862-4872.

Thatcher, W. (1979). Systematic inversion of geodetic data in central California, *J. Geophys. Res. 84*, 2283-2295.

Thatcher, W. (1984). The earthquake deformation cycle at the Nankai Trough, Southwest Japan, *J. Geophys. Res. 89*, 3087-3101.

# 11 Near-Field Tectonic Geodesy

ARTHUR G. SYLVESTER
*University of California, Santa Barbara*

ABSTRACT

Fault movements may be monitored by precise surveying of closely spaced arrays of permanent bench marks within 1 km of a fault. The geodetic data may complement data from tiltmeters and creepmeters as well as data from large aperature trilateration or triangulation arrays. If resurveys are temporally fortuitous, preseismic, coseismic, and postseismic movement data are obtained.

Closely spaced, linear arrays of nails in pavement across active faults provide a quick, simple, and inexpensive way to locate and measure horizontal displacement across narrow, well-defined zones of faulting.

Small-aperature trilateration and alignment arrays document horizontal creep across faults of the San Andreas system, especially in central California, where as much as 32 mm/yr right slip has taken place for more than two decades. Small-aperature triangulation arrays have also identified horizontal creep on faults elsewhere in California at rates of up to 5 mm/yr.

Short level lines may detect height changes of 0.5 mm. Crustal tilt may be measured to about 0.5 μrad if special attention is paid to type and stability of bench marks. Thus, Chinese precise leveling has documented several centimeters of vertical movement within a few hundred meters of faults a few days before surface rupture; 14-cm vertical afterslip was measured in the 10 weeks following the 1979 Imperial, California, earthquake; and 35 mm/yr nontectonic subsidence has occurred across a fault in Fremont Valley, California, for at least the last 9 yr.

Spirit-level optical tilt of triangular arrays of bench marks (dry-tilt) yields tilt data to a precision of about 1 μrad sufficient to document major movement, especially near volcanoes. From 10s to 1000s of microradians of tilt occurred over a few days or weeks prior to eruptions of the Kilauea and Mount St. Helens volcanoes.

## INTRODUCTION

Only a short while ago tectonic movements of the Earth's crust were generally considered to be too slow to be observed in a lifetime, and long periods of inactivity were believed to be punctuated only at the most inconvenient times and places for man by surficial fault ruptures accompanying large, infrequent earthquakes. To be sure, Reid (1910) estimated a steady movement rate of the Farallan Islands relative to Mount Hamilton, California, at about 5 cm/yr from 1850 to 1905, and in 1938 Icelanders commenced geodetic measurements to observe tectonic movements in the neovolcanic zone of north Iceland (Niemczyk, 1943). However, the discov-

ery in 1960 of aseismic slip on the central segment of the San Andreas Fault, manifested by offset buildings, irrigation ditches, and vineyard rows (Steinbrugge *et al.*, 1960), changed many of our notions about fault mechanics, because here was an example of a geologic process occurring at rates measureable on a human time scale.

Because the movements seemed to be limited to a zone only a few meters wide, Tocher and his colleagues (Tocher *et al.*, 1968; Nason and Tocher, 1970) initiated a variety of small-scale geodetic and instrumental studies to measure these minor, but significant movements close to the fault. Monitoring of several faults, chiefly in California but also in New Zealand (Lensen and Sugrate, 1969) led to the equally surprising discoveries of minor fault movements that preceded earthquakes (Allen and Smith, 1966), that followed earthquakes (Smith and Wyss, 1968; Wallace and Roth, 1968), and that were triggered by earthquakes (Allen *et al.*, 1972). In all cases the surficial displacements were confined to narrow zones less than 100 m wide along the fault. Although the U.S. Coast and Geodetic Survey (now the National Geodetic Survey) has conducted near-field triangulation monitoring of faults since about 1900 (Meade, 1971), several investigators including C. R. Allen, R. O. Burford, G. J. Lensen, R. D. Nason, J. C. Savage, A. G. Sylvester, and D. Tocher devised and initiated a variety of new near-field geodetic and instrumental techniques in the late 1960s and 1970s to determine the extent and rate of creep, whether creep may occur on other faults or on other kinds of faults, about the timing and magnitude of preseismic slip, the amount and duration of postseismic slip, and the significance of dynamically triggered slip.

These small movements, now found to measure from 1 to 30 mm/yr, have an impact on society as can be demonstrated by damage to buildings, streets, and subsurface pipelines in the town of Hollister, California, insofar as preseismic slip may provide information leading to the prediction of earthquakes and to the extent that earthquakes on a known active fault may trigger equal or greater movement on other faults presumed to be inactive. At the very least, understanding these movements may provide greater insight into earthquake mechanisms, knowledge of which will be requisite for eventual prediction of earthquakes.

## CREEP, AFTERSLIP, AND DYNAMICALLY TRIGGERED SLIP

It is useful to discuss briefly a preferred nomenclature for minor fault slip of very different origin, because ambiguities arise when the term "creep" is simply used for all these kinds of fault slip (Table 11.1).

TABLE 11.1 Earthquake Mechanics of Minor Movements

| Movement | Rate | References |
|---|---|---|
| Tectonic | | |
| creep | 1-30 mm/yr | Steinbrugge *et al.* (1960) |
| preseismic slip | 1-? mm/yr | Allen and Smith (1966) |
| coseismic slip | 1 to thousands of mm | Many authors |
| dynamically triggered slip | 1-30 mm | Allen *et al.* (1972) |
| afterslip | 1-300 mm/yr | Allen and Smith (1966) |
| Nontectonic | | |
| subsidence | 1-35 mm/yr | Many authors |

The great difference among these terms is illustrated in Figure 11.1, which shows the magnitude of slip as a function of time. *Creep* is aseismic fault slip: it may be stable and continuous or temporally and spatially episodic (Yamashita and Burford, 1973; King *et al.*, 1973; Nason *et al.*, 1974; Evans *et al.*, 1981), and the long-term rate may vary before or after earthquakes along the creeping fault segment (Nason and Tocher, 1971; Burford *et al.*, 1973). Fault creep precedes some earthquakes, as is summarized by Mjachkin *et al.* (1972), Scholz *et al.* (1973), and Whitcomb *et al.* (1973), and offers the hope that near-field geodetic observations

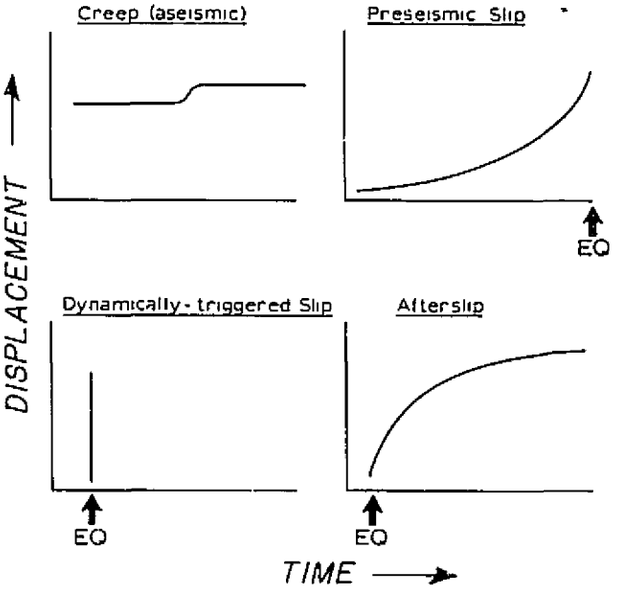


FIGURE 11.1 Types of tectonic creep.

TABLE 11.2 Near-Field Tectonic Geodesy

| Motion/Technique | Measured Changes | Typical Aperture | Required Precision | Frequency of Resurvey |
|---|---|---|---|---|
| Horizontal | | | | |
| alignment | Deflection | 100 m | +1 mm | Months |
| triangulation | Angles | 1000 m | +5 mm | Months to years |
| trilateration | Lengths | 1000 m | +5 mm | Months to years |
| Vertical | | | | |
| precise leveling | Heights | 1000 m | +1 mm | Months |
| Tilt | | | | |
| precise leveling | Heights | 500 m | +1 μrad | Months |
| dry tilt | Heights | 40 m | +10 μrad | Months to years |

may be one of the effective methods for earthquake prediction. The tectonic significance of creep is still a topic of debate: some investigators believe that creep relieves sufficient buildup of stress so that large earthquakes are precluded in a creeping segment of a fault (Brown and Wallace, 1968; Prescott and Lisowski, 1983), and that notion seems to have gained support by great accumulation of strain data over the last decade (Langbein, 1981). Alternatively, creep is postulated to be the first step in progressive failure leading to a major earthquake (Nason, 1973).

*Afterslip* is fault slip that occurs in the days, weeks, or even months following the main earthquake. Most reported (Nakamura and Tsuneishi, 1967; Ambrayses, 1970) and documented instances of significant afterslip are for strike-slip faults. The principal characteristic of afterslip is that the slip rate decreases logarithmically (Smith and Wyss, 1968; Wallace and Roth, 1968; Sylvester and Pollard, 1975; Bucknam *et al.*, 1978; Cohn *et al.*, 1982; Harsh, 1982). The magnitude of displacement may equal or exceed the coseismic slip, as has been observed in strike-slip earthquakes (Smith and Wyss, 1968; Burford, 1972; Bucknam *et al.*, 1978; Sharp and Lienkaemper, 1982), but in other kinds of earthquakes it is small relative to the coseismic slip (Lensen and Suggate, 1968; Lensen and Otway, 1971; Sylvester and Pollard, 1975; Stein and Thatcher, 1981). Whether afterslip is truly aseismic has not been clearly established, although Stein and Lisowski (1983) found that afterslip following the 1979 Homestead Valley, California, earthquake ($M_L$ = 5.8) was much greater than the summed $M_0$ of the aftershocks, and they concluded that the afterslip, which constituted about 10 percent of the seismic slip, was aseismic.

*Dynamically triggered slip* is coseismic slip on a fault or faults outside the epicentral area of the main shock. The phenomenon has been documented in moderate earthquakes in the Salton Trough, where up to 30 mm slip was found on faults as far as 40 km from the causative fault and epicenter (Allen *et al.*, 1972; Fuis, 1982; Sieh, 1982). Ambiguities inevitably arise in the definition, however, such as in cases of the May 1983 Coalinga ($M_L$ = 6.7) earthquake where aftershocks and surface ruptures occurred on faults distant from and not be-

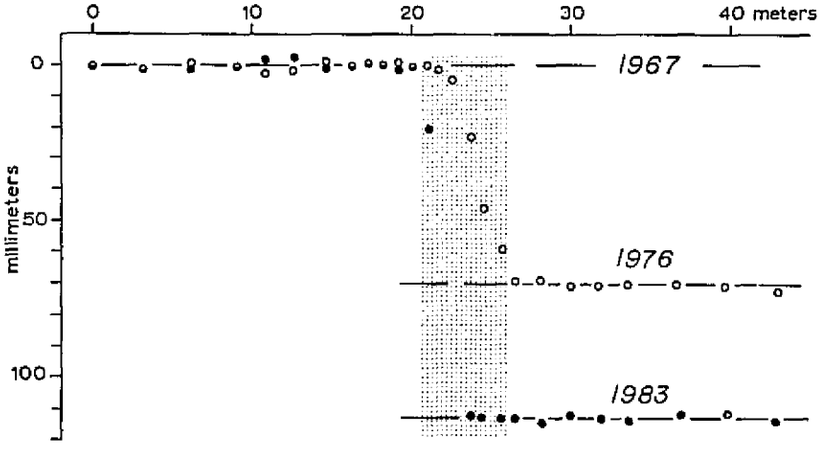


FIGURE 11.2 Offset of line of nails across San Andreas Fault near San Juan Bautista. Line was originally straight in 1967.

lieved to be directly related to the fault that caused the main earthquake (Hart and McJunkin, 1983; Stein, 1983). Some of the myriad of surface ruptures produced in the 1971 San Fernando ($M_L$ = 6.4) earthquake may have been dynamically triggered.

## METHODS, TECHNIQUES, AND RESULTS

Geodesists have classically documented the direction and magnitude of small crustal movements by repeated surveys of arrays of bench marks and by comparing changes in line lengths, angles, or heights among bench marks between an initial and a subsequent survey. If a surveying array covers a large area, then accumulated survey errors may yield changes of position that are nearly equal in magnitude to the actual movement. Thus the advantage of small fault-crossing networks is that they may yield more accurate displacement data; and because of their small size, they may be resurveyed more quickly and frequently, providing thereby, more nearly continuous sampling of movement (Table 11.2).

In the appraisal of fault movements, we wish to know where the movement occurs, which way the fault blocks move relative to each other, how much the offset is, and when it happens. Geologic rates of crustal movement and empirical determination of historic rates of fault displacements from progressive offset of cultural features show that a precision of at least 1 part per million is required to document ongoing tectonic movements in near-field geodetic work (NRC Panel on Recent Crustal Movements, 1981). That means reproducible resolution of at least 1 mm is generally necessary. At these high levels of precision, the question of bench-mark stability (Karcz *et al.*, 1976; Savage *et al.*, 1979b; Sylvester, 1983, 1984) also clouds interpretations of tectonic movements, because any small shift of a point that is assumed to be fixed or stable will yield systematic changes in other points that are not necessarily real.

All near-field geodetic arrays must be resurveyed periodically to establish bench mark and background and secular noise. Soviet scientists have found that earth background noise may be very unstable for a variety of known and unknown reasons; therefore, many repeated surveys are needed to characterize background noise (Nersesov, 1984). Out of several bench-mark stations, only a few may be good and reliable, but which ones can only be determined by observing them. Both the Soviet and Chinese experiences show that *networks* of instruments, especially a wide range of observations, together with good communication among participating scientists, are absolutely essential if earthquakes are ever to be predicted (Mei, 1984; Nersesov, 1984).

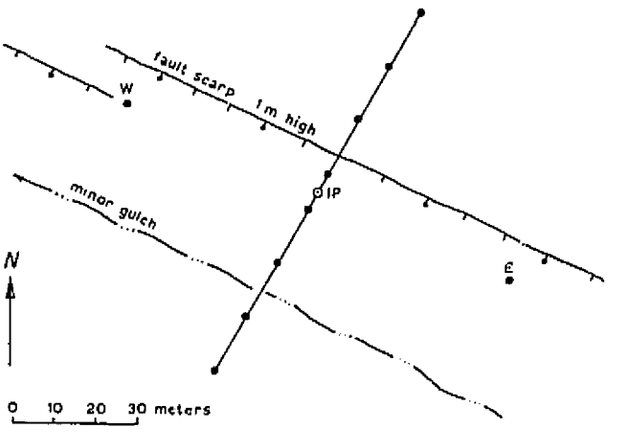


FIGURE 11.3 Alignment array across Nadeau branch of San Andreas Fault near Palmdale, California. E and W are wing stations, IP is the instrument point for the theodolite.

### *Horizontal Movements*

*Alignment Arrays* Perhaps the simplest and cheapest measurement technique for horizontal movements is to establish a line of nails in street pavement across a fault (Figure 11.2) and to measure their deflection over time relative to one or several arbitrarily fixed points (Rogers and Nason, 1971). If fault slip is discovered, then more expensive and rigorous techniques may be employed for more complete documentation of the spatial and temporal character of the movement. Typically nail lines, or "nail files" as they have come to be called (Louie *et al.*, 1985), contain from 10 to 50 nails in a line as long as 100 m established perpendicular to the fault strike. The position of each nail can be measured to within 1 mm with precision calipers relative to a straight line of sight provided by a theodolite.

Alignment arrays are also measured by triangulation. Using a theodolite, angles are turned from reference targets in directions parallel to the fault to nails driven into a line of utility poles, fences, or trees with a precision of 1 mm (Keller *et al.*, 1978; Aytun, 1980; Louie *et al.*, 1985). These kinds of arrays range in length from 100 to 500 m, are nearly perpendicular to the fault, and contain at least three points on each side of the fault (Figure 11.3). Their chief disadvantage is that their substandard bench marks will inevitably yield substandard results and thus limit their eventual utility for both coseismic and long-term changes.

Alignment arrays established by the U.S. Geological Survey (USGS) for more rigorous and precise determination of creep involve triangulation with a theodolite to specially designed targets placed above class B rod

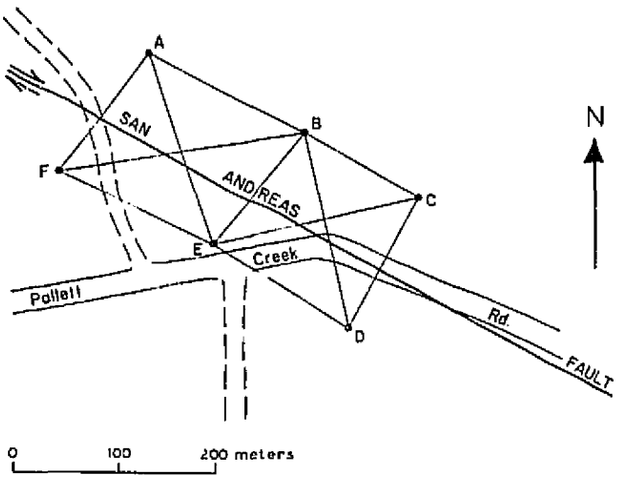


FIGURE 11.4 Doubly braced quadrilateral across the San Andreas Fault at Pallett Creek near Palmdale, California.

marks (Floyd, 1978) and yield a precision of 0.5 mm (Burford and Harsh, 1980). The USGS arrays were established in 1967-1974 along the creeping segment of the San Andreas Fault in central California to define the width of the creep zone more clearly as well as the variability of creep along strike. The arrays have about 15 bench marks in a line from 30 to 220 m long across the strike of the fault.

*Trilateration* The position of bench marks in closed arrays across faults (Figure 11.4) may be precisely determined by triangulation (e.g., Meade, 1971; Lensen and Otway, 1971; Henneberg, 1978, 1983) or trilateration. The former is tedious and time-consuming and still requires that a length be directly measured with high precision if displacements are to be resolved. More commonly, an array consisting of four bench marks—a quadrilateral—is established across a fault (Figure 11.4), and the lengths of each side and both diagonals are measured with an Invar tape or an electronic distance meter (EDM) with which a precision of 1 ppm is routinely achieved. Line lengths for EDM arrays range from 50 to 3000 m, depending on the topography and

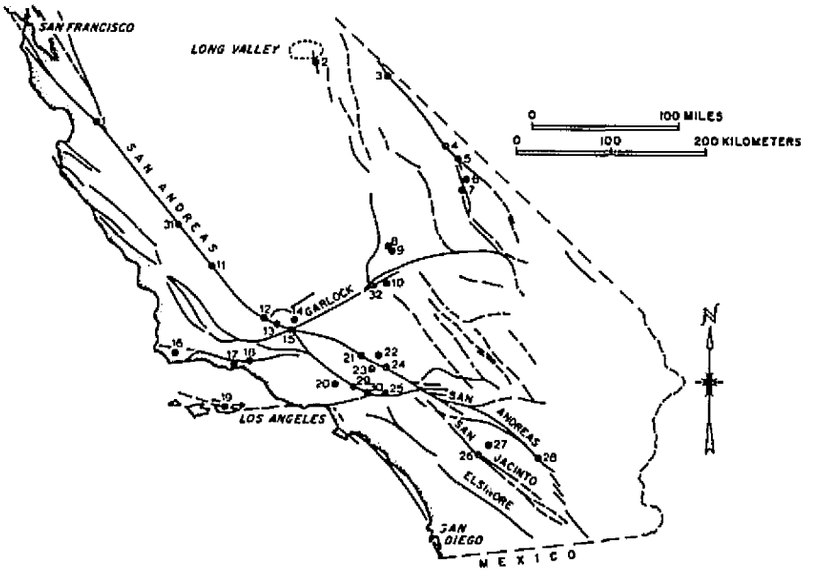


FIGURE 11.5 Locations of University of California, Santa Barbara, leveling arrays in central and southern California relative to major faults.

Key to Figure 11.5: Locations of UCSB Level Lines

(1) San Juan Bautista
(2) McGee Creek
(3) Fish Lake Valley
(4) Triangle Spring
(5) Sewage Plant
(6) Artist's Drive
(7) Shorty's Well
(8) SNORT
(9) Airfield
(10) Duravan Ranch
(11) Wallace Creek
(12) Camp Dix
(13) Caballo
(14) Grapevine
(15) Mesa Valley Farm
(16) JM Quarry
(17) Santa Barbara
(18) Jameson Lake
(19) Santa Cruz Island
(20) San Fernando
(21) Una Lake
(22) Llano
(23) Big Rock Springs
(24) Pallett Creek
(25) Dalton Canyon
(26) Anza
(27) Pinyon Flat
(28) Painted Canyon
(29) Arroyo Seco
(30) Santa Anita Canyon
(31) Parkfield
(32) Koehn Lake

the apparent width of the fault zone. The dimensions of taped quadrilaterals are smaller, from 1 to 50 m.

Horizontal displacements of bench marks are measured by resurveys of the array, and single bench-mark displacement-rate vectors and their standard deviations are computed from a variation of coordinates adjustment using all line-length change-rates and their standard deviations (Lisowski and Prescott, 1981).

The small-aperature trilateration studies complement creepmeter, strainmeter, alignment array, and broad-scale geodolite measurements (e.g., Savage *et al.*, 1979a) to show that (1) the creep rate in the central segment of the San Andreas Fault varies stepwise from less than 1 mm/yr at each end of the fault segment to 30 mm/yr at the center (Lisowski and Prescott, 1981); (2) the width of the main zone of slip is generally less than 70 m (Burford and Harsh, 1980); (3) episodic creep occurs in the Salton Trough at rates ranging from 1 to 10 mm/yr (Keller *et al.*, 1978; Louie *et al.*, 1985), although the infrequency of surveys there does not clearly show whether the fault slip is dynamically triggered or is truly tectonic creep (Goulty *et al.*, 1978); and (4) creep has been observed outside of California only on the North Anatolian Fault in eastern Turkey, where dextral creep of 10 mm/yr has taken place during the 10 years of geodetic monitoring (Aytun, 1980).

### *Vertical Movements*

Precise leveling is the most common method used to detect and document vertical crustal movements over periods of days to decades, because when compared with currently available alternatives, leveling is more stable over longer periods of time and long distances and is less costly and more accurate over short and moderate distances (Brown and Reilinger, 1980). If repeated sufficiently frequently, precise leveling may aid other geophysical techniques for earthquake prediction, as has been demonstrated in China (Tanaka, 1978; Mei, 1984; Zhu *et al.*, 1984). Preseismic fault offsets of 1- to 4-mm amplitude and from 50 to 200 km from the epicentral area were observed in the year prior to each of four $M$ = 7+ earthquakes in China (Zhang and Fu, 1981).

Tryggvason (1968) was one of the first to establish and frequently resurvey short leveling arrays of closely spaced bench marks to study small vertical fault movements in detail, although the U.S. Coast and Geodetic Survey established lines of closely spaced bench marks across the southern San Andreas Fault in the 1930s. A few lines, with only three or four bench marks in 1 or 2 km, were also established across the Atwater and Wairau Faults in New Zealand in 1930 (Mackie, 1971).

Because so few investigators are involved in this kind of work, it is instructive to outline the procedures and techniques employed in our studies of near-field tectonic strain. Following Tryggvason's (1968) example and since 1970, my students and I have established a variety of fault-crossing leveling arrays across strike-slip, normal, reverse, and thrust faults throughout southern and central California (Figure 11.5) to document in time and space the vertical movements that occur near different kinds of faults and to understand tectonic processes leading to, and following, fault rupture. For example, our straight-line array at San Juan Bautista (Figure 11.6) measures vertical separation across the San Andreas Fault (Figure 11.7), where horizontal creep is monitored by creepmeters (Sylvester *et al.*, 1980); our W-shaped array in the Garlock area northeast of the Mojave Desert (Figure 11.8) monitors nontectonic fault slip caused by groundwater withdrawal (Sylvester, 1982; Holzer, 1984) and in 9 years shows a constant height change across the fault of 35 mm/yr (Figure 11.9); straight lines across the Punchbowl Fault at Pallett Creek and across the Pleito Fault at Grapevine (Figure 11.10) measure movement across reverse and thrust faults (Figure 11.11); an irregular-

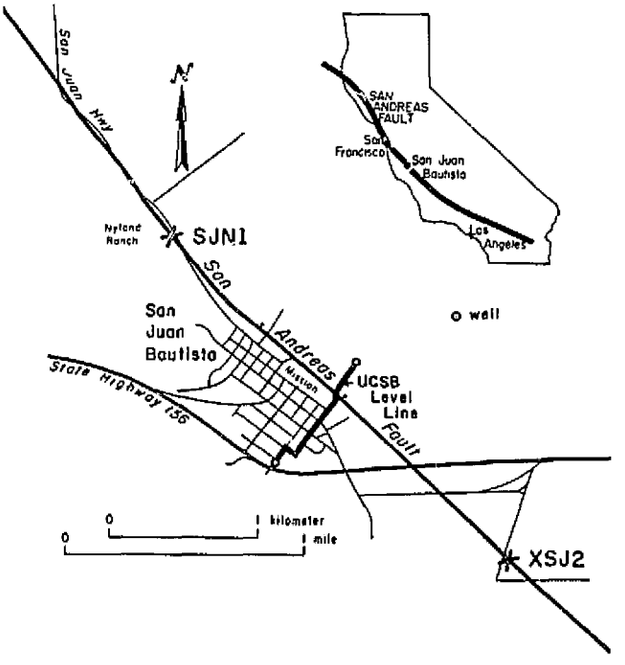


FIGURE 11.6 Site map for level line across San Andreas Fault at San Juan Bautista. SJN1 and XSJ2 are locations of the U.S. Geological Survey creepmeters for measurement of horizontal movement.

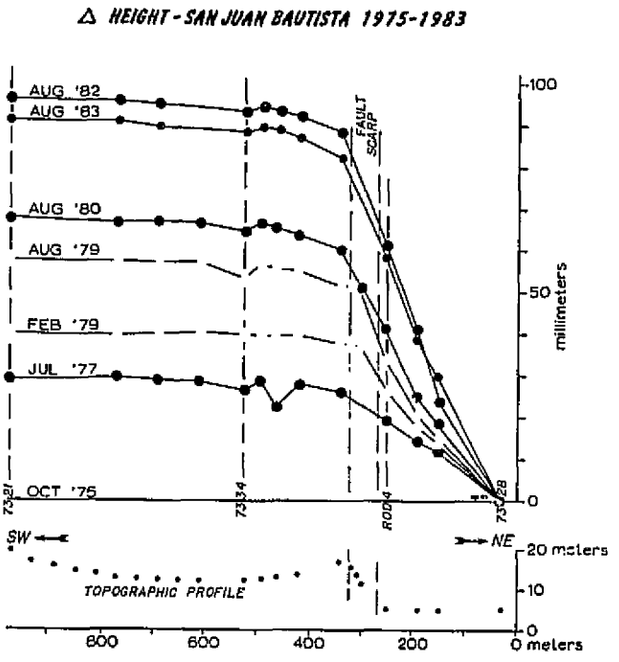


FIGURE 11.7 Height change data across San Andreas Fault at San Juan Bautista, 1975-1983. Bench mark 7328 is arbitrarily held fixed.

shaped array at Anza (Figure 11.12) detects minor vertical movements across a narrow, well-defined rift zone of the San Jacinto Fault (Figure 11.13); a closed quadrilateral across the San Andreas Fault at Wallace Creek (Figure 11.14) provides us two measurements of vertical offset across the fault as well as of the tilt of the fault blocks; lines in Death Valley and Long Valley are across youthful, normal faults; and the quadrilateral at the Pinyon Flat Geophysical Observatory (Figure 11.15) provides geodetic control for arrays of long-base fluid tiltmeters and other strain-measurement devices (Sylvester and Jackson, 1982; Sylvester, 1984).

We choose our surveying sites where geomorphic evidence shows that significant vertical movements have occurred in the recent geologic past, and we rely on other investigators to provide medium-range precursory information that identifies faults that may be in the preparation stages for a major earthquake. Then we establish arrays in the target area and resurvey them as frequently as possible and practical.

Like other investigators (e.g., Sharp and Lienkaemper, 1982), our procedure is to repeat precise leveling surveys of arrays of permanent bench marks established across active and potentially active faults. Comparison of surveys reveals height changes that then may be related spatially to surface faults and temporally to occurrences of earthquakes.

All our leveling arrays are relatively short—line lengths range from 200 to 2600 m and contain as many as 70 bench marks. Geometry of arrays is generally dictated by the terrain and property access and includes L-, Z-, W-, and closed, quadrilateral-shaped arrays (Sylvester, 1982). Some of the straight-line segments across faults are also aligned with a theodolite to document horizontal movement. Many of the fault-crossing arrays are quadrilateral-shaped to determine the tilt of each fault block independently by analyzing L-shaped subsets of bench marks (Figure 11.14).

Following Tryggvason (1968) and our accumulated

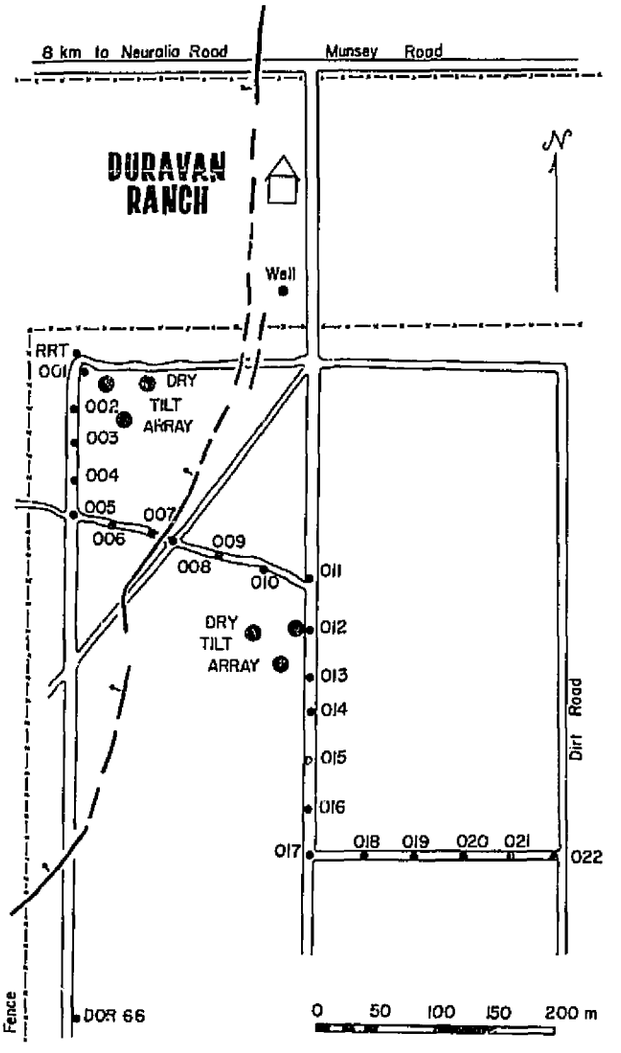


FIGURE 11.8 Site map of W-shaped leveling array across subsidence fault in Fremont Valley, California.

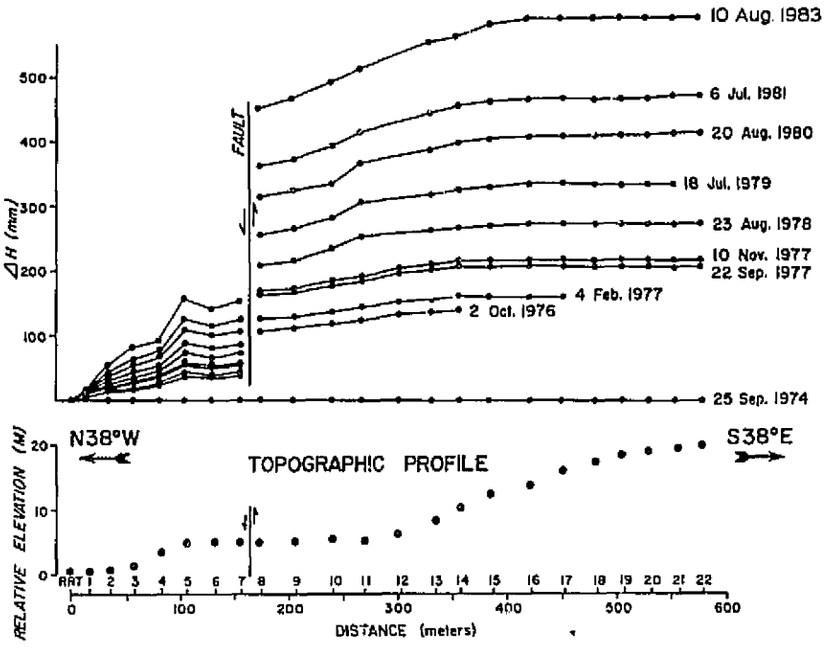


FIGURE 11.9 Height change data for subsidence fault at Duravan Range, Mojave Desert. Bench mark RRT is arbitrarily held constant.

experience, most turning points in our level are permanent bench marks no more than 40 m apart throughout the line, and permanently marked instrument points are exactly midway between bench marks. The relatively short, balanced sights minimize systematic errors from refraction and collimation, respectively, and assure that the rod images are sufficiently large to be read accurately. Our leveling is always double-run using a shaded precision automatic level and strut-supported Invar leveling rods. The same rod is always placed on the same bench mark in each successive survey, and our rods are annually calibrated every 10 cm along their entire length.

Perhaps because only a few investigators have been leveling in the near field for a short time in limited parts of the world, few reports of significant results are available in contrast to those from broad-scale leveling. A review of vertical preseismic, coseismic, and postseismic slip associated with U.S. earthquakes is given by Reilinger and Brown (1981). Vertical afterslip was indicated but not authenticated in two New Zealand earthquakes—the Murchison earthquake of 1929 (Henderson, 1937) and the Napier earthquake of 1931 (Henderson, 1933). Otherwise vertical afterslip has been documented in only four earthquakes. Sylvester and Pollard (1975) found that afterslip amounted to less than 1 percent of the coseismic vertical separation in the year following the 1971 San Fernando ($M$ = 6.4) earthquake; Sharp and Lienkaemper (1982) found that 14-cm afterslip, nearly equal to the coseismic slip of 16 cm, occurred in the 10 weeks following the 1979 Imperial Valley ($M$ = 6.5) earthquake; afterslip following the Alaskan ($M$ = 8.3) earthquake of 1964 reached 0.55 m over 10 years (Brown *et al.*, 1977; Prescott and Lisowski, 1977); Lensen and Suggate (1968) measured 12 mm of vertical afterslip in 2 months across the Inangahua Fault (New Zealand) after about 1 m of vertical separation in the 1968 Inangahua ($M$ = 7) earthquake. Near-field leveling revealed 54 μrad of crustal tilt 6 months before the Imperial Valley earthquake (Sharp and Lienkaemper, 1982), and significant tilt has also occurred before some Chinese earthquakes (Mei, 1984; Zhu *et al.*, 1984). Previous reports of regional tilt before Japanese earthquakes have been attributed to refraction errors in the leveling (Mogi, 1984).

Vertical movement across normal faults of the Asal-Ghoubbet rift, Dijoubti, East Africa, is regarded as aseismic creep by Ruegg *et al.* (1984), but vertical creep has not been observed elsewhere in spite of specific searches for it, especially in California (Sylvester, 1982).

## CRUSTAL TILT

Tilt of the Earth's surface has been observed prior to earthquakes by broad-scale leveling (e.g., Bendefy,

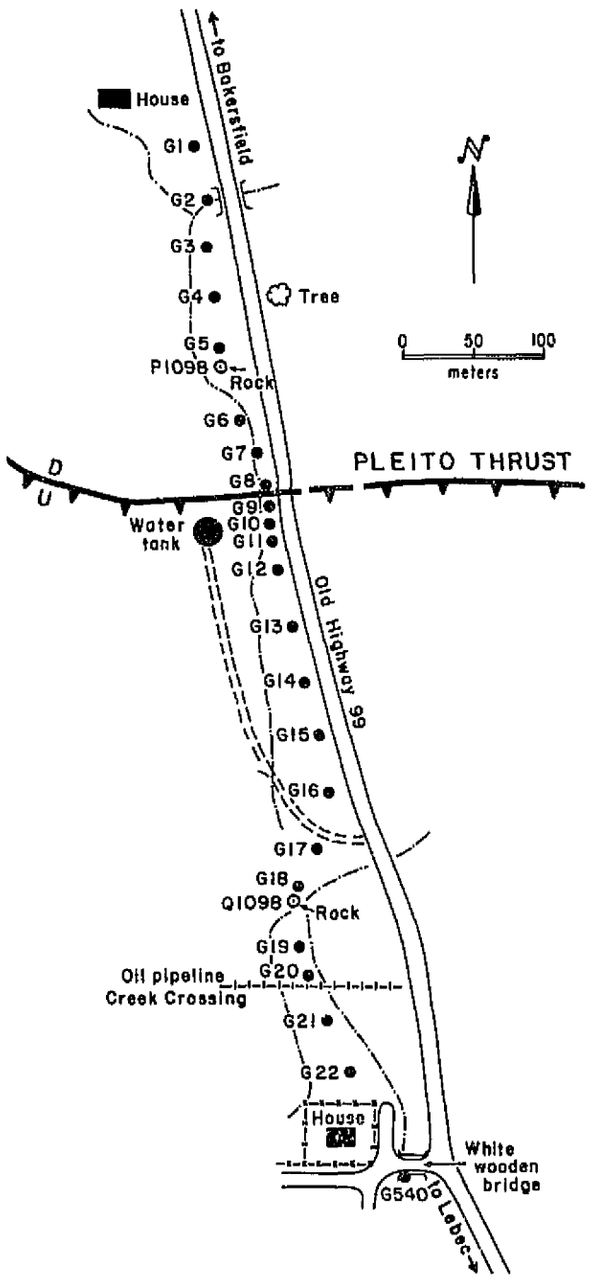


FIGURE 11.10 Site map of level line across Pleito thrust fault near townsite of Grapevine, California.

1958, 1965) and by near-field leveling (Sharp and Lienkaemper, 1982; Mei, 1984; Zhu *et al.*, 1984). Broad-scale leveling has also demonstrated recent influx of magma into the crust in the Yellowstone area (Pelton and Smith, 1982); beneath Long Valley caldera in eastern California (Savage and Clark, 1982); beneath Mount Etna (Murray and Guest, 1982); and in the rift zone of northern Iceland (Björnsson *et al.*, 1979). Magmatic inflation of volcanoes has been geodetically monitored for many years at Kilauea and Mauna Loa Volcanoes on Hawaii (Kinoshita *et al.*, 1974; Decker *et al.*, 1983) and more recently at Mount St. Helens (Chadwick *et al.*, 1983).

One of the small-scale, geodetic methods for monitoring fairly large tilt is spirit-level optical tilting (Kinoshita *et al.*, 1974) or dry-tilt as it is popularly termed. The dry-tilt method determines tilt of a plane defined by three or more bench marks by measuring height differences among the bench marks between two separate surveys (Sylvester, 1978; Yamashita, 1981). Both in our work and in Hawaii a shaded precision level is erected at the center of an array of at least three permanent bench marks on each of which three precise Invar leveling rods are erected simultaneously (Figure 11.16). We take care to choose sites for dry tilt that are reasonably flat; that have radial symmetry; and that are not near oil and water wells, landslides, or recently imposed construction loads such as bridges, buildings, and land fills. In our experience, the noisiest data are obtained from tilt sites on ridge crests and forested areas on bedrock, whereas data showing least noise are obtained from sites on wide open flats underlain by relatively thick deposits of alluvium.

In Hawaii the dry-tilt measurements complement those of borehole tiltmeters, and short-base (3 m) and long-base (50 m) water-tube tiltmeters. With superior equipment in good adjustment, with careful attention to detail, and with rigorous systematic measurement procedure, a resolution of from 2 to 3 μrad has been achieved in Hawaii as shown in comparative tests with the 50-m water-tube tiltmeter. In general, however, resolution of tilt with three point arrays ranges from 5 to 10 μrad (Isacks *et al.*, 1978; Björnsson *et al.*, 1979; Savage *et al.*, 1979b; Decker *et al.*, 1983; Otway *et al.*, 1984). Therefore, the dry-tilt method is best suited for monitoring large and fairly rapid tilts, from tens to hundreds of microradians per day which may be expected to accompany magmatic inflation of volcanoes (Dzurisin *et al.*, 1982a,b; 1983; Fiske and Shepard, 1982; Chadwick *et al.*, 1983). For more precise determination of tectonic tilt, long L- and T-shaped and closed arrays of bench marks having apertures of from 500 to 1000 m

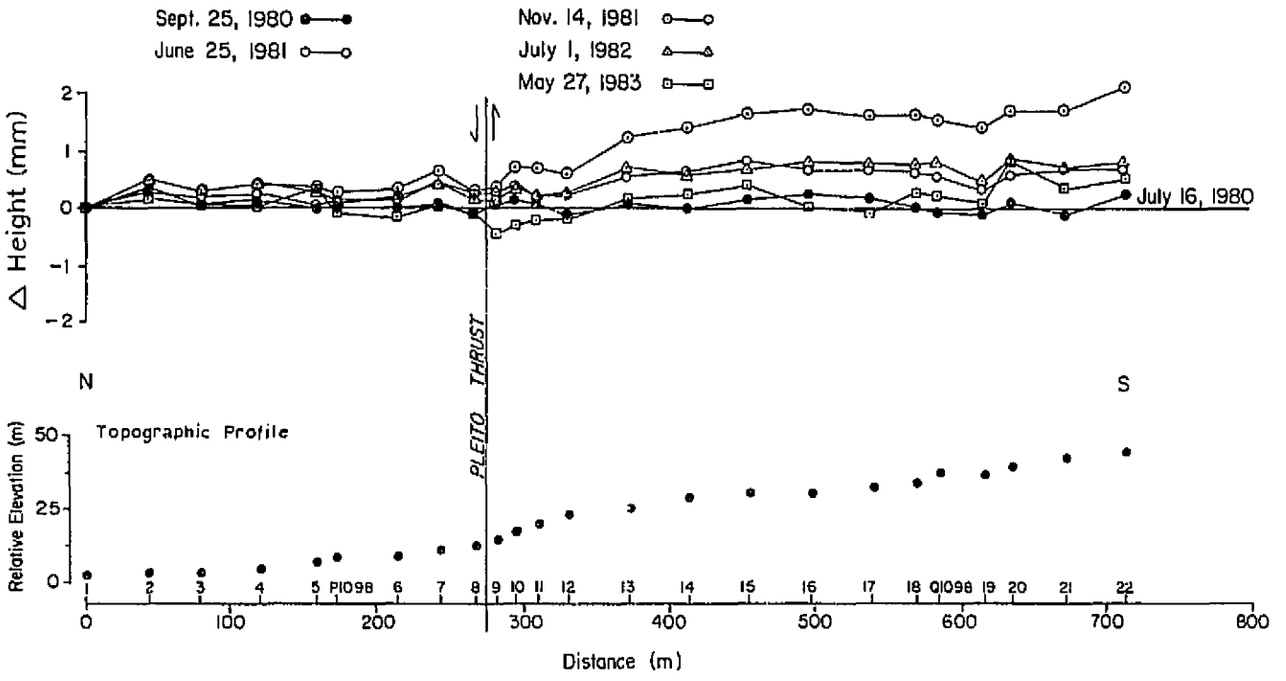


FIGURE 11.11 Height change data cross the Pleito thrust fault, 1980-1983. Bench mark 1 is arbitrarily held fixed.

are necessary (Savage *et al.*, 1979b). With such figures it is possible to achieve resolution approaching 0.5 $\mu$rad (Sylvester and Jackson, 1982).

## PROBLEMS

Although there is a fairly voluminous literature on the origin of creep and related minor fault movements, systematic near-field geodetic measurements of these movements have proceeded only about two decades—now only beginning to be a significant length of time. Thus it is imperative that this time base of data be lengthened to obtain empirical data to answer and refine earlier answers to the following questions.

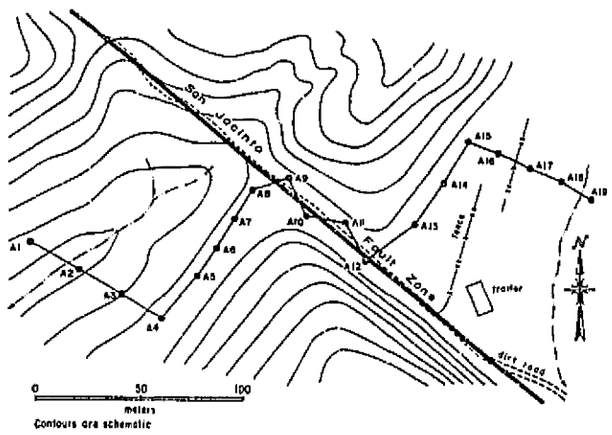


FIGURE 11.12 Site map of irregular leveling array across San Jacinto Fault near Anza, California.

### *Creep*

(1) Why, with but the exception of the North Anatolian Fault in Turkey (Aytun, 1980), is creep restricted to the central and southern segments of the San Andreas Fault? Is it because the fault is relatively straight and parallel to the lithospheric plate motion, that in its central segment it juxtaposes relatively weak, serpentine-bearing rocks as several authors have maintained?

(2) Why is vertical creep so uncommon? Is it simply because the search has not been sufficiently broad in scope and duration? Or are there more fundamental tectonic reasons?

(3) How does creep relate to the earthquake mechanism? Is it a safety valve that periodically releases stress, thus precluding great earthquakes as many authors believe? Or is creep a form of long-term, preseismic slip for a truly great earthquake?

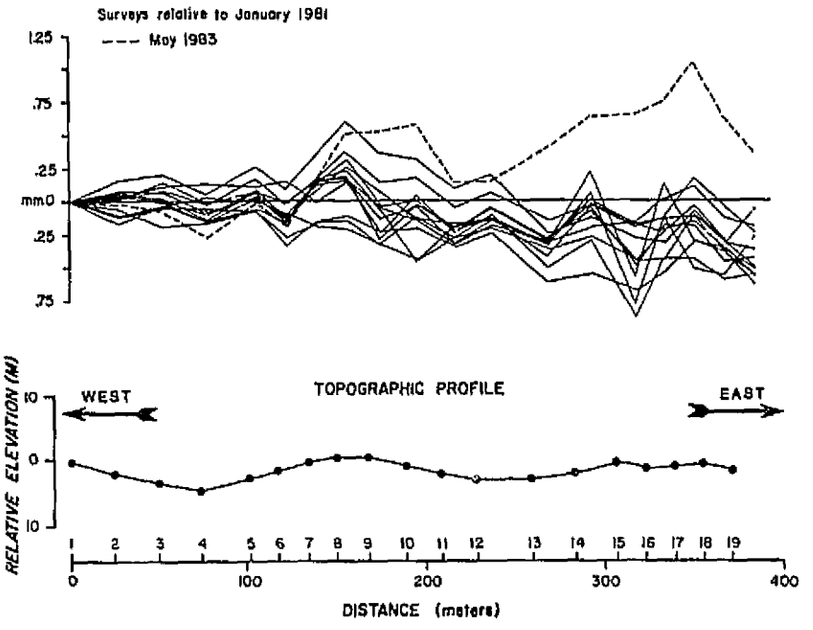


FIGURE 11.13 Height changes of bench marks across San Jacinto Fault near Anza, California, 1981-1983. Bench mark 1 is arbitrarily held fixed.

*Preseismic Slip*

Leveling evidence for vertical preseismic slip is generally sparse and ambiguous (Reilinger and Brown, 1981), but some fundamental questions arise.

(1) Does preseismic slip occur only on faults that are also characterized by creep?

(2) Does discrete vertical preseismic slip occur, or are preseismic movements typified only by bending, warping, or tilt?

(3) What is the temporal relation of onset and duration of creep to the impending main earthquake?

*Afterslip*

(1) Is afterslip truly aseismic, or is it caused incrementally by aftershocks? Continuously recording creepmeters may study this question, but the full range of the movement zone generally needs to be covered geodetically.

(2) Is significant afterslip restricted to strike-slip earthquakes? Afterslip is nearly equal to coseismic slip in strike-slip earthquakes, but less than 5 percent of coseismic movement in normal and reverse fault earthquakes. Why?

(3) Just what is the mechanism for afterslip? Some authors (e.g., Rundle and Jackson, 1977; Wahr and Wyss, 1980) maintain that it is a viscoelastic relaxation phenomenon, others regard afterslip as a quasi-static relaxation of stress changes (Matsu'ura and Iwasaki, 1983), while still others (e.g., Burford, 1972) regard afterslip as time-delayed propagation from bedrock offset through overlying cover rocks. The latter view is questioned (Sylvester and Pollard, 1975; Bucknam *et al.*, 1978), but more observations and measurements are clearly needed.

*Dynamically Triggered Slip*

(1) Does dynamically triggered slip represent release of a fraction of stored elastic strain energy along a given fault, or is it just a manifestation of jiggling of two fault blocks caused by shaking? A related question is how can quite small slips (1 to 30 mm) occur over such long (22 km) fault segments (Fuis, 1982; Sieh, 1982)?

(2) Why isn't dynamically triggered slip more common and widespread? Perhaps it is, but because of general preoccupation with the main fault rupture, seldom are careful investigations made of nearby faults. Certainly attention must be paid to surrounding faults following moderate and large earthquakes just to increase the base of data from the two clear examples at hand.

(3) Does dynamically triggered slip occur along segments of faults destined to be the loci of earthquakes in the near future? Thus, is dynamically triggered slip a

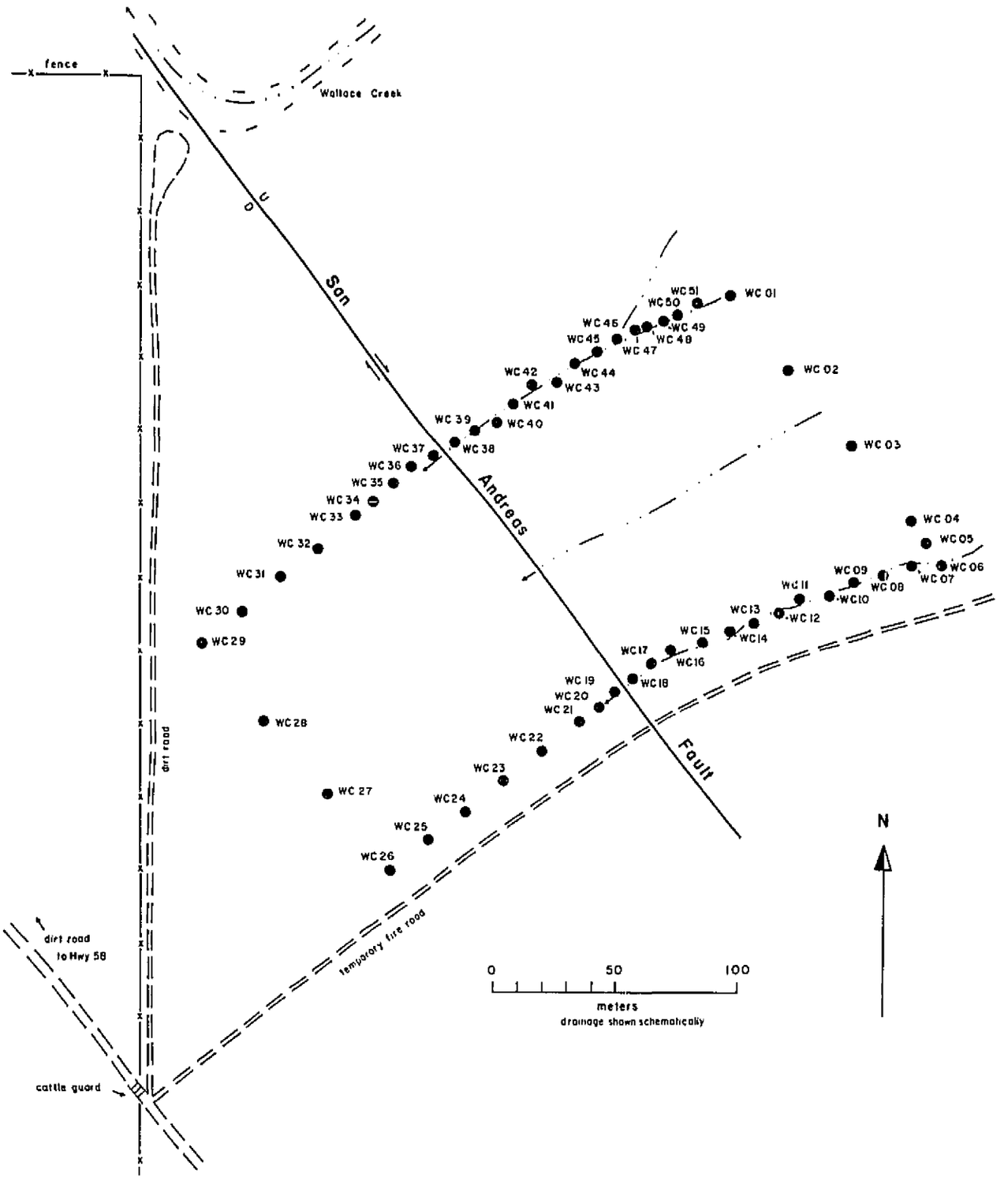


FIGURE 11.14 Site map of closed leveling array across the San Andreas Fault near Wallace Creek, Carizzo Plain, California.

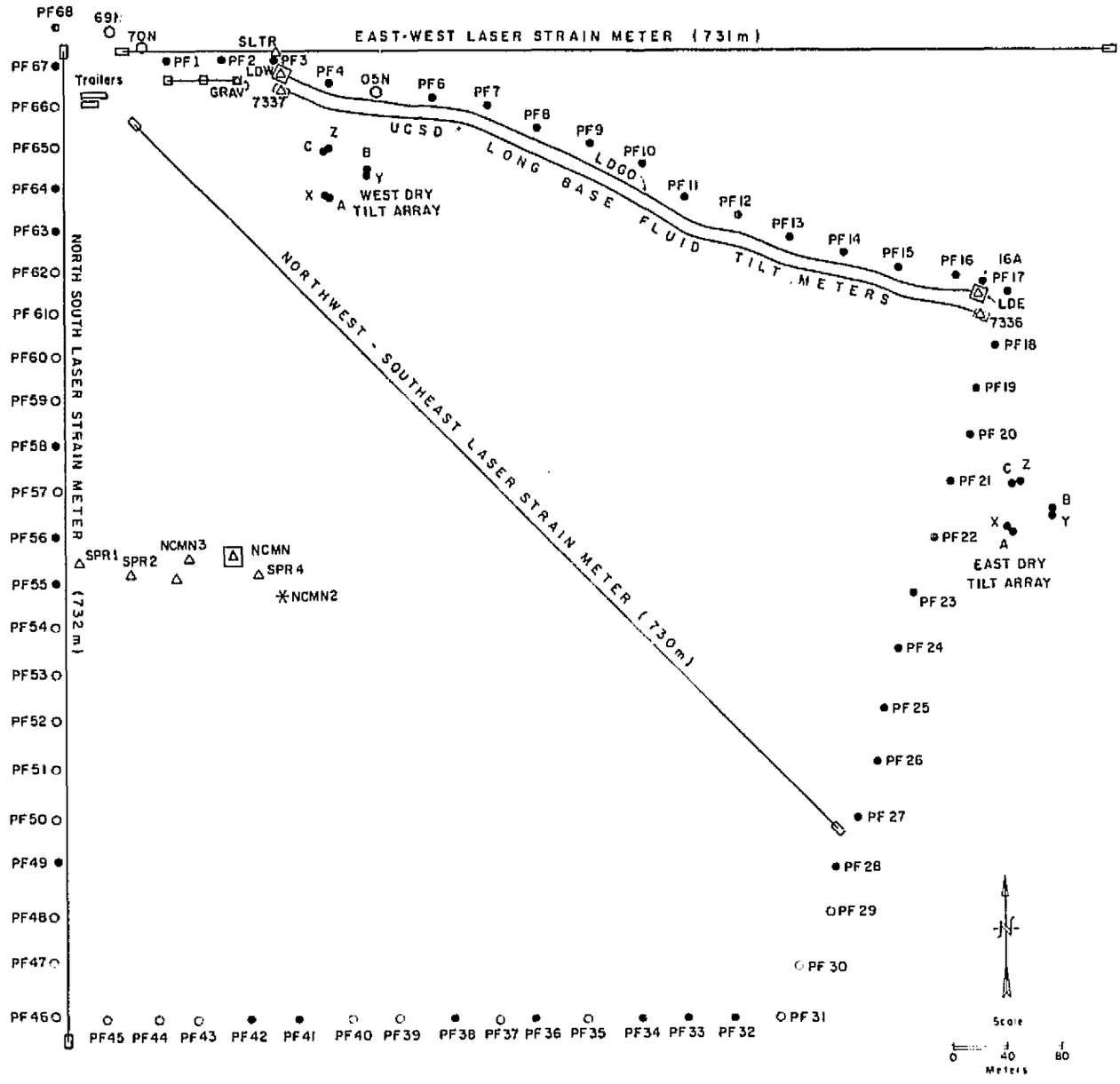


FIGURE 11.15 Site map of closed leveling array at Pinyon Flat Geophysical Observatory near Palm Springs, California. From Sylvester (1984) with permission of the American Geophysical Union.

form of precursory slip as suggested by Sieh (1982) from a limited base of observations? To date, dynamically triggered slip has been documented for only the Salton Trough of southern California. Is its identification there a function of good exposure, many postseismic investigations, and instrumental coverage? Or is it a function of the tectonics? Here, too, the data base must be increased considerably.

## CONCLUSIONS

Near-field tectonic geodesy has been instrumental in documentation of minor fault movements that follow earthquakes together with those that are aseismic and coseismic. Although continuously recording instruments such as creepmeters, strainmeters, and tiltmeters provide important time-history data, geodetic informa-

tion is required to know where to establish instruments in the first place, to provide a spatial range of observations intermediate between broad-range geodesy and the instruments, and to maintain a monitoring capability over periods of time far longer than are feasible or economic for continuous instrumental coverage.

Owing to the high degree of precision required for near-field measurements, careful attention must be paid to the kind and method of emplacement of bench marks. They must be made to have a half-life of at least 50 yr and should have secular movements of no more than about 0.25 mm.

In most cases, investigations seem to have required about 10 yr from the time of establishment of a given geodetic array to first publication of significant results. Such a length of time is probably necessary to quantify the noise—including bench-mark motions, survey errors, and Earth noise in the particular arrays, methods, and part of the world. Thus near-field geodetic studies are necessarily, or at least typically, long term, and agencies and institutions that provide initial support must realize the nature of the long-term commitment here to investigate a geologic phenomenon on a human time scale. It cannot be guaranteed that the Earth will cooperate and yield significant results in the course of a grant or contract period or soon enough to provide grist for a series of publications that will assist in promotion for a young assistant professor.

The Earth moves, often slowly and inexorably. To study these movements carefully requires time, patience, and not a little luck. To understand these movements requires long-time series of data—more than exist today.

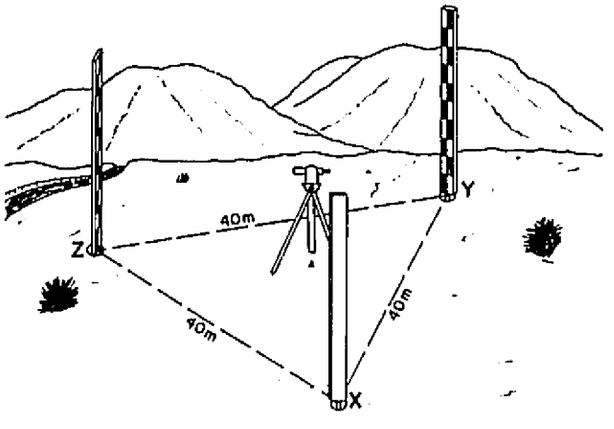


FIGURE 11.16 Diagrammatic representation of dry-tilt array.

## REFERENCES


Allen, C. R., and S. W. Smith (1966). Pre-earthquake and post-earthquake surficial displacements, in Parkfield earthquakes of June 27-29, 1966, Monterey and San Luis Obispo Counties, California, preliminary report, *Bull. Seismol. Soc. Am. 56*, 966-967.

Allen, C. R., M. Wyss, J. N. Brune, A. Grantz, and R. E. Wallace (1972). Displacements on the Imperial, Superstition Hills and the San Andreas Faults triggered by the Borrego Mountain earthquake, *U.S. Geol. Surv. Prof. Paper 787*, 87-104.

Ambrayses. N. N. (1970). Some characteristic features of the Anatolian Fault zone, *Tectonophysics 9*, 143-165.

Aytun, A. (1980). Creep measurements in the Ismetpasa region of the North Anatolian Fault zone, in *Proceedings, Multidisciplinary Approach to Earthquake Prediction*, A. M. Isikara and A. Vogel, eds., Friedr. Vieweg and Sohn, Braunswelg/Wiesbaden, pp. 279-292.

Bendefy, L. (1958). Seismotectonic examinations in the surroundings of Budapest (new points of view and methods to examine the connections between seismic disturbances and the Earth's crust), *Geogr. Anzeiger 7, Jg. Budapest.*

Bendefy, L. (1965). Elastic, plastic and permanent deformations of the earth's crust in connection with earthquakes, *Recent Crustal Movements, Finland.*

Björnsson, A., G. Johnsen, S. Siguardsson, G. Thorbergsson, and E. Tryggvason (1979). Rifting of the plate boundary in north Iceland 1975-1978, *J. Geophys. Res. 84*, 3029-3038.

Brown, L. D., and R. E. Reilinger (1980). Releveling data in North America, implications for vertical motions of plate interior, in *Dynamics of Plate Interiors*, A. W. Bally, P. L. Bender, T. R. McGetchin, and R. I. Walcott, eds., Geodynamics Ser. 1, Am. Geophys. Union, Washington, D.C., pp. 131-144.

Brown, L. D., R. E. Reilinger, S. R. Holdahl, and E. I. Balazs (1977). Post-seismic crustal uplift near Anchorage, Alaska, *J. Geophys. Res. 82*, 3369-3378.

Brown, R. D., and R. E. Wallace (1968). Current and historic fault movement along the San Andreas Fault between Paicines and Camp Dix, California, in *Proceedings, Conference on Geologic Problems of the San Andreas Fault System*, W. R. Dickinson and A. Grantz, eds., Stanford Univ. Publ. in Geol. Sci., Vol. 11, pp. 22-39.

Bucknam, R. C., G. Plafker, and R. V. Sharp (1978). Fault movement (afterslip) following the Guatemala earthquake of February 4, 1976, *Geology 6*, 170-173.

Burford, R. O. (1972). Continued slip on the Coyote Creek Fault after the Borrego Mountain earthquake, in The Borrego Mountain Earthquake of April 9, 1968, R. V. Sharp, ed., *U.S. Geol. Surv. Prof. Paper 787*, pp. 105-111.

Burford, R. O., and P. W. Harsh (1980). Slip on the San Andreas Fault in central California from alinement array surveys, *Bull. Seismol. Soc. Am. 70*, 1233-1262.

Burford, R. O., S. S. Allen, R. J. Lamson, and D. D. Goodreau (1973). Accelerated fault creep along the central San Andreas Fault after moderate earthquakes during 1971-73, in *Proceedings, Conference on Tectonic Problems of the San Andreas Fault System*, R. L. Kovach and A. Nur, eds., Stanford Univ. Publ. in Geol. Sci. 13, pp. 268-274.

Chadwick, W. W., Jr., D. A. Swanson, E. Y. Iwashubo, C. C. Heliker, and T. A. Leighley (1983). Deformation monitoring at Mount St. Helens in 1981 and 1982, *Science 221*, 1378-1380.

Cohn, S. N., C. R. Allen, R. Gilman and N. R. Goulty (1982). Pre-earthquake and post-earthquake creep on the Imperial Fault and the Brawley Fault zone, in The Imperial Valley, California, Earthquake of October 15, 1979, *U.S. Geol. Surv. Prof. Paper 1254*, pp. 161-168.

Decker, R. W., R. Y. Koyanagi, J. J. Dvorak, J. P. Lockwood, A. T. Okamura, K. M. Yamashita, and W. R. Tanigawa (1983). Seismicity and surface deformation of Mauna Loa Volcano, Hawaii, *EOS 64*, 545-547.

Dzurisin, D., K. Cashman, and A. G. Sylvester (1982a). Tilt measurements at Long Valley Caldera, California, May-August 1982, *U.S. Geol. Surv. Open-File Rep. 82-893*, 34 pp.

Dzurisin, D., D. J. Johnson, T. L. Murray, and B. Myers (1982b). Tilt networks at Mount Shasta and Lassen Peak, California, *U.S. Geol. Surv. Open-File Rep. 82-670*, 42 pp.

Dzurisin, D., K. J. Johnson, and R. B. Symonds (1983). Dry tilt at Mount Rainier, Washington, *U.S. Geol. Surv. Open-File Rep. 83-277*, 18 pp.

Evans, K. F., R. O. Burford, and G. C. P. King (1981). Propagating episodic creep and the aseismic slip behavior of the Calaveras Fault north of Hollister, California, *J. Geophys. Res. 86*, 3721-3735.

Fiske, R. S., and J. B. Shepard (1982). Deformation studies on Soufriere, St. Vincent, between 1977 and 1981, *Science 216*, 1125-1126.

Floyd, R. P. (1978). Geodetic bench marks, *NOAA Manual NOS NGT 1*, 50 pp.

Fuis, G. S. (1982). Displacement on the Superstition Hills Fault triggered by the earthquake, in The Imperial Valley, California, Earthquake of October 15, 1979, *U.S. Geol. Surv. Prof. Paper 1254*, 145-154.

Goulty, N. R., R. O. Burford, C. R. Allen, R. Gilman, C. E. Johnson, and R. P. Keller (1978). Large creep events on the Imperial Fault, California. *Bull. Seismol. Soc. Am. 68*, 517-521.

Harsh, P. W. (1982). Distribution of afterslip along the Imperial Fault, in The Imperial Valley, California, Earthquake of October 15, 1979, *U.S. Geol. Surv. Prof. Paper 1254*, 193-204.

Hart, E. W., and R. D. McJunkin (1983). Surface faulting northwest of Coalinga, California, June and July 1983, in *The 1983 Coalinga, California, Earthquakes*, J. H. Bennett and R. W. Sherburne, eds., Calif. Div. Mines and Geol. Spec. Publ. 66, pp. 201-219.

Henderson, J. (1933). The geological aspects of the Hawke's Bay earthquakes, *Bull. N.Z. Dep. Sci. Ind. Res. 43*.

Henderson, J. (1937). The West Nelson earthquakes of 1929, *Bull. N.Z. Dep. Sci. Ind. Res. 55*.

Henneberg, H. G. (1978). Local precision nets for monitoring movements of faults and large engineering structures, in *Proceedings of the 9th GEOP Conference: An International Symposium on the Applications of Geodesy to Geodynamics*, Ohio State Univ., Columbus, Ohio, pp. 113-130.

Henneberg, H. G. (1983). Geodetic control of neotectonics in Venezuela, *Tectonophysics 97*, 1-17.

Holzer, T. L. (1984). Ground failure induced by groundwater withdrawal from unconsolidated sediments, in *Man-Induced Land Subsidence*, T. L. Holzer, ed., Geol. Soc. Am. Rev. in Eng. Geol. VI, pp. 67-105.

Isacks, B. L., G. Hade, R. Campillo, M. Bevis, D. Chinn, J. Dubois, J. Rtecy, and J.-L. Saos (1978). Measurements of tilt in the New Hebrides island arc, in Proceedings of Conference VII, Stress and Strain Measurements Related to Earthquake Prediction, *U.S. Geol. Surv. Open-File Rep. 79-370*, 176-221.

Karez, I., J. Morreale, and F. Porebski (1976). Assessment of bench mark credibility in the study of recent vertical crustal movements, *Tectonophysics 33*, t1-t6.

Keller, R. P., C. R. Allen, R. Gilman, N. R. Goulty, and J. A. Hileman (1978). Monitoring slip along major faults in southern California, *Bull. Seismol. Soc. Am. 68*, 1187-1190.

King, C-Y., R. D. Nason, and D. Tocher (1973). Kinematics of fault creep. *Phil. Trans. R. Soc. London Ser. A, 274*, 355-360.

Kinoshita, W. T., D. A. Swanson, and D. B. Jackson (1974). The measurement of crustal deformation related to volcanic activity at Kilauea Volcano, Hawaii, in *Physical Volcanology*, L. Civetta, P. Gasperini, G. Luongo, and A. Rapolla, eds., Elsevier, New York, pp. 87-113.

Langbein, J. O. (1981). An interpretation of episodic slip on the Calaveras near Hollister, California, *J. Geophys. Res. 86*, 4941-4948.

Lensen, G. J., and P. M. Otway (1971). Earthshift and post-earthshift deformation associated with the May 1968 Inangahua earthquake, New Zealand, *R. Soc. N.Z. Bull. 9*, 107-116.

Lensen, G. J., and R. P. Suggate (1968). Preliminary reports on the Inangahua earthquake, New Zealand, May 1968, *Bull. N.Z. Dep. Sci. Ind. Res. 193*, 17-36.

Lensen, G. J., and R. P. Suggate (1969). Proposals for earth deformation studies, *Bull. N.Z. Dep. Sci. Ind. Res. 44*.

Lisowski, M., and W. H. Prescott (1981). Short-range distance measurements along the San Andreas Fault system in central California, 1975-1979, *Bull. Seismol. Soc. Am. 71*, 1607-1624.

Louie, J. N., C. R. Allen, D. C. Johnson, P. C. Haase, and S. N. Cohn (1985). Fault slip in southern California, *Bull. Seismol. Soc. Am. 75*, 811-834.

Macdonald, C., F. Wyatt, A. Sylvester, T. Owen, R. Bilham, and D. Jackson (1983). More tilt observations at Pinyon Flat Observatory, *EOS 64*, 679.

Mackie, J. B. (1971). Geodetic studies of crustal movement in New Zealand, *R. Soc. N.Z. Bull. 9*, 121-125.

Matsu'ura, M., and T. Iwasaki (1983). Study on coseismic and postseismic crustal movements associated with the 1923 Kanto earthquake, *Tectonophysics 97*, 201-215.

Meade, B. K. (1971). Horizontal movement along the San Andreas Fault system, *R. Soc. N.Z. Bull. 9*, 175-179.

Mei, Shirong (1984). Short-term and immediate precursors to continental earthquakes in China, in *A Collection of Papers of International Symposium on Continental Seismicity and Earthquake Prediction*, Gu Gongxu and Ma Xingyuan, eds., Seismological Press, Beijing, China, pp. 440-461.

Mjachkin, V. F., G. A. Sobolev, N. A. Dolbilkina, V. N. Morozow, and V. B. Preobrozensy (1972). The study of variations in geophysical fields near focal zones of Kamchatka, *Tectonophysics 14*, 287-293.

Mogi, K. (1984). Fundamental studies on earthquake prediction, in *A Collection of Papers of International Symposium on Continental Seismicity and Earthquake Prediction*, Gu Gongxu and Ma Xingyuan, eds., Seismological Press Beijing China, pp. 619-652.

Murray, J. B., and J. E. Guest (1982). Vertical ground deformation on Mt. Etna, 1975-1980, *Geol. Soc. Am. Bull. 93*, 1160-1175.

Nakamura, T., and Y. Tsuneishi (1967). Ground cracks at Matsushiro, probably of underlying strike slip origin, *Bull. Earthquake Res. Inst. (Tokyo Univ.) 45*, 417-471.

Nason, R. D. (1973). Fault creep and earthquakes on the San Andreas Fault, in *Proceedings, Conference of Tectonic Problems of the San Andreas Fault System*, R. L. Kovach and A. Nur, eds., Stanford Univ. Publ. in Geol. Sci. 13, pp. 275-285.

Nason, R. D., and D. Tocher (1970). Measurement of movement on the San Andreas Fault, in *Earthquake Displacement Fields and Rotation of the Earth*, L. Mansinha, *et al.*, eds., Reidel, Dordrecht, Holland.

Nason, R. D., and D. Tocher (1971). Anomalous fault slip rates before and after the April 1961 earthquake near Hollister, California, *EOS 52*, 278.

Nason, R. D., F. R. Philippsborn, and P. A. Yamashita (1974). Catalog of creepmeter measurements in central California from 1968 to 1972, *U.S. Geol. Surv. Open-File Rep. 74-31*.

Nersesov, I. L. (1984). Development of earthquake prediction in the

USSR, in *A Collection of Papers of International Symposium on Continental Seismicity and Earthquake Prediction*, Gu Gongxu and Ma Xingyuan, eds., Seismological Press, Beijing, China, pp. 373-383.

Niemczyk, O. (1943). *Spalten auf Island*, Konrad Witter, Stuttgart.

NRC Panel on Recent Crustal Movements (1981). *Geodetic Monitoring of Tectonic Deformation—Toward a Strategy*, National Academy Press, Washington, D.C., 109 pp.

Otway, P. M., G. W. Grindley, and A. G. Hull (1984). Earthquakes, active fault displacements and associated vertical deformation near Lake Taupo volcanic zone, *Bull. N.Z. Dep. Sci. Ind. Res. 110*, 73 pp.

Pelton, J. R., and R. B. Smith (1982). Contemporary vertical surface displacement in Yellowstone National Park, *J. Geophys. Res. 87*, 2745-2761.

Prescott, W. H., and M. Lisowski (1977). Deformation at Middleton Island, Alaska, during the decade after the Alaskan earthquake of 1964, *Bull. Seismol. Soc. Am. 67*, 579-586.

Prescott, W. H., and M. Lisowski (1983). Strain accumulation along the San Andreas Fault system east of San Francisco Bay, California, *Tectonophysics 97*, 41-56.

Reid, H. F. (1910). The California earthquake of April 18, 1906—Mechanics of the earthquake, *Carnegie Inst. Wash. Publ. 87*, Vol. 3.

Reilinger, R. E., and L. D. Brown (1981). Neotectonic deformation, near-surface movements and systematic errors in U.S. releveling measurements, in *Earthquake Prediction: An International Review*, D. W. Simpson and P. G. Richards, eds., M. Ewing Ser. 4, Am. Geophys. Union, Washington, D.C., pp. 422-440.

Rogers, T. H., and R. D. Nason (1971). Active fault displacement on the Calaveras Fault zone at Hollister, California, *Bull. Seismol. Soc. Am. 61*, 399-416.

Ruegg, J. C., M. Kasser, and J. C. Lepine (1984). Strain accumulation across the Asal-Ghoubbet rift, Dijoubti, East Africa, *J. Geophys. Res. 89*, 6237-6246.

Rundle, J. B., and D. D. Jackson (1977). A viscoelastic relaxation model for post-seismic deformation from the San Francisco earthquake of 1906, *Pure Appl. Geophys. 115*, 401-412.

Savage, J. C., and M. M. Clark (1982). Magmatic resurgence in Long Valley caldera, California; possible cause of the 1980 Mammoth Lakes earthquake, *Science 217*, 531-533.

Savage, J. C., W. H. Prescott, M. Lisowski, and N. King (1979a). Geodolite measurements of deformation near Hollister, California, 1971-1978, *J. Geophys. Res. 84*, 7599-7615.

Savage, J. C., W. H. Prescott, J. H. Chamberlain, M. Lisowski, and C. E. Mortenson (1979b). Geodetic tilt measurements along the San Andreas Fault in central California, *Bull. Seismol. Soc. Am. 69*, 1965-1981.

Scholz, C. H., L. R. Sykes, and Y. P. Aggarwal (1973). Earthquake prediction: A physical basis, *Science 181*, 803-810.

Sharp, R. V., and J. L. Lienkaemper (1982). Pre-earthquake and post-earthquake near-field leveling across the Imperial Fault and Brawley Fault zones, in The Imperial Valley, California, Earthquake of October 15, 1979, *U.S. Geol. Surv. Prof. Paper 1254*, pp. 169-182.

Sieh, K. E. (1982). Slip along the San Andreas Fault associated with the earthquake, in The Imperial Earthquake of October 15, 1979, *U.S. Geol. Surv. Prof. Paper 1254*, pp. 155-160.

Smith, S. W., and M. Wyss (1968). Displacement on the San Andreas Fault subsequent to the 1966 Parkfield earthquake, *Bull. Seismol. Soc. Am. 58*, 1955-1973.

Stein, R. S. (1983). Reverse slip on a buried fault during the 2 ? day 1983 Coalinga earthquake: Evidence from geodetic elevation changes, in *The 1983 Coalinga, California, Earthquakes*, J. H. Bennett and R. W. Sherburne, eds., Calif. Div. Mines and Geol. Spec. Publ. 66, pp. 151-163.

Stein, R. S., and M. Lisowski (1983). The 1979 Homestead Valley earthquake sequence, California: Control of aftershocks and post-seismic deformation, *J. Geophys. Res. 88*, 6477-6490.

Stein, R. S., and W. Thatcher (1981). Seismic and aseismic deformation associated with the 1952 Kern County, California, earthquake and relationship to the Quaternary history of the White Wolf Fault, *J. Geophys. Res. 86*, 4913-4928.

Steinbrugge, K. V., E. G. Zacher, D. Tocher, C. A. Whitten, and C. N. Clair (1960). Creep on the San Andreas Fault, *Bull. Seismol. Soc. Am. 50*, 396-404.

Sylvester, A. G. (1978). The dry tilt method of measuring crustal tilt, in Proceedings of Conference VII, Stress and Strain Measurements Related to Earthquake Prediction, *U.S. Geol. Surv. Open-File Rep. 79-370*, pp. 544-568.

Sylvester, A. G. (1982). Precise leveling across active faults in California, in *Proceedings, International Symposium on Geodetic Networks and Computations*, German Geodetic Commission of the Bavarian Academy of Science, Series B, Vol. 258/V, pp. 162-174.

Sylvester, A. G. (1983). Bench marks and tilt, Long Valley caldera, California, 1982-1983, *EOS 64*, 859.

Sylvester, A. G. (1984). Leveling precision and bench mark motions, Pinyon Flat Observatory, California, *J. Geophys. Res. 89*, 7949-7956.

Sylvester, A. G., and D. D. Jackson (1982). Precise Leveling at Pinyon Flat, 1978-1982, *EOS 63*, 1107.

Sylvester, A. G., and D. D. Pollard (1975). Afterslip on the Sylmar Fault segment, in *San Fernando California Earthquake of 9 February 1971*, G. B. Oakeshott, ed., Calif. Div. Mines and Geol. Bull. 196, 227-233.

Sylvester, A. G., A. H. Brown, and N. Riggs (1980). Vertical movements and aseismic horizontal creep on the San Andreas Fault at San Juan Bautista, California, in *Studies of the San Andreas Fault Zone in Northern California*, R. Streitz and R. Sherburne, eds., Calif. Div. Mines and Geol. Spec. Publ. 140, pp. 91-97.

Tanaka, Y. (1978). Reports on observations of crustal stress and crustal deformation, and their anomalous changes related to earthquakes in China, in Proceedings of Conference VII, Stress and Strain Measurements Related to Earthquake Prediction, *U.S. Geol. Surv. Open-File Rep. 79-370*, pp. 569-596.

Tocher, D., A. K. Cooper and R. D. Nason (1968). Fault creep measurements along the San Andreas Fault, *Geol. Soc. Am. Progr. Abstr.*, 72.

Tryggvason, E. (1968). Measurement of surface deformation in Iceland by precision leveling, *J. Geophys. Res. 73*, 7039-7050.

Wahr, J., and M. Wyss (1980). Interpretation of postseismic deformation with a viscoelastic relaxation model, *J. Geophys. Res. 85*, 6471-6477.

Wallace, R. E., and E. F. Roth (1968). Rates and patterns of progressive deformation, in The Parkfield-Cholame, California, Earthquake of June-August 1966, *U.S. Geol. Surv. Prof. Paper 579*, 23-40.

Whitcomb, J. H., J. D. Garmany, and D. L. Anderson (1973). Earthquake prediction: Variation of seismic velocities before the San Fernando earthquake, *Science 181*, 632.

Yamashita, K. M. (1981). Dry tilt: A ground deformation monitor as applied to the active volcanoes of Hawaii, *U.S. Geol. Surv. Open-File Rep. 81-523*, 21 pp.

Yamashita, P. A., and R. O. Burford (1973). Catalog of preliminary results from an 18-station creepmeter network along the San Andreas Fault system in central California for the time interval June 1969 to June 1973, *U.S. Geol. Surv. Open-File Rep.*

Zhang, Guomin, and Fu Zhengxiang (1981). Some features of medium- and short-term anomalies before great earthquakes, in *Earthquake Prediction: An International Review*, D. W. Simpson and P. G. Richards, eds., M. Ewing Ser. 4, Am. Geophys. Union, Washington, D.C., pp. 497-509.

Zhu Fenming, Quan Yingduo, Gu Haoding, Xu Xintong, and Guan Xingguo (1984). Re-examination of the anomalous phenomena taken as precursory before the Haicheng earthquake in 1975, in *A Collection of Papers of International Symposium on Continental Seismicity and Earthquake Prediction*, Gu Gongxu and Mu Xingyuan, eds., Seismological Press, Beijing, China, pp. 571-581.

# 12 Morphologic Dating and Modeling Degradation of Fault Scarps

DAVID B. NASH
*University of Cincinnati*

ABSTRACT

The pattern of degradation observed on some scarps formed by normal, range-front faulting of alluvial fan surfaces may be accurately modeled, and, when properly calibrated, these models provide a means for determining the ages of some scarps (morphologic dating). Two different degradation patterns are observed: some scarps recline, becoming more rounded with time, whereas others retreat with little or no decrease in gradient. Scarps that recline are generally covered with soil or loosened debris and are termed transport-limited because more loosened debris is produced than the transport processes are capable of removing. Retreating scarps are generally stripped bare of debris and are termed loosening-limited because debris is carried away as rapidly as it is loosened from the surface. These two different modes of degradation require two fundamentally different models.

Morphologic dating matches the observed morphology of a degraded scarp with that predicted by the appropriate calibrated model. The accuracy of the age calculated for a fault scarp is dependent on the accuracy of the calibration and the accuracy of the initial morphology assumed for the scarp prior to degradation (potentially complex for fault scarps). Despite some limitations, morphologic dating provides a means for dating fault scarps and other scarps resulting from active tectonism.

## INTRODUCTION

Most geologists have their first, and generally last, exposure to the subject of hillslope degradation in a discussion of landscape evolution during their introductory physical geology course. In that discussion, it is questioned whether hillslopes slowly progress through a series of evolutionary forms as they degrade as suggested by Davis (1899) or fairly rapidly reach an equilibrium form dependent on underlying structure as suggested by Hack (1960). It is further questioned, if hillslopes do in fact evolve slowly with time, what is that pattern of evolution? Do hillslopes retreat retaining a steep gradient as suggested by Bryan (1922) and King (1953) or progressively decrease in gradient, becoming more rounded as suggested by Davis (1899) and, to some extent, by Penck (1953)? Unfortunately, these diametrically opposed theories of hillslope degradation and the often acrimonious debates over the relative merits of each have convinced many geologists that little is known about the degradation of hillslopes.

Within the past 15 years, great progress has been made in our understanding of hillslopes. Much of this progress resulted from careful study of the degradation

processes active on hillslopes summarized in several excellent books, including those by Brunsden (1971), Carson and Kirkby (1972), and Young (1972), as well as by the rediscovery and popularization by Schumm and Mosley (1973) of several classic but generally forgotten works. Enough is now known about these processes that analytical modeling of the degradation of hillslopes has become possible. Two of these models have been tested and found to be sufficiently accurate for some hillslopes to be dated (*morphologic dating*) by matching their observed profile with that predicted by the properly calibrated model.

The hillslopes that will be modeled here are assumed to be closed systems, isolated from the surrounding landscape. Although this assumption is not valid for all hillslopes, it is appropriate for some. Scarps bounded by horizontal or gently inclined bases and crests, such as fault scarps produced by normal faulting, of alluvial fans, abandoned fluvial cutbanks (terrace scarps), and abandoned wave-cut bluffs, on which debris derived from the scarp face accumulates at its base (i.e., debris is not removed by fluvial or wave undercutting) and where degradation is by soil creep or by the raveling of sand and gravel may be modeled as a closed system.

## OBSERVED PATTERNS OF HILLSLOPE DEGRADATION

The degradation of most natural, vegetated hillslopes is extremely slow and difficult to observe directly, and the pattern of degradation observed on more rapidly eroding, man-made slopes, such as slag heaps and tailing piles, is not necessarily the same as on natural hillslopes. The degradation of natural hillslopes, however, may be observed *indirectly* by comparing the morphology of a series of different aged hillslopes assumed to have had the same initial morphology. This approach was probably first used by Savigear (1952), who studied differences in morphology among a series of coastal cliffs isolated from wave undercutting by the progressive lateral growth of a protective beach.

In similar studies, Welch (1970) documented the change in scarp morphology with time from observations of active and abandoned wave-cut bluffs along the north shore of Lake Erie, and Brunsden and Kesel (1973) presented differences between active and abandoned cut-banks along the Mississippi River. Nash (1980b) compared the morphology of wave-cut bluffs abandoned 10,500 yr before present (BP) and 4000 yr BP along the shore of Lake Michigan with that of nearby, actively forming wave-cut bluffs underlain by the same material (Figure 12.1). A pattern of degradation similar to that observed by Savigear (1952), Welch (1970), and

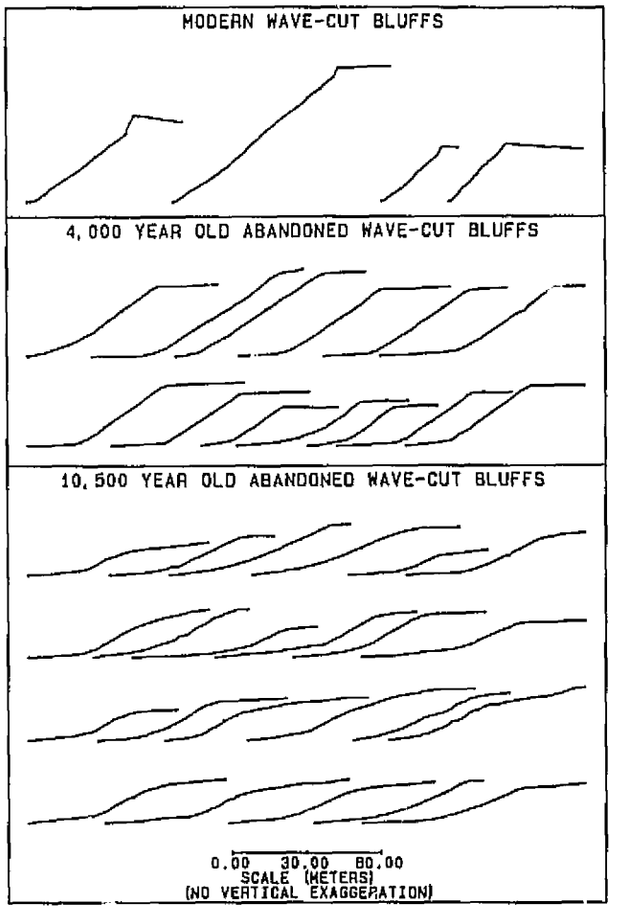


FIGURE 12.1 Profiles of modern, wave-cut bluffs similar to bluffs abandoned 4000 and 10,500 yr BP along the shores of Lake Michigan. All bluffs are underlain by a similar sandy morainal material.

Brunsden and Kesel (1973) is observed on the Lake Michigan bluffs—modern bluffs have a nearly horizontal *crest* and *base* separated from a straight, steeply inclined *midsection* by a sharp *crestal convexity* and *basal concavity* (Figure 12.2a). The midsection gradient of the 4000-yr-old bluff has decreased slightly from that of the modern bluff, and the crestal convexity and basal concavity of the profile have become more rounded. This pattern of degradation is more pronounced on the 10,500-yr-old bluffs. These hillslopes appear to have reclined with age, but did they also retreat?

Some fault scarps near the town of West Yellowstone in southwest Montana apparently did not retreat. In 1959 the Yellowstone earthquake occurred close to the town of West Yellowstone, Montana, forming numerous scarps in the overlying obsidian sand and gravel deposit. These scarps have a morphology similar to the

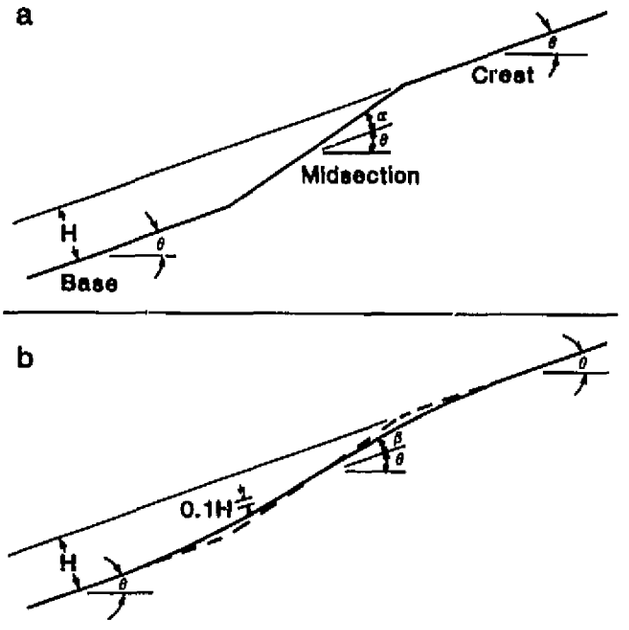


FIGURE 12.2 a, Profile of a scarp with a *simple* initial morphology: a straight base and crest inclined at the same angle, $\theta$, and a straight midsection at the angle of repose of the underlying debris. $\alpha$, the initial excess midsection slope angle is defined as the angle by which the initial midsection exceeds $\theta$. The scarp offset, $H$, is the perpendicular distance separating the parallel crest and base. b, With time, the curvature of the crestal convexity and basal concavity decrease on transport-limited hillslopes. The degraded excess midsection slope angle, $\beta$, is defined as the angle by which the degraded midsection exceeds $\theta$. The initial angle of the crest and base, $\theta$, and $H$ may be determined by analysis of the profile beyond the limits of the basal concavity and crestal convexity. From Nash (1984), reprinted from the *Bulletin of the Geological Society of America*, with permission.

modern wave-cut bluffs along the shores of Lake Michigan—straight midsections separated from gently inclined crests and bases by sharp crestal convexities and basal concavities (Figure 12.2a). Many of the 1959 scarps are superimposed on much older scarps produced by prehistoric earthquakes. These older scarps have a more rounded crestal convexity and basal concavity and lower midsection gradient than the modern scarps, indicating a pattern of degradation similar to that of the abandoned wave-cut bluffs along the shores of Lake Michigan (Figure 12.1). The 1959 scarps are generally located near the center of the midsection of the prehistoric scarp (Figure 12.3), suggesting that little retreat of the older scarp has occurred.

Scarp recline and rounding without significant retreat is fundamentally different from the pattern of scarp degradation reported by King (1953), Hamblin (1976), and Anderson (1977). King (1953) observed that the maximum gradient on hillslopes underlain by the same material is frequently the same on large, and presumably young, as on small, and presumably old, hillslopes and suggested that this demonstrates that once a stable angle has been reached, hillslopes no longer recline but retreat parallel to themselves. He further observed that the Drakensberg escarpment in Natal, South Africa, has "retreated back over 100 miles since the late Mesozoic and is still wall-like and over 4000 feet high." Hamblin (1976) and Anderson (1977) found evidence for scarp retreat in their investigations of a flight of faceted spurs above the Wasatch Fault near Salt Lake City, Utah. They suggested that the accordance in the elevations of these facets (Figure 12.4) indicates that the facets are remnants of once continuous scarps formed by past movements of the Wasatch Fault and concluded that the scarps have retreated significantly [Hamblin (1976) suggested that modest recline of the scarp face also occurred].

On a much smaller scale, a similar pattern of nearly parallel retreat may be observed on rapidly degrading, natural and man-made scarps underlain by cohesionless sands and gravels. Oversteepened walls of borrow pits in the obsidian sand and gravel deposit overlying the West Yellowstone area are observed to retreat back at a high angle, progressively burying their base with loosened debris (Figure 12.5). Similarly, scarps produced by normal faulting of the same material during the 1959 earthquake were observed by Wallace (1980) to have retreated, progressively burying their base with an accumulation of debris loosened from the scarp face. Following the usage of Wallace (1980), these retreating, oversteepened scarp faces underlain by cohesionless material will be referred to as *free faces*.

It is no wonder then that a controversy exists as to whether degrading hillslopes retreat or recline; there can be little doubt that *both* patterns of degradation may be observed. Why do some hillslopes recline with progressive rounding of their crestal convexity and basal concavity while others are apparently able to retreat considerable distances with little change in the morphology of their profiles?

## LOOSENING-LIMITED AND TRANSPORT-LIMITED HILLSLOPES

In his classic study of the geology of the Henry Mountains, Gilbert (1877) offered an explanation for why the summit of Mount Ellen is gently rounded while the summit of nearby Mount Holmes is precipitously steep and jagged despite the fact each is underlain by similar trachyte dikes. He observed that the summit of Mount Ellen is sufficiently high to be vegetated while the 2500

feet lower summit of Mount Holmes is too hot and dry to support continuous vegetation and thus has bare rock slopes. He further observed:

> . . . vegetation favors the disintegration of rocks and retards the transportation of disintegrated material. Where vegetation is profuse there is always an excess of material awaiting transportation, and the limit to the rate of erosion comes to be merely the limit to the rate of transportation. And since the diversity of rock texture, such as hardness and softness, affect only the rate of disintegration (weathering and corraision) and not rate of transportation, these diversities do not affect the rate of erosion in regions of profuse vegetation and do not produce corresponding diversities of form.
>
> On the other hand, where vegetation is scant or absent, transportation and corraision are favored while weathering is retarded. There is no accumulation of disintegrated material. The rate of erosion is limited by the rate of weathering, and that varies with the diversity of rock texture. The soft are eaten away faster than the hard; and the structure is embodied in the topographic forms.

This basic dichotomy between bare and debris mantled hillslopes has been largely overlooked by subsequent hillslope researchers until it was noted by Schumm (1956) in his study of the degradation of badland slopes. Schumm observed that *creep-dominated* slopes, those with a continuous cover of loosened debris, recline and become more rounded with time, whereas *wash-dominated* hillslopes, those on which wash processes sweep the surface bare of loosened debris, retreat with time. More recently Carson and Kirkby (1972) termed these two fundamentally different hillslope types *transport-limited* (hillslopes on which more loosened debris is available for removal than the transport processes are capable of removing) and *weathering-limited* (hillslopes on which the transport processes remove all debris as rapidly as it is loosened). Debris need not necessarily be loosened from the hillslope surface by *weathering*; sand and gravel are detached from the surface of the free face (Figure 12.5) by evaporation of pore water and by raveling. Because these are not weathering processes, the term *loosening-limited* will be used here instead of weathering-limited for hillslopes on which debris is removed as rapidly as it is loosened from the slope surface.

Both loosening-limited and transport-limited hillslopes can occur in all climates; transport-limited hillslopes, however, are more common on unconsolidated or weakly consolidated materials in humid-temperate climates with continuous vegetative cover, whereas loosening-limited hillslopes are more common on

FIGURE 12.3 The scarps formed during the 1959 West Yellowstone earthquak (indicated by the arrow) are generally found superimposed on the *center* of much older scarps indicating that little or no retreat of the older scarps has occurred (photo by J. R. Stacey, U.S. Geological Survey).

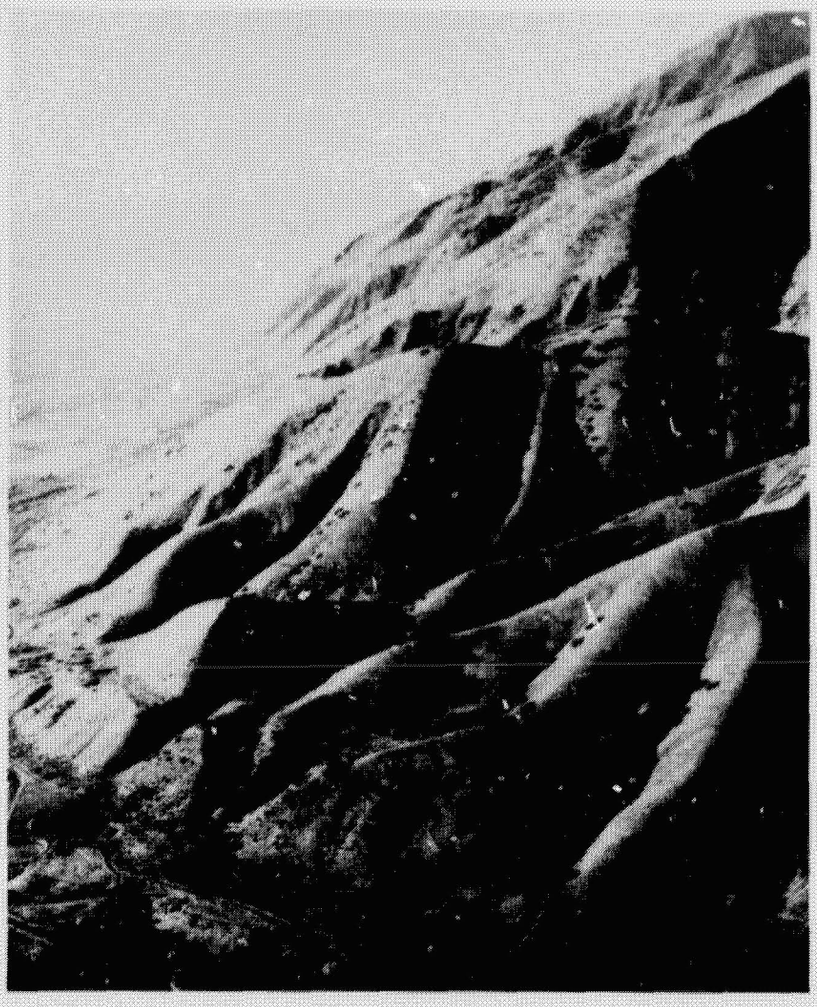

FIGURE 12.4 Flights of faceted spurs along the western front of the Wasatch Range. These facets are thought by Hamblin (1976) and Anderson (1977) to have formed by retreat of scarps produced by multiple movements of the Wasatch Fault (photo courtesy of W. K. Hamblin, Brigham Young University).

weathering-resistant rocks and in arid to semiarid regions with insufficient moisture to support a continuous vegetative cover. As will be discussed, loosening-limited hillslopes degrade by retreat, whereas transport-limited hillslopes degrade by recline and rounding. It is interesting to note that the advocates of parallel retreat, such as Bryan (1922) and King (1953), worked primarily in arid and semiarid regions, whereas the most notable proponent of hillslope recline, Davis (1899), worked primarily in temperate-humid regions.

## MODELING THE DEGRADATION OF TRANSPORT-LIMITED HILLSLOPES

The following model for describing the degradation of transport-limited hillslopes is not new; it has been proposed by many researchers including Culling (1960), Souchez (1964), Hirano (1968, 1975), and Pollack (1968). The model, sometimes termed the *diffusion* model of hillslope degradation, is based on the assumption that the volumetric rate at which debris moves downslope at a particular point on a hillslope profile is proportional to the gradient of the profile at that point. Although several transport mechanisms have been proposed for such debris transport, the most probable is soil creep (Culling 1963, 1965; Nash, 1980a).

### *Debris Transport by Creep*

The slow, steady downslope creep of material on transport-limited hillslopes is thought by many to result from alternate expansion and contraction within the de-

FIGURE 12.5 Walls of borrow pit in the obsidian sand and gravel deposit overlying the West Yellowstone Basin, Montana. The loosening-limited free face of the wall is observed to retreat, progressively burying its base with debris. From Nash (1984), reprinted from the *Bulletin of the Geological Society of America*, with permission.

bris mantle. This expansion and contraction may be the result of heating and cooling (Davison, 1888) or hydration and dehydration (Fleming, 1972) or freezing and thawing of pore water. If expansion occurs by heaving perpendicular to the slope surface and contraction by vertical dropping of the surface, a net downslope displacement of the debris cover results, which is proportional to the sine of the slope angle of the surface (Figure 12.6a). If the amount of expansion and contraction of the debris mantle is uniform throughout its thickness, the upward and downward displacement of debris decreases linearly with depth, and, therefore, the downslope movement of debris resulting from a single expansion and contraction episode will also decrease linearly with depth (Figure 12.6b). The depth to which an expansion and contraction cycle penetrates into the debris mantle, however, is highly variable. A light rain or light freeze may penetrate a few centimeters beneath the surface, but it will take the rarer, heavier rain or severe freeze to penetrate to greater depths. Thus we would expect the actual displacement profile within the debris mantle to reflect both the linear decrease in displacement with depth resulting from a single expansion-

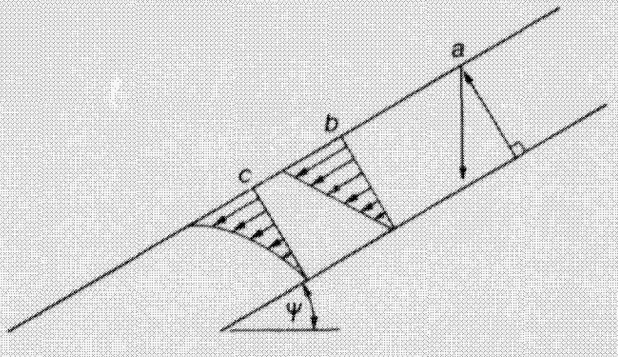


FIGURE 12.6 a, Downslope creep caused by expansion of the debris mantle perpendicular to the surface followed by vertical contraction. Alternate heating and cooling, freezing and thawing, or wetting and drying are thought to produce such creep. b, For a *single* episode of expansion and contraction, the displacement of soil downslope decreases linearly with depth (no displacement will occur beyond the depth of penetration of the expansion-contraction cycle). c, The frequency with which an expansion-contraction episode penetrates into the surface decreases rapidly with depth. When the linear downslope displacement of debris resulting from a single expansion-contraction episode is combined with the decreasing frequency of occurrence of penetration with depth, it produces a concave-downslope displacement profile after many episodes. This displacement profile has been observed in several field studies.

contraction episode *and* the decreasing *frequency* of penetration at greater depths to produce a concave-downslope displacement profile (Figure 12.6c). This prediction is verified by several field studies of creep displacement summarized by Carson and Kirkby (1972).

If the depth of penetration is uniform over the hillslope surface during a single expansion-contraction event then the volumetric, downslope flux of debris, $q$, per unit length of contour at a point on a transport-limited hillslope will be proportional to the sine of the slope angle ($\psi$) at that point, or

$$q = c \sin \psi, \tag{12.1}$$

where $c$ is the coefficient of proportionality. Debris will seldom remain on slopes steeper than 30°, so little error is introduced by assuming that $q$ at a point on a transport-limited hillslope is proportional to the tangent of the local slope angle, or

$$q = c \tan \psi = c \frac{\partial y}{\partial x} \tag{12.2}$$

in two spatial dimensions, where $x$ is the horizontal and $y$ is the vertical coordinate of the point. Field studies by Schumm (1967) and others verify that the observed creep rate may be described by Eq. (12.2).

### *Downslope Conservation of the Debris Flux*

A hillslope profile may be thought of as a series of linear segments each receiving debris at its upslope end and discharging debris at its downslope end. If more debris enters a segment than leaves, conservation of mass requires that the debris within the segment must increase, resulting in an increase in the elevation of the segment (Figure 12.7a). Conversely, if more debris leaves than enters a segment, its elevation must decrease (Figure 12.7b). Thus the downslope change in the debris flux, $q$, determines the change in elevation at a point on a hillslope. Debris will accumulate and the elevation will increase where $q$ decreases downslope, such as at basal concavities. Debris will be depleted and the elevation will decrease where $q$ increases downslope. In spatial dimension, $x$, the change in elevation, $y$, with time, $t$, on a hillslope profile is therefore equal to the downslope divergence of the debris flux, or

$$\frac{\partial y}{\partial t} = \nabla q = \frac{\partial y}{\partial x} = c \frac{\partial^2 y}{\partial x^2}. \tag{12.3}$$

This equation predicts the pattern of degradation shown in Figure 12.8; the gradient of the midsection decreases and the curvatures of the basal concavity and crestal convexity decrease (become more rounded) with time.

Equation (12.3) is not appropriate for loosening-limited slopes because the transportational processes are capable of sweeping the slope surface completely clear of debris, nor is it appropriate for all transport-limited hillslopes. Although Eq. (12.2) is probably appropriate for describing raindrop-induced, surficial creep on bare sand (e.g., Savat and DePloey, 1968), it is probably not appropriate for wash erosion on transport-limited hillslopes (such erosion is rarely effective on continuously vegetated hillslopes underlain by cohesionless sands and gravels).

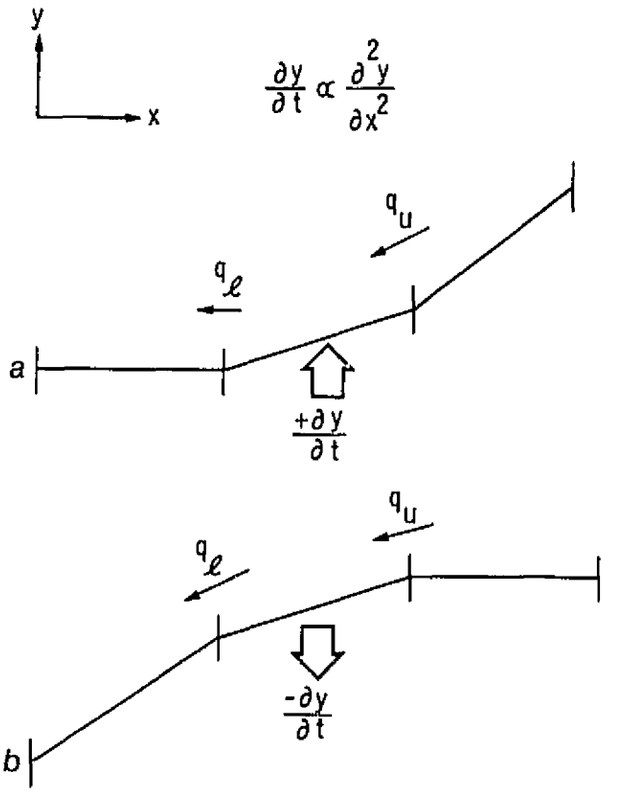


FIGURE 12.7 Conservation of debris on a transport-limited hillslope. a, If the debris flux entering a hillslope segment, $q_u$, exceeds the flux leaving $q_l$, there will be a net accumulation of debris within the segment and its elevation will increase with time. b, If $q_l$ exceeds $q_u$, there will be a net depletion of debris within the segment and its elevation will decrease with time.

Nash (1980b, 1984) demonstrated that Eq. (12.3) fits the pattern of degradation observed on abandoned wave-cut bluffs along the shore of Lake Michigan (Figure 12.1) and on fluvial terrace scarps along the Madison River near West Yellowstone (Figure 12.9). Hanks *et al.* (1984) fit the pattern of degradation observed on Lake Bonneville scarps and a fault scarps near Drum Mountain, Utah, abandoned sea cliffs along the Califor-

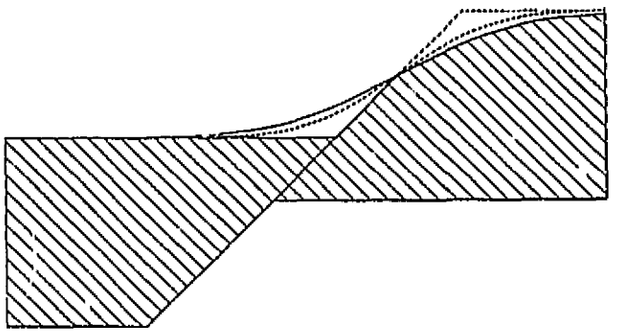

FIGURE 12.8 Model for the degradation of a transport-limited hillslope. The crestal convexity and basal concavity become more rounded and the midsection reclines.

nia coast near Santa Cruz, and fault scarps near the Fish Spring Range, the Oquirrh Mountains, and the Sheeprock Mountains, Utah, with the pattern of degradation predicted by Eq. (12.3). Hanks and Wallace (in press) demonstrate that the degradation pattern observed on shoreline scarps formed by Lake Lahontan in western Nevada may be closely modeled with Eq. (12.3). The model also predicts that the degradation of a transport-limited scarp is not accompanied by retreat, which would explain why the scarps formed during the 1959 West Yellowstone earthquake are generally located near the center of much older scarps formed by previous offsets of the same fault (Figure 12.3). The model also successfully predicts the inverse relationship between scarp height and the slope angle documented by Bucknam and Anderson (1979) in a study of a degraded fault scarp near Drum Mountain, Utah (Nash, 1980b; Colman and Watson, 1983; Hanks *et al.*, 1984; Hanks and Wallace, in press).

## MODELING THE DEGRADATION OF LOOSENING-LIMITED HILLSLOPES

### *Loosening of Debris from a Bare Scarp Face*

Numerous researchers believe that a uniform thickness of material is loosened from the surface of a uniformly inclined scarp face underlain by homogeneous material during a given unit of time. Penck (1953) suggested the following:

> . . . On a slope of *uniform gradient* and equal exposure, a profile of reduction is formed which shows everywhere the same development and the same thickness. In the same time that the uppermost horizon of that profile has taken to acquire the mobility necessary for migration, a rock layer of the same thickness throughout has become reduced. At the close of a further equal interval of time, a further layer of rock, again of the same thickness and of equal thickness at every part of the slope, passes over into the reduced form.

Removal of a uniform thickness of loosened debris from the scarp face results in parallel retreat with no rounding of the crestal convexity or basal concavity. The pattern of degradation, however, is dependent on whether the loosened debris accumulates at the base of the scarp or is removed.

### *Accumulation of a Basal Debris Apron*

As long as debris is swept clear of the base of a scarp, the scarp retreats parallel to itself. This process may be observed on active fluvial cut-banks and wave-cut bluffs. When undercutting ceases and debris is no longer removed, an apron of debris inclined at a characteristic angle of repose will progressively grow, ultimately burying the retreating scarp face.

The first analytical model of parallel retreat with accumulation of a basal debris apron was formulated by Fisher (1866) to describe the degradation of coastal chalk cliffs. Fisher's model assumed a vertical scarp face and a horizontal crest and base. Lehmann (1933) modified the model to permit the treatment of nonvertical scarp faces and to allow for changes in volume of the debris as it moves from the scarp face to the debris apron. The model was further modified by Nash (1981a) to permit the treatment of scarps with nonhorizontal crests and bases. The pattern of degradation predicted by this model is shown in Figure 12.10. Note that the model predicts the development of an uneroded, parabolic core of debris beneath the debris apron. Immediately adjacent to the base of the retreating scarp face, the surface of the uneroded core of material is thinly buried and nearly parallel to the overlying surface of the debris apron.

The predicted pattern of degradation of the scarp face is nearly identical to that documented by Wallace (1980) for scarps formed during the 1959 Yellowstone earthquake (Figure 12.11). It can also be used to explain the origin of the flight of faceted spurs along along the Wasatch Front above the Wasatch Fault noted by Hamblin (1976) and Anderson (1977) (Figures 12.4 and 12.12) and to provide a possible explanation for the origin of pediment surfaces. Pediments are bare or thinly veneered bedrock surfaces frequently found at the bases of loosening-limited ranges (Cooke and Warren, 1973). In numerous areas where the retreating face has been completely or extensively removed and the alluvial cover has been completely stripped away, the pediment

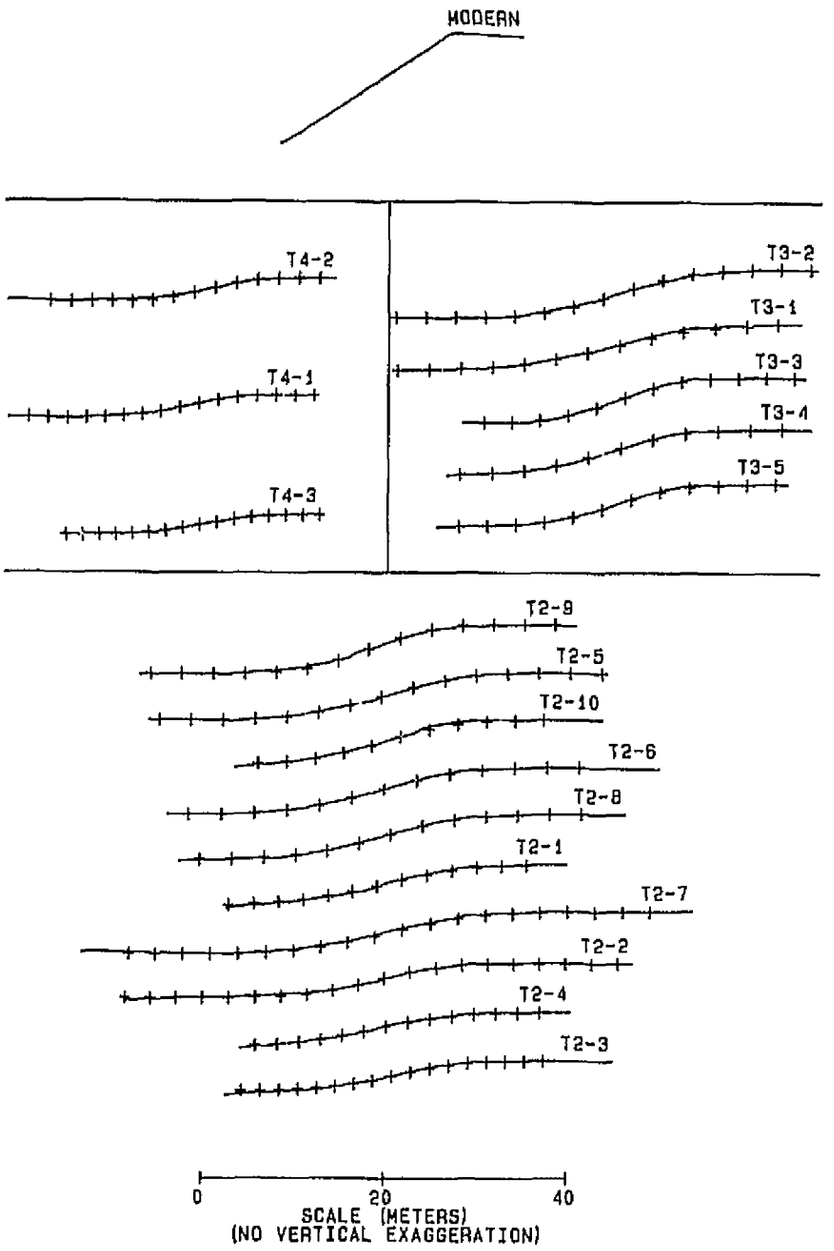


FIGURE 12.9 Comparison of the profiles measured on terrace scarps above the Madison river near West Yellowstone, Montana (solid lines), with the profiles predicted by the degradation model for transport-limited hillslopes (crosses). From Nash (1984), reprinted from the *Bulletin of the Geological Society of America*, with permission.

surface is observed to have a parabolic shape. In fact, Fisher (1866) proposed the model to explain the origin of what he terms "parabolic noses" of chalk at the base of the chalk cliffs along the English coast. He suggested that the noses formed beneath a debris apron that was able to accumulate at the base of the retreating cliff during a prehistoric period of lower sea level. The subsequent rise of the sea to its present level removed the basal debris apron, exposing the uneroded chalk nose.

## USING THE HILLSLOPE DEGRADATION MODELS TO DATE SIMPLE FAULT SCARPS

Both the transport-limited and the weathering-limited hillslope models offer a means for *morphologic dating* of some prehistoric fault scarps. Before this can be done, the initial morphology of a scarp must be accurately estimated and the models must be calibrated. Neither of these tasks is simple, nor are they even possi-

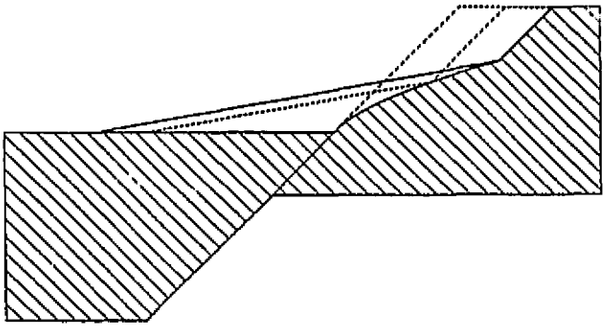

FIGURE 12.10 Model for retreating, loosening-limited scarp. The retreating free face is progressively buried by a basal apron of debris shed from its surface.

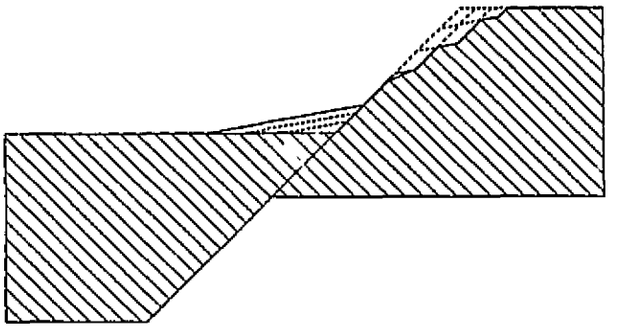

FIGURE 12.12 If a basal debris apron is not allowed to accumulate, the free face can retreat great distances. Subsequent movements of the fault may produce a new scarp before the older scarp is eliminated (compare with Figure 12.4).

ble in many cases. Although dating can be performed on several different types of scarp underlain by different kinds of materials, the following discussion of fault scarp dating is limited primarily to scarps produced by normal faulting of relatively cohesionless alluvium such as those produced by range-front faulting of alluvial fans in the Basin and Range region of the western United States. The initial morphology of such scarps can be quite complex. Frequently the fault surface will splay close to the ground surface to produce an assemblage of smaller scarps rather than producing a single scarp. Repeated faulting often superimposes younger scarps on much older ones. The initial morphology of these complex scarps is difficult or impossible to determine with an accuracy sufficient to permit morphologic dating. Nash (1984) suggested that independent geologic evidence (e.g., from trenching) be used to determine whether a scarp had a complex initial morphology and, if so, to reject it for morphologic dating. The analysis below is for simple scarps. Recently, however, Hanks *et al.* (1984) have proposed a method for dating more complex scarps produced by repeated fault movements.

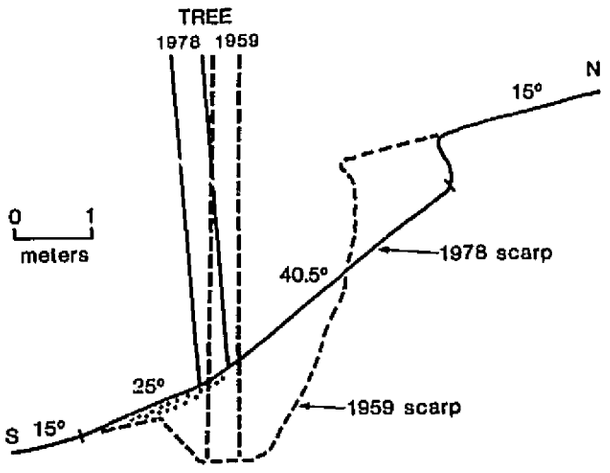


FIGURE 12.11 Comparison of the profile of a scarp produced by the 1959 West Yellowstone earthquake with its profile observed 20 years later. The free face of the retreating scarp is nearly buried (compare with Figure 12.10). (Photo courtesy of R. E. Wallace, U.S. Geological Survey.)

### *Initial Morphology of Fault Scarps*

It is assumed here that the initial morphology consists of a single scarp that offsets a straight crest and base inclined at the prefaulting slope of the fan surface (Figure 12.2a). Scarps formed by normal faulting of cohesionless sands and gravels result from active Rankine failure producing failure planes inclined at $45 + \Phi/2$ to the horizontal. $\Phi$, the angle of internal friction, generally varies from 30° to 35° so initial scarp angles range from 60° to 62°. Theoretically, for a purely cohesionless material, a slope cannot exceed $\Phi$ (Carson, 1977), therefore, the initial fault scarp should rapidly recline to $\Phi$. A rapid recline to $\Phi$, however, is frequently not observed on normal fault scarps underlain by "cohesionless" sands and gravels, probably because of a weak, ephemeral cohesion among grains resulting from pore water in capillary tension and from minute amounts of cementing at contact points between grains. Instead, a loosening-limited free face is produced that retreats, progressively burying its base with debris. The time necessary for the retreating free face to be completely buried, producing a continuous debris apron that at $\Phi$, varies with

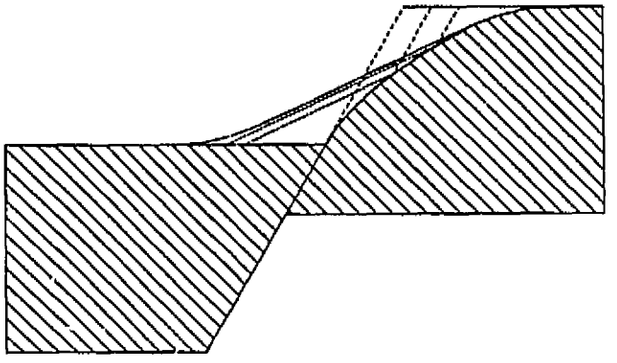

FIGURE 12.13 Scarps produced by normal faulting of alluvial fans degrade in two stages. In the first, the loosening-limited free face retreats. After the free face has been buried, the second, transport-limited stage of degradation begins.

the height of the scarp, the type of material, and the climate. Wallace (1980) found that the free face of most of the fault scarps produced by the 1959 earthquake in West Yellowstone are now nearly buried. On the other hand, the free face of the scarp produced by faulting during the 1915 Pleasant Valley, Nevada, earthquake is still clearly visible, and Wallace (1977) estimated that 300 yr will be required for it to be completely buried. The time necessary for the complete burial of the retreating free face may be from seconds to centuries but is probably most often on the order of decades.

Degradation thus proceeds in two stages. During the first stage, the retreating free face may be described with the loosening-limited model. The second stage begins when the free face has been completely buried by the debris apron. Subsequent degradation of this apron may be described with the transport-limited model (Figure 12.13). Although the scarp retreats during the first stage, the center of the initial free face and the center of the debris apron that it produces are nearly the same, so that future movements of the fault will nearly bisect the debris apron (Figures 12.10 and 12.3).

### *Morphologic Dating of Loosening-Limited Scarps*

Dating of fault scarps in the initial loosening-limited stage of degradation is simple in principle but difficult in practice: the distance that the free face has retreated from the fault is divided by the rate of scarp retreat. The accuracy of the calculated age is dependent on the accuracy of the retreat rate used, which varies not only from scarp to scarp but also along a given scarp face. The average retreat rate of the free faces resulting from the 1959 Yellowstone earthquake derived from data presented by Wallace (1980) is about 7-8 cm/yr, which is intermediate to the values derived from Wallace's (1977) study of scarps in north central Nevada: a slower, 2 cm/yr for the 1915 Pleasant Valley scarp and a faster 10 cm/yr for the nearby scarp produced by the 1954 Dixie Valley earthquake. A large variation in the retreat rate along the Pleasant Valley scarp is quite evident; in some locations the free face is still standing immediately adjacent to a fresh-appearing basal graben, while nearby it has been completely buried. Retreat rates are probably a function of variations in the cohesion of the alluvium and of the climate. It is also likely that rate of retreat varies over relatively short periods of time (a great deal of retreat may occur during a particularly severe storm). Despite these limitations, when the effects that underlying material and climate have on retreat rates are understood well enough to permit accurate calibration of the loosening-limited model, it is likely that relatively accurate dates may be derived for some fault scarps in the first, retreating stage of degradation.

### *Morphologic Dating of Transport-Limited Scarps*

With the burial of the free face by the basal debris apron, the scarp becomes transport-limited and dating must be based on Eq. (12.3). The first technique proposed for such dating (Nash, 1980a) uses the relationship between scarp height and rate of degradation to date the Drum Mountain, Utah, fault scarp observed by Bucknam and Anderson (1979). The method requires that a scarp of known age be located nearby and that both are underlain by the same material and show a continuous range of heights along their length. These requirements greatly limit the applicability of the technique. More flexible methods have subsequently been proposed by Nash (1981b), Colman and Watson (1983), and Hanks *et al.* (1984). The Nash (1981b) method is presented here, but all techniques based on Eq. (12.3) will yield similar ages for a given scarp.

As it enters the second, rounding stage of degradation, the scarp is assumed to have a straight midsection at the angle of repose of the underlying debris, $\Phi$, separating a straight base and crest equally inclined at an angle of $\theta$, the original slope of the faulted fan surface (Figure 12.2a). The scarp offset, $H$, is defined as the perpendicular distance separating the crest, and base and the initial *excess midsection slope angle*, $\alpha$, is defined as the angle by which the midsection slope angle exceeds $\theta$ (so $\Phi = \alpha + \theta$). As it degrades, the crestal convexity and basal concavity of the scarp become more rounded but $\theta$ may still be observed beyond the extent of this rounding

and thus $H$ may still be measured from the degraded profile (Figure 12.2b). The midsection of the degraded profile is defined as the straight inflection segment separating the basal concavity from the crestal convexity. The degraded excess midsection slope angle, $\beta$, is defined as the angle by which the inclination of the degraded midsection exceeds $\theta$.

For hillslopes with horizontal crests and bases (i.e., $\theta = 0$, a definite relationship exists among $H$, $c$, $\alpha$, $\beta$, and $t$, the elapsed time since the initiation of the second stage of scarp degradation. A single value of $\tan \alpha / \tan \beta$ is the unique result of a *single* value of $(tc/H^2) \tan^2 \alpha$ (Nash, 1984). This relationship (Figure 12.14) may be used as the basis for morphologic dating. Although the relationship breaks down for hillslopes with steeply inlined crests and bases ($\theta > 20°$), negligible errors (less than 2 percent in the calculated value of $t$) result from using the following dating procedure on scarps on which $\theta < 10°$ and where $\alpha + \theta < 35°$. According to Figure 12.14, one-quarter as much time is required for a scarp to degrade from $\alpha$ to $\beta$ if $c$ is quadrupled *or* if $H$ is halved. To date a scarp, $H$, $\beta + \theta$, and $\theta$ are measured from a profile of the scarp, and $\alpha + \theta$ is found indirectly by measuring the angle of repose, $\Phi$, of the underlying debris. $\tan \alpha / \tan \beta$ is calculated and the corresponding value of $(tc/H^2) \tan^2 \alpha$ is taken from Figure 12.14. This value of $(tc/H^2) \tan^2 \alpha$ is multiplied by $H^2$ and divided by $\tan^2 \alpha$ to yield $tc$. If $t$ is known then $c$ may be calculated. If $c$ has been calculated for a nearby scarp of known age or has been derived by some other means, $t$ may be calculated. Because the time required for completion of the first, loosening-limited stage of degradation is relatively short (rarely more than a few centuries), $t$ is generally assumed to be equal to the total age of the scarp.

The accuracy of $t$ is dependent on the validity of assuming that a scarp had an initial morphology similar to that shown in Figure 12.2a and on the accuracy of $c$. Calculated values of $c$ vary widely: $12 \times 10^{-3}$ m$^2$/yr for wave-cut bluffs underlain by sandy morainal material in Michigan (Nash, 1980b); $2 \times 10^{-3}$ m$^2$/yr for fluvial terrace scarps underlain by cohesionless obsidian sand and gravel near West Yellowstone, Montana; to a minimum of $(0.9\text{-}1.0) \times 10^{-3}$ m$^2$/yr calculated for the Lake Bonneville scarps by Colman and Watson (1983) and Hanks *et al.* (1984). [Hanks *et al.* (1984) also proposed that 1 m$^2$/1000 yr be termed a G.K.G. in recognition of G. K. Gilbert's contribution to the study of hillslopes.] Pierce and Colman (in press) observe a correlation between scarp aspect and $c$ and also find a disturbing relationship between $c$ and scarp height. It is likely that $c$ is a function of underlying material, climate, and scarp aspect and thus is highly site specific. The identical values for $c$ determined by Hanks and Wallace (in press) for the Lake Bonneville and Lake Lahontan shoreline scarps, however, suggest that a value of $c = (1.0\text{-}1.1) \times 10^{-3}$ m$^2$/yr may be appropriate for many scarps underlain by alluvium in the Basin and Range province. Ideally, the value used for $c$ should be derived from a nearby scarp of known age, underlain by the same material, and having the same aspect as the scarp to be dated. It is assumed that $c$ does not change with time—questionable given the extent to which Holocene climatic conditions differed from those of the Pleistocene. Pre-Holocene dates are thus suspect, and it is possible that the moderation of climate during the xerotherm 4000 yr BP may have been sufficient to have changed $c$ significantly.

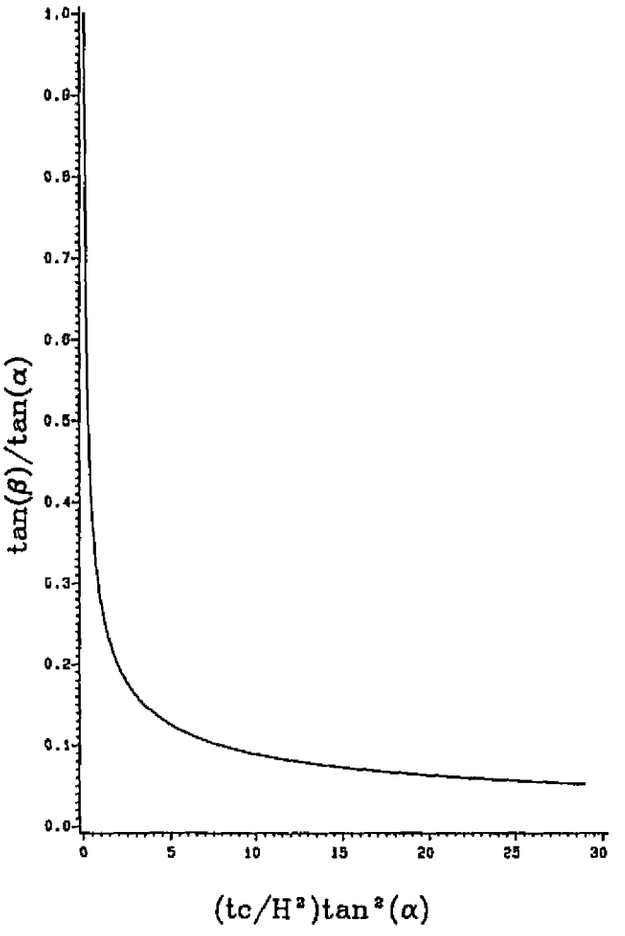


FIGURE 12.14 The relationship among initial excess midsection slope angle, ; degraded excess midsection slope angle, $\beta$; scarp offset, $H$; $c$; and elapsed time since the start of the second stage of scarp degradation, $t$. This relationship forms the basis of the morphologic dating technique used here for dating transport-limited scarps. From Nash (1984), reprinted from the *Bulletin of the Geological Society of America*, with permission.

Given the simple initial scarp morphology shown in Figure 12.2a, Eq. (12.3) predicts that curvature of the crestal convexity and basal concavity should be identical at any future time. If a significant asymmetry of the crestal convexity and basal concavity is observed, dating should be attempted with great caution [slope wash processes probably cannot be modeled with Eq. (12.3) and are likely to produce a profile with a more rounded basal concavity than crestal convexity].

## RECOMMENDATIONS FOR FUTURE RESEARCH

Although the validity of the models for loosening-limited and transport-limited hillslopes is fairly well established and accepted, widespread application of the models for morphologic dating of fault scarps is hampered by the lack of a means for accurately calibrating either model for a particular site. Both $c$ and the rate of retreat of a free face are probably a function of factors such as climate, underlying material, and scarp aspect and therefore are highly site specific. Currently, both parameters must be determined from a nearby scarp having the same aspect and underlain by the same material as the scarp to be dated (generally such a scarp will not be available). If the effects of climate, material, and aspect on the retreat rate and $c$ could be determined accurately, however, appropriate values for either parameter could be estimated by measurement of these factors. To determine these effects, retreat and rounding rates must be found for a large number of dated transport- and loosening-limited hillslopes in various climates, with a variety of aspects and underlying materials.

The study of initial scarp morphology and rates of retreat of the free face would be helped considerably if a continuous set of photogrammetric quality stereo images were taken at *ground level* along each scarp immediately after faulting and at 10-yr intervals thereafter. This set of imagery would also permit future investigators to make measurements of morphologic parameters not considered by the initial investigators.

## CONCLUSIONS

Degradation of scarps formed by normal faulting of alluvial fan surfaces occurs in two stages. In the first, the steep, loosening-limited free face retreats back, progressively burying itself with a basal apron of debris. The second stage of degradation begins when the free face is completely buried by debris to yield a midsection uniformly inclined at the angle of repose of the debris. Degradation of this transport-limited scarp proceeds by progressive rounding of the basal concavity and crestal convexity and recline of the midsection gradient. Both the parallel retreat of the free face in the first stage and the rounding of the scarp in the second stage can be described by two simple models. If the initial morphology of the scarp can be accurately estimated and if the models are properly calibrated, they can be used to date a scarp in either stage of degradation.

The applicability of morphologic dating is limited by the need to recalibrate the models for each scarp to be dated, currently only possible by analysis of a nearby similar scarp of known age. With additional investigation, it is likely that the influence that climate, underlying material, and aspect have on $c$ and on the rate of retreat will be known with sufficient accuracy that the models can be calibrated directly from measurements of these factors.

Morphologic dating is not applicable to all scarps formed by normal faulting of alluvial fans. Degradation by slope wash cannot be described with either model, so dating of wash eroded scarps should probably be avoided (such scarps will often have a more rounded basal concavity than crestal convexity). It is also likely that the pre-Holocene climate was sufficiently different from the present that $c$ was also different, making pre-Holocene dates suspect. Morphologic dating should not be applied to fault scarps that cannot be assumed to have had a simple initial morphology comprising an equally inclined crest and base separated by a straight midsection. Despite these limitations, morphologic dating, when used with considerable care, should prove itself to be a valuable tool for determining the deformational history of areas of active tectonism.

## ACKNOWLEDGMENTS

My research in the area of morphologic dating of fault scarps was sponsored by the U.S. Geological Survey, Earthquake Hazards Reduction Program, under Contract 14-03-0001-19109. Arvid M. Johnson and Thomas C. Hanks are thanked for their critical reviews of this manuscript. Rebecca Chavlot-Talmon is thanked for her assistance with the drafting.

## REFERENCES

Anderson, T. C. (1977). Compound faceted spurs and recurrent movement in the Wasatch Fault zone, north central Utah, *Brigham Young Univ. Geol. Stud. 24*, 83-101.

Brunsden, D., ed. (1971). *Slopes Form and Process*, Institute of British Geographers, Special Publ. No. 3, 178 pp.

Brunsden, D., and R. H. Kesel (1973). Slope development on a Mississippi River bluff in historic time, *J. Geol. 81*, 576-597.

Bryan, K. (1922). Erosion and sedimentation in the Papago Country, Arizona, *U.S. Geol. Surv. Bull. 730-B*, 19-90.

Bucknam, R. C., and R. E. Anderson (1979). Estimation of fault-scarp ages from a scarp-height-slope-angle relationship, *Geology 7*, 11-14.

Carson, M. A. (1977). Angles of repose, angles of shearing resistance and angles of talus slopes, *Earth Surface Processes 2*, 363-380.

Carson, M. A., and M. J. Kirkby (1972). *Hillslope Form and Processes*, Cambridge Univ. Press, Cambridge, 475 pp.

Colman, S. M., and K. Watson (1983). Ages estimated from a diffusion equation model for scarp degradation, *Science 221*, 263-265.

Cooke, A. V., and A. Warren (1973). *Geomorphology in Deserts*, University of California Press, Berkeley, 394 pp.

Culling, W. E. H. (1960). Analytical theory of erosion, *J. Geol. 68*, 336-344.

Culling, W. E. H. (1963). Soil creep and the development of hillside slopes, *J. Geol. 71*, 127-161.

Culling, W. E. H. (1965). Theory of erosion on soil-covered slopes, *J. Geol. 73*, 230-254.

Davis, W. M. (1899). The geographical cycle, *Geogr. J. 14*, 481-504.

Davison, C. (1888). Note on the movement of scree-material, *Q. J. Geol. Soc. Lond. 44*, 232-238.

Fisher, O. (1866). On the disintegration of a chalk cliff, *Geol. Mag. 3*, 354-356.

Fleming, R. C. (1972). Soil creep in the vicinity of Stanford University, Ph.D. dissertation, Stanford Univ., 148 pp.

Gilbert, G. K. (1877). *Geology of the Henry Mountains*, U.S. Geographical and Geological Survey, 160 pp.

Hack, J. T. (1960). Interpretation of erosional topography in humid regions, *Am. J. Sci. 258A*, 80-97.

Hamblin, W. K. (1976). Patterns of displacement along the Wasatch Fault, *Geology 4*, 619-622.

Hanks, T. C., and R. E. Wallace (in press). Morphological analysis of Lake Lahontan shoreline and beachfront fault scarps, Pershing County, Nevada.

Hanks, T. C., R. C. Bucknam, K. R. Lajoie, and R. E. Wallace (1984). Modification of wave-cut and fault-controlled landforms, *J. Geophys. Res. 89*, 5771-5790.

Hirano, M. (1968). A mathematical model of slope development—an approach to the analytical theory of erosional topography, *J. Geosci. Osaka City Univ. 11*, 13-52.

Hirano, M. (1975). Simulation of development process of interfluvial slopes with reference to graded form, *J. Geol. 83*, 113-123.

King, L. C. (1953). Canons of landscape evolution, *Geol. Soc. Am. Bull. 64*, 721-751.

Lehmann, O. (1933). Morphologische Theorie der Verwitterung von Steinschlagwanden, *Vierteljahresschr. Naturforsch. Ges. Zurich 78*, 83-126.

Nash, D. B. (1980a). Forms of bluffs degraded for different lengths of time in Emmet County, Michigan, U.S.A, *Earth Surface Processes 5*, 331-345.

Nash, D. B. (1980b). Morphologic dating of degraded normal fault scarps, *J. Geol. 88*, 353-360.

Nash, D. B. (1981a). FAULT: A FORTRAN program for modeling the degradation of active normal fault scarps, *Comput. Geosci. 7*, 249-266.

Nash, D. B. (1981b). Fault scarp morphology: Indicator of paleoseismic chronology, Final Tech. Rep., U.S. Geol. Surv. Contract Number 14-08-0001-19109, 132 pp.

Nash, D. B. (1984). Morphologic dating of fluvial terraces scarps and fault scarps near West Yellowstone, Montana, *Geol. Soc. Am. Bull. 95*, 1413-1424.

Penck, W. (1953). *Morphological Analysis of Land Forms*, H. Czeck and K. C. Boswell, translators, Macmillan, London, 429 pp.

Pierce, K. L., and S. M. Colman (in press). Effect of orientation and height rates of scarp degradation, central Idaho.

Pollack, H. N. (1968). On the interpretation of state vectors and local transformation operators, State Geol. Surv. of Kansas Computer Contrib. 22, 43-46.

Savat, J., and J. DePloey (1968). Contribution à l'étude de l'érosion par le splash, *Z. Geomorphol. 12*, 174-192.

Savigear, R. A. G. (1952). Some observations on slope development in South Wales, *Trans. Inst. Brit. Geogr. 18*, 31-51.

Schumm, S. A. (1956). The role of creep and rainwash on the retreat of badland slopes, *Am. J. Sci. 254*, 693-706.

Schumm, S. A. (1967). Rates of surficial creep on hillslopes in western Colorado, *Science 155*, 560-561.

Schumm, S. A., and M. P. Mosley, eds. (1973). *Slope Morphology*, Dowden, Hutchinson and Ross, Inc., Stroudsburg, Pa., 454 pp.

Souchez, R. (1964). Viscosité, plasticité et rupture dans l'evolution des versants, *Ciel Terre 80*, 3-24.

Wallace, R. E. (1977). Profiles and ages of young fault scarps, north-central Nevada, *Geol. Soc. Am. Bull. 88*, 1267-1281.

Wallace, R. E. (1980). Degradation of the Hebgen Lake Fault scarps of 1959, *Geology 8*, 225-229.

Welch, D. M. (1970). Slope Analysis and Evolution on Protected Lacustrine Bluffs, Ph.D. dissertation, Univ. of Western Ontario, 184 pp.

Young, A. (1963). *Slopes*, Oliver and Boyd, Edinburgh, 288 pp.

NOTE: A BASIC language computer program (for an IBM PC) has been developed by the author for the morphologic dating of transport-limited scarps. Copies of the program are available without cost. Send the author a self-addressed, stamped envelope for details (Department of Geology, University of Cincinnati, Cincinnati, OH 45221).

# 13 Dating Methods

KENNETH L. PIERCE
*U.S. Geological Survey, Denver*

ABSTRACT

Geologic assessment of active tectonism depends on two key measures: the age and the amount of deformation of a given stratigraphic unit. The amount of deformation can normally be measured with greater accuracy than the age. Adequate age control is thus a limiting factor in studies of active tectonism.

About 26 dating techniques can be applied to dating deposits and deformation of late Cenozoic age (past few million years). These techniques can be grouped as numerical, relative dating, and correlation. Numerical techniques are best, but datable materials are often lacking, and in these cases age estimation must be made using relative-dating or correlation techniques. Relative-dating techniques are nearly always applicable but are not precise and require calibration. Correlation techniques are locally useful and depend on recognition of an event whose age is known, such as a volcanic eruption or a paleomagnetic reversal.

Geologic studies of active tectonism are greatly aided by definition and time calibration of local stratigraphic sequences. Because all dating techniques may be subject to considerable error, reliability should be assessed by stratigraphic consistency between results of different dating methods or of the same method. Numerical ages may have large, nonanalytical errors. For example, radiocarbon dating is one of the most useful techniques in the 0-50-ka range (ka = thousand years old), but contamination can result in dates as young as 15 ka for deposits that should be isotopically dead (>40-70 ka).

Improvements in our ability to date active tectonism and define its rates will come from continued refinement of established techniques, such as carbon-14 dating, and development of experimental techniques, of which thermoluminescence seems to offer special promise. Experimental isotopic-dating techniques such as $^{10}Be$, $^{36}Cl$, and $^{26}Al$ also offer potential for dating faulting and other deformation. However, refinement of relative-dating techniques, such as soil development, rock weathering, and progressive landform modification are likely, because of their general applicability, to provide much of the needed age control.

For a given fault or other feature of active tectonism, deformation rates need to be determined over different time spans to recognize any variations in deformation rate and how attempts at prediction of future deformation may relate to these variations. If grouping of faulting events has occurred, hazard assessment based on deformation rates depends on the combination of the pattern of deformation and the time window of observation.

## INTRODUCTION

Dating is a critical tool in the assessment of active tectonism. The two primary measures of active tectonism are the age and the amount of deformation of a stratigraphic unit, which together define rates of deformation. Although slip or other deformation rates may vary through time, such rates are still one of the most useful measures of active tectonism (Slemmons, 1977).

Dating of active tectonism is commonly accomplished by dating surficial or volcanic deposits. In addition to dating conventional stratigraphic units, materials such as calcite infillings may be deposited in a fault plane and dating of these infillings used to determine the history of faulting. With either conventional stratigraphic units or materials infilling a fault zone, if the material is unbroken its age provides a minimum age for the last faulting; and if it is broken, it provides a maximum age for the last faulting. Although individual fault offsets obviously occur in jumps, the overall slip rate can be determined from the amount of offset, especially for multiple events, divided by the geologic time interval involved.

In the past few decades, our ability to date geologically young deformation and associated deposits has improved greatly. In this time, dozens of dating techniques (Tables 13.1 and 13.2) have been either developed or greatly refined. As few as 10 yr ago, estimates of the age of Quaternary deposits were commonly in error by severalfold, and it was not uncommon for age estimates to have been off by a factor of 10. Although we have recently learned much about the ages of young deposits and deformation, we still have a long way to go, for one of the greatest constraints in our understanding active tectonism is accurate and reliable dating in order to define rates of past deformation and times of past earthquakes (Allen, Chapter 9, this volume).

An appreciation of the amount of dating control needed is illustrated in Figure 13.1, which shows one model of fault activity through time. Predictions based on such a model require multiple dates to determine (1) the slope of the line shown as "accumulation rate," (2) the interval between fault movements, and (3) the time since the last movement. To define a fault history involving multiple events, at least one age is needed to define each event. This kind of model depends on the assumption of a constant accumulation or slip rate; dating control spanning different time intervals is needed to know if the assumption of a constant slip rate is warranted.

More than one age determination is required to establish reliable age control. Numerical ages are preferred, but relative-dating and correlation methods are important because they can provide age control in the absence

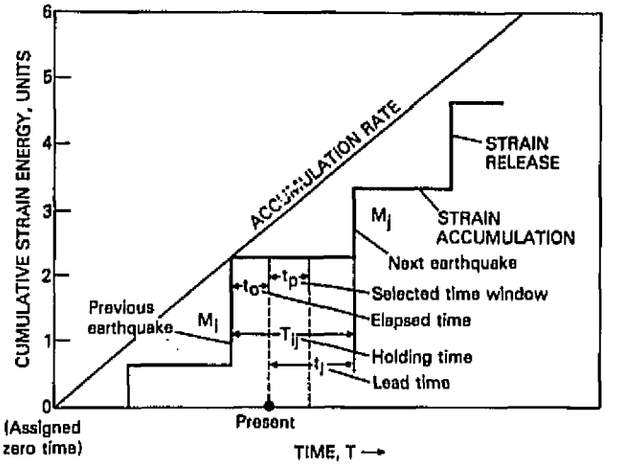


FIGURE 13.1 Diagram of the earthquake-generation process of Cluff *et al.* (1980) showing importance of time (horizontal scale) in earthquake history and prediction. In order to predict the time of a future earthquake based on this model, note how much dating control is needed to define holding time, accumulation rate (similar to slip rate), and elapsed time, even for this example in which accumulation rate is assumed to be constant.

of numerical techniques, or they can be used to evaluate the numerical ages, which can be subject to large nonanalytical errors. Surficial geologic studies and local time-calibrated stratigraphies are vital in the study of active tectonism, both to provide dating control and to evaluate the reliability of specific age estimates for tectonic events.

## OVERVIEW OF DATING METHODS

About 26 different dating methods can be used in dating active tectonism. Table 13.1 categorizes these methods as primarily numerical, relative dating, or correlation (Table 13.1). The numerical methods are based on processes that do not require further calibration. Relative-dating methods are applied to a local sequence of deposits that differ in age but are similar in other characteristics, such as a sequence of glacial moraines or a flight of alluvial terrace deposits. Relative-dating methods provide information on the magnitude of age differences between stratigraphic units. If calibrated, relative-dating methods can be used to estimate numerical ages. This normally requires calibration by numerical methods and an understanding of the process being measured and its relevant history (e.g., temperature, precipitation). The correlation methods do not directly yield a numerical age, but if a feature can be correlated with an event whose age is known, such as a volcanic ash

TABLE 13.1 Classification of Methods Applicable to Dating Active Tectonism[a]

| Numerical Methods | | | Relative Dating Methods | | Correlation Methods |
|---|---|---|---|---|---|
| 1. Annual | 2. Radiometric | 3. Other Radiologic | 4. Simple Process | 5. Complex Processes | 6. Correlation |
| 1. *Historical records* | 4. *Carbon-14* | 8. *Uranium trend* | 11. *Amino-acid racemization* | 15. *Soil development* | 21. *Stratigraphy* |
| 2. Dendrochronology | 5. *Uranium series* | 9. *Thermoluminescence and electron-spin resonance* | 12. *Obsidian hydration* | 16. *Rock and mineral weathering* | 22. *Tephrochronology* |
| 3. Varves | 6. *Potassium-argon* | | 13. Tephra hydration | 17. *Progressive landform modification* | 23. *Paleomagnetism* |
| | 7. *Fission track* | 10. *Cosmogenic isotopes other than carbon-14* ($^{10}$Be, $^{36}$Cl, $^{26}$Al, and others) | 14. Lichenometry | 18. Deposition rate | 24. *Fossils and artifacts* |
| | | | | 19. Geomorphic position and incision rate | 25. Stable isotopes |
| | | | | 20. Deformation rate | 26. Tektites and microtektites |

[a]All methods listed are briefly described in Table 13.2. Methods given in italics are discussed in the text.

eruption or a paleomagnetic reversal, precise age control can be obtained.

A dating technique, whether it be primarily a numerical, relative-dating, or correlation method, may be converted to the other two categories of methods (Table 13.1). For example, the relative-dating methods of amino-acid racemization or soil development can also serve either as local correlation techniques or, if calibrated by numerical dating, as numerical techniques.

Table 13.2 briefly summarizes 26 different dating methods noting their general applicability to studies of active tectonism, the age range of each method and the *optimum* accuracy within parts of this age range, and the basis of the method and the key problems in its use. The six columns (Table 13.1) are discussed in the next six sections. Beyond those given in Table 13.2 , the criteria for selecting individual methods for discussion include at least two of the following: (1) the method is particularly applicable to dating active tectonics, (2) the method provides a good illustration of the six general categories (columns of Table 13.1), and (3) the method has complexities or problems that merit discussion.

After this manuscript was completed, two books on Quaternary dating methods became available (Mahaney, 1984; Rutter, 1985). The reader interested in more extensive description and references to the literature may wish to consult these books.

## ANNUAL METHODS

Annual methods (Table 13.1, column 1), generally accurate to the nearest year, provide the most precise dating of active tectonism. But excepting varve chronology, annual methods span too short a time interval to assess active tectonism, particularly in the western hemisphere. Only limited use has been made of dendrochronology and varve chronology.

In the western hemisphere, historical records of faulting are restricted to about 200 yr (Bonilla, 1967). Based on the long historical records of seismicity from China (3000 yr) and Japan and the Middle East (2000 yr), Allen (1975, p. 1041) concluded that historical seismicity there shows "surprisingly large long-term temporal and spatial variations. The very short historical record in North America should, therefore, be used with extreme caution in estimating possible future seismic activity. The geologic history of late Quaternary faulting is the most promising source of statistics on frequency and location of large shocks."

## RADIOMETRIC METHODS

Because radiometric methods (Table 13.1, column 2) yield accurate numerical ages, samples for such dating are searched for in geologic studies of active tectonism. In many cases datable materials cannot be found. Additionally, radiometric methods may be subject to major errors and should be evaluated in their geologic context by other methods that, although not as precise, will normally be a valid indicator of the general age.

### *Carbon-14 Dating*

Carbon-14 dating is generally the most precise and applicable numerical method for dating prehistoric faulting. Indeed, the chronology of the late Quaternary and particularly the Holocene (past 10 ka) is based on this method (for review, see Grootes, 1983). The analytical uncertainty is generally less than a few percent.

Two applications of carbon-14 dating to active tec-

TABLE 13.2 Summary of Quaternary Dating Methods and Their Applicability to Dating Active Tectonism (from Colman and Pierce, 1979)

| Method | Applicability | Age Range and Optimum Resolution ($10^2$ $10^3$ $10^4$ $10^5$ $10^6$) | Basis of Method and Remarks |
|---|---|---|---|
| 1. Historical records | X to XXX | ═══ | Requires preservation of pertinent records; applicability depends on quality and detail of records. Limited to several hundred years in western hemisphere. |
| 2. Dendrochronology | XX | ═══ | Requires either direct counting of annual rings back from present or construction of a chronology based on variation in annual ring growth. Restricted to areas where trees of the required age and (or) environmental sensitivity are preserved. |
| 3. Varve chronology | X | ═══+++ | Requires either direct counting of varves back from present or construction of a chronology based on overlapping successions of continuous varved lake sediments. Subject to errors in matching separate sequences and to misidentification of annual layers. |
| 4. Carbon-14 | X to XXX | o•–+++═══? | Depends on availability of carbon. Based on decay of $^{14}C$, produced by cosmic radiation, to $^{14}N$. Subject to errors due to contamination, particularly in older deposits and in carbonate material (such as mollusk shells, marl, soil carbonate). See text. |
| 5. Uranium series | XX | ••–––+++– | Used to date coral, mollusks, bone, cave carbonate, and carbonate coats on stones. Potentially useful in dating travertine and soil carbonate. A variety of isotopes of the U-decay series are used including $^{230}Th/^{234}U$ (most common and method described to left), $^{234}U/^{238}U$ (with a range back to 600,000 yr), $^{231}Pa/^{235}U$ (10,000-120,000 yr), U-He (0-2 m.y.), and $^{226}Ra/^{230}Th$ (<10,000 yr). Errors due to the lack of a closed chemical system are a common problem, especially in mollusks and bone. |
| 6. Potassium-argon | X | •••––+++ | Directly applicable only to igneous rocks and glauconite. Requires K-bearing phases such as feldspar, mica, and glass. Based on decay of $^{40}K$ to $^{40}Ar$. Subject to errors due to excess argon, loss of argon, and contamination. |
| 7. Fission track | X | •••–––+++ | Directly applicable only to igneous rocks (including volcanic ash); requires uranium-bearing material (zircon, sphene, apatite, glass). Based on the continuous accumulation of tracks (strained zones) caused by recoiling U fission products. Subject to errors due to track misidentification and to track annealing. |
| 8. Uranium trend | XXXX | ooo••–––– | Based on open-system flux of uranium through sediment and soil; $^{238}U$, $^{234}U$, $^{230}Th$, and $^{232}Th$ must be measured on about five different samples from a given aged deposit and a isochron constructed to determine age. |
| 9. Thermoluminescence (TL) and electron-spin resonance (ESR) | XXXX | ooo••••••––––––– | Based on displacement of electrons from parent atoms by alpha, beta, and gamma radiation. Applicable to feldspar and quartz in sediments and carbonate in soils. TL based on amount of light released as sample is heated compared with that released after known radiation dose. TL precision better than indicated for ceramics in 400-10,000-year range. |
| 10. Cosmogenic isotopes other than carbon-14 | X | –?–?–?–?–?–?–?–?–? | Dating methods analogous to $^{14}C$-dating are based on the cosmogenic isotopes (half-life in hyears in parentheses) $^{32}Si$ (300), $^{41}Ca$ ($1.3 \times 10^5$), $^{36}Cl$ ($3.08 \times 10^5$), $^{26}Al$ ($7.3 \times 10^5$), $^{10}Be$ ($1.5 \times 10^6$), $^{129}I$ ($1.6 \times 10^7$), and $^{53}Mn$ ($3.7 \times 10^6$). Dating requires knowledge of the generation rates, flux rates, and retention efficiency of the deposit dated. These radio-isotopes occur in very low abundances and are measured by accelerator mass spectrometry. |

TABLE 13.2 Continued

| Method | Applicability | Age Range and Optimum Resolution | Basis of Method and Remarks |
|---|---|---|---|
| 11. Amino acid racemization | XX | 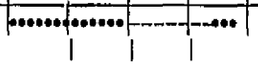 | Requires shell or skeletal material. Based on release of amino acids from protein and subsequent inversion of their stereoisomers. Shells tend to be more reliable than bone, wood, or organic-rich sediment. Is strongly dependent on other variables, especially temperature and leaching history. Commonly used as a relative dating or correlation technique, but yields numerical ages when calibrated by other techniques. |
| 12. Obsidian hydration | X | 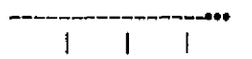 | Based on thickness of the hydrated layer along obsidian crack or surface formed during given event. Age proportional to the thickness squared. Calibration depends on experimental determination of hydration rate or numerical dating. Subject to errors due to temperature history and variation in chemical composition. |
| 13. Tephra hydration | X | 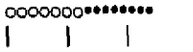 | Requires volcanic ash. Based on the progressive filling of bubble cavities in glass shards with water. Subject to the same limits as obsidian hydration, plus others, including the geometry of ash shards and bubble cavities. |
| 14. Lichenometry | X to XXX | 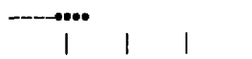 | Requires exposed, stable rock substrates suitable for lichen growth. Most common in alpine and arctic regions, where lichen thallus diameter is proportional to age. Subject to error due to climatic differences, lichen kill, and misidentification. The limit of the useful range varies considerably with climate and rock type. |
| 15. Soil development | XXXX | 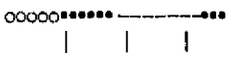 | Encompasses a number of soil properties that develop with time, all of which are dependent on other variables in addition to time (parent material, climate, vegetation, topography). Is most effective when these other variables are held constant or can be evaluated. Precision varies with the soil property measured; for example, accumulation of soil carbonate locally yields age estimates within ±20 percent. |
| 16. Rock and mineral weathering | XX | 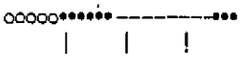 | Includes a number of rock and mineral-weathering features that develop with time, such as thickness of weathering rinds, solution of limestone, etching of pyroxene, grussification of granite, and buildup of desert varnish. Has the same basic limitations as soil development. Precision varies with the weathering feature measured. |
| 17. Progressive landform modification | XXX | 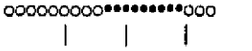 | In addition to time, depends on factors such as climate and lithology. Depends on reconstruction of original landform and understanding of processes resulting in change of landform, including creep and erosion. |
| 18. Rate of deposition | XX |  | Requires relatively constant rate of sedimentation over time intervals considered. Numerical ages based on sediment thickness between horizons dated by other methods. Quite variable in alluvial deposition. |
| 19. Geomorphic position and incision rate | XXX |  | Geomorphic incision rates depend on stream size, sediment load, bedrock resistance to erosion, and uplift rates or other base-level changes. If one terrace level is dated, other terrace levels may be dated assuming constant rate of incision. |
| 20. Rate of deformation | XXX | 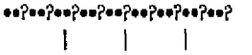 | Dating assumes deformation rate constant over interval of concern and requires numerical dating for calibration. At spreading centers and plate boundaries, nearly constant rates may be valid for intervals of millions of years. |

TABLE 13.2 Continued

| Method | Applicability | Age Range and Optimum Resolution | Basis of Method and Remarks |
|---|---|---|---|
| 21. Stratigraphy | XXXX | RESOLUTION DEPENDS ON RECOGNITION OF FEATURE AND ACCURACY OF DATING THAT FEATURE | Based on physical properties and sequence of units, which includes superposition and inset relations. Depends on the establishment of time equivalence of units; deposition of Quaternary units normally occurs in response to cyclic climatic changes. |
| 22. Tephrochronology | X | | Requires volcanic ash (tephra) and unique chemical or petrographic identification and (or) dating of the ash. Very useful in correlation because an ash eruption represents a virtually instantaneous geologic event. |
| 23. Paleomagnetism | XX | | Depends on correlation of remnant magnetic vector, which includes polarity, or a sequence of vectors with a known chronology of magnetic variation. Subject to errors due to chemical magnetic overprinting and physical disturbance. |
| 24. Fossils and artifacts | XX | | Depends on the availability of fossils, including pollen, and artifacts. Resolution depends on the rate of evolution or change of organisms or cultures and on calibration by other techniques. Subject to errors due to misidentification and interpretation. |
| 25. Stable isotopes | X | | Depends on correlation of the sequence of isotopic changes with an age-controlled master chronology. Oxygen isotopic record is useful in deep-sea and ice-cap cores and perhaps in cave deposits. |
| 26. Tektites and microtektites | X | | Depends on recognition and dating of glassy material (tektites) formed during impact of extraterrestrial masses. Tektites are scattered over large areas, such as the Australo-Asian tektite field, formed about 700 ka. |

APPLICABILITY

XXXX, nearly always applicable
XXX, very often applicable
XX, often applicable
X, seldom applicable

OPTIMUM RESOLUTION

=======, <2 percent
++++++, 2-8 percent
--------, 8-25 percent
••••••, 25-75 percent
oooooo, 75-200 percent

tonism illustrate powerful applications of this method. Along the San Andreas Fault 55 km northeast of Los Angeles at Pallet Creek, about 50 carbon-14 ages date 11 episodes of faulting in the 1700 yr prior to the 1857 historical rupture and define an average recurrence interval of about 145 yr (Figure 13.2; Sieh, 1984). For the south Boso Peninsula of Japan, carbon-14 dating defines four stepwise uplifts of land relative to sea level in the last 7000 yr (Figure 13.3). Shimazaki and Nakata (1980) concluded that the offset history supports a time-predictable recurrence model; that is, the larger the amount of the coseismic slip, the longer the interval before the next earthquake (Figure 13.3).

Carbon-14 ages may be in error by much more than the analytical uncertainty. Because of the extensive use of carbon-14 dating in studies of active tectonism, consideration should be given to the following three types of carbon-14 dating problems.

*Fluctuations in Atmospheric Carbon-14* Based on carbon-14 dating of tree rings whose absolute age is known, carbon-14 ages deviate from actual ages by amounts that are significant for some tectonic studies. For example, in the interval from 5000 to 8000 yr ago, carbon-14 ages are about 500-900 yr too young (Klein *et al.*, 1982). In the late Holocene, fluctuations in atmospheric carbon-14 introduce significant uncertainty in dating tectonic events (Figure 13.4). For example, a carbon-14 age of 150 + 20 ya (years before AD 1950) only defines an age in the interval from 0 to 295 *calendar* years before AD 1950 (Klein *et al.*, 1982, Table 2).

*Contamination with Old Carbon* Independent of the age of the sample, the effect of contamination with old carbon is constant (Figure 13.5, upper left half). Regardless of whether a sample is 1 or 30 ka, incorporation of 10 percent "dead" carbon will make ages 800 yr too

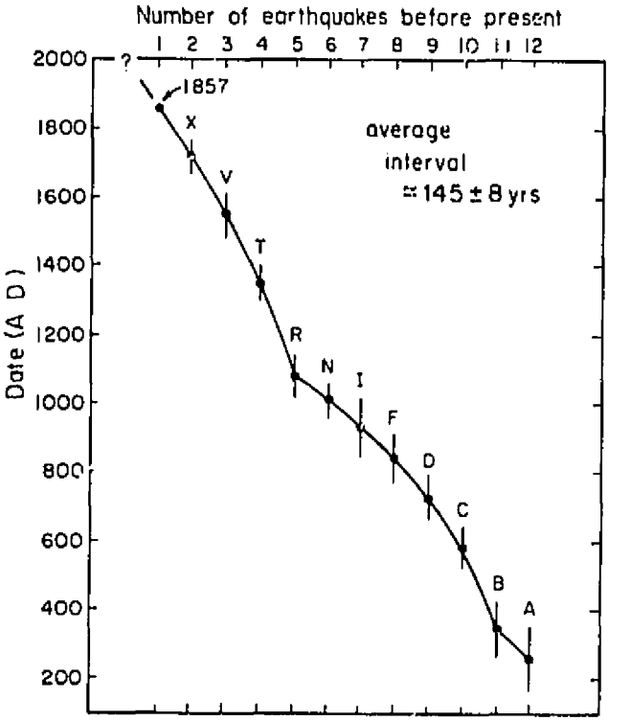


FIGURE 13.2 Ages of faulting events (letters) on San Andreas Fault at Pallet Creek (from Sieh, 1984). Ages are based on about 50 carbon-14 dates and detailed trench mapping.

old. Old carbon may contaminate a sample in two ways. First, detrital carbon, such as that from coal of pre-Quaternary age which contains no carbon-14 or that from humic soil material which may have an age of several thousand years, may be incorporated in a sample. Second, plants and animals living underwater can incorporate lower activity carbon from $CO_2$ in the water either because the water is old or because it has bicarbonate from old rocks. For marine mollusks from the North Atlantic, the age of $CO_2$ in ocean water increases ages by 400 to 750 yr (Mangerud and Gulleksen, 1975).

*Contamination with Young Carbon* Contamination with recent carbon can alter ages greatly. Samples whose ages are beyond the range of carbon dating (>75 ka) that are contaminated with only half a percent of recent carbon will yield an age of about 40 ka (Figure 13.5, lower right half). Even the most exacting of analyses can be in error: a carbon-14 enrichment age of 71 ka (representing only 0.014 percent of the original carbon-14 activity) was thought to date the Salmon Springs glaciation of northwest Washington State (Stuiver *et al.*, 1978) until associated ash deposits were fission-track dated at 700 and 800 ka (Easterbrook *et al.*, 1981).

Contamination with younger carbon may be responsible for many of the finite carbon-14 ages in the 20- to 70-ka range. Contamination of carbon samples with recent carbon produces effects that are not generally appreciated (Figure 13.5). Examination of this nonlinear effect also should provide a caution about assuming that "consistency" in age results necessarily is an argument for the validity of carbon-14 ages. For example, the consistency of many dates falling in the 25- to 40-ka range may only reflect contamination of samples older than about 50 ka with the equivalent of 0.5-2 percent of recent carbon (Figure 13.5). Several hundred carbon dates in the 25- to 40-ka range have been obtained from coastal deposits in the eastern United States. Many researchers (referenced in Bloom, 1983) have concluded that these samples date a mid-Wisconsin high stand of sea level, in part based on the apparent "consistency" of a large number of dates in this age range. After thorough analysis of this problem, Bloom (1983, pp. 215-218) concluded that these ages are invalid. Amino-acid racemization studies on mollusks asssociated with samples yielding caron-14 dates in the 25- to 40-ka range also indicate that the carbon-14 dates are erroneously young (Belknap, 1984).

Samples may be contaminated by in situ additions of younger carbon. Soil carbonate, mollusks, or corals are particularly susceptible to addition of young carbon, especially when subject to repeated wetting or drying. Contamination by microorganisms incorporating young carbon may occur either before or after a sample has been collected. Marine cores stored for 5 yr were found to be contaminated by enough terrestrial bacteria to account for 5-10 percent contamination with modern carbon (Geyh *et al.*, 1974). In-place contamination of samples is not well studied, but it may be possible if microbial activity consumes $CO_2$ from air or $HCO_3^-$ from water with a higher carbon-14 activity than the age of the sample. For example, methanogens participate in terminal stages of the degradation of organic matter, living on and presumably incorporating carbon dioxide and hydrogen produced by anaerobic bacteria into their tissue (see Maugh, 1977).

Extra care should be taken in order to minimize contamination with recent organic material during sampling and sample preparation. In addition, samples should be examined for visible contamination, particularly by roots. Removing modern roots will not, of course, remove contamination caused by older, largely decayed roots. Common sample pretreatment before carbon-14 dating removes base-soluble fulvic acids and acid-soluble humic acids, leaving a residue called

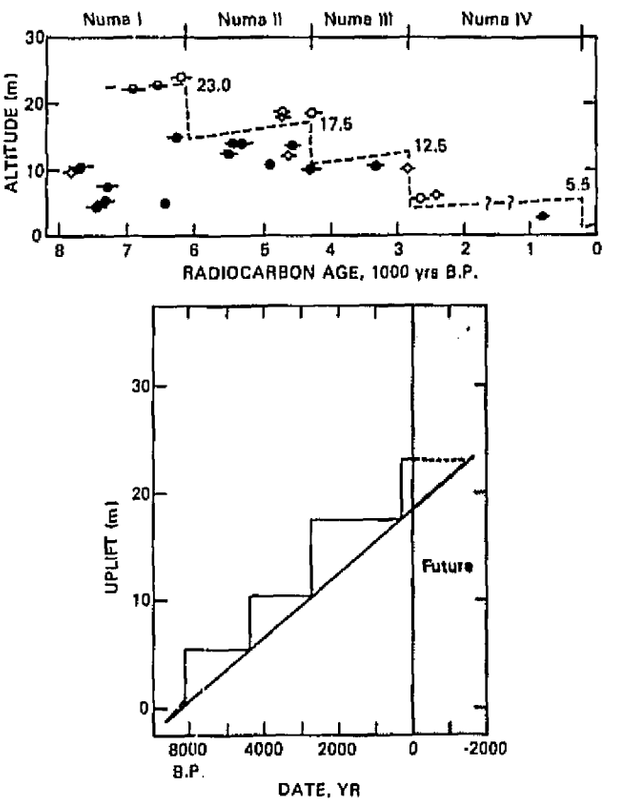


FIGURE 13.3 Four stepwise uplifts of the coast of the southern Boso Peninsula, Japan, determined by about 25 carbon-14 dates (from Shimazaki and Nakata, 1980). The open, half-closed, and closed circles indicate samples from above, near, and below the former sea level, respectively. Lower part of figure shows cumulative uplift versus time; line through corners of stairstep plot shows that uplift, inferred to be caused by coseismic faulting, conforms to a time-predictable model.

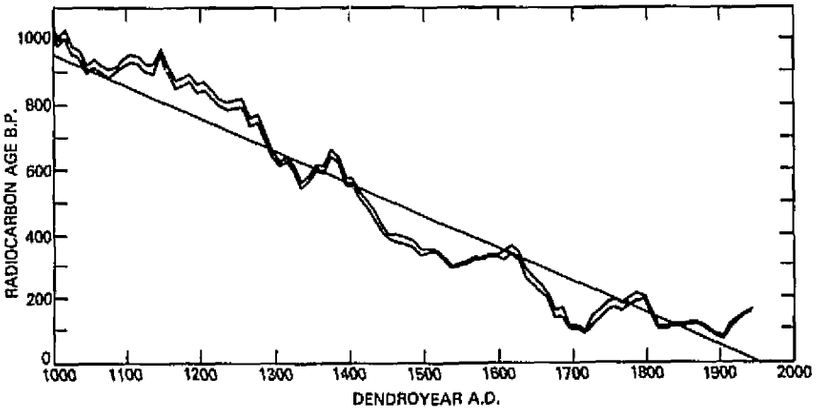


FIGURE 13.4 Carbon-14 age as a function of dendrochronological age for the past 1000 yr (from Stuiver, 1982). Note deviations from concordance line that have a 100-200-yr period.

humin or humate. Such pretreatment is commonly employed, but it does not remove all forms of contamination by younger carbon. For example, dating studies by Goh *et al.* (1977) have obtained ages as young as 17,750 ± 2050 ya on humin from deposits whose "best" carbon-14 ages are *more than* 40,600 ya.

### *Uranium-Series Dating*

The $^{230}Th/^{234}U$ disequilibrium method is the most commonly used dating technique of the many based on the radioactive decay series of uranium (Table 13.2; Ivanovich and Harmon, 1982). Because uranium is

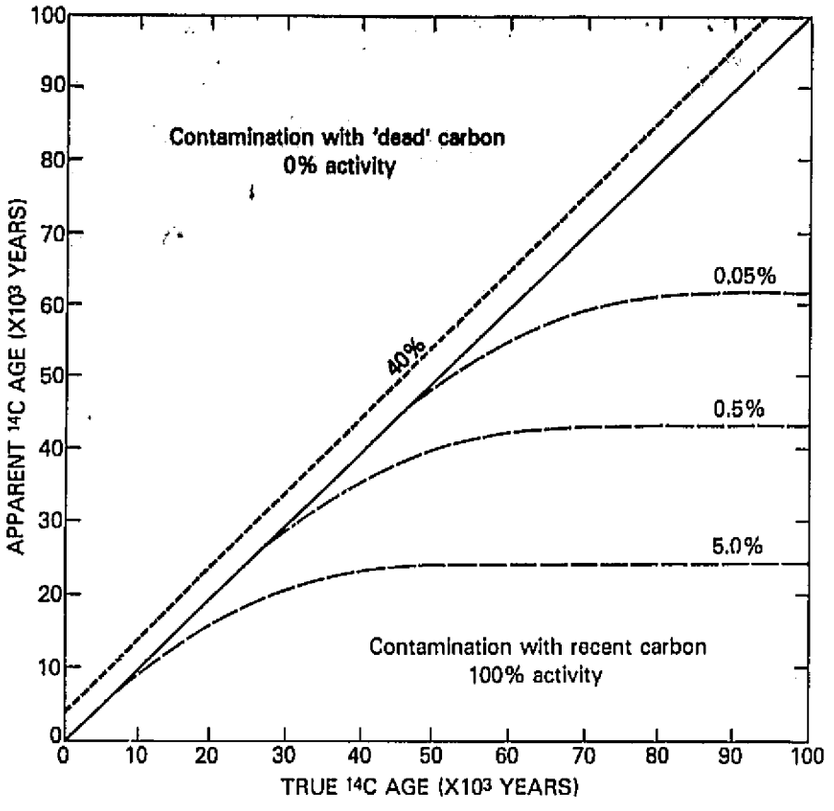


FIGURE 13.5 Unequal effects of contamination with recent and dead carbon on carbon-14 ages (from Grootes, 1983). For contamination with dead carbon (shaded area), effect is a simple ratio. But for samples with true ages older than a few tens of thousands of years, the apparent age can be dictated by only small amounts of contamination with recent carbon.

much more soluble than thorium, materials precipitated from solution such as corals, mollusks, calcic soils, carbonate deposits in caves and fault zones, and fossil bones are greatly enriched in uranium with respect to thorium. This provides a system in which radioactive growth of $^{230}$Th is a function of time until it reaches a steady-state relation with its parent $^{234}$U. The most reliable application of the method is to pure cave carbonate and to samples of corals in which the original aragonite is unaltered. For the time interval of 50 ka to about 300 ka, age control for deformation of coastal areas is largely based on uranium-series dating of corals.

For corals and cave deposits, uranium is incorporated in the sample at the time of deposition and, under appropriate conditions, the sample acts as a closed system with respect to uranium. Dating problems generally result from migration of uranium after initial deposition or contamination with thorium in detrital material at the time of deposition. Living mollusk shells or bones contain only about a tenth of the uranium that becomes incorporated after burial. If ages are calculated on the basis of a closed system, the uranium in the sample should ideally have been introduced in a time interval that is short relative to the age of the sample, and none of this secondary uranium should have been leached away. If uranium is incorporated at later times in the history of the sample, the apparent Th/U age is too young. Conversely, if uranium is leached during the later history of a sample, the apparent Th/U age is too old. Kaufman *et al.* (1971) concluded that for samples of known age, $^{230}$Th/$^{234}$U dating of mollusks gave ages within their analytical uncertainty no more than half the time.

For active tectonism in semiarid and drier areas, $^{230}$Th/$^{234}$U dating of carbonate may date fault movements. Soils may contain carbonate coats on the undersides of stones that can date faulted alluvial surfaces. Along the Arco fault scarp in central Idaho, a surface vertically offset about 19 m by faulting has 1-cm-thick carbonate coats that can be subdivided into outer, middle, and inner parts (Pierce, 1985). Analyses of both the soluble (carbonate) and insoluble (detrital residue) fractions from these layers yield ages as shown in Figure 13.6

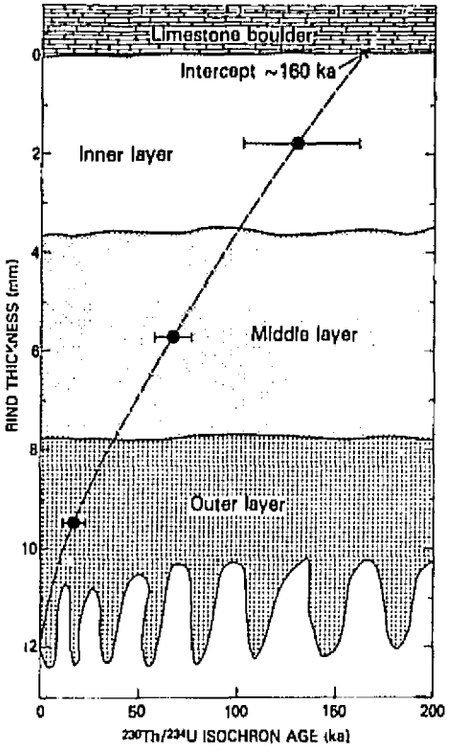


FIGURE 13.6 Three stratigraphically consistent $^{230}Th/^{234}U$ ages from a stratified carbonate coat. This plot of age versus thickness defines an age of about 160 ka for an alluvial fan surface offset about 19 m along the same range-front fault, but 50 km south of the part offset during the 1983 Borah Peak earthquake, central Idaho. $^{230}Th/^{234}U$ isochron ages from Szabo and Rosholt (1982, Figure 10.5) are plotted at midpoint of sampled layer. The carbonate coats form on the underside of stones in the soil on an alluvial fan.

(Szabo and Rosholt, 1982). These ages are stratigraphically consistent and indicate a time span of 160 ka for 19 m of offset and a long-term slip rate of about 1 m/ka.

### *Potassium-Argon Dating*

The potassium-argon (K-Ar) method is limited in its applicability to dating active tectonics by its primary use with igneous rocks and general lack of resolving power for rocks younger than a few tens of thousands of years. Nevertheless, most of the correlation methods (Table 13.1, column 6) and calibration of many of the relative-dating methods (Table 13.1, columns 4 and 5) depend on K-Ar dating for their age control. More important to the study of active tectonism, both the paleomagnetic time scale, which was critical in establishing the theory of plate tectonics, and the relative rates of plate motions are largely based on K-Ar dating.

### *Fission-Track Dating*

Fission-track dating is generally limited to rhyolitic volcanic rocks older than about 100 ka and is commonly better than the K-Ar method for dating volcanic ash.

Fission-track dating can also be used in areas of high relief and rapid uplift to estimate long-term rates of uplift. Because fission tracks in apatite anneal if warmer than about 120°C, fission-track dating of apatite determines the time a rock has been below this temperature and consequently at relatively shallow depths. If the geothermal gradient is known, the rate of uplift and erosion of a mountainous area can thereby be determined. Using this method, Naeser *et al.* (1983) estimated that the late Cenozoic rate of uplift of the Wasatch Mountains has averaged 0.4 m/ka over the past 10 Ma (million years).

## OTHER RADIOLOGIC METHODS

Other radiologic methods (Table 13.1, column 3) involve radioactive processes but may also depend on other nonradioactive processes that must be either estimated or accounted for by calibration using other numerical methods.

### *Thermoluminescence (TL) and Electron-Spin-Resonance (ESR) Dating*

Thermoluminescence (TL) dating (Wintle and Huntley, 1982) may be widely applicable to dating active tectonics, but the method has been used rarely in the United States. Owing to the effects of radiation, many minerals emit light when progressively heated, and the changing intensity of light emission yields a glow curve. A starting point for buildup of TL can be the time of crystallization of carbonate in a soil, the growth of a shell, the firing of a ceramic, the eruption of a lava flow, or the time of burial after exposure to sunlight. The glow curve becomes stronger the greater and longer the radiation exposure. The flux of radiation is related to the modern content of uranium, thorium, and potassium. The response of the dosimeter grains is calibrated by artificial irradiation (alpha, beta, and gamma) and measurement of the induced glow curves. Several hours of exposure to sunlight "zeros" the TL in grains of quartz and feldspar, which are nearly ubiquitous in surficial deposits. Thus, many surficial deposits offset by faulting are potentially datable by TL.

Because water adsorbs some of the gamma radiation, the amount of water present over the history of the sample needs to be measured or estimated and its effect on the in situ sample calculated. Also, radiogenic isotopes

are assumed not to have been added to or leached from the sample. Wintle and Huntley (1982) listed criteria for evaluating TL dates of sediment and discussed problems that merit further research.

TL dating of loesses has yielded reasonable results. Late Pleistocene loess in Germany yielded TL ages that are stratigraphically consistent and concordant with carbon-14 ages of an associated ash (Wintle and Brunnacker, 1982; Figure 13.7).

Electron spin resonance (ESR) dating is similar to TL dating in that a mineral acts as a dosimeter for local radiation, but differs in the feature measured and the method of measurement. ESR dating of corals from marine terraces of Japan yielded results in good agreement with carbon-14 (2-4 ka) and $^{230}Th/^{234}U$ (40->200 ka) dating (Ikeya and Ohmura, 1983).

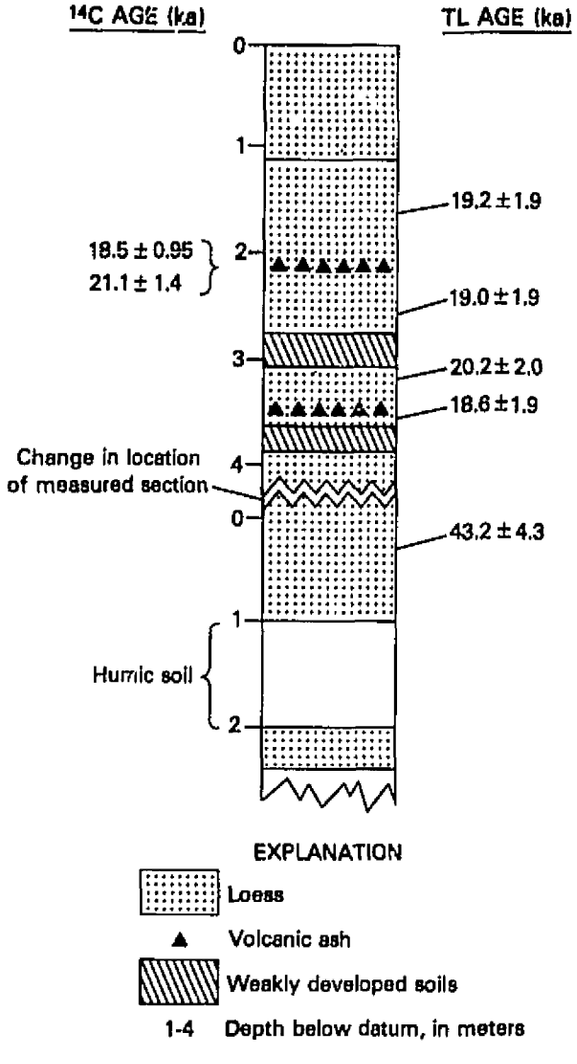


FIGURE 13.7 Thermoluminescence (TL) dating of loess deposits in West Germany showing that the TL ages are both stratigraphically consistent and concordant with existing carbon-14 ages on the volcanic ash that was dated elsewhere (redrawn from Wintle and Brunnacker, 1982).

### *Uranium-Trend Dating*

Uranium-trend dating is an isochron-type method for dating Quaternary sediments and soils (Rosholt, 1980; Szabo and Rosholt, 1982). Rather than requiring a closed system as do most uranium-series methods, this method depends on a flux of uranium (mostly $^{238}U$) through sediments and the consequent embedding of recoil products $^{234}U$ and $^{230}Th$ in the sediments. The method can be used on almost all sedimentary materials and has produced generally reasonable ages (Rosholt, 1980). The calibration of the method initially depended on ages determined by other methods, but ages can now be calculated using the established calibration. The method is expensive, requiring determination of $^{238}U$, $^{234}U$, $^{230}Th$, and $^{232}Th$ for five or more samples from a given deposit. Although widely applicable, the method has so far experienced limited use because of its newness, complexity, and cost.

### *Cosmogenic Isotopes Other Than Carbon-14*

Similar to carbon-14, several other radiogenic isotopes are generated by cosmic-ray bombardment and may be useful in tectonic studies. Dating rationales exist for $^{32}Si$, $^{41}Ca$, $^{36}Cl$, $^{26}Al$, $^{10}Be$, $^{129}I$, and $^{53}Mn$, which are analyzed by accelerator mass spectrometry (half-lives given in Table 13.2).

Beryllium-10 is produced by cosmic-ray bombardment and is carried to the Earth's surface by rain and dust. Pavich *et al.* (1984) showed that $^{10}Be$ is adsorbed onto clays in soils and systematically increases in abundance with soil age for at least the first 100 ka of soil development. More research is needed to evaluate this method for dating surface and buried soils.

## RELATIVE-DATING METHODS, SIMPLE PROCESS

These methods (Table 13.1, column 4) do not depend on radiogenic processes but are based on relatively simple chemical or biological processes whose rates are related to controlling variables such as temperature and chemical composition or species effects.

### *Obsidian-Hydration Dating*

Obsidian hydration has been used to date the last two glaciations in the Rocky Mountain region (Pierce *et al.*, 1976). If temperature and chemical composition are constant, hydration thickness increases proportional to the square root of time. Figure 13.8 shows the increase in hydration with time as determined by the hydration thicknesses of two K-Ar-dated rhyolite flows and carbon-14-dated recessional deposits. The deposits of the next to last, or Bull Lake, glaciation date at about 140 ka (Pierce *et al.*, 1976). This age for the Bull Lake glaciation is about 5 times older than the age considered correct 20 yr ago. The importance of the dating at West Yellowstone to studies of active tectonism is that these ages can be inferred for many deposits throughout the western United States if they can be correlated with those at West Yellowstone on the basis of criteria such as soil development, morphologic changes, and weathering rinds (see Figure 13.9).

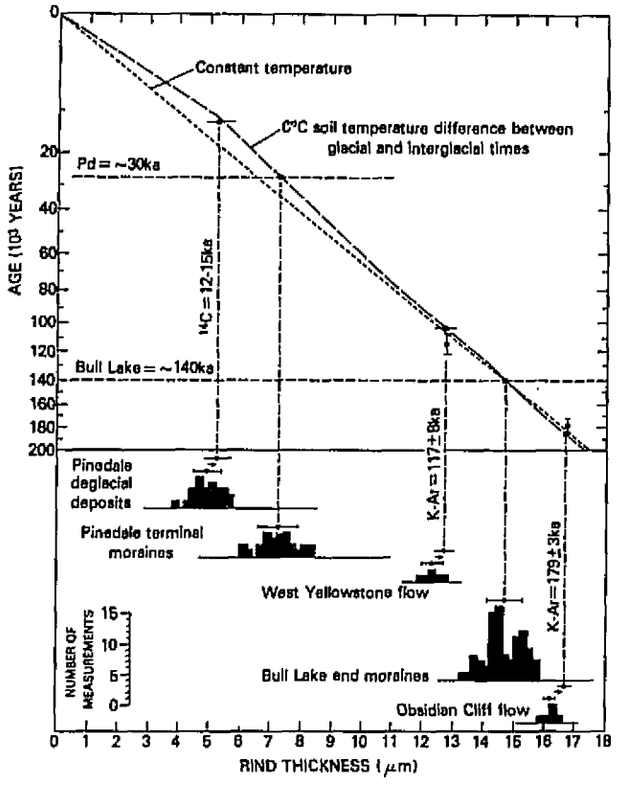


FIGURE 13.8 Obsidian-hydration dating of the Pinedale and Bull Lake Glaciations near West Yellowstone, Montana (from Pierce *et al.*, 1976). Dashed line shows increase in hydration thickness with age based on hydration thickness measured on deposits dated by K-Ar or $^{14}C$ methods. Above histograms, short lines with dots are means and standard deviations of hydration-thickness measurements, some of which are offset (small arrows) to account for small temperature differences between localities.

### *Amino Acid Racemization*

Amino acid racemization (and epimerization) has provided important age information for deciphering late Quaternary deformation along the West Coast of the United States (Lajoie, Chapter 6, this volume). Because racemization rates for a given species depend on temperature and a kinetic model (Wehmiller, 1982), the method works best if calibrated by numerical methods. On the California coast, uranium-series dating of corals has provided a few calibration points, but even with this calibration the amino acid ratios on mollusk samples did not allow distinction between three global sea-level culminations known from elsewhere to date at about 80, 95, and 125 ka. The problem of distinguishing these three high-sea stands has been resolved by combined studies using amino acid and uranium-series dating, temperature gradients along the coast, and paleontological identification of cool (oxygen isotope substages 5a or b) and warm (substage 5e) faunas (Lajoie, Chapter 6, this volume).

## RELATIVE-DATING METHODS, COMPLEX PROCESSES

This group of dating methods includes some of the most widely applicable methods (Table 13.1, column 5). Numerical ages can be empirically estimated by these methods. Rigorous evaluation of these complex methods would require modeling of each process and quantification of their relative effects. Nevertheless empirical quantification has been done, and some age estimates based on these methods (Table 13.1, column 4) may be more reliable than, if not so precise as, some carbon-14 ages.

### *Rock and Mineral Weathering*

Rock and mineral weathering (Table 13.1, column 5) includes such relative-dating techniques as mineral grain etching, seismic velocities in weathered stones, pitting on stone surfaces, and weathering rinds.

Weathering rinds on basaltic and andesitic stones from the B horizons of soils have yielded age information on middle and late Quaternary deposits at seven different areas in the western United States (Figure 13.9; Colman and Pierce, 1981). Multiple measurements of rind thicknesses from a given stratigraphic unit are consistent; and, for a succession of deposits, rind

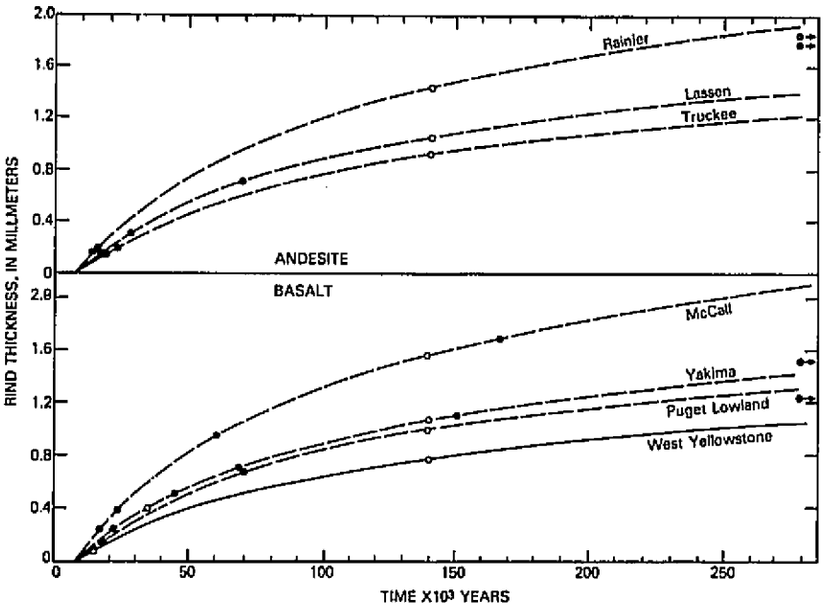


FIGURE 13.9 Use of weathering rinds to date and correlate glacial deposits in seven areas in the western United States. As shown by decreasing curvature of lines, rind thickness is assumed to increase logarithmically with time (from Colman and Pierce, 1984). Open circles are for deposits independently dated at West Yellowstone and for deposits correlated on basis of soils and other criteria with 140,000-yr-old deposits at West Yellowstone. Solid circles are for other glacial deposits plotted on the appropriate curve according to their rind thickness.

thickness increases with stratigraphic age. Local calibration by numerical dating indicates that rind thicknesses increase logarithmically with time. Based on a logarithmic increase in rind thickness and on the assumption that deposits with a certain relative moraine form and degree of soil development correlate with deposits of the Bull Lake glaciation at West Yellowstone (oxygen-isotope stage 6), ages can be estimated for all the deposits in seven glacial successions in the western United States. Deposits representing isotope stages 2 and 6 apparently are present in all areas sampled, but moraines representing stages 3 and 4 were apparently obliterated in many areas by glaciation during stage 2 (Figure 13.9).

Recent developments in the study of desert varnish suggest that systematic changes in varnish properties, such as decreasing ratios of leachable cations to manganese, occur with time (Dorn, 1983). With local calibration, age estimates on faults in desert environments may be obtained by this method.

### *Soil Development*

On land, soil development is nearly always pertinent to estimating the age of deformation. Soil development is a function of climate, parent material, organisms, topography, and time. If all the factors other than time can be held constant, the effect of time on soil development can be isolated and used to calibrate soil development with time at other sites.

Recently, Harden (1982) devised the soil "Profile Development Index" based on quantification of standard field descriptions of soils, including such features as color, clay content, texture, and soil-horizon thickness. Each of 10 or so soil properties is objectively quantified for each soil horizon on a scale that goes from zero to the maximum observed development. For the Merced, California, area, an individual soil property such as rubification (reddening and brightening of soil colors) shows a progressive increase with time from 100 yr to more than 1 m.y. (rubification, Figure 13.10A). The Profile Development Index (Figure 13.10B) combines several soil properties such as texture, pH, dry consistence, and soil structure and shows the cumulative effect of the development of many soil properties with time. Dating by this soil Profile Development Index is improved by using only soil properties that show the highest correlation with age (see Index of four best properties, Harden and Taylor, 1983).

Although calibration of soil Profile Development Index with age is best restricted to local areas where climate and parent material are the same, soils from four different areas of the United States appear to show similar Profile Development Index values with increasing age (Figure 13.10C). The soil Profile Development Index should prove useful in estimating ages of deformation, for it is based on readily describable field properties, provides an objective numerical basis for comparison between soils, and eliminates the need for subjective estimates of a soil's "development."

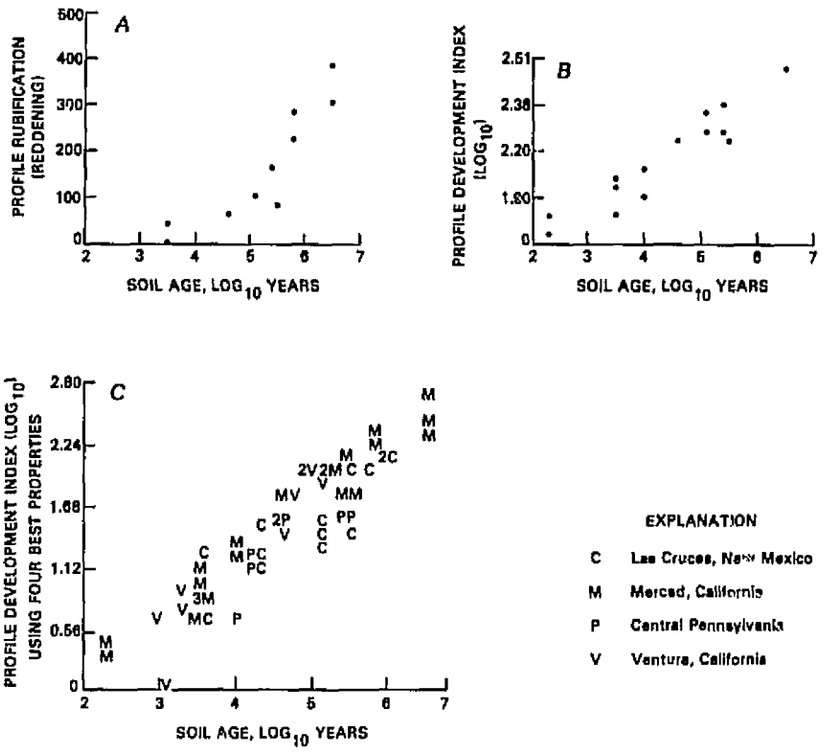


FIGURE 13.10 Increase in soil development with time (from Harden, 1982; Harden and Taylor, 1983). A, one soil property (rubification) in Merced, California, area. B, Soil Profile Index based on multiple properties in Merced area. C, Soil Profile Index for climatically different areas. Numbers indicate the number of points that plot in one place.

Some individual soil properties can be measured to estimate age. Such properties include increases in clay (Levine and Ciolkosz, 1983; Reheis, 1984; Pierce, 1979), secondary carbonate (Machette, 1978), secondary gypsum (Reheis, 1984), and secondary iron oxides (McFadden, 1982) as well as major-element chemistry (Harden and Taylor, 1983, Reheis, 1984). These measurements of changes are for an individual process and are like the simple-process, relative-dating methods (Table 13.1, column 4) but are discussed here because they are a component of soil development.

On the downwind and downthrown side of a fault offsetting a flat, former basin floor of the Rio Grande rift, New Mexico, fault movements were rapidly followed by deposition of eolian sand. During stable periods, five different calcic soils developed on these eolian sands and were subsequently buried (Figure 13.11). The time taken to form each soil is based on the total pedogenic $CaCO_3$ (g/cm$^2$-soil column) divided by the accumulation rate of pedogenic $CaCO_3$ determined from the 500-ka surface soil on the upthrown side of the fault. The deposit thickness indicates fault offset, whereas the amount of pedogenic $CaCO_3$ indicates the interval between fault episodes (Figure 13.11). The deformation history inferred from this information (Figure 13.12) shows an apparently decelerating rate of faulting.

### *Progressive Landform Modification*

Recognition of active tectonism commonly depends on detection of landforms created or modified by deformation, which is the subject area of tectonic geomorphology. To the trained eye, tectonic landforms tell much about the degree of tectonic activity, and new quantitative methods are making tectonic geomorphology a more exact science (Keller, Chapter 8, this volume). The effects may be subtle, such as alterations of river courses and gradients (Schumm, Chapter 5, this volume) or dramatic, such as bold, mountain-front escarpments (Keller, Chapter 8, this volume).

Geomorphic modification of fault scarps is particularly important to studies of active tectonism (Wallace, 1977; Nash, Chapter 12, this volume; Keller, Chapter 8, this volume). As with soils, the environmental variables such as lithology, climate, and vegetation need to be held constant or accounted for otherwise.

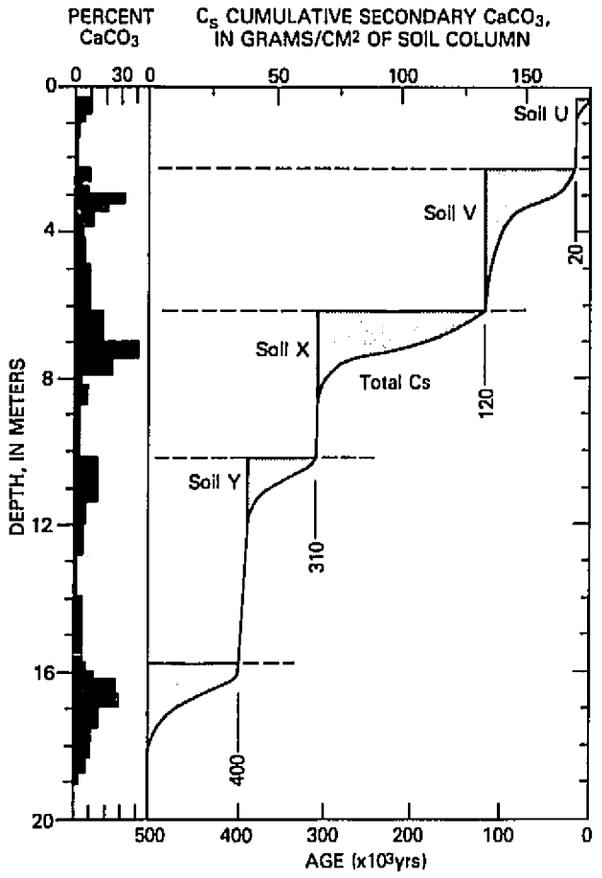


FIGURE 13.11 Dating of fault-related buried soils based on the accumulation of carbonate in calcic soils near Albuquerque, New Mexico (from Machette, 1978).

## CORRELATION METHODS

If a feature can be correlated with an event of known age, reliable and precise age control can be obtained. Methods such as those listed in Table 13.1 (column 6) may provide accurate numerical dates or exact correlation between deformed areas.

### *Stratigraphy*

Stratigraphy, including lithologic characteristics and the sequence of units, is basic to understanding the history of active tectonism. In surficial geology, the sequence of units may not be based on superposition but on geomorphic relations such as a sequence of successively lower and younger stream terraces. The origin of deposits also may be important in understanding the stratigraphy of surficial deposits. If the age of a unit can be determined in one place, that age can be applied to correlative units or be used to provide age constraints for sequentially younger or older units. Many surficial geologic units are causally related to the cycles of climatic change that characterize the Quaternary, such as successions of glacial till, sequences of loess separated by buried soils, and sequences of marine or alluvial terraces.

Numerical dating control is normally obtainable only at scattered localities, and extension of this dating control to sites of deformation depends on stratigraphic correlation over distances of tens to even hundreds of kilometers. The age of stratigraphic units in Quaternary geologic successions is the subject of much current research. Such research addresses many unresolved dating problems, results in new and commonly significantly revised ages, and leads to development of new strategies for obtaining ages. Studies centered on stratigraphy offer the best method to check a given dating technique through comparison with other age information from related stratigraphic units. Thus, although laboratory and numerical analyses are important in obtaining ages, stratigraphic work based on field studies is fundamental

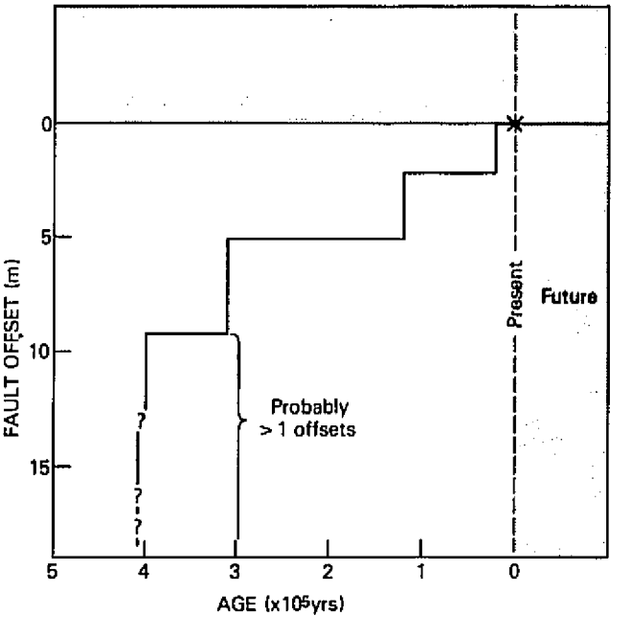


FIGURE 13.12 Fault offset versus time as determined by accumulation of soil carbonate in buried soils near Albuquerque, New Mexico (drawn from data in Machette, 1978).

in judging the reliability of these ages and relating ages to deformation of stratigraphic units.

### *Tephrochronology*

A volcanic ash can provide a time-parallel marker whose age is as accurate as the best dating either at any of its occurrences or of the correlative volcanic rocks in its source area. Recognition of a given ash bed should be based on multiple criteria, especially the petrography and chemistry of the glass and phenocrysts, as well as stratigraphy, paleomagnetism, paleontology, and radiometric dating (Westgate and Gorton, 1981). Tephrochronology has proved of great value in dating active tectonics. For example, in southern California deposits containing the 0.7-Ma Bishop ash are laterally offset about 6.6 km on the San Jacinto Fault (Sharp, 1981), and deposits containing 0.6-, 0.7-, and 1.2-Ma volcanic ashes are uplifted and tilted along the Ventura Fault (Yeats, Chapter 4, this volume). Tephrochronology is also important in calibrating other relative-dating and correlation methods, such as soil development, uranium-trend dating, amino-acid racemization, thermoluminescence dating, and dating of faunal boundaries. These calibrated methods can then, in turn, be used to date active tectonism.

Improvements in tephrochronology have led to major revisions in Quaternary stratigraphy and age assignments. In the 1960s, the Pearlette ash (known present distribution from California to Iowa) was considered to be of a single age, and the stratigraphy and paleontology of older Quaternary deposits all the way from the midcontinent to the Rocky Mountains were founded on the assumption that the Pearlette ash represented one eruption of late Kansan age. Careful petrographic and chemical study of the Pearlette ash has shown that it actually includes ashes from three different and distinct eruptions from the Yellowstone area that differ in age by a factor of 3 (Huckleberry Ridge ash, 2 Ma; Mesa Falls ash, 1.2 Ma; and Lava Creek ash, 0.6 Ma; Izett, 1981).

### *Paleomagnetism*

The orientation of the Earth's magnetic field is recorded by the orientation of magnetic minerals at the time of deposition of many fine-grained sedimentary deposits. Dating control can be obtained if the paleomagnetic record determined from a sequence of late Cenozoic sediments or volcanic rocks can be correlated with the established paleomagnetic polarity time scale (Mankinen and Dalrymple, 1979; see Barendregt, 1981, for a review). For example, the change from the Matuyama Reversed-Polarity Chron to the present Brunhes Normal-Polarity Chron occurred about 730 ka. This change provides a global datum for the assessment of long-term tectonic rates and calibration of relative-dating methods.

The established polarity time scale also dates the age of the ocean floor outward from the ocean-ridge spreading centers. The rates of movement of crustal plates away from these spreading centers is based on the age and width of the normal and reversed polarity stripes of the ocean floors.

Within the Brunhes Normal-Polarity Chron, potential age control may be provided excursions or reversed-polarity subchrons that lasted a few thousand years; about five such events have been suggested. In addition, secular variation in the geomagnetic field with periodicities of thousands to tens of thousands of years may provide a basis for local correlation and dating. The record of secular variation is best studied in lacustrine and other environments of continuous fine-grained sediment deposition. Such sediment dated by paleomagnetic criteria may also record sediment deformation associated with nearby earthquakes.

### *Fossils and Artifacts*

Fossils have been of limited value in dating young deposits because the amount of Quaternary evolutionary change has been small. Some organisms, such as the rapidly evolving microtine rodents, do show several changes each million years and can therefore be of great value in estimating long-term deformation rates. An example of dating active tectonics comes from east of San Francisco Bay where the Verona Fault offsets Livermore Gravel and is mapped within 60 m of the General Electric Test Reactor at Vallecitos (Herd, 1977). The age of this faulted gravel was poorly known until it was dated using small mammal faunas as about 500 ka (C. A. Repenning, U.S. Geological Survey, personal communication, 1984).

The cyclic climatic changes of the Quaternary Period resulted in cyclic changes in plant and animal populations. Such plant or animal changes also provide a basis for dating active tectonism. For example, pollen assemblages representing climate considerably colder than at present may be used to infer a pre-Holocene age (>10 ka).

## WHY DATING SPANNING DIFFERENT TIME INTERVALS IS NEEDED

Geologic prediction of future deformation requires enough dating control to understand if and how deformation has changed through time. For most active tec-

tonism, we know little about whether strain rates are uniform through time. Even with the simplifying assumption that strain and long-term slip rates are uniform, a fault scarp with evidence of recent movement can yield dramatically different predictions: (1) if the slip rate is fast, future movements are likely soon, or (2) if the slip rate is slow, future movements are unlikely soon.

Spreading rates at oceanic ridges and movement rates of crustal plates appear to be rather constant over the planning intervals of concern to man and his activities. Consequently, constant strain rates may be appropriate for some major tectonic features. For many individual faults, however, this assumption is probably not valid. Even for some faults in the boundary zone between crustal plates, slip rates have changed greatly. On the San Jacinto Fault southeast of Los Angeles, the slip rate for the past 730 ka has averaged about 9 mm/yr, whereas the rate between 0.4 and 6 ka averaged about one-fifth that (Table 13.3; Sharp, 1981). These large differences in rate may have resulted from differential movements between the Pacific and American plates being localized at times on the San Jacinto Fault and at other times on the nearby San Andreas Fault (Sharp, 1981).

On a fault in the Rio Grande rift near Albuquerque, New Mexico, the rates of deformation have decelerated over the last 400 ka. Recurrence intervals on this fault are quite long, averaging more than 100 ka (Figure 13.12).

For the total Basin and Range province encompassing the 700-km distance between the crests of the Wasatch Mountains of Utah and the Sierra Nevada of California, the overall rate of extension may be relatively constant. But Holocene and historical activity in the Basin and Range is spatially clustered in zones. Holocene tectonic events ($M_s$ about 7 or larger) define an eastern and western zone; these zones are separated by a zone about 300-km wide encompassing the Nevada-Utah border in which no late Quaternary scarps are recognized (Wallace, 1981).

Grouping of events in time may also occur. Some segments of the Wasatch Fault zone have had three or more Holocene (last 10 ka) offsets and exhibit slip rates during the Holocene of 1.3 + 0.1 m/ka, yet other sections of the Wasatch Fault zone have not been active in the Holocene (Schwartz *et al.*, 1983). In addition, based on fission-track annealing ages, the uplift rate of the Wasatch Mountains for the past 10 Ma has been about one-third the Holocene rate, or about 0.4 m/ka (Naeser *et al.*, 1983). Work in progress on deposits as old as 250 ka sheds light on the meaning of these rates (Machette, 1984). As dated by calcic-soil development, the slip rate has been on the order of 1 m/ka during the last 5 ka; this rate appears to have been more than 5 times greater than that over the past 250 ka, suggesting variable slip rates and temporal grouping of fault offsets (Machette, 1984).

TABLE 13.3 Variable Slip Rates Through Time, San Jacinto Fault, Southern California (from Sharp, 1981)

| Time Interval | Slip Rate (mm/yr) | Change in Slip Rate Through Time |
|---|---|---|
| 0-400 | $3.9 \pm 1.1$ | Twofold increase |
| 400-6000 | $1.7 \pm 0.3$ | Fivefold decrease |
| 0-730,000 | $9^{+3}_{-1}$ | |

Rates of fault slip or other deformation are dependent on both the deformation pattern through time *and the time window of observation*. To illustrate this point, Figure 13.13 shows the effect of short, medium, and long time windows on the slip rates for five patterns of deformation: accelerating, constant, decelerating, episodic-quiescent, and episodic-active. For convenience, the deformation patterns are shown as systematic, and the deformation rates are arbitrarily set at 1 for the longest interval. Depending on the time window, deformation rates for each pattern may differ by more than an order of magnitude. Also, although the long-term rate is arbitrarily set at 1, the short interval has rates that differ by more than 2 orders of magnitude (Figure 13.13B).

Deformation rates determined for differing time intervals will contribute to an understanding of deformation patterns through time in different tectonic settings. Few fault histories such as those shown by Figures 13.2, 13.3, and 13.12 have been determined. Deformation histories like that shown by lines for episodic-active and episodic-quiescent (Figure 13.13) have not been well documented, but, as discussed previously, some evidence suggests that these patterns of deformation have occurred.

Only by understanding the history of a fault can we better understand what can be expected in the future. Consequently, the deformation history needs to be defined by multiple dates. The simplifying assumption that tectonic events such as rates of faulting or rates of uplift are constant may be useful as a first approximation, but this assumption may be quite misleading in some tectonic environments. Few fault histories are well enough dated to know in what cases the assumption of constant slip rate is valid and in what cases it is not. By detailed documentation, we can construct predictive models appropriate to a given tectonic setting. If movements on a given fault are grouped in time, or if faults in an area alternate in activity, concepts such as constant

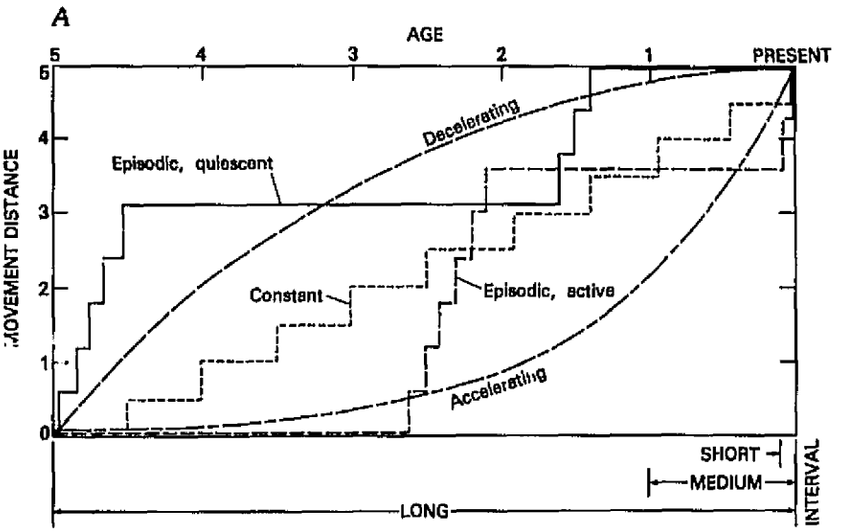


B

| PATTERN | | INTERVAL | | |
|---|---|---|---|---|
| | | Long * | Medium | Short |
| Accelerating | ——— | 1 | 3 | 4 |
| Constant | ------- | 1 | 1.6 | 5 |
| Decelerating | —— | 1 | 0.3 | <.1 |
| Episodic, quiescent | ——— | 1 | 0 | 0 |
| Episodic, active | —— | 1 | 1.4 | 14 |

* Long-term rate arbitrarily set at 1

FIGURE 13.13 A, five patterns of fault offset versus time. B, contrasting slip rates for these five patterns over short, medium, and long intervals of time. Slip rates are in arbitrary distance/time units, and long-term deformation for all patterns has been arbitrarily set at 1.

slip rate or constant recurrence intervals would be, of course, quite misleading.

Thus, sufficient dating related to deformation histories is required to understand the character of faulting in different tectonic settings and thereby to anticipate more intelligently the future deformation over time intervals of concern to man. Dating of a single fault history without concern for related faults may be examining too small a component, for relatively constant tectonic activity may be unevenly distributed among a group of faults.

The definition of rates and knowledge of the constancy or variation of these rates through time permit quantitative ranking of tectonic activity, both for the purposes of scientific understanding and hazard assessment.

## DATING METHODS IN FUTURE RESEARCH ON ACTIVE TECTONISM

All the dating methods discussed (Tables 13.1 and 13.2) have importance to studies of active tectonism. In the last decade, much improvement, refinement, and evaluation of the reliability of these methods have been associated with studies of active tectonism.

Because experimental methods such as $^{36}Cl$ and $^{26}Al$ are numerical and based on radioactive decay, some may consider such methods the most promising for future advances. But such methods also involve assumptions concerning nonradiometric processes—one assumes that the isotope measured both accumulated at a known rate and no subsequent leaching has occurred. These nonradiometric factors are difficult to evaluate rigorously and have similarities with, for example, the extremely complex process of soil development. For example, $^{10}Be$ accumulation in soils is influenced by the clays in the soil, which generally increase in quality and may change mineralogically as the soil develops. The recent quantification of soil development using the Profile Development Index, as well as analyses of changes in individual soil components such as soil carbonate or clay, can provide useful but not precise dating control; soil development is nearly always applicable to the dating of active tectonism.

Because of their nearly universal applicability, thermoluminescence and uranium-trend dating of sediments are promising methods for dating deformation, especially in the $10^4$- to $10^6$-yr range. Compared to this potential, research by laboratories on these methods and application to active tectonics have been limited.

Carbon-14 dating is the most important method in the range of about 30,000 yr to the present. Research using current methods of organic chemistry may help to resolve problems with the method and the mechanisms of contamination. Even before sample collection, microbes may have lived in organic material and incorporated younger carbon from the surrounding water or air. Important carbon-14 samples might be quantitatively examined for such microbes and other potential contaminants to estimate the importance of their effect, as was done by Geyh *et al.* (1974).

Carbon-14 dating using accelerator mass spectrometry permits the dating of milligram-sized samples (Grootes, 1983). If only small samples are present, this offers obvious advantages, but contamination within, for example, an individual grain of charcoal, may still be present. Special organic concentrates in combination with accelerator dating may offer real improvements. For example, a whale bone sample from northern Alaska has been carbon-14 dated, but considerable question remains about the reliability of the ages (D. L. Carter, USGS, personnal communication, 1984). Because one amino acid is common in bone but not in the likely contaminating materials, dating of this amino-acid sample may provide a reliable carbon-14 age. The amino acid concentrate will be small, requiring dating by accelerator mass spectrometry.

In the quest for better dating of active tectonism, the importance of local, time-calibrated stratigraphies should not be underestimated. Datable materials are commonly not found where a given stratigraphic unit is offset but may be found elsewhere in that stratigraphic unit. Because the stratigraphy of many Quaternary deposits reflects the cycles of climatic changes, the ages of faulted or uplifted datums can be inferred if relations between stratigraphic units and climatic cycles are known. Study of active tectonism and Quaternary stratigraphy should proceed together also because evidence of tectonism and climatic change is commonly similar. For example, gravel deposition may result from uplift, from climatic change, or from both uplift and climatic change.

In conclusion, knowledge of active tectonism of a given area progresses as both the amount and age of deformation are determined. Such knowledge commonly develops by documenting first the age and amount of the most recent movement; second, the history of the last several movements; third, deformation over contrasting time intervals, including long intervals; and last, the relation between the dated deformations on associated faults.

Dating control is commonly the limiting factor in understanding active tectonism. Normally, several dating methods need to be used because of (1) the limited range of a given technique, (2) the presence of appropriate materials, and (3) the need to check the reliability of any given dating technique by using another method. For studies of a fault segment, for example, dating control for Holocene activity can be determined by carbon-14, and studies of surface and buried soils can be made to provide dating control in the $10^4$- to $10^5$-yr range as well as to provide a check on the reasonableness of the carbon-14 dates. Tables 13.1 and 13.2 list 26 methods. Development or refinement of the methods, particularly those listed in columns 3 to 6 of Table 13.1, has advanced greatly in the past decade, in part because of the impetus to date active tectonics. With continued effort, comparable advances are possible in the future.

## REFERENCES


Allen, C. R. (1975). Geologic criteria for evaluating seismicity, *Geol. Soc. Am. Bull. 86*, 1041-1057.

Barendregt, R. W. (1981). Dating methods of Pleistocene deposits and their problems: IV, Paleomagnetism, *Geosci. Canada 8*(2), 56-64.

Belknap, D. F. (1984). Amino-acid racemization in the "mid-Wisconsin" C-14 dated formations on the Atlantic Coastal Plain, *Geol. Soc. Am. Abstr. Progr. 16*, 2-3.

Bloom, A. L. (1983). Sea level and coastal morphology of the United Statesthrough the Late Wisconsin glacial maximum, in *The Late Pleistocene*, S. C. Porter, ed. (Volume 1 of Late Quaternary Environments of the United States, H. E. Wright, ed.), University of Minnesota Press, Minneapolis, pp. 215-229.

Bonilla, M. G. (1967). Historic surface faulting in the continental United States and adjacent parts of New Mexico, *U.S. Geol. Surv. Open-File Rep.*, 36 pp.

Cluff, L. S., A. S. Patwardhan, and K. J. Coppersmith (1980). Estimating the probability of occurrences of surface faulting earthquakes on the Wasatch Fault zone, Utah, *Bull. Seismol. Soc. Am. 70*, 1463-1478.

Colman, S. M., and K. L. Pierce (1981). Weathering rinds on andesitic and basaltic stones as a Quaternary age indicator, western United States, *U.S. Geol. Surv. Prof. Paper 1210*, 56 pp.

Colman, S. M., and K. L. Pierce (1979). Preliminary map showing Quaternary deposits and their dating potential in conterminous United States, *U.S. Geol. Surv. Misc. Field Studies Map* MF-1052.

Colman, S. M., and K. L. Pierce (1984). Correlation of Quaternary glacial sequences in the western United States based on weathering rinds and related studies, in *Correlation of Quaternary Chronologies*, W. C. Mahaney, ed., Geo Books, Norwich, England, pp. 437-453.

Dorn, R. I. (1983). Cation-ratio dating: A new rock varnish age-determination technique, *Quaternary Res. 20*, 49-73.

Easterbrook, D. J., N. D. Briggs, J. A. Westgate, and M. P. Corton (1981). Age of the Salmon Springs Glaciation in Washington, *Geology 9*, 87-93.

Geyh, M. A., W. E. Krumbein, and H. R. Kudrass (1974). Unreliable

$^{14}C$ dating of long-stored deep sea-sediments due to bacterial activity, *Mar. Geol. 17*, M43-M50.

Goh, K. M., B. J. P. Molloy, and T. A. Rafter (1977). Radiocarbon dating of Quaternary loess deposits, Banks Peninsula, Canterbury, New Zealand, *Quaternary Res. 7*, 177-196.

Grootes, P. M. (1983). Radioactive Isotopes in the Holocene, in *The Holocene*, H. E. Wright, ed. (Volume 2 of Late Quaternary Environments of the United States), University of Minnesota Press, Minneapolis, pp. 86-105.

Harden, J. W. (1982). A quantitative index of soil development from field descriptions: Examples from a chronosequence in central California, *Geoderma 28*, 1-28.

Harden, J. W., and E. M. Taylor (1983). A quantitative comparison of the soil development in four climatic regimes, *Quaternary Res. 20*, 342-359.

Herd, D. G. (1977). Geologic map of the Los Positas, Greenville, and Verona Faults, eastern Alameda County, California, *U.S. Geol. Surv. Open-File Rep. 77-689*.

Ikeya, M., and K. Ohmura (1983). Comparison of ESR ages of corals from marine terraces with $^{14}C$ and $^{230}Th/^{234}U$ ages, *Earth Planet. Sci. Lett. 65*, 34-38.

Ivanovich, M., and R. S. Harmon, eds. (1982). *Uranium Series Disequilibrium: Application to Environmental Problems*, Clarendon Press, Oxford, 571 pp.

Izett, G. A. (1981). Volcanic ash beds: Recorders of upper Cenozoic silicic pyroclastic volcanism in the western United States, *J. Geophys. Res. 86*, 10200-10222.

Kaufman, A., W. S. Broecker, T. L. Ku, and D. L. Thurber (1971). The status of U-series methods on mollusk dating, *Geochim. Cosmochim. Acta 35*, 1155-1183.

Klein, J., J. C. Lerman, P. E. Damon, and E. K. Ralph (1982). Calibration of radiocarbon dates: Tables based on the consensus data of the workshop on calibrating the radiocarbon time scale, *Radiocarbon 24*, 103-150.

Levine, E. R., and E. J. Ciolkosz (1983). Soil development in till of various ages in northeastern Pennsylvania, *Quaternary Res. 19*, 85-99.

Machette, M. N. (1978). Dating Quaternary faults in the southwestern United States by using buried calcic paleosols, *U.S. Geol. Surv. J. Res. 6*(3), 369-381.

Machette, M. N. (1984). Preliminary investigations of late Quaternary slip rates along the southern part of the Wasatch Fault zone, in *Evaluation of Regional and Urban Earthquake Hazards and Risk in Utah*, W. W. Hayes and P. Gori, eds., U.S. Geol. Surv. Open-File Rep. 84-763, pp. 391-406.

Mahaney, W. C., ed. (1984). *Quaternary Dating Methods*, Elsevier, New York, 428 pp.

Mangerud, J., and S. Gulleksen (1975). Apparent radiocarbon ages of recent marine shells form Norway, Spitsbergen, and Arctic Canada, *Quaternary Res. 5*, 263-273.

Mankinen, E. A., and G. B. Dalrymple (1979). Revised geomagnetic polarity time scale for the interval 0-5 m.y. B.P., *J. Geophys. Res. 84*(B2), 615-626.

Maugh, J. H. (1977). Phylogeny: Are methanogens a third class of life? *Science 198*, 812.

McFadden, L. D. (1982). Impacts of Temporal and Spatial Climatic Changes on Alluvial Soils Genesis in southern California, Ph.D. dissertation, Univ. of Ariz., Tucson, 430 pp.

Naeser, C. W., B. Bryant, M. D. Crittenden, Jr., and M. L. Sorensen (1983). Fission-track ages of apatite in the Wasatch Mountains, Utah: An uplift study, *Geol. Soc. Am. Mem. 157*, 29-36.

Pavich, M. J., L. Brown, J. Klein, and R. Middleton (1984). $^{10}Be$ accumulation in a soil chronosequence, *Earth Planet. Sci. Lett. 68*, 198-204.

Pierce, K. L. (1979). History and dynamics of glaciation in the northern Yellowstone National Park area, *U.S. Geol. Surv. Prof. Paper 729-F*, 90 pp.

Pierce, K. L. (1985). Quaternary history of faulting on the Arco segment of the Lost River Fault, central Idaho, In *Proceedings of Workshop XXVIII on the Borah Peak Idaho, Earthquake*, R. S. Stein and R. C. Bucknam, eds., U.S. Geol. Surv. Open-File Rep. 85-290, pp. 195-206..

Pierce, K. L., J. D. Obradovich, and I. Friedman (1976). Obsidian hydration dating and correlation of Bull Lake and Pinedale glaciations near West Yellowstone, Montana, *Geol. Soc. Am. Bull. 87*, 703-710.

Reheis, M. C. (1984). Climatic and Chronologic Controls on Soil Development, Northern Bighorn Basin, Wyoming and Montana, Ph.D. dissertation, Univ. of Colo., Boulder, 346 p.

Rosholt, J. N. (1980). Uranium-trend dating of Quaternary sediments, *U.S. Geol. Surv. Open-File Rep. 80-1087*, 65 pp.

Rutter, N. W., ed. (1984). *Dating Methods of Pleistocene Deposits and Their Problems*, Geoscience Canada, reprint series No. 2.

Schwartz, D. P., K. L. Hanson, and F. H. Swan III (1983). Paleoseismic investigations along the Wasatch Fault zone: An update, in *Geologic Excursions in Neotectonics and Engineering Geology in Utah*, Utah Geological and Mineral Survey, Special Studies 62, pp. 45-55.

Sharp, R. V. (1981). Variable rates of late Quaternary strike slip on the San Jacinto Fault zone, southern California, *J. Geophys. Res. 86*, 1754-1762.

Shimazaki, K., and T. Nakata (1980). Time-predictable recurrence model for large earthquakes, *Geophys. Res. Lett. 7*, 279-282.

Sieh, K. E. (1984). Lateral offsets and revised dates of large prehistoric earthquakes at Pallet Creek, southern California, *J. Geophys. Res. 89*, 7641-7670.

Slemmons, D. B. (1977). State-of-the-Art for Assessing Earthquake Hazards in the United States, Report 6, Faults and Earthquake Magnitude, U.S. Army Engineers Waterways Experiment Station, Miscellaneous Paper S-73-1, 129 pp.

Stuiver, M. (1982). A high-precision calibration of the AD radiocarbon time scale, *Radiocarbon 24*, 1-26.

Stuiver, M., C. J. Heusser, and I. C. Yang (1978). North American glacial history extended to 75,000 years ago, *Science 200*, 16-21.

Szabo, B. J., and J. N. Rosholt (1982). Surficial continental sediments, in *Uranium Series Disequilibrium: Applications to Environmental Problems*, M. Ivanovich and R. S. Harmon, eds., Clarendon Press, Oxford, pp. 246-267.

Wallace, R. E. (1977). Profiles and ages of young fault scarps, north central Nevada, *Geol. Soc. Am. Bull. 88*, 1267-1281.

Wallace, R. E. (1981). Active faults, paleoseismology, and earthquake hazards in the western United States, in *Earthquake Prediction: An International Review*, Maurice Ewing Series 4, American Geophysical Union, Washington, D.C., pp. 209-216.

Wehmiller, J. F. (1982). A review of amino-acid racemization studies in Quaternary mollusks, *Quaternary Sci. Rev. 1*, 83-120.

Westgate, J. A., and M. P. Gorton (1981). Correlation techniques in tephra studies, in *Tephra Studies*, S. Self and J. Sparks, eds., Reidel, Dordrecht, Holland, pp. 73-94.

Wintle, A. G., and K. Brunnacker (1982). Thermoluminescence dating of loess from Wallertheim, West Germany, *Naturwissenschaften 69*, 181-183.

Wintle, A. G., and D. J. Huntley (1982). Thermoluminescence dating of sediments, *Quaternary Sci. Rev. 1*, 31-53.

# Seismic Hazards: New Trends in Analysis Using Geologic Data

# 14

DAVID P. SCHWARTZ *and* KEVIN J. COPPERSMITH*
*Woodward-Clyde Consultants*

## INTRODUCTION

Where? When? How large? These are the most frequently asked questions in evaluating seismic hazards. The ability to answer these, whether estimating a maximum earthquake, the amount of potential surface displacement on an active fault, or the probability of exceeding a particular level of ground motion, rests on the ability to recognize and characterize seismic sources Seismic source characterization is the quantification of the size(s) of earthquakes that a fault can produce and the distribution of these earthquakes in space and time. As such, source characterization provides the basis for evaluating the long-term seismic potential at particular sites of interest.

In the late 1960s and early 1970s—largely in response to expansion of nuclear power plant siting and the issuance of a code of federal regulations by the Nuclear Regulatory Commission referred to as Appendix A, 10CFR100—the need to characterize the earthquake potential of individual faults for seismic design took on greater importance. Appendix A established deterministic procedures for assessing the seismic hazard at nuclear power plant sites. Bonilla and Buchanan (1970), using data from historical surface-faulting earthquakes, developed a set of statistical correlations relating earthquake magnitude to surface rupture length and to surface displacement. These relationships, which have been refined and updated (Slemmons, 1977; Bonilla *et al.*, 1984) along with the relationship between fault area and magnitude (Wyss, 1979) and seismic moment and moment magnitude (Hanks and Kanamori, 1979), have served as the basis for selecting maximum earthquakes in a wide variety of design situations (Schwartz *et al.*, 1984). A related concept that developed at about the same time and that has also seen widespread use is the idea that a seismic source can produce two types of earthquakes, a "maximum credible" event or simply a "maximum" earthquake, which is the largest conceivable, and a "maximum probable" event, which is smaller and more frequent.

It is clear that the correlations between earthquake magnitude and fault parameters can provide reasonable estimates of the magnitude or surface displacement associated with future earthquakes on a fault when appropriate values for the parameters are used. However, in applying these correlations to actual siting situations, there is often much uncertainty, and there has frequently been great controversy, in the selection of the parameters used. Perhaps no better example can be found than the diversity of conclusions regarding the seismic design parameters for the proposed Auburn Dam on the American River east of Sacramento, California. Reports on these were issued by the U.S. Bureau

*David P. Schwartz's present address is U. S. Geological Survey, Menlo Park, California; Kevin J. Coppersmith's present address is Geomatrix Consultants, San Francisco, California.

of Reclamation, the U.S. Geological Survey, Woodward-Clyde Consultants, and five additional independent consultants to the Bureau of Reclamation. Estimates of the magnitude of the maximum earthquake on a fault in the vicinity of the dam ranged from 6.0 to 7.0; the closest approach of the source of the maximum earthquake ranged from less than 0.8 to 8 km; estimates of the focal depth of the maximum event varied from 5 to 10 km; the amount of the surface displacement expected during the maximum event varied from 25 cm to 3 m; and estimates of the recurrence interval of the maximum earthquake ranged from 10,000 to 85,000 yr. Characteristics of expectable faulting within the dam foundation similarly had a wide range of estimated values: the maximum earthquake was 5.0 to 7.0; displacement per event was less than 2.5 cm to 1 m; and the recurrence interval of an event in the foundation was 260,000 to about 1,000,000 yr. This clearly illustrates the differences in perception among the various consultants or groups regarding both the physical basis for quantifying a particular fault parameter and the general understanding of fault behavior.

During the past 10 yr the integration of geologic, seismologic, and geophysical information has led to a much better, though still far from complete, understanding of the relationships between faults and earthquakes in space and time. Geologic studies, especially a few highly focused fault-specific studies, have shown that individual past large-magnitude earthquakes can be recognized in the geologic record and that the timing between events can be measured. Such investigations of prehistoric earthquakes have developed into a formal discipline called paleoseismology (Wallace, 1981). Additionally, they have yielded information on fault slip rate, the amount of displacement during individual events, and the elapsed time since the most recent event. These data can be used in a number of different ways and have led to the development of new approaches to quantifying seismic hazards. Specifically, they have allowed us to begin to develop models of fault zone segmentation, which can be used to evaluate both the size and potential location of future earthquakes on a fault zone, and also earthquake recurrence models, which provide information on the frequency of different size earthquakes on a fault. At the same time, significant advances have been made in developing earthquake hazard models that use probabilistic approaches. These are particularly suited to incorporating the uncertainties in seismic source characterization and our evolving understanding of the earthquake process.

In the present paper we discuss new trends in seismic hazard analysis using geologic data, with special emphasis on fault-zone segmentation and recurrence models and the way in which they provide a basis for evaluating long-term earthquake potential.

## THE GEOLOGIC DATA BASE

Figure 14.1 is a schematic diagram showing the types of geologic data that can be obtained for individual faults and the applications of each to the evaluation of seismic hazards.

### *Slip Rate*

Slip rate is the net tectonic displacement on a fault during a measurable period of time. In recent years a great deal of emphasis has been placed on obtaining slip-rate data, and published rates are available for many faults. Slip rates are an expression of the long term, or average, activity of a fault. In a general way they can be used as an index to compare the relative activity of faults. Slip rates are not necessarily a direct expression of earthquake potential. Although faults with high slip rates generally generate large-magnitude earthquakes, those with low slip rates may do the same, but with longer periods of time between events. Slip rates reflect the rate of strain energy release on a fault, which can be expressed as seismic moment. Because of this they are now being used to estimate earthquake recurrence on individual faults, especially in probabilistic seismic hazard analyses.

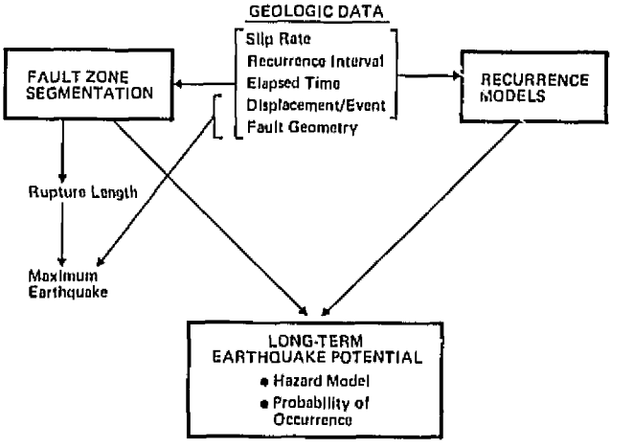


FIGURE 14.1 Relationship between geologic data and aspects of seismic hazard evaluation.

### *Recurrence Intervals*

A recurrence interval is the time period between successive geologically recognizable earthquakes. The excavation of trenches across faults has proven to be a tremendously successful technique for exposing stratigraphic and structural evidence of past individual earthquakes in the geologic record. The recognition of geomorphic features such as tectonic terraces and individual stream offsets, morphometric analysis of fault scarps, and evidence of past liquefaction also provide direct information on the number of past events for many faults. Where datable material is found, the actual intervals between successive events can be determined, although in many cases only average recurrence intervals can be estimated. Data on recurrence intervals can be combined with information on displacement during each event to develop fault-specific recurrence models.

### *Elapsed Time*

Elapsed time is the amount of time that has passed since the most recent large earthquake on a fault. Many faults have experienced repeated late Pleistocene and Holocene surface-faulting earthquakes but have not ruptured historically. With trenching and geomorphic analysis it is possible to identify and estimate the timing of the most recent event. Information on elapsed time is desirable because, when combined with data on recurrence intervals, it provides the basis for calculating real-time probabilities of the occurrence of future events on a fault. Differences in the timing of the most recent surface rupture along the length of a fault zone are also extremely useful in identifying segments that may behave independently.

### *Displacement per Event*

Displacement per event is the amount of coseismic slip that occurs at the surface during an individual earthquake. Geologic studies are providing this information for past earthquakes and assume that the measured displacement occurred coseismically, that is, simultaneously with seismic rupture rather than (to any significant extent) during a period of postseismic adjustment called afterslip. Displacements may be obtained, for example, from measurements of displaced stratigraphic horizons; the thickness of colluvial wedges observed in trenches, stream offsets, the heights of tectonic terraces on the upthrown side of faults; and inflections in fault scarp profiles. Displacement reflects the energy associated with an earthquake; displacement data can be used as input for calculating maximum earthquakes. Because the amount of coseismic slip generally varies in some systematic way along the length of a surface rupture, care must be taken to evaluate the degree to which a particular displacement value reflects a minimum, maximum, or average displacement for that event. Displacement per event data for repeated earthquakes at a point on a fault coupled with the timing of the events provide a basis for formulating recurrence models.

### *Fault Geometry*

The geometry of a fault is defined by its surface orientation, its dip, and its down-dip extent. For many faults, and particularly dip-slip faults, changes in the strike of the fault at the surface, especially when coupled with major changes in lithology, may aid in assessing the location of fault segment boundaries. For strike-slip faults dips are generally vertical, but for dip-slip faults the dip at depth may vary considerably from the surface dip. Some normal faults may decrease in dip with depth (become listric), whereas seismogenic thrust or reverse faults often steepen with depth. Seismic reflection data and seismicity data such as focal mechanisms can provide constraints on dip. The thickness of the seismogenic or brittle crust in a region determined from the depth distribution of seismicity also places constraints on the down-dip extent of the part of a fault that exhibits brittle behavior. Fault dip and down-dip seismogenic extent define fault width, which, along with fault length, are the key parameters for quantifying the fault area that is used to estimate magnitude and seismic moment.

## FAULT-ZONE SEGMENTATION

### *The Concept*

In evaluating the hazard posed by a specific fault or seismic source zone, a major concern is the location of future events on that zone. It is commonly observed that long fault zones do not rupture along their entire length during a single earthquake. Therefore, to what degree is the location of rupture random, or are there physical controls in the fault zone that define the location and extent of rupture and divide the zone into segments? If a zone is segmented, how long can segments persist as discrete units without overlap of rupture during successive faulting events? Even more importantly, can segments be recognized on the basis of geologic, seismologic, and geophysical data? Answers to these questions have the potential to provide new insights into understanding rupture propagation and also to provide a physical basis

for evaluating where along a fault the next rupture may occur. In addition, the ability to identify potential rupture segments places constraints on fault rupture length, which is a major geometric parameter used in the estimation of maximum earthquake magnitude. Inherent in the concept of segmentation is the idea of persistent barriers (Aki, 1979, 1984) that control rupture propagation.

### *Examples of Segmentation*

*Wasatch Fault Zone, Utah* The Wasatch is a 370-km-long normal-slip fault that has not had a historical surface-faulting earthquake. Based on historical surface ruptures on normal faults in the Great Basin, which have ranged in length from about 35 to 65 km, only a part of the Wasatch Fault zone will be expected to rupture in future earthquakes with lengths comparable to the historical examples. A segmentation model for the Wasatch Fault zone (Schwartz and Coppersmith, 1984) is shown on Figure 14.2. Each Wasatch segment is identified using surface fault geometry, fault scarp morphology, slip rate, timing of the most recent and prior events, gravity data, and geodetic data. From north to south, the length and orientation of the segments are (1) Collinston segment, 30 km, N20°W; (2) Ogden segment, 70 km, N10°W; (3) Salt Lake City segment, 35 km, convex east N20°E to N30°W; (4) Provo segment, 55 km, N25°W; (5) Nephi segment, 35 km, N11°E; and (6) Levan segment, 40 km, convex west. The Collinston segment has had no identifiable surface faulting during the past 13,500 yr. The Ogden segment has experienced multiple displacements, including two within the past 1580 $^{14}$C yr before present (BP) and with the most recent of these within the past 500 yr. The Salt Lake City and Provo segments have each had repeated Holocene events; the timing of the most recent event along the Salt Lake City segment is not known, and the youngest event on the Provo segment appears to have occurred more than 1000 yr ago. Along the Nephi segment one event has occurred within the past 1100 $^{14}$C yr BP and possibly as recently as 300 yr ago; two earlier events occurred on this segment between 4580 and 3640 $^{14}$C yr BP, and this event occurred less than 1750 $^{14}$C yr BP.

The proposed segment boundaries may represent structurally complex transition zones ranging from a few to more than 10 km across. To varying degrees, boundaries selected on the basis of paleoseismic and geomorphic observations are coincident with changes in the surface trend of the fault zone; major salients in the range front; intersecting east-west or northeast structural trends observed in the bedrock geology of the Wasatch Range; cross faults and transverse structural

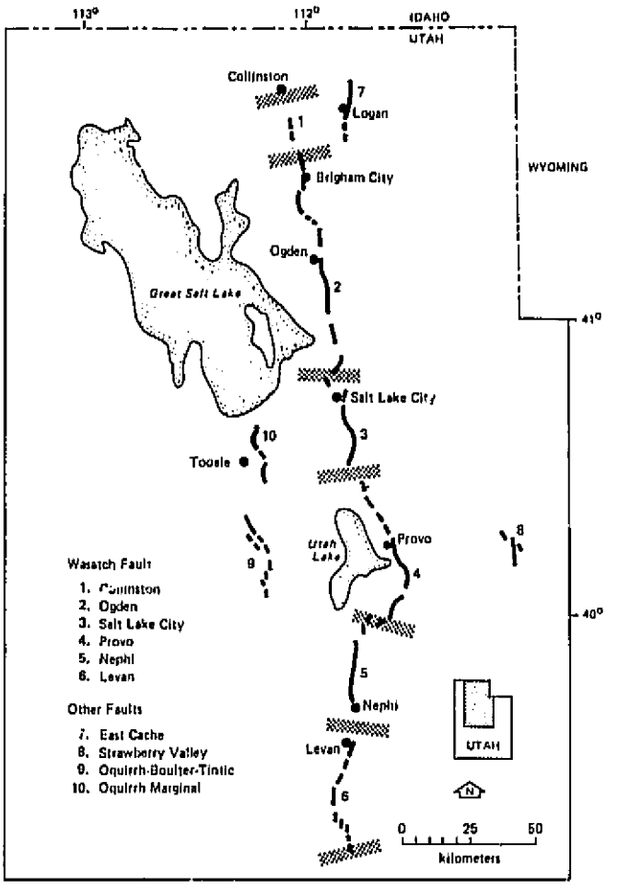


FIGURE 14.2 Segmentation model for the Wasatch Fault zone, Utah. Stippled bands define segment boundaries (modified from Schwartz and Coppersmith, 1984).

trends interpreted from gravity data (Zoback, 1983); and geodetic changes (Snay *et al.*, 1984). Smith and Bruhn (1984) showed a strong spatial correlation between segment boundaries and the margins of major thrust faults of Late Jurassic to Early Tertiary age.

*Oued Fodda Fault, Algeria* An excellent example of fault-zone segmentation is provided by the Oued Fodda Fault, which produced the El Asnam, Algeria, earthquake ($M_S$ = 7.3) of October 10, 1980. Yielding *et al.* (1981) and King and Yielding (1984) described this earthquake in terms of fault geometry and rupture propagation and termination. Basic features of the surface rupture and segmentation are shown in Figure 14.3. Thirty kilometers of coseismic surface faulting occurred on a northeast trending thrust fault, with secondary normal faulting on the upper plate. This rupture is

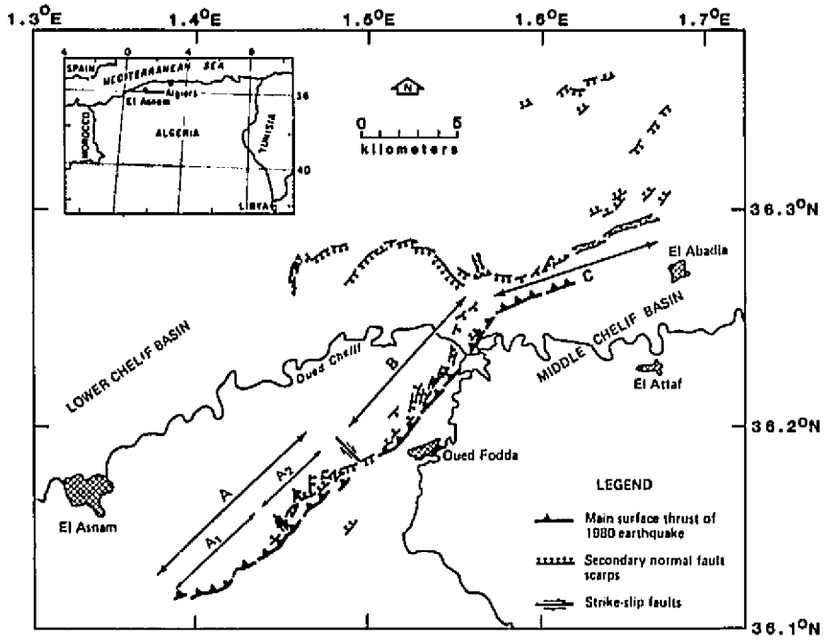


FIGURE 14.3 Map showing coseismic surface rupture from the 1980 El Asnam, Algeria, earthquake and the segmentation model for the Oued Fodda fault (modified from King and Yielding, 1984). Fault segments A, B, and C are defined by differences in geomorphic expression, seismicity, coseismic slip, geometry, and long-term rates of deformation.

composed of three distinct segments, referred to as A, B, and C. The southern segment contains two smaller segments, A1 and A2. Local and teleseismic data showed that the earthquake occurred at a depth of 10 to 15 km and was a complex rupture event. The main shock nucleated at the southwest end of segment A and propagated 12 km northeast, where a second rupture of equal seismic moment occurred and ruptured 12 km further northeast; a smaller third rupture occurred and propagated along segment C. Geologically, coseismic surface displacement during the 1980 earthquake decreases at each segment boundary, the strikes of the segments differ, and there is a gap in the main thrust rupture and an en echelon step between southern and central segments. There are also differences in long-term deformation along each as expressed by the degree of development of folds on the hanging wall of the thrust. A well-developed anticline with an amplitude of more than 200 m occurs along segment B, the amplitude of the anticline decreases to less than 100 m along A2, and the amplitude along A1 is less than 30 m before the anticline dies out toward the south end of segment. The slip distribution from the 1980 earthquake corresponds closely with the observed differences in the amount of long-term deformation. The average net slip in 1980 was greatest on segment B, decreased along A2, and decreased again along A1. Aftershocks show that strike-slip faulting normal to the trend of the surface rupture occurs at the segment boundaries, specifically between A1 and A2, and between A and B. In addition, aftershocks indicate differences in dip between segments, with segment A having a steeper dip than segment B. Based on these observations, Yielding *et al.* (1981) and King and Yielding (1984) concluded that the 1980 displacement pattern was similar to past surface ruptures and that features of fault geometry and barriers that control the nucleation and propagation of rupture on this fault have persisted through geologic time.

*Lost River Fault Zone, Idaho* Surface faulting associated with the October 28, 1983, Borah Peak, Idaho, earthquake ($M_S$ = 7.3) on the Lost River Fault zone provides another example for examining segmentation. The Lost River Fault is a normal-slip fault zone that extends for approximately 140 km from Arco to Challis. In 1983 it ruptured along 36 km of its length (Crone and Machette, 1984). Scott *et al.* (1985) suggested that the zone may be composed of five or six segments characterized by different geomorphic expression, structural relief, and timing of most recent displacement. The segmentation model for the fault zone is shown on Figure 14.4. At the southern end of the 1983 rupture zone, where surface rupture initiated, a 25-cm-high scarp that formed in 1983 is coincident with a fault scarp of approximately the same height that defines the pre-1983 event of this location. South of this point the strike of the range front changes sharply, transverse faults occur in the bedrock of the range, and a set of higher fault scarps

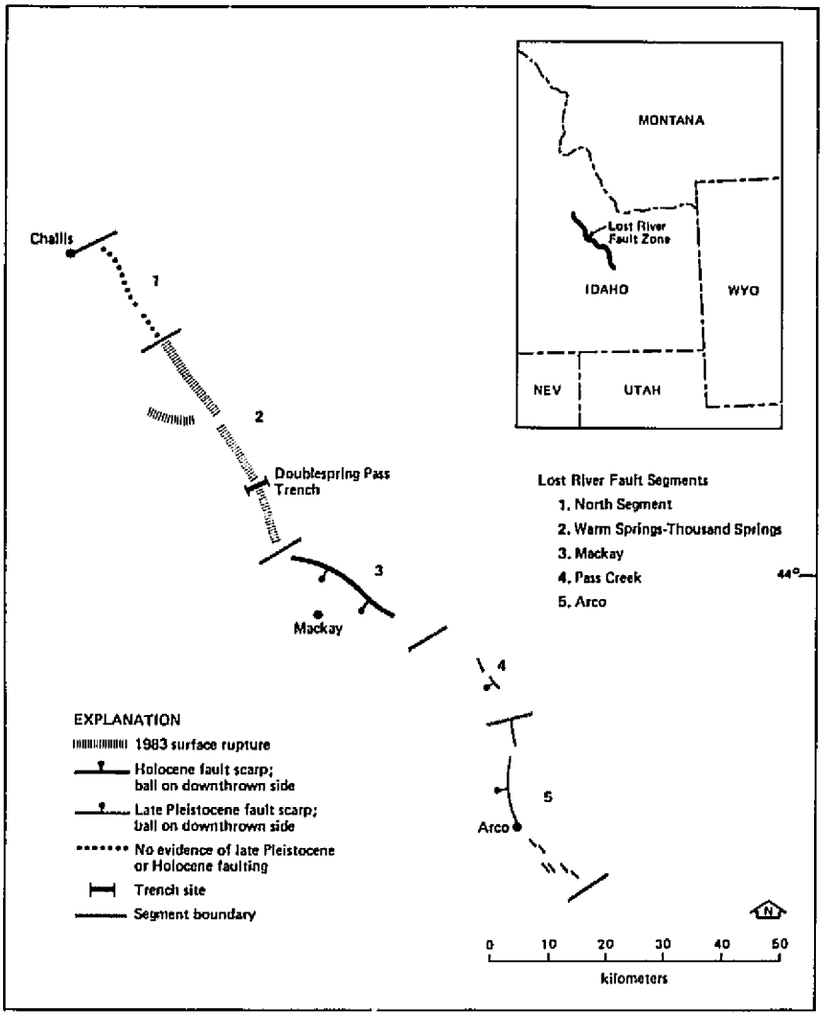


FIGURE 14.4 Segmentation model for the Lost River Fault zone, Idaho (modified from Scott *et al.*, 1985).

along which there was no slip in 1983 can be traced southward. These observations suggest that rupture may have initiated at the same point during the past two events and that a segment boundary occurs at the location of rupture initiation. Crone and Machette (1984) also suggested that a subsegment boundary may occur in association with a complex zone of bedrock structure near the northern end of the 1983 surface rupture.

*San Andreas Fault Zone, California* The San Andreas Fault zone also provides an example for evaluating segmentation, primarily because most of the fault has ruptured in historical time and the amount and extent of slip are known. Allen (1968) recognized differences in the historical behavior of various parts of the San Andreas Fault zone and identified four segments (Figure 14.5): a northern segment that was the location of the 1906 rupture, a central segment that is currently creeping and has been the location of repeated moderate earthquakes during this century, a south-central segment that was the location of the 1857 rupture, and a southern segment that has not generated large earthquakes during the historical period.

Recently developed historical and paleoseismicity data, particularly recurrence data developed from trenching studies and data on displacement per event gathered at different points along the zone (Sieh, 1978, 1984; Bakun and McEvilly, 1984; Hall, 1984; Sieh and Jahns, 1984), indicate that long-term differences in the behavior of individual segments do occur and that such behavior has remained relatively constant during the past few thousand years. This strongly suggests that the


FIGURE 14.5 Segmentation model for San Andreas Fault zone, California. The northern segment ruptured in 1906; the central segment has been the location of repeated moderate earthquakes during this century and is currently creeping; the south-central segment ruptured in 1857; and the southern segment has not generated large historical earthquakes.

historically defined segments have persisted as distinct units through at least the past several seismic cycles (Schwartz and Coppersmith, 1984).

### *Segmentation and Seismic Hazard Assessment*

Fault segmentation occurs on a variety of scales. Segments may represent the cumulative coseismic rupture during a single event on a long fault and be many tens of kilometers in length, they may represent a part of the rupture associated with an individual faulting event and be only a few kilometers long, or they may represent local inhomogeneities along a fault plane and be only a few tens or hundreds of meters in length. Because of their longer lengths, it is the first and second types of segments that have the most relevance to evaluating seismic hazards and are discussed here.

The identification of segments is not particularly easy, and methods for doing so are in the early stages of development. As more segmented faults are observed and studied, the physical characteristics and controls of segmentation will become more readily identifiable and better understood. The best types of data that provide information on segmentation are those that quantify differences in behavior along the length of a fault during its most recent seismic cycle. The most definitive is the difference in the timing of the most recent event, followed by differences in the timing of older events as indicated by paleoseismological recurrence data. Differences in representative slip rates, major changes in the strike of the fault, the occurrence of significant lithologic changes, and the presence of transverse geologic structures may spply additional information that can be used to recognize fault segments.

For many faults it appears that surface geology and changes in fault geometry frequently have a one-to-one correlation with, and are an expression of, rupture processes occurring at seismogenic depths. As a result, geologic, seismologic, and geophysical data can be used to define fault-specific segmentation models for individual faults. Implicit in segmentation modeling is the concept that segments can persist as generally discrete units through significant periods of time and, therefore, that each segment ruptures separately. There are no geologic data that currently preclude the possibility that some ruptures may cross segment boundaries or that adjacent segments may rupture completely during the same event. However, in instances where the amount of surface slip during a historical event can be compared with that from previous events at the same location it is observed often that displacement during successive events has been essentially the same. This indicates that the slip distribution along the fault, and by inferences the rupture length, has remained relatively constant. When the amount and rate of short-term (i.e., Holocene) deformation on a fault segment can be compared with the amount of long-term deformation, there is often a good correspondence. For example, Schwartz and Coppersmith (1984) showed that Wasatch Fault segments defined on the basis of paleoseismicity data are also reflected by systematic changes in the elevation of the Wasatch Range. The elevation of the range is highest where late Quaternary slip rates are fastest and recurrence intervals are shortest, the elevation of the range decreases at segment boundaries and where Holocene scarps die out, and the elevation of the range is lowest at each end where paleoseismicity data reveal the lowest Holocene slip rates and the longest recurrence intervals along the fault zone. Along the south-central segment of the San Andreas Fault, the parts of the segment that had the largest amounts of coseismic slip in 1857 also have the higher long-term slip rates. Aki (1979, 1984) suggested that strong, stable barriers to rupture propagation persist through many repeated earthquakes, and the observations noted above are consistent with this.

For dip-slip faults these barriers appear to be mainly transverse geologic structures inherited from previous stress regimes that permit decoupling of adjacent segments. The controls of segmentation on strike-slip faults are not so clear, and, because these faults propagate laterally, the longevity of individual segments may be shorter than for dip-slip faults.

The independent behavior of fault segments has important implications for seismic hazard evaluation. Segment identification provides a physical basis for the selection of rupture lengths used in the calculation of maximum earthquakes. Also, if a fault is segmented, the potential hazard posed by each segment may be different. For example, variability in segment length will mean variability in the size of the maximum earthquake. Moreover, recognition of segments and of the differences in the behavior of each will be extremely important for long-range earthquake forecasting. Information on the difference in the elapsed time and on the recurrence interval for each segment can be used to assess where along a fault zone the next major event will most likely occur and to calculate the probability of that event. This provides a basis for selecting parts of a fault zone for more intensive investigation for purposes of short-term earthquake prediction.

## THE CHARACTERISTIC EARTHQUAKE MODEL

Recent fault-specific geologic investigations have shown that many individual faults and fault segments tend to generate essentially the same size or characteristic earthquakes having a relatively narrow range of magnitudes at or near the maximum (Schwartz and Coppersmith, 1984). The characteristic earthquake model was developed from geologic observations that, at a point along a fault, the displacement during successive surface-faulting earthquakes remained essentially constant. This was observed in trenches along the Wasatch Fault zone, where past displacements could be measured using colluvial deposits derived from erosion of fault scarps. Similar behavior is observed along the south-central segment of the San Andreas Fault, where location-specific displacement during the 1857 earthquake appears to repeat the amount of displacement of at least the two previous events. This has been shown to be the case at Wallace Creek (Sieh and Jahns, 1984) as well as at other sites along the fault segment.

### *The 1983 Borah Peak, Idaho, Earthquake—A Characteristic Event*

Comparisons of observations of the October 28, 1983, Borah Peak, Idaho, earthquake ($M_S$ = 7.3) with paleoseismic observations provide strong support for the characteristic earthquake model. In 1976 a trench was excavated across a fault scarp of the Lost River Fault zone that was developed in a Pinedale-age outwash fan (approximately 15,000 yr old) at Doublespring Pass Road (Figure 14.4). Relationships in this trench suggested that only one major surface faulting event had occurred since formation of the fan surface and that this event was mid-Holocene (about 6000 yr) in age (Hait and Scott, 1978). As part of the evaluation of the 1983 earthquake, a parallel trench was excavated to re-expose the pre-1983 earthquake relationships and observe the changes that occurred in 1983. A generalized log of the 1984 trench is shown on Figure 14.6. Within this trench, correlative stratigraphic marker horizons occur on both sides of the main fault and can be traced across the graben. Because of this, the complete postfan faulting history is exposed, and measurement of pre-1983 displacements can be made and compared with those of 1983 displacements. Mapping and analysis of the stratigraphic and structural relationships in the trench (Schwartz and Crone, 1985) indicate the following sequence of events:

1. Pre-1983 surface faulting. The fan surface was displaced, and a series of graben and a horst were produced across a 40-m-wide zone west of the main scarp. The amount of displacement on individual faults formed during this event is the same across the base of a pedogenic carbonate horizon (Ck) that was near the surface of the fan and lithologic contacts at the base of the trench (for example, the top of the distinctive silty gravel).
2. Deposition of scarp-derived colluvium. This occurred at and west of the main fault (meters 5 through 10) and in graben (meters 15 through 19; 24 through 27). Fissure infills also developed (meters 24 and 39). These deposits are shown by the gray stippled pattern in Figure 14.6.
3. Continued colluviation and the development of an organic A-horizon (slanted pattern) at the pre-1983 ground surface.
4. 1983 surface faulting. All pre-1983 faults were reactivated, one new trace developed, and the existing colluvial wedge at the main fault was backtilted to the east.
5. Deposition of scarp-derived colluvium. Postfaulting colluvial deposits (dashed pattern) buried fault scarp free faces and are prominently developed at the main fault (meter 5) and in a graben (meters 15 and 19).

Important conclusions can be drawn from the new Doublespring Pass trench regarding the number and size of past events. Only one pre-1983 surface faulting earthquake occurred along this segment of the Lost

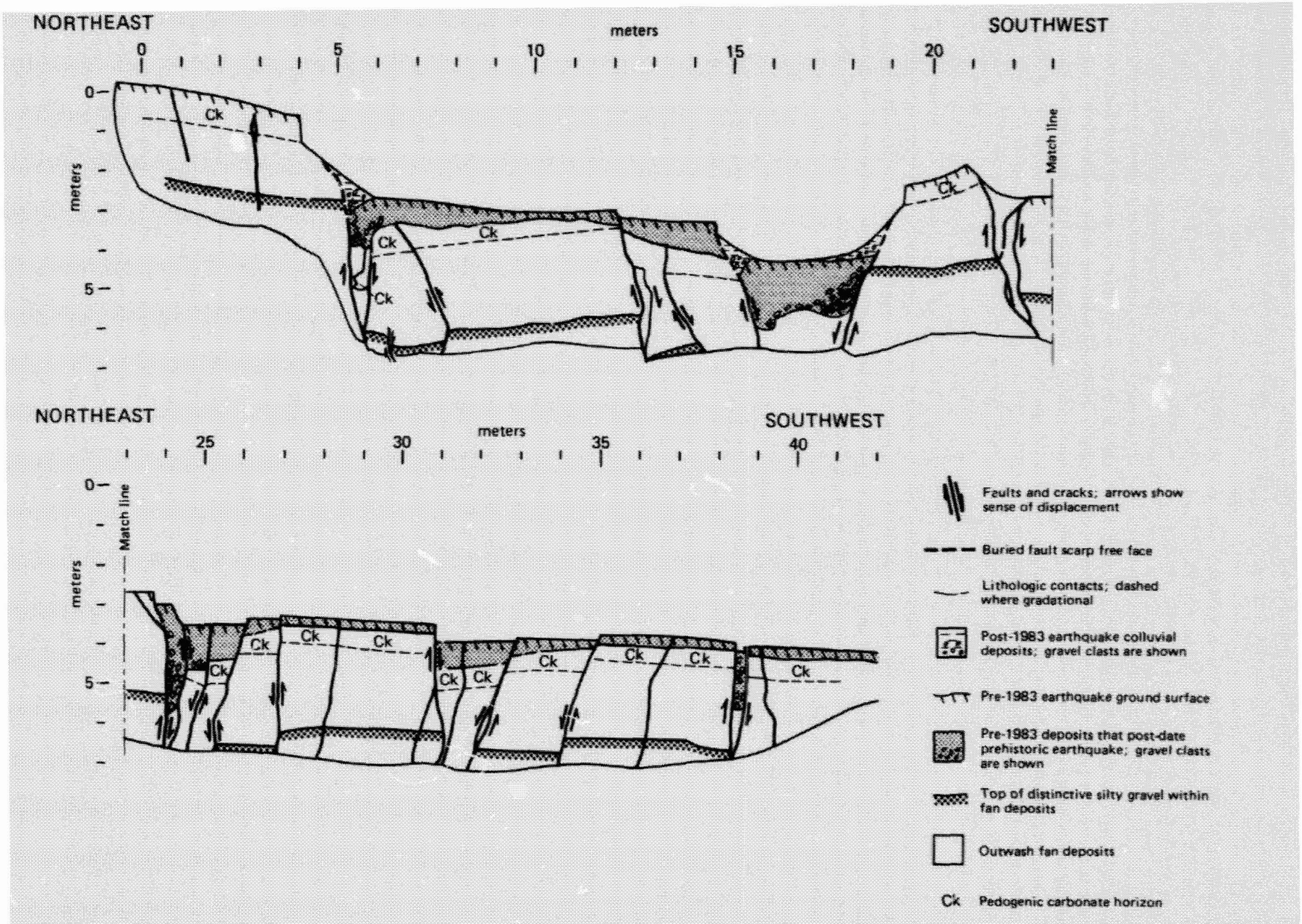


FIGURE 14.6 Generalized log of trench across the Lost River Fault and surface rupture from the 1983, Borah Peak, Idaho, earthquake at Doublespring Pass Road (from Schwartz and Crone, 1985). The trench location is shown on Figure 14.4.

River Fault zone between the time of formation of the surface of the Pinedale-age outwash fan and the 1983 event. Surface displacement that occurred in 1983 closely mimicked displacement from the previous event in both style and amount. All individual pre-1983 faults in the trench were reactivated, including small graben and the well-defined horst. Displacement across the main fault was similar for both events, as was displacement on many of the synthetic and antithetic faults.

Crone and Machette (1984) showed the distribution of displacement along the length of the 1983 surface rupture. Although measurements of pre-1983 displacements have not been made systematically, mapping suggests that scarp heights from 1983 were extremely similar to heights developed during the one pre-1983 event; small 1983 scarps are associated with small pre-1983 scarps and large 1983 scarps are associated with large pre-1983 scarps. The pattern of faulting is also remarkably consistent. This is shown not only in the trench but also at other locations along the fault where other graben and existing en echelon scarps were all reactivated in 1983. Therefore, it appears that point-specific displacement is essentially the same for the past two events. These observations, coupled with those of segmentation, support the characteristic earthquake model and imply that the 1983 earthquake was a characteristic event for this segment of the Lost River Fault zone.

## EARTHQUAKE RECURRENCE MODELS

An earthquake recurrence model describes the rate or frequency of occurrence of earthquakes of various magnitudes, up to the maximum, on a fault or in a region. We distinguish this from an earthquake hazard model, which describes the likelihood or probability of future earthquake occurrence. Statistical studies of the historical seismicity of large regions have shown that the number of earthquakes is exponentially distributed with earthquake magnitude. The general form of this recurrence model is the familiar Gutenberg-Richter exponential frequency magnitude relationship

$$\log N(m) = a - bm, \qquad (14.1)$$

where $N(m)$ is the cumulative number of earthquakes of magnitude $m$ or greater and $a$ and $b$ are constants. This is often termed a "constant $b$-value" model. In the general absence of fault-specific seismicity data, it has commonly been assumed that the exponential recurrence model is as appropriate to individual faults as it is to regions.

Recent geologic studies of late Quaternary faults strongly suggest that the exponential recurrence model is not appropriate for expressing earthquake recurrence on individual faults. The evaluation of geologic recurrence rests on the ability to recognize past events, date the interval between events, and evaluate the size of each event. By combining the recurrence intervals for large-magnitude earthquakes developed from geologic data with the recurrence for smaller-magnitude events developed from seismicity data, a characteristic earthquake recurrence model is derived that has the general form shown in Figure 14.7. Notice that the geologic data represented by the box on Figure 14.7 include the uncertainty in both the recurrence intervals and the magnitude of the paleoseismic events. The model has a distinctive nonlinear $b$ value that changes from values of about 1.0 in the small-magnitude range to lower values of about 0.2-0.4 in the moderate- to large-magnitude range. The low $b$ value reflects a recurrence curve anchored at the large-magnitude events and having relatively fewer moderate-magnitude earthquakes than would be expected for $b$ of about 1.0 (Schwartz and Coppersmith, 1984). The implications of this are that for an individual fault, estimates of the frequency of occurrence of large earthquakes based on extrapolation of the frequency of occurrence of small earthquakes may be subject to considerable error. Likewise, the concept

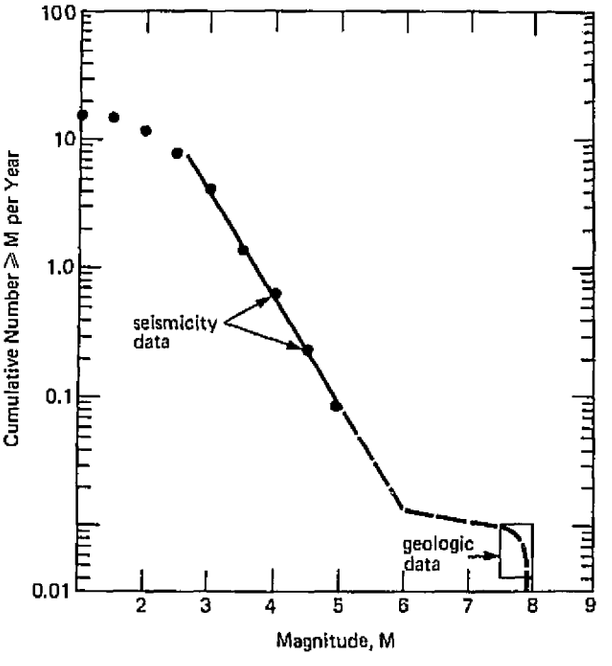


FIGURE 14.7 Diagrammatic cumulative frequency-magnitude recurrence relationship for an individual fault or fault segment. A low $b$ value is required to reconcile the small-magnitude recurrence with geologic recurrence, which is represented by the box (from Schwartz and Coppersmith, 1984).

of a "probable" earthquake that is somewhat more likely to occur than the maximum event, and is therefore usually assumed to be somewhat smaller, is probably erroneous.

Although it may be argued that the nonlinear slope of the recurrence curve in Figure 14.7 results from too short a sampling period of historical seismicity data, the distinctive nonlinear recurrence relationship suggested by the characteristic earthquake model has been observed solely from historical seismicity data along fault zones that historically have had repeated characteristic events. Examples are the Alaskan subduction zone (Utsu, 1971), the Mexican subduction zone (Singh *et al.*, 1983), Greece (Bath, 1983), Japan (Wesnousky *et al.*, 1983), and Turkey (Bath, 1981). These observations suggest that the nonlinear slope is real and not merely the result of an inadequate data base. From these data, Youngs and Coppersmith (1985) developed a recurrence density function for the characteristic earthquake model. This relationship is essentially a refinement of the generalized characteristic earthquake recurrence model and, unlike the exponential model, is appropriate for describing fault-specific recurrence.

### *Slip Rate and Earthquake Recurrence*

As discussed, geologic studies have been successful at identifying prehistoric earthquakes in the geologic record and at estimating recurrence intervals between surface-faulting earthquakes. Unfortunately, these types of paleoseismicity data are not currently available for most faults. The late Quaternary geologic slip rate, however, can frequently be obtained and is being used to constrain fault-specific earthquake recurrence relationships for seismic hazard analysis.

Fault slip rates offer the advantage over historical seismicity data of spanning several seismic cycles of large-magnitude earthquakes on a fault, and they can be used to estimate average earthquake frequency. Their use, however, requires a number of assumptions, and each of these must be carefully considered when using a slip rate to calculate recurrence on a specific fault. These assumptions are (1) all slip measured across the fault is seismic slip, unless fault creep has been recognized; (2) surface measurements of slip rate are representative of slip at seismogenic depths; (3) the slip rate is an average, which does not allow for short-term fluctuations in rate to be recognized; (4) the slip rate measured at a point is representative of the fault; and (5) the slip rate is applicable to the future time period of interest.

Two basic approaches have been developed for using geologic slip rates. The first, proposed by Wallace (1970), allows average earthquake recurrence intervals to be calculated by dividing the slip rate into the displacement per event. Slemmons (1977) developed this further and arrived at relationships between recurrence intervals, magnitude, and slip rate. This general approach assumes that only one size earthquake, usually the maximum, occurs and that the displacement per event used represents this event. However, because earthquakes with magnitudes less than the maximum also occur on the fault, less of the total slip rate is available for the maximum event. Therefore the maximum event may have a longer recurrence interval than would be calculated assuming that no other slip events occur.

The second approach is based on the assumption that the slip rate reflects the rate at which strain energy (seismic moment) accumulates along the fault and is available for release. Seismic moment, $M_0$, is the most physically meaningful way to describe the size of an earthquake in terms of static fault parameters:

$$M_0 = \mu AD, \tag{14.2}$$

where $\mu$ is the rigidity or shear modulus (usually taken to about $3 \times 10^{11}$ dyne/cm$^2$), $A$ is the area of fault plane undergoing slip during the earthquake, and $D$ is the average displacement over the slip surface (Aki, 1966). The seismic moment rate $\dot{M}_0$, which is the rate of energy release along a fault, is estimated by (Brune, 1968)

$$\dot{M}_0 = \mu AS, \tag{14.3}$$

where $S$ is the average slip rate along the fault (in centimeters per year). The seismic moment rate provides an important link between geologic and seismicity data. For example, seismic moment rates determined from fault slip rates in a region may be directly compared with seismic moment rates based on seismicity data (Doser and Smith, 1982).

Once a seismic moment rate has been calculated for a fault, it must be partitioned into various magnitude earthquakes according to an assumed recurrence model. Most commonly, an exponential magnitude distribution is used. Several authors (Smith, 1976; Campbell, 1977; Anderson, 1979; Molnar, 1979; Papastamatiou, 1980) have developed relationships between earthquake recurrence and fault or crustal deformation rates, assuming an exponential magnitude distribution.

As discussed, there is increasing evidence that, at least for some faults, a recurrence model based on the characteristic earthquake may be more appropriate than the exponential model for individual faults and fault segments. Youngs and Coppersmith (1985) developed a generalized recurrence density function for this model that can be used when fault slip rate data are available. The choice of either the exponential model or the characteristic earthquake model can have a significant im-

pact on the resulting recurrence relationship. Figure 14.8 compares the earthquake recurrence relationship for a single fault developed using an exponential magnitude distribution (solid curve) with that developed using the characteristic magnitude distribution (dashed curve). Both relationships were developed using the same maximum magnitude, *b* value (for the exponential distribution magnitude range), and fault slip rate. As shown in Figure 14.8, for the same slip rate, use of the characteristic earthquake model rather than a constant *b*-value model results in a significant reduction in the rate of occurrence of moderate-magnitude earthquakes and a modest increase in the rate of the largest events. This difference can have a significant impact on seismic hazard assessment at a site, depending on whether the moderate-magnitude events or the large events contribute most to the hazard.

One final consideration that is important in assessing earthquake recurrence from fault slip rate (moment rate) is sensitivity to the choice of maximum magnitude used in the analysis. As shown in Figure 14.9, for the same slip rate (constant moment rate), increasing the maximum magnitude from 6 to 8 results in a dramatic decrease in the recurrence rate for smaller events. This is

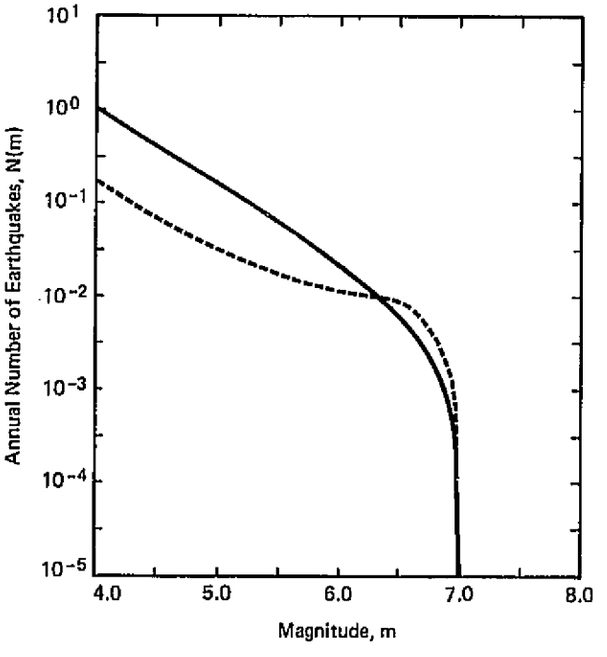


FIGURE 14.8 Comparison of recurrence relationships based on an exponential magnitude distribution (solid curve) and a characteristic earthquake distribution (dashed curve). Both relationships assume the same maximum magnitude, *b* value, and fault slip rate (from Youngs and Coppersmith, 1985).

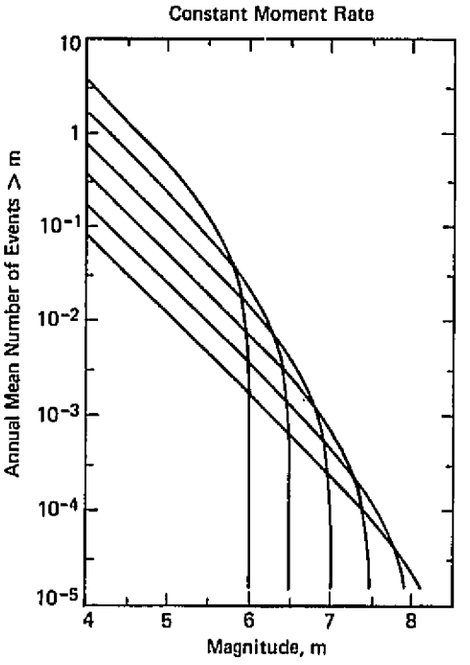


FIGURE 14.9 Effect of variations in maximum magnitude on the recurrence relationship for a fault when fault slip rate (moment rate) is held constant (from Youngs and Coppersmith, 1985).

because the largest earthquakes account for the major part of the total seismic moment rate and adding a single large earthquake requires the subtraction of many smaller events to maintain the same moment rate.

## EARTHQUAKE HAZARD MODELS

One primary goal of a seismic hazard analysis is to quantify the hazard in such a way that it can be used for engineering decisions regarding seismic design. For the seismic design of dams, power plants, hospitals, and schools it has been common practice to use deterministic design criteria. That is, the design is based on the assumption that a particular earthquake magnitude, level of ground motion, or amount of displacement on a fault will occur during the life of the facility. In recent years, probabilistic models have become increasingly used in evaluating seismic hazards.

Estimates of the likelihood or probability of future earthquake occurrence are quantified into probabilities through the use of earthquake hazard models. These models express assumptions regarding the timing and size of earthquake occurrence based on a physical and statistical understanding of the earthquake process. As

our understanding of fault behavior advances, the use of forecast models and the quantification of probabilities based on more refined geologic input will take on greater importance in guiding judgments regarding seismic design parameters. Some of the more common models are discussed below. They range from simple models that require few data constraints to complex models that, because of their large number of data constraints, have rarely been applied. It is expected that, with our evolving understanding of fault behavior and earthquake generation, increasingly sophisticated models will be put into more frequent use.

*Poisson-Exponential Model*

The most commonly used hazard model (see Cornell, 1968) is based on the assumption that earthquakes follow a Poisson process. That is, along a fault or within a seismic source zone, earthquakes are assumed to occur randomly in time and space. Coupled with this assumption is the exponential distribution of earthquake magnitudes. The Poisson-exponential model assumes that the times between earthquake occurrences are exponentially distributed and there is some time between occurrences of particular magnitudes. Therefore, the time of occurrence of the next earthquake is independent of the elapsed time since the previous one. Also, the Poisson process has no "memory" in that the magnitude of the next earthquake will not depend on the magnitude of any past events. Finally, the magnitude, locations, and times of occurrence of earthquakes along the fault are independent. This means, for example, that a long period of quiescence does not imply anything about the size of the next earthquake. Also, the next event is just as likely to occur on a segment of a fault that recently ruptured as on any other segment. Where data on faults and fault behavior are lacking, the Poisson-exponential model may be necessary and useful. However, in many cases the assumptions of the model may not be compatible with our understanding of the physical processes of earthquake generation.

For the Poisson-exponential model few data constraints are required. The probability of occurrence of $x$ number of events during time $t$ is only a function of the rate $\nu$ (the average number of events per unit time or the average recurrence interval):

$$P(x) = \frac{(\nu t)^x e^{-t}}{x!}. \qquad (14.4)$$

The rate $\nu$ may come directly from geologically derived estimates of earthquake recurrence.

*Time-Predictable Model*

The time-predictable model, as proposed by Shimazaki and Nakata (1980), is based on assumptions of constant rates of stress and strain accumulation and that stress accumulates to some relatively constant threshold at which failure occurs. From these assumptions, given the size of the most recent strain release (usually expressed as coseismic fault slip) and the rate of strain accumulation (slip rate), one can predict the time to the next earthquake Figure 14.10). In this regard, the time-predictable model is relatively deterministic, although some uncertainty may be introduced in the model parameters. For example, stochastic models of earthquake occurrence have been developed based on the time-predictable model (Anagnos and Kiremidjian, 1984).

The evaluation of seismic hazards would be greatly simplified if all faults followed a time-predictable behavior. However, it is likely that this is not the case. Rather, time-predictable behavior may be strongly dependent on tectonic environment. Along plate boundaries, such as major transform fault zones like the San Andreas, or subduction zones, where the rate and source of stress are relatively constant and the rate of strain accumulation is high, major faults and fault segments may approach a generally uniform behavior. In these cases, a time-predictable model may provide a reasonable approach to quantifying hazard, even if there is some uncertainty in the precision regarding the regularity of recurrence. Geodetic observations in Japan suggest that the rate of strain accumulation between large earthquakes is not constant, but if the true variations in rate can be measured, the time-predictable model may still be applicable (Thatcher, 1984). However, the time-predictable model does not appear to be applicable to interplate environments, where repeat times for the same-size earthquake on a fault can be highly variable.

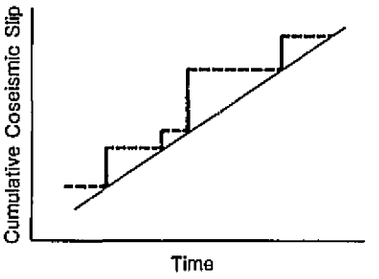


FIGURE 14.10 The time-predictable recurrence model. With information on the amount of the most recent coseismic fault slip (heavy line) and the assumption of linear strain accumulation (thin line), the time to the next earthquake (dashed line) can be estimated (from Shimazaki and Nakata, 1980).

*Renewal Models*

Renewal models, which are also referred to as real-time models, also imply a time-dependent accumulation of energy between major earthquakes. As opposed to the Poisson model, renewal models have a one-step "memory" that considers the time since the most recent event (Figure 14.11). That is, the likelihood of earthquake occurrence during a particular future period of interest, which is referred to as conditional probability, is related to the elapsed time since the most recent event and the average recurrence interval between major earthquakes. To use this model, the parameters required are the elapsed time, the average recurrence interval, and the uncertainty of dispersion about the average recurrence.

Renewal models and variations thereof have been widely used to describe earthquake occurrence (Veneziano and Cornell, 1976; Kameda and Ozaki, 1979; Savy *et al.*, 1980; Grandori *et al.*, 1984). More complex models that are based on an assumed renewal process have also been proposed. However, additional parameters are required to specify these models, for example, the semi-Markov two-step memory that relates the probability of future earthquakes of particular sizes to both the elapsed time since the most recent event and the magnitude of the prior event. This model has been used to assess probabilities of earthquake occurrence in Alaska (Patwardhan *et al.*, 1980), the Wasatch Fault zone (Cluff *et al.*, 1980), and the San Andreas Fault (Coppersmith, 1981).

In many instances, renewal models have the potential to provide the most realistic estimates of seismic hazard. Therefore, it should be the goal of hazard evaluation studies to provide the fault behavior data that best characterize seismic sources.

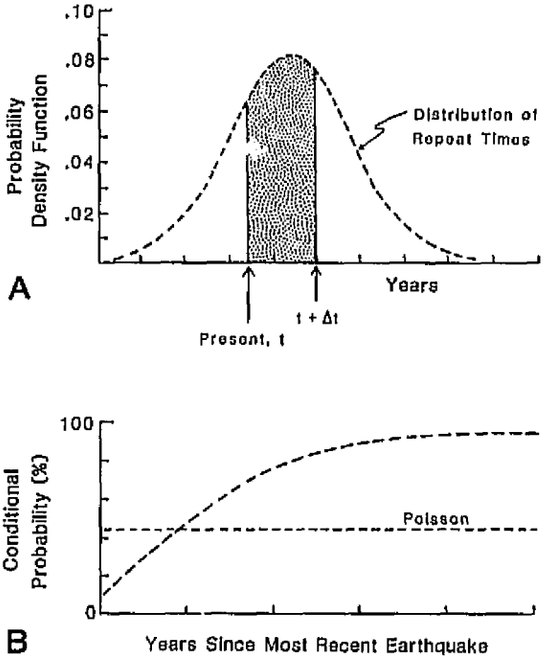


FIGURE 14.11 Schematic diagram of simple renewal model. A, The distribution of earthquake repeat times (recurrence intervals) is represented by the probability density function. The future period of interest is shown from present, $t$ to $(t + \Delta t)$. The conditional probability of earthquake occurrence is defined as area under the density function (stippled area) divided by the area under the curve to the right of the present. B, For the renewal model the conditional probability varies as a function of the elapsed time since the most recent earthquake, whereas the Poisson estimate is independent of the elapsed time.

## SOME FINAL THOUGHTS

In recent years there has been an evolution in the approach toward the evaluation of seismic hazards. Deterministic estimates of maximum earthquake size and associated ground motion that are based on a restricted data base are gradually being replaced by probabilistic assessments of future earthquake potential that incorporate information on earthquake recurrence intervals, displacement per event, fault slip rate, fault segmentation, and the uncertainties in these parameters. This is occurring, in large part, because of the progress that has been made in obtaining and using geologic data to quantify fault behavior and earthquake processes. We are optimistic that future geologic investigations, especially of faults or seismic sources associated with historical events that can be used for calibration, will provide even greater insights into understanding the space-time relationship between faults and earthquakes. Characterization of hazards in greater detail will increase our ability to make better informed and more realistic engineering decisions regarding seismic design.

## ACKNOWLEDGMENT

We thank Walter J. Arabasz and Robert D. Brown for their insightful and constructive reviews.

## REFERENCES

Aki, K. (1966). Generation and propagation of G-waves from the Niigata earthquake of June 19, 1964. 2. Estimation of earthquake movement, released energy, and stress-strain drop from G-wave spectrum, *Bull. Earthquake Res. Inst. (Tokyo Univ.)* 44, 23-88.

Aki, K. (1979). Characterization of barriers on an earthquake fault, *J. Geophys. Res.* 84, 6140-6148.

Aki, K. (1984). Asperities, barriers, and characteristic earthquakes, *J. Geophys. Res. 89*, 5867-5872.

Allen, C. R. (1968). The tectonic environments of seismically active and inactive areas along the San Andreas Fault system, in *Proceedings of the Conference on Geological Problems of the San Andreas System*, W. R. Dickinson and A. Grantz, eds., Stanford Univ. Publ. Geol. Sci., Vol. 11, pp. 70-82.

Anagnos, T., and A. S. Kiremidjian (1984). Temporal dependence in earthquake occurrence, in *Proceedings of the Eighth World Conference on Earthquake Engineering*, Prentice-Hall, Englewood Cliffs, N.J., pp. 255-262.

Anderson, J. G. (1979). Estimating the seismicity from geological structure for seismic-risk studies, *Bull. Seismol. Soc. Am. 69*, 163-168.

Bakun, W. H., and T. V. McEvilly (1984). Recurrence models and the Parkfield, California, earthquakes, *J. Geophys. Res. 89*, 3051-3058.

Bath, M. (1981). Earthquake recurrence of a particular type, *Pure Appl. Geophys. 119*, 1063-1076.

Bath, M. (1983). Earthquake frequency and energy in Greece, *Tectonophysics 95*, 1233-1252.

Bonilla, M. G., and J. M. Buchanan (1970). Interim report on worldwide historic surface faulting, *U.S. Geol. Surv. Open-File Rep.*, 32 pp.

Bonilla, M. G., R. K. Mark, and J. J. Lienkaemper (1984). Statistical relations among earthquake magnitude, surface rupture length, and surface fault displacement, *Bull. Seismol. Soc. Am. 74*, 2379-2411.

Brune, J. N. (1968). Seismic movement, seismicity and rate of slip along major fault zones, *J. Geophys. Res. 73*, 777-784.

Campbell, K. W. (1977). The use of seismotectonics in Bayesian estimation of seismic risk, Rep. No. UCLA-ENG-7744, School of Engineering and Applied Sciences, University of California, Los Angeles.

Cluff, L. S., A. S. Patwardhan, and K. J. Coppersmith (1980). Estimating the probability of occurrences of surface faulting earthquakes on the Wasatch Fault zone, Utah, *Bull. Seismol. Soc. Am. 70*, 463-478.

Coppersmith, K. J. (1981). Probabilities of earthquake occurrence on the San Andreas Fault based on geologic risk, *EOS 62*, 322.

Cornell, C. A. (1968). Engineering seismic risk analysis, *Bull. Seismol. Soc. Am. 58*, 1583-1606.

Crone, A. J., and M. N. Machette (1984). Surface faulting accompanying the Borah Peak earthquake, central Idaho, *Geology 12*, 664-667.

Doser, D. I., and R. B. Smith (1982). Seismic moment rates in the Utah region, *Bull. Seismol. Soc. Am. 72*, 525-555.

Grandori, G., E. Guargenti, and V. Petrini (1984). On the use of renewal processes in seismic hazard analysis, in *Proceedings of the Eighth World Conference on Earthquake Engineering*, Prentice-Hall, Englewood Cliffs, N.J., pp. 287-293.

Hait, M. J., Jr., and W. E. Scott (1975). Holocene faulting, Lost River Range, Idaho, *Geol. Soc. Am. Abstr. Program 10*, 217.

Hall, N. T. (1984). Holocene history of the San Andreas Fault between Crystal Springs reservoir and San Andreas Dam, San Mateo County, California, *Bull. Seismol. Soc. Am. 74*, 281-300.

Hanks, T. C., and H. Kanamori (1979). A moment magnitude scale, *J. Geophys. Res. 84*, 2981-2987.

Kameda, H., and H. Ozaki (1979). A renewal process model for use in seismic risk analysis, *Mem. Faculty of Eng. (Kyoto Univ.) VXLI*, 11-35.

King, G., and G. Yielding (1984). The evolution of a thrust fault system: Processes of rupture initiation, propagation and termination in the 1980 El Asnam (Algeria) earthquake, *Geophys. J. R. Astron. Soc. 77*, 913-933.

Molnar, P. (1979). Earthquake recurrence intervals and plate tectonics, *Bull. Seismol. Soc. Am. 69*, 115-133.

Papastamatiou, D. (1980). Incorporation of crustal deformation to seismic hazard analysis, *Bull. Seismol. Soc. Am. 70*, 1321-1335.

Patwardhan, A. S., R. B. Kulkarni, and D. Tocher (1980). A semi-Markov model for characterizing recurrence of great earthquakes, *Bull. Seismol. Soc. Am. 70*, 323-347.

Savy, J. B., H. C. Shah, and D. Boore (1980). Nonstationary risk model with geophysical input, *J. Struc. Div. ASCE 106*, 145-164.

Schwartz, D. P., and K. J. Coppersmith (1984). Fault behavior and characteristic earthquakes: Examples from the Wasatch and San Andreas Faults, *J. Geophys. Res. 89*, 5681-5698.

Schwartz, D. P., and A. J. Crone (1985). The 1983 Borah Peak earthquake: A calibration event for quantifying earthquake recurrence and fault behavior on Great Basin normal faults, in *Proceedings of Workshop XXVIII on the Borah Peak, Idaho, Earthquake*, R. S. Stein and R. C. Bucknam, eds., U.S. Geol. Surv. Open-File Rep. 85-290, pp. 153-160.

Schwartz, D. P., K. J. Coppersmith, and F. H. Swan III (1984). Methods for estimating maximum earthquake magnitudes, in *Proceedings of the Eighth World Conference on Earthquake Engineering*, Prentice-Hall, Englewood Cliffs, N.J., pp. 279-285.

Scott, W. E., K. L. Pierce, and M. H. Hait, Jr. (1985). Quaternary tectonic setting of the Borah Peak earthquake, central Idaho, *Bull. Seismol. Soc. Am. 75*, 1053-1056.

Shimazaki, K., and T. Nakata (1980). Time-predictable recurrence model for large earthquakes, *Geophys. Res. Lett. 7*, 279-282.

Sieh, K. E. (1978). Prehistoric large earthquakes produced by slip on the San Andreas Fault at Pallett Creek, southern California, *J. Geophys. Res. 83*, 3907-3939.

Sieh, K. E. (1984). Lateral offset and revised dates of large earthquakes along the San Andreas Fault at Pallett Creek, southern California, *J. Geophys. Res. 89*, 7641-7670.

Sieh, K. E., and R. H. Jahns (1984). Holocene activity of the San Andreas Fault at Wallace Creek, California, *Geol. Soc. Am. Bull. 45*, 883-896.

Singh, S. K., M. Rodriguez, and L. Esteva (1983). Statistics of small earthquakes and frequency of large earthquakes along the Mexico subduction zone, *Bull. Seismol. Soc. Am. 73*, 1779-1796.

Slemmons, D. B. (1977). State-of-the-art for assessing earthquake hazards in the United States, Rep. 6: Faults and earthquake magnitude, U.S. Army Corps of Engineers, Waterways Experiment Station, Miscellaneous Paper S-73-1, 129 pp.

Smith, R. B., and R. L. Bruhn (1984). Intraplate extensional tectonics of the eastern Basin-Range: Inferences on structural style from seismic reflection data, regional tectonics, and thermal-mechanical models of brittle-ductile deformation, *J. Geophys. Res. 89*, 5733-5762.

Smith, S. W. (1976). Determination of maximum earthquake magnitude, *Geophys. Res. Lett. 3*, 351-354.

Snay, R. A., R. B. Smith, and T. Soler (1984). Horizontal strain across the Wasatch front near Salt Lake City, Utah, *J. Geophys. Res. 89*, 113-122.

Thatcher, W. (1984). The earthquake deformation cycle, recurrence, and the time-predictable model, *J. Geophys. Res. 89*, 5674-5680.

Utsu, T. (1971). Aftershocks and earthquake statistics (III), *J. Fac. Sci. (Hokkaido Univ.) Ser. VII (Geophys.) 3*, 1337-1346.

Veneziano, D., and C. A. Cornell (1976). Earthquake models with spatial and temporal memory for engineering seismic risk analysis, Department of Civil Engineering, MIT, R74-18, Cambridge, Mass.

Wallace, R. E. (1970). Earthquake recurrence intervals on the San Andreas Fault, California, *Geol. Soc. Am. Bull. 81*, 2875-2890.

Wallace, R. E. (1981). Active faults, paleoseismology and earthquake hazards in the Western United States, in *Earthquake Prediction: An*

*International Review*, D. W. Simpson and P. G. Richards, eds., Maurice Ewing Series 4, American Geophysical Union, Washington, D.C., pp. 209-216.

Wesnousky, S., C. H. Scholz, K. Shimazaki, and T. Matsuda (1983). Earthquake frequency distribution and the mechanics of faulting, *J. Geophys. Res. 89*, 9331-9340.

Wyss, M. (1979). Estimating maximum expectable magnitude of earthquakes from fault dimensions, *Geology 7*, 336-340.

Yielding, G., J. A. Jackson, G. C. P. King, H. Sinvhal, C. Vita-Finzi, and R. M. Wood (1981). Relations between surface deformation, fault geometry, seismicity and rupture characteristics during the El Asnam (Algeria) earthquake of 10 October 1980, *Earth Planet. Sci. Lett. 56*, 287-304.

Youngs, R. R., and K. J. Coppersmith (1985). Implications of fault slip rates and earthquakes recurrence models to probabilistic seismic hazard estimates, *Bull. Seismol. Soc. Am. 75*, 939-964.

Zoback, M. L. (1983). Structure and Cenozoic tectonism along the Wasatch fault zone, *Geol. Soc. Am. Mem. 157*, pp. 3-27.

# 15 Volcanoes: Tectonic Setting and Impact on Society

DONALD W. PETERSON
*U.S. Geological Survey, Vancouver*

ABSTRACT

Volcanic eruptions frequently interfere with human affairs; impacts range from minor nuisances to major disasters. Some 50 to 65 different volcanoes typically are active in any given year, and among these a small number may cause significant damage and human casualties. Eruptions of catastrophic proportions occur but a few times in a century. Volcanoes are a dramatic manifestation of tectonic processes, and the distribution of most of them is closely related to tectonic belts. Consequently only about 10 percent of the world's population lives in localities that may, at one time or another, be affected by volcanic activity. Near long-dormant volcanoes, public attitudes toward hazards commonly reflect unconcern. In contrast, the onset of activity may spawn unreasoning fear.

Geological studies of volcanic systems and monitoring of active volcanoes have revealed important insights into volcanic processes. Volcanologists can inform people about volcanoes and help improve responses to volcanic crises. But in so doing, volcanologists stray into unfamiliar terrain, dealing frequently with public officials, land managers, and members of the news media. Misunderstandings may arise among these groups because of differences in background, objectives, and perceptions, and at times even well-based scientific opinions may encounter skepticism. It is vital, however, for volcanologists to communicate effectively with civic leaders and journalists, for it is only through constructive and harmonious interactions that optimum public response to volcanic hazards can be developed.

## INTRODUCTION

Volcanic eruptions are among the most spectacular and awesome of all natural phenomena. From earliest human history they have both fascinated and terrorized mankind. Volcanoes have created some of the Earth's most beautiful scenery but also caused some of its greatest catastrophes. The geologic record reveals countless prehistoric eruptions that were orders of magnitude more voluminous and violent than any that have occurred in the brief span of human history; when such huge events occur again they will cause unprecedented disasters. The problems posed by known volcanism during recorded history and contemporary times, as well as those posed by the unknown but inevitable volcanism of the future, are compelling reasons to improve our understanding of volcanic phenomena. Even though little hope exists for controlling other than the most benign volcanic manifestations, some forms of volcanic energy can be harnessed for man's benefit; an example is the

utilization of geothermal energy as a source of heat and electrical power. Compared with many other fields of science, volcanology is in its infancy; yet substantial progress is being made both in understanding volcanic processes and in developing methods of forecasting eruptions.

This paper (1) reviews the relations that volcanoes bear to the tectonic belts of the Earth, (2) summarizes the major kinds of volcanic activity, (3) reviews principal methods that scientists have used to study and forecast volcanic activity, and (4) discusses the ways that people react to volcanic activity.

## VOLCANISM IN THE CONTEXT OF TECTONICS

The distribution of volcanoes throughout the world broadly parallels the major tectonic belts, although they do not precisely coincide (Figure 15.1). Epicenters of major earthquakes are much more widely scattered than are volcanoes, and large segments of active tectonic belts have no volcanoes at all. Nevertheless, all but a few of the world's active volcanoes lie close enough to the major zones of active earth movement to have long provoked speculation and discussion on the nature of and connection between earthquakes and volcanoes. The current theory of plate tectonics provides a unifying framework explaining the association.

Most volcanoes lie on or near two of the three principal types of boundaries between the moving crustal plates: (1) spreading boundaries, where plates move away from each other, and (2) compressive boundaries, where plates move toward each other and one overrides the other. The third type of boundary, transform, along which the plates slide laterally, is rarely associated with volcanism. But some volcanoes lie far from plate margins, and most of these are explained as a result of the plate moving across a stationary, magma-generating spot beneath the crust. Other intraplate volcanoes require a more elaborate explanation.

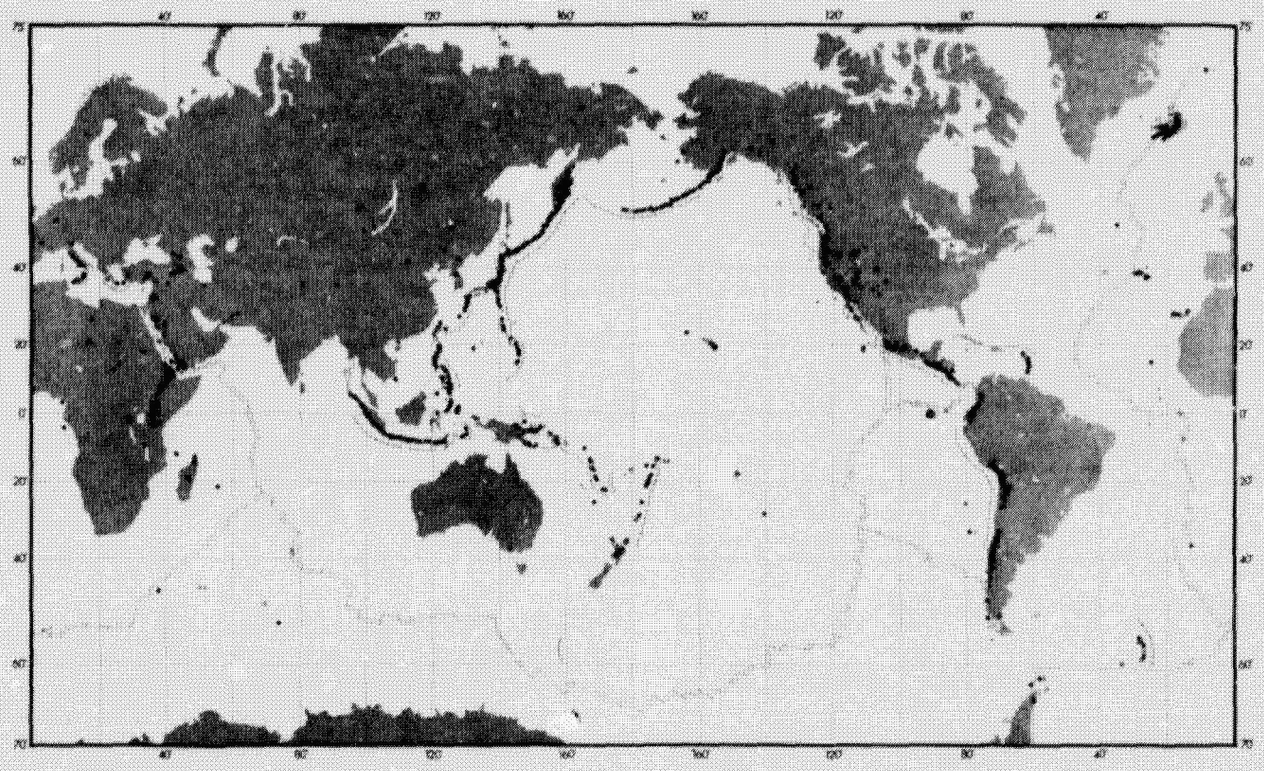

FIGURE 15.1 Map of the volcanoes of the world, showing the relation between volcanoes and tectonic belts. Solid circles are volcanoes with eruptions since 1880; open circles are volcanoes with dated eruptions prior to 1880; triangles are volcanoes with undated but geologically recent eruptions; small crosses are volcanoes with uncertain or solfataric activity. Light double lines are spreading boundaries; thin cross-hatched lines are compressive boundaries (adapted from Simkin and Siebert, 1984). Most spreading boundaries are sites of frequent volcanism, but most submarine eruptions go undetected (see text), hence few specific submarine volcanoes appear on this map.

The basic concepts of plate tectonics have been formulated during the past two decades through multidisciplinary efforts; useful summaries of the developments are found in Oxburgh (1971), Vine (1971), Wyllie (1971), and LePichon *et al.* (1973). An easily read summary of how volcanoes fit into plate-tectonics theory is provided by Decker and Decker (1981). The following discussion summarizes the concept and its relations to volcanism.

Most spreading boundaries lie on the floors of oceans (Figure 15.1), where they form a broad, linear ridge typically surmounted by a narrow trough or graben along the crest. As the opposing plates separate from each other, magma rises from depth along the tensional cracks to erupt as fluid basaltic lava on the ocean floor, thus forming new crust along the spreading boundary. Although no deep ocean-floor eruptions have been detected or observed in progress, bathymetric mapping of the seafloor, studies of the basalt recovered by deep-sea dredging, and photography and other observations from deep-diving submersible vehicles provide evidence demonstrating the close relations between volcanism and the spreading process.

Computations based on rates of seafloor spreading and the relative ages of mid-ocean ridge basalts show that the worldwide total volume rates of eruption from submarine volcanism are several times the totals from subaerial volcanism (Nakamura, 1974). However, this most common form of the Earth's volcanism has essentially no direct impact in the form of hazards on human society because of its depth and remote location beneath the ocean. Future technology may change this if attempts are made to recover mineral deposits believed to be associated with submarine volcanoes. However, in a few places, spreading-type volcanism does impinge on people: it has produced islands such as Iceland astride the mid-Atlantic ridge, and a spreading rift crosses part of East Africa.

Most compressive or convergent plate boundaries form a subduction zone along which one plate descends beneath the other. A linear submarine trench commonly marks the boundary between two such plates. Within, adjacent to, or above the downward-moving slab, partial melting occurs. The resulting magma migrates upward through the crust to emerge eventually at the surface, causing volcanic eruptions from a linear belt of volcanoes that typically lies inland from but parallel to the compressive boundary. The long-recognized circum-Pacific "ring of fire" is the result of subduction. More than 80 percent of the world's recorded historic volcanism has occurred along the Pacific margin and offshoots such as the Indonesian and Marianas arcs.

The third type of plate boundary, transform faults, does not seem to cause volcanism, but some transform faults may incidentally offset a spreading or compressive boundary along which volcanoes are located.

Although most active volcanism is associated with plate boundaries, some important volcanic centers lie within the interior of plates, in some cases thousands of kilometers from a boundary. An explanation of some intraplate centers of volcanism is the concept of a melting or hot spot—an inferred stationary source in the upper mantle producing magma that rises through the overlying moving plate to form volcanoes at the surface (Wilson, 1963, Morgan, 1971, 1972a,b). The melting-spot hypothesis has been further supplemented by the concept of "gravitational anchors," a model that explains both the processes at melting spots and many of the geophysical and geochemical data observed at intraplate volcanoes (Shaw and Jackson, 1973). The most fully documented example of such a system is that of the volcanic islands and seamounts of the Hawaiian-Emporer chain (Dalrymple *et al.* 1973). Several other volcanic centers in the mid-Pacific Ocean may be associated with melting spots.

Other intraplate volcanic centers lie in the western United States, central and eastern Asia, west Africa, and west-central Europe. Most of these show no apparent evidence for being related to a melting spot, and how they fit the plate-tectonic theory requires special explanation. The structures and volcanic evolution of the western United States have been related to complex interactions among plates and subplates along the Pacific-North American margin throughout the past 30 m.y. (Christiansen and Lipman, 1972). The prehistoric but potentially active volcanic centers throughout this region are associated with an extremely complicated and continually changing state of stress, and pulses of motion along structural lineaments have been proposed as triggering the formation of magma (Smith and Luedke, 1984). These ideas demonstrate the important role of volcanism in the past and ongoing development of the concepts of plate tectonics.

## CHARACTERISTICS OF VOLCANOES AND ERUPTIONS

The term "volcano" is defined in two ways; both definitions are valid and are in common use. A volcano is (1) the opening or vent through which volcanic material (molten, solid, or gaseous) is emitted to the surface, and (2) the edifice—hill or mountain—built by the emitted material. The first definition applies chiefly to new volcanoes that have not yet emitted enough material to build an edifice and to those whose products have been dispersed by post-eruption processes. The second defini-

tion is perhaps the more familiar. The size, shape, and structure of volcanoes vary widely with the physical and chemical characteristics and amount of the emitted material, and they are classified according to these various factors. Examples of large volcanic edifices include composite cones and shield volcanoes. Composite cones are typically steep-sided structures, some of great beauty like Mayon in the Philippines and Fuji in Japan. Most large volcanoes associated with compressive plate boundaries are composite cones. They are built of lava flows alternating with layers of pyroclastic fall, pyroclastic flow, and other fragmental material. Shield volcanoes, in contrast, are broad, gently sloping structures, built of many overlapping tongues of lava that had great fluidity; Mauna Loa and Kilauea in Hawaii are examples. Descriptions of these and other volcanic landforms are in such textbooks on volcanoes as those by Macdonald (1972), Bullard (1976), Williams and McBirney (1979), and Decker and Decker (1981).

Material erupted by volcanoes is of widely diverse type and character. Eruptions cover the spectrum of size, violence, and rates of ejection and travel of the material. Hazards vary accordingly. Volcanic products assume a variety of forms, including lava flow, pyroclastic fall, pyroclastic flow, lahar, volcanic gas, and debris avalanche and a wide assortment of intermixtures and intergradations.

Lava flows originate by quiet welling from a vent or by more vigorous lava fountains, and they vary from fluid and mobile to viscous and slow. Fluid flows may travel long distances, they may be either sheetlike or lobate depending on topography, and they are thin relative to their length and breadth. On steep slopes, speeds may reach several tens of kilometers per hour. Viscous flows travel slowly and only short distances, and they are thick relative to fluid flows of comparable lateral dimensions. Speeds are typically a few meters to a few hundred meters per hour. Lava flows commonly destroy property, arable land, buildings, and other structures, but relatively few have taken human lives. A rare exception was the 1977 eruption of the African volcano Nyiragongo, from which a highly fluid, fast-moving lava flow overwhelmed several villages and killed about 300 people.

Pyroclastic falls result from violent ejection of fragmented or pulverized rock that travels through the air and falls to the ground. "Tephra" is a widely used term for this material. Mechanisms that cause fragmentation include explosive eruptions and vigorous streaming of gas from a vent. Fallout may be directly from eruption columns or from clouds produced by convective columns and transported by the wind. Convective clouds may rise above pyroclastic flows (see below) and be transported and deposited as pyroclastic falls. Pyroclastic falls probably constitute the most common of all volcanic hazards. A small to moderate amount of tephra, with thicknesses of up to a few centimeters, is a nuisance and causes damage and inconvenience by clogging machinery and covering buildings, roads, and vegetation. It causes breathing difficulties for humans and animals, and it can abrade tooth enamel. Voluminous tephra falls may be highly destructive; eruptions during historical and recent times have produced deposits many meters thick that collapsed structures and buried towns and farms. Fine material may be carried tens to hundreds of kilometers; some large prehistoric eruptions have deposits that can be recognized thousands of kilometers from their source.

Pyroclastic flows, also known in various forms as ash flows, pumice flows, glowing avalanches, and *nuées ardentes*, are gravity-controlled ground-hugging masses of rapidly moving hot particulate matter. Their high mobility is the result of fluidization of the mass of particles, thought to be caused by both dissolved gases escaping from the hot particles during travel and the rapid expansion of suddenly heated air engulfed by the advancing mass. The size and shape of source vents, volume-rate of ejection, temperature of material, and mechanism of transport all vary widely, and each is a factor in determining the characteristics of the resulting deposit. Pyroclastic-flow deposits may range from narrow and lobate to broad and sheetlike, and thicknesses may vary from a fraction of a meter to hundreds of meters. Particularly high-temperature and/or voluminous pyroclastic flows may result in the flattening and welding of particles within parts of the deposit to form welded tuffs.

The rapid ejection of large volumes of material from a magma reservoir may cause the overlying surface area to collapse, producing a caldera. Calderas are circular to elongate depressions that are from one to several tens of kilometers across with walls that may be hundreds of meters high. Crater Lake, Oregon, is an example of this process. Relatively few caldera-forming eruptions have occurred during historical time, but they include some of the more notable eruptions such as Tambora (in 1815); Krakatau (in 1883), and Katmai (in 1912). These voluminous eruptions represent perhaps the most severe of all known volcanic hazards, and localities throughout the circum-Pacific belt and elsewhere have the potential for producing such eruptions. Their frequency of occurrence, fortunately, is very low by human time standards. Several times during the past million years, however, calderas have formed during truly immense eruptions of pyroclastic flows with volumes one or two orders of magnitude larger than those of historic erup-

tions. For example, calderas at Yellowstone National Park, Long Valley (California), Lake Taupo (New Zealand), and Lake Toba (Sumatra) all developed during pyroclastic-flow eruptions with volumes of tens to hundreds of cubic kilometers. General summaries of pyroclastic-flow deposits are provided by Smith (1960a,b) and Ross and Smith (1961); summaries of the concepts of relations between pyroclastic-flow deposits and calderas include those of Williams (1941), Smith (1960a, 1979), Smith and Bailey (1966, 1968), and Fisher and Schminke (1984).

Pyroclastic surge is a type of flow of particulate matter characterized by a relatively low ratio of solids to gas. Consequently surges are less dense, and they tend to be of relatively low temperature; their deposits are commonly sorted and stratified and display assorted bedforms, such as crossbedding. In contrast, typical pyroclastic flows have a high ratio of particulate matter to gas and have relatively high temperatures; deposits are typically nonsorted and nonstratified. Surges tend to be pulsating, whereas other pyroclastic flows are more continuous. Like pyroclastic flows, surges may travel at high speed, commonly in the range of 50 m per second but sometimes exceeding 100 m per second. Large historical surges have traveled as much as 30 km from the source. Surges may occur either separately or together with pyroclastic flows, and sometimes surges precede or follow pyroclastic flows, forming intergradational deposits. For these reasons, pyroclastic surge is here considered as a variant form of pyroclastic flow, even though some authors regard it as a distinct process. Several different types of surge have been described, and the development of the concept and additional references are found in Moore (1967), Sparks (1976), Wohletz and Sheridan (1979), and Fisher and Schminke (1984). Both flows and surges are highly destructive of property, crops, and natural resources; they have taken many human lives. The eruption of Pelée in 1902, for example, which included both flow and surge phenomena, claimed 28,000 lives.

Lahars are dense slurries of water-saturated volcanic debris that travel downslope, occasionally at velocities as high as 40 m/sec. They are sometimes called volcanic mudflows; but because they consist of material of all sizes, including blocks as much as several meters in diameter, the Indonesian term lahar is preferred. They may be generated during eruptions when fragmented volcanic material becomes intermixed with water, such as from a crater lake or any other body of water or from eruption-induced melting of snow and ice or from eruption-induced rainfall. They may also be generated during quiet periods between eruptions when heavy rain or breaching of ponds or lakes mobilizes unconsolidated tephra. Historically, lahars have been one of the most destructive of all volcanic agents, with a high toll of both lives and property. Some historical deposits are tens of cubic kilometers, and some prehistoric deposits are hundreds of cubic kilometers in volume, and large lahars can travel over 100 km from their source. Kelut Volcano, Indonesia, is a notorious example where dozens of historical eruptions have been accompanied by lahars; in 1919 more than 100 villages were destroyed and over 5000 people were killed. Ruiz volcano (Colombia) had a moderate eruption in November 1985; melted snow and ice generated lahars that destroyed cities and towns greater than 50 km from the volcano, and more than 20,000 people were buried.

During volcanic eruptions gases are not only a major product of emission, but they are considered to be the chief agent that propels the eruption. The most abundant volcanic gases include $H_2O$, $CO_2$, CO, $SO_2$, $SO_3$, $H_2S$, HCl, and HF, and minor amounts of many other gases have been identified. Gas emissions often continue between eruptions, and some vents issue volcanic gas continually for years and decades. Several of the gases are poisonous, and some are corrosive; and in developed areas near gas vents humans, animals, plants, and property may be adversely affected. Certain forest trees and agricultural crops may become stunted or fail to survive gas emissions, such as during the 1783 eruption of Laki, Iceland, when fluorine-poisoned crops resulted in a famine that led to 10,000 deaths. At some volcanoes heavy gases have accumulated in basins or flowed down valleys, displacing oxygen and killing humans and animals. At Dieng, Indonesia, such gas emitted during a small eruption in 1979 killed 150 people.

Another important volcanic process, which became much more widely recognized as a result of the 1980 eruption of Mount St. Helens, is the debris avalanche. At Mount St. Helens, an earthquake triggered the unstable, oversteepened north flank of the volcano into motion, and a catastrophic large landslide ensued that deposited some 2.8 $km^3$ of debris in the nearby river courses and lake basin (Voight *et al.* 1981). Although large landslide deposits had previously been identified at a number of volcanoes, many additional deposits of similar origin have subsequently been recognized throughout the world. The experience at Mount St. Helens demonstrates that not only is the avalanche itself destructive, but the abrupt removal of material can depressurize an underlying phreatomagmatic system, which may then explode with cataclysmic violence (Lipman and Mullineaux, 1981). At Mount St. Helens, the debris avalanche launched a whole array of additional volcanic processes, including pyroclastic surges, flows and falls, and lahars.

## IMPACT OF VOLCANOES ON PEOPLE

### *Distribution of Volcanoes in Relation to Human Population*

Concentration of volcanoes along relatively narrow belts means not only that a relatively small proportion of the land area of the world is close to volcanoes but also that a relatively small proportion of the human population has direct exposure to volcanic activity. Table 15.1 shows an approximation of the percentage of the world's population under risk from volcanic activity, either continuously, often, or only occasionally. It is assumed that people living within, say, about 300 km of an active volcano would be the most aware of and concerned about volcanoes. The table shows a total world population of 3709 million persons, of whom approximately 357 million live near volcanoes. As a result, somewhat less than 10 percent of the world's population is likely to experience risk from volcanic activity, and many of these for only relatively brief periods. Hence efforts to generate support for research and surveillance of volcanoes frequently encounter only apathy and disinterest because the great majority of people have not directly experienced the problems. Only after major volcanic disasters does general interest become widespread, such as that generated by the 1980 eruption of Mount St. Helens.

A high proportion of those countries having large segments of the population living in hazardous areas are developing countries, such as Indonesia, the Philippines, and countries in Central and South America (Table 15.1). These countries have but limited resources for dealing with the problems posed by volcanoes. Some developed countries with volcanic problems, such as New Zealand and Iceland, have but small populations. In western Europe, only Italy has historically active volcanoes located in areas that affect major population centers. The United Kingdom and France have overseas possessions with volcanoes (Caribbean and Indian Ocean regions), but these island colonies have small populations and lie far from the centers of government and industry. Similarly, the volcanoes of Spain and Portugal lie in the Canary and Azore Islands, well removed from national centers. Geologically young volcanic districts in France and West Germany have had no activity during human recorded history. Most of the volcanoes of the Soviet Union lie in a remote region of eastern Siberia thousands of kilometers from the center of government. The historically active volcanoes of the United States lie only in Hawaii and Alaska and in the Cascade Range of California, Oregon, and Washington. They directly affect less than 5 percent of the people of the United States. Other volcanic centers throughout the western United States have the potential for extremely destructive eruptions (Smith and Luedke, 1984), but because they have had no historical activity, public perception of their hazard is low. Among the largest powers, only Japan has active volcanoes in areas where they have direct and frequent influence on a high proportion of the population near the centers of national life. This selective distribution of volcanoes relative to centers of major influence in world affairs appears to be a cause of the rather low level of concern and understanding of volcanic hazards among the people of the world.

### *Effects of Volcanoes on People and Their Activities*

In spite of the widespread lack of concern, nearly 10 percent of the world's people do live and work near active volcanoes. Among the discussions of volcanic hazards and their implications to society are those by Macdonald (1972, 1975), Murton and Shimaburuko (1974), Warrick (1975, 1979), Marts (1978), Hodge *et al.* (1979), Sheets and Grayson (1979), Williams and McBirney (1979), Blong (1984), Crandell *et al.* (1984), and Tomblin and Fournier d'Albe (in press). Each provides insight into the hazards and risks posed by volcanoes. Most conclude that except during and shortly after crises, most people in risk-prone regions have little concern even about their own neighborhood, although they may be aware that elsewhere major eruptions cause serious consequences.

The adverse effects of volcanoes are partly offset by often-overlooked beneficial effects. Volcanoes are builders of land. Many oceanic islands throughout the world owe their very existence to volcanic activity, and in these and other coastal areas volcanoes occasionally add new land. Even greater benefits are the water and air of the planet. Ancient volcanoes transferred volatile components from the molten depths to the surface to form the primitive oceans and atmosphere, and these were gradually modified to form the environment in which living things could develop. Hence volcanoes are one of the agents to which life itself owes its existence.

Fertile soils develop from volcanic rock, and products from eruptions naturally renew them from time to time. In Indonesia the heaviest population is concentrated in the parts of Java and Bali that experience frequent damage or destruction by volcanic ejecta, for these are also the areas that sustain the richest agriculture. Where the climate is compatible, virtually every volcanic region on Earth is noted for its agricultural productivity. Volcanoes also produce outstanding scenery, and many volcanic areas support thriving tourist industries.

The common proximity of volcanic belts to coastlines

TABLE 15.1 Tabulation of Estimated Population Dwelling Near Volcanoes in Each Continent or World Region Compared with Total Population for Each Region

| Continent or Region | | Country or Section Within Continent or Region That Has Volcanoes[b] | | | |
|---|---|---|---|---|---|
| Name | Total Population[a] (in millions) | Name | Total Population | Population Near Volcanoes[c] | Subtotals |
| Africa | 354 | Ethiopia | 26 | 2 | |
| | | Other E. Africa | 74 | 4 | |
| | | Central Africa | 37 | 1 | |
| | | West Africa | 104 | 2 | 9 |
| Asia (except USSR) | 2,104 | Indonesia | 125 | 105 | |
| | | Philippines | 39 | 32 | |
| | | Japan and Ryukyus | 106 | 95 | 232 |
| North America (including Hawaii) | 229 | Alaska | 0.3 | 0.2 | |
| | | Washington | 2.9 | 2.9 | |
| | | Oregon | 1.8 | 1.8 | |
| | | California | 18.8 | 6 | |
| | | Hawaii | 0.7 | 0.7 | 11 |
| Middle America | 96 | Mexico | 53 | 40 | |
| | | Central America | 17 | 13 | |
| | | Caribbean Islands | 26 | 4 | 57 |
| South America | 195 | Colombia | 22 | 7 | |
| | | Ecuador | 6 | 6 | |
| | | Peru | 14 | 5 | |
| | | Chile | 10 | 3 | 21 |
| Europe (except USSR) | 466 | Iceland, Jan Mayan | 0.3 | 0.3 | |
| | | Italy | 54 | 22 | |
| | | Greece | 9 | 0.4 | |
| | | Canary Is., Azores | 1.3 | 1 | |
| USSR | 245 | Kamchatka | 0.4 | 0.2 | 24 |
| Oceania | 20 | New Zealand | 3 | 1.5 | |
| | | Papua New Guinea | 3 | 0.5 | |
| | | Island groups (i.e., Mariannas, Solomons, New Hebrides, Samoa) | 1 | 1 | 3 |
| Total World Population | 3,709 | Total Population Near Volcanoes | | | 357 |

[a]Population figures are for early 1970s and have been adapted from Ehrlich and Ehrlich (1972). Some sectional figures have been derived from various geographic atlases.

[b]Precise data not available in convenient references; figures are estimates based on broad distribution of populations both within and outside volcanic belts.

[c]The countries and sections listed are derived from those having appreciable historic activity as shown in Simkin *et al.* (1981).

means that some volcanoes lie near heavily used transportation and shipping routes. Geographic location and the benefits of volcanoes thus combine to attract human populations and activities to certain eruption-prone regions. Agriculture, tourism, shipping, and accompanying commercial and industrial activities may grow and flourish, especially near volcanoes with long eruption-recurrence intervals.

At some places the activity is frequent and people learn to coexist with the volcanoes, carrying out mitigating measures as necessary. When the activity is mild, eruptions are an inconvenience, but more vigorous activity may cause minor to major destruction. Repeated destruction in some areas has led to adoption of land-use zoning, where frequently damaged areas are left undeveloped or minimally developed. Relatively successful adaptations are found in Japan, Philippines, Indonesia, and Iceland, but even in these countries some authorities are concerned over excessive development in places susceptible to damage by volcanoes. Volcano observatories have been established at a several frequently active volcanoes throughout the world, where systematic sur-

veillance and monitoring are carried out to provide advance warnings of impending activity.

At many volcanoes, however, intervals between eruptions may be so long that the hazards are overlooked or forgotten. Commercial, industrial, agricultural, and residential development may proceed without regard to the potential threat of the volcano. When indications of potential activity commence, it may be difficult to evaluate their significance. Many such signs either subside with no activity or lead only to mild activity. However, sometimes precursory signs are followed by major disastrous eruptions that destroy both lives and property. Several well-known, large eruptions that followed quiet intervals of decades to centuries are Vesuvius (Italy, AD 79); Krakatau (Indonesia, 1883); Pelée (Martinique, 1902); Lamington (Papua New Guinea, 1951); Agung (Indonesia, 1963); Mount St. Helens (United States, 1980); and El Chichon (Mexico, 1982). Each of these eruptions cost human lives. Minor symptoms precede almost all large eruptions, but at infrequently active volcanoes they may be either ignored or misinterpreted. Even at Mount St. Helens, where the early minor symptoms were extensively studied, it was not possible to forecast the time or character of the cataclysmic event. However, precursors have been successfully interpreted to predict more than a dozen subsequent eruptions (Swanson *et al.*, 1983).

Cataclysmic events, although uncommon, have a far greater influence on human perceptions than do the many lesser eruptions that occur each year throughout the world. Major eruptions arouse the awareness of people everywhere to this natural process and its capacity for destruction. Such eruptions demonstrate the need for improved understanding of the processes that cause volcanic activity. The interest generated by new major eruptions generally leads to temporary modest increases in support of research on volcanic processes and improvement of surveillance techniques.

## VOLCANO MONITORING

From a world total of about 540 volcanoes with identified historical activity (Simkin *et al.*, 1981), about 50 to 65 different volcanoes erupt every year. Many eruptions occur in remote regions where their impact on human affairs is minimal, and many of those reported are small and cause but minor damage. Even so, on the average about a dozen volcanoes per year cause appreciable damage and sometimes human casualties, and from one to a few times per decade volcanic eruptions cause major damage and disruption with many casualties.

In spite of the subordinate ranking of volcanic hazards in public consciousness, most countries with active volcanoes have been able to organize some effort to observe and study them. The United Nations and several of the more developed countries with foreign aid programs have given occasional assistance to countries whose own resources are small, and efforts are being made to improve and continue these programs. However, in every country decisions must be made on how to allocate the limited available resources in the most effective way. For example, it must be decided whether to achieve broad but dilute coverage for an entire region or instead to concentrate on one or a few frequently active volcanoes. The ideal goal would be to monitor them all, but this is rarely possible. Decisions on priority are reached by fitting the available surveillance program to known patterns of volcanic behavior. Even with abundant resources, it is difficult to achieve fully satisfactory warning capabilities. While great strides have been made in monitoring procedures and general volcanic processes are becoming better understood, each volcano has a wide range of individual behavior, and few volcanoes exhibit the same precursors or eruptive style. Virtually every eruption at every volcano adds new information to the scope of possibilities.

Within this framework of limitations and difficulties, a wide array of tools and techniques has proven important for study, monitoring, and forecasting. Some techniques have universal applicability, whereas others prove useful only at some volcanoes or for certain eruptive episodes. Hence monitoring techniques applied at any volcano are best established by trial and error, gradually discovering the most effective techniques and adapting them to local behavior patterns. As more data are collected, perhaps more universal behavior patterns will be recognized.

### *Monitoring Techniques*

The most basic of all techniques, and one frequently overlooked or ignored in these times of high technology, is that of careful, systematic, visual observation. Descriptions by trained and practiced observers for background and quiet conditions, for precursory periods, for eruptive activity, and for changes caused by eruptions constitute the most essential surveillance technique of all. Such observations are the starting point from which all other techniques begin. It is desirable for the observations to be supplemented by topographic maps at several scales, aerial photographs with stereographic coverage, and systematic documentary photographs—all made at appropriate time intervals. But even when these valuable supplements are not available, the records of keen and diligent observers are vital.

An extensive literature describes the multitude of in-

strumental techniques utilized in volcano monitoring. Useful summaries and applications of common techniques are provided by Stacey (1969), UNESCO (1971), Civetta *et al.* (1974), Lipman and Mullineaux (1981), Martin and Davis (1982), and Tazieff and Sabroux (1983). Citations to individual papers within these collections will not be given in this abbreviated summary.

Seismic monitoring is the single most essential instrumental technique used in volcano surveillance. As magma rises toward the surface before eruption, stresses forming in the adjacent rocks are relieved by fracturing and slippage, which seismographs detect as earthquakes. Most of these are of very small magnitude (less than Richter magnitude 1), although these microearthquakes may be interspersed with some quakes of larger magnitude (1 to 5). Another type of signal commonly recorded is a fairly continuous, low-frequency rhythmic vibration that is termed *volcanic tremor* (more commonly but slightly erroneously called *harmonic tremor*). It is generally thought to be associated with the movement of fluid through passageways in rock, though the mechanism that generates volcanic tremor is not fully understood.

At most volcanoes the numbers of earthquakes per unit time and the rate of seismic energy release show systematic increases prior to eruptions. Such increases, particularly when accompanied by or interspersed with volcanic tremor, are one of the most important techniques in forecasting volcanic eruptions (Figure 15.2). They are used with most confidence where repeated similar patterns have been observed prior to earlier eruptions. Each volcano seems to have an individual set of characteristic signals, so although the general principles are common to all, the details recorded at one volcano do not necessarily apply at any other. Not every increase in seismic activity at a volcano precedes an eruption, which sometimes greatly complicates the forecasting process and emphasizes the importance of utilizing multiple techniques for surveillance. However, rarely if ever does an eruption begin without being preceded by an increase in seismicity; hence any volcano with even primitive seismic instrumentation will likely give some warning before eruption.

Nearly as important as seismic monitoring are various techniques of measuring ground deformation. As magma rises, it displaces rock, and these displacements are transmitted through intervening rock and expressed at the surface. Displacement of the surface may also be caused by pressure exerted by gases exsolving from the magma. These displacements cause points on the surface of the ground to move in relation to one another, both vertically and horizontally, and the amounts and rates of movement can be detected by a variety of techniques. The simplest of these is a measuring tape; if cracks or faults develop, distances between fixed points on opposite sides of the break can be measured periodically, and rates, and sometimes directions, can be determined and plotted. Across distances from tens of meters to tens of kilometers, horizontal displacement between fixed points can be monitored by electronic distance meters; modern precise instruments utilize a laser beam. Vertical changes can be determined by repeated leveling along survey lines. Changes in slope of the ground are determined by tilt measurements by precise surveying techniques, water-tube devices, or electronic tiltmeters. High-precision photogrammetry is now capable of detecting ground displacements to within fractions of a

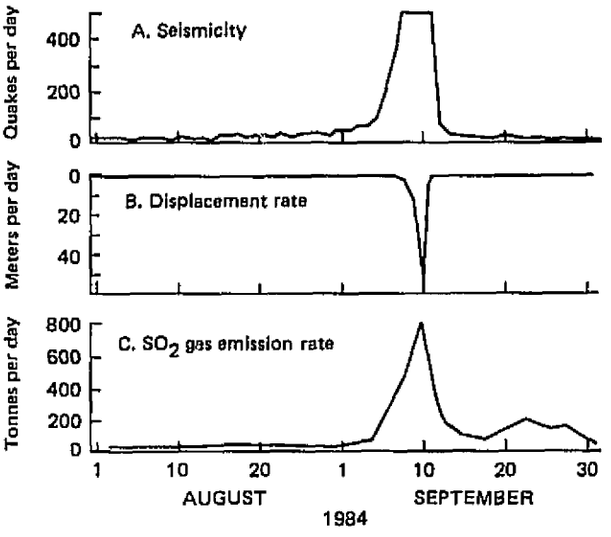


FIGURE 15.2 Plot showing data as detected by three different monitoring methods spanning a 2-month period at Mount St. Helens. The period includes an episode of lava extrusion during September 1984. Increases in seismicity, rate of ground displacement, and rate of gas emission were associated with this extrusion. The extrusion of lava began about September 10 and continued for a few days. Signals commonly increase at accelerating rates during days prior to the onset, and decrease when extrusion begins. A, Seismicity as shown by daily earthquake count at a seismograph located in the crater. Counts began to increase in late August and progressively increased for several days; signals saturated the record from about September 8 to 11. Seismicity returned to background about September 14. B, Maximum daily rate of displacement of selected target on lava dome. Prior to September 1, the background rate was from about 2 to 5 cm/day; from September 2 to 8 the rate increased from 10 cm/day to about 3.5 m/day. The displacement rate exceeded 50 m/day just prior to onset of extrusion and declined rapidly after extrusion began. C, $SO_2$ gas emission rate as measured by aircraft-mounted COSPEC. Data are not continuous because flights are made at irregular intervals. This extrusion was preceded and accompanied by a pronounced increase in emission rate, but some events show little or no change.

meter, so it holds promise of being a useful supplement in detecting deformation, particularly in places where access is difficult. Repeated measurements by any of these techniques may give an indication of when swelling of the volcano is occurring, but ideally a combination of all of them is employed, preferably with multiple stations and lines to attain a broad coverage. Constant rates of displacement indicate steady inflation or deflation of the volcano. Days to weeks before an eruption, rates of displacement may increase or total displacement may reach some critical level. Such changes, especially when correlated with seismic observations, are important in predicting eruptions (Figure 15.2). When observations are made over a wide enough area, displacement vectors can estimate the location of the center of swelling, and further analysis may give indications of the depth, size, and behavior of the magma body. Ground deformation studies are, therefore, important both to forecasting and to improving understanding of volcanic processes.

The chemical and mineralogical composition of the erupted products is important in assessing the character of an eruption and the general state of the volcano, and systematic collection and analysis of lava and tephra samples are critical activities. Any change in composition during an eruption provides clues to magmatic processes and may hint of potential changes in eruptive behavior.

Changes in the gravitational-field strength are caused by a change in elevation or a change in the density of nearby rocks or both. At a volcano the altitude of points on the surface may change in response to intrusion or withdrawal of magma, and the nearby mass distribution may also change in response to the same processes. Eruptions add new rock to the surface, and other volcanic processes may cause collapse or other redistribution of material, which affects the local gravity field. Changes in the level of groundwater associated with eruptions, rainfall, or accumulated snow and ice can cause changes in the gravitational-field strength. Because of these complexities, it is unlikely that gravity measurements can be used as a forecasting tool. But when coupled with other techniques, especially ground-deformation measurements, they can be useful in constraining and better defining models for movement of magma and other volcanic processes.

Gases are significant components of magma, and their chemistry, rate of emission, and relative proportions provide clues to magmatic behavior and to volcanic processes in general. The manner and rate at which gases are liberated from the magma are primary factors determining the type and style of any eruption. Moreover, during the times between eruptions, gases being exhaled from vents and fumaroles provide the only component of magma that can be readily sampled. Hence gases have long been recognized as an important subject for study, both for potential value in eruption forecasting as well as in improving the understanding of volcano behavior. Modern collecting and analytical techniques can yield reliable results for gas composition, and changes in ratios among different gases can help scientists to infer the eruptive potential of a volcano. Changes in the absolute emission rates of volcanic gas empirically would seem to reflect the likelihood of eruption because, as magma rises, confining pressure decreases and cracks develop in adjacent rocks, which should tend to increase gas flux. Use of the correlation spectrometer (COSPEC) at Mount St. Helens and other volcanoes has helped to confirm this concept. The COSPEC, an instrument originally designed to monitor air pollution, can be utilized to measure the flux rate of $SO_2$ gas, and results have demonstrated broad, and sometimes specific, fluctuations that correlate with volcanic behavior (Figure 15.2). Electronic probes to detect hydrogen emissions and transmit data via telemetry have been deployed at a few volcanoes.

Changes in the strength of the magnetic field at a volcano can be caused either by the underground movement of magma or by changes in the stress patterns in the adjacent rocks. Regardless of the cause, a change in field strength should be a useful supporting technique to forecast eruptions. Studies have been carried out at a number of volcanoes, generally by deploying an array of magnetometers at sites on the volcano with one instrument established at a site remote from the volcano; the readings are systematically telemetered to a recording station. In addition to the absolute magnetic field measurements, the field-strength differences between the distant and near sites are recorded so as to neutralize nonvolcanic fluctuations such as magnetic storms and diurnal variations. Promising results have been obtained at several volcanoes, showing some changes in field strength associated with volcanic events, but assorted difficulties with instruments, telemetry, and volcano-induced damage have not yet allowed the technique to achieve its full potential.

Several kinds of study have been performed at volcanoes using a variety of electrical and electromagnetic techniques. Electrical resistivity of magma and molten lava is low, whereas that of dry solidified lava is high; resistivity is further modified by the variable conductivity of permeating groundwater. The contrasts are adaptable to a wide variety of studies and experiments with different kinds of instruments and equipment. Self-potential, very-low-frequency electromagnetic, resistivity, and induced polarization are a few of the tech-

niques that have been used for experiments and studies at volcanoes.

Measurement of temperature changes at the surface seems to be an obvious method of detecting change within a volcano, but it must be applied with caution. Under certain conditions at some volcanoes, increases in temperature occur at hot springs, fumaroles, and crater lakes, and systematic temperature surveillance is a useful monitoring tool. But surface temperatures can be affected by many nonvolcanic factors—rainfall, snow, changing groundwater levels, vegetation, weather conditions such as clouds and wind, and diurnal changes—so measurements must be carefully interpreted. A number of methods may be used to determine temperature; the simplest being direct measurements using thermometer, thermistor, or thermocouple, depending on the temperature range. Care must be taken on successive readings to occupy the same location under as consistent environmental conditions as possible. Thermal infrared techniques have been used at some volcanoes; measurements can be made remotely, either from ground stations or by aerial survey. These methods are useful in detecting broad changes in thermal patterns, but unless expensive calibrated equipment is used they do not yield quantitative results. Readings depend heavily on atmospheric conditions; clouds, rain, dust, and volcanic fume will affect results. In spite of these difficulties, efforts are under way at some volcanoes to establish consistent calibrated thermal surveys. Fluctuating temperatures at some crater lakes have preceded some eruptions; such changes can supplement symptoms revealed by other techniques to help forecast activity.

## PUBLIC RESPONSE TO VOLCANIC ERUPTION

Most people, in areas impacted by a volcanic eruption, are not especially interested in the research that keeps volcanologists occupied. During an emergency, they are concerned chiefly with the practical matters that affect them directly. Their questions are: Will the volcano erupt again? Will the lava (or volcanic ash) come in our direction? How often will it happen? How long will the eruption last? When can we go home? When can we resume our regular work? People generally expect scientists to answer these questions, yet they rarely can be answered with confidence.

When confronted with the stark conditions of displacement, discomfort, and perhaps survival, people may be surprised that the volcanologists are concerned with such seemingly esoteric matters as rock chemistry, tiny motions of survey markers, and wiggly lines on paper charts. While some people are interested and understanding, others will regard such activities as irrelevant, inane, or futile, and scientists may be viewed with indifference, skepticism, or hostility. It is difficult for some people to comprehend that answers to the scientific questions are ultimately the chief hope for answering their own questions. For a more beneficial outlook, people need information and education, both about volcanoes and about methods used in their study. Hence in regions likely to experience volcanic eruptions, it is important for regular programs of education to be carried out before times of crisis. It is in the interest of scientists themselves to provide impetus, encouragement, and even to sponsor such education. In making long-range plans for appropriate use and development of land, zones may be established as defined by relative degrees of volcanic hazard (Crandell *et al.*, 1984).

Various ways can be utilized to inform people about volcanoes, such as special meetings; talks to schools, civic groups, and clubs; and through booklets and pamphlets, displays at museums and visitor centers, newspaper articles, television and radio programs, and open houses at volcano observatories or other research facilities. The specific means can be adapted to local conditions.

In the broad scheme of interactions between a volcano and the people, three other groups besides the scientists play key roles: public officials, land and property managers, and representatives of the news media. When a nearby volcano is quiet, all groups have the opportunity to participate in the important functions of education about volcanoes and preparation for crises, both for their own enlightment and for the benefit of the people they serve. When the volcano becomes active, all become responsible for critical functions. In many branches of science, scientists have but minimal or casual dealings with public officials, land managers, and news media, but when working with an active volcano, scientists must deal regularly with them all. Each group will find it advantageous to attain a good understanding of the role of the other and to gain appreciation and respect for the requirements, capabilities, and limitations of one another. While each group performs a different role, all have the common goal of promoting the welfare of the community.

### *Interactions Between Volcanologists, Public Officials, and Property and Land Managers*

Wide variations exist from one country to another in the type of government and land ownership. Regardless of the prevailing system, however, those vested with appropriate responsibility each have an essential role to play when confronting problems posed by volcanoes. In areas of high volcanic risk, public officials and property

and land managers will be wise to gain at least minimal knowledge about the nature, characteristics, and range of behavior of the volcanoes in and near their jurisdiction. Ideally volcanologists will assist them, and members of each group will establish acquaintance and a good working relationship during times when the volcano is quiet. All can foster education, both for children in schools and for adults in meetings and forums by public and private groups. Officials can formulate contingency plans that prescribe courses of action for all departments in the event of a volcanic emergency. Property and land managers can anticipate questions regarding operations and access on their property and develop contingency policies in conjunction with public officials. Drills may be held by all groups for practice and to test and improve the plans. At some volcanoes, the hazards affect two or more local jurisdictions, in which case the adjoining governments should cooperate in developing the plans and in practicing the procedures. Volcanologists may serve as advisors in such exercises.

In most societies, elected or appointed officials hold authority for making the decisions on common action in response to a volcanic crisis (Warrick, 1979; Blong, 1984; Tomblin and Fournier d'Albe, in press). Depending on the situation and conditions, the officials may be at the local, regional, or national level. They must decide if and when people are to be evacuated; designate the boundaries of the evacuated area; determine routes and transportation methods; arrange for food, shelter, sanitation, medical care, and other needs of the evacuees; and pay the costs. An evacuation is an economic loss in terms of the cost of evacuation, care of those evacuated, and interrupted productivity; it is a social disruption because of the displacement of people from their homes and occupations. Officials face grave decisions when confronted with a volcanic crisis: to fail to evacuate during early activity when a destructive eruption follows may result in lives lost; yet to evacuate when no eruption follows results in social and economic loss. Either circumstance is inevitably followed by a hail of criticism (Hodge *et al.*, 1979; Blong, 1984; Fiske, 1984; Tomblin and Fournier d'Albe, in press).

Officials themselves are rarely able to judge independently whether the condition of a volcano warrants evacuation; they must depend on the advice of scientists. At frequently active volcanoes, especially those where an observatory keeps the volcano under regular surveillance, the advice of the scientists is usually reliable. At these volcanoes, procedures for a warning and subsequent decisions and actions are generally well established; familiarity and frequent practice aid officials in making sound decisions. Several correct decisions on warning and evacuation will build up public confidence and likely some tolerance for an occasional incorrect decision. Officials tend to lean toward the side of caution when issues of public safety are involved. The expenses incurred in unnecessary evacuations may help to convince officials that costs of volcano research are sound investments. But all should realize that even well-monitored volcanoes produce surprises.

In contrast, at volcanoes that are little studied, infrequently active, or believed to be extinct, the onset of unrest may create confusion and uncertainty. Public officials are likely to be unsure over the proper steps to protect the people and to uphold the public interest. They desperately need sound scientific advice, yet volcanologists brought in to evaluate such situations must often make conclusions based on inadequate data gathered quickly. Any resulting advice to officials may be heavily qualified with uncertainties. Unless mutual understanding has been established earlier, such advice may be perceived as inadequate or incompetent. During such situations, controversy may develop between scientists and public officials. Sometimes the officials want the scientists to make and be responsible for the decisions on evacuation and degree of allowable public access; more commonly the officials prefer not to relinquish this authority. Such decisions involve economic and social consequences about which scientists generally have little expertise, and the officials must weigh carefully the degree of hazard against the consequences of various choices. The volcanologists have the responsibility to state the degree of risk in language that is as clear and unambiguous as possible, recognizing that few officials are familiar with technical terminology or with scientific methods of judging uncertainties based on scant evidence. However, if evidence is compelling that hazards are severe or unequivocal, volcanologists must make this clear by making appropriate recommendations. Yet all parties should understand that, unless authority is otherwise vested, the ultimate decisions about public safety are in the hands of the public officials.

### *Interactions Between Volcanologists and the News Media*

Newspapers, magazines, television, and radio constitute the principal means by which people learn about potential or actual eruptive activity at any particular volcano. The degree and type of news coverage is determined by the size and character of the volcano or eruption, its accessibility, and the size and distribution of the local population. Journalists are generally more interested in the impact of an event on people than in the scientific aspects. Major eruptions in isolated regions of-

ten receive little or no notice by the press, whereas even minor events in populated areas receive much attention.

It is important that public officials, property and land managers, and scientists have effective means for communicating with the press, because the public welfare requires that prompt, reliable, accurate information be conveyed to the news media. Both public officials and large land managers deal with the press regularly, so channels and procedures are normally already in place. Volcanologists, however, may be unfamiliar with media procedures, so it is important that they prepare themselves.

If a group of scientists is studying an erupting volcano or one showing signs of erupting, it is well to designate a single member of the group to communicate with the news media; if the team is small the person may be the leader. Having a single representative ensures continuity and consistency and permits mutual confidence and rapport to develop while minimizing the chances for misunderstandings. Ideally this scientist-for-information is fully informed on the status of the volcano and on the activities, findings, and opinions of every team member and reports to the press regularly after consultation with the other scientists. Reports should be as complete and factual as possible, emphasizing what has happened and is happening. The scientist must be prepared on how to respond to questions regarding the timing, nature, and magnitude of future events. These are important questions, and seeking their answers is one of the principal reasons for the scientists' activities; yet most of the time these questions do not have clearly defined answers. The scientist must still respond in a factual, helpful manner, stating the range of possibilities and the degrees of uncertainty in terms of ongoing processes that are understood. Many reporters will be dealing with an unfamiliar subject, and information should be presented, insofar as possible, in straightforward, everyday language. The scientist should be patient with reporters as they learn and be genuinely concerned in helping them to produce complete and accurate stories. Honesty and sincerity inspire confidence from media members, which in turn enhances the quality of the news stories.

Departures from this ideal sometimes occur. Controversies between scientists may arise, sometimes when two or more groups come from different institutions or different countries. It is best to try to resolve such controversies privately. But if the news media learn of them, the controversies can still be handled constructively by showing that volcanology is a young, inexact science and that progress is made by testing opposing hypothesis. Sometimes, however, such public disagreements become antagonistic; the disagreement may rival the story of the eruption, relations between scientists and media deteriorate, the public becomes confused or angry, and scientists lose credibility. Such a controversy occurred at La Soufrière Volcano on Guadeloupe in 1976 (Fiske, 1984).

While constructive and mutually supportive relations between scientists and the news media are the ideal goal, it is sometimes not achieved. Most scientists who have experienced more than a few interviews can cite examples of misquotations, quotations out of context, or news stories that are flatly inaccurate. On the other hand, reporters have equally valid complaints about scientists who talk in obtuse language, refuse to see them, or are perceived to be arrogant. Differences in perceptions and goals between scientists and journalists are probably the cause of most of this antagonism and controversy. In an effort to help members of each group better understand the other, Table 15.2 outlines some of the complaints scientists and journalists have expressed about each other. These problems stem partly from the basically different personalities attracted by the contrasting professions. Their respective job requirements are different. Scientists must be accurate, analytical, and deliberate, and they must consider many lines of evidence before reaching conclusions. Statements of their conclusions are commonly hedged with qualifiers. In contrast, journalists must be quick and decisive, and while they strive for accuracy it must be achieved within a framework of perpetual deadlines. Further, they must quickly identify the key factors, emphasize them, and reduce a body of information to its simplest terms. Table 15.2 is arranged to illustrate opposite but corresponding complaints, which demonstrate how mutual misunderstandings develop from particular situations. Obviously not every aspect of these problems can be covered in an abbreviated and generalized table, but even so it implies ways to improve understanding between scientists and journalists.

When scientists understand the reporters' needs to get quickly to the main point, they can dispense with lengthy preambles and excessive qualifiers. Scientists can minimize jargon and be sure that those technical terms that are necessary are clearly defined. It is useful for them to remember that they are not delivering a paper at a scientific meeting but instead are conveying information, through the reporter, to people from all walks of life. Reporters in turn have the responsibility to strive for accuracy in expressing the information. Nothing is more frustrating to the scientist than to find himself misquoted or to have his statements used in a wrong context. He is put in the position of seeming to provide incorrect, perhaps damaging, information to the public. Reporters should not be reluctant to check back to

TABLE 15.2 Some Common Sources of Friction Between Scientists and Journalists

| Complaints by Scientists About Reporters | Complaints by Reporters About Scientists |
|---|---|
| We get misquoted in news stories | Scientists talk in jargon that no one else can understand |
| Reporters are too pushy and aggressive | Scientists are aloof, hard to reach, uncooperative |
| Reporters are not satisfied with what we tell them; they are always looking for hidden angles; they are too suspicious | Scientists do not tell the whole story, they hold back and conceal information |
| Many reporters are poorly prepared; they know nothing about the subject or even about what has already happened here | Scientists expect us to be experts in their subject, they are impatient in giving us the background we need |
| Reporters interrupt our work schedules; they do not seem to see how they themselves are hindering us in trying to find answers to their (and everyone's) questions | Scientists do not understand the time deadlines under which we are required to operate |
| Reporters do not really listen to the whole story we try to tell them; their coverage is shallow; they omit the all-important qualifiers to our statements; they think all answers should be black and white but ignore all the intermediate shades of gray | Scientists are too long-winded; they talk all around the subject and never get to the point. They do not understand that we need to use straightforward simple statements; we have to convert their complicated discourses to words that people can read |
| Reporters seek out differences of opinion between scientists and overemphasize them; they try to make a story by fabricating discord | When we try to verify our story with a second opinion, we cannot get any consistency between different scientists. How do we know who to believe? |

NOTE: This table shows examples of attitudes and actions that lead to antagonism between scientists and journalists. Their listing here is not intended as criticism of either group nor to fuel controversy. Instead they are intended to help each group recognize how its own attitudes and actions impinge on the other, thereby aiding members of each group to seek ways to improve the perceptions of the other. Happily, the complaints are not universal, and many members of both groups understand and accommodate the others' viewpoints and requirements.

verify the accuracy of their stories; scientists should welcome such opportunities. Many of the hard-to-reach scientists about whom the reporters complain are those who have been embarrassed by past misquotations. These potential problems demonstrate the value of having a specified scientist to provide information; this person can become practiced in responding to reporters' needs, seek ways to improve each presentation and avoid past mistakes, and build up friendly rapport. Likewise it is helpful if the same reporters stay on the story long enough to gain knowledge and build consistency; when new reporters are assigned, they can avoid many problems if they acquire appropriate background before starting their interviews.

It is important that each group understand the work requirements and time schedules of the other. Newspapers and television have deadlines at different times, and neither necessarily fits the normal working schedule of a field volcanologist. When the scientific staff is small, stopping work to grant interviews interferes with the acquisition and interpretation of data. However, when both groups better understand the others' legitimate requirements and limitations, it is almost always possible for them to accomodate each other. When such cooperation is achieved, the public reaps the benefits.

### *Summary of the Volcanologist's Role in Enhancing Public Understanding*

People properly informed about the character and behavior patterns of volcanoes are best prepared to deal with volcano emergencies when they arise. Only near volcanoes that either erupt frequently or have just recently erupted, however, are members of the general public likely to have much awareness of volcano hazards (Murton and Shimaburuko, 1974). In areas distant from volcanoes, or in areas near long-dormant volcanoes, people are unlikely to be aware of problems posed by volcanoes. Even at times of volcanic crisis elsewhere, the general reaction is commonly, "aren't we lucky those things don't happen here."

Among all groups of people, volcanologists and other earth scientists are the most likely to be aware of the troublesome potential of nearby volcanoes. Many recognize the responsibility to raise the general awareness of the hazards, yet their efforts are often misunderstood or misconstrued. For example, when the now-renowned report by Crandell and Mullineaux (1978) on volcanic hazards at Mount St. Helens first appeared, it received considerable local criticism for being scarey and potentially adverse to the economy. Then, in spite of the les-

sons learned at Mount St. Helens in 1980, a storm of criticism arose when a notice of potential hazard was issued in 1982 at Mammoth Lakes, California, in response to repeated earthquake swarms (the hazards are summarized in Miller *et al.*, 1982). The warnings were perceived by some of the local population and the press as self-serving to the scientists as well as highly damaging to property values and local business. Even in Hawaii, where, if anywhere, people should be aware of problems posed by volcanoes, a report describing volcanic hazards of the Island of Hawaii (Mullineaux and Peterson, 1974) was severely criticized by some community leaders for depressing the local economy and hampering development in volcano-prone areas. Similar reactions have occurred during recent seismicity and deformation at both Rabaul, Papua New Guinea, and Pozzuoli, Italy. Such reactions demonstrate traits typical of human nature and emphasize the attitudes of indifference or hostility induced when receiving information about potentially unpleasant matters.

They also underscore the challenge that faces scientists as they attempt to inform the public about volcano hazards. The importance of the message is great enough that the scientists must not only be willing to face the adverse reactions but also to persist in finding truly effective ways of conveying information that is important to societal needs. Competent scientific information does little good if it is ignored, scorned, or disbelieved. It is important for scientists to be tactful, patient, and perservering as they deal with the news media and public officials on matters concerning volcano hazards. They must find ways to employ the same qualities of innovation and resourcefulness that they normally display in scientific research if their hazard messages to the public are to be heard and heeded.

## ACKNOWLEDGMENTS

This paper reflects the experience, ideas, and opinions developed during service at both the Hawaiian Volcano Observatory and the Cascades Volcano Observatory (CVO). I am grateful to my colleagues at each facility for support, discussions, and constructive debate on both the scientific and societal issues associated with hazardous volcanoes. I am also grateful to the public officials, land managers, and representatives of the press in both regions, with whom we explored together to find positive ways to solve the problems that we faced. The paper was reviewed by D. R. Mullineaux, R. W. Decker, and several colleagues at CVO, and it has been greatly improved by their suggestions.

## REFERENCES

Blong, R. J. (1984). *Volcanic Hazards*, Academic Press, Sydney, Australia, 424 pp.

Bullard, F. M. (1976). *Volcanoes of the Earth*, Univ. of Texas Press, Austin, Texas, 579 pp. (2nd ed. published 1984, 629 pp.).

Christiansen, R. L., and P. W. Lipman (1972). Cenozoic volcanism and plate-tectonic evolution of the western United States, II. Late Cenozoic, *Philos. Trans. R. Soc. Lond. 271*, 249-284.

Civetta, L., P. Gasparini, G. Luongo, and A. Rapolla, eds. (1974). *Physical Volcanology*, Elsevier, Amsterdam, 333 pp.

Crandell, D. R., and D. R. Mullineaux (1978). Potential hazards from future eruptions of Mount St. Helens Volcano, Washington, *U.S. Geol. Surv. Bull. 1383-C*, 26 pp.

Crandell, D. R., B. Booth, K. Kazumadinata, D. Shimozuru, G. P. L. Walker, and D. Westercamp (1984). *Source Book for Volcanic-Hazard Zonation*, UNESCO, Paris, 97 pp.

Dalrymple, G. B., E. A. Silver, and E. D. Jackson (1973). Origin of the Hawaiian Islands, *Am. Sci. 61*, 294-308.

Decker, R. W., and B. Decker (1981). *Volcanoes*, Freeman, San Francisco, Calif., 244 pp.

Ehrlich, P. R., and A. H. Ehrlich (1972). *Population, Resources, Environment: Issues in Human Ecology*, Freeman, San Francisco, Calif., 509 pp.

Fisher, R. V., and H.-U. Schminke (1984). *Pyroclastic Rocks*, Springer-Verlag, New York, 472 pp.

Fiske, R. S. (1984). Volcanologists, journalists, and the concerned local public: A tale of two crises in the eastern Caribbean, in *Explosive Volcanism: Inception, Evolution, and Hazards*, Geophysics Study Committee, National Research Council, National Academy Press, Washington, D.C., pp. 170-176.

Hodge, D., V. Sharp, and M. Marts (1979). Contemporary responses to volcanism: Case studies from the Cascades and Hawaii, in *Volcanic Activity and Human Ecology*, P. D. Sheets and D. K. Grayson, eds., Academic Press, New York, pp. 221-248.

LePichon, X., J. Francheteau, and J. Bonnin (1973). *Plate Tectonics*, Elsevier, Amsterdam, 300 pp.

Lipman, P. W., and D. R. Mullineaux, eds. (1981). *The 1980 Eruptions of Mount St. Helens, Washington*, U.S. Geol. Surv. Prof. Paper 1250, 844 pp.

Macdonald, G. A. (1972). *Volcanoes*, Prentice-Hall, Englewood Cliffs, N.J., 510 pp.

Macdonald, G. A. (1975). Hazards from volcanoes, in *Geological Hazards*, B. A. Bolt, W. L. Horn, G. A. Macdonald, and R. F. Scott, eds., Springer-Verlag, New York, pp. 63-131.

Martin, R. C., and J. F. Davis, eds. (1982). Status of Volcanic Prediction and Emergency Response Capabilities in Volcanic Hazard Zones of California, Calif. Div. Mines and Geology, Special Publ. 63, 275 pp.

Marts, M. E. (1978). Social implication of volcano hazard case studies in the Washington Cascades and Hawaii, Dept. of Geography, University of Washington, Seattle, NSF-RANN Project Rep. ENV-76-20735, 364 pp.

Miller, C. D., D. R. Mullineaux, D. R. Crandell, and R. A. Bailey (1982). Potential hazards from future volcanic eruptions in the Long Valley-Mono Lake area, east central California and southwest Nevada—A preliminary assessment, *U.S. Geol. Surv. Circ. 877*, 10 pp.

Moore, J. G. (1967). Base surge in recent volcanic eruptions, *Bull. Volcanol. 30*, 337-363.

Morgan, W. J. (1971). Convection plumes in the lower mantle, *Nature 230*, 42-43.

Morgan, W. J. (1972a). Deep mantle convection plumes and plate motions, *Am. Assoc. Petrol. Geol. Bull. 46*, 203-213.

Morgan, W. J. (1972b). Plate motions and deep mantle convection, *Geol. Soc. Am. Mem. 132*, pp. 7-22.

Mullineaux, D. R., and D. W. Peterson (1974). Volcanic hazards on the island of Hawaii, U.S. Geol. Surv. Open-File Rep. 74-239, 61 pp.

Murton, B. J., and S. Shimaburuko (1974). Human adjustment to volcanic hazard in Puna District, Hawaii, in *Natural Hazards, Local, National, and Global*, G. F. White, ed., Oxford Univ. Press, New York, pp. 151-159.

Nakamura, K. (1974). Preliminary estimate of global volcanic production rate, in *Utilization of Volcanic Energy*, J. Colp and A. S. Furimoto, eds., U. of Hawaii and Sandia Corp., Hilo, Hawaii, pp. 273-286.

Oxburgh, E. R. (1971). Plate tectonics, in *Understanding the Earth*, J. C. Cass, P. J. Smith, and R. C. L. Wilson, eds., 2nd ed., MIT Press, Cambridge, Mass., pp. 263-285.

Ross, C. S., and R. L. Smith (1961). *Ash-flow Tuffs—Their Origin, Geologic Relations, and Identification*, U.S. Geol. Surv. Prof. Paper 366, 81 pp.

Shaw, H. R., and E. D. Jackson (1973). Linear island chains in the Pacific: Result of thermal plumes or gravitational anchors? *J. Geophys. Res. 78*, 8634-8652.

Sheets, P. D., and D. K. Grayson, eds. (1979). *Volcanic Activity and Human Ecology*, Academic Press, New York, 644 pp.

Simkin, T., and L. Siebert (1984). Explosive eruptions in space and time: Duration, intervals, and a comparison of the world's active volcanic belts, in *Explosive Volcanism: Inception, Evolution, and Hazards*, Geophysics Study Committee, National Research Council, National Academy Press, Washington D.C., pp. 110-121.

Simkin, T., L. Siebert, L. McClelland, D. Bridge, C. Newhall, and J. H. Latter (1981). *Volcanoes of the World: A Regional Directory, Gazetteer, and Chronology of Volcanism During the Last 10,000 Years*, Hutchinson Ross, Stroudsburg, Pa., 240 pp.

Smith, R. L. (1960a). Ash flows, *Geol. Soc. Am. Bull. 71*, 795-841.

Smith, R. L. (1960b). Zones and zonal variations in welded ash flows, *U.S. Geol. Surv. Prof. Paper 354-F*, pp. 149-159.

Smith, R. L. (1979). Ash-flow magmatism, in *Ash-Flow Tuffs*, C. E. Chapin and W. E. Elston, eds., Geol. Soc. Am. Spec. Paper 180, pp. 5-27.

Smith, R. L., and R. A. Bailey (1966). The Bandelier Tuff: A study of ash-flow eruption cycles from zoned magma chambers, *Bull. Volcanol. 20*, 83-104.

Smith, R. L., and R. A. Bailey (1968). Resurgent cauldrons, in *Studies in Volcanology*, R. R. Coats *et al.*, eds., Geol. Soc. Am. Mem. 116, pp. 613-662.

Smith, R. L., and R. G. Luedke (1984). Potentially active volcanic lineaments and loci in western conterminous United States, in *Explosive Volcanism: Inception, Evolution, and Hazards*, Geophysics Study Committee, National Research Council, National Academy Press, Washington D.C., pp. 47-66.

Sparks, R. S. J. (1976). Grain size variations in ignimbrites and implications for the transport of pyroclastic flows, *Sedimentology 23*, 147-188.

Stacey, F. [illegible] 969). *Physics of the Earth*, Wiley, New York, 324 pp.

Swanson [illegible], T. J. Casadevall, D. Dzurisin, S. D. Malone, C. G. New[illegible], and C. S. Weaver (1983). Predicting eruptions at Mount St. Helens, June 1980 through December 1982, *Science 221*, 1369-1376.

Tazieff, H., and J. C. Sabroux, eds. (1983). *Forecasting Volcanic Events*, Elsevier, Amsterdam, 635 pp.

Tomblin, J., and E. M. Fournier d'Albe (in press). *Principles of Volcanic Emergency Management*, UNESCO, Paris.

UNESCO (1971). *The Surveillance and Prediction of Volcanic Activity*, UNESCO, Paris, 166 pp.

Vine, F. J. (1971). Sea-floor spreading, in *Understanding the Earth*, J. C. Bass, P. J. Smith, and R. C. L. Wilson, eds., 2nd ed., MIT Press, Cambridge, Mass., pp. 233-249.

Voight, B., H. Glicken, R. J. Janda, and P. M. Douglass (1981). Catastrophic rockslide avalanche of May 18, in *The 1980 Eruptions of Mount St. Helens, Washington*, P. W. Lipman and D. R. Mullineaux, eds., U.S. Geol. Surv. Prof. Paper 1250, pp. 347-377.

Warrick, R. A. (1975). *Volcano Hazard in the United States: A Research Assessment*, Institute of Behavioral Science, University of Colorado, Monograph NSF-RA-E-75-012, 144 pp.

Warrick, R. A. (1979). Volcanoes as hazards: An overview, in *Volcanic Activity and Human Ecology*, P. D. Sheets and D. K. Grayson, eds., Academic Press, New York, pp. 161-194.

Williams, H. (1941). Calderas and their origin, *Calif. Univ. Dep. Geol. Sci. Bull. 25*, 239-346.

Williams, H., and A. R. McBirney (1979). *Volcanology*, Freeman, Cooper and Co., San Francisco, Calif., 397 pp.

Wilson, J. T. (1963). A possible origin of the Hawaiian Islands, *Can. J. Phys. 41*, 863-870.

Wohletz, K. H., and M. F. Sheridan (1979). A model of pyroclastic surge, in *Ash-Flow Tuffs*, C. E. Chapin and W. E. Elston, eds., Geol. Soc. Am. Spec. Paper 180, pp. 177-194.

Wyllie, P. H. (1971). *The Dynamic Earth*, Wiley, New York, 416 pp.

# 16 Volcanic Hazard Assessment for Disposal of High-Level Radioactive Waste

BRUCE M. CROWE
*Los Alamos National Laboratory*

ABSTRACT

Volcanic hazard studies for disposal of high-level radioactive waste pose a number of unique problems. These include the long time frame of hazard assessment ($10^4$ to $10^6$ yr), the limited geologic record of volcanic activity at disposal sites and the political sensitivity of this national problem. The major variables affecting volcanic hazards are the structure of magma feeder systems at repository depths and the magma fragmentation and dispersal energy of eruptions. The latter is generally controlled by magma composition and the presence or absence of groundwater. Long-lived volcanic fields (>1 m.y.) provide the greatest potential risk for waste disposal, but these can be avoided by proper site selection. Short-lived volcanic fields are more difficult to avoid but are generally mafic in composition, which results in smaller disruption zones and explosive eruptions of lower energy than those of long-lived centers.

Volcanic hazards are evaluated through risk assessment, which is a product of probability and consequences. These studies have been completed for a potential waste disposal site in the Nevada Test Site (NTS). Cenozoic volcanism of the NTS region is divided into three distinct episodes. The youngest episode, 3.7 to 0.3 m.y., comprises scattered, monogenetic Strombolian centers of small volume (<1 $km^3$). Rates of volcanic activity for the NTS region are estimated to be about $10^{-6}$ event/yr, based on vent counts through time and calculation of rates of magma production. The conditional probability of disruption of the possible waste disposal site at the NTS by basaltic volcanism is bounded by the range of $10^{-6}$ to $10^{-10}$ $yr^{-1}$. Consequences, expressed as radiological release levels, were evaluated by assuming disruption of a repository by basaltic magmas fed along narrow dikes. Limits are placed on the volume of waste material incorporated in magma by analogy to the abundance of lithic fragments in basalt scoria and lava. These consequences would be increased if rising magma encountered water and produced magma/water vapor explosions, which can eject large volumes of country rock. Such a mechanism would be important only if the vapor explosions excavated a crater to repository depths (380 m)—an unlikely event, based on the dimensions of hydrovolcanic craters. The total expected release from disruption of a repository by basaltic magma for a $10^4$-yr period is 1.8 Ci for spent fuel and 1.3 Ci for high-level waste.

## INTRODUCTION

Regardless of the current or future use of nuclear power reactors for the generation of electricity, one of the major national problems facing scientists across a range of disciplines is the safe disposal of high-level radioactive wastes. (High-level radioactive waste refers to heat-producing waste.) By current definitions, this includes two by-products of nuclear reactors—spent fuel assemblies and reprocessed spent-fuel assemblies. The current consensus of the scientific community is that the most viable means of waste isolation is through deep burial in selected rock formations. This is the present policy of the U.S. Department of Energy. The suitability of a number of sites for storage of high-level radioactive waste is now being actively investigated. Two of the sites that have undergone thorough geologic investigations are the Hanford site in southern Washington (waste burial in the Columbia River Basalt) and the Nevada Test Site (NTS) in southern Nevada (waste burial in ash-flow sheets of the Timber Mountain-Oasis Valley caldera complex).

Geologic investigations leading to selection of sites for burial of radioactive wastes pose several problems. First, detailed characterization of a block of the Earth's crust is required on a level that is unprecedented in the science. This characterization has unique requirements. First, the repository block must be defined with a high degree of confidence, and yet penetrations of the block by exploratory drilling or tunnels must be limited so the integrity of the block is not compromised. This restriction requires an emphasis on geophysical techniques as a primary means of site exploration. Second, the potential effects of construction of a repository tunnel complex and the thermal disturbance of the rock from the emplacement of heat-producing waste must be evaluated with respect to induced changes that could alter the isolation properties of the rocks. Third, the rates of operation of natural geologic processes on the block, such as groundwater movement and tectonic uplift or erosion, must be defined to evaluate the suitability of the block for containment of radioactive waste elements. Finally, possible future changes from naturally occurring but more catastrophic tectonic processes such as seismicity or volcanism must be evaluated for the required isolation period of high-level waste. This last topic, which falls in the regime of predictive geology is the focus of this paper. More and more frequently, geologists are being asked by other scientists and the public to make specific predictions on the future activity of geologic phenomena. Although some progress has been made in prediction of earthquake and volcanic activity, most predictions are valid for periods of months or at most a few tens of years. In contrast, geologic predictions required for waste disposal must encompass a period of thousands of years. We have limited experience in the geologic methods used to make such predictions and even less experience in communicating and defending decisions based on geologic predictions in a public forum. This chapter describes recent work concerned with prediction of tectonic processes for one specific problem—volcanic hazards related to permanent isolation of high-level radioactive wastes. Two topics are emphasized: (1) the special problems posed by volcanic hazard assessment for waste disposal and (2) the use of risk-assessment techniques to evaluate volcanic hazards for the storage of high-level radioactive waste in tuff in southern Nevada (Nevada Nuclear Waste Storage Investigations).

## SPECIAL PROBLEMS INHERENT IN VOLCANIC HAZARD ASSESSMENT FOR WASTE DISPOSAL SITES

Perhaps the most novel aspect of volcanic hazard assessment for radioactive waste disposal is the length of time for which hazards must be forecast. The required containment period of high-level v[illegible]tive waste is $10^4$ yr as defined in the draft version [illegible] Environmental Standards for Management and [illegible]sposal of Spent Nuclear Fuel, High-Level and Transuranic Radioactive Wastes [U.S. Environmental Protection Agency (1982) 40 CFR 191]. This standard, which has not yet been formally approved, is based on a radiological comparison of the projected mass of radioactive waste [$10^5$ metric tons of heavy metal (MTHM)] with an equivalent amount of unmined uranium ore. A $10^4$-yr period has been chosen as the required interval for radioactive waste to decay to a level where the risk is about the same as the smallest estimate of the risk from an equivalent amount of uranium ore (EPA 520/1 82-025, p. 29). However, Bredehoeft *et al.* (1978) noted that $10^4$ yr provides adequate containment for the short-lived radionuclides such as $^{90}Sr$ or $^{137}Cs$ but allows for only a limited reduction in the potential hazards of long-lived radionuclides like $^{129}I$. Gera (1982) argued that the waste should be allowed to decay until the radiotoxicity levels are equal to the levels from the amount of uranium consumed in a reactor. This would require an isolation time of about $10^5$ yr. Whatever the required isolation period of high-level waste, this period becomes the minimum length of time for which future volcanic hazards must be forecast. Both $10^4$ and $10^5$ yr are long compared to the rates of operation of volcanic processes.

The long time frame of hazard assessment is a special problem of waste disposal. There is neither an estab-

lished methodology nor scientific experience to draw on to test data conclusions. Because the regulatory guidelines for volcanic hazards are general, it is difficult to decide what types of data best satisfy licensing requirements. This ambiguity has led to increased pressure to quantify the interpretations because numeric data are more easily judged in licensing decisions. However, no matter how the arguments are constructed, these calculations have large uncertainties that are difficult to evaluate within the constraints of the existing general guidelines for site licensing. Moreover, the development of safe methods to permanently isolate radioactive waste is closely linked to the future use of nuclear power reactors, a highly sensitive national issue. Studies dealing with the suitability of a site for waste disposal are subjected to intense public scrutiny.

Another problem that applies to most tectonic processes and to volcanism in particular is the relatively limited record used to forecast future activity. Licensing requirements of the U.S. Nuclear Regulatory Commission (document 10 CFR 60) specify that a site under consideration for disposal of high-level radioactive waste must have limited Quaternary igneous activity. Although this is logical for siting considerations, it presents a dilemma for forecasting future rates of volcanism. Either subjective assumptions must be made to estimate numerical rates of volcanism from the limited Quaternary record, or the time scale of the volcanic assessment must be lengthened to include more volcanic events. Neither approach is satisfactory and both increase the possibility that the data do not adequately represent possible future volcanic activity at a repository site.

## FORECASTING VOLCANIC HAZARDS: NATIONAL PERSPECTIVE

Examination of the distribution of volcanic rocks in the United States shows that all Quaternary and, in fact, all major Cenozoic sites of volcanic activity are restricted to the western conterminous United States (for example, Suppe *et al.*, 1975; Smith and Luedke, 1984). Giletti *et al.* (1978) noted that for the area east of the Rocky Mountains ". . . the probability for a magmatic incursion into a waste repository during the next million years has been taken as astronomically low, but numerically uncertain." The obvious conclusion, therefore, is that siting a waste repository east of the Rocky Mountains eliminates volcanism as a licensing issue. However, all current potential waste disposal sites, with the exception of an unspecified site in domal salt in Louisiana or Mississippi, are west of the Rocky Mountains and within the broad region identified by Smith and Luedke (1984) as having the potential for future volcanic eruptions.

Crowe (1980) reviewed the major factors controlling the disruption of a repository by volcanism. He noted that the significant variables are the structure of magmatic intrusions or feeder systems at repository depths (>300 m) and the eruptive style of surface activity. The latter is generally controlled by magma composition and the presence or absence of groundwater. Magma feeder systems range from narrow dikes to diapirs; the controlling variables are the viscosity and yield strength of the melt and the rate of heat exchange between the wall rock and the magma. It must be possible for the magma to ascend to the surface before falling temperatures or crystallization prevent eruption (Wilson and Head, 1981). Basaltic magmas ascend along linear dikes because of their low viscosities and Newtonian fluid behavior. Calculated ascent rates based on the presence of high-density nodules, geophysical data, and theoretical considerations are about 1 to 10 cm/sec (Crowe *et al.*, 1983b). In contrast, silicic magmas must ascend as diapirs as a result of their high viscosity. The rate of rise is controlled by the diapir size and the viscosity of the wall rock; ascent velocities are $10^{-2}$ to $10^{-6}$ cm/sec (Marsh, 1984).

Monogenetic volcanic centers are single-cycle volcanoes with eruptive durations of days, months, or years. Magmas associated with these centers are generally of basaltic composition with variations toward andesite. Field studies of the roots of monogenetic centers show that they are fed by narrow dikes (aspect ratios of $10^{-2}$ to $10^{-3}$), which is consistent with their composition (Crowe *et al.*, 1983b). Eruptive activity in these centers is transitory, and the flux of magma is insufficient to maintain a magma chamber at shallow crustal levels (Fedotov, 1981). The disruption zone associated with monogenetic volcanic centers is limited, therefore, to the feeder dikes. Magma along these dikes must directly intersect a repository to disrupt and disperse waste radionuclides. In contrast, shield volcanoes, stratavolcanoes, or large silicic centers, such as caldera complexes, are long-lived features with multiple eruption cycles and life spans of several million years. Field and geophysical evidence shows that they are fed from shallow-reservoir magma chambers. The presence of shallow magma chambers, multiple feeder systems, and hydrothermal circulation systems above a magma chamber means that the potential effect of repository disruption by these magmas is much greater than that by magmas from monogenetic volcanic centers.

The potential effect of eruption mechanisms on disruption and dispersal of the inventory of a waste repository is illustrated in Figure 16.1. This figure, which is

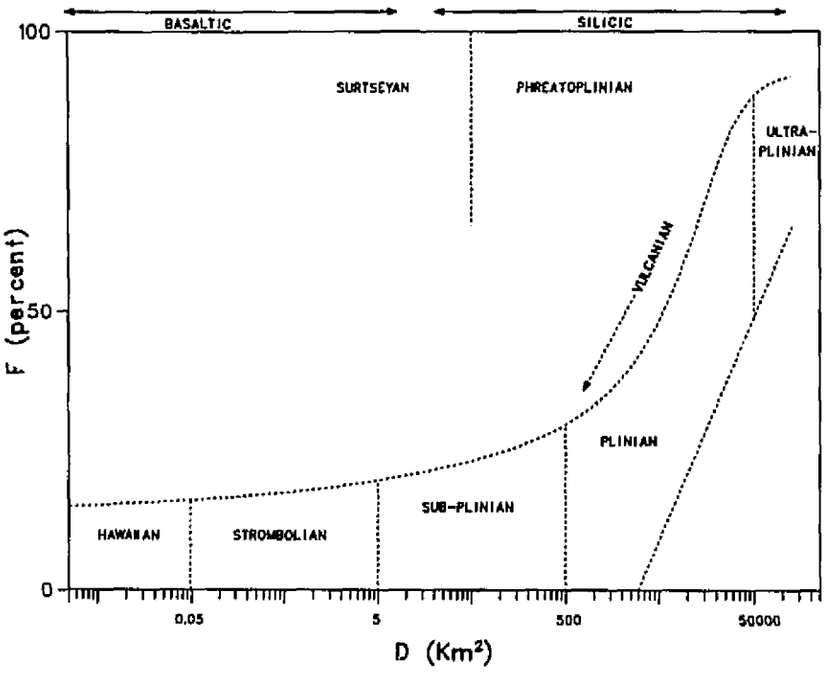


FIGURE 16.1 Classification diagram for pyroclastic eruptions (after Walker, 1973; Wright *et al.*, 1980). The $F$ is the weight percent of material finer than 1 mm on the axis of dispersal, where it is crossed by the $0.1T_{max}$ isopach. The $D$ is the area inclosed by the $0.01T_{max}$ isopach.

used for classification of eruption types based on the properties of the pyroclastic component (Walker, 1973; Wright *et al.*, 1980), can be viewed as a measure of the explosiveness of an eruption. Positive displacement along the $x$ axis represents increased particle dispersal, and height along the $y$ axis represents increased particle fragmentation. Volcanic eruptions of basaltic composition have low dispersal and fragmentation values because of their low water contents (0.1 to 2 wt. %), lower viscosities ($10^2$ to $10^3$ P), and Newtonian fluid properties. These eruptions fall into the Hawaiian and Strombolian fields in the lower left part of Figure 16.1. The limited dispersal and fragmentation characteristics of basaltic eruptions result in the smallest potential for disruption effects should a repository be penetrated by basaltic magma. The only important exception is hydrovolcanic activity, when basalt magma mixes at shallow levels with water and is fragmented and dispersed by water/magma vapor explosions. These eruptions have greatly increased particle fragmentation and somewhat increased dispersal and fall within the Surtseyan field of Figure 16.1. In marked contrast, andesitic to silicic volcanic activity spans the sub-Plinian, Plinian, Vulcanian, and Ultraplinian fields of Figure 16.1. These eruptions have orders of magnitude greater dispersal of pyroclastic debris than that of basaltic eruptions. Silicic eruptions have the potential for disrupting the entire area of a waste repository and dispersing waste radionuclides on a global scale (Crowe, 1980).

We thus have two end members of volcanic activity with very different potential effects on a buried radioactive waste repository: (1) monogenetic volcanoes of mafic composition, which have limited dispersal and disruptive effects, and (2) long-lived silicic volcanoes, which have large dispersal and disruptive effects. The potential risk from the latter type of volcanic activity can and should be greatly reduced by careful selection of sites for a repository. Large-volume, long-lived volcanic centers are generally confined to distinct volcanic zones. For example, continental arc volcanoes form aligned volcanic chains that are located above active subduction zones. The long-term existence of the arc itself and the host of tectonic features associated with an active subduction zone make arc volcanism relatively easy to recognize and avoid (for example, the Cascade volcanic arc in the Pacific Northwest). Similarly, we now recognize that many if not all of the major silicic volcanic fields of the western United States exclusive of the Cascade chain (for example, the Jemez field in New Mexico, the Yellowstone field in Wyoming, and the Long Valley field in California) occur in distinct volcanic lineaments (Smith and Luedke, 1984). These volcanic zones appear to form from melting of the lower crust within areas of upwelling of mantle-derived basaltic magmas (Smith, 1979;

Hildreth, 1981). The large flux of basaltic magma required to raise crustal rocks to their melting temperatures and the apparent need for extensional deformation to provide storage space for the basalts mean that sites of silicic magmatism are zones of high heat flow and tectonic activity. Again, these are relatively easy to recognize and avoid in selection of sites for waste storage. The problem of choosing a site for waste disposal in the western United States and minimizing potential effects of future volcanism becomes a matter of determining the risk of future volcanic eruptions in recognized volcanic zones.

## SITE-SPECIFIC TECHNIQUES OF VOLCANIC HAZARD ASSESSMENT

There are two methods for assessing the hazards of volcanism at a site being investigated as a repository for high-level radioactive waste. The first and generally more traditional approach is to study the past record of volcanism at and around a site by using the current tools available to geologic sciences (field mapping, geochronology, petrology, geochemistry, and geophysics). Whereas this approach provides essential data for understanding the past record of volcanism, it does not provide a direct means for deciding whether volcanism represents a significant threat to waste disposal. The second method, which is used increasingly in geological studies for waste disposal, is risk assessment (for example, Crowe and Carr, 1980; D'Alessandro *et al.*, 1980). In this sense, risk is defined as the product of probability and consequences. Probability determinations provide a means of specifying levels of risk as a function of time, and consequences give a perspective for judging acceptable probability levels. In the following sections, the use of risk assessment is described for a potential waste disposal site on and adjacent to the NTS.

### *Volcanic Geology of the Nevada Test Site Region*

The NTS is located in southcentral Nevada approximately 80 km northwest of Las Vegas (Figure 16.2). The current proposed site for burial of high-level radioactive wastes is Yucca Mountain, a linear range upheld by a thick accumulation of ash-flow and air-fall tuff and associated volcaniclastic rocks derived from the Timber Mountain-Oasis Valley caldera complex (Christiansen *et al.*, 1977). The identified volcanic hazards for the Yucca Mountain site are twofold: the hazards of future silicic volcanism and the hazards of basaltic volcanism. The hazards of silicic volcanism are considered to be negligible for a number of reasons (Crowe *et al.*, 1983a):

1. There has been no silicic volcanism within the NTS region for at least the last 7 million years (m.y.). The youngest silicic volcanic activity (7 to 8 m.y.) was associated with the Black Mountain caldera, which is located approximately 80 km north-northwest of Yucca Mountain.
2. There has been a dramatic regional decrease, and in most areas a cessation, of silicic volcanic activity within the southern Great Basin during the last 10 to 20 m.y. (Stewart *et al.*, 1977).
3. Silicic volcanic activity of Quaternary age is restricted entirely to the margins of the Great Basin.

The hazards of basaltic volcanism are much more difficult to define and have been the subject of detailed studies (Crowe and Carr, 1980; Vaniman and Crowe, 1981; Crowe *et al.*, 1982, 1983a,b). The NTS region is in a zone of active volcanism referred to as the Death Valley-Pancake Range (DV-PR) volcanic zone. This zone extends from the Lunar Crater volcanic field in central Nevada south-southwestward to southern Nevada and adjoining areas of eastern California (Figure 16.2). The zone merges at its southern end with the Western Cordilleran rift zone of Smith and Luedke (1984). The DV-PR volcanic zone has been active since the cessation of silicic volcanism in the southern Great Basin, about 8 m.y. ago. At that time, basaltic volcanism surpassed silicic volcanism in erupted volume. Centers of active basaltic and minor silicic volcanism shifted progressively to the margins of the southern Great Basin, whereas intermittent activity continued within the DV-PR volcanic zone (Crowe *et al.*, 1983a). Centers of Quaternary volcanic activity in the volcanic zone include the Cinder Hill scoria cone in southern Death Valley (0.7 m.y.), the Lathrop Wells scoria center (0.3 m.y.) located 20 km south of the waste disposal site at Yucca Mountain, four basalt centers (1.2 m.y.) aligned along a north-northeast trending arc in Crater Flat immediately west of Yucca Mountain, two small scoria cones named the Sleeping Butte cones (0.3 m.y.) located 10 km south of Black Mountain caldera, and at least 10 centers in the Lunar Crater volcanic field.

Two major types of volcanic fields are present in the DV-PR volcanic zone. Type-I fields include long-lived volcanic fields that are active over a period of several million years. Mafic centers in these fields are clustered, with vent densities of $10^{-1}$ to $10^{2}$ vents/km. Magma volumes of individual centers are approximately 1 to 2 $km^3$, and the total volume of the fields exceeds 10 $km^3$. The range of rock types in type-I fields includes basaltic andesite and trachyte that probably evolved through fractionation from basalt and bimodal basalt-rhyolite as-

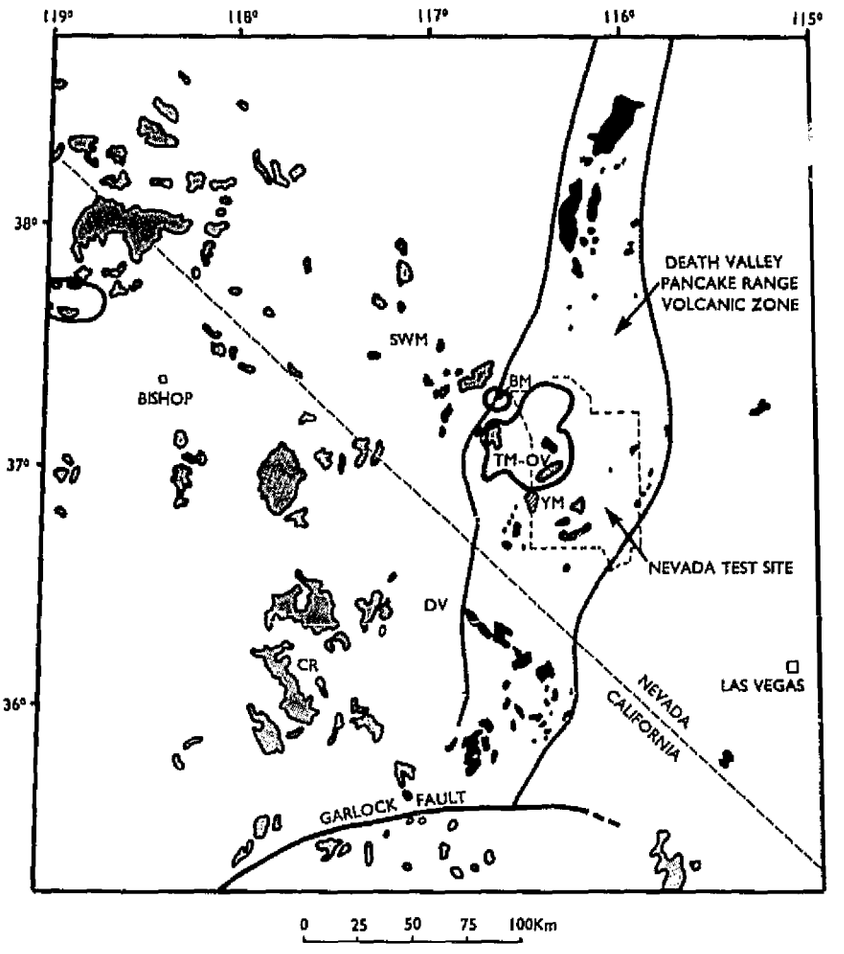


FIGURE 16.2 Generalized geologic map of the Death Valley-Pancake Range volcanic zone. SWM: Stonewall Mountain; BM: Black Mountain; TM-OV: Timber Mountain-Oasis Valley caldera complex; YM: Yucca Mountain exploration block; DV: Death Valley; and CR: Coso Range.

semblages. Type-I volcanic fields in the DV-PR volcanic zone include the Greenwater and Black Ranges in southern Death Valley (8 to 4 m.y.), the oldest episode of basaltic volcanism in the NTS region (11 to 8.5 m.y.), the Reveille Range (6 to 5 m.y.), and the Lunar Crater volcanic field (4 m.y. to Recent). Type-II volcanic fields include small-volume ($<1$ km$^3$) monogenetic centers, which consist of clusters of scoria cones and small-volume lava flows. Vent densities of these fields are low and average about $10^{-3}$ to $10^{-4}$ vent/km$^2$. Lava compositions are predominantly hawaiite with lesser amounts of alkalic olivine basalt. The hawaiites tend to be of evolved composition (Vaniman *et al.*, 1982) with Mg numbers [Mg/(Mg + $Fe^{2+}$)] generally $<0.55$. Parental basalts (Mg number $>0.68$) are rare. Type-II volcanic fields in the DV-PR volcanic zone include southernmost Death Valley, the NTS region, and Kawich Valley (Figure 16.2).

Crowe *et al.* (1983a) divided the basaltic rocks of the NTS area surrounding the Yucca Mountain site into three episodes; each episode spans several million years and includes basalt from many eruptive centers. The volume relations of these episodes versus time are shown on Figure 16.3. The oldest episode of basaltic volcanism includes the basalts of the silicic episode, which erupted during the waning phase of silicic volcanic activity (11 to 8.5 m.y.). These basalts form bimodal basalt-rhyolite centers that crop out in a northwest-trending zone extending from the south moat zone of the Timber Mountain caldera to Stonewall Mountain (Figure 16.2). Volumes of basaltic magma associated with the basalts of the silicic episode are large, and individual centers exceed 10 km$^3$ in volume. The basalts of the silicic episode were replaced gradationally in time by the older rift basalts. The older rift basalts are either distinctly younger than or spatially separate from the silicic volcanic cen-

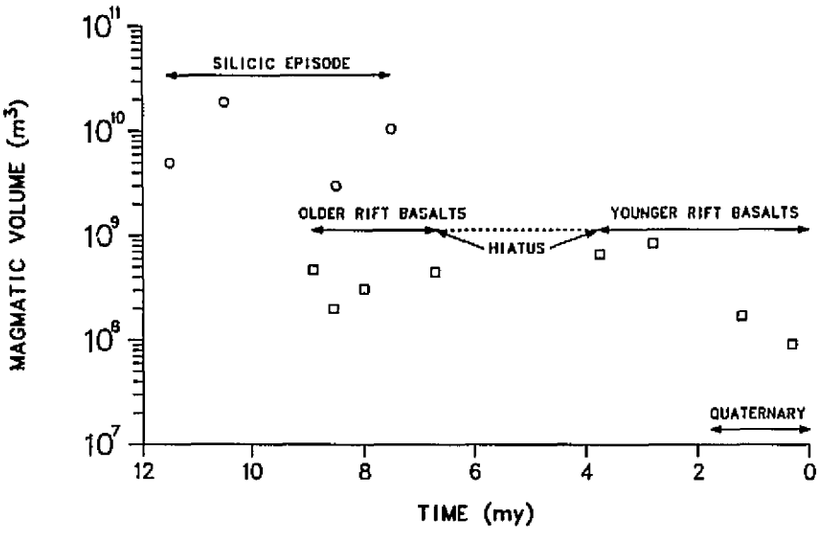


FIGURE 16.3 Plot of magma volume versus time for volcanic episodes of the NTS region. Volumes for the silicic episode are average estimations for a 1 m.y. period. Volumes of the rift basalts are for individual volcanic cycles. The identification of the volcanic hiatus is based on extensive age determinations of volcanic rocks in the NTS region.

ters. They consist of small-volume ($<1$ km$^3$) monogenetic Strombolian centers that erupted during the probable peak of extensional faulting. Magma volumes during this episode declined drastically, then stabilized at low but uniform rates (Figure 16.3). There was a brief but important pause in volcanic activity between 6.5 and 3.7 m.y. This hiatus was followed by eruption of the younger rift basalts. These basalts form widely scattered, small-volume centers identical to those of the older rift basalts. They are separated from the older rift basalts on the basis of their age (3.7 m.y. to Recent) and their enrichment in incompatible trace elements, with the exception of Rb (Vaniman *et al.*, 1982). The younger rift basalts record an interval of declining magma production rates (Figure 16.3). The decline may coincide with a declining rates of tectonism in the NTS region and increased activity in the adjoining southwestern areas of the Great Basin (Death Valley and Owens Valley, Figure 16.2).

Figure 16.4 is a geologic map of the Lathrop Wells center. This center illustrates a number of characteristic features of Strombolian centers of both the younger and older rift basalts. Each center consists of a main scoria cone flanked by several smaller satellite cones. The satellite cones are generally older and are located south or southeast of the main scoria cone. This suggests a north to northeastward migration of active vents during an eruption cycle. The number of vents per center averages 2 to 3 for the Quaternary centers of the NTS region (Crowe *et al.*, 1983b). Blocky aa lava flows vented from the flanks of the main scoria cone and traveled short distances. Measured flow lengths of Quaternary flows in the NTS region range from 0.6 to 1.9 km with a mean length of 1.1 km. It is inferred that scoria fall sheets extended downwind from the main scoria cone. These are entirely removed by erosion at all but the youngest centers in the NTS region. The only exception is the 270,000-yr-old scoria fall sheet of the Lathrop Wells center, and only minor remnants of this sheet are preserved. The cumulative volume of individual centers in the NTS region (dense rock equivalent) was calculated assuming a scoria fall sheet-to-cone ratio of 5:1. Magma volumes for the Quaternary cones of the NTS region range from $10^5$ to $10^8$ m$^3$ with a mean of $3 \times 10^7$ (Crowe *et al.*, 1983b, p. 269).

## PROBABILITY AND CONSEQUENCE ASSESSMENT

### *Probability*

Several aspects of the history of basaltic volcanism in the NTS region provide justification for a probabilistic approach to volcanic hazards. First, there has been a consistency or decline in the rates of basaltic volcanism for the past 8.5 m.y. Second, all basalt centers formed during the past 8.5 m.y. are small-volume Strombolian centers. Third, the petrology of the erupted basalts is broadly similar throughout this period, which is indicative of similar conditions of magma genesis. The consistency in rates, eruptive style, and petrology for this extended period provides a basis for forecasting rates of future volcanism for the required containment period of high-level radioactive waste.

The probability of disruption of a repository by basal-

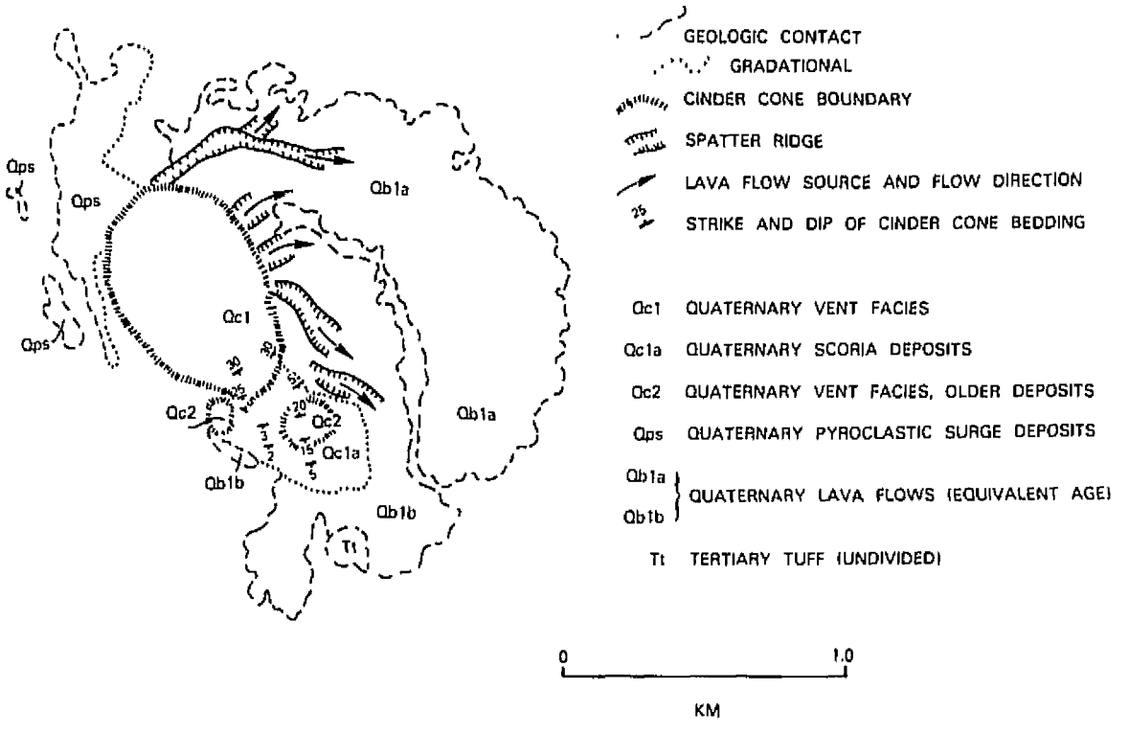


FIGURE 16.4 Geologic map of the Lathrop Wells basalt center located 20 km south of Yucca Mountain. From Vanlman and Crowe (1981).

tic magma can be formulated as a case of conditional probability

$$Pr = \{E2 \text{ given } E1\}, \tag{16.1}$$

where $Pr$ is the probability of repository disruption, $E1$ is the rate of occurrence of volcanic events, and $E2$ is the probability of intersection of a repository by magma, given $E1$. This probability can be expressed as (Crowe *et al.*, 1982)

$$Pr[\text{no disruptive event before time } t] = \exp(-\lambda t p), \tag{16.2}$$

where $\lambda$ is the rate of volcanic activity and $p$ is the probability that an event is disruptive. This formulation assumes that the time between events is exponentially distributed, and the number of events in time intervals of length $t$ has a Poisson distribution with a mean of $\lambda t$. The $p$ can be estimated as the ratio $a/A$, where $a$ is the area of a repository or of an assigned volcanic disruption zone (whichever is larger) and $A$ is some minimal area that encloses the repository and the volcanic events used to describe $\lambda$. For the case of basaltic volcanic activity, $a$ is the area of the repository. It is estimated to be about 6 to 8 km$^2$, based on the size of the exploration block at Yucca Mountain (Crowe *et al.*, 1982). The $A$ can be selected in a number of ways. Crowe and Carr (1980) defined $A$ as the area enclosed by circles of 25- and 50-km radii with centers at the Yucca Mountain exploration block. This approach, although computationally simple, does not consider the spatial trends in the distribution of volcanic centers that are controlled by tectonic features. Crowe *et al.* (1982) developed a numerical approach to find the minimum area circle and the minimum area ellipse that contain the volcanic centers of interest and the repository site. Differing combinations of ellipses and circles were obtained using geologic assumptions concerning the tectonic setting of volcanic centers. Disruption probability values are calculated and tabulated in table form (Crowe *et al.*, 1982), which allows a range of values $p$ to be used in Eq. (16.2). The preferred definition of $p$ is based on the distribution of volcanic centers in the DV-PR volcanic zone.

The most difficult parameter to estimate for probability calculations is $\lambda$, the rate of volcanic activity. Ideally, rates should be determined from an understanding of the controlling processes of volcanic activity. Although this is not now possible, a number of studies suggest that rates of volcanism are related in a direct but as yet poorly understood way to the regional stress-strain pattern. That is, rates of volcanism, similar to regional

seismicity, reflect the degree of tectonic activity of a region. For example, Shaw (1980) related rates of magma production at Hawaii to seismic moment—a measure of the volume change represented by the release of seismic energy. He assumed that the potential energy available in a tectonic system may be released through both seismic radiation and the generation and ascent of magma. The demonstration of a connection between the release of seismic energy per year and the annual rate of magma production suggests that the two tectonic processes are closely related and that, by inference, magmatism may be an important process in regulating mantle stress levels (Shaw, 1980, p. 259). Similarly, Feigensen and Spera (1981) recognized a correlation between the occurrence of tholeiitic and incompatible-element-enriched alkalic magmas and eruption frequency in Hawaiian lavas. They related magma production to shear-stress deformation (viscous deformation of Shaw, 1973) and suggested that a reduction in shear stress caused a decrease in the degree of partial melting and an increase in the time between eruptions. Bacon (1982) documented a time-predictable relation among the basalts and high-$SiO_2$ rhyolites of the Coso volcanic field. He suggested that the magma production rate for the field is controlled by a constant strain rate. A minimum strain value equal to the failure strength of the crustal rocks must be exceeded to allow ascent of magma.

These studies, although promising, are not yet sufficiently developed to allow estimates of volcanism rates, particularly for relatively inactive regions such as the NTS. We thus are forced to forecast future rates of volcanic activity on the basis of past activity. Crowe *et al.* (1982) estimated rates of volcanic activity in two ways: through counts of age-controlled volcanic centers and through variations in magma volume versus time. The first technique involves field mapping vent zones for Quaternary volcanic centers. Each vent is treated as one volcanic event, and time control is provided by the K-Ar age and the magnetic polarity of the volcanic center. A somewhat similar approach, with less rigorous age controls, was used to determine the probability of faulting for a potential waste disposal site in Italy (D'Alessandro *et al.*, 1980). Estimated rates of volcanic activity are calculated by counting vents within the areas defined in the determination of $A$. These rates durir g Quaternary time ($< 1.8$ m.y.) are about $8 \times 10^{-6}$ volcanic events per year for the NTS region, $7 \times 10^{-5}$ volcanic events per year for the DV-PR volcanic zone, and $8 \times 10^{-5}$ volcanic events per year for the southern Great Basin (Crowe *et al.*, 1982). The latter two calculations are strongly effected by the high cone density of the Lunar Crater volcanic field at the northern end of the DV-PR volcanic zone.

The calculation of volcanic rates by using rates of magma production is based on Figure 16.5, an expanded version of Figure 16.3. Figure 16.5 shows magma volume (dense rock equivalent) versus time for the past 3.7 m.y. The basaltic eruptions show a linear decrease in magma volume with time. Regression analysis, treating magma volume as the dependent variable, gives a coefficient of determination of 0.8 and a rate of magmatic production of 210 $m^3$/yr. This magma production rate is used to calculate the times required to generate magma volumes that are equal to representative volumes of past magmatic cycles in the NTS region. These times, corrected for the time since the last basaltic

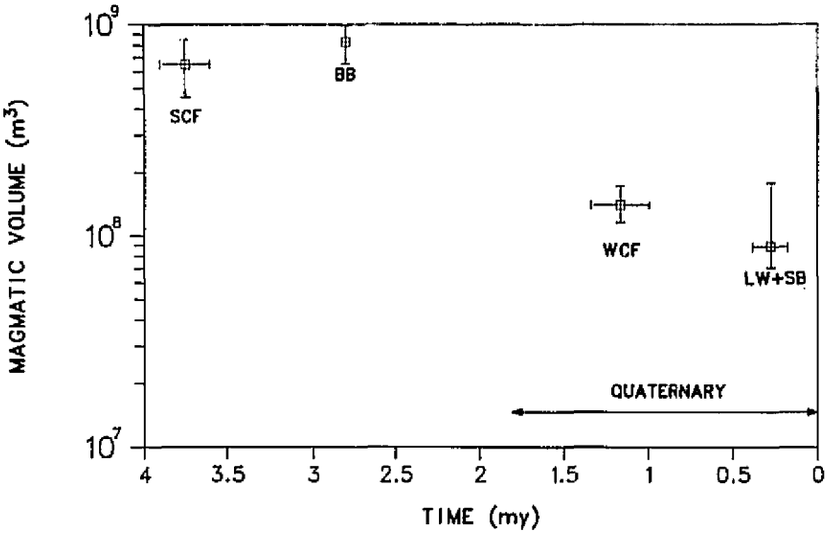


FIGURE 16.5 Plot of magma volume (dense rock equivalent) versus time for the younger rift basalts. Error bars for time are the standard deviation (1) of replicate age determinations. Error bars for the volume are estimates of errors in volume calculations. From Crowe *et al.* (1982).

eruption ($2.7 \times 10^5$ yr) give predicted occurrence times or rates of future activity (Crowe *et al.*, 1982).

The conditional probability for the combined occurrence of a future basaltic event and that event to directly intersecting a buried radioactive waste repository at Yucca Mountain is calculated using Eq. (16.2) and the data tables for $\lambda$ and $p$. Because of the large uncertainties in the probability calculations, little emphasis is placed on individual calculations. Rather, a range of probability values is assembled by using a matrix of area ratios and rate determinations. Probability bounds are established by the extremes of the calculated probabilities. These bounds are $5 \times 10^{-8}$ to $3 \times 10^{-10}$ yr$^{-1}$ for the Yucca Mountain site (Crowe *et al.*, 1982).

*Consequence*

Consequence analysis involves identification of volcanic processes that could lead to failure of a waste-isolation system and calculation of the results of failure expressed as radiological levels of released waste elements. Crowe *et al.* (1983b) suggested that the most likely event to affect a buried repository at Yucca Mountain would be intrusion of the repository by rising basaltic magma, followed by Strombolian eruptions of waste-contaminated magmas. They argued, based on field evidence, that the most likely intrusion structure for basalt at repository depths (>300 m) would be linear dikes, that there would be 2 to 3 dikes per volcanic event, and that the dike widths and lengths would be 0.3 to 4 m and 0.5 to 5 km, respectively. Using these background parameters, the important questions become: (1) How much waste material would be incorporated in the basalt magma, and (2) how would the waste material be dispersed with the magma at the surface?

The mechanisms of intrusion of basalt magma into a waste repository are difficult to predict. Magma could completely flood a repository tunnel or intrude as narrow dikes with the only magma/waste contact being along the dike walls. In either case, the number of waste canisters that would be contacted by magma and potentially carried to the surface ranges from 0 to more than 400 (Logan *et al.*, 1982). It is possible to establish limits on the volume of waste material incorporated in basalt magma by assuming that the repository is intersected by a dike of random orientation and tracing the pathways of waste incorporated in magma through analogy with the distribution of lithic (country-rock) fragments in basalt scoria. Studies of the distribution of these fragments in basaltic rocks revealed that they are derived from shallow levels and are concentrated in the pyroclastic component (Crowe *et al.*, 1983b). This latter conclusion is based on the fact that particles in a magma exsolving volatiles are preferential sites of bubble nucleation (Sparks, 1978) and that lithic fragments are present in small amounts in cone scoria but are extremely rare in lava. Two mechanisms are proposed for the incorporation of lithic fragments in basaltic magma: (1) during magma fragmentation when the gas-to-magma ratio reaches 0.75 and the magma disrupts (Wilson and Head, 1981) and (2) during hydrovolcanic explosions associated with a predominantly Strombolian eruptive cycle. Assuming that waste particles are dispersed in an eruption in the same pattern as country-rock lithic fragments would be, Crowe *et al.* (1983b) calculated that 600 to 1100 m$^3$ of a repository inventory would be dispersed in a pyroclastic eruption. Of that inventory, 15 to 20 percent will be deposited in the scoria cone (less than 1 percent will be exposed at the surface during a time period of $10^4$ yr), 50 to 80 percent will be deposited in the scoria fall sheet, and 2 to 5 percent will be regionally dispersed with the fine-grained particle component (windborne). These calculations are based on an average lithic fragment abundance of 0.032 percent by volume in studied scoria deposits of the NTS region and the San Francisco volcanic field in northern Arizona (Crowe *et al.*, 1983b).

An additional eruptive process in basaltic eruptions is hydrovolcanic vapor explosions. This type of eruption occurred at three basalt centers in the NTS region during the past 10 m.y. The increased dispersal distance and the greater particle fragmentation of hydrovolcanic explosions, as noted previously, could greatly increase the consequences of repository disruption. Crowe and Carr (1980) originally argued that hydrovolcanic activity was unlikely at Yucca Mountain. This was based on the depth to the groundwater table at Yucca Mountain (>300 m below the surface) and the lack of surface water as a result of the arid climate and steep drainage gradients. Moreover, the moisture content of the unsaturated zone at Yucca Mountain is insufficient to allow initiation or maintenance of hydrovolcanic explosions except under extreme saturation conditions (Crowe *et al.*, 1983b). New data on hydrovolcanic activity have caused re-examination of this question. Although field evidence indicates that lithostatic load has an inhibiting effect on the formation of hydrovolcanic activity (probably because the vapor phase of water is suppressed), this may not always be the case. In the geologic setting of Yucca Mountain, groundwater may mix in a supercritical state with magma below the repository level. As the magma/water mix ascends and the pressure drops, vapor explosions may occur throughout an interval extending from the water table through the repository horizon to the surface. Studies of fuel-coolant interactions and experimental work using thermite melt mixed with

water to simulate volcanic eruptions (Wohletz and McQueen, 1984) show that the major control of hydrovolcanic explosions is the mass ratio of water to magma. Eruptions may vary between Surtseyan and Strombolian, depending on this ratio. The optimum ratio for development of Surtseyan explosions is about 0.3 (Wohletz and McQueen, 1984).

The occurrence of lithic fragments in basalt scoria of the Lathrop Wells center may be due, as noted above, to hydrovolcanic explosions. Such explosions would require a water-to-magma ratio of less than about 0.3 so that the eruptions would have been predominantly Strombolian with only a minor hydrovolcanic component. This is suggested by the irregular distribution of fragments in scoria (intermittent explosions) and the fact the initial eruptions of the center were hydrovolcanic (Vaniman and Crowe, 1981). If it is assumed that the fragments were produced by a hydrovolcanic component, possible effects of hydrovolcanic explosions were included in the calculations of lithic fragment abundance. In this case, the consequences of a hydrovolcanic component can be shown to be small (Logan *et al.*, 1982). A more extreme case, having major negative consequences for waste isolation, would be the possibility of exhumation of a buried repository during crater-forming hydrovolcanic explosions. This possibility is tested by data summarized in Figure 16.6, which is a relative-frequency diagram of crater depth for hydrovolcanic centers (maars and tuff rings) based on the data of Pike and Clow (1981). The crater-depth data are positively skewed, and the mean depth is 91 ± 67 m. The average depth to the repository horizon at Yucca Mountain is about 380 m (the depth varies throughout the exploration block because of the 6 to 8° eastward dip of the currently favored repository horizon). A depth of 380 m is greater than 4 standard deviations from the mean depth of hydrovolcanic craters and exceeds the maximum listed crater depth in the data catalog of Pike and Clow (1981). The low probability of repository disruption ($10^{-8}$ to $10^{-10}$ $yr^{-1}$), coupled with the low probability of exhumation of a repository by explosive cratering, suggests that the risk of hydrovolcanic explosions is of limited concern at Yucca Mountain.

The radiologic consequences of basaltic volcanism have been calculated for the disruption of two hypothetical repositories, both located at Yucca Mountain (Logan *et al.*, 1982). The first contained unreprocessed spent fuel and the second reprocessed waste. The calculations assumed a repository storage capacity of half the estimated volume of spent fuel or reprocessed waste generated by commercial power reactors through the year 2000. It was estimated that the repository area would be 1640 $m^2$ and would contain waste aged for 10 yr at the time of emplacement. A range of geometric arguments is used to determine the number of canisters that would be intersected by a linear basalt dike. The preferred approach was to assume a random orientation of the dikes

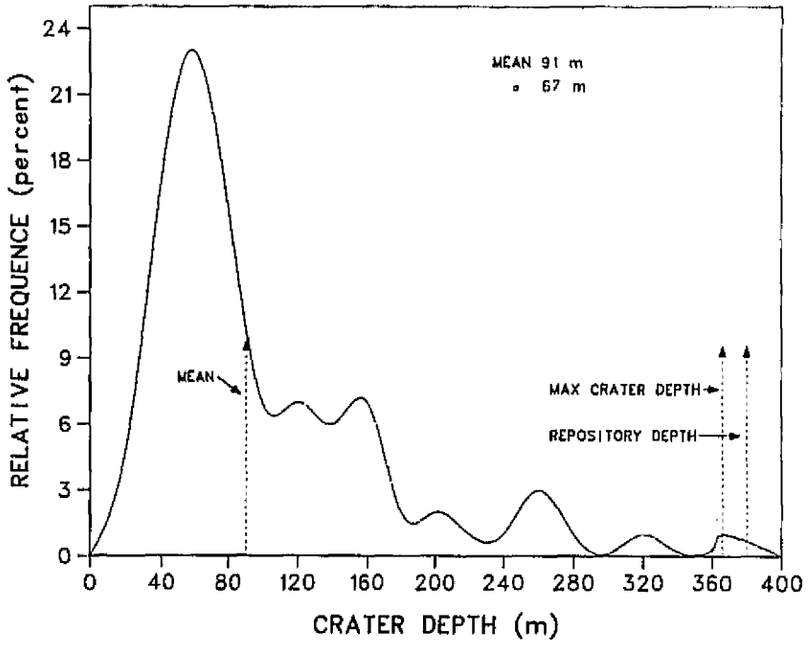


FIGURE 16.6 Relative-frequency diagram of crater depth for hydrovolcanic craters. The data are positively skewed with a mean of 91 m. Repository depth is the estimated average depth to the repository horizon at Yucca Mountain. Maximum crater depth is the deepest measured crater. Data on crater depths are from Pike and Clow (1981).

encountering the repository tunnel complex. Accordingly, magma would intersect about seven canisters of spent fuel and about one cannister of high-level waste—equivalent to an inventory fraction in both cases of about $8 \times 10^{-5}$ (Logan *et al.*, 1982, p. 32). There are no data on the behavior of a waste canister in rising and vesiculating magma. Therefore, it was assumed that all waste contacted by magma would be incorporated uniformly in the magma and carried to the surface to be erupted preferentially with the pyroclastic component. Radiological dose was examined in two forms: the dose resulting from the waste entrained in the basalt eruption column and the dose resulting from exposure to waste-bearing scoria deposits, resuspended particles, and radionuclides entering the food chain. Population, agricultural, and meteorological data from Yucca Mountain were used to calculate doses from the airborne component. The worst case for the airborne dose resulted in a cumulative total of 25 health effects in $10^6$ yr (Logan *et al.*, 1982, p. 6). Dose effects were calculated from scoria deposits that formed the scoria cone and the scoria fall deposits downwind of a hypothetical eruption and include effects of erosional transport during a period of $10^6$ yr. The worst case here yields about 2800 health effects in $10^6$ yr. Finally, Logan *et al.* (1982) calculated the total activity that would be transported to the surface, normalized to $10^3$ MTHM. The values vary for the type of waste and the time of eruption relative to emplacement and closure of the repository. Stepwise integration of the release fraction by radionuclide with the annual probability of volcanic disruption of a repository using the computer code AMRAW (Logan and Berbano, 1978) gives total expected releases as a function of time. The total expected release for $10^4$ yr is 1.8 Ci or 0.038 Ci/$10^3$ MTHM for spent fuel and 1.3 Ci or 0.034 Ci/$10^3$ MTHM for high-level waste (Logan *et al.*, 1982, p. 163).

## DISCUSSION

A variety of evidence shows that there is a finite risk of volcanism with respect to storage of radioactive waste at Yucca Mountain. In particular, the site is located in a zone of active volcanism—the Death Valley-Pancake Range volcanic zone and five Quaternary volcanic centers (1.2 to 0.3 m.y.) are present within a range of 8 to 20 km of the exploration block. Geologic data show that there has been a consistency in the rates, eruptive style, and petrology of basaltic volcanism in the NTS region for the past 8 m.y. Volcanic activity in the region was characterized by formation of scattered small-volume Strombolian scoria cones and lava flows. Rates of volcanism have been low, and there is some evidence of a decline in the rate of magma production during the past 3.7 m.y. The consistency in the geologic record provides some degree of confidence that future volcanic patterns can be projected for periods of $10^4$ to $10^5$ yr. These circumstances provide a reasonable basis for applying risk-assessment techniques to define the magnitude of volcanic hazards. Probability estimates of the likelihood of the combined occurrence of a future volcanic event and the likelihood that the volcanic event will intersect a buried repository at Yucca Mountain are very low—$10^{-8}$ to $10^{-10}$ per year. The consequences of penetration of a repository by basaltic magma followed by eruption of the magma at the surface are limited, perhaps surprisingly limited. This is due to the small subsurface area of basalt feeder dikes, the probable limited intrusion effects of these dikes, and the limited surface dispersal of basaltic particulates in Strombolian eruptions. The combination of the low probability and limited consequences indicate that the risk of volcanism at this particular site is low.

The suitability or unsuitability of the Yucca Mountain site will be decided by the U.S. Nuclear Regulatory Commission if the Department of Energy recommends the site as a formal candidate for a waste repository. Certainly many other criteria other than volcanism will be considered in any licensing decisions; this paper emphasizes the methods followed to define the magnitude of volcanic hazards. In the Nevada case, geologic, geochronologic, petrologic, geochemical, and geophysical data are used in combination with techniques of risk assessment to evaluate volcanic hazards. Some but not all of these methods may be useful for hazard assessment at other sites under consideration for disposal of high-level radioactive waste.

How reliable are the geologic data used for risk assessment? Certainly the field, geophysical, and laboratory data have been gathered as carefully as possible, and the reliability of this work must be judged by research standards established in the current geologic literature. Research data have been evaluated at review meetings where hazard data were presented to a panel of scientists. The volcanic hazard work has also been published in the scientific literature to provide a wide exposure to the scientific community. An additional item of concern is the built-in bias in the work. That is, the purpose of the Nevada Nuclear Waste Storage Investigations is to attempt to find and prove a site for disposal of radioactive waste. As studies of a site progress and increased funding is invested, there is mounting pressure to "prove" the site. The presentation of both positive and negative evidence of the hazards of volcanism (Crowe *et al.*, 1983b) is an attempt to overcome this bias.

There is a continuing controversy over the use of

probabilistic studies in geology. Indeed, the special problems of hazard prediction in waste disposal have brought this question to the forefront (for example, Marsily and Merriam, 1982). Questions have been raised whether geologic process are truly random and suitable for probabilistic analyses (D'Alessandro and Bonne, 1982). Certainly, with respect to the Nevada work, the data used for probability calculations are limited at best. The number of data points for rate calculations are small, and it is difficult to include effects of tectonic setting in localizing sites of volcanism. What is the time sensitivity of the data? For the Nevada site, future rates of volcanism are forecast on the basis of the geologic history of the region during the past 3.7 m.y. The isolation period of radioactive waste is 3 to 0.3 percent of this time, and, thus, it is not clear how sensitive this approach is to short-term variations in tectonic processes. Because of these data uncertainties, the probability is presented as a range spanning 3 orders of magnitude and the data assumptions are biased toward the worst case to provide conservative estimates (Crowe *et al.*, 1982). Similar questions are raised about the results of consequence analyses. The detailed effects of intrusion of a repository by volcanism are not clear. Variations in the strike of linear dikes intersecting a repository result in differences in the number of contacted cannisters, ranging from 0 to more than 400 (Logan *et al.*, 1982). Equally, we can only speculate how waste could be incorporated in a magma. It may be maintained in its cladding, may be fragmented as a particulate, or may be geochemically dispersed in the magma. Any of these possibilities results in major changes in the calculated radiological dose levels through time.

## ACKNOWLEDGMENTS

Much of the work on the volcanic hazards of the NTS site was completed with Will Carr (U.S. Geological Survey) and Dave Vaniman (Los Alamos National Laboratory); probability studies were completed with Mark Johnson and Richard Beckman (Los Alamos National Laboratory). I have been greatly aided by their cooperation and numerous discussions. The manuscript was reviewed critically by B. D. Marsh, G. D. Robinson, D. T. Vaniman, and K. H. Wohletz. Funding for the NTS work was provided by the Nevada Nuclear Waste Storage Investigations and the Office of Basic Energy Sciences through the U.S. Department of Energy.

## REFERENCES

Bacon, C. R. (1982). Time-predictable bimodal volcanism in the Coso Range, California, *Geology 10*, 65-69.

Bredehoeft, J. D., W. W. England, D. B. Stewart, N. J. Trask, and I. J. Winograd (1978). Geologic disposal of high-level radioactive wastes—earth science perspective, *U.S. Geol. Surv. Circ. 779*.

Christiansen, R. L., P. W. Lipman, W. J. Carr, F. M. Byers, Jr., P. P. Orkild, and K. A. Sargent, (1977). The Timber Mountain-Oasis Valley caldera complex of southern Nevada, *Geol. Soc. Am. Bull. 88*, 943-959.

Crowe, B. M. (1980). Disruptive event analysis: Volcanism and igneous intrusion, Battelle Pacific Northwest Laboratory Rep. PNL-2882.

Crowe, B. M., and W. J. Carr (1980). Preliminary assessment of the risk of volcanism at a proposed nuclear waste repository in the southern Great Basin: *U.S. Geol. Surv. Open-File Rep. 80-375*, 15 pp.

Crowe, B. M., M. E. Johnson, and R. J. Beckman (1982). Calculation of the probability of volcanic disruption of a high-level radioactive waste repository within southern Nevada, USA, *Radioactive Waste Management 3*, 167-190.

Crowe, B. M., D. T. Vaniman, and W. J. Carr (1983a). Status of volcanic hazard studies for the Nevada Nuclear Waste Storage Investigations, Los Alamos National Laboratory Rep. LA-9325-MS, 47 pp.

Crowe, B. M., S. Self, D. Vaniman, R. Amos, and F. Perry (1983b). Aspects of potential magmatic disruption of a high-level radioactive waste repository in southern Nevada, *J. Geol. 91*, 259-276.

D'Alessandro, M., and A. Bonne (1982). Fault-tree analysis for probabilistic assessment of radioactive-waste segregation: An application to a plastic clay formation at a specific site, in *Predictive Geology with Emphasis on Nuclear-Waste Disposal*, G. Marsily and D. F. Merriam, eds., Pergamon Press, New York.

D'Alessandro, M., M. Murray, C. N. Bertozzi, and G. F. Girardi (1980). Probability analysis of geologic processes: A useful tool for the safety assessment of radioactive waste disposal, *Radioactive Waste Management 1*, 25-42.

Environmental Protection Agency (1982). Draft Environmental Impact Statement 40 CFR Part 191: Environmental Standards for Management and Disposal of Spent Nuclear Fuel, High Level and Transuranic Radioactive Wastes, 228 pp.

Fedotov, S. A. (1981). Magma rates in feeding conduits of differing volcanic centers, *J. Volcanol. Geotherm. Res. 9*, 379-394.

Feigensen, M. D., and F. J. Spera (1981). Dynamic model for temporal variation in magma type and eruption interval at Kohala volcano, Hawaii, *Geology 9*, 531-533.

Gera, F. (1982). Geologic predictions and radioactive waste disposal: A time limit for the predicted requirements, in *Predictive Geology with Emphasis on Nuclear Waste Disposal*, G. Marsily and D. F. Merriam, eds., Pergamon Press, New York.

Giletti, B., R. Siever, J. Handin, J. Lyons, and G. Pinder (1978). State of geological knowledge regarding potential transport of high-level radioactive waste from deep continental repositories, *Environmental Protection Agency Rep. 520/4-78-004*, 53 pp.

Hildreth W. (1981). Gradients in silicic magma chambers: Implications for lithospheric magmatism, *J. Geophys. Res. 86*, 10153-10192.

Logan, S. E., and M. C. Berbano (1978). Development and application of risk assessment method for radioactive waste management, *Environmental Protection Agency Rep. 520/6-78-005*.

Logan, S. E., R. Link, H. S. Ng, F. A. Rockenbach, and K. J. Hong (1982). Parametric studies of radiological consequences of basaltic volcanism, Sandia National Laboratories Rep. SAND81-2375, 219 pp.

Marsh, B. D. (1984). Mechanics and energetics of magma formation and ascension, in *Explosive Volcanism: Inception, Evolution, and*

*Hazards*, Geophysics Study Committee, National Research Council, National Academy Press, Washington, D.C., pp. 67-83.

Marsily, G., and D. F. Merriam, eds. (1982). *Predictive Geology with Emphasis on Nuclear Waste Disposal*, Pergamon Press, New York, 206 pp.

Pike, R. J., and G. D. Clow (1981). Revised classification of terrestrial volcanoes and catalog of topographic dimensions, with new results on edifice volume, *U.S. Geol. Surv. Open-File Rep. 81-1038*, 40 pp.

Shaw, H. R. (1973). Mantle convection and volcanic periodicity in the Pacific: Evidence from Hawaii, *Geol. Soc. Am. Bull. 84*, 1505-1526.

Shaw, H. R. (1980). The fracture mechanisms of magma transport from the mantle to the surface, in *Physics of Magmatic Processes*, R. B. Hargraves, ed., Princeton University Press, pp. 201-264.

Smith, R. L. (1979). Ash-flow magmatism, in *Ash-Flow Tuffs*, C. E. Chapin and W. E. Elston, eds., Geol. Soc. Am. Spec. Paper 180, pp. 5-27.

Smith, R. L., and R. G. Luedke (1984). Potentially active volcanic lineaments and loci in western conterminous United States, in *Explosive Volcanism: Inception, Evolution and Hazards*, Geophysics Study Committee, National Research Council, National Academy Press, Washington, D.C., pp. 47-66.

Sparks, R. S. J. (1978). The dynamics of bubble formation and growth in magmas: A review and analysis, *J. Volcanol. Geotherm. Res. 3*, 1-37.

Stewart, J. H., W. Moore, and I. Zietz (1977). East-west patterns of Cenozoic igneous rocks, aeromagnetic anomalies, and mineral deposits, Nevada and Utah, *Geol. Soc. Am. Bull. 88*, 67-77.

Suppe, J., C. Powell, and R. Berry (1975). Regional topography, seismicity, Quaternary volcanism, and the present-day tectonics of the western United States, *Am. J. Sci. 275-A*, 397-436.

Vaniman, D., and B. M. Crowe (1981). Geology and petrology of the basalts of Crater Flat: Applications to volcanic risk assessment for the Nevada Nuclear Waste Storage Investigations, Los Alamos National Laboratory Rep. LA-8845-MS.

Vaniman, D., B. M. Crowe, and E. S. Gladney (1982). Petrology and geochemistry of hawaiite lavas from Crater Flat, Nevada, *Contrib. Mineral. Petrol. 80*, 341-357.

Walker, G. P. L. (1973). Explosive volcanic eruption—A new classification scheme, *Geol. Rund. 62*, 431-466.

Wilson, L., and J. W. Head (1981). Ascent and eruption of basaltic magma on the Earth and Moon, *J. Geophys. Res. 86*, 2971-3001.

Wohletz, K. H., and R. G. McQueen (1984). Experimental studies of hydromagmatic volcanism, in *Explosive Volcanism: Inception, Evolution, and Hazards*, Geophysics Study Committee, National Research Council, National Academy Press, Washington, D.C., pp. 158-169.

Wright, J. V., A. L. Smith, and S. Self (1980). A working terminology of pyroclastic deposits, *J. Volcanol. Geotherm. Res. 8*, 315-336.

# Index